UNIVERSITÉ DU QUÉBEC EN ABITIBI-TÉMISCAMINGUE

INVESTIGATING THE HYDROGEOTECHNICAL AND MICROSTRUCTURAL PROPERTIES OF CEMENTED PASTE BACKFILL USING THE CUAPS APPARATUS

ÉTUDE DES PROPRIÉTÉS HYDROGÉOTECHNIQUES ET MICROSTRUCTURALE DES REMBLAIS CIMENTÉS EN PÂTE À L'AIDE DE L'APPAREIL CUAPS

THESIS PRESENTED IN PARTIAL FULFILLMENT OF THE REQUIREMENTS FOR THE DEGREE OF DOCTOR OF PHILOSOPHY IN ENVIRONMENTAL SCIENCES

BY

EROL YILMAZ

MARCH 2010

This thesis is dedicated to
my late father, Ismail YILMAZ,
who passed away on January 1, 2006

UNIVERSITÉ DU QUÉBEC EN ABITIBI-TÉMISCAMINGUE

Library Release Form

Name of Author: Erol YILMAZ

Title of Thesis: Investigating the hydrogeotechnical and microstructural properties of cemented paste backfill using the CUAPS apparatus

Degree: Doctor of Philosophy (Ph.D.) in Environmental Sciences

Year this Degree was granted: 2010

UNIVERSITÉ DU QUÉBEC EN ABITIBI-TÉMISCAMINGUE

Doctor of Philosophy in Environmental Sciences

The undersigned certify that they have read, and advise to the Doctorate Program in Environmental Sciences for acceptance, a Ph.D. thesis entitled "Investigating the hydrogeotechnical and microstructural properties of cemented paste backfill using the CUAPS apparatus" submitted by Erol YILMAZ in partial fulfilment of the requirements for the degree of Doctor of Philosophy in Environmental Sciences.

Approved by the jury members below:

President of the jury:	Dr. Li Zhen CHENG, UQAM
Thesis examiners:	Dr. Tikou BELEM (Supervisor), UQAT
	Dr. Mostafa BENZAAZOUA (Co-supervisor), UQAT
	Dr. Bruno BUSSIÈRE (Co-supervisor), UQAT
External evaluator:	Dr. Andy B. FOURIE, The University of Western Australia
Internal evaluator:	Dr. Gérard BALLIVY, The University of Sherbrooke

March 2010

Major Subject: Mine backfill hydrogeotechnics

"If we knew what it was we were doing, it would not be called research, would it?"

– Albert EINSTEIN

ACKNOWLEDGEMENTS

I would like to express my sincere gratitude to my supervisor Dr. Tikou Belem for his help, guidance, supervision, encouragement, patience, and constant technical and financial support during the course of this doctoral program. I would also like to thank my co-supervisors Dr. Mostafa Benzaazoua and Dr. Bruno Bussière for their financial support, assistance, guidance, encouragement, patience, confidence and advice. As thesis committee members, Dr. Mamert Mbonimpa and Dr. Vincent Cloutier are gratefully acknowledged for their invaluable help and guidance during the course of the study. Significant contributions to enhance the quality of this thesis were also made by Dr. Andy B. Fourie of the University of Western Australia as external evaluator, Dr. Gérard Ballivy of the University of Sherbrooke as internal evaluator, and Dr. Li Zhen Cheng of the Université du Québec à Montréal as jury president.

I am also indebted to my former colleagues, Omar El Aatar, Fanta Cissokho, Dr. Anne-Marie Dagenais, Dr. Isabelle Demers, Dr. Thomas Deschamps, Elaine Fried, Reza Sadat Hosseini, Dr. Raphael Mermillod Blondin, Dr. Serge Ouellet, Geneviève Pépin, Dr. Benoit Plante and Dr. Robin Potvin, and to my student colleagues, Akué Sylvette Awoh, Hassan Bouzahzah, Samuel Coussy, Virginie Derycke, Weidan Ding, Marie-Pier Ethier, Thomas Genty, Jovette Godbout, Dr. Venceslas Goudiaby, Ichrak Hadimi, Aissa Zalagou Moussa Hamani, Jalila Hamdi, Dr. Jian-Guo Huang, Azmul Huda, Vincent Martin, Saloumeh Momenipour, Drissa Ouattara, Dr. Evgeniya Smirnova, Yadav Uprety, Huaitong Xu, Lihong Zhai and Yiqin Zhou. A special thanks goes out to Denis Bois, the principal of the unité de recherche et de service

en technologie minérale (URSTM), for giving me the opportunity to use experimental facilities, to the URSTM professional people, Hugues Bordeleau, Mélanie Bélanger, David Bouchard, Franck Gagnon, Nil Gaudet, Caroline Germain, Mélinda Gervais, Dr. Abdelkabir Maqsoud, Yvan Poirier, Alain Perreault, Dr. Olivier Peyronnard and Mathieu Villeneuve for their technical help, humour and ingenuity, to Monique Fay for her constant assistance and guidance in every way, to Françoise Bégin and Gaston Blanchette for their material and mail services, to Gisèle Neas for her invaluable help in providing technical documents, to Jimmy Maciejewski for his useful discussions about general issues, and to Louise Labbé for her outstanding hospitality during my first days in Rouyn-Noranda.

This research would not have been possible without the financial support provided jointly by the Natural Sciences and Engineering Research Council of Canada – NSERC Discovery Grant Program, the Industrial NSERC-Polytechnique-UQAT Chair on Environment and Mine Waste Management, and the Canada Research Chair on Integrated Management of Sulphidic Mine Tailings using Backfill Technology. The Canada Foundation for Innovation is gratefully acknowledged for its generous financial support for the manufacture of the ten CUAPS set-ups for my Ph.D. test program. I would like to express thanks Pierre Trudel of G+PLUS INDUSTRIAL PLASTIC Inc. for his collaborative assistance in improving the CUAPS apparatus. Special acknowledgements are also extended to Margaret McKyes for her overall revision of the Ph.D. thesis and to the anonymous referees for their constructive and practical comments, which have enhanced notably the quality of the thesis manuscripts.

Last, but certainly not least, I would like to express my deepest gratitude to all my friends and family for supporting me and for their patience throughout the four years of the program. I am also grateful to a unique person, Melissa Hamel, for things too numerous to count. I could not have completed this work without the motivating encouragement of the Hamel family (Pierrette – I call her Mamy québécoise, Marianne, Vanessa and Nathalie), the Karslioglu family (Karen and Huseyin), Sevil Yalcin and my beloved mother, Havva Yilmaz.

TABLE OF CONTENTS

LIST OF FIGURES

LIST OF TABLES

LIST OF ABBREVIATIONS, INITIALISMS AND ACRONYMS

AES	atomic emission spectrometer
AMD	acid mine drainage
ARD	acid rock drainage
ASTM	American Standard of Testing Material
atm	standard atmosphere
BET	Brunauer-Emmett-Teller (method)
cc	cubic centimetre
CFI	Canada Foundation for Innovation
CGS	centimetre-gram-second system
CPB	cemented paste backfill
CRC	Canada Research Chair
C-S-H	calcium silicate hydrate (gel)
CUAPS	curing under applied pressure system
CV	coefficient of variation
DIN	Deutsches Institut für Normung (German Institute for Standardisation)
DOS	degree of saturation
DTA	differential thermal analysis
DTG	differential thermogravimetry
EDS	energy-dispersive X-ray spectrometry
EFL	extra fast loading

Eq, Eqn	equation
ESL	extra slow loading
EVA	enterprise virtual array
FL/RL	fast/rapid loading
GGBFS	ground granulated blast furnace slag
GSD	grain size distribution
GU	general use Portland cement
GWC	gravimetric water content
HDPE	high density polyethylene
HI	hydraulic index
ICP	inductively coupled plasma
ICP-AES	inductively coupled plasma-atomic emission spectrometry
LIR	load increment ratio
LID	load increment duration
log	logarithm (common)
LVDT	linear variable displacement transducer
max	maximum
min	minimum, minute
MIP	mercury intrusion porosimetry
MKS	meter-kilogram-second system
ML	low plastic silt
ml, mL	millilitre
mmHg	millimetre of mercury (pressure)
MRTS	most represented troat size
MTS	material testing system
NSERC	Natural Sciences and Engineering Research Council of Canada
ºC	degrees Celsius
ODC	one-dimensional consolidation

PCI	Type I or general use Portland Cement (GU)
PCI-Slag	Type I Portland cement blended with blast furnace slag
PCI-PFA	Type I Portland cement blended with pulverized fly ash
pH	negative log of hydrogen ion concentration
ppm	parts per million
PSD	pore size distribution
PVC	polyvinyl chloride
PFA	Pulverized fly ash
PWP	pore water pressure
RH	relative humidity
sat, satd	saturated
sd	standard deviation
SEM	scanning electron microscopy
SG	specific gravity
SI	International System of Units
SSA	specific surface area
SWC	self-weight consolidation
TDC	time-dependent consolidation
TG/DSC	thermo-gravimetric / differential scanning calorimeter
UCS	uniaxial / unconfined compressive strength
UQAM	Université du Québec à Montréal
UQAT	Université du Québec en Abitibi-Témiscamingue
URSTM	Unité de recherche et de service en technologie minérale
USCS	Unified Soil Classification System
w/c	water-to-cement ratio
wt	weight
XRD	X-ray diffraction
VCL	virgin compression line

LIST OF SYMBOLS

a_v	coefficient of compressibility or coefficient of compression (L^2F^{-1})
B, R_w, I_L	liquidity index (–)
B_v	binder content by volume (–)
B_w	binder content by weight (–)
c	cohesion (FL^{-2})
c_f	compression rate (FL^{-3})
C_c	compression index (–)
C_r	recompression index (–)
C_z	coefficient of curvature (–)
C_U	coefficient of uniformity (–)
c_v	coefficient of consolidation (L^2T^{-1})
C_v	slurry concentration by volume (–)
C_w	slurry concentration by weight (–)
D	diameter (L)
D_{10}	diameter corresponding to 10wt% passing on the cumulative GSD curve (L)
D_{30}	diameter corresponding to 30wt% passing on the cumulative GSD curve (L)
D_{50}	diameter corresponding to 50wt% passing on the cumulative GSD curve (L)
D_{60}	diameter corresponding to 60wt% passing on the cumulative GSD curve (L)
D_{85}	diameter corresponding to 85wt% passing on the cumulative GSD curve (L)
D_{90}	diameter corresponding to 90wt% passing on the cumulative GSD curve (L)

D_e, D_{10}	effective diameter (L)
D_r, I_D	relative density in compaction (–)
E	elastic modulus or young's modulus (FL^{-2})
e	void ratio (–)
e_{cuaps}	void ratio of CUAPS consolidated samples (–)
e.g.	exempli gratia or for example
e_{min}	minimum void ratio (–)
e_{max}	maximum void ratio (–)
e_0	initial void ratio (–)
e_f	final void ratio (–)
g	gravitational acceleration (MT^{-2})
G_s	specific gravity of solids (–)
$G_{s\text{-}t}$	specific gravity of the tailings (–)
$G_{s\text{-}bkf}$	specific gravity of the backfill (–)
G_w	specific gravity of water (–)
H, $H_{dr/avg}$	drainage distance for the range of loading considered (L)
h, H, L	equivalent backfill height (L)
i.e.	id est or that is
I_c, C_R	relative consistency (–)
I_w, I_P	plasticity index (–)
k	hydraulic conductivity or coefficient of permeability (LT^{-1})
k_{sat}	saturated hydraulic conductivity (LT^{-1})
K_0	coefficient of earth pressure at-rest, no lateral deformation (–)
LL, L_w, w_L	liquid limit (–)
M_d	dry mass of a soil/tailings sample (M)
M_s	mass of solids (M)
Mt	million tons (M)
m_v	coefficient of volume compressibility or modulus of volume change (L^2F^{-1})

M_w	mass of water (M)
n	apparent porosity (–)
n_e	effective porosity or effective drainage porosity (–)
p_{cr}	critical pressure or stress (FL^{-2})
p_v	vertical applied overburden pressure or stress (FL^{-2})
p_e	pre-consolidation pressure or pre-stress (FL^{-2})
q_u, C_0	compressive strength or unconfined compression strength UCS (FL^{-2})
PL, P_w, w_P	plastic limit (–)
Q	quantity of flow (L^{-3})
r	coefficient of correlation
r_f	CPB filling rate (LT^{-1})
R_h	relative humidity (–)
R_e	relative degrees of reduction in initial void ratio (–)
S_m	mass specific surface area (L^2M^{-1})
S_r	degree of saturation or percent saturation (–)
t	elapsed time, curing time (T)
t_n	reduced or normalized time factor (–)
t_{90}	time for 90 percent consolidation to occur (T)
T_v, T	time factor (–)
UCS_{cuaps}	UCS of CUAPS-consolidated backfills (FL^{-2})
$UCS_{cuaps\ (h)}$	CUAPS-predicted UCS at a corresponding stope depth *h* (FL^{-2})
UCS_{udm}	UCS of undrained mould backfills (FL^{-2})
u, u_0, u_w	pore water pressure or pore pressure or neutral stress (FL^{-2})
w_{opt}	optimum water content (–)
w_0	initial water content (–)
w	gravimetric water content (–)
ν	Poisson's ratio (–)

σ', p', f'	effective stress or effective pressure or inter-granular pressure (FL^{-2})
σ, p, f	total stress or pressure or inter-granular pressure (FL^{-2})
σ_1	major principal stress (FL^{-2})
σ_2	intermediate principal stress (FL^{-2})
σ_3	minor principal stress (FL^{-2})
σ_h	horizontal stress (FL^{-2})
σ_v	vertical stress (FL^{-2})
σ_θ	hoop stress (FL^{-2})
τ	shear stress (FL^{-2})
ϕ	angle of internal friction (–)
δ_r	radial expansion (–)
ρ	bulk density of soil or tailings (ML^{-3})
ε_r	radial strain (–)
η	dynamic viscosity of water (10^{-6} kPa.sec at 20 °C)
μ	micron (–)
θ	volumetric water content (–)
γ_d	dry unit weight (FL^{-3})
θ_r	residual volumetric water content (–)
θ_s	saturated volumetric water content (–)
ρ_s	density of solid particles (ML^{-3})
ρ_w	density of water (ML^{-3})
γ_w	unit weight of water (FL^{-3})
γ_{wet}	wet unit weight (FL^{-3})
γ_z	zero air voids unit weight (FL^{-3})

RÉSUMÉ

Dans l'industrie minière et des minéraux, un grand volume et une large variété de résidus miniers qui se compose de fractions grossières et fines et pouvant être soit réactifs (production d'acide) ou non réactifs sont produits à travers le monde chaque jour. La plupart des opérations minières utilise la fraction grossière des résidus miniers pour le remblayage souterrain alors que les fines sont généralement déposées en surface dans des parcs à résidus ou derrière des digues de retenue. Il est toutefois bien connu que les digues de retenue sont à risque de rupture dû à une fuite, l'instabilité, la liquéfaction et d'un défaut de conception. En outre, les rejets générateurs d'acidité peuvent causer des dommages importants à l'environnement sous la forme de drainage minier acide en libérant des métaux lourds, s'ils ne sont pas correctement gérés. Pour résoudre ces problèmes, la solution de gestion des résidus miniers est d'adopter une approche qui est techniquement approprié, économiquement viable, écologiquement durable et socialement responsable. Le remblai cimenté en pâte (RCP) est l'une des plus récentes méthodes novatrices de gestion des résidus et se compose généralement d'un mélange des résidus miniers tout-venant sans deslamage (70-85% solides), un liant hydraulique (3-7% en poids) pour répondre aux critères de stabilité requise et d'eau de mélange (20-25% d'eau).

La plupart des travaux de recherche a été jusqu'à présent effectuée en focalisant sur les propriétés physico-chimiques, minéralogiques, mécaniques et microstructurales des RCP. La plupart du temps, des moules en plastique conventionnels non drainés sont généralement utilisés pour déterminer les paramètres de conception du remblai minier en pâte qui dépendent du pourcentage solides, de la granularité des résidus, du type de liant et de sa teneur, et du temps de cure. Toutefois, des études récentes ont montré que pour une même recette de remblai utilisée au laboratoire et in situ après un temps de cure donné, la performance mécanique du remblai préparé au laboratoire était toujours inférieure à celle du remblai in situ.. La raison principale derrière ce phénomène est que la cure du remblai en pâte in situ se serait faite sous l'action des contraintes effectives qui se serait progressivement développées dans le chantier remblayé en raison de leur consolidation (sous poids propre ou par surcharge) et ainsi, entraîne l'amélioration du taux de d'acquisition de la résistance mécanique finale. La mise en place et les propriétés des remblais in situ ne peuvent être reproduits à l'aides des moules classiques. Par conséquent, il existe un besoin évident de développer de nouveaux équipements et de procédures d'essai capables de reproduire de façon réaliste les conditions de cure in situ des remblais cimentés en pâte dans un environnement de laboratoire contrôlé. Dans ce cas le but étant d'être en mesure d'atteindre des résistances mécanique les plus élevées possibles et/ou au moins équivalentes pour une meilleure conception de remblai.

Cette thèse est composée principalement de quatre articles/manuscrits de journaux avec comité de révision par les pairs. Le premier papier essaye d'investiguer les différences dans les propriétés hydromécaniques des RCP observées entre les échantillons qui curent dans les conditions de laboratoire et in situ par le biais de la première version d'un nouvel appareil d'essais en laboratoire appelé CUAPS (système de cure sous pression appliquée). Il aborde substantiellement les propriétés physiques, hydrotechniques et géochimiques d'échantillons de RCP préparés avec des résidus catégorisés comme grossiers (15 wt% ≤ grains de moins de 20 μm < 35 wt%) provenant d'une mine polymétallique européenne. Le deuxième papier présente davantage l'évaluation de l'appareil CUAPS modifié qui permet d'estimer certaines propriétés hydromécaniques des RCP incluant la compression anisotrope (consolidation 1-D) et la perméabilité. L'appareil CUAPS modifié capture bien la déformation axiale qui se produit dans le remblai pendant sa compression (soit par surcharge ou par son poids propre) et cela permet de réaliser des essais de consolidation unidimensionnelle, mais aussi des essais de dissipation de la pression interstitielle, de perméabilité (mesure de la conductivité hydraulique saturée), de cure sous contrainte effective appliquée et de cure sous différents taux de compression. Les résultats préliminaires illustrent bien l'efficacité, l'utilité et la capacité de cet appareil CUAPS modifié dans l'optique de l'optimisation réaliste des recettes de RCP à être utilisées pour le remblayage souterrain. Le troisième papier focalise particulièrement sur les propriétés de consolidation unidimensionnelle à l'aide de l'appareil CUAPS modifié. Les échantillons de remblai en pâte ont préparés avec de résidus catégorisés comme fins (35 wt% ≤ grains de moins de 20 μm < 60 wt%). Le quatrième papier et dernier présente les résultats de l'étude sur les effets des conditions de cure (consolidée et non consolidée) sur les propriétés microstructurales du RCP au moyen de la porosimétrie par intrusion de mercure (PIM) et la détermination de la surface spécifique. Quelques modèles empiriques de prédiction de la résistance en compression uniaxiale (UCS) en fonction de certains paramètres de la microstructure des RCP ont été proposés.

Cette thèse de doctorat a non seulement permis une meilleure compréhension des propriétés des remblais en pâtes préparés au laboratoire, mais il a également permis d'évaluer avec succès l'appareil CUAPS modifié qui peut être un outil précieux pour la collecte de données équivalentes à celles du remblai in situ mais à l'échelle du laboratoire. Ce travail est considéré comme une étude originale qui a investigué le comportement en consolidation unidimensionnelle des échantillons de RCP à différents temps de cure et aussi le comportement d'échantillons de RCP curés sous une série d'incréments de pressions en permettant le développement graduel de la contrainte effective dû au drainage (simulant les chantiers souterrains remblayés). Cette recherche a donc contribué à une meilleure compréhension du comportement de ce matériau relativement complexe qu'est le RCP et a mis au point une procédure d'essai pour évaluer la performance mécanique qui pourrait être considérée lors du processus de conception de tout remblai cimenté en pâte. Enfin, l'appareil CUAPS modifié aidera les chercheurs et les opérateurs des remblais à mieux comprendre les propriétés de consolidation des CPB frais ou durcis qui devraient être préparés en laboratoire.

Mots clés: Résidus miniers, Remblai cimenté en pâte, Consolidation unidimensionnelle, Conductivité hydraulique saturée, Pression des pores, Hydration des ciments, Contrainte de cure, Résistance en compression

ABSTRACT

In the mining and mineral industry worldwide, large volumes and many varieties of mine tailings consisting of coarse and fine fractions that are either reactive (acid generating) or non-reactive are produced every day. Most mining operations use the coarse fraction of the tailings for underground backfill, while the fines are usually deposited on the surface into tailings impoundments or dams. However, it is well known that these dams are at risk of failure due to leakage, instability, liquefaction and inadequate design. Moreover, unless they are properly managed, acid-generating tailings can cause significant environmental damage by generating acid mine drainage that releases heavy metals. Overcoming such problems requires tailings management approaches that are technically suitable, economically viable, environmentally sustainable and socially responsible. Cemented paste backfill (CPB), an engineering material, is used in a recent, innovative tailings management method. Typically, CPB is a mixture of total mill tailings without removing the fines, or desliming (70–85 wt% solids), and single, binary and ternary hydraulic binders (3–7 wt%) in order to meet stability requirements and combined with mixing water (20–25 wt%).

Most studies to date have focused on the physicochemical, mineralogical, mechanical and microstructural properties of CPB. Conventional undrained plastic moulds (non-perforated) are usually used to determine mine backfill design parameters, depending on the solids mass concentration, grain size grading, binder type and content, and curing time. However, recent studies have shown that for identical backfill recipes used in the laboratory and in situ after a given curing time, the performance (i.e., mechanical strength) of laboratory-prepared CPB samples is consistently lower than that obtained from in situ CPB samples. The primary reason is that in situ backfill material is cured under effective stresses that develop gradually in a stope due to self-weight and/or time-dependent consolidation loads, which accelerate the rate of final strength development. In situ CPB placement and properties cannot be replicated using conventional moulds. Therefore, innovative equipment and test procedures that allow realistic reproduction of in situ curing conditions of CPB materials in a controlled laboratory setting are needed. The aim is to obtain higher or at least equivalent mechanical strength, and consequently a better backfill design.

This thesis comprises four separate peer-reviewed journal manuscripts. The first paper investigates differences in CPB hydromechanical properties between laboratory and in situ

curing conditions using the original version of a recently developed laboratory apparatus called CUAPS (curing under applied pressure system). It consists of an in-depth examination of the physical, hydrogeotechnical and geochemical properties of CPB samples prepared using a coarse-grained tailings (15 wt% ≤ finer than 20 μm < 35 wt%) sample from a European polymetallic mine. The second paper assesses an improved CUAPS apparatus that allows estimating certain in situ hydromechanical properties of CPB, including anisotropic compression and permeability behaviour. The improved CUAPS apparatus accurately captures the axial deformation that occurs in backfill as it compresses (either by surcharge load or self-weight). This allows performing not only one-dimensional consolidation testing, but also pore water pressure (PWP) dissipation testing, permeability testing (saturated hydraulic conductivity), and curing under applied effective stresses and compression rate dependent curing conditions. Preliminary results show the capacity, efficiency and usefulness of this improved CUAPS apparatus: it can be used to optimize more realistic paste backfill mix designs for use in underground backfilling. The third paper investigates the one-dimensional consolidation properties of early age CPB material, which are closely related to their permeability (saturated hydraulic conductivity), using the improved CUAPS apparatus. CPB samples were prepared using a medium-grained tailings (35 wt% ≤ finer than 20 μm < 60 wt%). The fourth and last paper investigates the effect of curing conditions (consolidated and non-consolidated) on CPB microstructural properties using empirical mercury intrusion porosimetry (MIP) results and specific surface area measurements. Some predictive equations for unconfined compressive strength of CPB materials are proposed based on the certain microstructural parameters.

This Ph.D. thesis not only provides a better understanding of the properties of laboratory-prepared CPB samples, but also assesses the improved CUAPS apparatus, a valuable tool for collecting equivalent in situ mine backfill data at laboratory scale. It constitutes an original study on the one-dimensional consolidation behaviour of CPB samples at various curing times as well as the behaviour of samples cured under a series of incremental pressures, which allows the effective stress to develop gradually (simulating CPB-filled underground stopes). This research effort has contributed to a better understanding of the behaviour of CPB, a relatively complex material. Moreover, it proposes a strength performance testing procedure that can be incorporated into the design process of any CPB material. Finally, the improved CUAPS apparatus can help backfill researchers and practitioners better understand the consolidation properties of fresh or hardened laboratory-prepared CPB samples.

Keywords: Mine tailings, Cemented paste backfill, One-dimensional consolidation, saturated hydraulic conductivity, Pore pressure, Cement hydration, Curing stress, Compressive strength

CHAPTER I

GENERAL INTRODUCTION

1.0 PROBLEM STATEMENT

The three principal activities of the mining industry – blasting, mineral processing or milling, and metallurgical extraction – produce significant quantities of mine wastes such as mill tailings, waste rocks and water treatment sludge (Lottermoser, 2007). Mine wastes produced and disposed at mine sites are problematic, because they contain harmful substances (e.g., heavy metals, metalloids, acids and process chemicals) and require monitoring, treatment and safe disposal. Accordingly, effective and economical disposal of these wastes has become a major issue for all mining operations (Aubertin et al., 2002; Yilmaz, 2007). Various methods have been developed in the mining industry in order to prevent, rectify, lessen or eliminate the potential environmental impacts of mine wastes (Grice, 1998; Bussiere, 2007). One practical mine waste management method for underground mines involves refilling, which is, depositing wastes as mine backfill into underground voids created by ore extraction (stopes). Mine backfill, categorized mainly as rock fill (RF), hydraulic fill (HF) and cemented paste backfill (CPB), is extensively used in most successful underground mine operations, reducing volumes of surface-disposed mine wastes (Hassani and Archibald, 1998; Potvin et al., 2005).

This environmental benefit has spurred the acceptance of the CPB materials as an economical alternative to both rock fills and hydraulic fills (Rankine et al., 2006; Stone, 2007). Unlike hydraulic slurry, the CPB can be composed of mill tailings without fine particles removal, thereby maximizing the amount of tailings that can be used regardless of the size distribution. CPB offers a number of advantages over other backfill materials in operational, financial and environmental terms. Further information on the design and application of CPB technology for underground mines can be found elsewhere (Belem and Benzaazoua, 2007; Grabinsky and Bawden, 2007; Dirige and De Souza, 2007).

Most investigations to date have been conducted on the physical, chemical, mineralogical, mechanical, geotechnical and microstructural properties of laboratory-prepared CPB samples, and have focused mainly on the effects of tailings specific gravity, grain size and grading, binder type, and proportion and curing time (Landriault, 1995; Amaratunga et al., 1997; Pierce et al., 1998; Benzaazoua et al., 1999, 2002, 2004a; Archibald et al., 1999; Bertrand et al., 2000; Belem et al., 2000, 2001, 2002; Hassani et al., 2001; Kesimal et al., 2003, 2004, 2005; Yilmaz, 2003; le Roux, 2004; Klein and Simon, 2006; Ouellet, 2007; Tarig and Nehdi, 2007; Fall et al., 2008; Dirige et al., 2008; Cihangir et al., 2008; Ercikdi et al., 2009a,b). However, the CPB technique presents some difficulties in terms of the representativeness of laboratory samples and data to actual in situ materials. In fact, replicating in situ backfill mixing, placement and curing conditions in a laboratory using conventional moulds is a challenging task, first, because it is impossible to exactly duplicate in situ conditions, and second, due to the lack of suitable laboratory equipment and procedures (Servant, 2001). The mechanical and curing properties of in situ CPB material vary, to a great extent, principally depending on the method of preparation (continuous or batching), placement method and particular mine conditions (Cayouette, 2003; le Roux et al., 2005). Recent studies have indicated that for a given mine backfill recipe and curing time, the unconfined compressive strength (UCS) of the CPB produced at the surface backfill plant and placed underground can be 4 to 6 times higher than samples of the identical CPB recipe prepared in the laboratory and cast in the conventional moulds (Belem et al., 2002; le Roux et al., 2002; Cayouette, 2003; Yilmaz et al., 2004a, Revell, 2004), in contrast to what some other authors have observed (le Roux et al., 2005; Grabinsky and Bawden, 2007). The observed differences between the UCS

of laboratory-prepared samples and in situ backfill material are attributable to scale effects, placement methods and in situ curing conditions (curing under self-weight/time-dependent consolidation due to drainage of excess free water within the paste backfill and temperature). However, there have been few studies on in situ CPB (Ouellet and Servant, 2000; le Roux et al., 2005; Harvey, 2004; Belem et al., 2004; Hassani et al., 2004; Grabinsky and Bawden, 2007; Helinski et al., 2007a). Moreover, most of these studies have been either confidential or limited to providing knowledge on the site conditions. More information is needed to gain a better understanding of in situ backfill properties. In situ testing is essential to obtain a real mechanical CPB response in order to improve the design of backfilled stopes. In addition, measuring and understanding the field material properties is vital for optimizing different CPB recipes in order to improve safety and cut costs. Fortunately, these properties can be well simulated in the laboratory using the CUAPS apparatus which allows for the application of different pressure increments to backfill samples during or after curing. To the author's knowledge, only a few works have indicated that the consolidation affects the quality and behaviour of fresh or hardened CPB materials (Belem et al., 2002, 2006; le Roux et al., 2005; Fourie et al., 2006, 2007; Helinski et al., 2006; 2007c, 2009; Fahey et al., 2009). As a result, aspects linked to in situ properties and conditions of the CPB materials that affect its strength and stability performance need to be further investigated.

1.1 DESCRIPTION OF CEMENTED PASTE BACKFILL

Cemented paste backfill (CPB) is a mixture of the total filtrated wet mill tailings, hydraulic binder and mixing water. The percentage of filtered tailings solids ranges from 75 to 85 wt%. The binder is made of a general use (GU) Portland cement or a blend of GU cement and either granulated blast furnace slag (GBFS) or fly ash. The binder proportion varies from 2 to 7 wt% and mixing water is added to reach the targeted slump, which should vary in the range of 15–25 cm (6–10 in.) to facilitate paste transport to underground stopes by either gravity or pumping. CPB are frequently used for backfilling stopes in underground mines. This may allow a safer management of potentially acid generating mine tailings, while at the same time provide ground support to the surrounding rock mass (e.g., Brackebusch, 1994; Landriault, 1995; Hassani and Archibald, 1998; Amaratunga and Hmidi, 1998; Benzaazoua et al., 1999,

2002, 2004a; Belem and Benzaazoua, 2007; Evans et al., 2007; Hassani et al., 2007; Cooke, 2007). Surface paste disposal (with or without binder) has lately been proposed in the mining industry as an alternative to conventional tailings disposal methods for above ground storage (Cincilla et al., 1997; Verburg, 2002; Grabinsky et al., 2002; Yilmaz, 2003; Benzaazoua et al., 2004b; Bussière, 2007; Deschamps et al., 2008; Deschamps, 2009). To date, surface paste tailings disposal was used merely by a few mines. The Bulyanhulu mine (Tanzania) was the first gold mine to adopt this technology (Shuttleworth et al., 2005; Martin et al., 2006).

Moreover, it has been experimentally shown that tailings in a paste backfill mixture should contain at least 15 wt% of particles finer than 20 µm, which act as lubricant (colloidal water retention) and so facilitate plug flow in pipelines (Landriault, 1997). Paste material properties such as water retention and flow resistance are not only controlled by grain size distribution (GSD), but also their chemical and mineralogical composition. Thus, each CPB mix must be tested separately to determine the paste backfill behaviour (Benzaazoua et al., 2002, 2004; Kesimal et al., 2005; Fall et al., 2007; Nasir, 2008). The three main GSD categories are considered in the design of CPB mixtures for most mine tailings worldwide: coarse, medium and fine tailings (Landriault, 1995, 2001). Coarse-grained tailings contain between 15 and 35 wt% particles finer than 20 µm. For a given binder content, high solids content creates good paste backfill strength. Medium-grained tailings contain between 35 and 60 wt% particles finer than 20 µm, and produce a good CPB material, but with lower strength than CPB made with coarse-grained tailings. Fine-grained tailings contain 60 to 90 wt% particles finer than 20 µm. Depending on their mineralogy, these fine-grained tailings show high water retention, which create CPB with good flow properties but relatively lower strength. By adding coarse material to the tailings, the GSD of CPB is increased due to the lower porosity.

The mine tailings used in a CPB must be analyzed for mineralogical composition (zinc, lead, pyrite and pyrrhotite), which can affect the binder chemical reactions (Levens et al., 1996). Some minerals can induce strength retardation, strength reduction and long-term strength loss due to internal sulphate attack (Benzaazoua et al., 1999; Petrolito et al., 2005; Benkendorff, 2006). CPB made of this type of tailings should be laboratory tested for short- and long-term strength before it can be used for underground CPB. Furthermore, the health and safety of

mine workers must be considered when designing CPB for mines. When pyritic tailings are used to prepare CPB, their exothermic properties must be investigated in order to prevent self-heating (Kwong, 2004). For instance, pyrrhotite and pyrite can react chemically in favourable underground water and oxygen conditions. Such reactions can cause internal heating to temperatures that may ignite the sulphur content of the material and cause a self-sustaining underground fire that produces toxic sulphide gas (Landriault, 2000; Moerman et al., 2001; Yilmaz et al., 2004a; Ouellet et al., 2006; Nehdi and Tarig, 2007; Godbout et al., 2009). Readers interested in the general area of CPB are advised to consult the relevant literature (e.g., Henderson et al., 2005).

1.2 A BRIEF LITERATURE REVIEW OF CPB TECHNIQUE

The following review covers the published results of laboratory testing undertaken on CPB materials. Most of the data concern the consolidation, saturated permeability coefficient (hydraulic conductivity), curing under effective stress conditions, hydromechanical behaviour and pore structure of CPB samples. Because CPB is a relatively new integrated mine waste management method, much of the literature usually focuses on the preparation and transport rather than the hydrogeotechnical characteristics such as one-dimensional consolidation.

1.2.1 The theory of consolidation

When a loading is applied on a saturated soil stratum, the incompressible pore water initially supports this loading (pore water pressure, PWP) and no volume change takes place. As time passes, water from locations with higher heads flows towards locations with lower heads, and the excess PWP dissipates. In this process, loading that was originally supported by the water is transmitted to the soil grains (effective stress). This results in the increase of the effective stress of soils. As no hole is to develop in the ground, the volume of the pore water that flows away equals to the soils' volume reduction, and the ground settles. As the permeability of a cohesive soil is rather small, the process of excess PWP dissipation and the ground settlement takes time to develop. This time-dependent process is called consolidation. When the load is removed from a consolidated soil, the soil will rebound, regaining some of the volume it had

lost in the consolidation process. If stress is reapplied, the soil will consolidate along a recompression curve, defined by the recompression index. The soil which had its load removed is considered to be over-consolidated (OC). This is the case for soils which have previously had glaciers on them. The highest stress that it has been subjected to is termed pre-consolidation stress σ'_{cp}. A soil is often considered under-consolidated instantly after a new load is applied but before the excess PWP has had time to dissipate. The rate of consolidation is governed by the speed of PWP dissipation and this is related to the permeability of a soil quantified by the coefficient of permeability k_{sat}, which has the same unit as velocity (cm/s). The coefficient of permeability is dependent on several factors: fluid viscosity, pore-size distribution, grain-size distribution, void ratio, roughness of the mineral particles and degree of soil saturation. In clayey soils, structure plays an important role in permeability. Besides that, other major factors that affect the permeability of clays are the ionic concentration and the thickness of the layers of water held to the clay particles. The higher the permeability coefficient the higher the rate of consolidation due to the facts that pore water can escape. For coarse-grained soil, consolidation complete as rapidly as loads are applied on it owing to the structure of coarse-grained soils that is relatively pervious. For fine-grained soils, it requires a long time for the consolidation process as a result of low permeability.

Consolidation is one of the three major aspects of soil engineering, the other two being the shear strength and permeability of soils. Since deformation is one of the design criteria for structures founded on cohesive soils, the consolidation test is important in order to determine a number of consolidation characteristics, such as the coefficient of consolidation c_v, the compression index C_c, the recompression index C_{cr}, the coefficient of volume change m_v, and the coefficient of compressibility a_v (McCarthy, 2007). To predict the rate of settlement of soils, it is necessary to know the value of c_v. In the literature, numerous methods are available for the determination of c_v from laboratory one-dimensional compression test data. Most of the available methods depend on one-dimensional consolidation theory which was developed initially by Terzaghi (1923). Terzaghi's theory was based on experimental tests conducted on a thin layer of soil under small strain and a mathematical formulation driven with many assumptions was known to simplify the engineering behaviours of compressible soil. Many settlement and soil deformation problems were solved by geotechnical engineers and

overcome by this classic theory. However, the process of consolidation was simplified in the theory with several necessary assumptions made to solve the problem reasonably. With the precise measurement of soil compression behaviour in the laboratory on a thin layer of soil under one dimensional loading, engineers have managed to predict in some cases, very closely the performance, whereas in many cases predictions are off by more than ± 20 % variation even with very good judgment (Bo, 2008). This variation is due to a number of factors; *i*) the behaviour of consolidation in the field has departed from the assumptions made in the one-dimensional theory, *ii*) the environmental conditions differ from the laboratory conditions under which the compression and consolidation parameters are obtained, *iii*) the rate of loading and the rate of strain differ between laboratory and field conditions *iv*) more importantly the limitations of the one dimensional theory itself and many others.

In all graphical procedures, some characteristic features of the theoretical time factor T_v – degree of consolidation U relationship is identified in the experimental relationship and used to locate salient points on the experimental curves. This forms the basis for most of the graphical techniques that are available in the literature (Taylor, 1948; Casagrande, 1964; Parkin, 1978; Sridharan et al., 1987; Pandian et al., 1992). Most of the current methods attempt to fit the characteristic features of average degree of consolidation (U) versus time factor (T) relationship from the Terzaghi consolidation theory to the observed compression versus time data obtained in the laboratory oedometer test with incremental loading. The two conventional methods, namely the Casagrande logarithm of time fitting and the Taylor square root of time fitting methods, are still having much greater acceptance and use in geotechnical engineering practice as the standard methods in spite of their limitations (Terzaghi et al., 1996). Other alternative methods such as inflection point (Cour, 1971; Mesri and Shahein, 1999), velocity (Parkin, 1978), rectangular hyperbola fitting (Sridharan and Rao, 1981; Sridharan et al., 1995) and revised logarithm of time fitting (Robinson and Allam, 1996; Feng and Lee, 2001; Chan, 2003) methods are also based on rational approaches and have potential for predicting reliable values, sometimes even better than the values obtained by standard methods. Mainly, due to the lack of comparisons with field observations of time rate of settlement, and also to some extent because of more data reduction effort and sophistication of the method, the alternative methods have not been found suitable for routine applications.

Many sophisticated theories on consolidation have been proposed which take into account various factors that were not considered by Terzaghi's theory. However, Terzaghi's theory called one-dimensional consolidation is still widely used, mainly due to its simplicity. This theory is based on the following assumptions: *i*) the coefficient of permeability k_{sat} is constant during the process, *ii*) the soil is homogenous and fully saturated with water, *iii*) the soil skeleton and pore water are incompressible, *iv*) Darcy's law for the velocity of flow of water through soil is valid, *v*) soil is laterally confined in order that compression is one dimensional, *vi*) excess pore water drains out in a vertical direction only, *vii*) linear relationship between effective stress and void ratio exists so that the coefficient of compressibility and the coefficient of volume change are constant for every stages of consolidation, *viii*) the time interval of consolidation is due entirely to the low permeability of soil, and therefore, the secondary consolidation is disregard, and *ix*) the soil properties do not vary with stress and strain. Terzaghi (1936) proposed the effective stress ($\sigma - u_w$) as the stress variable to describe the behaviour of a saturated soil. The governing equation for one-dimensional consolidation is as follows (Terzaghi, 1943):

$$\frac{\partial u}{\partial t} = c_v \frac{\partial^2 u}{\partial z^2} \tag{1.1}$$

$$c_v = \frac{k_{sat}}{m_v \gamma_w} = \frac{1+e_0}{a_v} \frac{k_{sat}}{\gamma_w} \tag{1.2}$$

where u is the excess pore water pressure, t is the elapsed time, c_v is the coefficient of consolidation, z is the depth, k_{sat} is the saturated hydraulic conductivity, m_v is the coefficient of volume compressibility, and γ_w is the unit weight of water.

In this approach the coefficient of consolidation c_v is assumed to be constant, whereas, in reality, it varies as the coefficients of volume compressibility m_v and permeability k_{sat} change during the consolidation process. Some empirical curve-fitting procedures are also used to find out the coefficient of consolidation where different procedures assess different values for c_v, for the same experimental data. These limitations lead to an uncertainty in the prediction of consolidation rate (Duncan, 1993). Alternatively, recent advances in numerical solution of complex and non-linear partial differential equations have lead to more realistic solutions

with minimum simplifying assumptions for physical phenomena such as consolidation. In the last few decades, efforts have been made to overcome the main shortcomings of Terzaghi's theory of consolidation. Researchers have attempted to improve graphical interpretation of the oedometer test results (Rendulic 1936; Biot, 1941; Gibson et al., 1967; Olson, 1977; Fredlund and Hasan, 1979; Schiffman et al., 1984; Robinson and Allam, 1996; Mesri and Shahein, 1999; Feng and Lee, 2001; Chan, 2003; Hsu and Lu, 2006). Others have tried to predict the coefficient of consolidation based on the index properties of soils (Carrier, 1985; Raju et al., 1995). Numerous researchers (Leroueil et al., 1985; Laloui et al., 2008) developed a numerical model to use a strain-rate dependent compressibility law and a permeability-void ratio law. They concluded that the pore pressure isochrones maintain the same shape during controlled-gradient or creep test, in particular when the effective stresses correspond to the pre-consolidation pressure. It has also been established that the strain rate behavior is controlled by a unique effective stress-strain rate concept. Leroueil (2006) also showed that the compressibility is influenced by several factors: strain rate, temperature, sampling disturbance, stress path, and restructuring factors. In the normally consolidated range, major factors are strain rate and temperature, and their effect can be evaluated. In some cases, however, structuring phenomena can exist and decrease the viscous effects. In recent times, Sridharan and Nagaraj (2004) reported that the coefficient of consolidation has a correlation with the shrinkage index, I_s, which is the difference between liquid and shrinkage limits and proposed a simple equation for the determination of c_v using shrinkage index only. Although in these studies, it has been attempted to overcome problems involved in the determination of c_v in the consolidation test, the limitations related to its variability during consolidation process have not been considered. Other researchers have attempted to present more realistic nonlinear theories with consideration of variability of c_v during the consolidation process and as a result, a number of different numerical and analytical solutions have been proposed for the solution of non-linear equations (Mesri and Rokhsar, 1974; Basak, 1979; Gibson et al., 1967; Morris, 2002). Lekha et al. (2003) derived a theory for consolidation of a compressible medium of finite thickness neglecting the effect of self-weight of soil and creep effects but considering variation in compressibility and permeability. They proposed an analytical closed form solution to determine the relation between degree of consolidation and time factor. Zhuang et al. (2005) presented a non-linear analysis and a semi-analytical solution for

consolidation with variable compressibility and permeability. Although Lekha et al. (2003) and Zhuang et al. (2005) attempted to consider the variation of c_v during consolidation, but their solutions give the relation between degree of consolidation with time factor which is related to real time via the coefficient of consolidation c_v. As Terzaghi's theory was unable to solve for the large strain consolidation process which the characteristics of compressible soils are changing during the consolidation process, Gibson et.al. (1981) proposed the large strain theory, which takes into consideration the changes of the soil parameter during consolidation. Carrillo (1942) and Barron (1948) proposed another consolidation theory, which takes into consideration both radial and vertical flow, which is generally much faster than vertical flow alone. Biot (1955) presented a more comprehensive theory, which took into consideration the flow towards three dimensions with 3-D deformation. Consolidation generally starts with the level of effective stress, which is equivalent to the overburden stress, so this theory is unable to realistically solve the problem of self-weight consolidation in which natural deposit of soil is still undergoing consolidation with stresses caused by its self-weight. Been and Sills (1981) and Lee and Sills (1981) have widely studied self-weight consolidation and proposed a new theory. However, in many cases the application of load may be applied before the completion of self-weight consolidation. Compression and deformation of soil upon additional load, which is still undergoing self-weight consolidation, is different from deformation of normally consolidated natural soil. Consequently, Bo et al. (1999) proposed a model and a few sets of equations which can solve the compression and consolidation characteristics of the soil, which have a natural moisture content greater than the liquid limit.

To overcome some of the limitations of the conventional test and to incorporate some of the controls of modern soil test, two new methods of performing a consolidation test were reported previously: the controlled gradient test of Lowe et al. (1969) and the constant rate of strain test of Smith and Wahls (1969). Aboshi et al. (1970) reported on the use of a constant rate of loading. Wissa et al. (1971) developed a general purpose consolidometer to analysis the conditions in the constant rate of strain consolidation (CRSC) test where specimens can be saturated at constant volume under a back pressure and loaded, with no lateral strain, by incremental loads, at a constant rate of strain, or at a constant rate of stress. The solution includes both the initial transient portion of the test and the steady state conditions. One of

the peculiarities of loading a sample at a constant rate of strain is that immediately as the piston is set in motion a transient condition develops in the soil and must be dissipated before steady state conditions are established. Smith and Wahls (1969) have analysed their data from a constant rate of strain consolidometer using a solution that applies after the transient has dissipated. They assumed that the permeability of the soil is constant over the depth of the sample at any time and that the void ratio of the soils varies linearly with depth. They also assumed that the change in void ratio with time is so small and thus ignorable. Analyzing the related test at a constant hydraulic gradient, Lowe et al (1969) assumed that the permeability is independent of depth at any time and that only infinitesimal strains exist. Their solution does not consider transient conditions and assumes implicitly that the soil skeleton is linearly elastic at any time. Wissa et al. (1971) have tried to find a theoretical solution that would include transient behaviour, which would describe the behaviour of soil as generally as possible without excessive mathematical difficulties, and whose assumptions could be verified from the results of the consolidation test itself. Consequently, it was assumed that infinitesimal strains exist and that the coefficient of consolidation c_v is independent of depth at any time. This implies that c_v is insensitive to small changes of strain but not necessarily to large ones. These assumptions have been previously justified and used for conventional one-dimensional consolidation situations at constant load (Davis and Raymond, 1965; Janbu, 1965). Unless soil is to be consolidated directly from a slurry, the assumption of infinitesimal strains is reasonable. Gibson et al. (1967) have showed that an extension of consolidation theory to large strains requires, in addition to mathematical difficulties, a redefinition of c_v, which must still be nearly constant for solutions to be obtained.

1.2.2 One-dimensional consolidation behaviour

This subsection assesses mechanisms associated with the behaviour of early age CPB during and/or after placement and highlights the importance of consolidation. Some studies have shown that effective stress may greatly affect the barricade loads, arching and consolidation rate that assist in replicating in situ curing conditions (Helinski et al., 2007a; Fourie et al., 2007; Yumlu and Guresci, 2007; Sainsbury and Revell, 2007). The stiffness or rigidity of CPB samples being cured under self-weight or time-dependent consolidation loads increases

significantly with increased cement hydration rate and reduced void ratio. With increased stiffness, there is less deformation of CPB as the cement hydrates fill some of the void spaces within the backfill (Belem et al., 2002, 2006, 2010; le Roux et al., 2002, Helinski et al., 2006; Grabinsky and Bawden, 2007; Yilmaz et al., 2008a, 2010a). It has been well documented that curing cemented materials under an effective stress (gives rise to water lost by drainage) increases the mechanical strength acquisition, depending on the binder type and proportion (Belem et al., 2002, 2006; Consoli et al., 2000, 2006, 2007; Rotta et al., 2003; Helinski et al., 2006, 2009; Yilmaz et al., 2008a, 2009a, 2010a). It should be however noted that the duration of application of the effective stress (with respect to curing time) plays a key role in the CPB strength. Fourie et al. (2006) showed that if the effective stress is applied immediately before the commencement of curing, CPB gains more strength than when the effective stress is applied after hydration is complete. This is mainly attributable to the cement bonds that form during hydration (increased stiffness). If the CPB is subjected to curing stress after a couple of days (up to the first 4 days) then the cement bonds that are forming may break down, reducing the material strength and stiffness (Yilmaz et al., 2006, 2008a, 2010a,b).

Applying curing pressure to backfill after it has cured assumes that the backfill is unable to consolidate at all prior to curing. Whether or not this is representative of what occurs in situ depends on the curing rate relative to the filling rate. Mitchell and Smith (1979) and Mitchell et al. (1982) found that the rate of strength gain within cemented hydraulic fills exceeds the stress increase due to the filling. In this case, hydraulic fill cures before it has a chance to consolidate from self-weight, and it would therefore be reasonable to apply pressures after curing. However, this may not be true for CPB, mainly due to its rapid rate of delivery and placement, as well as the absence of the need to wait for excess water to drain from the stope. Hydraulic fill usually requires special pre- and post- placement techniques than CPB. This leads to a significant delay for self-weight consolidation within hydraulic fills where curing pressures are applied at very early ages (typically 2-3 days, an elapsed time for the removal of excess water from the backfilled-stope via vertical and horizontal drainage conditions). Pierce (1997) showed that a significant amount of the self-weight stress can be applied to CPB prior to curing. This results in greater consolidation prior to curing, because the backfill is more compressible at this time. The application of pressure after longer curing (typically

more than 2-3 weeks, depending on the binder types and content and curing conditions) is hence not entirely representative of in situ conditions for CPB material, except for the case of sequential filling separated by a curing pause (up to 7 days). In this case, the CPB material is still considered "fresh" because cement hydration is not fully completed.

The consolidation properties of the CPB material are influenced by the rate at which the load is applied vertically during curing. An understanding of how consolidation loading rates (or the rate of accumulation) interact to affect the final void ratio of CPB samples was developed by le Roux et al. (2002) and Yilmaz et al. (2008b, 2010a). The faster the loading rate, the steeper the consolidation curves. On the contrary, the slower the loading rate, the flatter the consolidations curve. It was also shown that the higher the binder content, the greater the consolidation resistance and the higher the final void ratio within the cemented paste backfill for a given loading rate. Considering the undrained loading conditions in which paste backfill samples are cured under zero effective stress (0 kPa), the self-desiccation process caused by the cement within the backfill results in reduced pore water pressure. This reduction produces an increase in effective stress. As the effective stress increases, the vertical stresses within the CPB material are reduced. The coarser the paste, the more quickly pore water pressures are dissipated, and the more quickly the arching and effective stresses develop. More information on this process can be found elsewhere (e.g., Grabinsky and Simms, 2006; Helinski et al., 2007b; Simms and Grabinsky, 2009; Belem et al., 2010a,b).

1.2.3 Saturated hydraulic conductivity behaviour

The saturated hydraulic conductivity (a.k.a., permeability, k_{sat}) of cemented tailings backfills such as CPB is a key factor, as it represents the material's capacity to permit water flow and prevent pollutants from escaping from the stabilized tailings to the environment. Numerous studies have examined the change in k_{sat} as a function of grain size, binder type and content, curing under pressure and curing time (Pierce, 1997; Belem et al., 2001; Jones et al., 2001; Mohamed et al., 2002; le Roux, 2004; Godbout, 2005; Godbout et al., 2007; Yilmaz et al., 2008b, 2009a). The test results show that k_{sat} decreases rapidly at early ages of curing (up to 7 days) and then tends to stabilize over the time. The reduction in k_{sat} is attributable to micro-

structural changes caused by cement hydration and mineral precipitation during curing, which give rise to the changes in the pore-size geometry and its distribution. As well, these studies indicated that k_{sat} values for consolidated CPB samples usually vary between 10^{-5} and 10^{-7} cm/s, depending on the grain size of the tailings (fine, medium or coarse) and the curing conditions (under applied pressure or not) of the tested samples.

Several approaches have been proposed to predict the permeability of cemented materials, using various control factors such as fluid properties, pore size distribution and solids surface characteristics (Aubertin et al., 1996; Belem et al., 2001; Mbonimpa et al., 2002; Chapuis and Aubertin, 2003; Godbout et al., 2007). Permeability is expressed as a function of porosity, tortuosity, the constrictivity factor and the critical pore radius of cemented materials from mercury intrusion porosimetry results (Ait-Mokhtar et al., 2002; Kumar and Bhattacharjee, 2003; Ouellet et al., 2007). Such predictive equations can be very useful to estimate the k_{sat} during the preliminary stages of a project, and to determine the validity of laboratory results. However, predictive equations are not meant to replace testing on representative samples.

1.2.4 Uniaxial compressive strength behaviour

One of the most important parameters in designing a CPB operation for underground mines is uniaxial compressive strength (UCS). Other important design issues are material properties and flow and dewatering characteristics (Archibald et al., 1993; Hassani and Archibald, 1998; Potvin et al., 2005). To obtain the real UCS response of a CPB-filled stope so as to develop an optimal stability design, it is vital to properly assess the "intrinsic" (the CPB ingredients) and "extrinsic" factors that influence the overall performance of the backfill:

- Intrinsic factors include all the parameters of the three main backfill ingredients (tailings, cement and water) and their interrelationships during curing;

- Extrinsic factors include all the events that occur in a backfilled mine stope as a function of stope dimension, CPB-rock wall interaction, placement and curing conditions, self-weight or time-dependent consolidation, and drainage or bleeding of excess water.

1.2.4.1 Influence of intrinsic factors

The physical, chemical and mineralogical properties of the backfill ingredients (mine tailings, binding agent and mixing water) have a profound effect on the strength and durability of the CPB material (Belem et al., 2000, 2001; Benzaazoua et al., 2002, 2004a; Yilmaz et al., 2004a, Kesimal et al., 2005; Klein and Simon, 2006). For instance, grain size distribution (GSD) of the tailings determines in part some of the CPB final bulk properties. Overall, a sample with a small spread of grain sizes is referred to as "poorly graded", whereas a sample with a wide spread would be "well graded". Numerous authors (Kesimal et al., 2003; Benzaazoua et al., 2004a; Fall et al., 2005; Sivakugan et al., 2005; Yilmaz et al., 2003a,b, 2004b, 2005, 2007; Celestin, 2008; Belem and Benzaazoua, 2008) have shown that for a given water:cement *w/c* ratio, a CPB with coarse- and medium-grained tailings is more liable to produce higher UCS than a CPB with fine-grained tailings, mainly due to the lower void ratio and consequently higher solids content (UCS_coarse > UCS_medium > UCS_fine). Fall et al. (2004) indicated that the highest UCS was obtained only with medium-grained tailings. GSD is directly related to the flow properties, permeability and pumpability of CPB materials. Hence, the higher the fines content (<20 µm), the lower the permeability coefficient k_{sat} (Henderson and Revell, 2005). Fine-grained particles, with their relatively high specific surface area, have a greater water-holding capacity and are transported together with coarse-grained particles in a pipeline. CPB frequently produces a plug flow when transported through a pipeline. The annulus of fine-grained particles naturally-formed in the plug flow condition acts as a lubrication layer along the pipe wall, reducing flow resistance and pipe wear. Coarse-grained particles are naturally forced to the center of pipeline and transported in the fine-material carrier. This phenomenon allows coarse material to be transported through a pipeline by a fluid material with paste flow properties where granular material must have at least 15 wt% finer than 20 µm to produce sufficient colloidal water retention (Landriault, 2000).

The mineralogy of tailings and binders can also affect backfill strength by influencing certain chemical reactions that occur during curing (Benzaazoua et al., 1999, 2002, 2004a, Bertrand et al., 2000; Yilmaz et al., 2004a; Bernier et al., 1999). When CPB is created from sulphide-rich tailings, certain events may occur, such as pyrite oxidation in the presence of oxygen and

water, forming acid and sulphate. Sometimes, these chemical interactions between sulphate ions and cement hydrate products can cause internal heating to temperatures that ignites the sulphur content of the materials and result in a self-sustaining underground fire that produces toxic sulphide gas. All these events may affect damagingly paste backfill strength (Ouellet et al., 1998; Landriault, 2000; Hassani et al., 2001; Benzaazoua et al., 2002, 2004; Yilmaz et al., 2003a, 2004a,b; Kesimal et al., 2005; Fall and Benzaazoua, 2005). Minerals such as sericite, micas and clay can reduce CPB strength and stability due to their water absorbent mineral layers. Sulphide minerals raise the specific gravity, while the strong of abrasiveness of silica minerals causes serious pipeline wear. Mixing water also affects CPB mechanical strength with regard to the *w/c* ratio and cement hydration mechanisms (see Appendix A). The effects of municipal, lake and process waters on CPB strength were assessed in detail by Benzaazoua et al. (2002) using different binder agents. The authors found that the best strengths were obtained from combinations of general use Portland cement and blast furnace slag, the CPB materials and lake and municipal waters, compared to mixtures using process water.

1.2.4.2 Influence of extrinsic factors

The preparation, transport and placement of in situ CPB can influence the overall quality and properties of the backfill. Recently, some investigators have published field works on in situ CPB material (Ouellet and Servant, 2000; Cayouette, 2003; Harvey, 2004; Belem et al., 2004; le Roux et al., 2002, 2005; le Roux, 2004; Yumlu and Guresci, 2008; Grabinsky and Bawden, 2007; Grabinsky et al., 2008; Belem, 2009). The results show that geomechanical designs of in situ CPB are excessively conservative in terms of backfill recipes, barricade design, and filling and curing strategies. Overall, in situ observations have shown lower void ratios, higher solids concentration and higher UCS values near the bottom of the stope, as well as higher void ratios, lower solids concentration and lower UCS values near the top of the backfilled stope. This is mainly caused by self-weight or time-dependent consolidation, interaction between CPB and rock, and the effective curing conditions (curing under pressure and removal of excess water within CPB through cracks at the bottom, or water absorption by soft rocks or materials placed in side walls). These processes enhance the CPB mechanical strength development mainly due to pore water pressure dissipation and solids skeleton

settlement (le Roux, 2004; Belem et al., 2002, 2006, 2010a; Yilmaz et al., 2009a; Helinski et al., 2006, 2009; Fourie et al., 2007; El Aatar, 2009).

The measurement of volume change or chemical shrinkage at early age CPB materials is important because it can cause significant reductions in excess PWP during cement hydration (Helinski et al., 2007b), playing a role on the backfill stiffness and consequently strength development. Justness et al. (1994, 1996) stated that the chemical shrinkage is closely related to the multiple stage cement hydration reactions happened at very early ages of curing and the gradual formation of the stiffness development of CPB. It is well-known that the volume of the non-hydrated cement is relatively lower than the sum of the hydrated cement and water volumes. The chemical shrinkage (also referred to as self-desiccation) is observed within the CPB materials through the PWP measurements and/or matric suction increase because of capillary depression (Grabinsky and Simms, 2006; Fourie et al., 2006; Helinski et al., 2007b; Simms and Grabinsky, 2009; Witteman and Simms, 2010). Belem et al. (2010b) has also showed experimentally using the dilatometry (or volumetric method) to quantify the chemical shrinkage from direct measurements that the higher *w/c* ratios of cemented backfills can give rise to less efficiency of the hydration reactions at curing ages of less than 30 days. The effectiveness of short-term hydration decreased drastically when the solid (i.e., tailings and sand is added to cement and when the *w/c* ratios became higher. Further discussions on these original test results of the chemical shrinkage can be found in Belem et al. (2010b).

It is well known that it is difficult to conduct paste backfill testing in the field, because mines generally do not want to risk the safety of personnel or cause property damage or production losses and delays. Therefore, laboratory testing should be designed so that when the CPB is prepared, cured and tested at laboratory, all the physical and mechanical conditions present in underground backfilled stopes are reproduced, resulting in an equivalent CPB performance. A new laboratory apparatus called the CUAPS (curing under applied pressure system) was designed at UQAT for exactly this purpose: to better investigate the in situ properties of CPB (Benzaazoua et al., 2006; Yilmaz et al., 2008a, 2009b). The CUAPS can be effectively used to conduct a series of tests on CPB during curing, including *i*) one-dimensional consolidation testing, *ii*) pore water pressure dissipation testing, *iii*) permeability testing and *iv*) curing

under pressure testing. Further information on the improved CUAPS apparatus and individual studies can be found in Yilmaz et al. (2006, 2008a,b, 2009a,b, 2010a,b).

1.2.5 Microstructural (pore structure) behaviour

Pore structure is an important microstructural characteristic of a porous matrix, as it affects the physical and mechanical properties and controls the durability of cemented materials such as CPB. The behaviour of a porous material is strongly affected by the distribution of pores of various sizes within the solid (Aligizaki, 2006). Pore size distribution (PSD), which is in turn influenced by the tailings grain size and packing, plays a role in permeability and pore water pressure within the CPB in response to loading (Belem et al., 2001; le Roux, 2004). Characterization of the pore structure (e.g., total porosity, macropores, mesopores, PSD, threshold diameter and critical pore diameter) of CPB is complicated by the presence of pores having different shapes and sizes and by the connectivity between pores. Among the many methods reported in the literature to characterize the pore structure (microstructural), mercury intrusion porosimetry (MIP) is one of the most frequently used because it provides good repeatability and covers almost the whole range of pore sizes to be analyzed in the hydrated material (Cook and Hover, 1999; Diamond, 2000; Ait-Mokhtar et al., 2002).

MIP results are influenced not only by the microstructure of the specimen, but also by the experimental parameters, such as pre-treatment technique, sample size, pressure build-up rate, pore structure alteration, surface tension of mercury and contact angle (Galle, 2001; Kumar and Bhattacherjee, 2003). The effects of microstructural changes on the pore structure parameters of CPB using MIP have been well studied by many researchers (Benzaazoua, 1996; Ouellet et al., 1998; 2005, 2007, 2008; Benzaazoua et al., 2000; Belem et al., 2001; Mohamed et al., 2003; le Roux 2004; Ramlochan et al., 2004; Fall et al., 2005; El Aatar et al., 2007; Deschamps et al., 2008; Yilmaz et al., 2008c, 2009b). From the results, it was shown that the CPB pore structure is affected by tailings grain size, *w/c* ratio, binder type, binder proportion, curing conditions and drainage conditions with curing time. These studies showed that as *w/c* ratio decreases or as curing time increases, total MIP porosity is reduced, mainly due to the reduction in the number of larger-sized pores, which have been filled or connected

by hydrate precipitates in the originally water-filled space. The presence of sulphate also contributes to reduce porosity by increasing pore fineness.

1.3 RESEARCH SCOPE AND OBJECTIVES

The main objective of this doctoral thesis was to provide theoretical and experimental bases for evaluating the in situ properties and curing conditions of laboratory-prepared CPB using the improved CUAPS apparatus. More specifically, an attempt is made to examine the one-dimensional consolidation characteristics of CPB as a function of curing time and binder types and contents. The specific objectives and scope of the thesis are as follows:

- To provide a review of the recent literature on CPB techniques, with an emphasis on one-dimensional consolidation, saturated hydraulic conductivity (permeability coefficient), uniaxial compressive strength and microstructure;

- To investigate the hydromechanical, geotechnical and geochemical properties of CPB materials cured under equivalent overburden pressure using the CUAPS apparatus and to appraise the utility and capacity of the apparatus;

- To present and assess the improved CUAPS apparatus for investigating in situ properties of laboratory-prepared CPBs, and to validate the functions of the improved CUAPS with a series of tests: one-dimensional consolidation with and without pore water pressure measurement, permeability tests and curing under pressure tests;

- To study the one-dimensional consolidation characteristics (i.e., compression index C_c, coefficient of volume compressibility m_v, coefficient of compressibility a_v and coefficient of consolidation c_v) of CPB and to propose some empirical models for predicting these consolidation parameters;

- To demonstrate the effect of curing conditions on the pore structures of consolidated and undrained CPB samples using mercury intrusion porosimetry (MIP) and specific surface

area (SSA) measurements, and to propose some empirical models for predicting the UCS from the MIP parameters (i.e., porosity, threshold diameter and critical pore diameter).

The research scope covers a widespread investigation of the consolidation, curing conditions and placement methods for different CPB samples using different laboratory equipments (see Appendix J). The conventional backfill recipe designs tend to underestimate CPB strength properties, because they do not truly simulate underground stope conditions, often failing to account for consolidation, effective stress and curing conditions. An effective stress develops over time within the CPB placed in an underground stope due to self-weight consolidation. The application of stress during curing increases the mechanical strength development of the CPB materials (see Appendices H and I). This thesis makes an original contribution by using an innovative CUAPS apparatus as part of a reasonable approach to curing samples under pressure and to design an effective mix recipe. CUAPS more accurately estimates CPB in situ conditions. Due to space limitations, the scope of this thesis project study does not allow for a study of curing loading rates, scale effects, mixing techniques, curing and drainage conditions (just for mould investigations), although such investigations are needed to better evaluate and implement CPB materials.

1.4 ORGANIZATION OF THE THESIS

This Ph.D. thesis is organized into six chapters and four of them (chapters 2, 3, 4 and 5) are peer-reviewed journal manuscripts that address the different properties of CPB for a practical mine backfill design. Chapter 1 provides a general introduction.* General shortcomings of the current paste backfill characterization methods are identified, the research aims and scope are presented, and the general resources for issues of interest are provided. Chapter 2 describes the effects of curing under pressure on the compressive strength development of CPB using the original CUAPS apparatus and conventional plastic moulds. The principal processes that occur within paste backfill that is cured under overburden pressure over time are explained and testing methods are reviewed. Additionally, the original CUAPS apparatus is thoroughly

* References in the Introduction are presented in the General References section.

assessed in terms of the hydromechanical, geotechnical and geochemical properties of CPB. Chapter 3 introduces the improved CUAPS apparatus designed to investigate in situ CPB behaviour and presents some preliminary results on consolidation, permeability coefficient, pore water pressure dissipation, curing stress and compression rates. Chapter 4 addresses the consolidation characteristics of early age paste backfill samples using the improved CUAPS. It provides important insights into the understanding of what occurs in a stope over time, based on consolidation settlement and therefore the grain rearrangement that notably reduces final porosity. Chapter 5 describes the microstructural (pore structure) behaviour of CUAPS-consolidated and mould-unconsolidated (undrained) CPB samples using mercury intrusion porosimetry and specific surface area (SSA) measurements. Some simple empirical models are proposed for predicting compressive strength from microstructural parameters. Chapter 6 presents the summary, general conclusions and directions for future research.

CHAPTER II

EFFECT OF CURING UNDER PRESSURE ON COMPRESSIVE STRENGTH DEVELOPMENT OF CEMENTED PASTE BACKFILL

Erol Yilmaz, Mostafa Benzaazoua, Tikou Belem and Bruno Bussiere

Paper published in

Minerals Engineering, Vol. 22, No. 9–10, pp. 772–785 (August–September 2009)

2.0 RÉSUMÉ

La performance mécanique du remblai cimenté en pâte (RCP) mise en place dans des vides souterrains (par example, chantiers miniers) diffère souvent de celle prédite en laboratoire, même dans des conditions atmosphériques de cure similaires (mêmes température ambiante et humidité relative). Cela est probablement dû spécifiquement à la consolidation gravitaire, aux différentes conditions de drainage et aux pressions de confinement rencontrées dans les chantiers miniers remblayés. Un nouveau système d'essai appelé CUAPS (système de cure sous pression appliquée) a été conçu à l'Université du Québec en Abitibi-Témiscamingue (UQAT) pour évaluer la performance hydromécanique du RCP in situ à partir d'échantillons à l'échelle du laboratoire. Le dispositif expérimental CUAPS permet une cure efficace des échantillons de RCP soumis à une gamme de pressions verticales appliquées (cure sous contraintes appliquées) qui peuvent simuler la mise en place et les conditions de consolidation in situ du RCP. L'acquisition de la résistance à la compression des échantillons de RCP préparés à partir de résidus miniers sulfurés de la mine polymétallique de Garpenberg (Suède) a été étudiée en utilisant le dispositif expérimental CUAPS et les moules en plastique conventionnels (échantillons non drainés) en parallèle. L'effet de la contrainte de cure (c.-à simulant différentes conditions de consolidation) sur les paramètres géotechniques index et les propriétés hydromécaniques des échantillons de RCP qui en résultent a été analysé. La principale observation est la confirmation que l'acquisition de la résistance à la compression des échantillons de RCP consolidés (donc drainés) est plus élevée que celle des échantillons non drainés (moules en plastique). Ceci pourrait être attribué à l'élimination de l'eau interstitielle excédentaire due principalement à la pression appliquée au cours du processus cure efficace, ce qui semble améliorer le processus de consolidation du matériau remblai en pâte. Les résultats représentent aussi les différences observées au niveau de la résistance du RCP entre les échantillons de laboratoire et ceux in situ. Ainsi, le CUAPS serait plus approprié que les moules en plastique conventionnels pour recueillir des données pour la conception préliminaire et final des systèmes de remblayage.

Mots clés: Résidus miniers, Remblai en pâte, Consolidation, Contrainte de cure, Résistance en compression

2.0 ABSTRACT

The mechanical performance of cemented paste backfill (CPB) placed in underground openings (mine stopes) usually differs from laboratory-predicted performance, even under the same atmospheric curing conditions (ambient temperature and relative humidity). This is probably due to the specific self-weight consolidation and the different drainage conditions and confinement pressures encountered in paste backfilled stopes. A new test system called CUAPS (curing under applied pressure system) was designed at the Université du Québec en Abitibi-Témiscamingue (UQAT) to assess the hydro-mechanical performance of in situ CPB samples at laboratory scale. CUAPS apparatus allows the effective curing of CPB samples subjected to an assortment of vertical pressure applications (curing under stress) that can mimic well the in situ placement and consolidation conditions. The compressive strength development of CPB samples prepared from sulphide-rich mine tailings from the Garpenberg polymetallic mine (Sweden) was investigated using the CUAPS apparatus and conventional plastic moulds (undrained samples) in parallel. The effect of curing stress (using different simulated consolidation conditions) on the resultant geotechnical index parameters (bulk properties) and hydromechanical properties of CPB samples was investigated. The main finding is that the compressive strength development of consolidated CPB samples is higher than that of undrained CPB samples. This could be attributed to the removal of excess pore water, mainly as a result of the applied pressure during the effective curing process, which appears to improve the consolidation of CPB. The results also account for differences in CPB strength observed between laboratory and in situ samples. The CUAPS would therefore be more suitable than conventional plastic moulds to collect data in developing preliminary and final designs for backfill systems.

Keywords: Mine tailings, Paste backfill, Consolidation, Curing stress, Compressive strength

2.1 INTRODUCTION

Cemented paste backfill (CPB) technology has become well established in the Canadian hard rock mining industry over the past three decades, and has been extensively used as an alternative tailings management method for the safe disposal of the tailings produced during mineral processing operations (Landriault and Lidkea, 1993; Brackebusch, 1994; Hassani and Archibald, 1998). Basically, mine backfill consists of an efficient secondary ground support system for underground mine stopes that provide a secure working environment for mine operators. As a substitute for all other types of underground mine backfill (e.g., hydraulic fill and rock fill), CPB provides a number of advantages from the operational, financial, and environmental perspectives (Hassani and Archibald, 1998; Bussière, 2007). Given the strict environmental regulations and increasing public awareness, CPB allows a safe underground disposal of potentially detrimental wastes such as sulphide-rich mine tailings, consequently limiting the well known problem of acid mine drainage (Aubertin et al., 2002; Yilmaz et al., 2004). Accordingly, the vast majority of underground mines worldwide contemplate using CPB as a proven, cost–effective, and high–quality backfill system (Cayouette, 2003; Belem and Benzaazoua, 2008).

Paste backfill is a relatively complex material consisting of a mixture of dewatered mill tailings (75–85 wt% solids, depending on mineralogy and specific gravity), binding agent to meet the backfill strength (uniaxial compressive strength, UCS) requirements, and sufficient water to reach the desired consistency for transporting the paste to the mine backfilled stope (Amaratunga and Yaschyshyn, 1997; Benzaazoua et al., 1999). Even if the understanding of backfill behaviour has improved, CPB still continues to attract a great deal of attention, as testified by a number of works authored by mining practitioners, consultants, academics, and researchers (e.g., Belem et al., 2000; Benzaazoua et al., 2002, 2004; Yilmaz, 2003; Kesimal et al., 2003, 2004; Godbout, 2005; Fall et al., 2005; Rankine and Sivakugan, 2007; Ouellet, 2007). However, some aspects of CPB materials need to be further investigated such as the effects of placement (i.e., behaviour under self–weight or time–dependant consolidation) and the evolution of the geotechnical properties with curing time.

Nonetheless, numerous investigations indicated that well–drained backfilled stope conditions generate better mechanical strength development and long–term stability than poorly drained ones (Belem et al., 2002; Helinski et al., 2007). Furthermore, compared to field data, laboratory studies using conventional plastic (non–perforated) mould, which is typically used to determine mine backfill design values, tend to underestimate the mechanical strength of a given CPB mixture over the same curing period (Cayouette, 2003; Revell, 2004; le Roux et al., 2005; Belem et al., 2006; Grabinsky and Bawden, 2007). This phenomenon could be attributed to the settling and hardening processes occurring within the CPB material and the removal of its excess pore water. After placement of the mine fill material in the stope, the self-weight consolidation controls these phenomena (Belem et al., 2006). Binder hydration can also notably influence the pore water pressure (PWP) and the development of effective stress within the CPB through early age chemical shrinkage (Helinski et al., 2006, 2007; Grabinsky and Simms, 2006; Simms et al., 2007). Helinski et al. (2006) and Grabinsky and Simms (2006) observed experimentally that as PWP dissipates the effective stress increases and the total vertical stress in the stopes decreases. Consequently, the reduction of PWP gives rise to a reduction in horizontal total stresses and barricade loads. In most cases, these underground conditions are neglected in backfill studies except for a few investigations (le Roux et al., 2005; Grabinsky and Simms, 2006; Belem et al., 2006, 2007; Helinski et al., 2006, 2007; Fourie et al., 2007; Grabinsky and Bawden, 2007), apparently as a result of difficulties with appropriate laboratory equipments and test procedures in order to examine the improved behaviour of the CPB materials subjected to the different placement techniques.

A small number of works are reported in the literature on self-weight / time-dependent consolidation characteristics of non-cemented or cemented tailings materials (Mitchell and Smith, 1981; Bussière, 1993; Belem et al., 2006, 2007; Yilmaz et al., 2006, 2008a,b,c). The literature in general focuses mainly on odometer tests (Pierce et al., 1998; le Roux et al., 2005; Grabinsky and Bawden, 2007) in order to determine the consolidation parameters. The one-dimensional consolidation tests are also performed using modified triaxial cells (Mitchell and Smith, 1981) or triaxial cells (Grabinsky and Simms, 2006; Helinski et al., 2006). Due to the fact that triaxial cells do not give flexible working conditions, an affordable and efficient

experimental setup that allows understanding of in situ curing conditions (controlling curing stress) of CPB materials was developed and named CUAPS (Curing Under Applied Pressure System; Benzaazoua et al., 2006).

The originality of this paper consists in the evaluation of the effect of pressure application (during curing) on the properties of CPB, using the CUAPS apparatus. The main parameters investigated during the tests are geotechnical index parameters and the UCS for both standard moulds (undrained) and CUAPS-consolidated samples. The quality of drainage water is also presented to better understand the geotechnical results. Several mix recipes (different binder types and proportions) are tested using Garpenberg poly-metallic Mine tailings (Sweden).

2.2 MATERIALS AND METHODS

2.2.1 CUAPS apparatus

The experimental setup used to simulate backfill consolidation tests is the CUAPS (curing under applied pressure system) apparatus which was developed to mimic in situ placement and effective curing conditions at laboratory scale (Benzaazoua et al., 2006). This apparatus was inspired from a previous consolidation setup used by Belem et al. (2002). CUAPS apparatus can be used to assess the actual strength performance of CPB under loading by applying pneumatic pressure (up to 500 kPa) to the upper portion of sample. The operating principle of CUAPS consists of one–dimensional compression of CPB sample in a pressure vessel (Perspex cylinder) by vertical pressure application. The applied pressure allows the excess pore water to escape from CPB material through a drainage port located at the bottom of the unit. During the consolidation, drainage water is collected and the drainage rate can be calculated. This equipment is simple to operate, readily portable, and relatively affordable.

Figure 2.1a presents a schematic illustration of CUAPS apparatus and a photograph is shown in Figure 2.1b. Specifically designed for laboratory scale tests, it can capture time–dependent sensitivity of the evolution of CPB materials in a variety of consolidation loading schemes

and drainage conditions. The CUAPS tool consists of three main components (Benzaazoua et al., 2006): a rigid top plate with an axial loading piston that applies a pneumatic pressure and equipped with a dial gauge and pressure valve; a rigid Perspex mould (i.e. transparent polycarbonate round tube) protected by a metal cylinder to hold CPB specimen; and a bottom plate with a central port equipped with a ceramic plate and drainage port to drain the CPB sample excessive pore water. It was proven that under the range of applied pressure (0–500 kPa) the Perspex mould radial deformation is less than 1%. This allows simulating the at-rest condition (K_0 consolidation), which is the most realistic conditions for in situ CPB. Perspex cylinders of 102 mm (4") diameter and 204 mm (8") height are used as backfill specimen holders. Once the CUAPS apparatus is filled with the paste material, the loading piston is installed at the top and a small bottle is plugged to the drainage port at the bottom to collect drainage water at a constant time interval. The chemical composition of drainage water can then be analyzed.

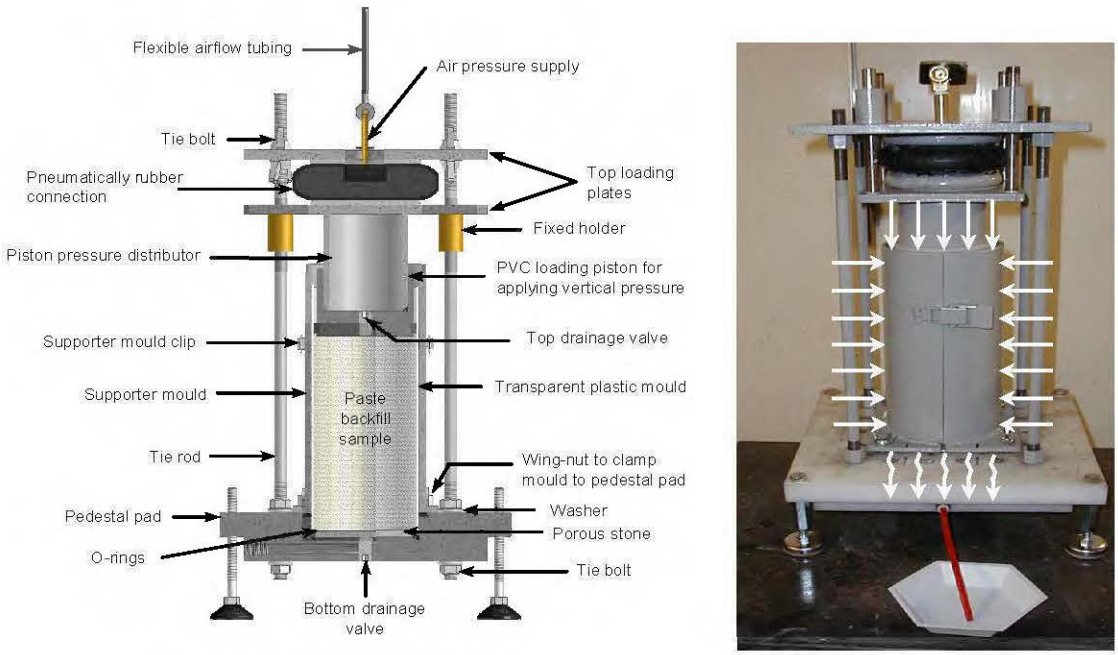

Figure 2.1 CUAPS (curing under applied pressure system) apparatus developed for CPB consolidation and drainage tests (Benzaazoua et al., 2006).

2.2.2 Materials characterization

The tailings sample used for CPB preparation is coarse-grained tailings from the Garpenberg Mine (Stockholm, Sweden), one of the world's largest zinc mines. Approximately 1.1 million tonnes (Mt) of ore are mined yearly, resulting in a production of approximately 0.6 Mt of sulphidic tailings per year; nearly 45% of the total mine tailings are returned underground as CPB (Lindqvist et al., 2006). The physical properties (grain size distribution, solids specific gravity, and specific surface area), chemical and mineralogical analyses of the tailings were determined. The average initial water content of the tailings was 15.2 wt% and was used to set paste properties such as solids content and slump, in accordance with ASTM D 2216 standard. Mixing water was analyzed for chemical composition (ICP-AES), and for pH.

2.2.2.1 Grain size distribution of tailings sample

Grain size distribution (GSD) of tailings is an important property since it can affect the resultant paste consistency, chemical reactivity, and the overall hydromechanical properties. The GSD curves of tailings samples were determined using a Malvern Laser Mastersizer S 2000® where particles between 0.05 µm and 880 µm can be measured with an accuracy of ±1%, according to both ASTM D421 and ASTM D422 standards. Figure 2.2 presents the GSD curves of the Garpenberg tailings, comparing to a typical range of GSD curves of 11 mine tailings sampled from the underground mines located in the province of Quebec and Ontario, Canada (Ouellet, 2007). The D_{85} (particle size at 85% passing) of tailings was 0.16 mm, with a highest particle size of 0.88 mm. According to the Unified Soil Classification System (McCarthy, 2007), the tailings can be classified as a non–plastic silt, like most of the tailings produced in hard rock mines (Bussière, 2007). The amount of particles finer than 20 µm (fine fraction) was 26 wt%, indicating a good ability to retain sufficient water to form a paste. According to Landriault (2001), the studied mine tailings samples may be classified as coarse-grained. The Garpenberg Mine tailings have C_u and C_c values of 13.4 and 2.1 respectively, and can be categorized as a well–graded material, following the standard criteria (e.g., Hassani and Archibald, 1998; McCarthy, 2007).

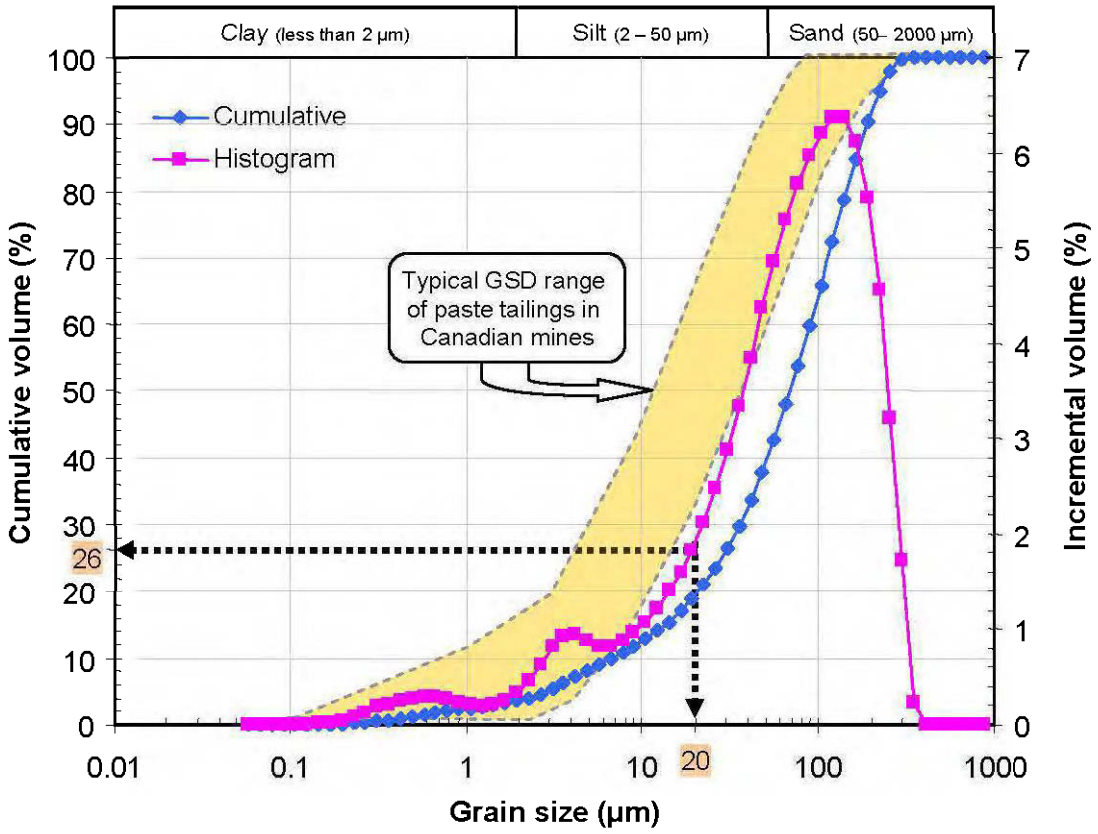

Figure 2.2 Grain size distribution (GSD) curves of the Garpenberg Mine tailings, compared to a typical range of GSD curves of 11 tailings sampled from Canadian hard rock mines.

2.2.2.2 Solids specific gravity and specific surface area

The specific gravity of the tailing solids $G_{s\text{-}t}$ is important for the mixture proportioning and geotechnical index parameters calculation. Specific gravity ($G_{s\text{-}t}$) of the tested tailings sample was determined to be 2.96, using a Micromeritics® AccuPyc 1330 helium pycnometry in accordance to standard ASTM C128. Specific surface area by mass (SSA) is a good indicator of material fineness. As particle size becomes smaller, specific surface area per unit mass or weight of solids increases, and so paste consistency increases. The most common approach to obtain the SSA value is the isothermal adsorption of nitrogen, using either a single point or multipoint calculation method. In this study, the BET (Brunauer, Emmett, and Teller) theory

of multilayer gas adsorption behaviour by means of multipoint calculation was used to better evaluate the SSA value of the mine tailings, using a Micromeritics® Gemini surface analyzer, which was 1.032 m^2/g.

2.2.2.3 Chemical composition of tailings sample and mixing water

The sulphide content of mine tailings is of prime importance in the CPB operation, since it controls tailings specific gravity and therefore the binder content by weight to be added per unit volume, along with the short– and long–term strength durability of the CPB materials (Kesimal et al., 2005; Klein and Simon, 2006). The elemental analysis of the Garpenberg Mine tailings was done from digested samples using a Perkin-Elmer Inductively Coupled Plasma – Atomic Emission Spectroscopy (Optima 3100 RL ICP–AES). As shown in Table 2.1, the tailings sample contained largely silica (32.7 wt%) and, to a lesser extent, magnesium (2.62 wt%), calcium (3.55 wt%), aluminium (2.59 wt%), and iron (6.91 wt%), with a relatively low total sulphur content (4.69 wt%).

Table 2.1 Chemical composition of the Garpenberg Mine tailings

Element	Grade (%)	Element	Grade (%)
Al	2.590	Fe	6.910
As	0.018	Mg	2.620
B	0.020	Mn	0.697
Ba	0.041	Na	0.656
Ca	3.550	Pb	0.191
Cd	0.001	S	4.690
Co	0.001	Se	0.144
Cr	0.004	Si	32.70
Cu	0.009	Zn	0.210

Table 2.2 presents the chemical analysis of the tailings interstitial water (derived from the Garpenberg tailings slurries) by means of ICP–AES. Tailings water contains some metal species (e.g. 0.016 mg/L of Al, 5.18 mg/L of Mg, 0.056 mg/L of Cu and 0.116 mg/L of Zn)

and relatively high sulphate concentration (4344 mg/L, based on a stochiometric conversion assuming all sulphur ions in sulphate form), signifying an expected aggressiveness towards cement durability according to standard DIN 4030. The water also contains a relatively high level of calcium (805 mg/L), presumably due to the addition of lime for pH control during mineral processing. An Orion Model 920A pH meter equipped with a Thermo Orion Triode combination electrode (Orion Inc., Boston, MA) was used for pH measurements. The pH value for the mixing water was 7.88.

Table 2.2 Tailings pore-water chemical analysis

Element	Content (mg/L)	Element	Content (mg/L)
S	1450	Na	94.3
As	0.143	Ca	805
Ba	0.033	Mg	5.180
Bi	***	Al	0.016
Mn	0.339	Fe	***
Cd	***	Si	6.330
Co	***	Cr	***
Se	0.118	Cu	0.056
Mo	0.009	Pb	***
[a]SO_4^{2-}	4344	Ni	0.010
Ti	0.003	Zn	0.116

*** The ICP-AES detection limit

[a] Total sulphur was assumed expressed exclusively as SO_4^{2-}

2.2.3.4 Mineralogical composition of tailings sample

Information on the mineralogy of the tailings sample was obtained from X–Ray Diffraction (XRD) analysis, using a Bruker AXS D8 Advance diffractometer equipped with a Cobalt anticathode. Data collection was performed at angle 2θ varying from 5° to 70° with a step width of 0.005° and a counting time of 0.5 s per step. The diffractograms used to quantify the detectable mineral phases of the tailings specimen (using EVA identification software) were evaluated by Rietveld fitting method using TOPAS software (Rietveld, 1993). The analysis

results are listed in Table 2.3. The mineralogical composition reveals that the Garpenberg tailings sample was dominated by quartz (62.35 wt%). Minor quantities of aluminosilicate minerals including actinolite (12.29 wt%), anorthite (8.41 wt%), muscovite (6.7 wt%) and chlorite (3.17 wt%) were detected as well as small amount of sulphides (mainly pyrite; 7.09 wt%). The amount and type of sulphides within the tailings may affect both the short– and long–term strength development of CPB and the selection of binder type, considering the water retention potential of the phyllosilicates and the sulphate generation potential of the iron sulphides (Benzaazoua et al., 2002; Fall and Benzaazoua, 2005).

Table 2.3 Mineralogical composition of the Garpenberg Mine tailings

Element	Formula	Grade (wt%)
Quartz	SiO_2	62.35
Actinolite	$Ca_2(Mg, Fe^{2+})_5(Si_8O_{22})(OH)_2$	12.29
Anorthite	$Ca[Al_2Si_2O_8]$	8.41
Muscovite	$KAl_2[(OH)_2AlSi_3O_{10}]$	6.70
Chlorite	$(Fe^{2+}, Mg)_5Al[(OH)_8AlSi_3O_{10}]$	3.17
Pyrite	FeS_2	7.09

2.2.2.5 Binder characterization

The primary binder used for the present study was ordinary Portland cement (PCI) supplied by ST-LAURENT CEMENT. Mineral additive such as blast furnace slag, supplied by LAFARGE CEMENT, was also used for blending with PCI as a binding agent to harden CPB samples. Two mixtures of binder were used: ordinary Portland cement (PCI) and Slag blend binder (PCI-Slag). The blending ratio is 20:80 wt% of PCI and Slag. The binder content ($B_{w\%}$) used ranges from 3wt% to 10wt%, representing the lower and upper limits encountered in mining applications. Table 2.4 presents the chemical composition of Portland cement (PCI) and slag binders (by ICP-AES analysis), and some physical properties. The Portland cement (PCI) shows a typical chemistry for this type of cement, and the calculated Bogue's composition is 64.4% for C_3S, 6.6% for C_2S, 8.7% for C_3A and 7.4% for C_4AF. The hydraulic modulus [$CaO/(SiO_2+Al_2O_3+Fe_2O_3)$], which quantifies the hydraulic activity or the self-cementing characteristics of binders (Kamon and Nontananandh, 1991) calculated for both ordinary

Portland cement and blast furnace slag are 2.28 and 0.66, respectively. The higher the hydraulic modulus, the higher the overall self-cementing ability of the binder. However, numerous researchers (Wang et al., 1994; Pal et al., 2003; Belem et al., 2010) showed that the correlation between hyradulic modulus and the compressive strength of blended cements is not always good. There are some other factors (cement fineness, specific surface area, and water/cement ratio) that may affect greatly the last mechanical strength (Hewlett, 2001). Slag conforms to Taylor's (1990) recommendation to prevent sulphate attack with the use of a binder containing an Al_2O_3 percentage lower than 11%. In addition, PCI must contain a maximum MgO value of 5%. Slag has the highest BET specific surface area (SSA) with a value of 3.54 m^2/g, compared to PCI with a SSA value of 1.58 m^2/g. PCI and Slag binders have specific gravities of 3.08 and 2.89, respectively.

Table 2.4 Characteristics of Portland cement and slag used in the mixtures

Property	Ordinary Portland cement, PCI	Granulated blast furnace Slag	Blended binder PCI-Slag (20-80%)
Al_2O_3 (%)	4.82	10.28	8.39
CaO (%)	60.59	31.34	42.82
Fe_2O_3 (%)	2.42	0.51	0.64
MgO (%)	2.19	11.18	6.19
Na_2O (%)	2.10	2.01	2.03
SO_3 (%)	3.92	3.20	3.35
SiO_2 (%)	19.25	36.37	30.91
TiO_2 (%)	0.26	0.61	0.56
Loss on ignition (%)	2.97	2.83	2.96
Hydraulic modulus	2.28	0.66	1.07
Solids specific gravity G_s	3.08	2.89	2.93
BET specific surface area (m^2/g)	1.58	3.54	2.85

2.2.3 Experimental procedures

2.2.3.1 Mixing, casting, and curing of paste backfill

A total of 60 CPB cylinders having a diameter of 102 mm (4") and a height of 204 mm (8") were prepared with different binder contents (3, 5, 7, and 10wt%). The tailings, binder, and water were mixed during about 7 minutes in a concrete mixer. The targeted slump was 178

mm (7"), conducted following the ASTM C 143 standard. Water-to-cement (w/c) ratio and volumetric solids concentration C_v obtained from each CPB are listed in Table 2.5.

Table 2.5 Constant slump paste mix properties (slump = 178 mm; solid content = 78 wt%)

Mixture number	Binder type	Blending	Binder content B_w (%)	Volumetric binder content B_v (%)	Volumetric solids content C_v (%)	Water-to-cement ratio (w/c)
# 1	PCI	1	3	3.54	50.8	11.38
# 2	PCI	1	5	5.90	50.7	6.99
# 3	PCI	1	7	8.26	53.5	4.54
# 4	PCI	1	10	11.79	52.3	3.42
# 5	PCI –Slag	1–4	3	3.85	50.2	11.64
# 6	PCI –Slag	1–4	5	6.41	49.9	7.21
# 7	PCI –Slag	1–4	7	8.98	50.7	5.07
# 8	PCI –Slag	1–4	10	12.83	52.8	3.34

For the range of binder contents used in the study, the C_v value varies between 50.8 and 52.3 %v/v for PCI binder, and between 50.2 and 52.8 %v/v for slag blend binder (PCI–Slag). The corresponding w/c ratios were 11.4–3.4, and 11.6–3.3 for PCI and PCI–Slag binder types, respectively. The prepared pastes were poured into both conventional plastic and CUAPS Perspex moulds. CPB samples were then sealed and stored in a humidity chamber maintained at ~80% relative humidity and 24°C ± 2 in order to mimic curing conditions sustained in the underground mines. Figure 2.3 shows the CUAPS consolidation test preparation steps, from backfill casting to test running in the humidity chamber.

2.2.3.2 CUAPS reproducibility tests

A series of uniaxial compression tests were first performed on CPB samples in order to verify the CUAPS apparatus reproducibility from one setup to another. For that purpose, the PCI–Slag binder type was used at a binder content of 7 wt%. Ten CUAPS cells were used to obtain ten CPB cylinders. After 14 days of curing, the backfill cylinders were subjected to uniaxial compression tests. Figure 2.4 presents the UCS variability of CPB samples, taking into account the effect of the ambient air curing.

Figure 2.3 Photos illustrating CPB preparation steps: (a) filling Perspex cylinders with CPB material; (b) Perspex cylinder (mould) with supporting cover and PVC loading piston; (c) upper plate equipped with pneumatic pressure application system; and (d) CUAPS cells running tests in a controlled humidity chamber.

The first 5 CUAPS cells were cured inside the controlled humidity chamber (condition 1) while the remaining 5 CUAPS cells were cured outside of the humidity chamber (condition 2). From these test results submitted to two different curing environments, it was inferred that there was no significant UCS difference between "inside" samples and "outside" samples,

CPB moulds being well sealed. Moreover, a mean UCS value μ of 3167 kPa and a standard deviation σ of 376.8 kPa were observed. Calculated coefficient of variation *CV* (= σ/μ) is approximately 12%. This relatively low *CV* value confirmed that CUAPS cells give reliable and repeatable results.

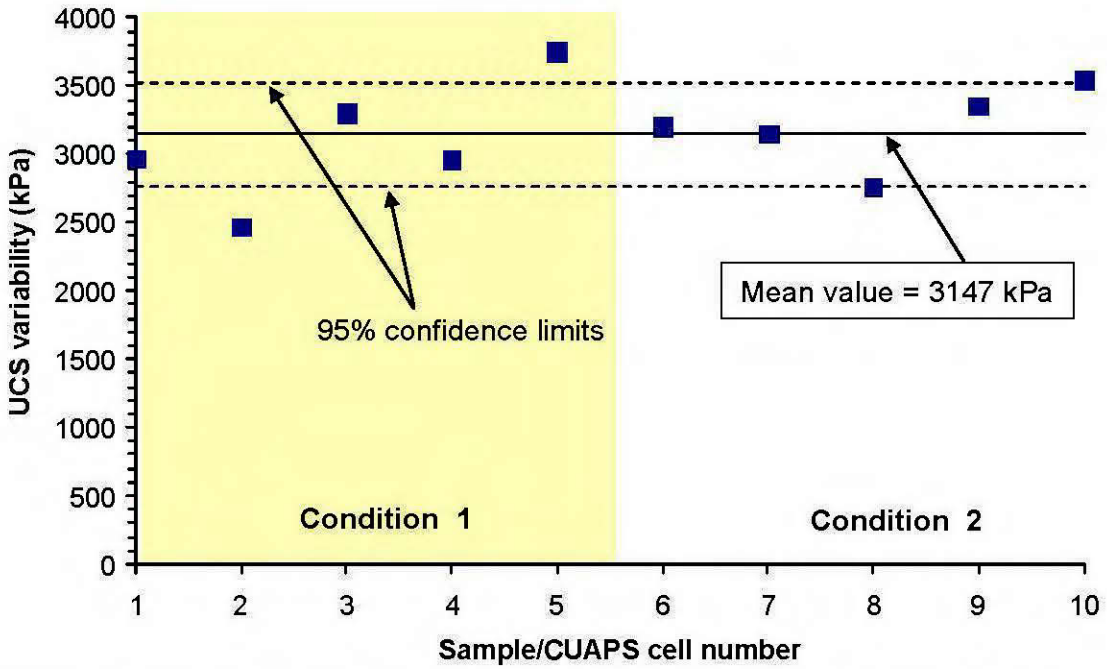

Figure 2.4 The consolidated CPB samples UCS variability over ten test samples/CUAPS cells. The first 5 CUAPS cells were cured inside of the humidity chamber (condition 1) while the remaining 5 CUAPS cells were cured outside of the humidity chamber (condition 2).

2.2.3.3 Pressure application scheme

After validating CUAPS cells, two final constant pressures were chosen for two sequential stope filling scenarios: p_v = 250 kPa for scenario A and p_v = 375 kPa for scenario B. Table 2.6 and Figure 2.5a present the pressure application scenarios simulating a backfilled stope sequential backfilling over four days. The applied pressure (p_v) generated during stope filling and corresponding equivalent backfill height h (where $h = p_v/\gamma$) are also given (Figure 2.5b).

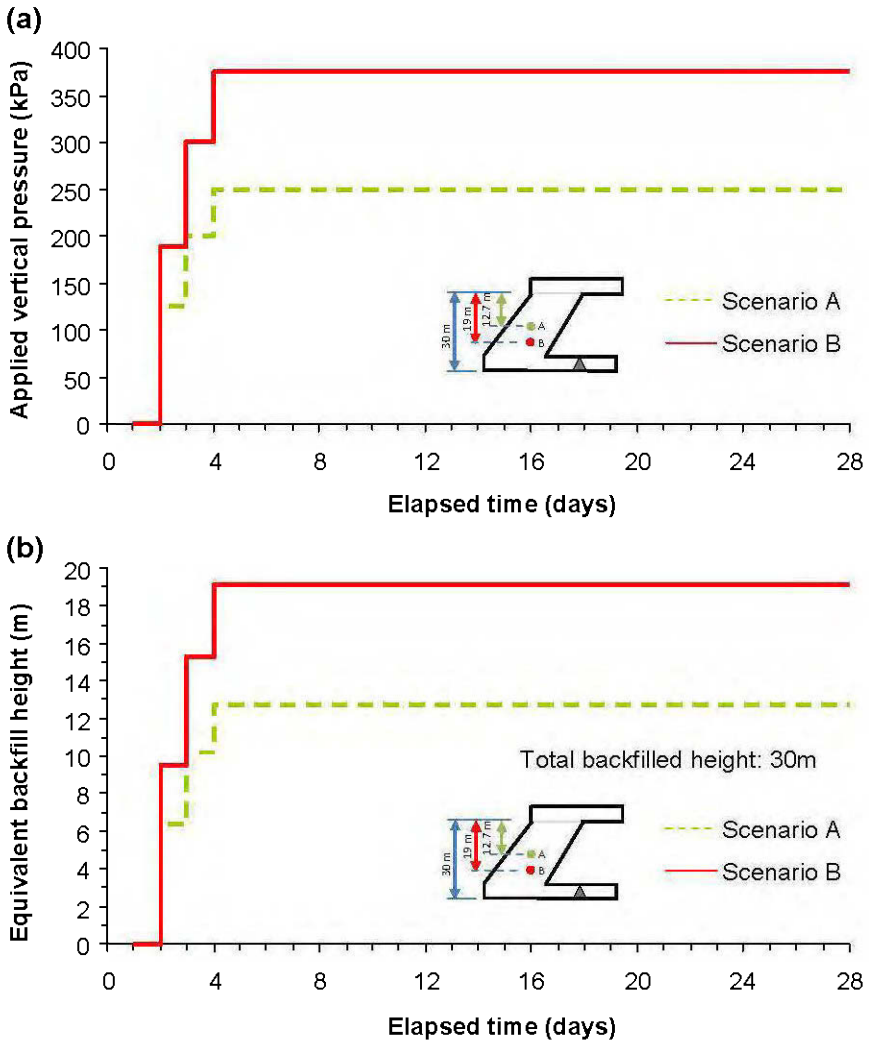

Figure 2.5 Comparison of the two simulated scenarios: a) vertical pressure application scheme, b) corresponding equivalent CPB height of surcharge.

Notice that equivalent backfill height depends on the CPB bulk unit weight γ which was taken to be 19.63 kN/m^3 (in this case, arching effect was not taken into account, only at-rest condition with K_0 consolidation). It should be stated that during the first 24 hours after the sample placement, no pressure was applied. Then, pressure was incrementally increased up to final pressure of 250 kPa (scenario A) and 375 kPa (scenario B) at an average compression rate of 2.6 kPa/hour (filling rate of 0.133 m/hour) for scenario A and 3.9 kPa/hour (filling rate

of 0.199 m/hour) for scenario B. These stresses correspond to an equivalent CPB overburden pressure of about 12.7 m for 250 kPa (scenario A) and 19.1 m for 375 kPa (scenario B), respectively. Note that the pressure range applied in the tests was determined by the mine and the equivalent CPB heights were back–calculated from the pressure range.

Table 2.6 CUAPS pressure application scheme and scenarios simulating a stope filling sequences and filling rate

Elapsed time (day)	Applied vertical pressure p_v (kPa)	(psi)	Equivalent height h (m)	Equivalent filling rate (m/hr)
		Scenario A		
1	0	0	0	0
2	125	18	6.4	0.133
3	200	29	10.2	0.142
4	250	36	12.7	0.133
		Scenario B		
1	0	0	0	0
2	187.5	27	9.6	0.199
3	300	44	15.3	0.212
4	375	54	19.1	0.199

2.2.3.4 Measurement of drainage water

The volume of free water within CPB has a strong influence on the strength development. Although excess pore water is necessary to transport the paste in pipelines to underground, it negatively affects the strength development of the CPB material. Excess pore water tends to bleed (if no drain present) or to drain through the backfill material on the placement (Belem et al., 2006). Bleed and drainage waters will in turn reduce initial *w/c* ratio and eventually the mechanical strength of CPB (Benzaazoua et al., 2004; Grabinsky and Bawden, 2007). In order to increase the reliability and validity of test results, two different methods for drainage water collection were followed. The first method consists of weighing each consolidated CPB mould at the beginning and the end of testing. The second method, used in the present study, consists of measuring the volume of drained waters from consolidated backfill samples at specific time intervals as a function of pressure application.

2.2.3.5 Uniaxial compression tests

For this laboratory investigation, only one curing time of 28 days was chosen arbitrarily. Following this curing time, CPB cylinders were subjected to uniaxial compression tests described in the ASTM C 39 standard for determining the unconfined compressive strength (UCS). After backfill cylinder faces rectification (both sides were smoothed with a cutter), the length and weight of CPB samples were first recorded and then were placed between the two plates of a mechanical press for compression test. In this study, a computer–controlled stiff testing machine (MTS Sintech Material Testing Work-station, Sintech 10/GL load frame) with a 50 kN loading capacity was used for compression tests. Each sample was broken at a constant deformation rate of 1 mm/min. The applied loading to the CPB material was measured using a pressure cell having a full–scale precision of 1%. The UCS value corresponds to the maximum stress value (failure peak) reached during the compression test.

2.3 RESULTS AND INTERPRETATION

2.3.1 Analysis of drainage water of consolidated CPB samples

Figure 2.6 shows the variation of drainage water proportion with elapsed time since the beginning of drainage for consolidated samples prepared with 3, 5, 7, and 10 wt% of ordinary Portland cement (PCI) binder. During the first 24–hour period (no applied pressure), samples were allowed to settle under self–weight consolidation and curing conditions, and only a limited amount of water (between 3.4 and 5.4 wt% of total water) was drained from the CPB samples having different binder contents. After the initial period (no pressure), CPB samples were cured inside the CUAPS apparatus under incrementally applied pressure from 125 kPa to a final confining pressure of 250 kPa to simulate overburden backfill weight during a stope filling (Scenario A). When the final pressure of 250 kPa was applied to CPB samples during a 26–hour curing period, a large increase in water drainage was observed (Figure 2.6). Total drainage water volume seems to depend on the binder proportion being used within the CPB. The volume of drainage water from CPB samples prepared with 3 wt% binder (PCI) was 9.2 wt% (133 mL) compared with 3.9 wt% (51.2 mL) for those prepared with 10 wt% of binder.

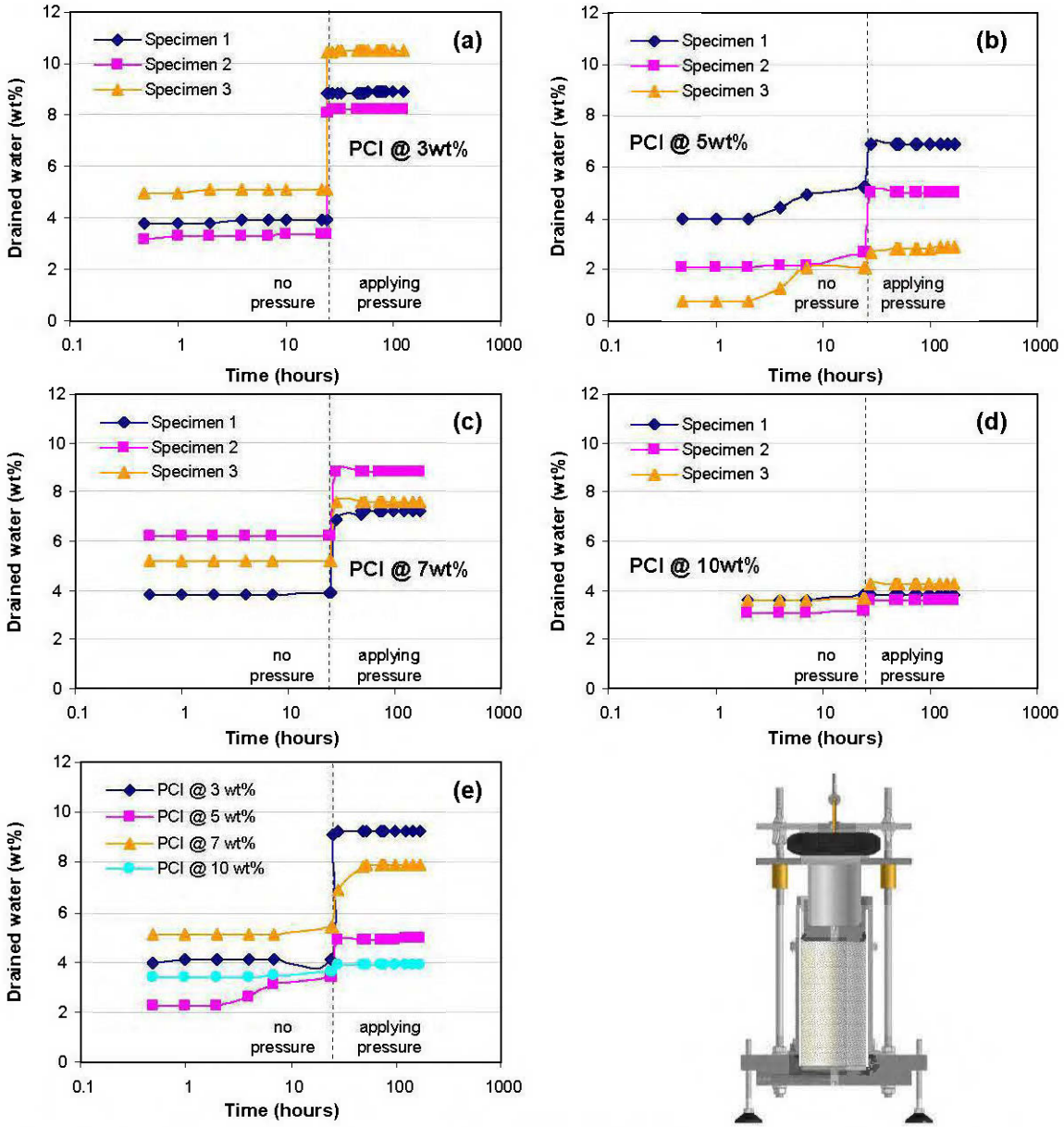

Figure 2.6 Variation of drainage water proportion with time elapsed from the beginning of drainage of CPB samples prepared with PCI@100 wt%: a) 3 wt% binder; b) 5 wt% binder; c) 7 wt% binder; d) 10 wt% binder; and e) the mean values.

This could be attributed to the higher amount of water required for hydration at 10 wt% binder. The water drainage pattern for the CPB materials prepared using PCI-Slag binder (Figure 2.7) is not comparable with that of ordinary Portland cement alone.

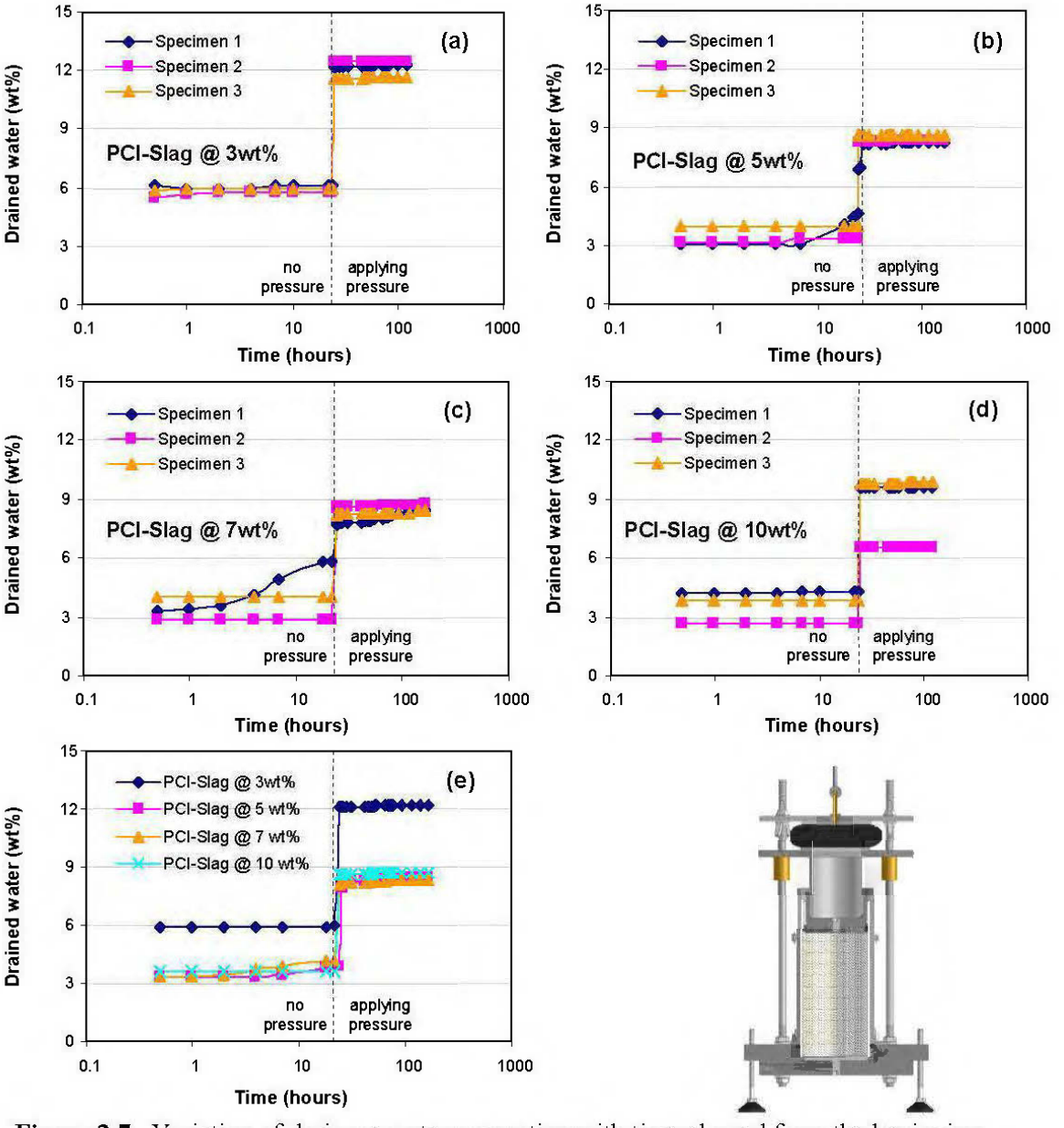

Figure 2.7 Variation of drainage water proportion with time elapsed from the beginning of drainage of CPB samples with a slag blend binder PCI–Slag@20:80 wt%: a) 3 wt% binder; b) 5 wt% binder; c) 7 wt% binder; d) 10 wt% binder; and e) the mean values.

Indeed, over the first 24–hour period (no applied pressure), water drainage is slightly higher than with PCI alone, presumably due to low water consumption capacity of PCI-Slag binder compared with PCI. In this case, the average total volume of drainage water from the CPB

materials with PCI-Slag binder decreased from 189.9 mL (12.2 wt%) to 116.5 mL (8.7 wt%) when binder content was increased from 3 wt% to 10 wt%. Figures 2.6 and 2.7 illustrate that, for a given binder content (curing time of 28 days), the amount of drainage water collected from consolidated CPB samples prepared with PCI-Slag binder was approximately 1.5 times higher than the amount drained from the ones prepared with PCI. This could be attributed to the inherent hydration characteristics of each binder type, i.e. slower hydration process of slag blend binder at early age curing time (up to 28 days) due to the pozzolanic effect. In addition, the GSD of the Garpenberg Mine tailings, categorized as coarse–grained tailings according to the fine fraction content, appeared to largely contribute to the relatively high amount of water drainage. The degree of water retention would be expected to depend on the hydration products formed within the CPB material at an early age depending on the type of binder used. Benzaazoua et al. (2004) has noticed that the drainage of excess water can positively contribute to binder hydration, and consequently a higher strength development in the CPB material.

2.3.2 Analysis of geotechnical index parameters

Table 2.7 presents the mechanical and geotechnical index parameters (bulk properties) of the CUAPS-consolidated samples after 28 days of curing. It can be observed that the porosity n and degree of saturation S_r decreased with the increase in binder content (3 to 10 wt%) while the modulus of deformation E and specific surface S_m increased with the increase of binder content for PCI and PCI–Slag binders. There is a major variation in S_r (98–69%), porosity n (0.45–0.37), and S_m (3.975–14.775 m^2/g). Specific gravity $G_{s\text{-}bkf}$, water content w and solid concentration C_w of CPB are affected by the applied pressure during curing, so it is generally expected that the water content of the paste will decrease (26 to 16%) with increased solids concentration (79.2 to 86.8) when binder content is increased from 3 to 10 wt%. However, there was marginal change (2.895 to 2.806) of the $G_{s\text{-}bkf}$ of CPB at similar range of binder content. In addition, n and S_m values are affected by the drainage ability of freshly produced CUAPS-consolidated CPB samples. The CPB strength development is remarkably consistent with water content. The highest binder content (10 wt%) of CPB samples exhibits the lowest water content and degree of saturation, regardless of binder type.

Table 2.7 Bulk properties of CUAPS-consolidated CPB samples after 28 days of curing

CPB identification and sample no	B_w (%)	w † (%)	C_w (%)	$G_{s\text{-}bkf}$ ⌂	S_m ‡ (m^2/g)	S_r (%)	n	E (MPa)	UCS (kPa)
PCI (100%) #1	3	22.1	81.9	2.888	4.427	94	0.40	737.4	307
PCI (100%) #2	3	26.3	79.2	2.888	3.975	94	0.45	153.3	237
PCI (100%) #3	3	25.4	79.7	2.888	3.859	93	0.44	197.2	281
PCI (100%) #1	5	26.9	78.8	2.856	5.229	94	0.45	247.7	403
PCI (100%) #2	5	25.1	79.9	2.856	4.854	92	0.44	201.5	362
PCI (100%) #3	5	26.1	79.3	2.856	4.717	93	0.44	176.4	316
PCI (100%) #1	7	22.4	81.7	2.831	5.962	88	0.42	179.6	563
PCI (100%) #2	7	23.6	80.9	2.831	5.371	89	0.43	263.2	671
PCI (100%) #3	7	23.7	80.8	2.831	4.939	92	0.42	403.4	667
PCI (100%) #1	10	23.5	80.9	2.797	9.256	89	0.43	479.8	1140
PCI (100%) #2	10	20.5	82.9	2.797	7.683	82	0.41	341.9	1031
PCI (100%) #3	10	20.0	83.3	2.797	7.210	80	0.41	360.7	994
PCI–Slag@20:80 #1	3	26.0	79.4	2.895	5.491	98	0.44	429.4	1104
PCI–Slag@20:80 #2	3	25.5	79.7	2.895	5.526	97	0.43	480.5	1181
PCI–Slag@20:80 #3	3	25.5	79.7	2.895	5.208	89	0.45	509.4	1200
PCI–Slag@20:80 #1	5	25.2	79.8	2.879	8.558	97	0.43	854.8	2545
PCI–Slag@20:80 #2	5	27.3	78.5	2.879	9.324	96	0.45	800.3	2479
PCI–Slag@20:80 #3	5	23.8	80.8	2.879	8.734	94	0.42	948.4	2378
PCI–Slag@20:80 #1	7	24.5	80.3	2.854	10.458	92	0.43	896.9	3011
PCI–Slag@20:80 #2	7	24.9	80.1	2.854	11.618	96	0.43	938.6	3262
PCI–Slag@20:80 #3	7	22.6	81.6	2.854	11.612	95	0.40	894.4	3104
PCI–Slag@20:80 #1	10	15.2	86.8	2.806	11.157	75	0.36	1163.4	3525
PCI–Slag@20:80 #2	10	15.7	86.4	2.806	12.257	69	0.39	1035.5	3558
PCI–Slag@20:80 #3	10	16.1	86.1	2.806	14.775	78	0.37	1057.1	2806

† Water content w determination was done on a representative CPB sample being taken after each UCS test. Samples were oven-dried for about 3 days at 105°C standard temperature.

⌂ Solids specific gravity G_s was determined using an AccuPyc 1330 helium pycnometry. Testing parameters: temperature, cell volume, equilibration rate, and number of purges were taken as 27-30 °C, 12.09 cm^3, 0.005 psig/min, and 5 respectively.

‡ Specific surface area S_m was determined using a Gemini 2375 nitrogen adsorption instrument. Testing parameters: evacuation rate, saturation pressure, and equilibration time were constantly taken as 500 mmHg/min, 767.08 mmHg, and 3 sec, respectively.

This observation is readily explained by the different initial w/c ratios (see Table 2.5) and amounts of water required for binder hydration. Also, specific gravity of the CPB solids ($G_{s\text{-}bkf}$) slightly decreased with an increase in binder proportions within mixture. It is well known that a high–quality CPB should have a high S_m, low n and degree of saturation S_r.

Figure 2.8 shows that there is a clear relationship between bulk properties and binder contents for both consolidated and undrained CPB samples in terms of specific surface area, porosity, degree of saturation, specific gravity, water content, and void ratio vs degree of saturation.

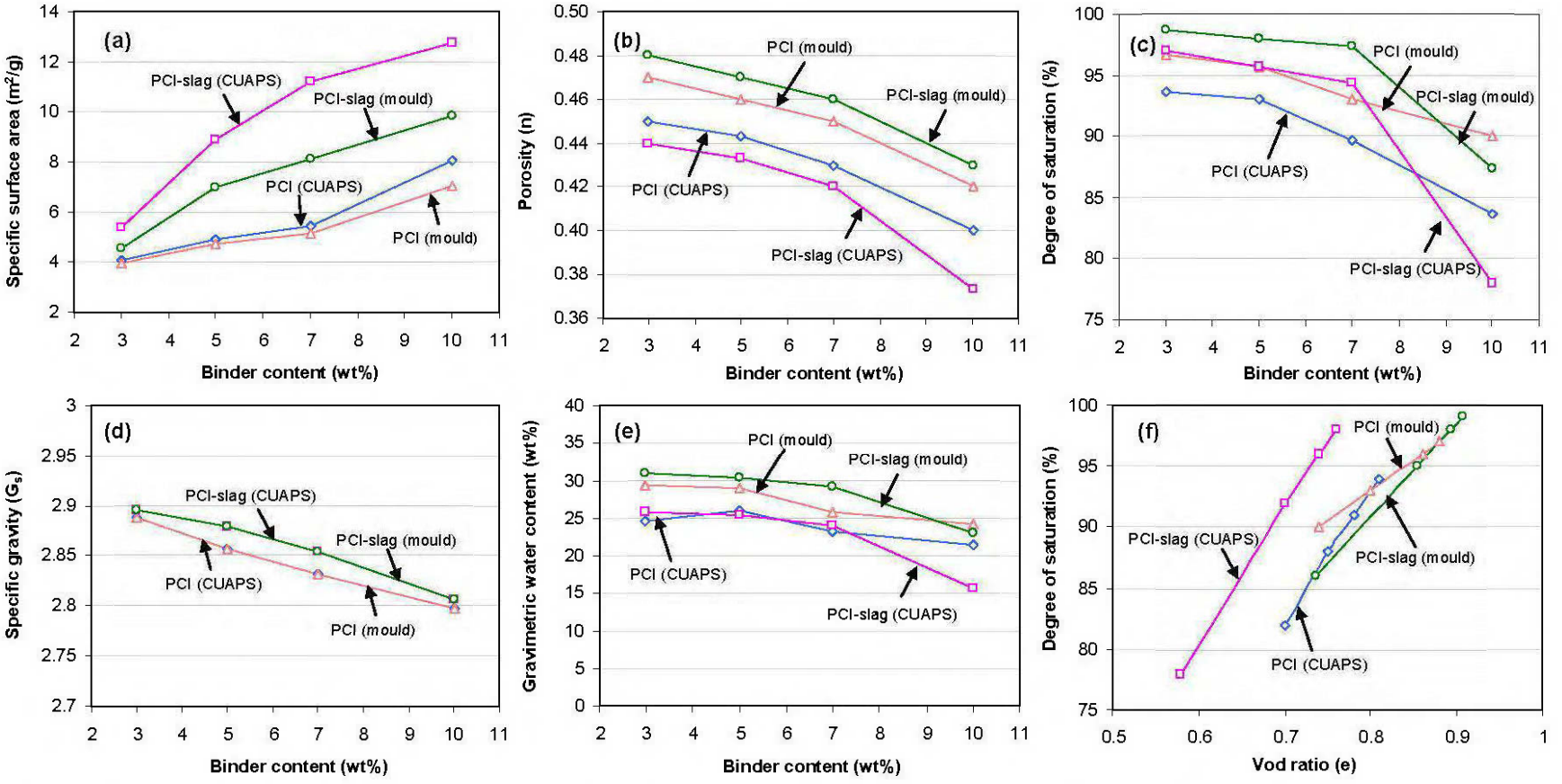

Figure 2.8 Summary of the bulk properties of consolidated and undrained CPB samples in terms of: (a) specific surface area; (b) porosity; (c) degree of saturation; (d) specific gravity; (e) gravimetric water content; and (f) void ratio vs degree of saturation.

Overall, the backfill porosity (or void ratio) is strongly influenced by the drainage ability of early age CPB (up to 3-5 days). The consolidated backfills show less porosity and smaller degree of saturation than undrained ones for a given binder type (Figures 2.8b and 2.8c). This is probably due to the fact that the reduced pore size distribution and population of the CPB materials cured under stress improves the physical properties of the composites by decreasing the paste backfill porosity (see Figure 2.8f), and consequently increasing the backfill strength and stiffness. During binder hydration, the capillary voids available in the CPB sample due to consolidation will be filled with hydrated products, thus increasing the internal cohesion.

Table 2.8 Bulk properties of mould-undrained CPB samples after 28 days of curing

CPB identification and sample no	B_w (%)	w † (%)	C_w (%)	$G_{s\text{-}bkf}$ ⌂	S_m ‡ (m^2/g)	S_r (%)	n	E (MPa)	UCS (kPa)
PCI (100%) #1	3	29.5	77.2	2.888	4.148	97	0.47	100.4	147
PCI (100%) #2	3	29.2	77.4	2.888	3.932	97	0.47	52.2	187
PCI (100%) #3	3	29.2	77.4	2.888	3.855	96	0.47	36.4	184
PCI (100%) #1	5	28.9	77.6	2.856	4.849	95	0.47	129.6	256
PCI (100%) #2	5	28.9	77.6	2.856	4.814	96	0.46	132.1	255
PCI (100%) #3	5	29.2	77.4	2.856	4.452	96	0.47	116.1	275
PCI (100%) #1	7	25.8	79.5	2.831	5.469	90	0.45	316.9	448
PCI (100%) #2	7	25.3	79.8	2.831	5.348	92	0.44	303.4	467
PCI (100%) #3	7	26.3	79.2	2.831	4.712	93	0.44	284.1	463
PCI (100%) #1	10	24.1	80.6	2.797	7.390	91	0.43	449.1	920
PCI (100%) #2	10	25.0	80.0	2.797	7.159	92	0.43	371.2	924
PCI (100%) #3	10	23.2	81.2	2.797	6.624	90	0.42	376.1	863
PCI–Slag@20:80 #1	3	31.1	76.3	2.895	4.889	99	0.48	220.1	549
PCI–Slag@20:80 #2	3	30.5	76.6	2.895	4.844	98	0.47	268.2	555
PCI–Slag@20:80 #3	3	31.1	76.3	2.895	3.988	99	0.48	286.8	594
PCI–Slag@20:80 #1	5	30.6	76.6	2.879	7.403	98	0.47	655.9	1507
PCI–Slag@20:80 #2	5	29.7	77.1	2.879	7.511	96	0.47	768.4	1487
PCI–Slag@20:80 #3	5	30.3	76.7	2.879	6.983	98	0.47	556.4	1487
PCI–Slag@20:80 #1	7	29.5	77.2	2.854	8.098	99	0.46	769.7	2131
PCI–Slag@20:80 #2	7	28.9	77.6	2.854	7.697	96	0.46	798.4	2032
PCI–Slag@20:80 #3	7	28.9	77.6	2.854	6.989	97	0.46	801.6	2129
PCI–Slag@20:80 #1	10	22.1	81.9	2.806	9.854	86	0.42	948.7	3067
PCI–Slag@20:80 #2	10	22.9	81.4	2.806	8.258	87	0.43	974.1	3026
PCI–Slag@20:80 #3	10	23.8	80.8	2.806	7.007	89	0.43	944.1	3088

† Water content w determination was done on a representative CPB sample being taken after each UCS test. Samples were oven-dried for about 3 days at 105°C standard temperature.

⌂ Solids specific gravity G_s was determined using an AccuPyc 1330 helium pycnometry. Testing parameters: temperature, cell volume, equilibration rate, and number of purges were taken as 27-30 °C, 12.09 cm^3, 0.005 psig/min, and 5 respectively.

‡ Specific surface area S_m was determined using a Gemini 2375 nitrogen adsorption instrument. Testing parameters: evacuation rate, saturation pressure, and equilibration time were constantly taken as 500 mmHg/min, 767.08 mmHg, and 3 sec, respectively.

Accordingly, the volume of water available for drainage will extremely be reduced and the coefficient of consolidation will increase. Gravimetric water content of CPB samples is proportional to corresponding porosity values (Figure 2.8e). The higher the gravimetric water content, the greater the CPB porosity becomes. It can be inferred from Figure 2.8a that, as binder content increases, the specific surface area of consolidated CPB samples are higher than those of undrained ones because of the more efficient cement hydration under stress. This is also valid for specific gravity, but in the negative way (Figure 2.8d). With increasing binder content, the specific gravity slightly reduces. This reduction is less with ordinary Portland cement than with slag blend cement.

Similar observations are also made for plastic mould-undrained CPB samples obtained using conventional plastic moulds (Table 2.8). By comparing Tables 2.7 and 2.8, it is observed that the porosity of consolidated CPB samples were lower than those of the undrained ones. It was also observed that the CPB prepared from coarse–grained tailings (Figure 2.2) induced lower porosities. Therefore, less water was required to fill the relatively small amounts of voids between particles, which in turn increased the solids concentration. This phenomenon is greatly related to the lower *w/c* ratio and higher strength for a given binder content.

2.3.3 Effects of binder type and proportion on strength development

Figure 2.9 illustrates the UCS differences observed between consolidated paste backfills and undrained paste backfills as a function of binder type and content (for a constant slump value of 178 mm (7") and curing time of 28 days). Note that scenario A is applied to the backfill samples presented well in Figure 2.9. As expected, the samples' strength increases with the increase of binder added to the mixture. For the consolidated paste backfills, ordinary Portland cement (PCI) produced lower mechanical strengths than the ones obtained from slag blend binder (PCI–Slag) for the range of binder content 3–10wt% after 28 days of curing. When compared to undrained backfills, the consolidated backfills provided a compressive strength increase of 27.1%, 27.3%, 27.5%, and 14.5% for PCI binder (Figure 2.9a), and of 51.4%, 39.5%, 32.9%, and 7.2% for PCI-Slag binder (Figure 2.9b) for the binder contents of 3wt%, 5wt%, 7wt% and 10wt%, respectively.

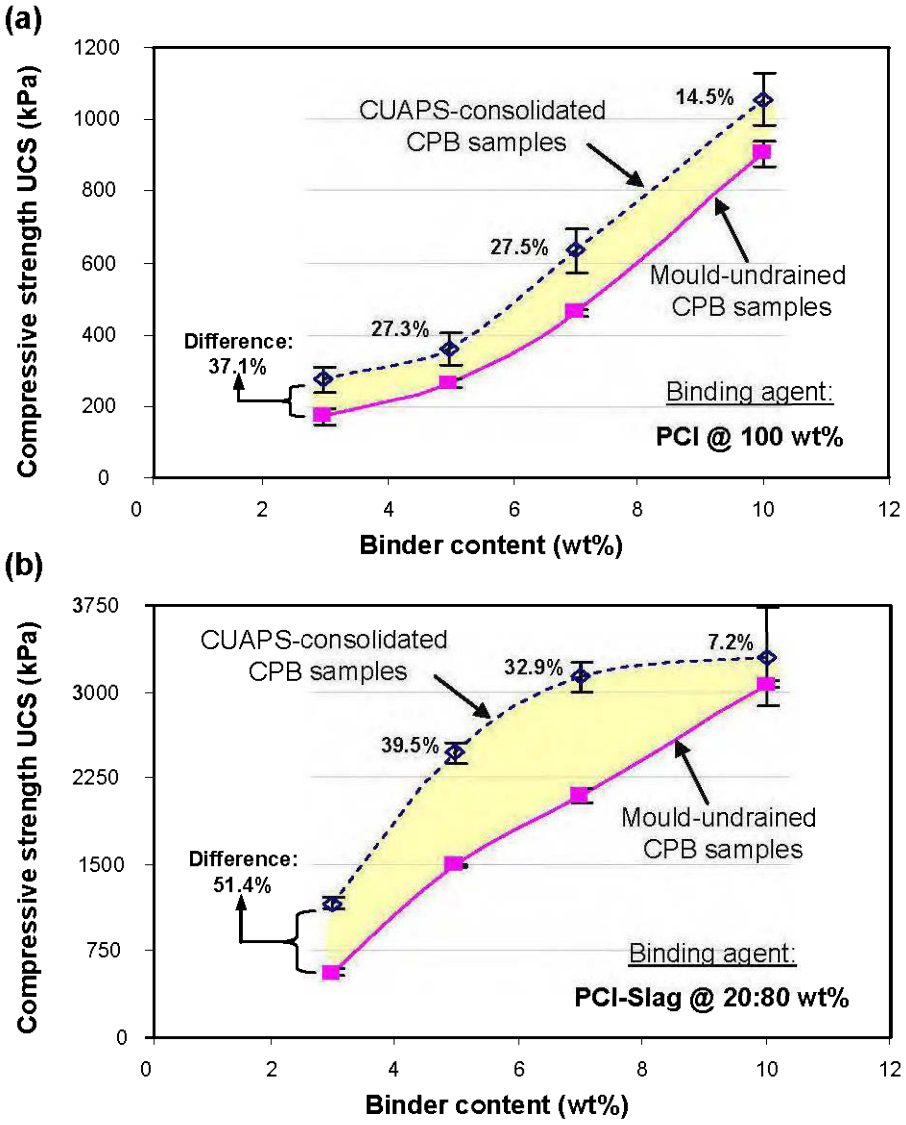

Figure 2.9 Variation in UCS with binder content for all CPB samples prepared using for two binder types: a) ordinary Portland cement (PCI@100 wt%); b) Slag blend binder (PCI-Slag@20:80 wt%). Results shown are the average of three tests for each binder proportionb and error bars represents standard error of the mean values.

The CPB strength varies between 237 kPa and 1140 kPa for PCI binder, and between 1104 kPa and 3558 kPa for PCI–Slag binder. Overall, slag blend binder produces higher UCS values than only PCI binder. This is because slag contains more pozzolanic material whose reaction gives rise to a formation of more C-S-H that is known to increase the mechanical

strength development of the paste backfill materials involved. One can also say that early age hydration process or the self-cementing ability depends on the hydraulic modulus (see Table 2.4). The higher the hydraulic modulus, the higher the binder self-cementing and therefore the higher the early age mechanical strength development. In addition, the short-term strength is determined mainly by the fineness of cement and increases with increasing amount of fine particles and increasing specific surface area (at constant *w/c* ratio). In contrast, the long-term strength is only slightly dependent on the fineness of the binder and for a given *w/c* ratio is determined mainly by the compostion of the cement (Hewlett, 2001). It is worthy mentioning that the PCI is vulnerable to sulphate attack although it is a commonly used binder. However, the blast furnace slag (used as partial replacement of PCI up to 80%) blend binder is known to develop better cohesion in CPB matrix (pores refinement), but exhibits slow hydration rate at an early age before attaining higher strengths for short-, mid- and long-term curing periods (Belem et al., 2000; Benzaazoua et al., 2000; Petrolito et al., 2005; Ouellet et al., 2007).

It appears from Figure 2.9 that consolidated CPB samples always develop better compressive strength than undrained ones, regardless of the curing time. This difference in the mechanical strength development is interpreted mainly as a result of the following phenomena:

- Consolidation reduces the porosity of the CPB compared to the undrained backfill sample (Belem et al., 2002). This observation was confirmed by a variety of mercury intrusion porosimetry (MIP) tests performed on both consolidated and undrained CPB samples (El Aatar et al., 2007; Yilmaz et al., 2008c). Figure 2.10 is a schematic representation of the effect of curing stress on the resultant CPB microstructure, regardless of the binder type and its proportion. The CPB samples produced with fine-grained tailings give in general a lower saturated hydraulic conductivity and a lower modulus of elasticity, giving rise to slower consolidation rate.

- In addition, saturation indices regarding some ions (such as sulphates) is more easily reached since lower water contents are observed in the consolidated CPB backfills, and no (or marginal) cement species are lost during the drainage (Belem et al., 2007). This

leads to more dense cementitious matrices (i.e. the filling of the pore size occurred due to hydration) which is reflected by a better cohesion.

- Garpenberg mine tailings are relatively coarse-grained (Figure 2.2), which may help faster consolidation (high drainage ability). Numerous authors (e.g. Kesimal et al., 2003; Fall et al., 2005; Yilmaz et al., 2007; Belem and Benzaazoua, 2008) showed that for a given *w/c* ratio, the CPB material prepared using coarse–grained tailings generates higher UCS than CPB made of fine–grained tailings due to lower void ratio or porosity.

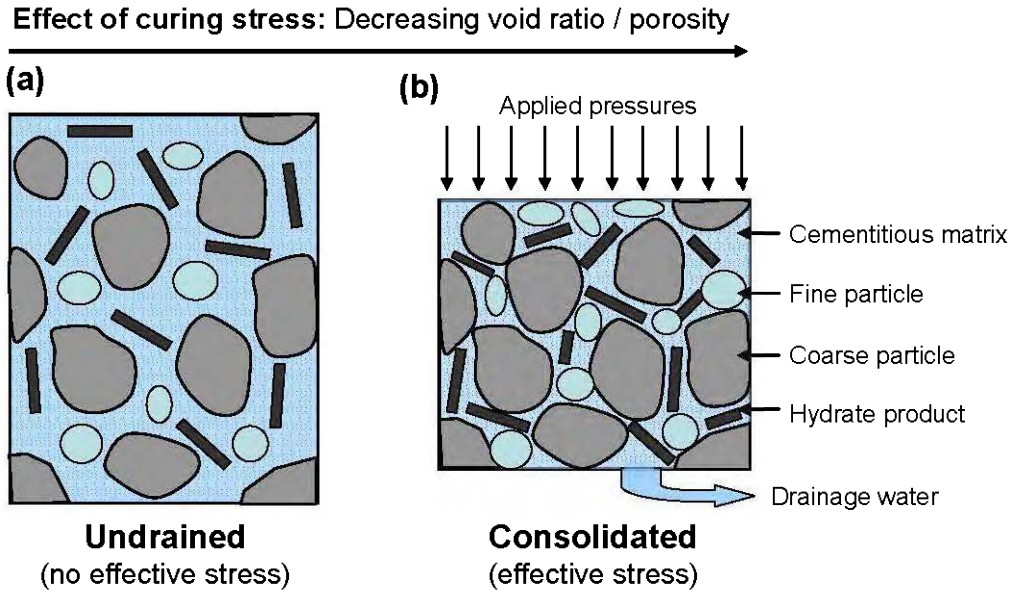

Figure 2.10 Schematic representation of the effect of curing stress on the paste backfill performance: a) undrained CPB sample; b) consolidated CPB sample.

The results of this study illustrate that this newly developed laboratory apparatus (CUAPS), can investigate the compressive strength differences observed between laboratory backfill samples and in situ backfill samples. Consequently, in order to obtain a better knowledge on the overall performance of fresh and hardened CPB materials, CUAPS can advantageously replace conventional plastic (non-perforated) moulds for a better CPB mix design.

2.4 DISCUSSION AND ANALYSIS

2.4.1 Assessment of chemical analysis of drainage water

Water quality (interstitial and mixing water) is an important parameter for determining the quality and transportation characteristics of any CPB, since the water-to-cement ratio affects the strength and stability of the prepared backfill samples, and the cement hydration process is greatly affected by the chemical composition of waters used in the mixtures (Benzaazoua et al., 2002). Accordingly, the tailings interstitial water and water drained from CUAPS-consolidated samples were collected during the first 7 days of testing for chemical analysis and pH measurement. Results are presented in Table 2.9.

Table 2.9 Chemical analysis of drainage water from CUAPS-consolidated CPB samples

Sample identification	pH	Al	Ca	Fe	Mg	Na	*SO_4^{2-}	Si	Zn
					(mg/L)				
PCI@3 wt% binder	12.55	0.155	864	0.276	0.195	27.4	5842	27.8	0.173
PCI@5 wt% "	11.78	0.129	657	0.301	0.056	105	2019	24.8	0.082
PCI@7 wt% "	12.50	0.086	592	0.307	0.033	103	1486	18.1	0.525
PCI@10 wt% "	12.34	0.078	495	0.509	0.035	159	1435	13.45	0.634
PCI–Slag@3 wt% "	11.64	0.185	798	0.101	0.656	24.7	9167	34.5	0.047
PCI–Slag@5 wt% "	11.62	0.156	688	0.128	0.544	103	14859	38.5	0.061
PCI–Slag@7 wt% "	12.30	0.104	686	0.123	0.319	118	12103	36.1	0.082
PCI–Slag@10 wt% "	11.00	0.105	631	0.138	0.262	122.8	6771	21.5	0.051

* SO_4^{2-} was estimated from the total sulphur: $[SO_4^{2-}] = 2.9956*[S]$

For a given binder type, the analysis results showed that iron Fe (0.1–0.5 mg/L), magnesium Mg (0.6–0.03 mg/L), and aluminium Al (0.1–0.07 mg/L) concentrations remained negligible in drainage water, attesting of their stability within CPB solid matrix. Sodium Na (24.7–159 mg/L) content is important, as well as calcium Ca (864–495 mg/L) and sulphate SO_4^{2-} (14859–1435 mg/L). Silicon Si (34.5–13.4 mg/L) concentrations decreased with increasing binder content in the CPB (3–10 wt% binder). Ca and Si participate in C–S–H gel phases

formation and remain trapped in the porous media (CPB sample) during the early age hydration, since only negligible Ca and Si losses were observed in the drained waters. The chemical differences observed between the different waters collected can be attributed to the different chemical compositions of the two binder types. These factors affect the hydration and hardening process at early ages. The hardening reaction during the first days of hydration is progressive due to both anhydrous cement direct hydration and oversaturated phases precipitation, providing continuous internal cohesion growth over months and/or years (Benzaazoua et al., 2004). Slag blend binders have a 2.5–3 times higher SiO_2/CaO ratio than ordinary Portland cement (see Table 2.4); this explains the well–known vulnerability of the later in acidic and sulphate-rich waters. In fact, the high amount of anhydrous silicates leads to less Portlandite and more C–S–H gels formation that are more stable at lower pH. Backfill water retention can be mitigated by controlling the hydration process, which are in turn controlled by the pH and dissolved cations in the medium (Kesimal et al., 2005). The cement buffers in the backfill were at pH values of 11–13. Ca and Fe in drainage water were at high concentrations. Besides, SO_4^{2-} concentration is relatively low since the sulphates participate in the cementation process and remain in the solid state (as in this case).

The binder chemistry combined with mixing-water chemistry (mainly sulphate concentration) strongly affects the hydration processes depending on the binder type in the course of curing time. CPB strengthening was proven to be conditioned mainly by the hydration of unhydrated cement as well as the precipitation of secondary hydrated phases (like gypsum). Slag blend binder hydration seems to be inhibited by the presence of very high soluble sulphate concentration in contrast to Portland cement blend binder. In general, slag blend binders give the best strength for low and medium sulphide-rich tailings for which Portland blend blends have a relatively low strength. The sulphate concentration levels and their effect on paste hardening were discussed in depth in Benzaazoua et al. (2002, 2004). According to the DIN 4030 standard, the sulphate content in water drained from CPB with 5–10wt% PCI was classified as "highly aggressive" and the remaining sulphate levels (3wt% PCI and 3-10wt% PCI-Slag) were "very highly aggressive" at concentrations varying between 5842 and 15167 mg/L (Table 2.9).

2.4.2 Effects of compression rate on CPB performance

Figure 2.11a shows that the compressive strength values of the CPB samples increase with increasing vertical pressure. The highest UCS increase was obtained with 5wt% binder, notably increasing from 2467 kPa to 2673 kPa when the applied p_v value was increased from 250 kPa to 375 kPa. A 50% increase in the vertical pressure produced an 8.3% increase of UCS (Figure 2.11b). Increasing the applied pressure leads to an increase of drainage water, which may have favoured better hydration process due to over-saturation of dissolved ions.

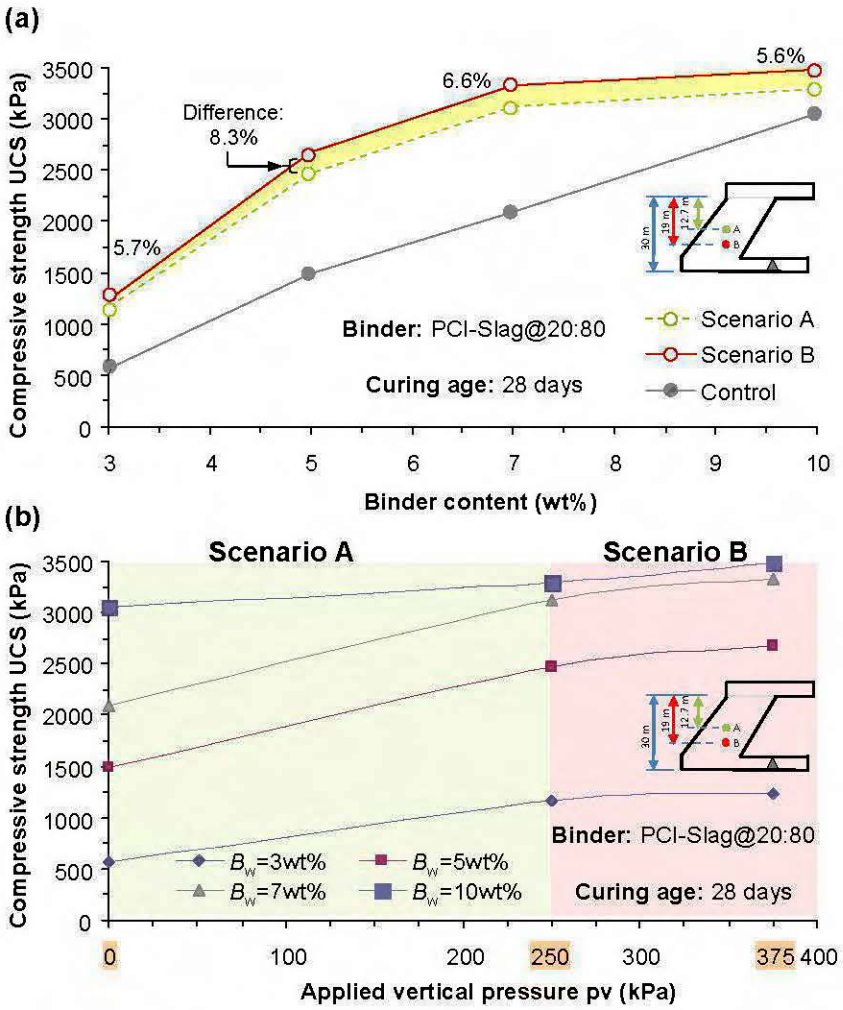

Figure 2.11 Comparison of the UCS of the two simulated scenarios: a) evolution of UCS as a function of binder content, b) evolution of UCS as a function of applied vertical stress.

The aim of the load applied in the CUAPS is to evaluate the effect incremental pressure on the properties of CPBs. In situ observations have shown a lower void ratio, higher solids concentration, and higher compressive strength near the bottom of a backfill stope and a higher void ratio, lower solids concentration, and lower compressive strength near the top of the backfilled stope (Cayouette, 2003). The effect of pressure increment on the compressive strength development of CPB was investigated following two different scenarios (A and B) that are simulating two different CPB heights (or filled-stope depth) based on a maximum aplied pressure p_v and CPB bulk unit weight γ using slag blend binder (CPI-Slag@20:80 wt%). Scenario A is the one presented in the previous section (pressure of 0, 125, 200, and 250 kPa applied after 1, 2, 3, and 4 days of curing respectively; corresponds to a depth of about 12.7 m). Scenario B was similar to scenario A, but with a 50% pressure increase which vary from 0 to 375 kPa (corresponding to a point located below top surface at about 19.1 m). The simulated total height of the backfilled stope was 30 m (Figure 2.11).

However, further work is needed to better understand the effects of binder type and content on the improved behaviour of CPB materials cured under different drainage configurations / curing stresses or loading rates which enable operators to simulate the different heights of the backfill material placed in an underground stope, and how these properties affect the overall quality and performance of fresh and hardened CPB materials over the different curing times.

2.5 CONCLUSIONS

A new paste backfill consolidation setup named CUAPS was used to simulate in situ curing conditions of CPB under self–weight consolidation settlement and/or time–dependent stress to enable better characterization of the mechanical, physical, and chemical properties of lab-prepared CPBs. CUAPS was used to evaluate the properties of CPB prepared with sulphide-rich tailings using two different binder types: slag blend binder (PCI–Slag @ 20:80 wt%) and ordinary Portland cement (PCI @ 100 wt%) alone at binder contents varying from 3 wt% to 10 wt%. The effects of vertical pressure on compressive strength development of CPB were analyzed. Based on the different results presented, the following conclusions can be drawn:

- Drainage water measurements revealed that the amount of water recovered from CPB samples was higher (by 31%) for slag blend binder than for ordinary Portland cement. In other words, the water to cement ratio in the interstitial water is lower for the recipes made of slag blend binder.

- Chemical analyses of drainage water for sulphate content showed that the water obtained from CPB with 5–10 wt% PCI is classified as "highly aggressive" and the remaining sulphate levels (3-10 wt% PCI-Slag and 3 wt% PCI) were "very highly aggressive" at concentrations varying between 5842 and 15167 mg/L according to DIN 4030 standards.

- Geotechnical index parameters showed that porosity, degree of saturation, and specific surface area of consolidated CPB samples were respectively 11.9%, 4.9%, 7.1% lower, and 19.3% higher than those of the undrained ones, for a given binder type and content.

- The consolidated CPB samples containing slag blend binder gave a 51.4% and 7.2% higher UCS than the undrained ones at 3 wt% and 10 wt% binder contents respectively. For ordinary Portland cement, consolidated CPB samples provided a 37.1% and 14.5% higher UCS than undrained ones at 3 wt% and 10 wt% binder contents respectively.

- The incremental compression rate test results showed that CPB strength increases with higher pressure rate applied to samples (e.g. 8.3% increase in the compressive strength when the pressure was increased from 250 kPa to 375 kPa at 5 wt% binder).

This preliminary study demonstrated that the newly developed CUAPS apparatus can be a valuable tool for the collection of reliable data at laboratory scale, and for the assessment of the effects of in situ conditions on the CPB performance. This setup should be a useful device for backfill researchers and practitioners striving to better realize the quality of laboratory-prepared fresh / hardened CPB samples.

2.6 ACKNOWLEDGEMENTS

The authors would like to express their sincere appreciation to Fredrik Ogren from Boliden Mineral AB (Garpenberg Mine, Sweden) for partially funding the project, providing tailings material, and granting permission to publish the results of the tests performed. This project was also funded via a doctoral grant under the NSERC (Natural Sciences and Engineering Research Council of Canada) Discovery Grant Program, the Canadian Research Chair on Integrated Management of Sulphidic Mine Mailings using Backfill Technology, and the Industrial NSERC-Polytechnique-UQAT Chair on Environment Mine Wastes Management. A special acknowledgment goes out to the Canada Foundation for Innovation (CFI) for the manufacture of the ten CUAPS apparatus, Hugues Bordeleau for unconfined compression testing, Mathieu Villeneuve for chemical and mineralogical analyses. The authors also thank Dr. Haci Deveci and two anonymous reviewers for their constructive and useful comments that significantly improved the quality of the manuscript.

2.7 REFERENCES

Amaratunga, L.M., Yaschyshyn, D.N., 1997. Development of a high modulus paste fill using fine gold mill tailings. *Geotechnical and Geological Engineering,* Vol. 15, No. 3, pp. 205–219.

ASTM Designation C128–97, 2002. Standard test method for density, specific gravity, and absorption of fine aggregate. In: *Annual Book of ASTM Standards,* Vol. 04.01, ASTM International, West Conshohocken, PA, pp. 45–52.

ASTM Designation C143–90, 2002. Standard test method for slump of hydraulic cement concrete. In: *Annual Book of ASTM Standards,* Vol. 04.01, ASTM International, West Conshohocken, PA, pp. 68–76.

ASTM Designation C39–98, 2002. Standard test method for compressive strength of cylindrical concrete specimens. In: *Annual Book of ASTM Standards,* Vol. 04.01, ASTM International, West Conshohocken, PA, pp. 15–23.

ASTM Designation D2216–92, 1999. Standard test method for laboratory determination of water (moisture) content of soil and rock. In: *Annual Book of ASTM Standards,* Vol. 04.08, ASTM International, West Conshohocken, PA, pp. 188–191.

ASTM Designation D422–63, 1999. Standard test method for particle size analysis of soils. In: *Annual Book of ASTM Standards,* Vol. 04.01, ASTM International, West Conshohocken, PA, pp. 10–17.

ASTM Designation D421–85, 1999. Standard practice for dry preparation of soil samples for particle size analysis and determination of soil constants. In: *Annual Book of ASTM Standards,* Vol. 04.01, ASTM International, West Conshohocken, PA, pp. 8–9.

Aubertin, M., Bussière, B., Bernier, L., 2002. Environnement et gestion des résidus miniers. In: *CD–ROM,* Presses Internationales Polytechnique, Montréal, Québec, Canada.

Belem, T., Benzaazoua, M., Bussière, B., 2000. Mechanical behaviour of cemented mine paste fill. In: *Proceedings of 53rd Canadian Geotechnical Conference "geotechnical engineering at the dawn of the third millennium*", vol 1, Montreal, Quebec, Canada, October 15–18, pp. 373–380.

Belem, T., Bussière, B., Benzaazoua, M., 2001. The effect of microstructural evolution on the physical properties of paste backfill. In: *Proceedings of the 8th International Conference on Tailings and Mine Waste,* Vail, Fort Collins, Colorado, USA, AA Balkema, Rotterdam, January 16–19, pp. 365–374.

Belem, T., Benzaazoua, M., Bussière, B., Dagenais, A.M., 2002. Effects of settlement and drainage on strength development within mine paste backfill. In: *Proceedings of the 8th International Conference on Tailings and Mine Waste,* Vail, Fort Collins, Colorado, USA, AA Balkema, Rotterdam, January 27–30, pp. 139–148.

Belem, T., El Aatar, O., Bussière, B., Benzaazoua, M., Fall, M., Yilmaz, E., 2006. Characterization of self–weight consolidated paste backfill. In: *Proceedings of the 9th International Seminar on Paste and Thickened Tailings,* Limerick, Ireland, ACG, April 3–7, pp. 333–345.

Belem, T., El Aatar, O., Benzaazoua, M., Bussière, B., Yilmaz, E., 2007. Hydrogeotechnical and geochemical characterization of column consolidated cemented paste backfill. In: *Proceedings of the 9th International Symposium in Mining with Backfill,* Montreal, Quebec, Canada, April 29–May 2, pp. 1–8.

Belem, T., Benzaazoua, M., 2008. Design and application of underground mine paste backfill technology. *Geotechnical and Geological Engineering,* Vol. 26, No. 2, pp. 147–174.

Belem, T., Benzaazoua, M., 2008. Predictive models for pre-feasibility cemented paste backfill mix design. In: *Post-Mining'08,* February 6-8, Nancy, France, pp. 1–13.

Belem, T., Peyronnard, O., Benzaazoua, M., 2010. A model of formulation of blended binders for use in cemented mine backfills. In: *Proceedings of the First International Seminar on the Reduction of Risk in the Management of Tailings and Mine Waste,* Sheraton Perth Hotel, Western Australia, September 29 to October 1, pp. 1–14.

Benzaazoua, M., Ouellet, J., Servant, S., Newman, P., Verburg, R., 1999. Cementitious backfill with sulphur content: physical, chemical and mineralogical characterization. *Cement and Concrete Research,* Vol. 29, No. 5, pp. 719–725.

Benzaazoua, M., Belem, T., Jolette, D., 2000. Investigation de la stabilité chimique et de son impact sur la qualité des remblais miniers cimentés. In: *Institut de Recherche Robert-Sauvé en Santé et en Sécurité du Travail Report* R–260, Montreal, pp. 1–172.

Benzaazoua, M., Belem, T., Bussière, B., 2002. Chemical factors that influence the performance of mine sulphidic paste backfill. *Cement and Concrete Research,* Vol. 32, No. 7, pp. 1133–1144.

Benzaazoua, M., Fall, M., Belem, T., 2004. A contribution to understanding the hardening process of cemented pastefill. *Minerals Engineering,* Vol. 17, No. 2, pp. 141–152.

Benzaazoua, M., Belem, T., Yilmaz, E., 2006. Novel lab tool for paste backfill. *Canadian Mining Journal,* Vol. 127, No. 3, pp. 31–31.

Brackebusch, F.W., 1994. Basics of paste backfill systems. *Mining Engineering,* Vol. 46, No. 10, pp. 1175–1178.

Bussière, B., 1993. Evaluation des propriétés hydrogéologiques de résidus miniers utilisés comme barrières de recouvrement. *M.Sc. Thesis,* Université de Montréal École Polytechnique, Montreal, Québec, Canada, pp. 1–171.

Bussière, B., 2007. Colloquium 2004: Hydrogeotechnical properties of hard rock tailings from metal mines and emerging geoenvironmental disposal approaches. *Canadian Geotechnical Journal,* Vol. 44, No. 9, pp. 1019–1052.

Cayouette, J., 2003. Optimization of the paste backfill plant at Louvicourt mine. *CIM Bulletin,* Vol. 96, No. 1075, pp. 51–57.

DIN Designation 4030, 2001. Standard assessment of water, soil, and gases for their aggressiveness to concrete; principles and limiting values. *Construction Materials and Building,* German Standard, Berlin, pp. 35–46.

El Aatar, O., Belem, T., Bussiere, B., Benzaazoua, M., Yilmaz, E. 2007. Microstructural properties of column consolidated paste fill. In: *Proceedings of the Joint 60th Canadian Geotechnical and 8th IAH-CNC Conferences,* Ottawa, Ontario, Canada, October 21-24, pp. 45–52.

Fall, M., Benzaazoua, M., 2005. Modeling the effect of sulphate on strength development of paste backfill and binder mixture optimization. *Cement and Concrete Research,* Vol. 35, No. 2, pp. 301–314.

Fall, M., Benzaazoua, M., Ouellet, S., 2005. Experimental characterization of the influence of tailings fineness and density on the quality of cemented paste backfill. *Minerals Engineering,* Vol. 18, No. 1, pp. 41–44.

Fourie, A.B., Fahey, H., Helinski, M., 2007. Using effective stress theory to characterize the behaviour of backfill. *CIM Bulletin,* Vol. 100, No. 1103, pp. 1–9 (Paper 27).

Godbout, J., 2005. Évolution des propriétés hydriques des remblais miniers cimentés en pate durant le curage. *M.Sc. Thesis,* École Polytechnique de Montréal, Université de Montréal, Quebec, Canada, pp. 1–190.

Grabinsky, M., Simms, P., 2006. Self-desiccation of cemented paste backfill and implications for mine design. In: *Proceedings of the 9th International Seminar on Paste and Thickened Tailings,* Limerick, Ireland, April 3–7, pp. 323–332.

Grabinsky, M.W.F., Bawden, W.F., 2007. In situ measurements for geomechanical design of cemented paste backfill systems. *CIM Bulletin,* Vol. 100, No. 1103, pp. 1–8.

Hassani, F.P., Archibald, J.F., 1998. *Mine Backfill Handbook.* Canadian Institute of Mining, Metallurgy and Petroleum (CIM), Montreal, Quebec, Canada.

Helinski, M., Fourie, A.B., Fahey, M., 2006. Mechanics of early age cemented paste backfill. In: *Proceedings of the 9th International Seminar on Paste and Thickened Tailings,* Limerick, Ireland, ACG, April 3–7, pp. 313–322.

Helinski, M., Fahey, M., Fourie, A.B., 2007a. Numerical modelling of cemented paste backfill deposition. *Journal of Geotechnical and Geoenvironmental Engineering,* Vol. 13, No. 10, pp. 1308–1319.

Helinski, M., Fourie, A.B., Fahey, F., Ismail, M. 2007b. Assessment of the self-desiccation process in cemented mine backfills. *Canadian Geotechnical Journal,* Vol. 44, No. 10, pp. 1148–1156.

Hewlett, P.C., 2001. *Lea's Chemistry of Cement and Concrete.* 4th ed., Elsevier Butterworth Heinemann, Oxford, United Kingdom.

Kamon, M., Nontananandh, S., 1991. Combining industrial wastes with lime for soil stabilization. *Journal of Geotechnical Engineering,* Vol. 117, No. 1, pp. 1-17.

Kesimal, A., Ercikdi, B., Yilmaz, E., 2003. The effect of desliming by sedimentation on paste backfill performance. *Minerals Engineering,* Vol. 16, No. 10, pp. 1009–1011.

Kesimal, A., Yilmaz, E., Ercikdi, B., 2004. Evaluation of paste backfill test results obtained from different size slumps with varying cement contents for sulphure rich mill tailings. *Cement and Concrete Research,* Vol. 34, No. 10, pp. 1817–1822.

Kesimal, A., Yilmaz, E., Ercikdi, B., Alp, I., Deveci, H., 2005. Effect of properties of tailings and binder on the short and long terms strength and stability of cemented paste backfill. *Materials Letters,* Vol. 59, No. 28, pp. 3703–3709.

Klein, K., Simon, D., 2006. Effect of specimen composition on the strength development in cemented paste backfill materials. *Canadian Geotechnical Journal,* Vol. 43, No. 3, pp. 310–324.

Landriault, D.A., Lidkea, W., 1993. Paste fill and high density slurry fill. In: *Proceedings of the International Conference on Innovative Mine Design for the 21st century,* Kingston, Ontario, Canada, August 23–26, pp. 111–118.

Landriault, D.A., 2001. Backfill in underground mining: underground mining methods engineering fundamentals and international case studies. In: *Society for Mining, Metallurgy and Exploration,* Hustrulid, W., Bullock, R.L. (eds), Littleton, Colorado, Chapter 69, pp. 601–614.

le Roux, K.-A., Bawden, W.F., Grabinsky, M.W.F., 2005. Field properties of cemented paste backfill at the Golden Giant mine. *Mining Technology,* Vol.114, No. 2, pp. 65–86.

Levens, R.L., Marcy, A.D., Boldt, C.M.K., 1996. Environmental impacts of cemented mine waste backfill. In: *ISBM Report RI 9599,* USBM, Washington, pp. 1–23.

Lindqvist, T., Nystrom, B.A., Norling, L., 2006. Paste backfill at Garpenberg North Mine. In: *Proceedings of the 9th International Seminar on Paste and Thickened Tailings,* Limerick, Ireland, ACG, April 3–7, pp. 303–311.

McCarthy, D.F., 2007. Essentials of soil mechanics and foundations: Basic geotechnics (7th edn), *Pearson Prentice Hall,* Toronto, Canada, pp. 1–864.

Mitchell, R., Smith, J., 1981. The compression–percolation test for mine tailings backfill. *CIM Bulletin,* Vol. 74, No. 833, pp. 85–89.

Ouellet, S., Bussiere, B., Aubertin, M., Benzaazoua, M. 2007. Microstructural evolution of cemented paste backfill: Mercury intrusion porosimetry test results. *Cement and Concrete Research,* Vol. 37, No. 12, pp. 1654–1665.

Ouellet, S., 2007. Mineralogical characterization, microstructural evolution and environmental behaviour of mine cemented paste backfills. *PhD Dissertation,* Université du Québec en Abitibi-Témiscamingue, Rouyn–Noranda, Quebec, pp. 1–310.

Pal., S.C., Mukherjee, A., Pathak, S.R., 2003. Investigation of hydraulic activity of ground granulated blast furnace slag in concrete. *Cement and Concrete Research,* Vol. 33, No. 9, pp. 1481–1486.

Petrolito, J., Anderson, R.M., Pigdon, S.P., 2005. A review of binder materials used in stabilized backfills. *CIM Bulletin,* Vol. 98, No. 1085, pp. 1–7.

Pierce, M.E., Bawden, W.F., Paynter, J.T., 1998. Laboratory testing and stability analysis of paste backfill at the Golden Giant Mine. In: *Proceedings of the 6th International Symposium on Mining with Backfill,* Australia, April 14–16, pp. 159–165.

Qui, Y.J., Sego, D.C., 2001. Laboratory properties of mine tailings. *Canadian Geotechnical Journal,* Vol. 38, No. 2, pp. 183–190.

Rankine, R.M., Sivakugan, N., 2007. Geotechnical properties of cemented paste backfill from Cannington Mine, Australia. *Geotechnical and Geological Engineering,* Vol. 25, No. 4, pp. 383–393.

Revell, M.B., 2004. Paste – How strong is it? In: *Proceedings of the 8th International Symposium on Mining with Backfill,* Beijing, China, Nonferrous Metals Society of China, September 19–21, pp. 286–294.

Rietveld, H.M., 1993. *The Rietveld method.* Oxford University Press, London, pp. 1–321.

Simms, P., Grabinsky, M.W., Zhan, G., 2007. Modelling evaporation to optimize surface deposition of paste tailings at the Bulyanhulu mine. *Canadian Geotechnical Journal,* Vol. 44, No. 12, pp. 1417-1432.

Taylor, H.F.W., 1990. *Cement Chemistry, 3rd ed.,* Academic Press, New York, pp. 1–475.

Wang, S.D., Scrivener, K., Pratt, P.L., 1994. Factors affecting the strength of alkali-activated slag. *Cement and Concrete Research,* Vol. 24, No. 6, pp. 1033–1043.

Yilmaz, E., 2003. Experimental investigaton of the compressive strength behaviour of the cemented paste backfill samples prepared from sulphidic mine tailings. *M.Sc. Thesis,* Black Sea Technical University (KTU), Institute of Science and Technology, Trabzon, Turkey, pp. 1–117.

Yilmaz, E., Kesimal, A., Ercikdi, B., 2004. Evaluation of acid producing sulphidic mine tailings as a cemented paste backfill component. *Turkish Journal of Earth Science Review,* Vol. 17, No. 1, pp. 11–19.

Yilmaz, E., El Aatar, O., Belem, T., Benzaazoua, M., Bussière, B., 2006. Effect of consolidation on the performance of cemented paste backfill. In: *Proceedings of the 21st Underground Mine Support Conference,* Val d'Or, Quebec, Canada, April 11–12, pp. 1–14.

Yilmaz, E., Belem, T., Benzaazoua, M., Kesimal, A., Ercikdi, B., 2007. Evaluation of the strength properties of deslimed tailings paste backfill. *Minerals Resources Engineering,* Vol. 12, No. 2, pp. 129–144.

Yilmaz, E., Belem, T., Benzaazoua, M., Bussière, B. 2008a. Experimental characterization of the influence of curing under stress on the hydromechanical and geotechnical properties of cemented paste backfill. In: *Proceedings of the 12th International Conference on Tailings and Mine Waste,* Vail, Fort Collins, Colorado, USA, October 18–23, 139–152.

Yilmaz, E., Belem, T., Bussière, B., Benzaazoua, M. 2008b. Consolidation characteristics of early age cemented paste backfill. In: *Proceedings of 61st Canadian Geotechnical Conference and the 9th Joint CGS/IAH-CNC Groundwater Conference,* Edmonton, Alberta, Canada, September 21–24, pp. 797–804.

Yilmaz, E., Belem, T., Bussière, B., Benzaazoua, M. 2008c. Evaluation of strength, microstructure and consolidation properties of cemented paste backfill using new laboratory equipment. In: *Proceedings of the 3rd International Symposium on Mines and the Environment,* Rouyn Noranda, Quebec, Canada, November 2–5.

CHAPTER III

ASSESSMENT OF THE MODIFIED CUAPS APPARATUS TO ESTIMATE IN SITU PROPERTIES OF CEMENTED PASTE BACKFILL

Erol Yilmaz, Tikou Belem, Mostafa Benzaazoua and Bruno Bussiere

Paper published in

Geotechnical Testing Journal, Vol 33, No.5, pp. 351–362 (September 2010)

3.0 RÉSUMÉ

Cet article évalue certaines améliorations dans la conception d'un appareil de laboratoire appelé CUAPS (système de cure sous pression appliquée), conçu pour étudier les propriétés in situ des RCP. Cet appareil est efficace dans la conduite des essais suivants sur des échantillons de remblai pendant leur cure: *i*) essai de consolidation unidimensionnelle avec ou sans mesure de la pression d'eau interstitielle (PWP), *ii*) essai de dissipation de la pression d'eau interstitielle, *iii*) essai de perméabilité (conductivité hydraulique saturée), et *iv*) cure sous pression verticale constante ou variable. En outre, des essais de compression uniaxiale peuvent être réalisés sur les échantillons de RCP déjà consolidés après chacun de ces essais. Dans cet article, le dispositif expérimental CUAPS modifié est évalué. Les résultats préliminaires sont prometteurs et valident la fonctionnalité de l'appareil CUAPS qui contribuera à l'acquisition des connaissances sur le comportement en consolidation du matériau remblai en pâte in situ.

Mots clés: Remblai en pâte, CUAPS, Consolidation, Pression interstitielle, Perméabilité, Résistance en compression

3.0 ABSTRACT

This paper evaluates some improvements in the design of a laboratory apparatus called CUAPS (curing under applied pressure system) designed to estimate in situ properties of cemented paste backfill (CPB). This apparatus is effective in conducting the following tests on samples during curing: *i*) one-dimensional consolidation test with or without pore-water pressure (PWP) measurement, *ii*) PWP dissipation test, *iii*) saturated hydraulic conductivity (permeability) test, and *iv*) curing under constant or variable vertical pressure. Uniaxial compression tests can be also performed on consolidated CPB samples after each of these tests. The modified CUAPS apparatus is assessed in this paper. Preliminary results are promising and validate the functionality of the CUAPS apparatus, which will contribute to the knowledge on consolidation behaviour of in situ CPB material.

Keywords: Paste backfill, CUAPS, Consolidation, Pore pressure, Permeability, Compressive strength

3.1 INTRODUCTION

Cemented paste backfill (CPB) is used in most modern mines worldwide to refill voids created by underground ore extraction. Mine backfill provides local ground support and a secure working platform for workers and machinery, and allows more complete excavation and removal of ore bodies. It also allows disposing large quantities (up to 60%) of mine tailings underground, which in turn decreases surface tailings storage requirements, thereby reducing environmental hazards and costs linked to future tailings management (e.g., Potvin et al., 2005; Belem and Benzaazoua, 2008). CPB is manufactured by mixing the required amounts of filtered mine tailings (70–85 wt% solids) and mix water (recycled process water or tap water) to obtain the required slump (6–10"). A certain amount of binding agents, usually varying from 3% to 7% by dry weight, is added to achieve geomechanical objectives. Binding agents typically consist of general use Portland cement (GU) blended with different types and amounts of supplementary cementitious materials such as blast furnace slag and fly ash (Benzaazoua et al., 2002, 2004). The CPB material prepared at the surface paste backfill plant is then transported by gravity and/or pumped underground. The structural stability of CPB-filled underground mine stopes depends on the long-term mechanical strength performance of the CPB mass. The required long-term strength (in terms of unconfined compressive strength, UCS) and stability depend on different factors such as stope geometry, ore extraction method and CPB end-use application (waste disposal, pillar recovery, ground support, self-supporting backfill, drift seal in backfill mass, or working platform). UCS is usually used as the quality control parameter in the final evaluation of the CPB mechanical properties, generally varying from 0.1 to 5 MPa (Belem and Benzaazoua, 2008).

To determine the required strength for paste backfill design, UCS is generally obtained from laboratory-prepared CPB samples. Samples are usually poured into conventional plastic capped moulds and cured under undrained condition in a humidity chamber at constant relative humidity and temperature. However, many laboratory and in situ tests have shown that for a given mix recipe and curing time, the UCS of in situ CPB samples can be two to six times higher than the UCS of lab samples using the same CPB mix poured into conventional moulds (Servant, 2001; Belem et al., 2002; le Roux et al., 2002; Cayouette, 2003; Revell,

2004). This unforeseen difference between lab and in situ results cannot be ignored when optimizing a CPB recipe (Belem et al., 2002, le Roux, 2004, Belem and Benzaazoua, 2008).

The cogent reasons supporting this enormous discrepancy between the UCS of mould and stope samples could be well explained by the combined effects of placement, curing under stress, drainage, self-weight and/or time-dependent consolidation and cement hydration (Belem et al., 2002, 2010; Helinski et al., 2006, 2007a; Yilmaz et al., 2008a, b, 2009a, b). However, in most cases, only the paste backfill ingredients (e.g., tailings, cement and water) are considered in investigations of CPB properties. This is due to a lack of suitable laboratory apparatuses and test procedures, except for some investigations in which the apparatus used allowed backfill sample consolidation due to drainage, thus improving the CPB mechanical properties (e.g., Mitchell and Smith, 1981; Belem et al., 2002, 2006, 2007; Helinski et al., 2006, 2007a; Fourie et al., 2007; Yilmaz et al., 2009a). Few studies in the literature have attempted to better understand the effects of pressure and consolidation on the evolution of CPB properties (Pierce, 1997; Belem et al., 2002; le Roux, 2004). Therefore, there is a clear need to develop innovative and adequate experimental setups and appropriate procedures for preparing laboratory samples of CPB that realistically represent in situ conditions (i.e., CPB-filled stopes). An apparatus called CUAPS (curing under applied pressure system) was designed and developed for this purpose at Université du Québec en Abitibi-Témiscamingue (UQAT). This apparatus was initially intended for examining the mechanical strength development of CPB samples cured under equivalent overburden pressure (Benzaazoua et al., 2006; Yilmaz et al., 2008a, 2009a).

The objective of this paper is to present and assess the modified CUAPS apparatus, which allows estimating the in situ conditions and properties of CPB materials. More specifically, the modified CUAPS apparatus measures deformation within CPB samples (allowing one-dimensional consolidation testing), pore-water pressure and saturated hydraulic conductivity. The impact of curing under pressure on CPB strength performance can also be quantified. Validation tests of the modified CUAPS apparatus were performed using a typical CPB recipe. Preliminary results show the utility and capacity of the modified CUAPS apparatus in optimizing the CPB recipes for use as underground backfill.

3.2 EXPERIMENTAL APPARATUS

3.2.1 Standard CUAPS setup

3.2.1.1 Background

Conventional plastic mould-cured CPB does not allow obtaining either one-dimensional consolidation parameters or curing under pressure. Hence, the traditional approach is not representative of in situ conditions for CPB-filled stopes. The first study to address this problem was conducted by Belem et al. (2002). It consisted of a laboratory investigation of the effect of curing under pressure on CPB behaviour. A basic high-density polyethylene (HDPE) device was designed to allow axial loads to be applied to samples (D/H = 0.5) during curing. To overcome the limitations of this relatively simple laboratory apparatus, a more sophisticated apparatus was developed based on the principle of a standard consolidometer (Benzaazoua et al., 2006). This apparatus, called CUAPS (curing under applied pressure system), was better suited to investigate the evolution of UCS of CPB samples cured under applied constant or variable vertical pressure.

3.2.1.2 Brief description

The main parts of the standard CUAPS apparatus are a pressure application system equipped with a piston (at the top plate), a consolidation cell and a free drainage system equipped with a porous stone (at the bottom plate). The top plate is connected to a Firestone® single convoluted air spring with steel bead rings (pneumatic pressure controller), allowing the CPB sample to consolidate one-dimensionally under a maximum allowable pressure of 600 kPa in order to simulate different placement and curing conditions. The consolidation cell is a rigid transparent polycarbonate round tube (Perspex mould) 101.6 mm (4 in.) in diameter and 203.2 mm (8 in.) in height (D/H = 0.5), retained by a protective metal tube. The transparent tube allows visual observation of the backfill sample during testing. The free drainage system and its port are machined into the bottom HDPE plate of 250 mm thickness and 250 mm width to allow drainage water collection during the compression test. A detailed description

of the standard CUAPS and preliminary results are provided in Yilmaz et al. (2008a, b, 2009a, b) and Yilmaz (2010). Initial studies showed that the standard CUAPS apparatus had some technical limitations and needed to be modified to improve measurement quality and obtain more information on overall CPB properties. One such limitation was the frictional resistance that developed between loading piston and the Perspex mould sidewall, affecting vertical displacement at low applied vertical pressure. Other limitations were due to the lack of instrumentation, such as a pore water pressure (PWP) transducer and a linear variable displacement transducer (LVDT). Moreover, the CUAPS apparatus was unable to measure saturated hydraulic conductivity.

Note that a triaxial chamber could also be used to conduct 1-D consolidation tests under oedometer condition (K_0 condition). However, the authors did not opt for this feature due to the high cost and low operational flexibility of a triaxial chamber compared with the CUAPS apparatus (10 CUAPS available versus one mechanical press). Instead, the objective was to develop an efficient experimental apparatus that was easy to operate, readily portable and affordable.

3.2.2 Modified CUAPS setup

Various improvements were made to the standard CUAPS apparatus. Figure 3.1 presents a schematic illustration of the modified CUAPS apparatus and Figure 3.2 presents a photo of four modified CUAPS setups. The following subsection presents the main characteristics of the modified CUAPS apparatus.

3.2.2.1 Frictional resistance of the loading piston

To reduce and/or eliminate the frictional resistance of the loading piston during vertical pressure application, three specific improvements were made. First, the PVC loading piston dimension was redesigned, with three plastic O-rings (instead of two) placed equidistant to prevent any deflection of loading piston. This ensures a monotonous load and homogenous distribution of pressure on the top of the CPB sample under applied pressure (proven to

appreciably reduce frictional resistance). Second, a top porous stone was added to ensure good contact between the loading piston and the top of the CPB sample. This provides accurate and complete pressure application, as confirmed by a test procedure whereby a seating (pre-contact) pressure of approximately 15 kPa was applied prior to each test to ensure perfect contact between the loading piston, the top porous stone and the top of the CPB sample. Third, a polycarbonate round tube (Perspex mould) with a wall thickness of 1/4" was employed as a solid CPB sample container. The sidewall of Perspex mould is lightly lubricated with a thin coat of silicone grease to reduce sidewall friction resistance.

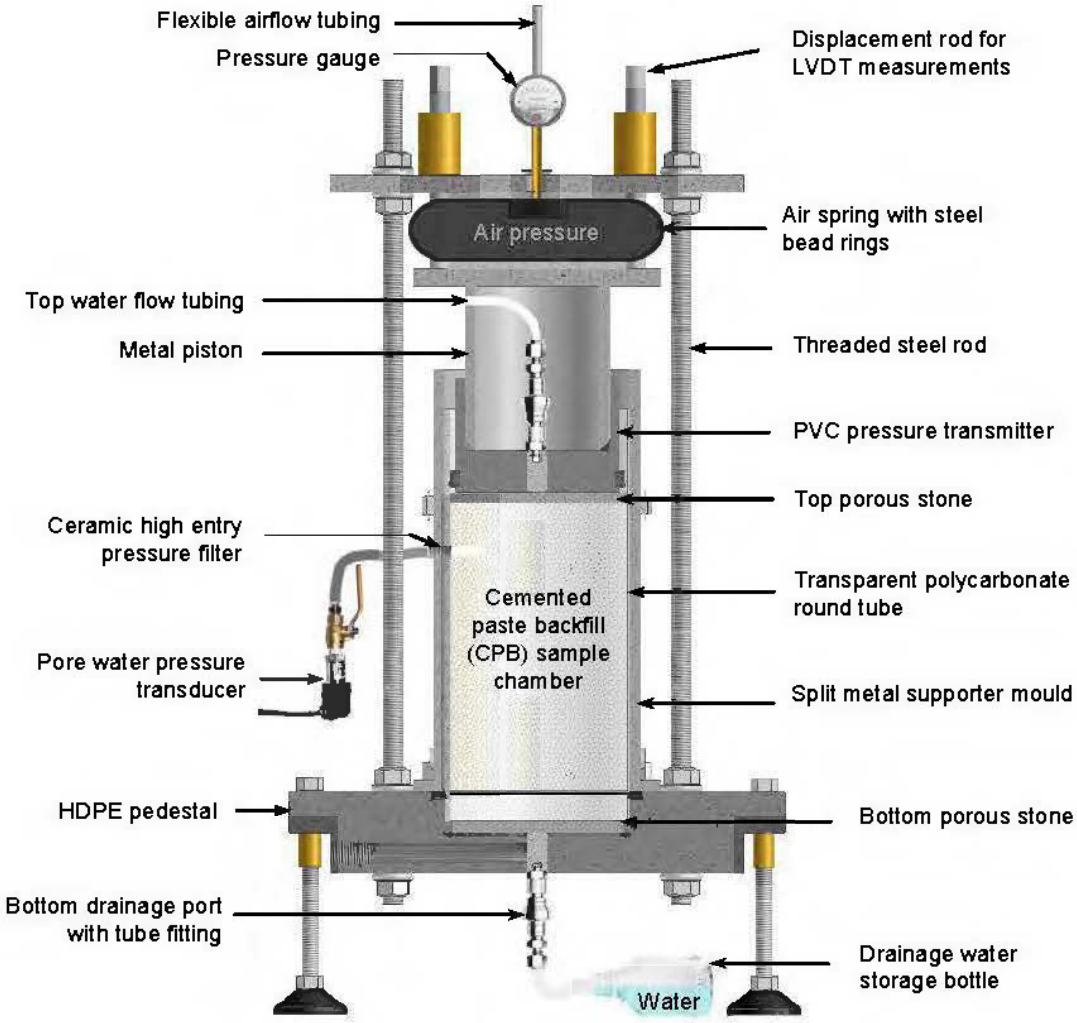

Figure 3.1 Schematic diagram of improved CUAPS (adapted from Benzaazoua et al. 2006).

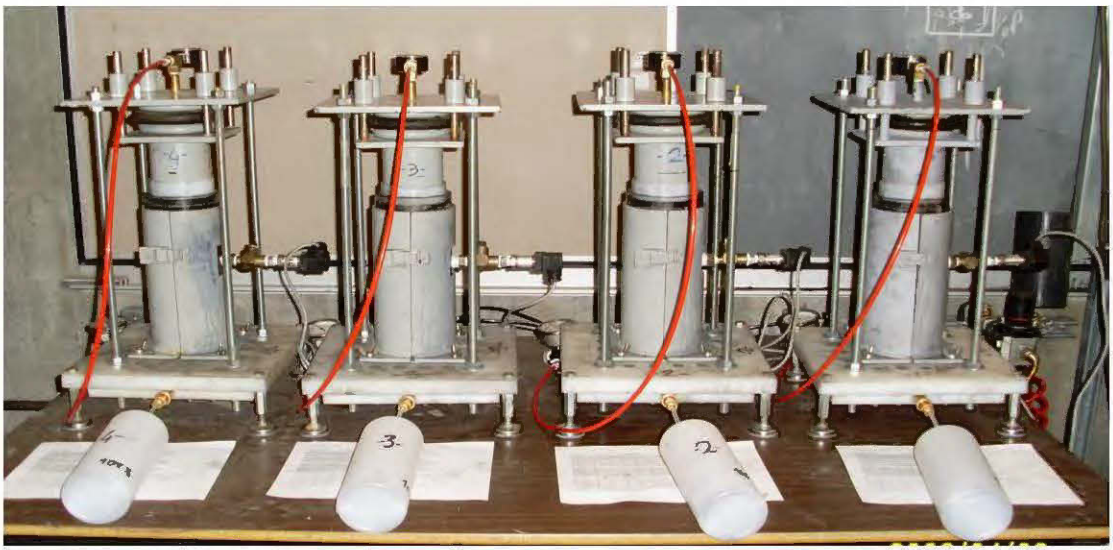

Figure 3.2 Photograph of modified CUAPS consolidation tests in progress. Permeability tests are conducted on one-dimensionally consolidated CPB samples (falling head method).

3.2.2.2 Perspex mould

To enable visual observation and prevent metal oxidation, the sample container is made of Perspex (clear polycarbonate). The container is also used for the consolidation tests to accurately measure initial sample height H_0. The CUAPS apparatus was modified to fit two different mould sizes [$D \times H$ = 101.6 × 101.6 mm (4" × 4") and 101.6 × 203.2 mm (4" × 8")]. In conventional consolidometers, the diameter-to-height ratio (D/H) is usually from 1.5 to 3. The D/H ratio of 1 is used for conventional consolidation, whereas D/H = 0.5 is used for silty materials such as CPB studied in the literature (Qui and Sego, 2001; le Roux, 2004). Despite this low D/H ratio, the calculated Perspex tube friction factor λ using Taylor's formula (Taylor, 1942), assuming a Poisson's ratio ν = 0.2 for CPB (Helinski et al., 2007b) and a coefficient of friction μ = 0.2–0.3 for concrete/plastic (Gorst et al., 2003), ranges from 0.75 to 0.82, compared to the recommended factor λ of 0.95–0.98. Therefore, the Perspex tube friction factor λ is considered acceptable, knowing that a thin coat of silicon grease is applied inside the tube to further reduce friction between backfill and Perspex. Moreover, λ is known

to increase with increasing consolidation pressure. To meet at-rest condition (i.e., no lateral deformation or K_0 consolidation), which is the more realistic in situ condition, the transparent Perspex tube should not deform significantly during the consolidation test. By considering the polycarbonate properties and an applied pressure range of 50–800 kPa, the calculation using the analytical equation shows that for the maximum allowed pressure of 600 kPa in the CUAPS, the lateral strain ε_r was 0.99% (lateral deformation = 0.53 mm). This observation was also verified numerically using the ABAQUS code, which gives almost the same average ε_r (0.98%) as the analytical solution. This confirms that the lateral deformation of the Perspex mould induced by a maximum pressure of 600 kPa is considered negligible ($\varepsilon_r < 1\%$), and that the K_0 condition is therefore met when the 1-D compression stresses are applied. Table 3.1 presents a comparison of analytical and numerical calculations of the lateral mould deformation under applied pressure.

Table 3.1 Analytical and numerical calculations for lateral mould deformation

Applied pressure p_v (kPa)	Calculated horizontal stress σ_h (kPa)	Hoop stress σ_θ (MPa)	Lateral deformation δ_r (mm)		Lateral strain ε_r (%)	
			Analytical	Numerical	Analytical	Numerical
50	21.3	0.18	0.04	–	0.08	–
200	85.3	0.72	0.18	–	0.33	–
375	159.9	1.36	0.33	–	0.62	–
400	170.6	1.45	0.35	0.35	0.66	0.65
600	255.9	2.17	0.53	0.53	0.99	0.98
800	–	–	0.71	0.69	1.31	1.27

3.2.2.3 Vertical displacement measurement

Displacements of the top rigid loading plate are measured using a linear variable displacement transducer (LVDT, Solartron Model AX/1/S). A total of four LVDTs are included in each CUAPS apparatus to monitor the vertical deformation of the sample with increasing pressure. The LVDTs have a gauge length of 40 mm and are accurate to within

0.001 mm. The average calibration curve of the LVDT measurement is presented in Figure 3.3, showing a perfect coefficient of correlation $r = 1$.

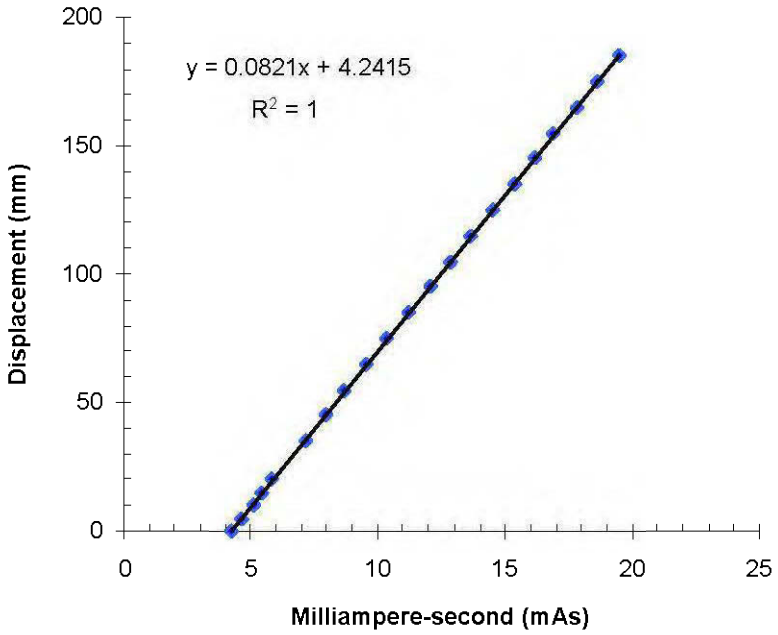

Figure 3.3 Linear variable displacement transducer (LVDT) calibration test curve.

3.2.2.4 Pore water pressure (PWP) measurement

Pore pressure is measured using PWP transducers (HOSKIN, model E13-5-4-B20R-25) having a pressure range of 0–600 kPa with an accuracy of ±0.25%. The PWP transducers are equipped with a ceramic high entry pressure filter having a saturated hydraulic conductivity of about 10^{-5} cm/s. The ceramic filter was chosen over a metallic filter to avoid potential corrosion. Each PWP transducer is mounted directly on the upper side of the Perspex mould (Figure 3.1). PWP transducers are calibrated by filling the Perspex tube with water and applying a normal pressure of 0–200 kPa. Figure 3.4 shows the calibration equations and the coefficient of correlation obtained ($r = 0.99$).

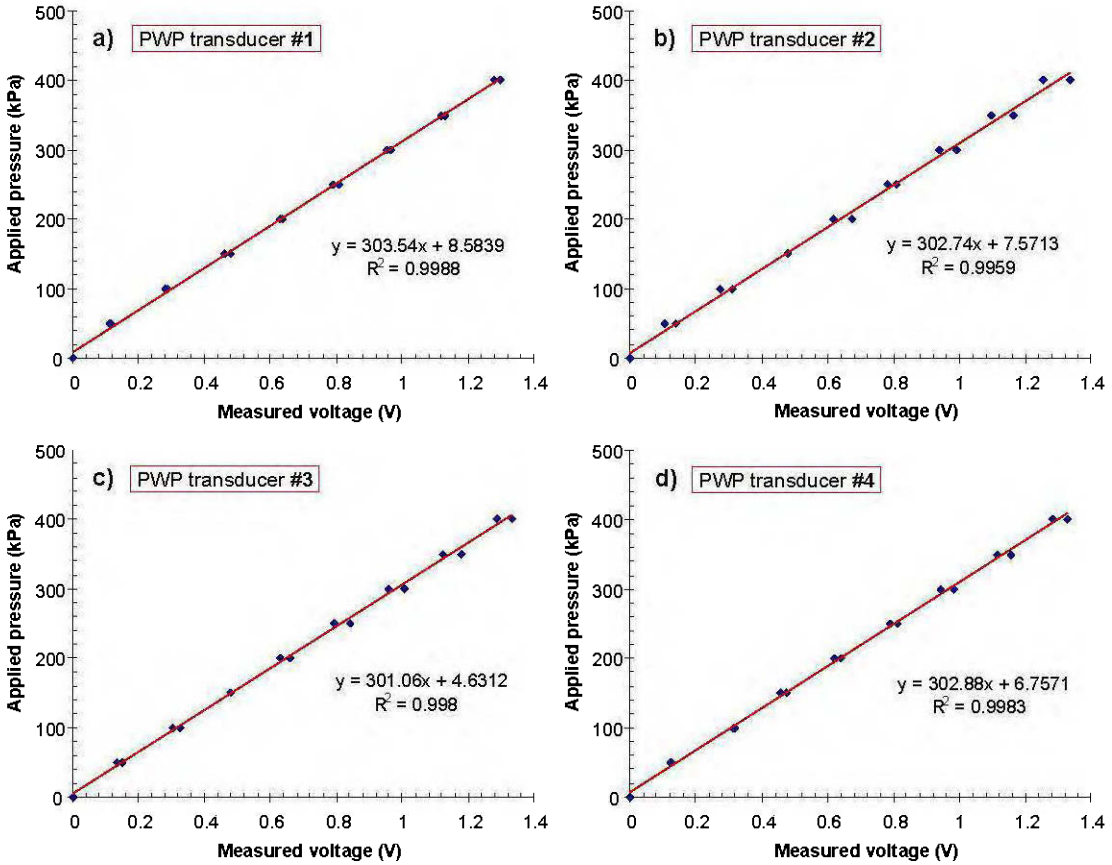

Figure 3.4 PWP transducer calibration curves for the four different transducers.

3.2.2.5 Drainage port system and permeability tests

The CUAPS was modified slightly to allow conducting permeability tests on CPB specimens before or after consolidation (see Figure 3.1). Saturated hydraulic conductivity k_{sat} is a key parameter for understanding water movement and consolidation in CPB samples from underground stopes. To prevent uncontrolled water loss, the free drainage system port is plugged with a Swagelok® tube fitting. When the one-dimensional consolidation tests are performed, the top drainage port valve is kept closed (no tube fitted) and the drainage tube is fitted with a tube. This tube is simply placed into a bottle under atmospheric pressure to allow drainage as pressure is applied to the top of sample (one-way drainage). In this study, no back

pressure was applied to either force drainage or to ensure sample saturation by measuring Skempton's pore pressure parameter B. Because the samples were initially fully saturated, it was assumed that they were almost saturated during testing (proportional to void ratio change). When rigid wall permeability tests were performed, the top and bottom drainage port valves were kept open and a back pressure was applied to the base of the sample to ensure saturation. Depending on the binder content (0 – control or 4.5 wt%) and curing time (0–7 days), the back pressure varied between 35 kPa and 100 kPa, which generated $B \approx 0.9$ and $S_r > 95\%$. The back pressure was used only to increase the hydraulic gradient to meet Darcy's law (constant volume condition), and was halted at the start of the permeability measurements. Porous stones 12.7 mm thick are also placed above and below each CPB sample to facilitate drainage during the consolidation test and to prevent solid loss.

3.3 EXPERIMENTAL VALIDATION

The CUAPS apparatus was assessed by conducting 1-D consolidation tests with and without pore water pressure (PWP) measurement, saturated hydraulic conductivity tests, and CPB specimen curing under constant or variable vertical pressure testing. Uniaxial compression tests were performed on CPB samples after each series of laboratory tests.

3.3.1 Materials, specimen preparation and curing

The materials used to assess the modified CUAPS are mine tailings (control samples with zero binder content) and CPB material prepared from tailings. Grain size distribution (GSD) of the homogenized tailings sample was determined using a Malvern Mastersizer S 2000® laser particle analyzer. Figure 3.5 presents the GSD curve of the tailings sample compared to typical Canadian hard rock mine GSD curves (Ouellet, 2006). The GSD analysis showed that approximately 44% of the mine tailings sample is finer than 20 µm, with only 4.7% clay-sized particles (< 2 µm). Most of the GSD falls into medium to fine sand and silt-sized grains. From the GSD curve, the coefficients of uniformity C_U (= D_{60}/D_{10}) and curvature C_C (= $D_{30}^2/D_{60}\times D_{10}$) are 7.9 and 1, respectively (the tailings being classified as well-graded).

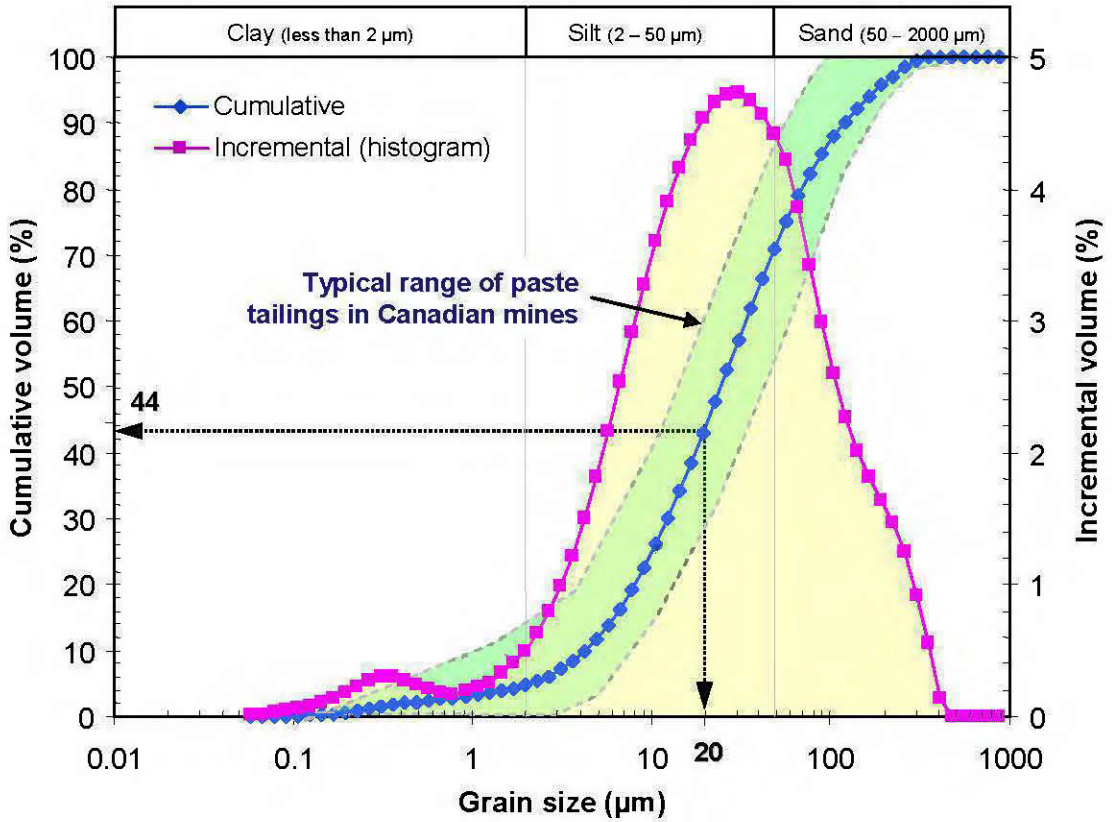

Figure 3.5 Grain size distribution (GSD) curves of the mine tailings sample used.

Table 2 also summarizes the geotechnical properties of the tailings used. The experimental results show that the tailings sample has a specific gravity of 3.71, a gas adsorption isotherm (Brunauer-Emmett-Teller or BET method) specific surface area of 2.17 m^2/g, a liquid limit of 23% and a plastic limit of 18%. The results of the grain-size analysis indicate that the tailings sample contains only 4.7% clay-sized particles. Most of the GSD falls into the silt to fine sand range. According to the Unified Soil Classification System (USCS; e.g., McCarthy, 2007), the tested mine tailings sample can be classified as low plastic silt (ML). Further details on physicochemical and mineralogical properties of the tested mine tailings can be found in Yilmaz (2010).

Table 3.2 Summary of tailings geotechnical properties

Element (unit)	Value
Gravimetric water content w (%)	23.45
Specific gravity G_s	3.71
Specific surface area S_s (m^2/g)	2.17
Clay size particles (< 2μm; %)	4.7
Silt size particles (2–50 μm; %)	66.13
Sand size particles (50–2000 μm; %)	29.18
Fines content (< 20 μm; %)	43.87
D_{10} (effective particle size; μm)	4.26
Coefficient of uniformity	7.88
Coefficient of curvature	1.04

Various CPB mixes were prepared by thoroughly mixing the tailings, binding agent and water for about 7 minutes in a concrete mixer with a double spiral. The binding agent was a blend of 20 wt% general use or type I Portland cement (PCI) and 80 wt% blast furnace slag (Slag). A single binder content of 4.5 wt% was tested (named PCI-Slag@4.5 wt%). After mixing, CPB materials were cast in both conventional moulds ($D \times H$ = 101.6 × 203.2 mm = 4" × 8") and lubricated Perspex moulds in three layers and each layer was puddled 25 times using a steel rod. The Perspex moulds were lubricated with silicon grease to facilitate extrusion without deteriorating the CPB sample after curing. Paste backfill samples were prepared and cured at different curing times in a controlled humidity chamber set at constant 24°C and 80% relative humidity (RH), mimicking underground mine curing conditions for CPB-filled stopes. The CPB material had a stable initial gravimetric water content of 28.2 wt%, which corresponds to a slump varying from 8" to 9". The resultant bulk (or wet) unit weight γ_{wet} of fresh CPB material was 22.7 kN/m^3.

3.3.2 Experimental procedures

Five types of tests were performed to assess and validate the modified CUAPS apparatus. All tests are summarized in Table 3.3.

Table 3.3 Summary of laboratory tests performed

Test type	Objective	Number of tests
1-D consolidation tests	Determine consolidation properties	16
Post-consolidation saturated hydraulic conductivity (k_{sat}) tests	Determine the evolution of k_{sat} with curing time	8
1-D consolidation tests with pore water pressure (PWP) dissipation measurements	Determine pore water pressure and consolidation properties	8
Curing under applied pressure test	Perform curing process of CPB samples under pressure	3
Unconfined compression tests	Determine mechanical strength properties	21
Compression rate tests	Simulate in situ paste backfill properties and conditions	9

3.3.2.1 One-dimensional consolidation tests

Procedures inspired by ASTM standards D2435 and D4186 were used to determine the magnitude and consolidation rate of CPB samples restrained laterally and drained axially while subjected to incremental applied controlled-stress loading.

The ASTM standard recommends that this test method be performed with constant load increment duration of 24 h. However, owing to the combined effects of the silty nature of the CPB material and the hardening process that occurred during curing, preliminary test results showed that the most appropriate load increment duration would be 2 h. Immediately after the samples were placed into the consolidometer, a seating pressure of 15 kPa was applied to the samples to eliminate sidewall friction between the loading piston and Perspex mould, and hence ensure a uniform pressure distribution on CPB sample. A pressure load sequence of 25, 50, 100, 200 and 400 kPa was then applied at a load increment ratio (LIR) of 1. Each pressure increment was maintained until near equilibrium (most often reached within 2 h).

Vertical displacement was recorded at time intervals of 2, 4, 6, 8 and 10 hours. Each sample was loaded to a maximum of 400 kPa and later unloaded, again at LIR equal to 1. A HOBO® datalogger, model U12 (from Onset® Computer Corporation, USA) was used to automatically record test data. Two sample sizes (D/H ratios of 0.5 and 1) and four curing times (0, 1, 3 and

7 days) were investigated. Curing times (short-term) were selected based on the hardening process of fresh CPB samples. Beyond the 7-day curing time, no drainage water was observed, similar to the behaviour observed by Belem et al. (2002; 2006), Benzaazoua et al. (2004), and Yilmaz et al. (2009a, b). Note that the incremental pressure sequence was applied to the CPB immediately after these curing times.

3.3.2.2 Saturated hydraulic conductivity tests

Saturated hydraulic conductivity or permeability k_{sat} tests were performed on samples submitted to one-dimensional consolidation tests in accordance with ASTM D5856 test procedure using the falling head method (see Figure 3.2). Distilled water was pumped to the top of CPB sample (upward flow) at a constant flow rate while a constant applied pressure was maintained at the base of the CUAPS apparatus.

In this study, the ratio of low hydraulic gradient ($i = (h_1\text{-}h_2) / L$, where i is the hydraulic gradient, h_1 and h_2 are the differential head loss, and L is the sample height) was relatively constant at 0.1.Two different sample types, control samples (tailings without binder) and 4.5 wt% binder CPB samples (PCI-Slag@20:80 wt%), were tested at curing times of 0, 1, 3 and 7 days. The k_{sat} tests were conducted in a relatively short period of time (approximately less than 2.5 hours). At least two tests were carried out on the consolidated CPB samples for each mixture and curing time to assess the repeatability of the k_{sat} tests.

3.3.2.3 Consolidation with PWP measurement

During the one-dimensional consolidation tests, pore water pressure (PWP) measurements were also performed. After each consolidation step, PWP data were recorded for each curing time (0, 1, 3, and 7 days) and measurements were converted into kPa units using the calibration equations obtained from the tailings samples, as given in Figure 3.4. PWP values were used to calculate the equivalent coefficients of consolidation c_v, which can be used to back-calculate k_{sat} values for laboratory-tested samples.

3.3.2.4 Curing under applied pressure tests

These tests were run to simulate the mechanical behaviour of in situ stope CPB samples and compare it to of CPB samples in standard laboratory conditions. Three CUAPS setups were filled with freshly prepared CPB material. For the first half an hour, no pressure was applied to the sample, with pressure gradually increased thereafter up to 400 kPa for a total duration of 35 h. Average compression rate was 11.4 kPa/h, for a filling rate of 0.5 m/h. The final applied pressure of 400 kPa corresponds to an equivalent overburden of 17.6 m in height of CPB in an underground stope. Each CUAPS sample was left to cure under the final pressure of 400 kPa for relatively short-term curing times (7, 14 and 28 days), chosen arbitrarily.

3.3.2.5 In situ backfill properties simulation

These tests aimed to better simulate the effect of different stope filling rates and backfill heights on the resultant strength properties of CPB. This scenario considers the backfilling of four different underground stopes at different heights h of 5, 10, 15 and 20 m for a total duration of 50 h, corresponding to a compression rate sequence c_f of 2.3, 4.5, 6.8 and 9.1 kPa/h. Table 3.4 lists the calculations of the equivalent overburdens $p_v = \gamma_{wet}h$ (kPa) and corresponding CPB filling rate r_f (m/h) (assuming no arching effect). Each sample was then left to cure for 7, 14 and 28 days under final overburden pressures of 113.5, 227, 340.5 and 454 kPa which correspond to the stope heights h of 5, 10, 15 and 20 m, respectively.

Table 3.4 Summary of compression rates used for CUAPS-consolidated samples

Backfill height in the stope h (m)	Equivalent overburden stress* p_v (kPa)	Equivalent filling rate** r_f (m/h)	Equivalent compression rate c_f (kPa/h)
5	113.5	0.1	2.27
10	227.0	0.2	4.54
15	340.5	0.3	6.81
20	454.0	0.4	9.08

*The wet unit weight of CPB is $\gamma_{wet} = 22.7$ kN/m^3
**for a total time period of 50 hours

3.3.2.6 Uniaxial compression tests

Following the prescribed curing times of 7, 14 and 28 days, the consolidated CPB samples were extruded from the clear polycarbonate Perspex mould (Figure 3.6a) using an adequate manual push sample extruder (Figure 3.6b). The two ends of the Perspex mould filled with backfill samples were open and the two porous discs were placed at these ends (Figure 3.6c). After the backfill cylinder faces were rectified in order to provide a flat surface, CPB samples were measured for length and weight and then subjected to uniaxial compression tests in order to determine the mechanical strength gain.

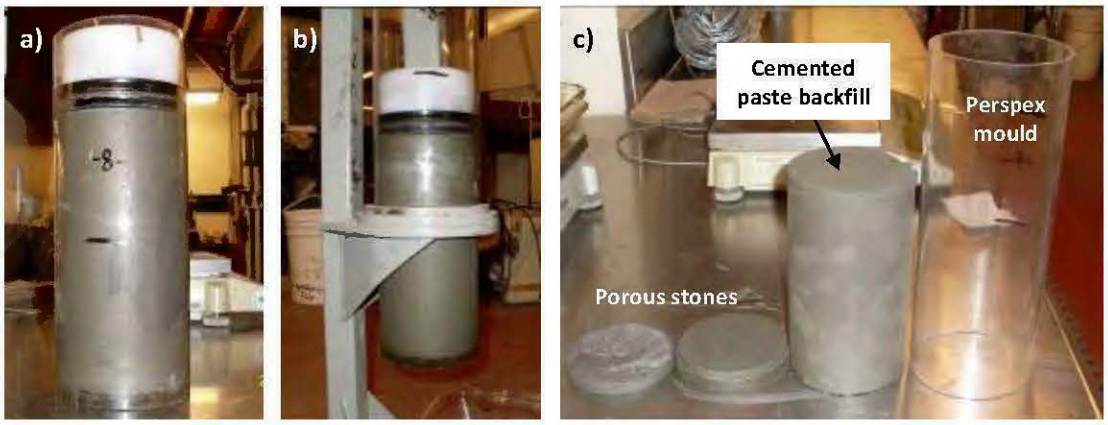

Figure 3.6 Photos of (a) a Perspex cylinder filled with backfill material, showing loading piston and bottom and top porous discs; (b) the manual push CPB sample extruder; and (c) the extruded CPB sample ready for UCS testing.

The UCS tests were performed using a computer-controlled mechanical press (MTS Sintech 10/GL load frame) with a load capacity of 50 kN and a displacement speed of 1 mm per minute. Axial deformations were digitally recorded by a real-time data acquisition system. The observed UCS value corresponds to the maximum stress (failure peak) reached during the compression test.

3.4 RESULTS AND DISCUSSION

3.4.1 One-dimensional consolidation of CPB samples

Loading pressure increments that correspond to typical in situ CPB conditions were applied after curing for 0, 1, 3 and 7 days. Some consolidation parameters such as initial void ratio e_0 (i.e., the void ratio during cementation at the end of curing times: 0, 1, 3 and 7 days), compression index C_c, recompression index C_r and the coefficient of consolidation c_v are listed in Table 3.5 as well as Appendices B and D. The compressibility of porous materials such as CPB is significantly affected by e_0, which is related to sample placement and compaction method as well as in situ overburden pressure.

Table 3.5 Summary of consolidation test results for tailings and backfill samples

Initial void ratio, e_0	Compression index, C_c	Recompression index, C_r	Coefficient of consolidation, c_v (cm^2/s)	References
*Mine tailings samples**				
2.3–1.64	0.308–0.75	0.037	$0.15–2\times10^{-3}$	Stone et al. 1994
0.56–0.8	0.05–0.13	0.003–0.01	$2.8–5\times10^{-3}$	Aubertin et al. 1996
0.76–0.64	0.02–0.18	0.002–0.012	$2.68–3.62\times10^{-3}$	Morris et al. 2000
0.5–1.6	0.083–0.156	—	$4.3\times10^{-3}–2.6\times10^{-2}$	Qui and Sego 2001
0.5–0.95	0.038–0.132	0.017–0.026	3.5×10^{-3}	Crowder 2004
0.5–1.6	0.005–0.3	0.003–0.03	$1\times10^{-1}–1\times10^{-3}$	Bussière 2007
0.96–1.05	0.33–0.49	0.004–0.008	7.9×10^{-2}	Present study
*Cemented paste backfills***				
1.1–1.4	0.05–0.34	—	1.6-4.8	Pierce 1997
0.85–1.1	0.064–0.25	0.02	0.2–5	le Roux 2005
0.99–1.2	0.05–0.45	0.0027–0.006	$1.5\times10^{-2}–8.5\times10^{-2}$	Present study

*Only hard rock mine tailings classified as ML are shown in this evaluation;
**The range of binder content was from 3 to 7 wt% and the curing time varies from 7 to 112 days.

Values in Table 3.5 are in the same range as those reported for similar hard rock mine tailings samples (Stone et al., 1994; Aubertin et al., 1996; Morris et al., 2000; Qui and Sego, 2001; Crowder, 2004; Bussière, 2007). Results also compare fairly well with those obtained on the CPB samples with similar GSD (Pierce, 1997; le Roux, 2004). It should be mentioned that a

slight difference in initial void ratio e_0 was observed, which was probably generated during paste backfill pouring into the CUAPS apparatus (different initial packing). It was then decided to present modified compression curves using normalized void ratio e/e_0 to eliminate the variation in initial void ratio e_0, as originally suggested by Kassim and Huey (2000). Figure 3.6 presents the evolution of the normalized void ratio e/e_0 with effective vertical stress (σ'_v) for CPB prepared with 4.5 wt% of binder type PCI-Slag@20:80 wt% at different curing times (0, 1, 3, and 7 days) compared to uncemented tailings (control sample). The two different D/H ratios of 0.5 and 1 are evaluated. The tested samples show similar behaviour regardless of aspect ratio D/H. The observed reduction in normalized void ratio can be attributed to the particle re-arrangement process at the early stage of compression (removal of water leads to increased density or a decrease in voids within the sample) followed by the gradual weakening of cement bonds that were previously formed or were being formed due to applied pressure. However, the cementation process was not measured directly.

Figure 3.6 shows that the virgin compression line VCL slope (corresponding to the modified compression index C_{cm}) almost always starts at a corresponding σ'_v = 50 kPa for aspect ratio D/H of 0.5 (Figure 3.7a), and that this value changes with curing time (from approximately 49 to 102 kPa) for D/H = 1 (Figure 3.7b). The observed horizontal portion of the loading curves in Figure 3.7a is attributed to the greater stiffness ("initial resistance" to consolidation) observed with D/H = 0.5, because no deformation is generated due to σ'_v = 50 kPa. Beyond this stress value it is assumed that the cement bonds begin to destruct. It therefore appears that the CPB stiffness response to compression was better captured with D/H = 1 due to the scale effect. However, the effect of binder addition on CPB compression behaviour can be seen in the variation of normalized void ratio, more specifically in the modified compression index C_{cm} (VCL slopes) for the different curing times. Indeed, from Figs. 3.7a and 3.7b show that the VCL slope flattens with increasing curing time (or stiffness due to hardening). We also see that the modified compression index C_{cm} decreases (from its initial value obtained with uncemented tailings) with increased curing time (dotted arrows). As cement hydration progresses, the particles in the CPB may be partially locked in place by cement bonds, which resist further consolidation (flattening of VCL with increased curing time).

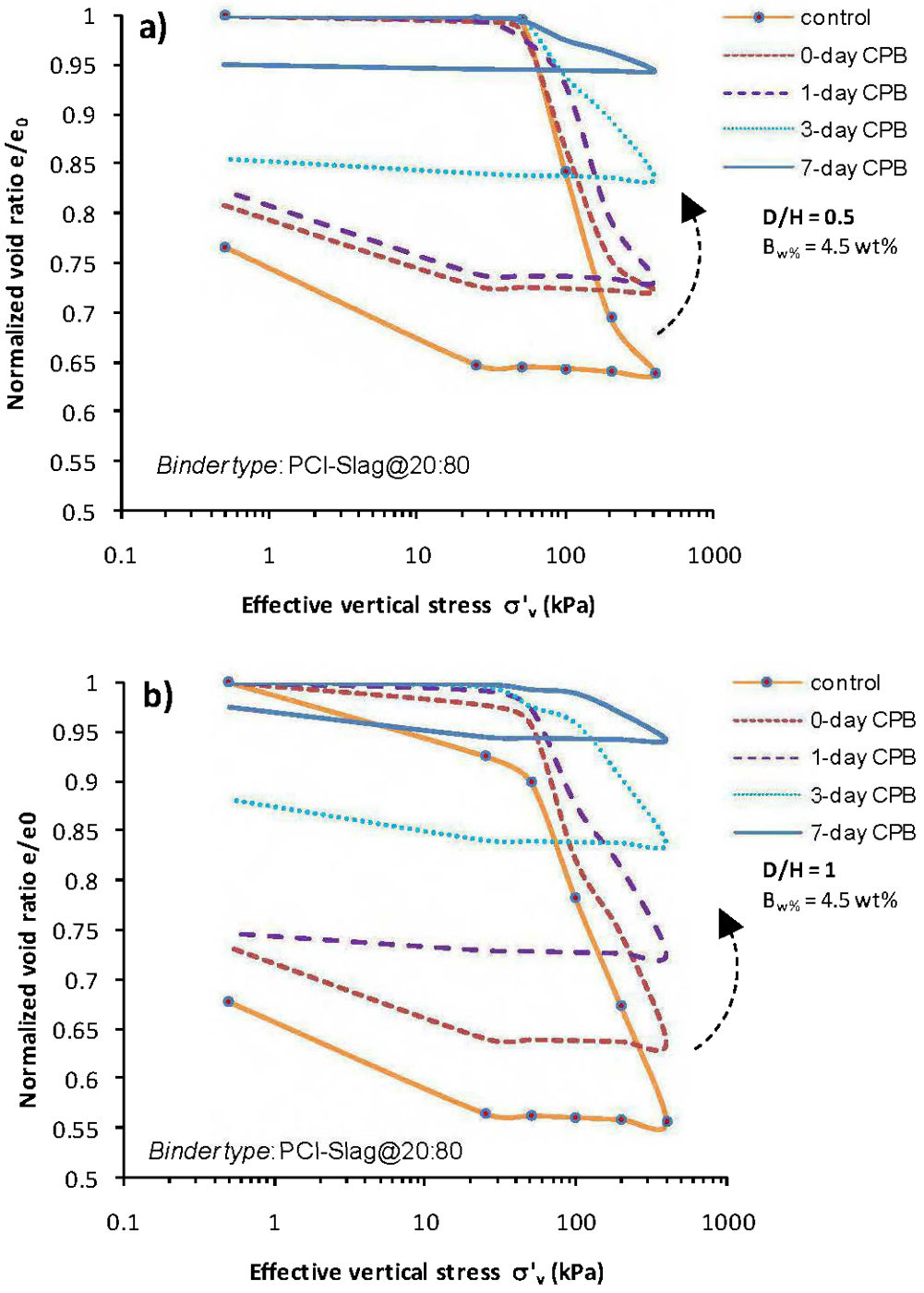

Figure 3.7 Typical normalized one-dimensional compression curves on CPB samples prepared with binder type PCI-Slag@20:80 wt% at 4.5 wt% for four different curing times and two diameter-to-height (D/H) ratios: (a) D/H of 0.5 and (b) D/H of 1.

These results show that the modified CUAPS apparatus captures the effect of binder amount on consolidation properties of cemented backfills such as CPB. From the experimental results, it appears that the most appropriate aspect ratio D/H would be 1 rather than 0.5, where a scale (along with a potential frictional resistance) effect on stiffness behaviour was observed due to the initial height of the sample.

3.4.2 One-dimensional consolidation with PWP measurement

It is critical to understand PWP (or u_w) behaviour when assessing CPB stability, particularly for designing barricades. The degree of PWP dissipation is closely related to factors such as chemical shrinkage, sometimes referred to as self-desiccation (Helinski et al., 2007b; Simms and Grabinsky, 2009), water volume consumption (mainly due to cement hydration) and CPB drainage conditions. However, insofar as the binder hydration (and hence the CPB hardening) was considered during the compression, it was decided to perform this test on an uncemented tailings sample only. Accordingly, sample saturation was expected to be slightly reduced from its initial condition due to water consumption by binder hydration at early ages. Note that immediately after mixing and pouring into the Perspex mould, the uncemented tailings specimen was fully saturated, because no drainage was allowed. However, when vertical pressure increments are applied to a sample in CUAPS cell, where the drainage valve is open, part of the water is drained. By assuming that the volume of drainage water is equivalent to the void ratio change, it can be assumed that the sample remained saturated (although no specific measurements were made, such as pore pressure parameter B).

Figure 3.8 presents typical excess PWP dissipation curves for control (uncemented tailings) samples at very early curing times (0, 1, 3 and 7 days). PWP values were recorded at 5.1 cm from the top of the Perspex mould and following the previous incremental pressure loading sequence of 25, 50, 100, 200 and 400 kPa. From this figure it can be seen that no PWP dissipation was recorded by PWP transducer for the first two pressure (total stress) increments of 25 and 50 kPa (first 240 minutes), although tailings sample underwent deformation. This is presumably explained by the fact that the drainage valve should have been closed during the incremental loading process, but was unfortunately left open by error.

For this reason, the instantaneously recorded u_w is lower ($u_w < \sigma_v$) than that it would have been if the drainage valve had been closed ($u_w = \sigma_v$). Overall, u_w dissipation takes almost one hour to return to equilibrium. This was confirmed by the total duration of the water discharge from the CPB samples. Recall that PWP is proportional to the rate of settlement, which is a function of initial water content (28.2 wt%) and the rate of effective stress.

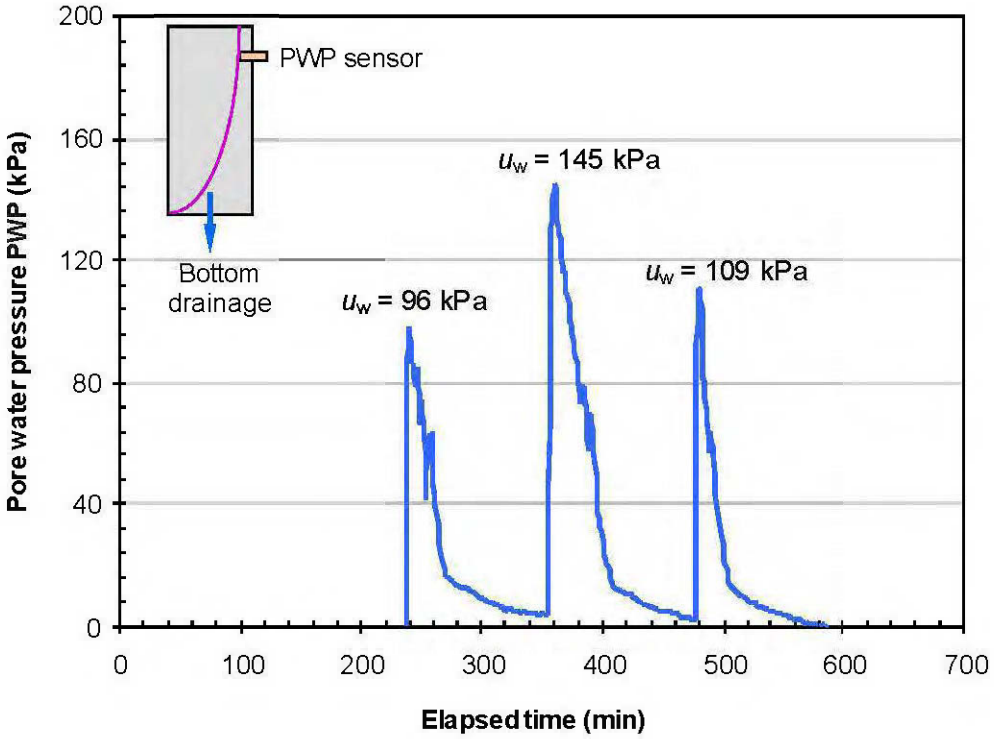

Figure 3.8 Pore water pressure vs elapsed time for uncemented tailings (control sample).

Figure 3.8 also shows that the excess PWP recorded immediately after the applied pressure increment (peak u_w values shown in the figure) is a certain percentage of this incremental pressure $p_v = \sigma_v$. The percentage is 96% for p_v = 100 kPa, 72.5% for p_v = 200 kPa and 27.3% for p_v = 400 kPa. The corresponding decrease percentages are 4, 27.5 and 72.8% for p_v = 100, 200 and 400 kPa, respectively. This gradual decrease after the application of three successive p_v can be explained largely by water drainage. However, as mentioned previously, the

drainage valve was unfortunately left open by error during the loading process. A second possible contributing factor to the apparent drop in peak PWP would be the sampling time interval (every 75 seconds), which was probably too large to systematically record peak u_w. Nevertheless, similar behaviour (in soils) has been reported in the literature (Chakrabarti and Horvath, 1986).

3.4.3 Saturated hydraulic conductivity of cemented paste backfill

The saturated hydraulic conductivity k_{sat} values of CPB and control (uncemented mine tailings) samples were determined directly from permeability measurements according to ASTM D2435. Figure 3.9 shows the evolution of the k_{sat} value as a function of curing time (0, 1, 3 and 7 days) for both uncemented tailings (control) and CPB (4.5 wt% binder) samples.

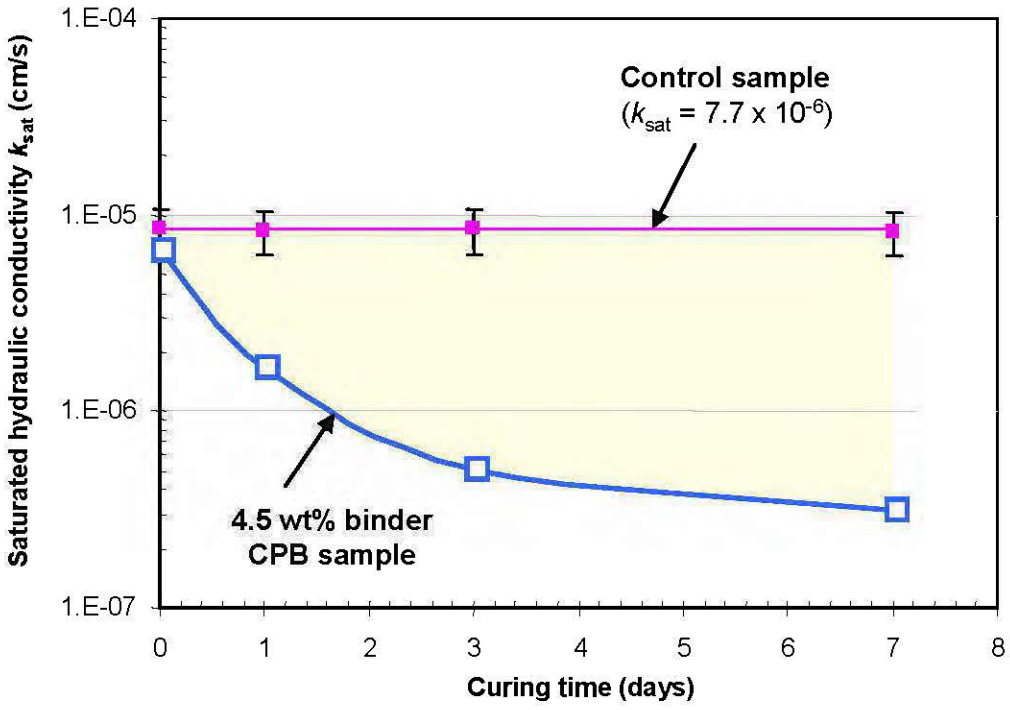

Figure 3.9 Evolution of saturated hydraulic conductivity k_{sat} with curing time for CUAPS-consolidated uncemented tailings (control) and CPB (4.5 wt% binder content) samples.

Results show a nearly constant k_{sat} (7.7×10^{-6} cm/s) for control samples with curing time, considering the precision associated with the k_{sat} test, which is typically half an order of magnitude (see Chapuis, 2004). These results are validated by the typical range (from 10^{-5} cm/s to 10^{-7} cm/s) of k_{sat} for compacted and consolidated tailings (classified as ML) reported in the literature (Aubertin et al., 1996; Qiu and Sego, 2001; Bussière, 2007). Moreover, with the addition of 4.5 wt% binder, k_{sat} decreased rapidly during the first 3 days of curing, from 6.6×10^{-6} cm/s to approximately 5.1×10^{-7} cm/s (a decrease of nearly one order of magnitude). After 7 days of curing time, k_{sat} continued to decrease to 3.1×10^{-7} cm/s, a major change of nearly 100%. It is noteworthy that similar k_{sat} evolutions were observed by Godbout et al. (2007) in CPB samples prepared with a similar binder type and content and for similar curing ages. However, those samples were not consolidated under incremental pressure loadings during curing, unlike the CPB samples tested in the present study. The results of this study show that the modified CUAPS apparatus effectively captures the evolution of k_{sat} with curing time for both uncemented tailings (control samples) and cemented backfills.

3.4.4 Compressive strength investigation in CUAPS-consolidated samples

Figure 3.10 shows that the consolidated CPB samples have higher UCS (compared to standard non-drained moulds) for all curing times tested. Similar behaviour was observed by Yilmaz et al. (2009a, b) using the CUAPS apparatus. For early-age curing (7 days), the consolidated samples show a UCS of 1506 kPa, which is 46.6% and 52.3% higher than those obtained on both drained and undrained CPBs (803.6 kPa and 718.4 kPa, respectively). For the CUAPS-consolidated CPB samples, relatively high UCS of about 2856 kPa and 3087 kPa were obtained after curing times of 14 days and 28 days, respectively. Corresponding UCS was 1621 kPa (14 days) and 2196 kPa (28 days) for drained mould samples, and 1307 kPa (14 days) and 1486 kPa (28 days) for undrained mould samples. Because it is common practice to obtain UCS values from plastic mould (drained or undrained) CPB samples, we initially considered a relationship that would allow predicting, as a first approximation, UCS accounting for the effect of curing under applied pressure. However, at this stage of our knowledge, it appeared more appropriate to propose an empirical model for predicting UCS_{cuaps} from known UCS_{mould} (drained or undrained mould backfills).

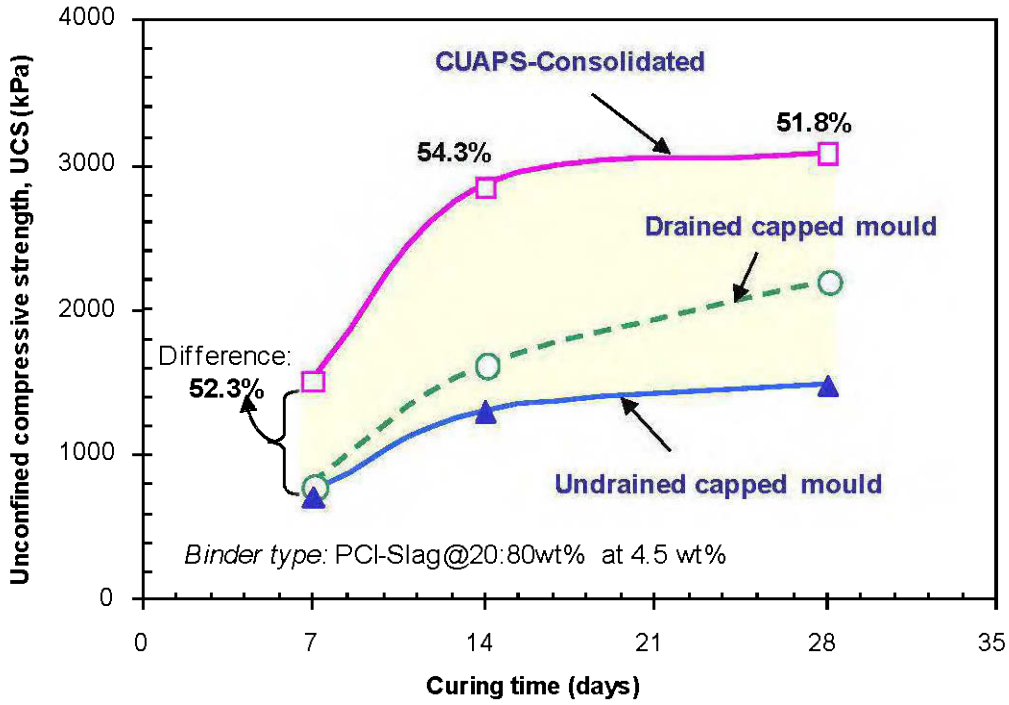

Figure 3.10 Comparison of compressive strengths obtained on 4.5 wt% CUAPS-consolidated CPB samples, drained and undrained CPB samples.

Figure 3.11a presents a plot of the differential strength UCS_{cuaps} against UCS_{mould}, showing no exploitable correlation. Before performing a regression analysis to determine an empirical relationship, a master-curve must be obtained from Figure 3.11a through a variable change by normalizing UCS_{cuaps} and UCS_{mould} while keeping units consistent. First, we defined a normalized time factor $t^* = t \times B_w / t_{min}$, or the combination of curing time and binder content effects, where t is curing time (day), t_{min} is a minimum curing time arbitrarily taken as equal to 1 day and B_w is the fractional binder content (percentage of binder divided by 100).

Second, we defined the normalization parameters $a_{c1} = p_a \times (t^*)^6$ (for the dependent variable UCS_{mould}, i.e., UCS_{mould}/a_{c1}) and $a_{c2} = p_v \times (t^*)^6$ (for the independent variable UCS_{cuaps}, i.e., UCS_{cuaps}/a_{c2}), where p_a is the atmospheric pressure (= 101 kPa) and p_v is the applied vertical pressure or effective stress (in kPa). The final variable change was $X = (UCS_{mould}/a_{c1})^{1/8}$ and $Y = Ln(UCS_{cuaps}/a_{c2})$, where the exponents 6 (in a_{c1} and a_{c2}) and 1/8 and the natural logarithm

were chosen to obtain the best possible fitting. Figure 3.11b presents the variable Y plotted against variable X, showing good correlation between normalized UCS_{pv} and UCS_{mould}. The data in Figure 3.11b are well fitted with a logarithm function (r^2 = 0.9967), as follows:

$$Y = a + bLn(X) \tag{3.1}$$

where a and b are fitting parameters.

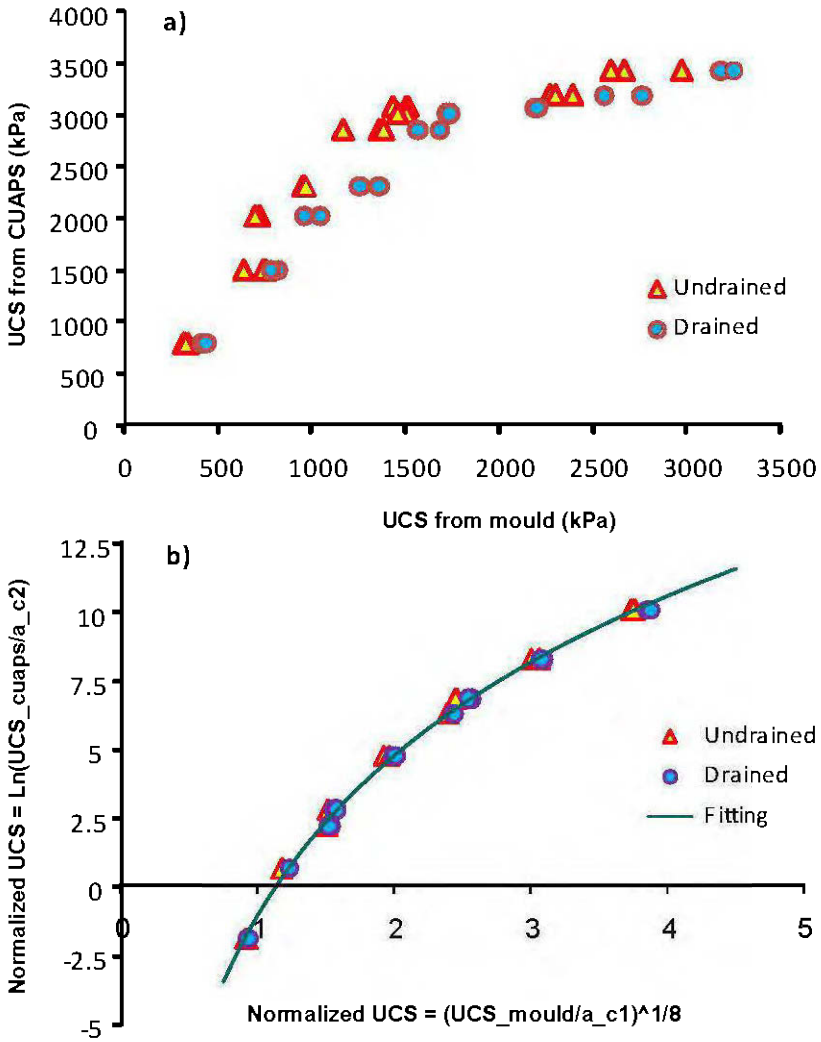

Figure 3.11 Variation in UCS_{cuaps} with UCS obtained from mould samples: a) direct relationship; b) normalized variables.

Replacing the variables X and Y with their expression into Eq. (3.1) and rearranging yields the proposed general empirical model for predicting the equivalent CUAPS-consolidated CPB sample strength (UCS_{cuaps}) from known drained or undrained plastic mould sample strength (UCS_{mould}), given as follows:

$$UCS_{cuaps(kPa)} = \Omega \cdot p_v \cdot \left(\frac{t \cdot B_w}{t_{\min}} \right)^n \cdot \left(\frac{UCS_{mould}}{p_a} \right)^m \tag{3.2}$$

where p_v = the final applied vertical pressure (kPa), which can be taken as the overburden pressure ($\gamma_{wet}h$) or vertical stress σ_v taking into account the arching effect, p_a = atmospheric pressure (= 101 kPa), B_w = binder content = ratio of mass of binder on mass of dry tailings (fraction), t = curing time (day), t_{min} = minimum curing time = 1 day, and Ω, n and m are fitting constants (unitless). For the data set used (4.5 wt% binder of PCI-Slag@20:80 wt% and applied vertical pressure in the range 0–400 kPa), the constants Ω, n and m are $\Omega = 0.33$; $n = -0.26$ and $m = 1.08$, with a good coefficient of correlation $r = 0.9984$. It is noteworthy that the vertical pressure range 0–400 kPa is also typical for compressive stress measured within CPB-filled stopes (Belem et al., 2004; le Roux et al., 2005; Li and Aubertin, 2009).

Based on existing CUAPS test data, it was observed that Eq. 3.2 can be used with a 75% confidence limit (±25% range). Although constants Ω, n and m in Eq. 3.2 were determined based on tests where the maximum effective stress was limited to 400 kPa, it is clear that this equation can also be used at higher pressure. The proposed Eq. 3.2 is useful given that laboratory CPB is usually prepared as either undrained or drained samples using conventional plastic capped cylinder moulds. However, the CUAPS-consolidated paste backfills can more accurately mimic in situ conditions, as explained above, so that effective stress can be applied during curing by allowing excess water to drain from capillary pores within CPB material, thereby improving the hardening process (better cohesion and strength development).

These results show that the CUAPS apparatus can overcome the limitations of standard laboratory-prepared CPB strength optimization tests and procedures, thereby providing

higher design strength. Hence, the CUAPS can be used to estimate in situ behaviour of in-stope CPB based on laboratory-prepared CPB samples.

3.4.5 Simulated in situ backfill strength

Determining the mechanical strength that develops within CPB-filled stopes is of paramount importance to assess the overall structural stability of pillars and backfill material. Figure 3.12 shows the evolution of UCS with curing time for 4.5 wt% binder paste backfills placed in a "virtual" stope, obtained at different depths from the top.

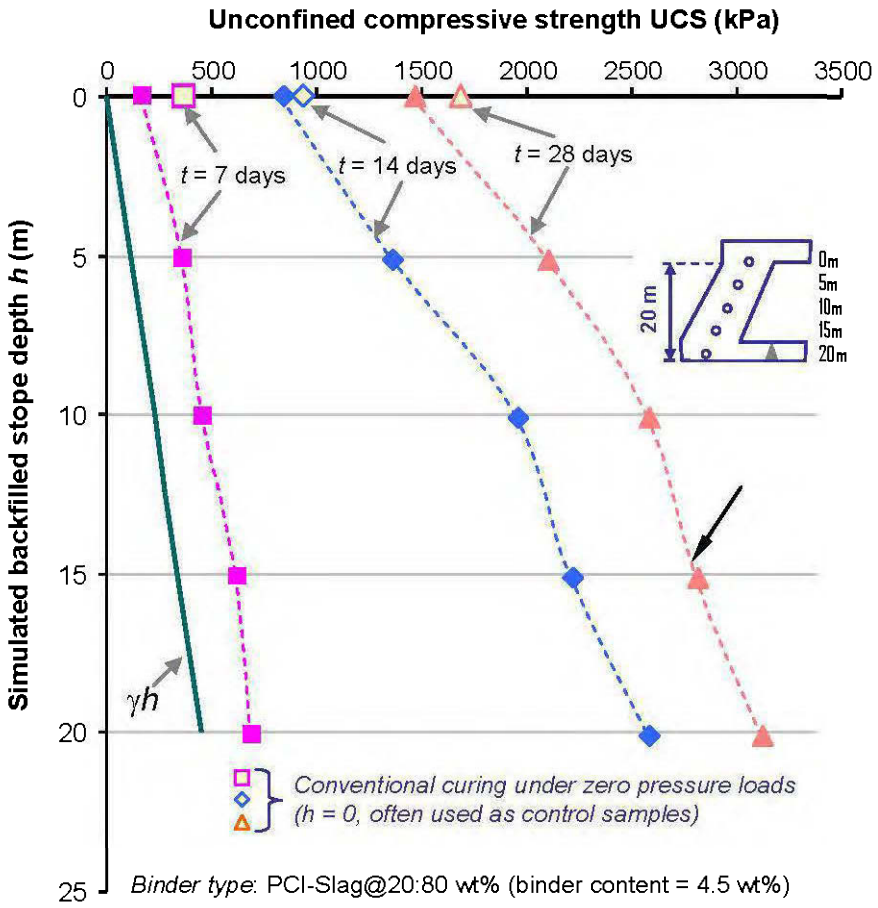

Figure 3.12 Variation in UCS obtained from 4.5 wt% CPB samples at different simulated stope depths as a function of curing time.

Overall, and as expected, UCS increases with increasing stope depth for a given curing time, following the same trend as the overburden pressure ($\sigma_v = \gamma_{wet} h$). At 28 days of curing, UCS of 1.5 MPa, 2.1 MPa, 2.6 MPa and 3.1 MPa were obtained on samples at stope depths of 0 m, 5 m, 10 m, 15 m and 20 m, respectively. This confirms that the UCS of CPB-filled stopes increases from top to bottom due to the self-weight consolidation effect. For curing times of 7, 14 and 28 days, this increase was estimated at 75%, 68% and 53%, respectively.

It was proven that the relative density ($D_r = [e_{max} - e_{cuaps}]/[e_{max} - e_{min}]$) increases with increasing stope depth, thus decreasing the corresponding void ratio e_{cuaps} (or porosity) as a result of applied consolidation pressure during curing. This is because the lower the void ratio e, the closer the CPB particle packing, and accordingly, the lower the friction angle ϕ that develops and the stronger the material (high cohesion c). Figure 3.12 also shows that conventional non-perforated moulds, commonly used to determine CPB design values, produce UCS similar to those obtained at the top of a backfilled stope (Caouyette, 2003; Thakur, 2008; El Aatar, 2009). On-top UCS were 351 kPa, 909 kPa and 1680 kPa for curing times of 7, 14 and 28 days, respectively. This confirms that the UCS of conventional mould-cured CPB samples is unfortunately unsuitable for use in CPB design, as it is representative of only the top of paste backfilled stopes.

Along with the experimental testing validations, one empirical general equation (Eq. 2) was proposed to predict the UCS of CUAPS-consolidated backfills from the known UCS of undrained or drained mould paste backfill samples. This equation was defined as a function of curing time t and binder content $B_{w\%}$, and it has a 75% confidence limit.

3.5 CONCLUSIONS

This paper presents an assessment of a recently developed laboratory apparatus called CUAPS (curing under applied pressure system) designed to better estimate in situ CPB properties and behaviour. The modified CUAPS apparatus can be used to evaluate four

different types of parameters, using a one-dimensional (1-D) consolidation test, a 1-D consolidation test with PWP measurements, permeability tests, and curing under constant or variable applied pressure testing. Physical (microstructure) and strength properties of tested samples can be determined after each test at various curing times. The preliminary results validate the accuracy and functionality of the modified CUAPS apparatus. Therefore, this apparatus enables the production of useful and more realistic CPB properties than those currently obtained from conventional plastic moulds, which consistently give lower UCS for a given CPB mixture recipe. A limitation of the CUAPS apparatus is that the applied pressure loading system allows applying a maximum pressure of 600 kPa (25–30 m height in the simulated stope, depending on the tested material's wet unit weight) and a D/H ratio of 0.5, i.e., a paste backfill sample size 100 mm in diameter and 200 mm in height. Further modifications in the near future will make the modified CUAPS apparatus more flexible by allowing a higher maximum pressure ($\geq$ 1200 kPa) application and/or larger backfill sample sizes for better representation of in situ conditions in mine stopes. These changes would enhance the utility and versatility of the modified CUAPS setup and allow an improved test protocol for laboratory-prepared CPB materials.

3.6 ACKNOWLEDGEMENTS

The authors would like to express their appreciation to the NSERC Discovery Grant Program, the Industrial NSERC-Polytechnique-UQAT Chair on Environment and Mine Wastes Management and the Canadian Research Chair on Integrated Management of Mine Tailings for their generous financial support for this research. The authors gratefully acknowledge the Canada Foundation for Innovation (CFI) for manufacturing the ten CUAPS apparatuses. We would also like to acknowledge Pierre Trudel of G+Plus Industrial Plastic Inc. for his collaborative assistance in modifying the CUAPS apparatus, David Bouchard, Yvan Poirier and Nil Gaudet (UQAT-URSTM technicians) for their technical support, and Nathan Mutch of Lafarge North America Inc. for kindly providing the cement materials.

3.7 REFERENCES

ASTM Designation D2435, 1999. Standard test method for one-dimensional consolidation properties of soils. In: *Annual Book of ASTM Standards,* Vol. 04.08, ASTM International, West Conshohocken, PA, pp. 207–216.

ASTM Designation D4186, 1999. Standard test method for one-dimensional consolidation properties of soils using controlled-strain loading. In: *Annual Book of ASTM Standards,* Vol. 04.08, ASTM International, West Conshohocken, PA, pp. 477–481.

ASTM Designation D5856, 2002. Standard test method for measurement of hydraulic conductivity of porous material using a rigid-wall, compaction-mould permeameter. In: *Annual Book of ASTM Standards,* Vol. 04.08, ASTM International, West Conshohocken, PA,, pp. 77–84.

Aubertin, M., Bussière, B., Chapuis, R.P., 1996. Hydraulic conductivity of homogenized tailings from hard rock mines. *Canadian Geotechnical Journal,* Vol. 33, No. 3, pp. 470–482.

Belem, T., Benzaazoua, M., Bussière, B., Dagenais, A-M., 2002. Effects of settlement and drainage on strength development within mine paste backfill. In: *Proceedings of the 9th International Conference on Tailings and Mine Waste,* Vail, CO, A.A. Balkema, Swets and Zeilinger B.V., Lisse, The Netherland, pp. 139–148.

Belem, T., Harvey, A., Simon, R., Aubertin, M., 2004. Measurement and prediction of internal stresses in an underground opening during its filling with cemented paste backfill. In: *Proceedings of the 5th International Symposium on Ground support in Mining and Underground Construction,* Perth, WA, Australia, Taylor and Francis Group, London, UK, A.A.Balkema, Leiden, the Netherlands pp. 619–630.

Belem, T., El Aatar, O., Bussière, B., Benzaazoua, M., Fall, M., Yilmaz, E., 2006. Characterization of self–weight consolidated paste backfill. In: *Proceedings of the 9th International Seminar on Paste and Thickened Tailings,* Limerick, Ireland, Australian Centre for Geomechanics, Nedlands, WA, Australia, pp. 333–345.

Belem, T., Benzaazoua, M., 2008. Design and application of underground mine paste backfill technology. *Geotechnical Geological Engineering,* Vol. 26, No. 2, pp. 147–174.

Belem, T., Fourie, A., Fahey, M., 2010. Time-dependent failure criterion for cemented paste backfills. *Proceedings of the 13rd International Seminar on Paste and Thickened Tailings,* Toronto, Ontario, Australian Centre for Geomechanics (ACG), Nedlands, WA, Australia pp. 1–14.

Benzaazoua, M., Belem, T., Bussière, B., 2002. Chemical factors that influence the performance of mine sulphidic paste backfill. *Cement and Concrete Research,* Vol. 32, No. 7, pp. 1133–1144.

Benzaazoua, M., Fall, M., Belem, T., 2004. A contribution to understanding the hardening process of cemented paste backfill. *Minerals Engineering,* Vol. 17, No. 2, pp. 141–152.

Benzaazoua, M., Belem, T., Yilmaz, E., 2006. Novel lab tool for paste backfill. *Canadian Mining Journal,* Vol. 127, No. 3, pp. 31–31.

Bussière, B., 2007. Colloquium 2004: Hydro-geotechnical properties of hard rock tailings from metal mines and emerging geo-environmental disposal approaches. *Canadian Geotechnical Journal,* Vol. 44, No. 9, pp. 1019–1052.

Cayouette, J., 2003. Optimization of the paste backfill plant at Louvicourt mine. *CIM Bulletin,* Vol. 96, No. 1075, pp. 51–57.

Chakrabarti, S., Horvath, P. 1986. Conventional consolidation tests on two soils. *Proceedings on Consolidation of soils: testing and evaluation; ASTM STP 892,* Baltimore, Maryland, ASTM International, West Conshohocken, PA, pp. 451–464.

Chapuis, R.P., 2004. Predicting the saturated hydraulic conductivity of sand and gravel using effective diameter and void ratio. *Canadian Geotechnical Journal,* Vol. 41, No. 5, pp. 787–795.

Crowder, J.J., 2004. Deposition, consolidation, and strength of non-plastic tailings paste for surface disposal. *Ph.D. Dissertation,* University of Toronto, Ontario, Canada.

El Aatar, O., 2010. Consolidation behaviour of cemented paste backfill material (in French). *M.Sc. Thesis*, Université du Québec en Abitibi-Témiscamingue, Rouyn-Noranda, Québec, Canada.

Fourie, A.B., Fahey, H., Helinski, M., 2007. Using effective stress theory to characterize the behaviour of backfill. *CIM Bulletin,* Vol. 100, No. 1103, pp. 1–9 (Paper 27).

Godbout, J., Bussiere, B., Aubertin, M., Belem, T., 2007. Evolution of cemented paste backfill saturated hydraulic conductivity at early curing time. In: *Proceedings of the 60th Canadian Geotechnical Conference,* Ottawa, Ontario, Canadian Geotechnical Society, Richmond pp. 1–7.

Gorst, N.J.S., Williamson, S.J., Pallett, P.F., Clark, L.A. 2005. Friction in temporary works. *The Health and Safety Executive HSE, Research Report 071,* Edgbaston, Birmingham (UK), University of Birmingham, pp. 1-62.

Helinski, M., Fourie, A.B., Fahey, M., 2006. Mechanics of early age cemented paste backfill. In: *Proceedings of the 9th International Seminar on Paste and Thickened Tailings,* Limerick, Ireland, ACG, Nedlands, WA, Australia, pp. 313–322.

Helinski, M., Fahey, H., Fourie, A.B., 2007a. An effective stress approach to modelling mine backfilling. *CIM Bulletin,* Vol. 100, No. 1103, pp. 1–8 (Paper 29).

Helinski, M., Fourie, A.B., Fahey, M., Ismail, M., 2007b. Assessment of the self-desiccation process within cemented paste backfills. *Canadian Geotechnical Journal,* Vol. 44, No. 10, pp. 1148–1156.

Kassim, K.A., Huey C.S., 2000. Consolidation characteristics of lime stabilised soil. *Journal Kejuruteraan Awam* (Journal of Civil Engineering), Vol. 12, No.1, pp. 31–42.

le Roux, K-A., Bawden, W.F., Grabinsky, M.F., 2002. Comparison of the material properties of in situ and laboratory prepared cemented paste backfill. In: *Proceedings of the 104th CIM Conference,* Vancouver, British Columbia, Canada, Canadian institute of Mining, Metallurgy and Petroleum (CIM), Montreal, pp. 201–209.

le Roux, K.-A., Bawden, W.F., Grabinsky, M.F., 2005. Field properties of cemented paste backfill at the Golden Giant mine. *Min. Techn. Trans. Ins. Min. Metal. Sect. A,* Vol. 114, No. 2, pp. 65–86.

le Roux, K-A., 2004. In situ properties and liquefaction analysis of cemented paste backfill. *Ph.D. Dissertation*, University of Toronto, Ontario, Canada.

Li, L., Aubertin, M., 2009. A three-dimensional analysis of the total and effective stresses in submerged backfilled stopes. *Geotech. Geol. Eng.,* Vol. 27, No. 4, pp. 559–569.

McCarthy, D.F., 2007. *Essentials of soil mechanics and foundations: Basic geotechnics (7th ed.).* Pearson Prentice Hall, Toronto, Ontario, Canada.

Mitchell, R., Smith, J., 1981. The compression-percolation test for mine tailings backfill. *CIM Bulletin,* Vol. 74, No. 833, pp. 85–89.

Morris, P.H., Lockington, D.A., Apelt, C., 2000. Correlations for mine tailings consolidation parameters. *International Journal of Mining, Reclamation and Environment,* Vol. 14, No. 2, pp. 171–182.

Pierce, M.E., 1997. Laboratory and numerical analysis of the strength and deformation behaviour of paste backfill. *M.Sc. Thesis,* Queen's University, Ontario, Canada.

Potvin, Y., Thomas, E.H., Fourie, A.B., 2005. *Handbook on Mine Fill.* Australian Centre for Geomechanics (ACG), Western Australia, Perth, Australia.

Qui, Y.J., Sego, D.C., 2001. Laboratory properties of mine tailings. *Canadian Geotechnical Journal,* Vol. 38, No. 2, pp. 183–190.

Revell, M.B., 2004. Paste – How strong is it? In: *Proceedings of the 8th International Symposium on Mining with Backfill,* Beijing, China, The Nonferrous Metals Society of China and The Nonferrous Metals Industry Association of China, Changsha, pp. 286–294.

Servant, S., 2001. Détermination des paramètres mécaniques des remblais miniers faits de résidus ciments (*In English:* Determination of mechanical parameters of mine backfills made of cemented mine tailings). *M.Sc. Thesis,* McGill University, Mining Engineering Department, Montreal, Quebec, Canada.

Simms, P., Grabinsky, M., 2009. Direct measurement of matric suction in triaxial tests on early-age cemented paste backfill. *Canadian Geotechnical Journal,* Vol. 46, No. 1, pp. 93–101.

Stone, K.J.L., Randolph, Toh, S., Sales, A.A, 1994. Evaluation of consolidation behaviour of mine tailings. *Journal of Geotechnical Engineering,* Vol. 120, No. 3, pp. 473–490.

Taylor, D.W., 1942. Research on consolidation of clays. *Civil and Sanitary Engineering Department,* MIT, Cambridge, MA, Publication Serial 82.

Thakur, N., 2008. Characterization of physico-mechanical properties of consolidated paste backfill columns of LaRonde Mine. *Summer Work Report*, Report No. 02, Université du Québec en Abitibi-Témiscamingue, Rouyn-Noranda, Québec, Canada.

Yilmaz, E., Belem, T., Benzaazoua, M., Bussière, B, 2008a. Experimental characterization of the influence of curing under stress on the hydromechanical and geotechnical properties of cemented paste backfill. In: *Proceedings of the 12th International Conference on Tailings and Mine Waste,* Vail, CO, Taylor and Francis Group plc, London, UK, A.A.Balkema Publishers, Leiden, the Netherlands, pp. 139–152.

Yilmaz, E., Belem, T., Bussière, B., Benzaazoua, M., 2008b. Consolidation characteristics of early age cemented tailings paste backfill. In: *Proceedings of the 61st Canadian Geotechnical Conference,* Edmonton, Alberta, Canada, Canadian Geotechnical Society, Richmond, pp. 797–804.

Yilmaz, E., Benzaazoua, M., Belem, T., Bussière, B., 2009a. Effect of curing under pressure on compressive strength development of cemented paste fill. *Minerals Engineering,* Vol. 22, No. 9-10, pp. 772–785.

Yilmaz, E., Belem, T., Bussière, B., Benzaazoua, M., 2009b. Relationships between microstructural properties and strength of consolidated and unconsolidated cemented paste backfill. *Cement Concrete Composites* (submitted in October 2009).

Yilmaz, E., 2010. Investigating the hydrogeotechnical and microstructural properties of cemented paste backfill using the CUAPS apparatus. *Ph.D. Thesis,* Université du Québec en Abitibi-Témiscamingue (UQAT), Rouyn-Noranda, Québec, Canada.

CHAPTER IV

EVALUATION OF THE ONE-DIMENSIONAL CONSOLIDATION BEHAVIOUR OF EARLY AGE CEMENTED PASTE BACKFILLS

Erol Yilmaz, Tikou Belem, Bruno Bussière, Mamert Mbonimpa and Mostafa Benzaazoua

Paper submitted in January 2010 to

Canadian Geotechnical Journal

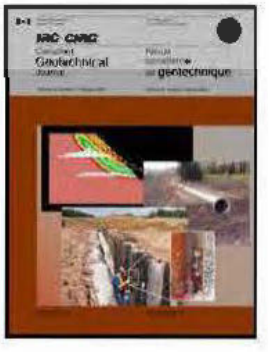

4.0 RÉSUMÉ

Les propriétés de consolidation 1-D des remblais cimentés en pâte (RCP) est utile pour l'estimation des paramètres de conception d'un chantier souterrain à remblayer ainsi que pour des fins de modélisations numériques. De nombreuses études ont été réalisées sur le comportement en consolidation des résidus miniers, mais pas sur les RCP principalement parce que la consolidation n'a pas été initialement considérée comme une propriété essentielle et les équipements d'essais existants n'étaient pas adaptés. Dans ce papier, les effets de différents types de liant ainsi que leur teneur sur les caractéristiques de consolidation des RCP jeunes (temps de cure entre 0–7 jours) a été étudiée à l'aide d'un appareil de laboratoire novateur modifié appelé CUAPS (système de cure sous pression appliquée). Puisque les propriétés de conductivité hydraulique saturée sont intimement liées à la consolidation, son évolution a également été étudiée pour les résidus (témoin) et les RCP. Les résultats montrent que l'ajout de liant affecte grandement l'indice des vides et augmente la rigidité du matériau. Les données de pression interstitielle montrent que l'ajout de liant réduisait la valeur de pic mesurée pour tous les incréments de pression tandis que le coefficient de perméabilité k_{sat} décroissait rapidement avec le temps de cure. Enfin, des relations empiriques pour l'estimation des paramètres de consolidation unidimensionnelle des RCP ont été proposées et leur applicabilité discutée.

Mots clés: Remblai en pâte, CUAPS, Consolidation, Pression interstitielle, Hydratation des liants

4.0 ABSTRACT

The one-dimensional consolidation properties of cemented paste backfill (CPB) are useful for the estimation of design parameters for underground stope filling purpose as well as for numerical modeling purposes. Many studies have examined the consolidation characteristics of mine tailings, but not in CPBs, mainly because consolidation was not initially considered as an essential property and the available testing equipment was not suitable. In this paper, the effect of different types of binder and their content on the one-dimensional consolidation characteristics of CPB samples at early ages of curing (between 0–7 days) were investigated using an improved laboratory apparatus called CUAPS (curing under applied pressure system). As the drainage ability and the saturated hydraulic conductivity are closely linked with consolidation, the change in the k_{sat} at the end of the consolidation process was also investigated for tailings (control) and CPB materials. Results indicate that adding binder to the mixtures considerably affects the void ratio and increases compression resistance. The excess PWP indicates that binder reduces the peak value reached for all pressure increments while the k_{sat} decreases with time. Some empirical equations to estimate the one-dimensional consolidation characteristics of CPB samples are finally proposed and discussed.

Keywords: Paste backfill, CUAPS, Consolidation, Pore pressure, Binder hydration

4.1 INTRODUCTION

Each year, large volumes of fine-grained and sulphide-rich mine tailings are generated by mining and milling operations. How to effectively and economically dispose of these problematic tailings is a major issue facing mining industries worldwide (Yilmaz, 2007; Bussière, 2007). Numerous techniques have been developed to better manage mine tailings in the backfill form which contributes positively to the mining operations. Among these, cemented paste backfill (CPB) has become increasingly widespread, mainly because it reduces by 50–60 wt% the quantity of sulphidic tailings deposited on the surface, increases the ore recovery, and minimizes the stoping sequences (e.g., Potvin et al., 2005; Belem and Benzaazoua, 2008a,b).

CPB usually consists of mixing dewatered and filtered ("cake") total tailings (70–85 wt% solids) with single, binary and ternary hydraulic binders (typically 2–7 wt% for underground backfill) to meet the mechanical strength requirements. The CPB preparation requires also mixing water for the desired consistency (6"–12" slump height) to enable plug flow of the resultant paste to its emplacement site (Benzaazoua et al., 1999). A considerable amount of experimental works has been done on physical, chemical, mechanical and microstructural properties of CPB materials at laboratory and meso scales (e.g., Belem et al., 2000, 2001; Benzaazoua et al., 2002; 2004; Yilmaz, 2003; Kesimal et al., 2004; Fall et al., 2005; Klein and Simon, 2006; Ouellet et al., 2007; El Aatar et al., 2007; Ercikdi et al., 2009; Yilmaz et al., 2009b). Only a few studies have examined in situ properties of CPB, which differ greatly from those of laboratory-prepared and cured CPB (Ouellet and Servant, 2000; Harvey, 2004; Belem et al., 2004, 2008a; le Roux et al., 2005; Ouellet et al., 2006; Helinski et al., 2007a; Grabinsky and Bawden, 2007). It is common practice at most modern underground hard rock mines worldwide to hydraulically place the CPB mixture within the mined-out stope in two sequences. The first sequence, called "plug fill," contains the highest binder content (7 wt%) and is left to cure under self-weight (or gravity-driven) consolidation for a few days (2–7 days), while the second sequence, called "residual fill," has lower binder content (typically 3–4.5 wt%) and is often left to cure under self-weight for a longer time. As a result, the plug fill will support an additional surcharge loading that could damage the formed cement bonds.

The settlement of saturated fresh paste backfill depends on the material's coefficient of consolidation c_v, which combines permeability coefficient (saturated hydraulic conductivity k_{sat}) and stiffness, and on the filling rate (Fahey et al., 2009). As the stress ratio increases, the void ratio decreases (including pore refinement and cementation by the cement hydration and precipitation; Benzaazoua et al., 2004) and the permeability coefficient decreases, thereby increasing the time required for water to flow out from the backfill material voids (Belem et al., 2002, 2006; le Roux et al., 2005; Helinski et al., 2006; Fourie et al., 2007; Grabinsky and Bawden, 2007; Yilmaz et al., 2008a). However, the relationship between the filling rate and consolidation rate of fresh CPB material during underground placement remains to be more understood. Only a few studies have examined the consolidation and saturated hydraulic conductivity behaviour of CPB materials (e.g., Pierce et al., 1998; le Roux et al., 2002; le Roux, 2004; Godbout et al., 2007; Yilmaz et al., 2008b).

A further key issue in freshly placed CPB material is the excess pore water pressure (PWP) that build-up during filling. If some consolidation is allowed to occur (through free drainage and PWP reduction) during filling, the result is effective stress development within the CPB (Fahey et al., 2009). Following filling, the combined effects of what is assumed to be chemical shrinkage (also known as self-desiccation) and subsequent water drainage (increase of the effective stress) give rise to a reduction in total stresses (vertical and horizontal) due to the development of arching (Helinski et al., 2007b; Fahey et al., 2009). Uniaxial compressive strength (UCS) increases thereafter by a factor up to 2.4 or a difference of up to 58% compared to the UCS obtained from undrained plastic mould samples, depending on binder type and proportion (Belem et al., 2002; Rotta et al., 2003; Consoli et al., 2006; Helinski et al., 2006; Yilmaz et al., 2008a; 2009a,b; 2010). Accordingly, the knowledge of one-dimensional consolidation characteristics of early age CPB materials is of great interest for a rational backfill design for underground mines.

The primary objective of this study was to investigate the one-dimensional consolidation characteristics of early age (a maximum curing time of 7 days) CPB materials prepared from a sulphide-rich mine tailings sample and a range of binder types and contents. A blended Portland cement (mixture of 20% GU Portland cement and 80% blast furnace slag) was used

as a reference binder since it provides the best CPB strength development. The effect of five binder proportions (0 – control, 1, 3, 4.5 and 7 wt%) on consolidation (e–logσ'_v) and on excess PWP development and dissipation was evaluated at four curing times (0, 1, 3 and 7 days). These results were also compared with batches made of two other binder types (GU–FA@40:60 wt% and GU only) at binder contents of 1 and 4.5 wt%. Saturated hydraulic conductivity k_{sat} was also determined at the end-test of consolidation for both uncemented tailings and 4.5 wt% binder CPB samples (GU–Slag@20:80 wt%) as a function of curing time (0, 1, 3 and 7 days). For these samples, the coefficient of consolidation c_v was back-calculated from k_{sat}. The originality of the present work lies in the attempt to understand the evolution of CPB consolidation parameters at early curing ages (i.e., compression index C_c, excess PWP behaviour, coefficient of consolidation c_v) using an innovative laboratory apparatus called CUAPS (curing under applied pressure system) developed by the authors (Benzaazoua et al., 2006; Yilmaz et al., 2010). This information is essential to accurately predict CPB settlement in mine stopes. A single regression model to predict consolidation parameters is also proposed and discussed.

4.2 MATERIAL AND METHODS

4.2.1 Mine tailings physical characteristics

The filtered total mine tailings sample (after cyanide destruction) was obtained from the LaRonde Mine milling complex (Quebec, Canada). It comes from the treatment of a poly-metallic (gold-copper and zinc-silver mineralization) sulphides ore. The determination of the physical properties include specific gravity G_s, specific surface S_m, water content w (%), the grain size distribution (GSD) parameters, the maximum dry unit weight $\gamma_{d\text{-}max}$ and the liquid limit LL. The GSD of homogenized tailings was determined according to standards D421-85 and D422-63 (ASTM, 1999a, 1999b). The GSD analysis showed that approximately 44% of the tailings sample is finer than 20 µm, with only 4.7% clay-sized particles (< 2 µm). Most of the GSD fall into medium to fine sand- and silt-sized grains. From the GSD curve, the coefficients of uniformity C_u (= D_{60}/D_{10}) and curvature C_z (= $D_{30}^2/D_{60}\times D_{10}$) – symbol C_z are

determined instead of the commonly used C_c to avoid confusion with the compression index C_c, they give values of 7.9 and 1.1, respectively (the tailings sample being identified as well-graded). The specific gravity G_s and specific surface area S_m of the tailings determined based on standards C128-04 and D6556 (ASTM, 2002a, 2009) are 3.7 and 2.17 m^2/g, respectively. The Atterberg limits determined based on ASTM standard D4318 (ASTM, 1991a) show that the tailings sample has a liquid limit LL of 23%. Table 4.1 lists some physical properties of the mine tailings sample used in the present study. Based on the Unified Soil Classification System (USCS, McCarthy, 2007), the mine tailings material is non-plastic silt (ML).

Table 4.1 Basic physical properties of mine tailings used in this study

Parameter	Unit	Values
Specific gravity G_s	---	3.71
Fines content ($d < 20$ μm)	%	43.9
Clay size particles (< 2μm)	%	4.7
Silt size particles (2–50 μm)	%	66.1
Sand size particles (50–2000 μm)	%	29.2
D_{10} (effective particle size)	μm	4.26
D_{50} (average particle size)	μm	24.27
Coefficient of uniformity C_u	---	7.9
Coefficient of curvature C_z	---	1.1
Water content w	%	23.5
Liquid limit LL	%	23

4.2.2 Binders and mixing water

Binder and water were added to mine tailings to prepare CPB mixtures. The three different binders used in the CPB mixtures were general use Portland cement (GU), blast furnace slag (Slag) and type C fly ash (FA). GU was used alone, while GU and Slag, and GU and FA were blended in ratios of 20/80 and 60/40, respectively. The proportions were based on the ranges widely used by the mining industry for CPB preparation. The mixing water used was municipal tap water since the LaRonde mine use fresh water. The specific gravity G_s and specific surface area S_s for GU, GU-Slag and GU-FA binder are 3.08 and 1.58 m^2/g, 2.92 and 2.84 m^2/g, and 2.88 and 1.66 m^2/g, respectively. The as-received tailings interstitial water

sulfate (SO_4^{2-}) content was 4880 ppm, which is considered highly aggressive according to DIN 4030-1 standard (German DIN norm, 1991). In addition, this pore water was rich in soluble calcium Ca (560 ppm) because of the lime added during upstream ore processing, before and after the cyanide destruction process. The mixing water allowed thus dilution of the sulphated pore water.

4.2.3 Experimental procedures

4.2.3.1 Improved CUAPS apparatus

To investigate the mechanical strength properties of CPB materials cured under vertical stress in closely simulated in situ conditions (filling rate, placement and curing), an innovative laboratory apparatus called CUAPS (curing under applied pressure system) was developed (Benzaazoua et al., 2006), inspired by an earlier simple set-up for curing under external vertical loads used by Belem et al. (2002). The improved CUAPS apparatus is a versatile laboratory system that can perform several experimental tests, as follows: one-dimensional consolidation tests (step load or rapid load) with or without pore water pressure (PWP) measurement, direct permeability tests and CPB specimen curing tests under constant or variable vertical pressure (Yilmaz et al., 2010). The advantage of the CUAPS apparatus is that it offers the possibility to retrieve a sample that has already undergone one of several possible tests (one-dimensional consolidation, curing under stress, permeability coefficient) to perform compression tests (uniaxial or triaxial) for determining the mechanical properties of CPB material. A schematic illustration of the CUAPS apparatus is presented in Figure 4.1. The CUAPS apparatus consists of three main components: *i*) a top loading device for applying vertical stress to the top of a CPB sample at air pressures up to 600 kPa (with an LVDT for measuring vertical deformation and a loading piston), *ii*) a Perspex mould forming the middle part (as specimen holder and consolidation cell: ($D \times H$ = 101.6 × 203.2 mm) protected by a metal cylinder and *iii*) a bottom drainage hole (which can be fitted with a PWP transducer) to drain excess pore water from the paste backfill sample. The corresponding diameter-to-height ratio (D/H) is only 0.5.

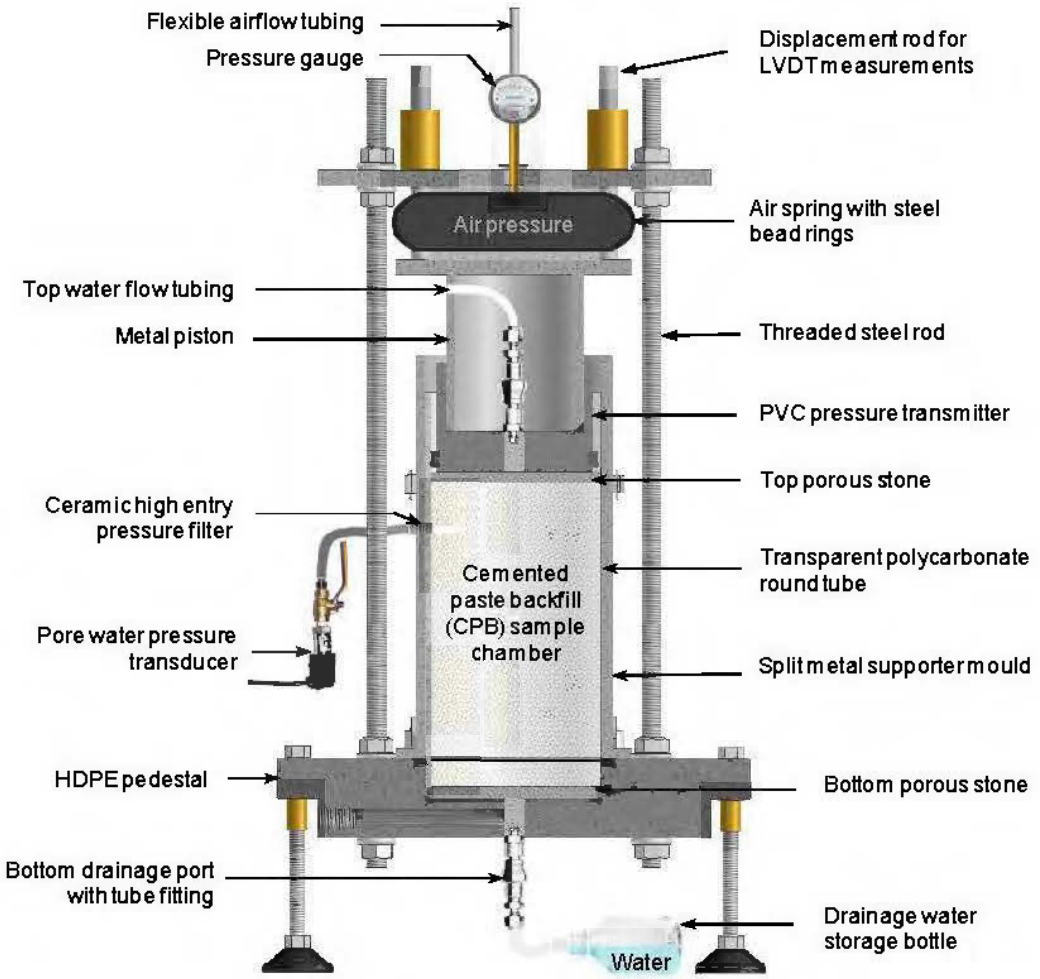

Figure 4.1 Schematic diagram of the modified CUAPS apparatus for one-dimensional consolidation and saturated hydraulic conductivity testing on uncemented tailings and CPB.

In conventional consolidometers, the D/H ratio typically varies between 1 and 4 (see ASTM, D2435, 1999c). These high ratios are used in order to reduce the friction between the sample and the ring and to avoid any soil disturbance. The D/H of 0.5 for the CUAPS was chosen to obtain a sample with a height-to-diameter ratio $H/D \geq 2$ for uniaxial or triaxial compression tests. It should be mentioned that in the literature, a ratio D/H of 0.5 was also used for silty materials such as CPB (Qui and Sego, 2001; le Roux, 2004). Despite this low D/H ratio, the calculated ring friction (or Perspex tube in the CUAPS) factor λ (Taylor, 1942), assuming a

Poisson's ratio ν = 0.2 for CPB and a coefficient of friction μ = 0.2–0.3 (concrete/plastic), ranges between 0.75 and 0.82 in comparison with the recommended factor λ of 0.95–0.98. The Perspex tube friction factor λ is acceptable knowing that a thin smear of silicon grease was applied inside the tube to further reduce friction. In addition, λ increases with increasing consolidation pressure. A full description of the CUAPS apparatus is beyond the scope of the present paper. However, detailed information on its features and some results can be found in Benzaazoua et al. (2006), Yilmaz et al. (2006; 2008a,b; 2009a,b; 2010) and Yilmaz (2010).

4.2.3.2 Paste backfill preparation: mixing, pouring and curing

To prepare the desired CPB consistency, the backfill ingredients (tailings, binding agent and tap water) were thoroughly mixed in a heavy-duty Hobart mixer (Model No. D 300-1) for approximately 12 minutes. The reference hydraulic binder consisting of a blend of 20 wt% general use Portland cement (GU) and 80 wt% blast furnace slag (Slag) was produced. For comparison purposes, two binder types, namely fly ash-based binders (GU-FA@60:40 wt% and Portland cement GU only) were also used. The CPB samples were prepared using five different binder contents: 0 – control, 1, 3, 4.5 and 7 wt%, resulting in water-to-cement *w/c* ratios ranging between 28.5 and 4.3 (note that only 1 and 4.5% binder proportions were used for the GU-FA and GU binders). The solid mass concentration for all samples was set at 78 wt% (corresponding to a gravimetric water content of 28.2 wt%), resulting in the average slump height of 177.8 mm (7") measured by a standard Abrams cone (ASTM, 2002b) The resultant average bulk (or wet) unit weight γ_{wet} of all fresh CPB samples was 22.3 kN/m^3. CPB mixes were poured into Perspex moulds ($D \times H$ = 101.6 × 203.2 mm) mounted on the bottom part of the ten CUAPS set-ups and covered by the top loading device. All samples were left to cure for 0, 1, 3 and 7 days in a controlled humidity chamber set at 23°C ± 2°C and 80% relative humidity. These external curing conditions replicate underground CPB-filled mine stope conditions. The main reasons for keeping the sample in CUAPS cells during the curing process are that *i*) they were also acting as curing cells and *ii*) any unnecessary additional manipulation of cured samples should be eliminated by avoiding their transfer from moulds to the CUAPS cells for consolidation testing.

4.2.3.3 One-dimensional consolidation tests

The one-dimensional consolidation state of CPB-filled underground stopes can occur during either continuous or sequential filling. During continuous filling, each CPB layer is suitably compressed by the weight of the overburden layer until the end of filling (loading before substantial cohesion). For sequential filling (e.g., plug fill followed by residual fill), the first backfilled sequence is left to cure under self-weight for a few days (generally 2–7 days) before pursuing with the second sequence (cementation before loading) deposited over the first one. In this study, the cementation before the loading case was selected, as it is more representative of paste backfilling systems used in Canadian underground hard rock mines. CPB samples were therefore left to cure for predetermined curing times (1, 3 and 7 days) before consolidation testing.

The main objective of these tests was to obtain experimental data on the void ratio–effective stress (e–σ'_v) and permeability–curing time (k–t) relationships for the CPB samples prepared with fine-grained, sulphide-rich tailings. These relationships are required for numerical modelling of one-dimensional consolidation behaviour of early age paste backfill materials. Procedures inspired by ASTM standards D2435 and D4186 (ASTM, 1999c, 1999d) were used to determine the one–dimensional consolidation properties of CPB sample using the modified CUAPS apparatus with a maximum vertical effective stress of 400 kPa, which corresponds to typical compression stress values measured within backfilled stopes (Belem et al., 2004; le Roux et al., 2005; Li and Aubertin, 2009). Immediately after CPB samples were placed into the CUAPS consolidometer, a pre-contact (seating) pressure of 15 kPa was applied in order to place the loading piston and the top porous stone in contact with the top of the sample. An increasing pressure increment was then applied to consolidate the sample. According to ASTM D2435 recommendations, a load (or pressure) increment ratio (LIR) of 1 was chosen. Thus, pressure increments of 25, 50, 100, 200 and 400 kPa were applied to the sample. Note that for each test an initial pressure of 0.5 kPa was applied immediately after each targeted curing time (0–7 days) to avoid log scale errors in the calculation. Each specimen was then loaded successively to a highest pressure of 400 kPa and later unloaded, again at LIR equal to 1. ASTM D2435 and D4186 standards recommend that each pressure

increment should be maintained for a minimum period of 24 h until primary consolidation is completed (called load increment duration, LID). In this study, because the material changes over time, it was decided to do the entire test within a 10-hour period based on preliminary testing on PWP dissipation measurements. Because the preliminary results showed that pressure equilibrium was reached after 2 h (Yilmaz et al., 2010), an LID of 2 hours was chosen. Each test was performed over a single day, and was therefore comparable to the rapid load test. During testing, the specimen's vertical deformation was automatically recorded by a linear variable displacement transducer (LVDT) at time intervals of 0, 2, 4, 6, 8 and 10 hours. During consolidation testing, all experimental data (i.e. pressure, vertical displacement and time, were concurrently and always recorded using an HOBO U12 data logger.

4.2.3.4 Pore water pressure measurement

Excess PWP measurements were performed only for the GU-Slag@20:80 wt% mixture. The CUAPS is a versatile apparatus that allows drainage at the bottom of the sample (rather than at the top) to facilitate leachate collection during curing under stress testing. Thus, the PWP transducers must be mounted close to the top end of the specimen. The type of transducer selected is a HOSKIN E13-5-4-B20R-25 transducer that captures a pressure range of 0–600 kPa with ±0.25% accuracy and is equipped with a ceramic high entry pressure filter. The transducer is placed in CPB and is normally mounted axially, but due to the configuration of the CUAPS pressure application device, the transducers were installed laterally on the Perspex tube at 5.1 cm from the top (or 15.22 cm from the bottom) of the CPB (see Figures 4.1 and 4.2). The excess PWP generated by the each pressure increment was allowed to dissipate for at least 2 hours before the next pressure increment was applied. Figure 4.2 presents a schematic diagram comparing the drainage and boundary conditions in the CUAPS (incremental loading consolidation) and in an oedometer with PWP measurement.

4.2.3.5 Permeability tests: direct measurement of k_{sat}

Saturated hydraulic conductivity k_{sat} has a considerable effect on the consolidation behaviour of saturated CPB materials, as it controls water flow characteristics.

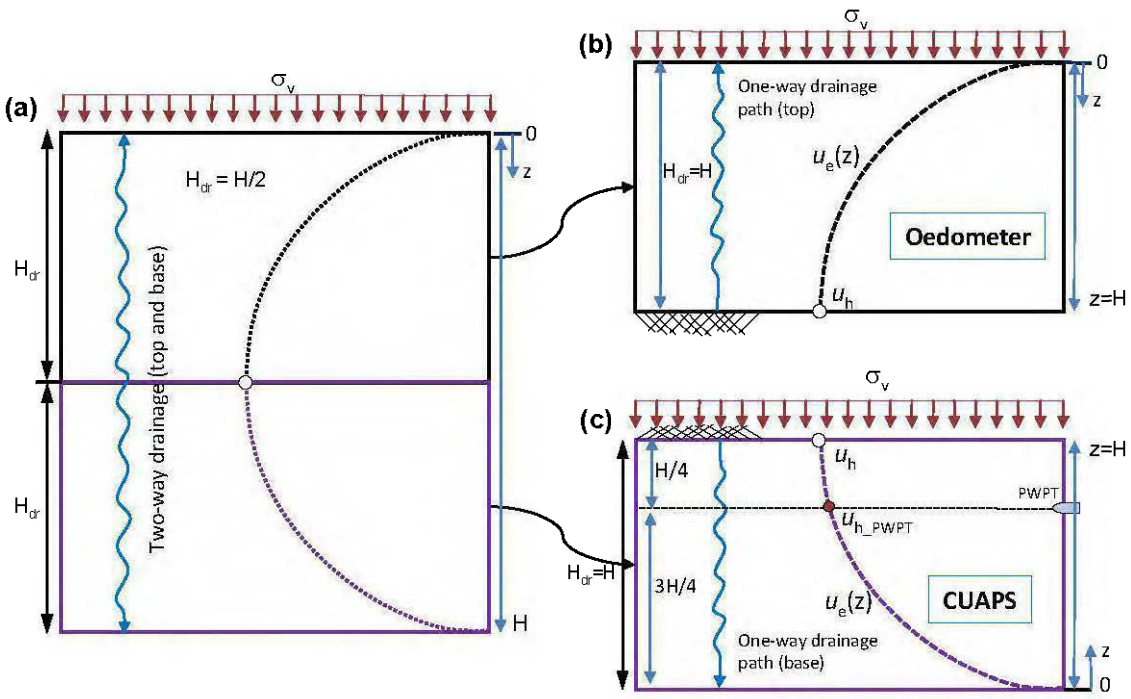

Figure 4.2 Drainage and boundary conditions during incremental load consolidation (ILC): a) general case of a two-way drainage system; b) one-way drainage in a conventional oedometer; c) one-way drainage in the CUAPS consolidation test.

In this study, the permeability tests were performed on samples that had undergone one-dimensional consolidation (after 10-hour consolidation testing), in accordance with ASTM standard D5856 (ASTM, 2002c) methods, using the falling head method (the CUAPS is used as a rigid wall permeameter). These tests were performed on two different sample types: control (uncemented tailings) and 4.5 wt% binder CPB samples (GU–Slag@20:80 wt%) according to curing times (0, 1, 3 and 7 days). Due to the nature of the compacted samples, a special laboratory technique was used to saturate the samples. Distilled water was pumped from bottom to top of the CPB samples (upward flow) at a constant flow rate while a constant pressure for each test was maintained at the base of the CUAPS apparatus (the calculated degree of saturation of paste backfill samples kept constant at values greater than 95%). The pumping was used only to raise the hydraulic gradient to meet Darcy's law (constant volume condition), and was halted at the start of the k_{sat} measurements. Depending on binder content

(0 – control or 4.5 wt% of GU-Slag@20:80) and curing time (0–7 days), the constant pressure varied between 35 kPa and 55 kPa, while elapsed time at constant pressure during each specified measurement recording varied from 2 to 23 minutes. Measured k_{sat} was corrected to that of 20 °C, k_{sat_20}, by multiplying k_{sat} by the ratio of water viscosity at test temperature T to water viscosity at 20 °C, R_T, as follows: $k_{sat\_20} = R_T \times k_{sat}$ (see ASTM, D5856, 2002c). A correction factor R_T of 0.976 was used for the water viscosity at a test temperature of 21 °C. The k_{sat} tests were performed within a relatively short time (less than 2.5 hours). To determine the average k_{sat}, at least two k_{sat} measurements were taken on consolidated samples for each recipe and curing time.

4.2.3.6 Determination of the coefficient of consolidation

For each pressure increment, c_v can be derived from the settlement s–time t data, back-calculated from the permeability coefficient k_{sat} and m_v data, or from the CUAPS excess pore water pressure data using Terzaghi's solution. In most cases, two methods are commonly used to determine c_v from s–t data: the logarithm of time method (logt or Casagrande's method), which assumes no creep and is based on 50% consolidation, and the square root of time method ($\sqrt{t}$ or Taylor's method), which allows for creep and is based on 90% consolidation (e.g. McCarthy, 2007). In this study, neither Casagrande's nor Taylor's method was used to derive c_v due to lack of sufficient settlement-time data. Instead, c_v was back-calculated from permeability coefficient k_{sat} and m_v. From Terzaghi's theory of consolidation (Terzaghi, 1925), the coefficient of consolidation c_v is expressed well in the Eq. 4.1. In this equation, the a_v and m_v can be determined from the void ratio e–effective stress σ'_v curve and the strain ε–effective stress σ'_v curve, respectively.

$$c_v = \frac{k_{sat}}{m_v \gamma_w} = \frac{1+e_0}{a_v}\frac{k_{sat}}{\gamma_w} \tag{4.1}$$

where c_v = coefficient of consolidation (cm^2/s), k_{sat} = permeability coefficient (cm/s), a_v = coefficient of compressibility (m^2/kN), m_v = coefficient of volume compressibility (m^2/kN), γ_w = unit weight of water (kN/m^3) and e_0 = initial void ratio (dimensionless value).

4.3 RESULTS AND INTERPRETATION

4.3.1 Effect of cementation on compression curves

Figure 4.3 presents the evolution of K_0 compression curves described by the normalized void ratio – effective stress (e/e_o –logσ'_v) relationships for CPB samples prepared with different binder contents B_w: (0 – control, 1, 3, 4.5 and 7 wt%; binder type: GU–Slag@20:80 wt%).

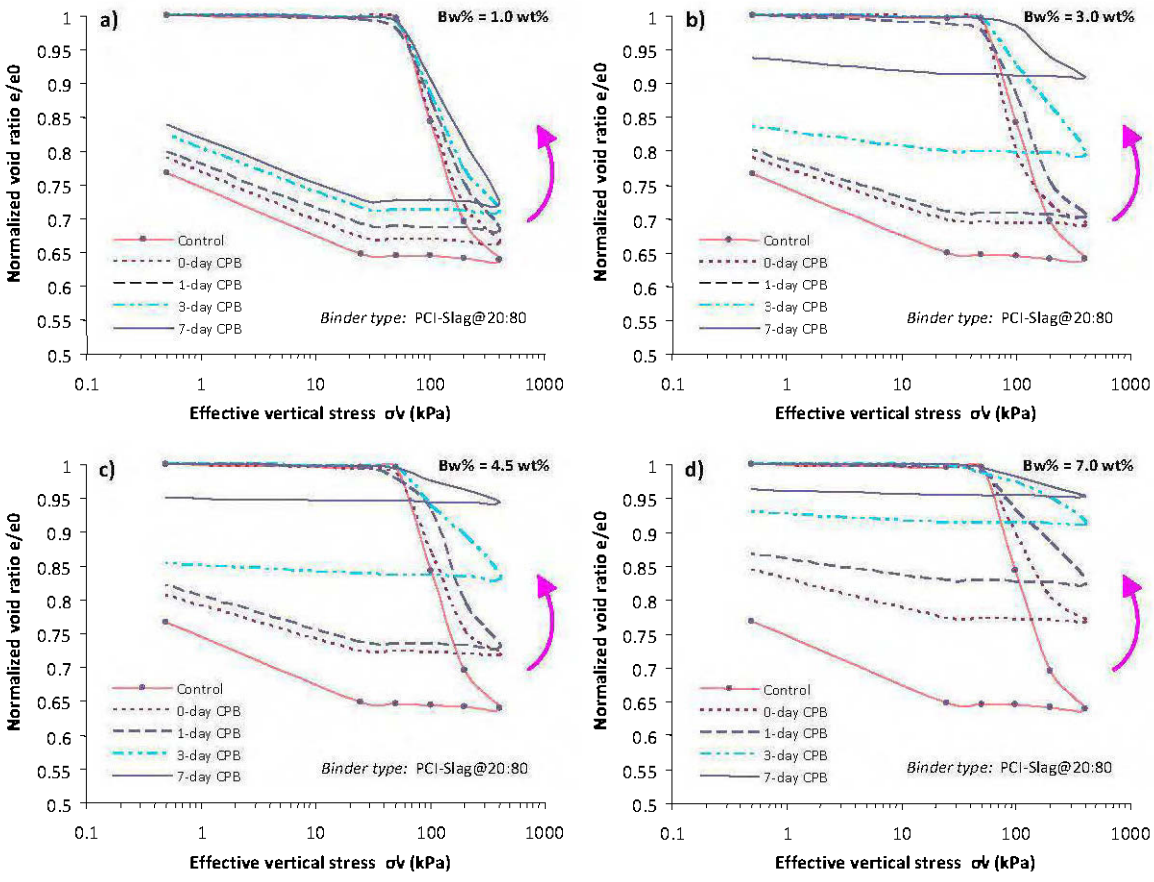

Figure 4.3 Evaluation of typical e/e_o–logσ'_v (compression) curves for CPB samples having different binder contents: a) 1 wt%; b) 3 wt%; c) 4.5 wt%; and d) 7 wt%. CPB samples are prepared using a slag blended binder (GU–Slag@20:80 wt%) and accompanied with uncemented mine tailings as a control sample.

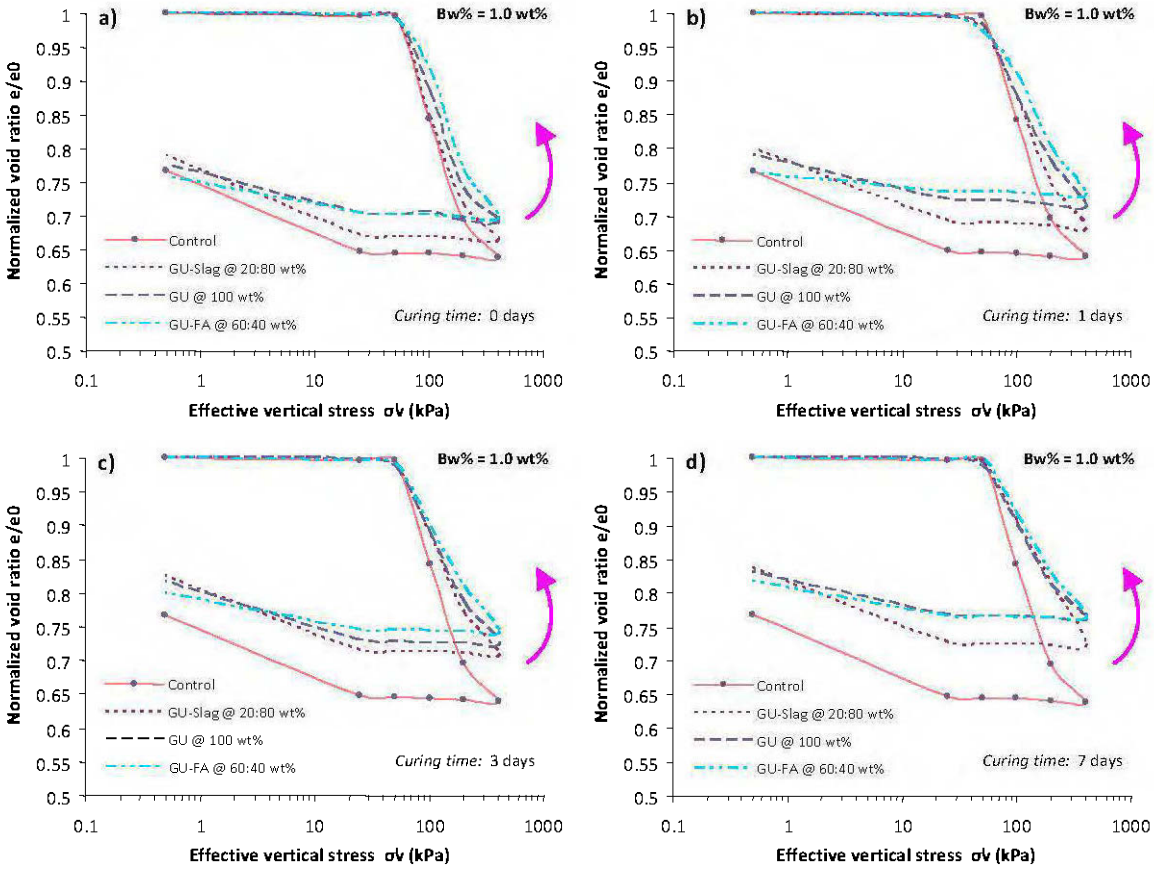

Figure 4.4 Comparison of typical e/e_0–logσ'_v (compression) curves for CPB samples with 1 wt% binder after different curing times: a) 0 days; b) 1 days; c) 3 days; and d) 7 days. CPB samples are prepared using three binder types (GU–Slag@20:80 wt%, GU@100 wt% and GU–FA@60:40 wt%) and accompanied with uncemented mine tailings as a control sample.

Figures 4.4 and 4.5 present a comparison of the K_0 compression curves for CPB samples prepared using two other binder types (GU–FA@60:40 wt% and GU@100 wt%) at binder contents of 1 and 4.5 wt% after the same curing times (see Appendix D). Figure 4.3 shows that when binder content B_w is relatively low (≤ 1 wt%), the initial void ratio e_0 is similar, regardless of curing time. However, e_0 is actually the void ratio during cementation at the end of curing times (0, 1, 3 and 7 days). The e_0 increases slightly when binder content increases more than 2 wt% (3 wt% < B_w < 7 wt%). This is probably due to the increase in volume of capillary pores with increased binder. Figure 4.3 also shows that, for a given binder content, the slope of virgin compression line (VCL) flattens with increasing curing time (or stiffness).

Overall, these curves show that once cement bonds between tailings particles are formed after the different curing times, CPB starts resisting to the applied vertical pressure and has almost the same e_0. The increased compression pressure then starts breaking some of the formed cement bonds, corresponding to primary yielding (Rotta et al., 2003). The applied pressure corresponding to this primary yielding is the yield stress σ_{vY} (or critical pressure). Below σ_{vY}, the hardened CPB behaviour is controlled mainly by cement bonds, whereas beyond σ_{vY}, a granular behaviour seems to play a major role in reducing void ratio prior to compression. Thus, after primary yielding, e_0 drops sharply due to the combined effect of the accelerated onset of cementitious matrix destruction and particle rearrangement due to drainage.

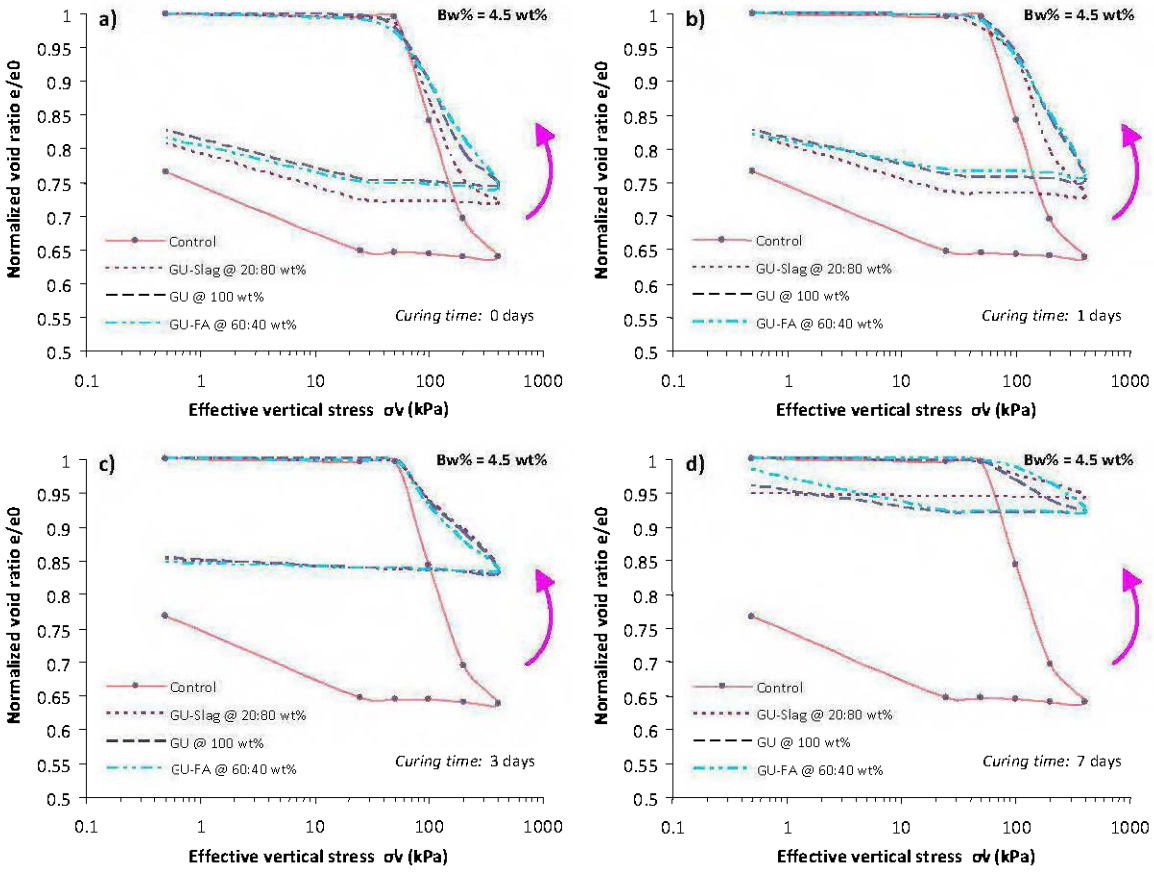

Figure 4.5 Comparison of typical e/e_0–logσ'_v (compression) curves for CPB samples with 4.5 wt% binder after different curing times: a) 0 days; b) 1 days; c) 3 days; and d) 7 days. CPB samples are prepared using three binder types (GU–Slag@20:80 wt%, GU@100 wt% and GU–FA@60:40 wt%) and accompanied with uncemented tailings as a control sample.

For example, the initial and final (after loading with 400 kPa pressure consolidation) void ratios of CPB samples (e_0, e_f) with 1 wt% binder are respectively (1.12, 0.89), (1.14, 0.92), (1.15, 0.95) and (1.15, 0.97) for curing times of 0, 1, 3 and 7 days. For 7 wt% binder, e_0 and e_f are respectively (1.17, 0.99), (1.18, 1.03), (1.20, 1.12) and (1.21, 1.17) at the identical curing times of 0, 1, 3 and 7 days. Table 4.2 presents the calculated relative degree of void ratio reduction $R_e = 100\times(e_0–e_f)/e_0$ for both binder type GU-Slag (B_w varies between 0 and 7 wt%) and binder types GU alone and GU-FA (only for a binder content of 1 and 4.5 wt% for comparison purposes) according to curing time (0–7 days). It can be seen that for a given curing time, R_e decreases with increasing binder content, and for a given binder content, R_e decreases in the course of curing time. The compression resistance is highest for a 7-day curing time, which can most likely be explained by bond development, mainly due to the progressive hardening of CPB with hydration.

Table 4.2 Calculated percent reduction in initial void ratio for the GU–Slag@20:80 wt% binder type (B_w varies between 0 and 7 wt%) and the GU 100 wt% and GU–FA@60:40 wt% binder types (only B_w values of 1 and 4.5 wt% for comparison purposes).

Curing time (days)	Relative reduction in initial void ratio, $R_e = 100\times(e_0 - e_f)/e_0$, (%)				
	Control	GU-Slag @ 20:80 wt%			
	B_w = 0 wt%	B_w = 1 wt%	B_w = 3 wt%	B_w = 4.5 wt%	B_w = 7 wt%
0	23	21	21	19	15
1	23	20	20	18	13
3	20	17	16	15	7
7	18	16	6	5	4

Table 4.2 (Continued).

Curing time (days)	Relative reduction in initial void ratio, $R_e = 100\times(e_0 - e_f)/e_0$, (%)				
	Control	GU 100 wt%		GU-Fly ash @ 60:40 wt%	
	B_w = 0 wt%	B_w = 1 wt%	B_w = 4.5 wt%	B_w = 1 wt%	B_w = 4.5 wt%
0	23	24	23	24	18
1	23	21	21	20	17
3	20	16	15	18	13
7	18	15	7	16	3

In addition, from Figures 4.4 and 4.5 and Table 4.2, it can be inferred that for a given binder content and curing time, the void ratio of slag-based binder (GU–Slag@20:80 wt%) backfills is lower than those obtained with type C fly ash-based binder (GU–FA@60:40 wt%) and general use Portland cement (GU@100 wt%) backfills. The change in terms of void ratio of CPB samples containing 1 wt% binder is slightly greater than for CPB with 4.5 wt% binder. For 1 wt% binder (see Figure 4.4 and Table 4.2), the relative degrees of reduction in initial void ratios of 0-day cured CPB samples is 21% for GU–Slag binders and 24% for GU cement and GU–FA binders. These variations in void ratio reduction are 20%, 21% and 20% for 1-day, 17%, 16% and 18% for 3 days, and 16%, 15% and 16% for 7 days, respectively. In the same way, for 4.5 wt% binder (see Figure 4.5 and Table 4.2), the changes in void ratio reduction are respectively 19%, 23% and 18% for 0-day, 18%, 21% and 17% for 1-day, 15%, 15% and 13% for 3 days, and 5%, 7% and 3% for 7 days for the same binder types. Meanwhile, the calculated percent reduction in initial void ratio for control samples is 23%, 23% and 20% and 18% for curing times of 0, 1, 3 and 7 days, respectively.

These results show that binder type plays an important role in the consolidation behaviour of CPB samples. It can be seen in Figures 4.3 to 4.5 that although the three different binder types exhibit fairly similar consolidation behaviour over the effective stresses, they have somewhat different curve shapes depending on the binder amount and curing time. In general, higher binder contents give lower void ratio reductions after 7-day curing, whatever binder type. The fact that slag-based binders consistently produce lower void ratios than general use Portland cements can be explained by their good performances, which in turn can be explained by their pozzolanic properties and their high hardening rate. The hardening is the result of cement hydration and precipitation of various hydrated and/or sulphated phases, contributing to the cohesion of the matrix by filling inter-granular voids. Considering that as curing time increases, cementitious products formation increase, thus the corresponding void ratios are significantly reduced.

4.3.2 Effect of cementation on compressibility behaviour

Compressibility parameters such as compression index C_c obtained from the slopes of the VCL portions and rebound of e–logσ'_v curves, as shown in Figures 4.3 to 4.5, are commonly used to determine consolidation settlement. In this study, only the change of C_c is considered, because the slope of the rebound curves does not vary with binder content or curing time.

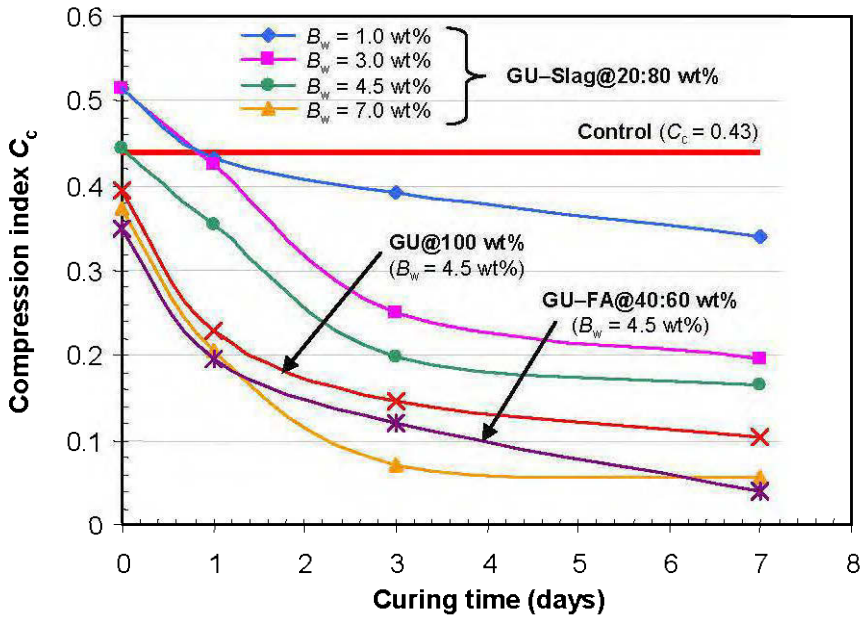

Figure 4.6 Variation in compression index with curing time for different CPB samples as a function of binder content. Samples are compared using three different binder types at a binder content of 4.5 wt%.

Figure 4.6 presents the variation in C_c with curing time for CPB samples containing slag based binders at five different binder contents (0 – control, 1, 3, 4.5 and 7 wt%), compared to specimens made with the two other binder types (GU cement and GU-FA binder), at binder contents of 4.5 wt%. Independently of binder content, the compression index C_c of CPB decreases non-linearly when curing time increases from 0 to 7 days. For control samples (uncemented tailings), C_c is nearly constant at 0.43 over the curing times, whereas for CPB

samples containing slag based binders, C_c is 0.52, 0.43, 0.39 and 0.34 for 1 wt% binder and 0.37, 0.21, 0.07 and 0.06 for 7 wt% binder, respectively for the same curing times of 0, 1, 3 and 7 days. Note that by increasing binder content from 1 to 7 wt%, C_c is reduced by 28% and 83% for curing times of 0 and 7 days, respectively. As well, C_c is reduced by 34% and 85% for binder contents of 1 and 7 wt%, respectively. The highest decrease in C_c with curing time is obtained from the highest binder content (B_w = 7 wt%), because the CPB matrix becomes gradually stiff due to the hardening processes. Moreover, by comparing the C_c values of 0.45, 0.35, 0.19, and 0.17 for slag-based binders with those of normal Portland cements (0.39, 0.23, 0.15, and 0.11) and fly ash-based binders (0.35, 0.19, 0.12, and 0.04), when curing age is increased from 0 to 7 days, it can be seen that the highest C_c is obtained from slag-based binders ($C_{c\_GU\text{-}Slag} > C_{c\_GU} > C_{c\_GU\text{-}FA}$). The measured C_c for control samples are consistent with those reported in the literature for similar tailings samples (Stone et al., 1994; Aubertin et al., 1996; Morris et al., 2000; Qui and Sego, 2001; Shamsai et al., 2007). The C_c of the CPB samples used in this study compares well with that obtained on CPB with similar GSD curves. In fact, the C_c of the CPB samples in the literature is between 0.05 and 0.34 (Pierce, 1997) and between 0.064 and 0.25 (le Roux, 2004).

4.3.3 Evaluation of pore water pressure behaviour

Typical excess dissipation curves are presented in Fig. 7a for the CPB containing 4.5 wt% slag based binder after 0- and 1-day curing times at incremental pressures σ_v = 100, 200 and 400 kPa. It should be mentioned that no excess PWP was recorded by the PWP transducer for CPB samples cured under applied pressures of 25 and 50 kPa. This can be explained by either the effects of wall friction or the zero offset on the PWP transducers during calibration testing (Yilmaz et al., 2010). From Figure 4.7a, it can be seen that the excess PWP measured immediately after the applied pressure increment (peak PWP) is of certain percent of the incremental pressure σ_v. For the uncemented mine tailings, this percentage is 98%, 73% and 28% of the incremental pressure σ_v = 100, 200 and 400 kPa, respectively. This drastic decrease after the application of three successive pressure increments can be explained largely by water drainage. In reality, the drainage valve should have been closed during the

loading process, but unfortunately, it was not. The other factor that might have contributed to the apparent drop in peak pore water pressure (PWP) is the sampling time interval, which was set at 75 seconds. This interval was most likely too large to systematically record peak PWP. However, similar behaviour has been reported in the literature, but in soils (Sonpal and Katti, 1973; Chakrabarti et al., 1986).

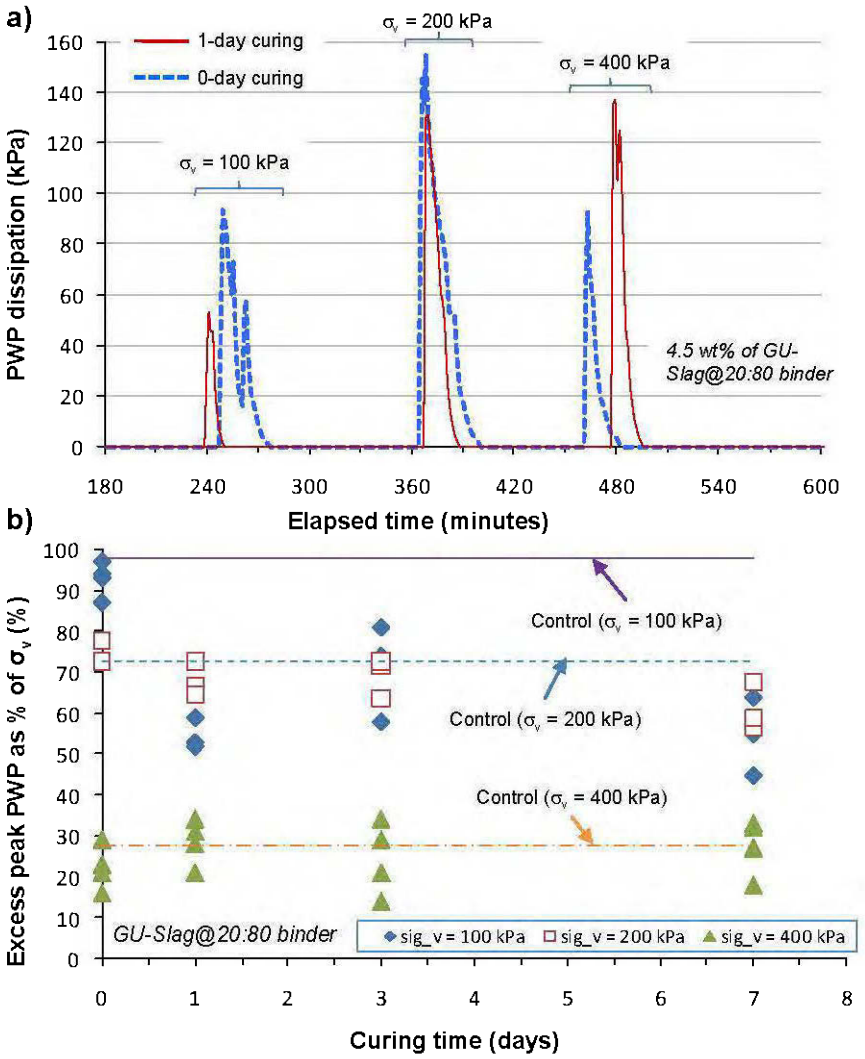

Figure 4.7 Plots of (a) change in pore water pressure (PWP) dissipation with time for CPB containing 4.5 wt% slag based binder based on only 0 and 1-day curing times and (b) variation in peak excess PWP as a percentage of applied pressure increment σ_v with curing time for control and CPB samples.

This behaviour is most likely due to specimen's microstructure changes with increasing compression stress, as well as the measurement system stiffness, air in the system, and the measurement method. When binder is added to the tailings, the percentage of PWP measured by the transducers is affected by both binder content (1 to 7 wt%) and curing time (0 to 7 days). For all CPB samples, the percentage range is 45–98%, 57–78% and 15–37% of the incremental pressure σ_v = 100, 200 and 400 kPa, respectively (see Figure 4.7b).

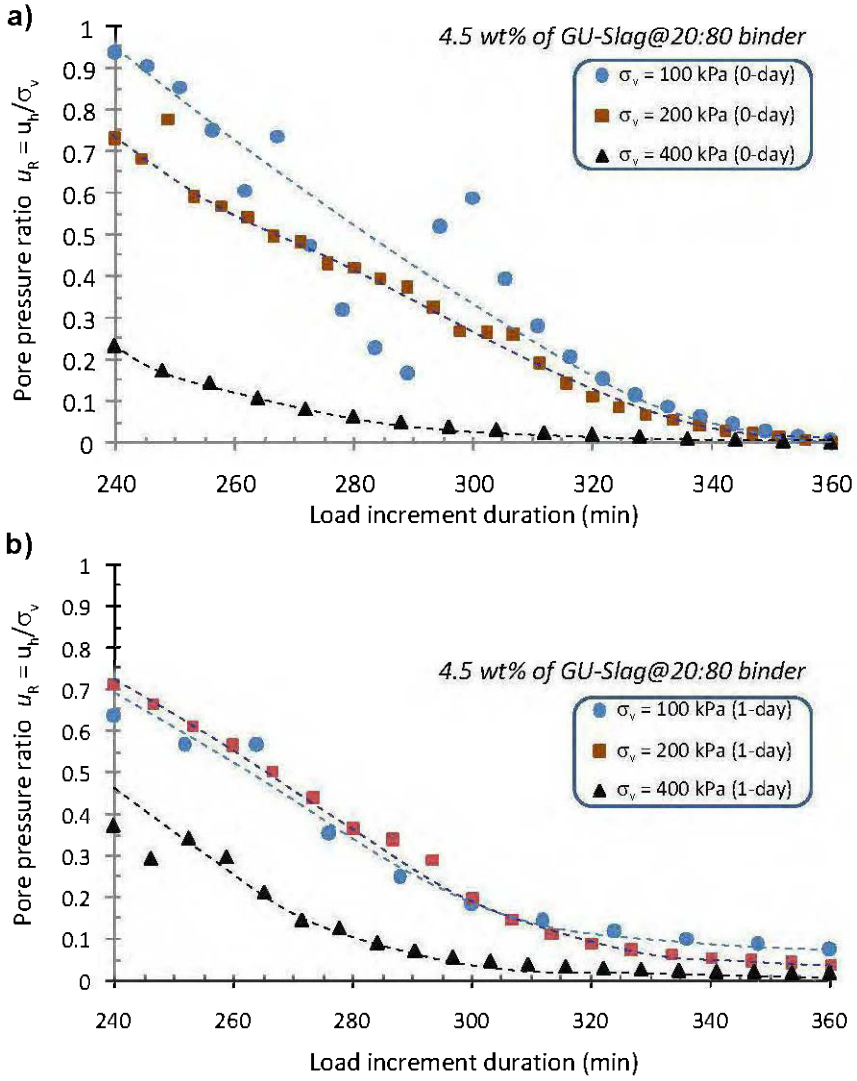

Figure 4.8 Variation in pore pressure ratio u_R with load increment duration for the CPB prepared with 4.5 wt% of GU-Slag@20:80 wt% and curing times: a) 0-day, b) 1-day.

From Figure 4.7b, the effect of added binder is evident when any amount of peak PWP reduction is compared to the one of uncemented tailings (horizontal lines), for all pressure increments. This is probably due to the hardening process within CPB samples. The excess PWP behaviour can also be investigated through the pore pressure ratio u_R, earlier defined as (u_h/σ_v). This parameter quantifies to some extent the degree of PWP development within the sample during consolidation. Figure 4.8 presents the variation in u_R versus LID for CPB samples prepared with 4.5 wt% of the GU-Slag@20:80 wt% binder and for two curing times (0 and 1 day). All data were plotted in the same LID, or 2 hours (i.e., between 240 and 360 min, which corresponds to 360 – 240 = 120 min) to facilitate identification of the effect of pressure increments on PWP build-up. From Fig. 8, it can be observed that the excess PWP significantly drops with the successive increments of vertical applied pressure, particularly between σ_v of 200 and 400 kPa. It should be also noted that the excess PWP developed immediately after CPB preparation (Figure 4.8a) is higher than the one within the 1-day cured samples (Figure 4.8b). These results suggest that particular attention should be paid to the method of PWP measurement to capture the whole behaviour of PWP development within CPB samples.

4.3.4 Saturated hydraulic conductivity of consolidated CPB

The saturated hydraulic conductivity k_{sat} (or saturated coefficient of permeability) of both CPB and control samples (uncemented mine tailings) was measured with permeability tests using the CUAPS (after consolidation testing). Figure 4.9 shows the variation of k_{sat} in the course of curing time for the CPB control sample and the 4.5 wt% binder CPB sample prepared with the GU-Slag@20-80 wt% binder type. First, the measured average k_{sat} for the consolidated uncemented mine tailings is 7.7×10^{-6} cm/s. When 4.5 wt% binder is added to the tailings, k_{sat} decreases rapidly during the first 3 days of curing from 6.6×10^{-6} cm/s to approximately 5.1×10^{-7} cm/s (a decrease of nearly one order of magnitude). Up to 7 days of curing, k_{sat} continues to decrease to 3.1×10^{-7} cm/s, a major change of nearly 100% compared to the initial k_{sat}. The k_{sat} reduction is due to the gradual changes of the microstructure of cemented tailings by hydration products and mineral precipitation during curing.

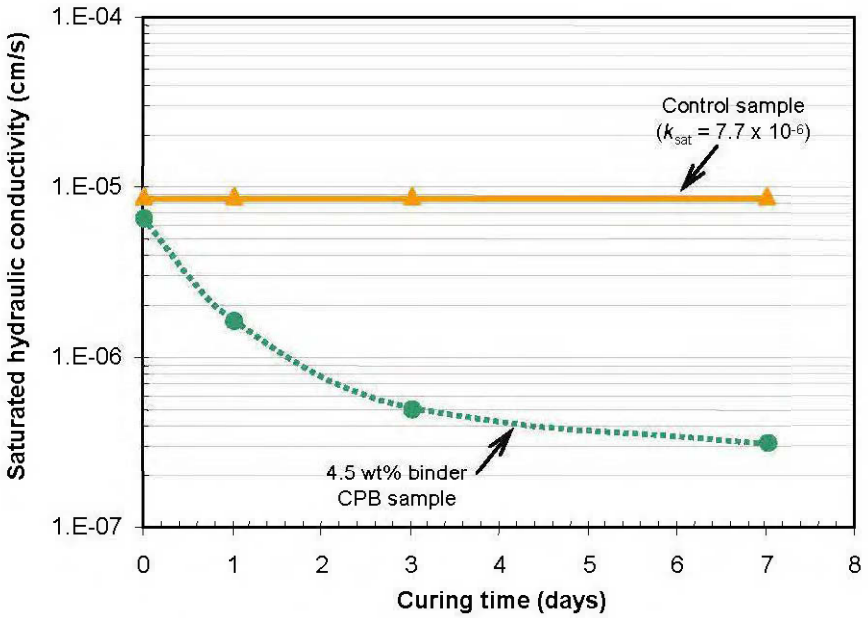

Figure 4. 9 Variation in saturated hydraulic conductivity k_{sat} with curing time for CPB samples prepared with 4.5 wt% of binder GU-Slag@20:80 wt% and uncemented tailings.

However, Godbout et al. (2007) suggest that k_{sat} variation is due not only to microstructure change, but likely depends on other factors as well, such as chemical water retention and gel formation. From the permeability tests, the measured k_{sat} of uncemented tailings falls into a typical range (between 1×10^{-4} and 1×10^{-7} cm/s) for consolidated tailings as it can be found in the literature (Bussière, 1993, 2007; Aubertin et al., 1996; Qiu and Sego, 2001; Shamsai et al., 2007). In addition, the k_{sat} obtained on CPB is fairly similar to those found by various researchers (Pierce et al., 1998; Belem et al., 2001; Mohamed et al., 2002; le Roux, 2004; Godbout et al., 2007). An experimental study by le Roux (2004) on early age CPB samples showed that CPB permeability reduces with curing time and stabilizes at about 5×10^{-6} cm/s. Belem et al. (2001) evaluated the k_{sat} of CPB having 5 wt% binder of slag blended binder with curing time (0, 1, 2, 5, 7, 14 and 28 days) and observed a rapid k_{sat} reduction from 10^{-5} to 10^{-8} cm/s during the first 7 days, which remained constant after 7 days of curing. Mohamed et al. (2002) examined backfills stabilized using a combination of lime, type C fly ash and aluminium and found permeability values ranging between 5×10^{-4} and 1.96×10^{-6} cm/s. Godbout et al. (2007) also observed a fairly similar change in the k_{sat} (similar to Figure 4.9)

within CPB using the same binder type and content at the same curing time, although values are slightly lower than the k_{sat} data of the present study.

4.3.5 Calculation of the coefficient of consolidation

The coefficient of consolidation c_v is an important parameter for estimating the settlement rate. Based on Terzaghi's theory (Eq. 1), c_v is back-calculated from the measured k_{sat}, m_v and γ_w. Table 4.3 contains the calculated m_v for the range 100–400 kPa of effective stress. Table 4.4 contains the directly measured k_{sat} using the CUAPS apparatus for the control sample and the CPB samples prepared with the binder 4.5 wt% of GU-Slag@20:80 wt% binder type and the corresponding back-calculated c_v. Figure 4.10 shows the evolution of back-calculated c_v based on measured k_{sat} (see Table 4.4). This figure shows that the calculated c_v for the control sample remains constant at 0.08 cm^2/s, whereas the c_v of the CPB containing 4.5 wt% binder tends to reduce over the curing time. c_v drops sharply from 0.081 cm^2/s initially to 0.014 cm^2/s after a curing time of 3 days, and reaches a plateau at 7 days thereafter. A significant change (82%) has taken place between the preparation time and last curing times.

Table 4.3 Calculated m_v value for CPB samples prepared with GU–Slag@20:80 wt% binder

Curing time (days)	Coefficient of volume compressibility, m_v (m^2/kN)				
	Control	B_w = 1 wt%	B_w = 3 wt%	B_w = 4.5 wt%	B_w = 7 wt%
0	9.89E-04	9.76E-04	9.63E-04	8.29E-04	6.91E-04
1	9.89E-04	8.11E-04	7.94E-04	6.56E-04	3.77E-04
3	9.89E-04	7.27E-04	4.67E-04	3.65E-04	1.30E-04
7	9.89E-04	6.36E-04	2.68E-04	2.10E-04	1.05E-04

Table 4.4 Back-calculated c_v from direct measurement of k_{sat} in both control samples and 4.5 wt% binder CPB samples prepared with GU–Slag@20:80 wt% binder

Curing time (days)	k_{sat} (cm/s) - direct		c_v back-calculated (cm^2/s)	
	B_w = 0 wt%	B_w = 4.5 wt%	B_w = 0 wt%	B_w = 4.5 wt%
0	7.74E-06	6.63E-06	7.97E-02	8.15E-02
1	7.74E-06	1.69E-06	7.97E-02	2.63E-02
3	7.74E-06	5.06E-07	7.97E-02	1.41E-02
7	7.74E-06	3.11E-07	7.97E-02	1.51E-02

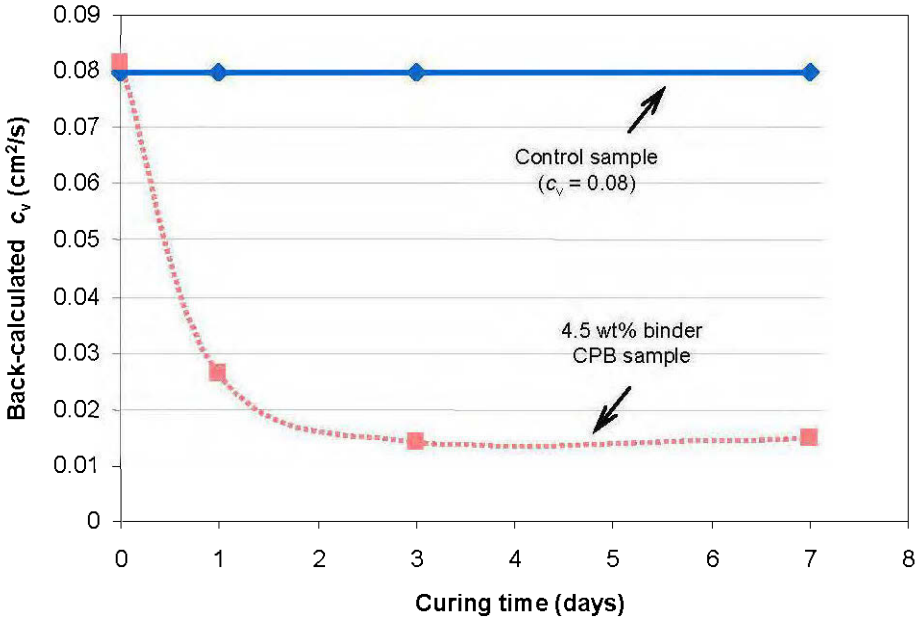

Figure 4.10 Variation in the back-calculated coefficient of consolidation c_v with time for CPB prepared with 4.5 wt% of binder GU-Slag@20:80 wt% and uncemented tailings.

It can be seen that with increasing quantity of binder added to the mixture, the material properties of CPB materials change drastically due to the gradual growth of the cement gels in the capillary pores over the curing time. With the rapid increase in stiffness of the backfill, the coefficient of consolidation increases rapidly as well.

The c_v data reported in the literature for uncemented tailings suggest that the consolidation coefficient usually varies between 1×10^{2} and 1×10^{-1} cm^2/s for coarse tailings and between 1×10^{-1} and 1×10^{-3} cm^2/s for fine tailings (Bussière, 1993; 2007; Aubertin et al., 1996). In the present study, the value obtained for the uncemented tailings (control sample) is typical for fine tailings, which is consistent with some literature findings: Stone et al. (1994), Morris et al. (2000) and Qui and Sego (2001). A recent study by Shamsai et al. (2007) on copper whole tailings tested for a range of initial void ratios e_0 between 0.3 and 1.1 found a c_v of 5×10^{-3} – 2×10^{-2} cm^2/s.

4.3.6 Preliminary single regression model for consolidation parameters

Knowledge of the one-dimensional consolidation parameters range variation (e.g., C_c and c_v) can be very useful in the pre-feasibility studies of any backfill operation and in numerical modeling using computational codes. The compression index C_c is used to predict the amount of settlement that will take place, and the coefficient of consolidation c_v is a rate factor used to predict how long it will take for a given amount of compression to take place (and to back-calculate saturated hydraulic conductivity). It is worth emphasizing that adding binder to mine tailings (CPB) largely changes its compressibility properties, mainly due to cementation during curing. However, the rational design of CPB requires the use of these parameters in basic calculations. An alternative to lengthy and costly laboratory testing would be to establish empirical or semi-empirical equations for predicting these parameters.

Accordingly, an optimal method for variables normalization was developed to obtain a single function describing the variation according to the curing or elapsed time for various binder contents. This function gives a good correlation between normalized parameters. The reduced or normalized time factor t_n, which is the combination of curing time and binder content effects, was first defined as follows (Eq. 4.2):

$$t_n = \frac{1+2t}{1+2B_w} \tag{4.2}$$

where t = curing time (day) and B_w = mass binder content (wt%).

It was also ascertained that any parameter λ_p whose variation is a function of both curing time t and binder content B_w is affected (proportionality) by the normalized time factor t_n raised to the exponent 3: $\lambda_p(t_n)^3$.

Hence, plotting a reduced variable $Y = \lambda_p(t_n)^3$ against the reduced time factor $X = t_n$ gives a power law function $Y = aX^b$ whose coefficients a and b can be readily determined by curve

fitting. Substituting Y and X [$\lambda_p(t_n)^3 = a(t_n)^b$] yields the single empirical model for predicting $\lambda_p = C_c$, c_v and e_f for curing times and binder contents, as follows (Eqs. 4.3 and 4.4):

$$\lambda_p(t_n)^3 = a(t_n)^b = a\left(\frac{1+2t}{1+2B_w}\right)^b \tag{4.3}$$

In Eq. 4.3 the final exponent will be $c = b–3$, hence

$$\lambda_p = a\left(\frac{1+2t}{1+2B_w}\right)^c \tag{4.4}$$

It should be mentioned that in the regression technique used the "independent" variable Y depends on the dependent variable X, mainly to concurrently take into account the double effect of binder content B_w and curing time t, which are described by the normalized time factor t_n. Figure 4.11 graphically presents the variation in the initial values of parameters C_c, c_v and e_f and their corresponding normalized values. It can be seen that the cubic function describes well all compression parameters, with a coefficient of correlation r close to 1. All the power law constants a and c and their corresponding coefficients of correlation r are listed in Table 4.5. From Eqs. 4.3 and 4.4, the C_c and c_v parameters can be predicted for estimating settlement magnitude or the rate at which it occurs for preliminary design needs. However, it should be mentioned that the range of effective stress is 100–400 kPa for the m_v calculation, and hence for the c_v back-calculation, curing times range between 0 and 7 days.

Table 4.5 Power law model parameters for the CPB samples tested

Parameters that can be predicted by the power law	X variable	Y variable	Constants Y = a*(X)^c		Coefficient
			a	*c*	*r*
Compression index C_c	$(1+2t)/(1+2B_w)$	$C_c\times(X)^3$	0.3921	-0.0298	0.999
Coefficient of consolidation c_v		$c_v\times(X)^3$	0.0148	-0.6526	1
Final void ratio e_f		$e_f\times(X)^3$	0.7811	0.0376	1

Abbreviations t and $B_{w\%}$ stand for curing time (days) and binder content (wt%), respectively.

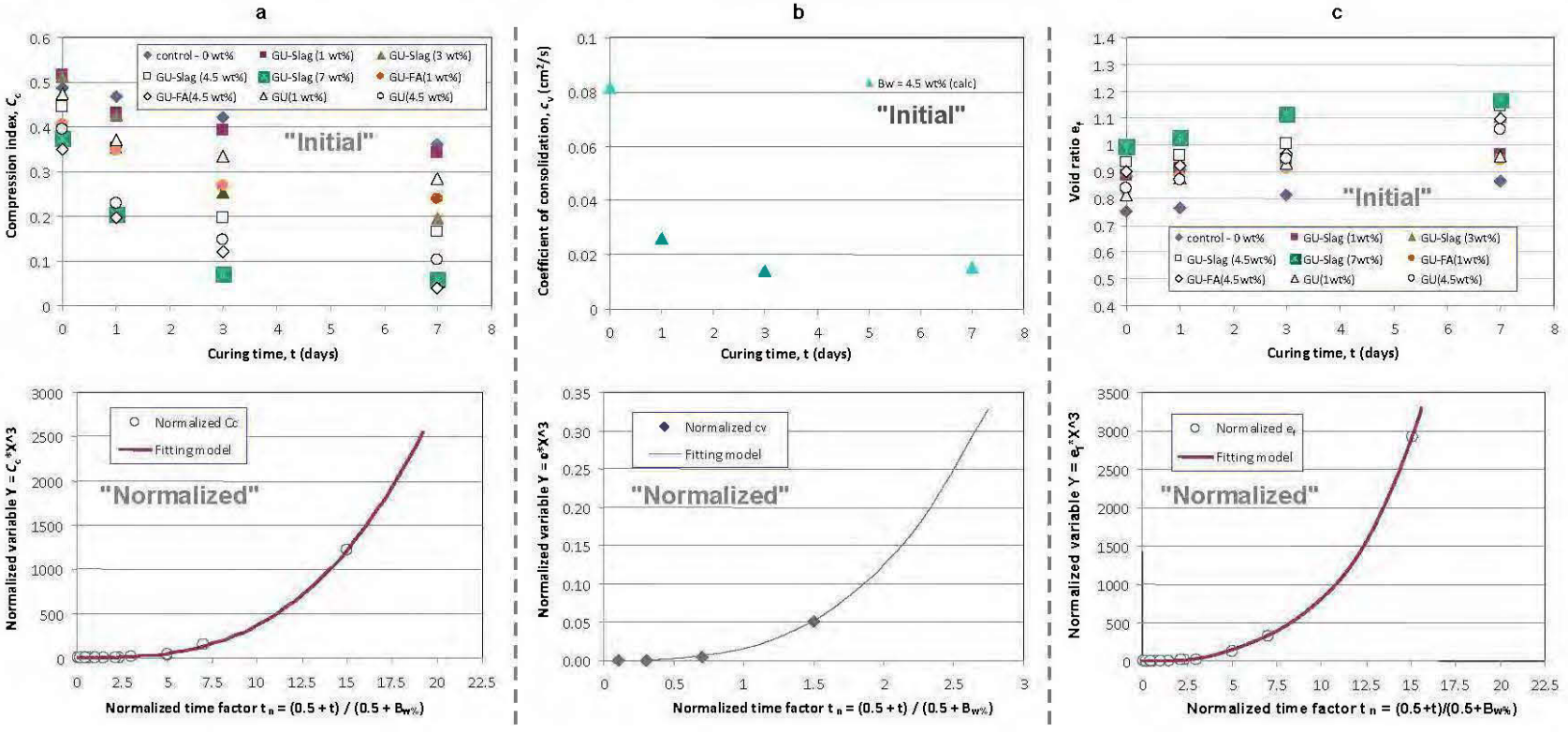

Figure 4.11 Variation in the compression index C_c, coefficient of consolidation c_v and void ratio e_f for three binder types (GU–Slag@20:80 wt%, GU–FA@40:60 wt% and GU@100 wt%) for four curing times (0, 1, 3 and 7 days) and five binder contents (0 – control, 1, 3, 4.5 and 7 wt%): a) initial and normalized C_c; b) initial and normalized c_v; and c) initial and normalized e_f.

4.4 DISCUSSION

The first issue for discussion is the difficulty of applying classical soil mechanics methods to CPB materials. The main challenge is the perpetual changes in terms of physical and mechanical properties that happen within CPB during curing. For instance, for the CPB material, there is no notion of disturbed or undisturbed soil, or even normally consolidated or over-consolidated soil. As mentioned above, CPB can be consolidated in the mine stope under several types of compression loading. To the authors' knowledge, the one-dimensional consolidation curves of CPB samples are the first attempt and regarded as an original contribution to the paste backfill materials. As shown in Figures 4.3 to 4.5, the curve shapes are typical of those obtained with oedometer testing. Instead of anisotropic K_0-consolidation, CPB could undergo isotropic compression. The argument for K_0-consolidation is based on the assumption that an underground stope is filled only at the end of the wall convergence. This means that, once CPB placed underground, it would be at rest state (K_0 condition). A potential issue concerning the compression curves presented in Figures 4.3 to 4.5 is that the primary yielding stress, which corresponds to the onset of cement bond destruction, appears to be constant at 50 kPa regardless of cement content or curing time. Only the slope of the VCL (straight line of the e–logσ'_v curve) and void ratios show apparent variation with the effect of hardening. In reality, this constant stress value of 50 kPa was also observed for the uncemented mine tailings (control sample), which appears improbable, even assuming some hardening due to other chemical reactions and precipitations (e.g., oxidation of sulphide minerals, sulfate precipitations, etc.). This type of behaviour has not been observed in the few existing previous works (le Roux et al., 2002). The observed constant yield stress is most likely owing to the rigidity of the modified CUAPS apparatus used in this study. Further research should be undertaken to overcome this shortcoming.

For preliminary design needs, Eqs. 4.3 and 4.4 and Table 4.5 can estimate the coefficient of compressibility C_c of CPB with good accuracy (Eq. 4.4), with a coefficient of correlation r = 0.999). The constants a and b given in Table 4.5 are obtained using additional data from the compression tests performed on CPB prepared with two different binder types: general use Portland cement GU@100 wt% and fly ash-based binder GU-Fly Ash@60:40wt%. Apart

from the effect of initial tailings GSD in the CPB mixtures, this predictive equation could be used for other types of cemented backfills, such as slurry and rock fills. Of course, the compression behaviour of CPB prepared with very fine tailings or tailings containing clay particles could differ greatly from that presented in this study. Constants a and c, as shown in Eq. 4.4, can be adjusted to reflect the GSD effect. In fact, the general power law model (Eq. 4.4) could always be improved by adding more data from different tailings sources and types to extend its use by reflecting a wider range of possible C_c values. However, this law provides a practical first approximation tool to predict the CPB compressibility parameters (for similar recipes) as a function of curing time and binder content.

Concerning the prediction of the coefficient of consolidation c_v (Eq. 4.4), it should be also mentioned that the limited number of data used for the regression analysis were back-calculated from directly measured k_{sat} values using the CUAPS apparatus after consolidation was completed (σ'_v = 400 kPa). Moreover, the final void ratio e_f of consolidated paste backfills is strongly affected by binder content and effective stress. As expected, the increase in curing time involves the increase in e_f, most likely due to the gradual formation of hydration products within the CPB. Note that the increased effective stress helps reduce the final void ratio for a given binder content and curing time. Overall, the above comments about C_c also hold true for c_v and e_f. The authors believe that for the same range of effective stress σ'_v (100–400 kPa), the same type of binder GU-Slag@20:80 and the same curing time range (0–7 days), Eq. 4.4 can be used to predict c_v and the final void ratio e_f with acceptable level of confidence.

4.5 CONCLUSIONS

A series of experiments, including the one-dimensional consolidation, pore water pressure dissipation and saturated hydraulic conductivity tests, were conducted on consolidated mine tailings and CPB materials cured before the application of different pressure increments (varying from 25 to 400 kPa) and prepared with different binder contents (0 – control, 1, 3, 4.5 and 7 wt%). All tests were performed using an innovative laboratory apparatus called

CUAPS (curing under applied pressure system). CPB samples were allowed to cure for time periods of 0, 1, 3 and 7 days. The results underscore the contribution of cementation and incremental pressure on consolidation behaviour (i.e., the compression index C_c and excess PWP dissipation) and hydrogeological properties (mainly saturated hydraulic conductivity k_{sat} measured with CUAPS and back-calculated coefficient of consolidation c_v) of uncemented tailings and CPB material. The main conclusions can be summarized as follows:

- With increased strength and stiffness due to cement hydration, the void ratio and deformation of CPB materials decreases noticeably. Less water thus needs to be expelled to dissipate pore water pressure during curing, producing an accelerated consolidation rate. The compression resistance of CPB samples increases with increased binder content for a given curing time. Consolidation characteristics (compression index C_c) of CPB samples are greatly affected by the content and type of binder as a function of curing time. Different binder types produce different consolidation behaviours, depending on binder content. The overall trend is that C_c decreases with increasing binder content and curing time. For the PCI-Slag @ 20:80 wt% binder, the C_c of CPB samples respectively decreases from 0.52 to 0.3 for 1 wt% binder and from 0.37 to 0.06 for 7 wt% binder when curing time increases from 0 to 7 days.When comparing binder types at 4.5 wt% binder content, the C_c of CPB samples respectively decreases from 0.44 to 0.16 for GU-Slag@20:80 wt% binder type, from 0.39 to 0.11 for GU@100 wt% binder, and from 0.35 to 0.04 for GU-FA@40:60 wt% binder type when curing times increase from 0 to 7 days. This shows that the C_c of slag-based binder samples is consistently higher than for other binder materials (i.e., Portland cement and fly ash-based binder samples) for a given binder content and curing time ($C_{c\_GU\text{-}Slag} > C_{c\_GU} > C_{c\_GU\text{-}Fly\ ash}$).

- The PWP dissipation tests show that excess PWP measured immediately after the applied pressure increment (peak PWP) is a certain percentage of the incremental pressure σ_v. For uncemented tailings, this percentage is 98%, 73% and 28% of the incremental pressure σ_v = 100, 200 and 400 kPa, respectively. For CPB samples, the ranges are 45–98%, 57–78% and 15–37% of the incremental pressure σ_v = 100, 200 and 400 kPa, respectively. Both

these drastic decreases after the application of three successive pressure increments can be largely explained by water drainage. In addition, the excess PWP consistently drops with the application of successive pressure increments. The PWP developed within the initially prepared CPB is higher than that within the 1-day cured samples, mainly due to microstructural changes.

- Measured saturated hydraulic conductivity k_{sat} indicates an average constant value (7.7×10^{-6} cm/s) for uncemented tailings. With the addition of 4.5 wt% binder, k_{sat} decreases rapidly over the first 3 days of curing, from 6.6×10^{-6} to 5.1×10^{-7} cm/s (a decrease of one order of magnitude). After 7 days of curing, k_{sat} continues to decrease to a value of 3.1×10^{-7} cm/s, representing a nearly 100% change.

- The coefficient-of-consolidation c_v (back-calculated from the measured k_{sat}, m_v and γ_w) for the control sample (uncemented tailings) remains constant at 0.08 cm^2/s, whereas the c_v of the CPB containing 4.5 wt% of GU-Slag@20:80 wt% binder type tends to reduce over the curing time. c_v drops sharply from 0.081 cm^2/s at 0-day curing time to 0.014 cm^2/s after 3-day curing time, reaching a plateau at 7 days thereafter. A significant change (82%) occurred between the first and last curing times. It appears with increasing quantity of binder added to the mix, the CPB material properties change drastically due to the gradual growth of cementation products in the capillary pores over time. With the rapid increase in stiffness of the backfill, the c_v decreases rapidly as well.

A general power law fitting model was proposed to predict the compressibility parameters required for the preliminary design needs of the CPB materials. This preliminary study has improved the understanding of changes in the one-dimensional consolidation properties of consolidated backfills and opened up several interesting avenues for future investigation, such as the use of different binder combinations and laboratory testing conditions.

4.6 ACKNOWLEDGEMENTS

This work was generously financed by doctoral research grants awarded to the first author from the NSERC (Natural Sciences and Engineering Research Council of Canada) Discovery Grant Program, the Industrial NSERC-Polytechnique-UQAT Chair on Environment and Mine Wastes Management, and the Canadian Research Chair on Integrated Management of Mine Wastes. The authors would also like to thank the Canada Foundation for Innovation (CFI) for funding and GENIVAR for manufacturing the ten CUAPS set-ups used in this study. Special acknowledgements are extended to Pierre Trudel of G+Plus Industrial Plastics Inc. for his collaborative support in modifying the CUAPS apparatus, to David Bouchard, Yvan Poirier and Nil Gaudet of UQAT-URSTM laboratory for their technical support, and to Nathan Mutch of Lafarge North America Inc. for kindly providing the cement materials.

4.7 REFERENCES

ASTM Designation D4318-84, 1991a. Standard test method for liquid limit, plastic limit, and plasticity index of soils. In: *Annual Book of American Society of Testing Material Standards,* Vol. 04.08, ASTM International, West Conshohocken, PA, pp. 573–583.

ASTM Designation D421-85, 1999a. Standard practice for dry preparation of soil samples for particle size analysis and determination of soil constants. In: *Annual Book of American Society of Testing Material Standards,* Vol. 04.08, ASTM International, West Conshohocken, PA, pp. 8–9.

ASTM Designation D422-63, 1999b. Standard test method for particle size analysis of soils. In: *Annual Book of American Society of Testing Material Standards,* Vol. 04.08, ASTM International, West Conshohocken, PA, pp. 10–16.

ASTM Designation D2435, 1999c. Standard test method for one-dimensional consolidation properties of soils. In: *Annual Book of American Society of Testing Material Standards,* Vol. 04.08, ASTM International, West Conshohocken, PA, pp. 207–216.

ASTM Designation D4186, 1999d. Standard test method for one-dimensional consolidation properties of soils using controlled-strain loading. In: *Annual Book of American Society of Testing Material Standards,* Vol. 04.08, ASTM International, West Conshohocken, PA, pp. 477–481.

ASTM Designation C128-04, 2002a. Standard test method for density, relative density (specific gravity), and absorption of fine aggregate. In: *Annual Book of American Society of Testing Material Standards,* Vol. 04.01, ASTM International, West Conshohocken, PA, pp. 45–52.

ASTM Designation C143–90, 2002b. Standard test method for slump of hydraulic cement concrete. In: *Annual Book of American Society of Testing Material Standards,* Vol. 04.01, ASTM International, West Conshohocken, PA, pp. 68–76.

ASTM Designation D5856, 2002c. Standard test method for measurement of hydraulic conductivity of porous material using a rigid-wall, compaction-mould permeameter. In: *Annual Book of American Society of Testing Material Standards,* Vol. 04.08, ASTM International, West Conshohocken, PA, pp. 77–84.

ASTM Designation D6556, 2009. Standard test method for carbon black-total and external surface area by nitrogen adsorption. In: *Annual Book of ASTM Standards,* Vol. 04.08, ASTM International, West Conshohocken, PA, pp. 411–428.

Aubertin, M., Bussière, B., Chapuis, R.P., 1996. Hydraulic conductivity of homogenized tailings from hard rock mines. *Canadian Geotechnical Journal,* Vol. 33, No. 3 pp. 470–482.

Belem, T., Benzaazoua, M., 2008a. Design and application of underground paste backfill technology. *Geotechnical and Geological Engineering,* Vol. 26, No. 2, pp. 147–174.

Belem, T., Benzaazoua, M., 2008b. Predictive models for pre-feasibility cemented paste backfill mix design. In: *Proceedings of the 3rd International Conference on Post-Mining'08,* Nancy, France, February 6–8, pp. 155–169.

Belem, T., Benzaazoua, M., Bussière, B., 2000. Mechanical behaviour of cemented paste backfill. In: *Proceedings of the 53rd Canadian Geotechnical Conference,* Montreal, Quebec, Canada, October 15–18, pp. 373–380.

Belem, T., Bussière, B., Benzaazoua, M., 2001. The effect of microstructural evolution on the physical properties of cement paste backfill. In: *Proceedings of the 8th International Conference on Tailings and Mine Waste,* Vail, Fort Collins, Colorado, USA, A.A. Balkema: Rotterdam, January 16–19, pp. 365–374.

Belem, T., Benzaazoua, M., Bussière, B., Dagenais, A.M., 2002. Effects of settlement and drainage on strength development within mine paste backfill. In: *Proceedings of the 9th International Conference on Tailings and Mine Waste,* Vail, Fort Collins, Colorado, USA, A.A. Balkema: Rotterdam, January 27–30, pp. 139–148.

Belem, T., Harvey, A., Simon, R., Aubertin, M., 2004. Measurement and prediction of internal stresses in an underground opening during its filling with cemented fill. In: *Proceedings of the 5th International Symposium on Ground support in Mining and Underground Construction,* Perth, Australia, September 28–30, pp. 619–630.

Belem, T., El Aatar, O., Bussière, B., Benzaazoua, M., Fall, M., Yilmaz, E., 2006. Characterization of self–weight consolidated paste backfill. In: *Proceedings of the 9th International Seminar on Paste and Thickened Tailings,* Edited by R. Jewell, S. Lawson, and P. Newman, Limerick, Ireland, April 3–7. pp. 333–345.

Belem, T., El Aatar, O., Benzaazoua, M., Bussière, B., Yilmaz, E., 2007. Hydro-geotechnical and geochemical characterization of column consolidated cemented paste backfill. In: *Proceedings of the 9th International Symposium in Mining with Backfill,* Montreal, Quebec, Canada, April 29–May 2, pp. 135–142.

Benzaazoua, M., Ouellet, J., Servant, S., Newman, P., Verburg, R., 1999. Cementitious backfill with high sulfur content: physical, chemical and mineralogical characterization. *Cement and Concrete Research,* Vol. 29, No. 5, pp. 719–725.

Benzaazoua, M., Belem, T., Jolette, D., 2000. Investigation de la stabilité chimique et de son impact sur la qualité des remblais miniers cimentés. In: *IRSST (Institut de recherche Robert-Sauvé en santé et en sécurité du travail) Report No R–260,* Montreal, Quebec, Canada, pp. 1–172.

Benzaazoua, M., Belem, T., Bussière, B., 2002. Chemical factors that influence the performance of mine sulphidic paste backfill. *Cement and Concrete Research,* Vol. 32, No. 7, pp. 1133–1144.

Benzaazoua, M., Fall, M., Belem, T., 2004. A contribution to understanding the hardening process of cemented pastefill. *Minerals Engineering,* Vol. 17, No. 2, pp. 141–152.

Benzaazoua, M., Belem, T., Yilmaz, E., 2006. Novel lab tool for paste backfill. *Canadian Mining Journal,* Vol. 127, No. 3, pp. 31–31.

Bussière, B., 1993. Evaluation des propriétés hydrogéologiques de résidus miniers utilisés comme barrières de recouvrement. *M.Sc. Thesis,* École Polytechnique de Montreal, Québec, Canada.

Bussière, B., 2007. Colloquium 2004: Hydrogeotechnical properties of hard rock tailings from metal mines and emerging geoenvironmental disposal approaches. *Canadian Geotechnical Journal,* Vol. 44, No. 9, pp. 1019–1052.

Chakrabarti, S., Horvath, P., 1986. Conventional consolidation tests on two soils. In: *Proceedings on Consolidation of soils: testing and evaluation; ASTM STP 892,* R.N. Yong and F.C. Townsend Eds., Philadelphia, USA, pp. 451–464.

Consoli, N.C., Rotta, G.V., Prietto, P.D.M., 2006. Yielding-compressibility-strength relationship for an artificially cemented soil cured under stress. *Géotechnique,* Vol. 56, No. 1, pp. 69–72.

DIN Designation 4030, 2001. Standard assessment of water, soil, and gases for their aggressiveness to concrete; principles and limiting values. In: *German Standard, Construction Materials and Building,* Berlin, Germany, pp. 35–46.

El Aatar, O., Belem, T., Bussière, B., Benzaazoua, M., Yilmaz, E., 2007. Microstructural properties of column consolidated paste fill. In: *Proceedings of the 60th Canadian Geotechnical Conference,* Ottawa, Canada, October 21–24, pp. 45–52.

Ercikdi, B., Kesimal, A., Cihangir, F., Deveci, H., Alp, I., 2009. Cemented paste backfill of sulphide-rich tailings: Importance of binder type. *Cement and Concrete Composites,* Vol. 31, No. 4, pp. 268–274.

Fahey, M., Helinski, M., Fourie, A., 2009. Consolidation in accreting sediments: Gibson's solution applied to backfilling of mine stopes. *Géotechnique* (Accepted on 2 October 2009).

Fall, M., Benzaazoua, M., Ouellet, S., 2005. Experimental characterization of the influence of tailings fineness and density on the quality of cemented paste backfill. *Minerals Engineering,* Vol. 18, No. 1, pp. 41–44.

Fourie, A.B., Fahey, H., Helinski, M. 2007. Using effective stress theory to characterize the behaviour of backfill. *CIM Bulletin,* Vol. 100, No. 1103, pp. 1–9 (Paper 27).

Godbout, J., Bussière, B., Aubertin, M., Belem, T. 2007. Evolution of cemented paste backfill saturated hydraulic conductivity at early curing time. In: *Proceedings of the 60th Canadian Geotechnical Conference,* Ottawa, Ontario, Canada, October 21–24, pp. 1–7.

Grabinsky, M.W., Bawden, W., 2007. In situ measurements for the geomechanical design of cemented paste backfill systems. *CIM Bulletin,* Vol. 100, No. 1103, pp. 1–8 (Paper 21).

Harvey, A. 2004. Étude comparative des contraintes triaxiales dans le remblai en pâte selon la portée des chantiers. *M.Sc. Thesis,* École polytechnique Montréal, Quebec, Canada, pp. 1–136.

Helinski, M., Fourie, A.B., Fahey, M., 2006. Mechanics of early age cemented paste backfill. In: *Proceedings of the 9th International Seminar on Paste and Thickened Tailings, Edited by* R. Jewell, S. Lawson, and P. Newman, Ireland, April 3–7, pp. 313–322.

Helinski, M., Fahey, F., Fourie, A.B., 2007a. Numerical modelling of cemented paste backfill deposition. *Journal of Geotechnical and Geoenvironmental Engineering,* Vol. 13, No. 10, pp. 1308–1319.

Helinski, M., Fourie, A.B., Fahey, F., Ismail, M., 2007b. Assessment of the self-desiccation process in cemented mine backfills. *Canadian Geotechnical Journal,* Vol. 44, No. 10, pp. 1148–1156.

Kesimal, A., Yilmaz, E., Ercikdi, B., 2004. Evaluation of paste backfill test results obtained from different size slumps with varying cement contents for sulphur rich mill tailings. *Cement and Concrete Research,* Vol. 34, No. 10, pp. 1817–1822.

Klein, K., Simon, D., 2006. Effect of specimen composition on the strength development in cemented paste backfill samples. *Canadian Geotechnical Journal,* Vol. 43, No. 3, pp. 310–324.

le Roux, K.-A., 2004. In situ properties and liquefaction analysis of cemented paste backfill. *Ph.D. Dissertation,* University of Toronto, Ontario, Canada, pp. 1–271.

le Roux, K.-A., Bawden, W.F., Grabinsky, M.F., 2002, Assessing the interaction between hydration rate and fill rate for a cemented paste backfill. In: *Proceedings of the 53rd Annual Canadian Geotechnical Conference,* Montreal, Ontario, Canada, October 15–18, pp. 201–209.

le Roux, K.-A., Bawden, W.F., Grabinsky, M.F., 2005. Field properties of cemented paste backfill at the Golden Giant mine. *Mining Technology: Transactions of the Institute of Mining and Metallurgy, Section A,* Vol. 114, No. 2, pp. 65–86.

Li, L., Aubertin, M., 2009. A three-dimensional analysis of the total and effective stresses in submerged backfilled stopes. *Geotechnical and Geological Engineering,* Vol. 27, No. 4, pp. 559–569.

McCarthy, D.F., 2007. *Essentials of soil mechanics and foundations: Basic Geotechnics* (7th Ed). Pearson Prentice Hall, Canada.

Mohammed, A., Hossein, M., Hassani, F., 2002. Hydromechanical evaluation of stabilized mine tailings. *Environmental Geology,* Vol. 41, No. 7, pp. 749–759.

Morris, P.H., Lockington, D.A., Apelt, C., 2000. Correlations for mine tailings consolidation parameters. *International Journal of Surface Mining, Reclamation and Environment,* Vol. 14, No. 2, pp. 171–182.

Ouellet, J., Servant, S., 2000. In situ mechanical characterization of paste backfill with a self-boring pressuremeter. *CIM Bulletin,* Vol. 93, No. 1042, pp. 110–115.

Ouellet, S., Bussière, B., Mbonimpa, M., Benzaazoua, M., Aubertin, M., 2006. Reactivity of an underground mine sulphidic cemented paste backfill. *Minerals Engineering,* Vol. 19, No. 5, pp. 407–419.

Ouellet, S., Bussière, B., Aubertin, M., Benzaazoua, M., 2007. Microstructural evolution of cemented paste backfill: Mercury intrusion porosimetry test results. *Cement and Concrete Research,* Vol. 37, No. 12, pp. 1654–1665.

Pierce, M.E., 1997. Laboratory and numerical analysis of the strength and deformation behaviour of paste backfill. *M.Sc. Thesis,* Queen's University, Kingston, Ontario, Canada, pp. 1–195.

Pierce, M.E., Bawden, W.F., Paynter, J.T., 1998. Laboratory testing and stability analysis of paste backfill at the Golden Giant Mine. In: *Proceedings of the 6th International Symposium on Mining with Backfill,* Australia, April 14–16, pp. 159–165.

Potvin, Y., Thomas, E., Fourie, A. 2005. *Handbook on Mine Fill.* Australian Centre for Geomechnanics, Western Australia, Australia.

Qui, Y., Sego, D.C., 2001. Laboratory properties of mine tailings. *Canadian Geotechnical Journal,* Vol. 38, No. 2, pp. 183–190.

Rotta, G.V., Consoli, N.C., Prietto, P.D.M., Coop, M.R., Graham, J., 2003. Isotropic yielding in a cemented soil cured under stress. *Géotechnique,* Vol. 53, No. 5, pp. 493–501.

Shamsai, A., Pak, A., Bateni, S.M., Ayatollahi, S.A.H., 2007. Geotechnical characteristics of copper mine tailings: A case study. *Geotechnical and Geological Engineering,* Vol. 22, No. 5, pp. 591–602.

Sonpal, R.C., Katti, R.K., 1973. Consolidation: an analysis with pore pressure measurements. In: *Proceedings of the 8th International Conference on Soil Mechanics & Foundation Engineering*. Moscow, Russia, Vol. 1.2, pp. 385–388.

Stone, K.J., Randolph, Toh, S., Sales, A.A., 1994. Evaluation of consolidation behavior of mine tailings. *Journal of Geotechnical Engineering,* Vol. 120, No. 3, pp. 473–490.

Taylor, D.W., 1942. Research on consolidation of clays. In: *Civil and Sanitary Engineering Department,* MIT, Cambridge, MA, Publication Serial 82.

Terzaghi, K., 1925, *Erdbaumechanik*, Franz Deuticke, Vienna

Yilmaz, E., 2003. Experimental investigaton of the compressive strength behaviour of the cemented paste backfill samples prepared from sulphidic mine tailings. *M.Sc. Thesis,* Black Sea Technical University (KTU), Trabzon, Turkey, pp. 1–117.

Yilmaz, E., 2007. How efficiently the volume of wastes produced from mining operations can be reduced without causing any important environmental impact? *Environmental Synthesis Report,* UQAT, Rouyn-Noranda, Quebec, Canada.

Yilmaz, E., 2010. Investigating the hydrogeotechnical and microstructural properties of cemented paste backfills using the CUAPS apparatus. *Ph.D. Thesis,* Université du Québec en Abitibi-Témiscamingue (UQAT), Rouyn-Noranda, Québec, Canada.

Yilmaz, E., El Aatar, O., Belem, T., Benzaazoua, M., Bussière, B., 2006 Effect of consolidation on the performance of cemented paste backfill. In: *Proceedings of the 21st Underground Mine Support Conference,* Val-d'Or, April 11–12, pp. 1–14.

Yilmaz, E., Belem, T., Benzaazoua, M., Bussière, B. 2008a. Experimental characterization of the influence of curing under stress on hydromechanical and geotechnical properties of cemented paste backfill. In: *Proceedings of the 12th International Conference on Tailings and Mine Waste,* Vail, Forth Collins, Colorado, USA, pp. 139–152.

Yilmaz, E., Belem, T., Bussière, B., Benzaazoua, M., 2008b. Consolidation characteristics of early age cemented tailings paste backfill. In: *Proceedings of the 61st Canadian Geotechnical Conference,* Edmonton, Alberta, Canada, pp. 797–804.

Yilmaz, E., Benzaazoua, M., Belem, T., Bussière, B., 2009a. Effect of curing under pressure on compressive strength development of cemented paste backfill. *Minerals Engineering,* Vol. 22, No. 9–10, pp. 772–785.

Yilmaz, E., Belem, T., Bussière, B., Benzaazoua, M., 2009b. Relationships between micro-structural properties and strength of consolidated and unconsolidated cemented paste backfills. *Cement and Concrete Composites* (submitted in October 2009).

Yilmaz, E., Belem, T., Benzaazoua, M., Bussière, B., 2010. Assessment of the modified CUAPS apparatus to estimate in situ properties of cemented paste backfill. *Geotechnical Testing Journal,* Vol. 33, No. 5, pp. 351–362.

CHAPTER V

RELATIONSHIPS BETWEEN MICROSTRUCTURAL PROPERTIES AND COMPRESSIVE STRENGTH OF CONSOLIDATED AND UNCONSOLIDATED CEMENTED PASTE BACKFILLS

Erol Yilmaz, Tikou Belem, Bruno Bussière and Mostafa Benzaazoua

Paper submitted in October 2009 to

Cement and Concrete Composites

5.0 RÉSUMÉ

Il est bien établi que le drainage de l'excès d'eau présente dans le remblai cimenté en pâte (RCP) joue un rôle essentiel dans l'acquisition de sa résistance à la compression due à la compaction des particules de résidus (réarrangement du squelette) et au durcissement de la matrice (microstructure). Les propriétés de résistance sont généralement obtenues à partir d'essais de compression uniaxiale, alors que la microstructure du RCP est caractérisée à l'aide de la porosimétrie par intrusion de mercure (PIM) ainsi que de la détermination de la surface spécifique (SSA). La PIM est largement utilisée par les chercheurs pour caractériser la structure des pores de matériaux cimentaires durcis, principalement en raison de sa simplicité d'utilisation et sa grande reproductibilité. Ce papier présente une étude expérimentale des effets des conditions de cure sur l'évolution de la microstructure des RCP et de leurs résistances à la compression uniaxiale (UCS) correspondantes. Deux types de RCP, consolidés drainés (échantillons consolidés et curés au CUAPS; CUAPS = système de cure sous pression appliquée) et non consolidés-non drainés (échantillons coulés dans des moules en plastique conventionnel non consolidés et curés sous aucune pression extérieure) ont été préparées en utilisant un liant qui est un mélange de 80 wt% de laitier de haut fourneau et de 20 wt% de ciment Portland à usage courant (GU) (GU-Slag@20:80 wt%). Les propriétés microstructurales du RCP sont comparées pour trois teneurs en liant (3, 4,5, et 7% wt%) et trois temps de cure (7, 14 et 28 jours). Les résultats du PIM montrent que les variations de la porosité d'intrusion (et donc les modifications de la microstructure) dépendent fortement du rapport eau-ciment (*w/c*) et des conditions de drainage (par exemple, application d'une pression pendant la cure et drainage de l'excès d'eau interstitielle). Quand *w/c* diminue ou lorsque le temps de cure augmente (avec une hydratation accrue qui en résulte), la porosité totale est réduite, en raison principalement de la réduction de plus grande taille des pores par leur remplissage partiel avec des phases cimentaires. Les mesures de la surface spécifique SSA montrent quant à elles une très bonne corrélation avec les valeurs d'UCS, ce qui implique que l'UCS des RCP non consolidés augmente avec une SSA croissante. Différents modèles de régression entre l'UCS et les paramètres de PIM (diamètre seuil, porosité total, mésoporosité et macroporosité) et de SSA d'échantillons de RCP sont également proposés et discutés.

Mots clés: Remblai en pâte; Porosimétrie par intrusion de mercure; Microstructure; Résistance en compression; Conditions de cure

5.0 ABSTRACT

It is well established that drainage of excess water present within cemented paste backfill (CPB) plays a critical role in its compressive strength development due to tailings particles packing (skeleton rearrangement) and matrix hardening (microstructure). Strength properties are generally obtained from uniaxial compression tests, while the CPB microstructure is characterized by mercury intrusion porosimetry (MIP) and specific surface area (SSA) determination. MIP is widely used by researchers to characterize the pore structure of hardened cementitious materials, mainly due to its simplicity of use and high reproducibility. This paper presents an experimental study of the effects of curing conditions on changes in CPB microstructure and corresponding unconfined compressive strengths (UCS). Two types of CPB, consolidated-drained (CUAPS-consolidated and cured samples; CUAPS = curing under applied pressure system) and unconsolidated-undrained (conventional plastic mould-unconsolidated and cured samples under no pressure) were prepared using a slag blended binder consisting of 20 wt% of general use Portland cement (GU) and 80 wt% of blast furnace slag (GU-Slag@20:80 wt%). CPB microstructural properties are compared for three binder contents (3, 4.5 and 7 wt%) and three curing times (7, 14 and 28 days). MIP results show that changes in intrusion porosity (and therefore changes in microstructure) strongly depend on the water-to-cement (*w/c*) ratio and drainage conditions (applied pressure during curing and excess pore water removal). As *w/c* ratio decreases or curing time increases (with consequent increased hydration), total porosity is reduced, mainly due to the reduction in larger-sized pores by partial filling with cementitious phases. SSA measurements show good correlation with UCS values, implying that the UCS of unconsolidated CPB increases with increasing SSA. Different regression models between UCS and MIP parameters (threshold diameter, total, meso- and macroporosity) and SSA of CPB samples are also proposed and discussed.

Keywords: Paste backfill; Mercury intrusion porosimetry; Microstructure; Compressive strength; Curing condition

5.1 INTRODUCTION

Cemented paste backfill (CPB) is increasingly used in the mining industry due to its several advantages: technical (provides ground support for cost-effective mining operations and greater safety for workers), economic (generates lower capital and operating costs than hydraulic and rock fills), and environmental (reduces surface tailings disposal by diverting them into underground stopes, thereby reducing both environmental hazards and tailings management costs) (Potvin et al., 2005; Bussière, 2007; Belem and Benzaazoua, 2008a,b). Given all these benefits, CPB is more cost effective and versatile than other backfill types.

CPB is a cementitious material produced with three ingredients: 1) filtered mine tailings (typically 70–85 wt%), 2) hydraulic binders (typically 1–7 wt%), and 3) mixing water to ensure the paste's flowability in pipeline for final deposition (Benzaazoua et al., 1999). The composition of CPB determines its long-term strength and durability. Many researchers have investigated the effects of different parameters (e.g., tailings granularity, binder type, and content) on the short- and long-term strength and stability of CPB over different curing times (Benzaazoua et al., 2002; 2004; Kesimal et al., 2003, 2004, 2005; Belem et al., 2000, 2008a; Fall et al., 2005; Godbout, 2005; Ouellet, 2006; Yilmaz et. al., 2007, 2008a, Ercikdi et al., 2009). The service life and durability of CPB also depend on its material properties, in situ placement, and curing conditions, and its self-weight consolidation. A number of researchers (Belem et al., 2002, 2006; le Roux, 2004; Yilmaz et al., 2006, 2008b, 2009a, 2010b, Fourie et al., 2007; Grabinsky and Bawden, 2007; El Aatar, 2009; Helinski et al., 2006, 2009) shown experimentally that curing CPB under pressure increases its unconfined compressive strength (UCS) development due to pore water pressure dissipation and solid skeleton settlement. Furthermore, some of these experimental studies showed that, in addition to UCS, other properties such as saturated hydraulic conductivity, specific surface area (SSA), porosity, and diffusivity change significantly during curing due to microstructure changes in hardened materials (Godbout, 2005; Garboczi, 1990; Belem et al., 2001; Ait-Mokhtar et al., 2002).

A number of recent studies have evaluated the microstructural properties of CPB materials by mercury intrusion porosimetry (MIP) testing (Fall et al., 2005; Ouellet, 2006; le Roux, 2004;

Belem et al., 2001; Benzaazoua, 1996; Ramlochan et al., 2003; Ouellet et al., 2007, 2008; El Aatar et al., 2007; Deschamps et al., 2008; Fall and Samb, 2008; Yilmaz et al., 2008c). Results show that CPB pore structure is greatly affected by the tailings grain size distribution (GSD), water-to-cement (*w/c*) ratio, mixing water quality, curing conditions (e.g., under applied pressure), binder type, and mix proportions over curing times. Ouellet (2006) showed that total porosity of CPB samples, indicated by mercury intrusion in conventional moulds, remained almost the constant during curing. Little information is available on the effects of curing under pressure on pore structure behaviour of CPB samples. To our knowledge, no microstructural investigation based on MIP has been conducted so far on CPB samples cured under applied pressure, probably due to the absence of appropriate laboratory equipment or test procedures. Consequently, aspects related to CPB in situ curing properties and conditions that can significantly affect its pore structure need further investigation.

The objective of this paper was to examine the effect of curing conditions (consolidated and unconsolidated) on microstructural (MIP porosities, pore size distribution, and SSA) and mechanical properties (UCS) of CPB samples. Three binder contents (3, 4.5, and 7 wt%) and three curing times (7, 14, and 28 days) were considered to compare the MIP parameters (total-, meso- and macroporosity, threshold diameter, and critical pore size) with UCS results obtained from both CUAPS-consolidated and mould unconsolidated-undrained backfills. The unconsolidated-undrained backfill samples were cast in conventional plastic moulds and the consolidated-drained samples were consolidated using a laboratory apparatus called CUAPS (curing under applied pressure system). Different formulations were proposed to predict compressive strength, knowing certain MIP pore-size distribution parameters.

5.2 MATERIALS AND METHODS

5.2.1 Paste backfill ingredients

5.2.1.1 Mine tailings

Sulphide-rich tailings were obtained from a polymetallic hard rock mine located in the province of Quebec, Canada. Characterization results indicate that the tailings sample has a

specific gravity G_s of 3.71 and a specific surface area S_m of 2.17 m^2g^{-1}. Atterberg limits were determined using an experimental procedure adapted from standard D4318 (ASTM, 1991a). Mine tailings showed only slight plasticity, with a liquid limit of 23% and a plastic limit close to zero (Table 5.1). Similar values have been reported by Bussiere (2007). These mine tailings can be categorized as non-plastic silt (ML) according to Unified Soil Classification System (USCS, McCarthy, 2007).

Table 5.1 Physico-chemical characteristics of the tailings sample

Physical properties	Value	Chemical elements	Value
Specific surface area S_s (m^2 kg^{-1})	2170	Aluminum *Al* (wt%)	2.82
Specific gravity G_s	3.7	Calcium *Ca* (wt%)	0.57
Moisture content *w* (wt%)	25.12	Silicon *Si* (wt%)	0.51
Liquid limit *LL* (wt%)	23	Iron *Fe* (wt%)	27.42
Effective grain size D_{10} (µm)	4.3	Total sulfur S_{tot} (wt%)	20.56
Average grain size D_{50} (µm)	24.3	Copper *Cu* (wt%)	0.04
Coefficient of uniformity C_u	8	Lead *Pb* (wt%)	0.11
Coefficient of curvature C_c	1.1	Zinc *Zn* (wt%)	0.35

Grain size distribution (GSD) of the tailings was obtained using a Malvern Laser Mastersizer S2000, and was compared (see Figure 5.1) to a typical range of GSD curves for 11 mine tailings from Quebec and Ontarian mines (Ouellet, 2006). Most of the GSD consisted of silt-sized (2–50 µm) particles (66.1%), with a sand-size particles of 29.2%. The GSD curve indicates that the tailings sample contains only 4.7% clay-sized (< 2 µm) particles. The effective diameter D_{10} (corresponding to 10% passing on cumulative GSD curve) and average grain size D_{50} are 4.3 µm and 24.3 µm, respectively.

Chemical composition of tailings was analyzed using inductively coupled plasma-atomic emission spectrometry (Optima 3100RL). Dilute HCl was used to extract sulfates and the obtained solution was analyzed (Table 5.1). Chemical analysis showed that iron Fe, total sulfur S, aluminum Al, and calcium Ca contents were 27.4 wt%, 20.6 wt%, 2.8 wt%, and 0.57 wt%, respectively. Mineralogy of tailings was obtained by X-ray diffraction (Bruker AXS D8 diffractometer) and quantified using the Rietveld method (TOPAS software).

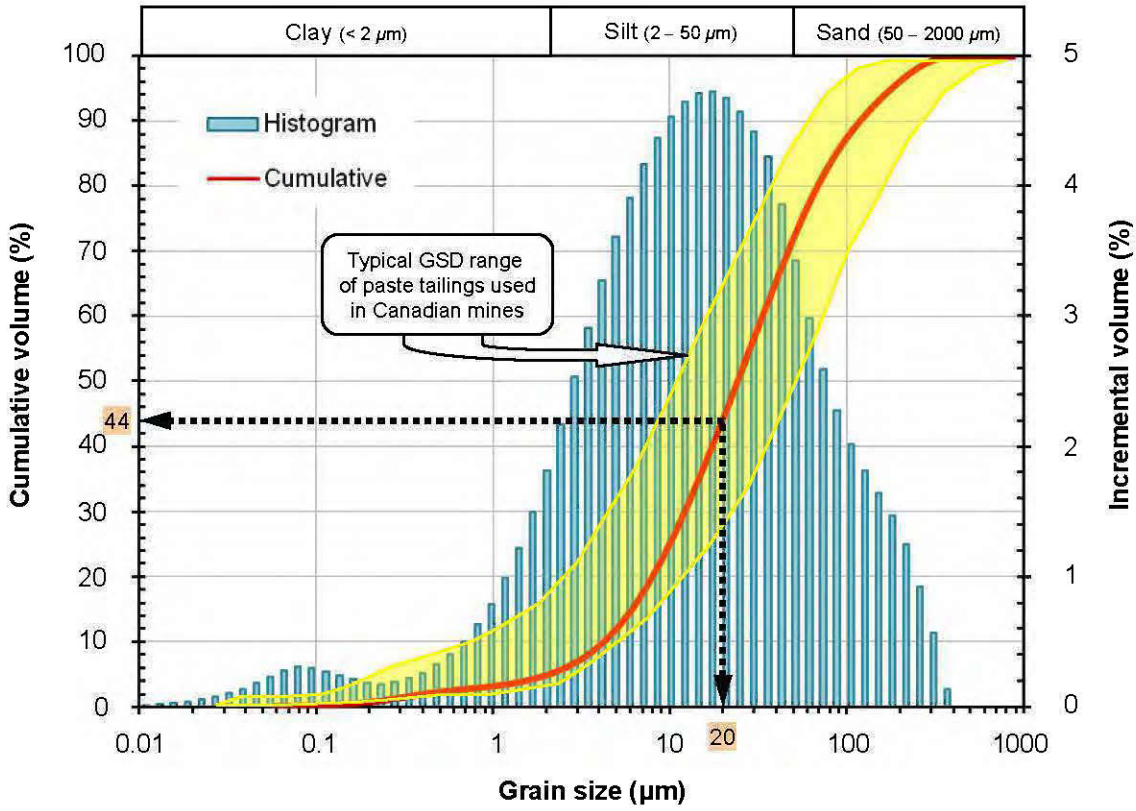

Figure 5.1 Grain size distribution (GSD) curves of the mine tailings sample compared to a typical range of GSD curves of eleven tailings sampled from Canadian hard rock mines.

The mineralogical composition reveals that the tailings sample was composed primarily of pyrite (47.1 wt%). Significant quantities of silicate minerals such as quartz (31.6 wt%), chlorite (8.9 wt%), and paragonite (7.3 wt%) were detected. More details on the mineralogy of the tested mine tailings can be found in Yilmaz (2010).

5.2.1.2 Hydraulic binders

The hydraulic binder used (GU-Slag@20:80 wt%) for CPB preparation was a blend of 80 wt% blast furnace slag (Slag) and 20 wt% general use Portland cement (GU). Three binder contents of 3, 4.5, and 7 wt% were used to produce the CPB mixtures. It is well known that slag exhibits good hardening properties when blended with GU, as it creates an alkaline

environment that activates the slag reaction (Petrolito et al., 2005). However, even when activated by GU cement, slag hydration is always slower than that of GU alone. The chemical composition (by ICP-AES analysis) and some physical properties of the components and the hydraulic binder mixture are given in Table 5.2. The cement chemistry results show that GU had a maximum MgO content of 5% and Slag had an Al_2O_3 content lower than 11%. Physical tests show that Slag had the highest BET specific surface at 3.54 m^2g^{-1}. GU alone and the tested hydraulic binder (GU-Slag@20:80 wt%) had a BET specific surface of 1.58 m^2 g^{-1} and 2.84 m^2 g^{-1}, respectively. The specific gravity of GU 100 wt% and GU-Slag@20:80 wt% was 3.1 and 2.8, respectively.

Table 5.2 Chemical composition and some physical properties of the experimental binders

Parameter	S_m (m^2/g)	G_s	Al_2O_3 (wt%)	CaO (wt%)	Fe_2O_3 (wt%)	MgO (wt%)	Na_2O (wt%)	SO_3 (wt%)	SiO_2 (wt%)
GU	1.58	3.1	4.86	65.76	2.44	2.21	2.11	3.67	19.51
Slag	3.54	2.8	10.24	31.41	0.55	11.3	2.01	3.27	36.22
GU-Slag	2.84	2.9	4.26	42.82	0.64	6.19	2.03	3.35	30.91

5.2.1.3 Mixing water

Table 5.3 summarizes the chemical composition of the as-received tailings interstitial water and mixing water (tap water), analyzed using the ICP-AES method. The as-received tailings interstitial water was highly aggressive, with high sulfate SO_4^{2-} content (4880 ppm). These sulfates were obtained mainly from a cyanide destruction process using SO_2/Air method. Additionally, the high concentration of soluble calcium Ca at 560 ppm is mainly due to the lime added at the ore processing plant. The pH, Eh (redox potential), and EC (electrical conductivity) of the mixing water were analyzed using a Benchtop pH/ISE Meter, Orion Model 920A with a Thermo Orion Triode combination electrode (see Table 5.3), and were determined at 9.4, +0.15 V, and 7.4 mS/cm for tailings interstitial water and 7.8, +0.43 V, and 0.3 mS/cm for tap water, respectively. Eh was first determined using a Pt/Ag/AgCl electrode and then converted into the standard hydrogen electron potential.

Table 5.3 Chemical and geochemical analysis of tailings interstitial water and tap water

Parameter	As-received tailings interstitial water	Municipal tap water
Chemical elements		
Silicon *Si* (ppm)	0.891	0.901
Magnesium *Mg* (ppm)	1.83	2.27
Calcium *Ca* (wt%)	559	40.9
Geochemical parameters		
Sulfate content SO_4^{-2} (ppm)	4883	138
Electrical conductivity *EC* (mS cm^{-1})	7.42	0.274
Corrected redox potential *Eh* (V)	0.147	0.431
pH (unitless)	9.4	7.8

5.2.2 Sample preparation, mixing, casting, and curing

The required amounts of CPB ingredients (as-received tailings, binding agent, and mixing water) were thoroughly mixed and homogenized in a double spiral concrete mixer for about 7 minutes to ensure homogeneity of the final paste. Initial water content for all CPB mixtures was set at 28.2 wt% (based on an equivalent percent solid of 78 wt%). Water-cement (*w/c*) ratios of 9.7, 6.5, and 4.3 corresponded to the binder proportions of 3, 4.5, and 7 wt%, respectively. Immediately after mixing, samples were cast in both conventional plastic (non-perforated) moulds and CUAPS Perspex (two open-ended sections) moulds. Both plastic and Perspex moulds had a diameter-to-height (*D*/*H*) ratio of 2 (*D* × *H*: 102 × 204 mm). Backfill was poured into plastic and Perspex moulds in three layers, each tamped 25 times with an iron rod to remove most of the air pockets within sample. Initial height was then recorded. CPB cylinders were then sealed and cured for 7, 14, and 28 days in a humidity chamber set at 24 °C and 80% RH to simulate typical curing conditions in underground mines.

5.2.3 Experimental procedures

5.2.3.1 Curing under applied pressure tests

To investigate the effects of curing under pressure on the pore structure of CPB materials across curing times, a recently designed laboratory apparatus called CUAPS (curing under

applied pressure system) was used (Benzaazoua et al., 2006, Yilmaz et al., 2010a). CUAPS apparatus (a total of 10 were used) allows simulating in situ placement properties and curing conditions for laboratory-prepared CPB. The CUAPS consists of three main parts: a sample holder (Perspex mould), a pneumatic pressure loading plate equipped with a piston, and a lower plate provided with a drainage port with an outlet for collecting excess pore water. The procedure is as follows. After mounting the CPB sample contained in the Perspex mould, no pressure is applied for the first half an hour, after which pressure is applied and gradually increased to 400 kPa. The final pressure corresponds to an equivalent overburden stress of 17.6 m in height of CPB within a stope and having a bulk unit weight of 22.7 kN/m^3. Figure 5.2 presents photos of consolidated and undrained samples cured in a foggy room.

Figure 5.2 Photos of (a) CUAPS-consolidated CPB samples and (b) conventional plastic mould unconsolidated-undrained CPB samples curing in the humidity chamber.

A detailed description of the improved CUAPS apparatus is beyond the scope of this study, but interested readers are referred to Benzaazoua et al. (2006), Yilmaz et al. (2006, 2008b, 2008c, 2009a, 2010a) and Yilmaz (2010).

5.2.3.2 Uniaxial compression tests

Following curing times of 7, 14, and 28 days, the hardened CPB samples (removed from plastic and Perspex molds) were subjected to uniaxial compression tests (based on method C39 (ASTM, 2002a)) to determine UCS using a computer controlled press (MTS 10/GL) with a normal load capacity of 50 kN and a deformation rate of 1 mm/min. Axial deformation was digitally recorded by a real-time data acquisition system. Observed UCS corresponds to the maximum stress (peak at specimen failure) reached during compressing. For a given CPB recipe, only one test was performed for consolidated samples, whereas three tests were done on average for unconsolidated samples. However, the reproducibility tests showed reliable and repeatable results across CUAPS apparatuses (Yilmaz et al., 2009).

5.2.3.3 Mercury intrusion porosimetry (MIP)

MIP apparatus and test procedure: CPB pore structure network was determined using a mercury intrusion porosimeter (MIP, Micromeritics Autopore III 9420). Applying pressures ranging from 0 to 414 MPa (60,000 psi) allows measuring throat pore diameter to 0.003 μm. MIP was analyzed according to standard D 4404 (ASTM, 2002b). After compression testing, representative samples weighing between 3.2 and 4.3 g ($D \times H$ = 12 × 24 mm) were taken from locations as far as possible from the shear plane to avoid stress concentration effects that could affect material properties. Samples were oven-dried at 50 °C for at least 96 hours and then stored in a dessicator over silica gel to minimize pore alteration due to hydration product destruction and moisture ingress. For a given CPB mixture, at least two MIP analyses were performed to obtain an average total porosity value.

Factors affecting MIP results: MIP is based on capillary law governing liquid penetration into small pores (Washburn, 1921). In the case of mercury, this law is expressed as follows:

$$d = -\frac{4\gamma \cos\varphi}{p} \tag{5.1}$$

where d = pore throat diameter (μm) into which mercury is intruded, p = mercury injection pressure (N/m^2), γ = surface tension of mercury (N/m), and φ = the contact angle between mercury and the sample surface (°).

MIP results are influenced not only by the microstructure of the specimen, but also by experimental factors such as pre-treatment technique, sample size, pressure build-up rate, pore structure alteration, mercury surface tension, and mercury contact angle (Galle, 2001; Kumar and Bhattacharjee, 2003a). In this study, surface tension γ and contact angle φ were taken as 0.485 N/m and 130°, respectively. According to the International Union of Pure and Applied Chemistry classification (IUPAC, 1972), there are three pore size categories for cement-based materials: *i*) micropores are smaller than 0.002 μm, *ii*) mesopores range between 0.002 μm and 0.05 μm and iii), and *iii*) macropores are larger than 0.05 μm. The MIP tests can measure mesopores and macropores.

5.2.3.4 Specific surface area determination

For any solid material, specific surface area (SSA or S_m), or the solid total surface area per weight unit (m^2/kg), includes the external geometrical surface as well as the internal surface area, which takes into account all surface irregularities at a molecular scale and the developed surfaces of pore structure walls (Xu, 2004). SSA is a good indicator of the fineness of the microstructure. So the finer the particles and the pore-size distribution, the higher the SSA.

In this study, the SSA was determined by measuring nitrogen N_2 multi-point adsorption isotherms based on the BET theory according to standard D 6556 (ASTM, 2009). A Gemini III 2375 from Micromeritics was used for surface analysis. Prior to measurement, samples were dried and out-gassed in a Micromeritics VacPrep 061 system at 50 ℃ for at least 12 h under atmospheric pressure.

5.3 RESULTS AND INTERPRETATION

5.3.1 Effect of curing conditions on pore size distribution and total porosity of CPB

Figure 5.3 shows the changes in cumulative and incremental pore size distribution (PSD) curves for 28-day cured CPB samples with binder contents of 3, 4.5, and 7 wt%. In the PSD curves, MIP total porosity n_{tot} corresponds to the last recorded point (or the highest intrusion pressure and the smallest equivalent pore throat size). Figures 3a, 3b, and 3c show that as binder content increases, pore throat openings become finer due to cementation by binder hydration products and applied pressures during curing. Cumulative PSD curves shift toward smaller average pore diameters with increasing binder proportion. This shift is more evident for CUAPS-consolidated samples than mold unconsolidated-undrained samples, for which cumulative PSD curves are consistently located above those of the consolidated backfills.

Figure 5.4 presents the change in average n_{tot} with curing time and binder contents for both mold unconsolidated-undrained samples and CUAPS-consolidated samples. Consolidated backfill consistently shows lower total porosity n_{tot} and hence higher bulk density than unconsolidated backfill. Moreover, n_{tot} decreases with increased curing time for undrained and consolidated samples, regardless of binder content. The range of variation in n_{tot} is 39%–41% for CUAPS-consolidated samples and 46%–47% for mold unconsolidated-undrained CPB samples. Accordingly, curing conditions (with and without applied pressure) appear to play a role in total mercury porosity n_{tot} and PSD of CPB samples for a given binder content.

MIP parameters of both consolidated and undrained CPB samples such as macroporosity, mesoporosity, total porosity, bulk density, crtical pore diameter, threshold diameter and stem volume are presented in Table 5.4 and Appendix G.

Figure 5.4 and Table 5.4 show that total porosity n_{tot} reduces slightly with increased binder content for the two different paste backfill types over the curing time, although the reduction percentage differs across types. Several factors may explain this:

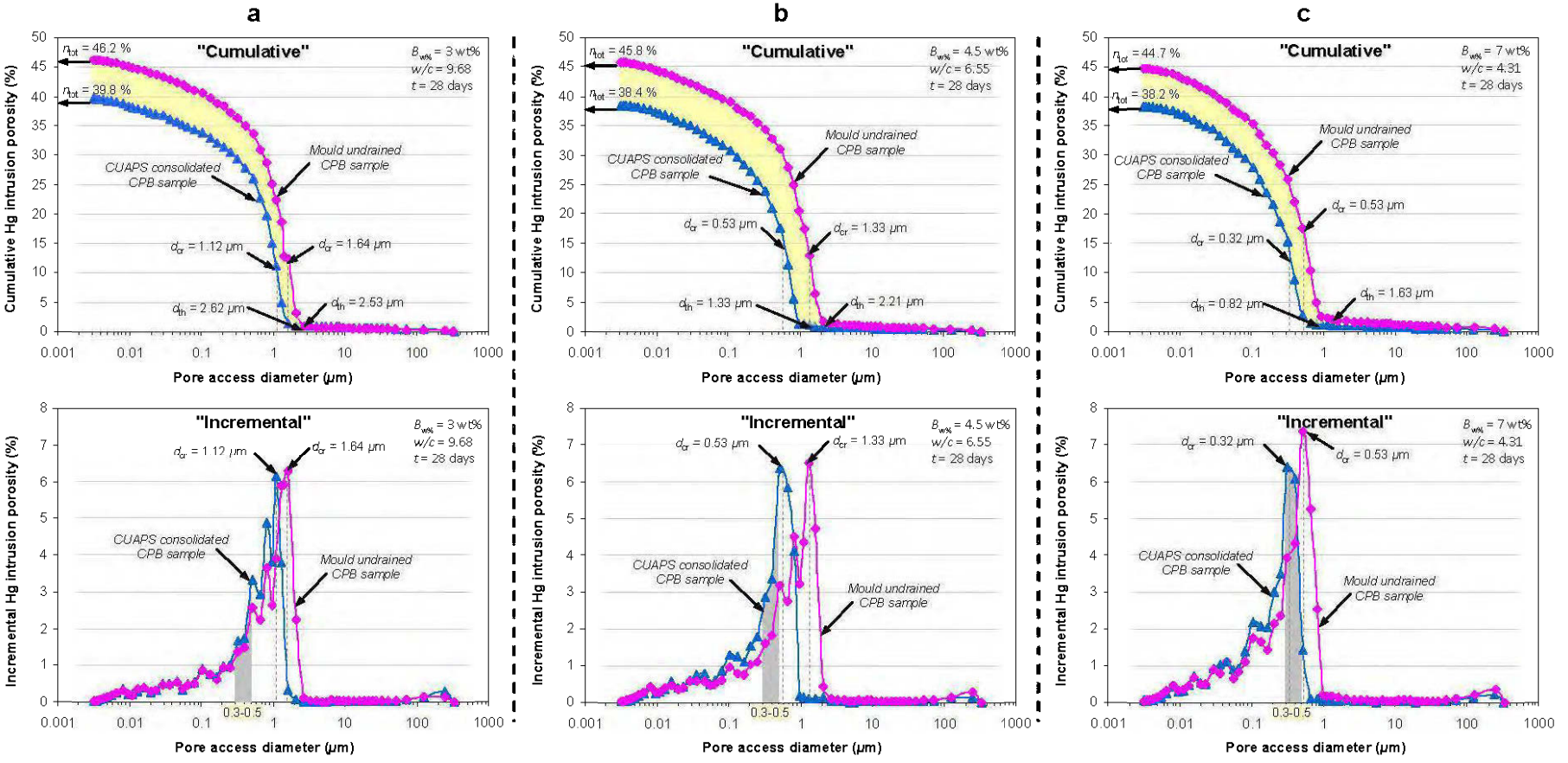

Figure 5.3 Effect of different curing conditions (with and without pressure) on pore size distribution (PSD) of CPB samples at 28-day curing for different binder contents: cumulative and incremental PSD curves for (a) 3 wt%, (b) 4.5 wt%, and (c) 7 wt%. Shadowed area in the incremental PSD graphs represents total volume in the specific pore range. In this case, the range is between 0.3 and 0.5 μm (B_w = binder content, wt %; t = curing time, day).

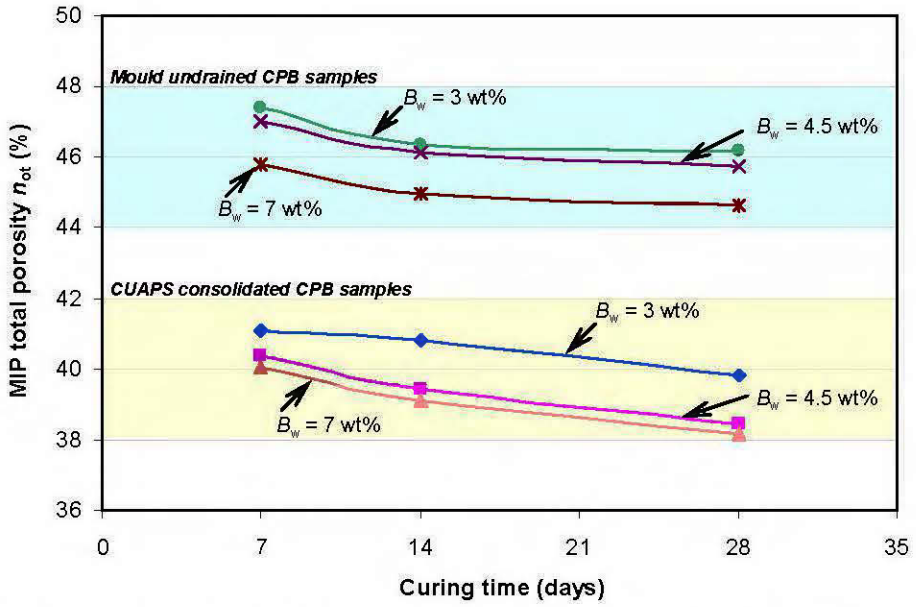

Figure 5.4 Change in MIP total porosity with curing time for CUAPS-consolidated and mould unconsolidated-undrained CPB samples.

- Figure 5.3 shows that the PSD curves depend on both *w/c* ratio (hence UCS, or cohesion) and curing conditions. Thus, Table 5.5 shows that the *w/c* ratio decreases from its initial value for a given curing time in the CUAPS-consolidated CPB samples. The *w/c* ratio of consolidated CPB decreases with the removal of excess water from samples due to the applied vertical pressure during curing and drainage. The reduction in the *w/c* ratio is accompanied by a slight reduction in n_{tot}, which could be explained by a reduction in pore size as pores are partially filled by hydrates and/or precipitates (C-S-H gel, gypsum).

- The effective curing conditions (the combined effects of applied pressure and water drainage on the consolidated paste backfill samples within the CUAPS apparatus) appear to accelerate the cementitious processes through the formation of increasing amounts of cementitious products in a mechanically reduced pore space. However, the hydration-precipitation appears to occur to a lesser extent in conventional mould CPB samples that are not allowed to drain. As a result, the porosity of unconsolidated-undrained samples is greater than that of CUAPS-consolidated samples.

Table 5.4 MIP test results for consolidated and undrained CPB samples as a function of cement content and curing time

Binder content (wt.%)	Curing time (day)	Mesopore[a] porosity n_{meso} (%)	Macropore[b] porosity n_{macro} (%)	Total porosity n_{tot} (%)	Bulk density ρ (g/mL)	Critical pore dia. d_{cr} (μm)	Threshold diameter d_{th} (μm)	Stem[c] volume V_{stem} (%)
CUAPS-consolidated backfill samples								
3	7	38.6	2.6	41.2	2.13	1.33	2.81	72
3	14	37.6	3.2	40.8	2.13	1.23	2.74	73
3	28	35.7	4.1	39.8	2.12	1.12	2.62	76
4.5	7	37.0	3.3	40.3	2.11	1.13	2.11	75
4.5	14	34.7	4.7	39.4	2.13	0.82	1.63	76
4.5	28	33.6	4.8	38.4	2.12	0.53	1.33	73
7	7	34.9	5.1	40.0	2.09	0.61	0.97	74
7	14	33.3	5.8	39.1	2.13	0.53	0.92	72
7	28	32.2	6.0	38.2	2.11	0.32	0.82	74
Mould unconsolidated-undrained backfill samples								
3	7	44.8	2.6	47.4	1.93	2.17	3.31	72
3	14	43.0	3.4	46.4	1.90	2.11	2.92	71
3	28	42.4	3.8	46.2	1.90	1.64	2.53	76
4.5	7	43.3	3.7	47.0	1.90	1.65	2.71	73
4.5	14	41.6	4.5	46.1	1.90	1.64	2.53	76
4.5	28	41.1	4.6	45.8	1.90	1.33	2.21	72
7	7	40.6	5.2	45.8	1.90	1.33	2.62	73
7	14	39.5	5.5	45.0	1.90	0.81	2.31	75
7	28	38.8	5.9	44.7	1.90	0.53	1.63	73

[a]Capillary mesopores range between 0.002 μm and 0.05 μm based on IUPAC classification.

[b]Macropores have pore size larger than 0.05 μm based on IUPAC classification.

[c]Maximum intrusion (stem) volume less than 25% or more than 90% suggests the need for a procedural change. The first instance indicates that a larger sample quantity might give better resolution and the second indicates that the capillary is on the verge of being depleted.

Table 5.5 Evaluation of water-to-cement (*w/c*) ratios of the CPB samples tested

Binder content (wt %)	Initial *w/c* ratio for all samples	Final *w/c* ratio for consolidated samples only		
		7 days	14 days	28 days
3	9.68	9.07	9.12	9.21
4.5	6.55	6.17	6.19	6.25
7	4.31	4.12	4.13	4.14

The modal distribution of the pore families present in the specimens can be determined from the incremental PSD curves. The graphs in Figures 3a, 3b, and 3c show only one pore family for all CPB sample types. They also show that as binder content increases, the proportion of pores sized 0.3–0.5 μm gradually increases for all samples. Thus, in this pore size range, the incremental porosity for 3, 4.5, and 7 wt% binder contents are respectively 3.2% and 2.5%, 5% and 3.1%, and 6.3% and 4.2% for both CUAPS-consolidated and mould unconsolidated-undrained samples (Figure 5.3). Furthermore, by increasing binder content from 3 to 7 wt%, the maximum incremental mercury porosity (corresponding to critical pore diameter d_{cr}, which can be obtained from the steepest slope of the cumulative PSD curves) increases from 6.1% to 6.4% for consolidated samples, and from 6.3 to 7.4% for unconsolidated-undrained samples. From these figures, it is apparent that samples cured under pressure produce greater pore refinement than samples cured traditionally (neither applied pressure nor drainage), mainly due to the accelerated development of cementitious phases.

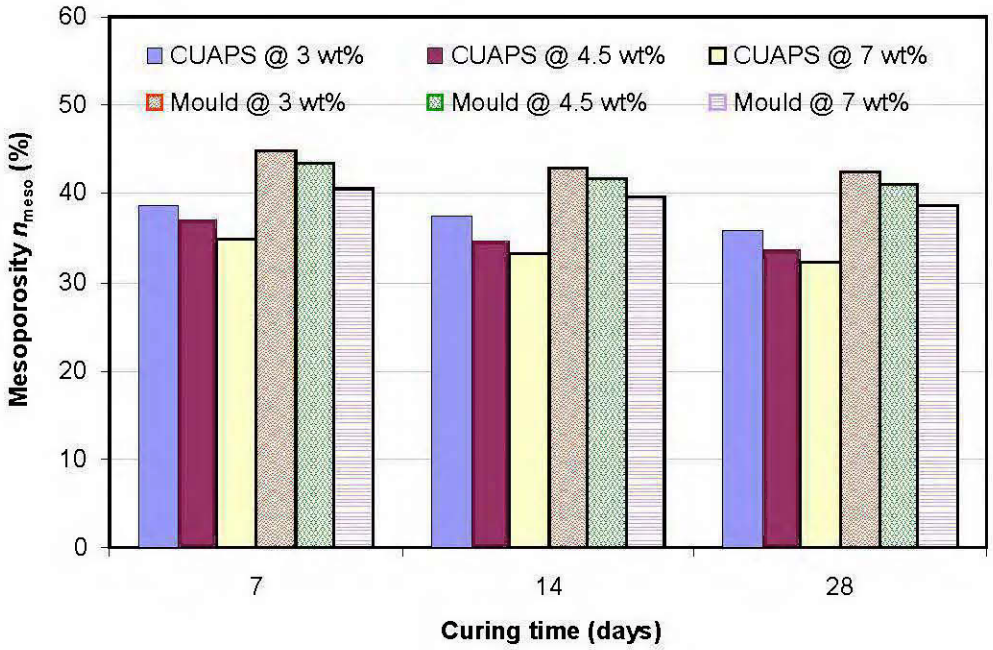

Figure 5.5 Change in mesoporosity with curing time for both CUAPS-consolidated and mould unconsolidated-undrained CPB samples using binder contents of 3, 4.5, and 7 wt%.

Figures 5.5 and 5.6 illustrate the change in mesoporosity n_{meso} (pore diameter range is 0.002–0.05 µm) and macroporosity n_{macro} (pore diameter > 0.05 µm) for CUAPS-consolidated and mold-undrained CPB samples with binder contents of 3, 4.5, and 7 wt% after curing for 7, 14, and 28 days. Figure 5.5 shows that the n_{meso} of undrained CPB samples are consistently higher than those of CUAPS-consolidated samples for a given binder content. Overall, n_{meso} decreases slightly with increasing binder content and curing time. For 4.5 wt% binder, the n_{meso} of CUAPS-consolidated samples decreases from 37 to about 34%, while the n_{meso} of undrained samples decreases from 43 to 41% when curing time increases from 7 to 28 days. Moreover, at early age (7-day curing), n_{meso} for 3, 4.5, and 7 wt% binders is 39%, 37%, and 35% for CUAPS-consolidated CPB samples, and 45%, 43%, and 41% for undrained CPB samples. For the same binder contents at 28 days, n_{meso} is 36%, 34%, and 32% for CUAPS-consolidated samples and 42%, 41%, and 39% for undrained samples. The n_{meso} for CUAPS-consolidated samples decreases at a higher rate (20%) than for mould-undrained samples (15%). The 5% difference could be explained by the CPB skeleton rearrangement due to applied pressure over the curing time (more fine pores and more binder hydrates).

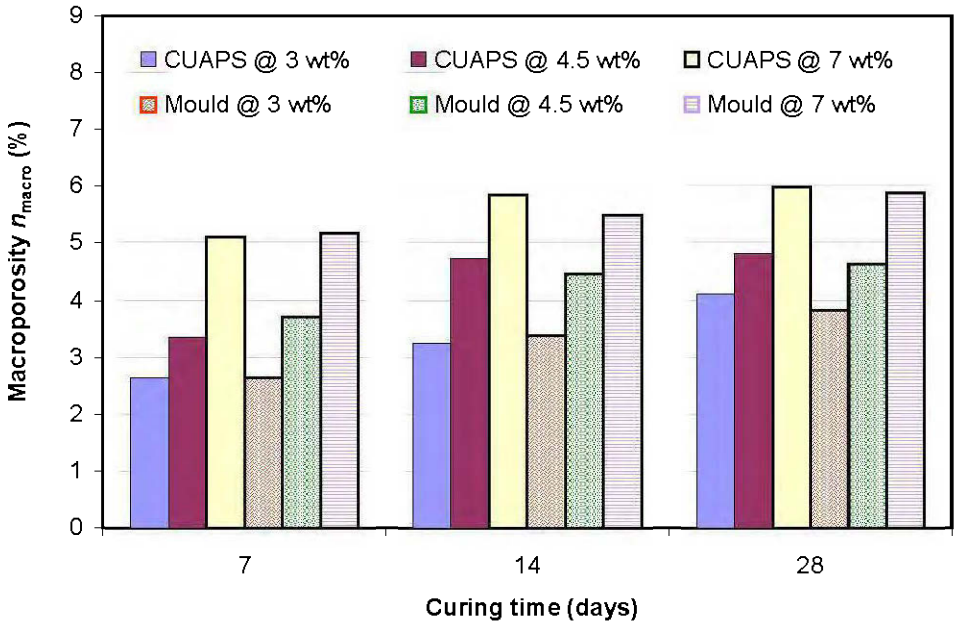

Figure 5.6 Evolution of macroporosity with curing time for both CUAPS-consolidated and mould unconsolidated-undrained CPB samples using binder contents of 3, 4.5, and 7 wt%.

Figure 5.6 shows relatively low macroporosity n_{macro} compared to n_{meso} for identical CPB samples under investigation. Changes in n_{macro} are almost the same (mainly a slight increase over time) for both CUAPS-consolidated samples and unconsolidated-undrained samples. For consolidated samples with 3, 4.5, and 7 wt% binder contents, n_{macro} increases from 2.6% to 4%, 3.3% to 4.8%, and 5% to 6%, respectively when curing time increases from 7 to 28 days. For unconsolidated-undrained samples, n_{macro} increases from 2.6% to 3.8%, 3.7% to 4.6%, and 5.2% to 5.9%, respectively, for 3, 4.5, and 7 wt% binder contents. However, these results show that macroporosity is less affected than mesoporosity by applied pressure.

5.3.2 Effect of curing conditions on critical pore size and threshold diameter of CPB

Other parameters can be used to characterize the pore structure of a cement-based material, such as critical pore size d_{cr} and threshold diameter d_{th} (Aligizaki, 2006). Critical pore size (or maximum continuous pore size) corresponds to the steepest slope of the cumulative porosity curve. The highest point of the steepest slope represents the mean size of pore entryways that allows maximum percolation throughout the pore system. The critical pore size d_{cr} controls the transmissivity of the material, and this parameter is most often used to examine the effect of factors such as *w/c* ratio, curing conditions, and time on pore structure change. The threshold diameter d_{th} is the minimum pore diameter that is geometrically continuous. More specifically, this diameter represents the pore size above which there is comparatively little mercury intrusion, and below which occurs the main intrusion; it could also be defined as the largest pore diameter at which significant intruded mercury volume is detected largest pore diameter (Diamond, 2000).

Figure 5.7 shows the change in d_{cr} with curing time for both plastic mold-undrained samples and CUAPS-consolidated samples. As can be seen clearly, d_{cr} decreases with increased binder content (3–7 wt%) and slightly decreases with curing time. Consolidated samples produce lower d_{cr} than mould-undrained samples. For 4.5 wt% binder content, d_{cr} at curing times of 7, 14, and 28 days is respectively 1.13 µm, 0.82 µm, and 0.53 µm for CUAPS-consolidated samples, and 1.65 µm, 1.64 µm, and 1.33 µm for mould-undrained samples (see Table 5.4).

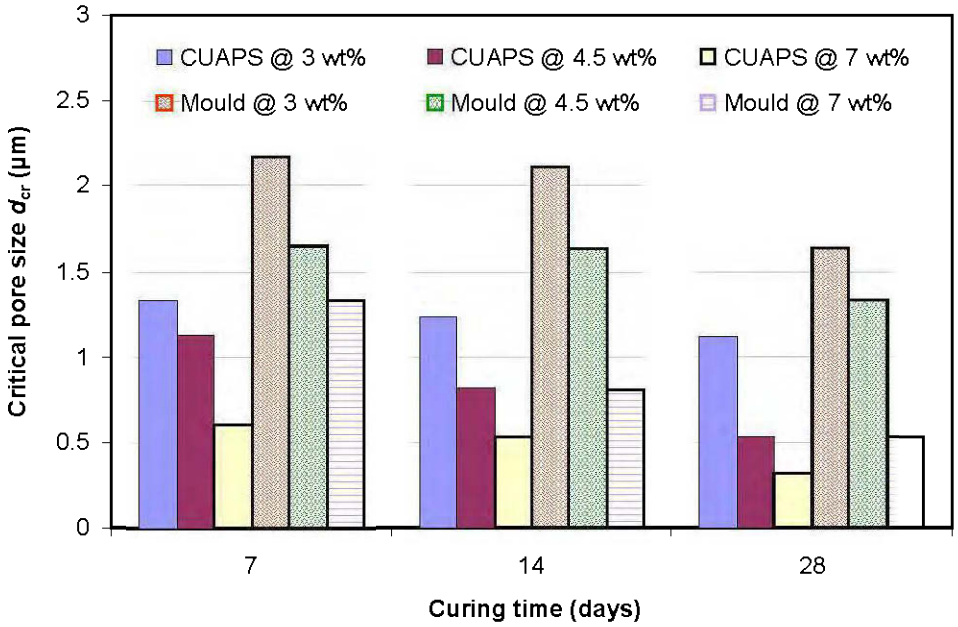

Figure 5.7 Change in critical pore diameter with curing time for both CUAPS-consolidated and unconsolidated-undrained CPB samples using binder contents of 3, 4.5, and 7 wt%.

Figure 5.8 shows that d_{th} decreases with increased binder content (3–7 wt%) and decreases slightly over curing time (7–28 days). After 28-day curing and for binder contents of 3, 4.5, and 7 wt%, consolidated samples show lower d_{th} at 2.62 µm, 1.33 µm, and 0.82 µm than unconsolidated-undrained samples at 2.53 µm, 2.21 µm, and 1.63 µm, respectively. For the highest binder (7%), d_{th} for undrained samples is respectively 2.62 µm, 2.31 µm, and 1.63 µm for curing times of 7, 14, and 28 days. For consolidated samples, d_{th} is respectively 0.97 µm, 0.92 µm, and 0.82 µm, corresponding to a decrease of 170%, 151%, and 99% after 7, 14, and 28 days of curing. This confirms that curing under applied vertical pressure contributes to refine the microstructure of the hardened CPB materials. Pores constrict during the curing process as precipitation/hydration phenomena happening in the pores progresses. Hence, d_{th} values lessen as curing time increases and *w/c* ratio decreases, as reported by numerous authors (Cook and Hover, 1999; Ouellet et al., 2007; Deschamps et al., 2008). In summary, MIP results show that threshold diameter ranges from 3.31 µm to 0.82 µm, which is fairly similar to the findings of Ouellet et al. (2007).

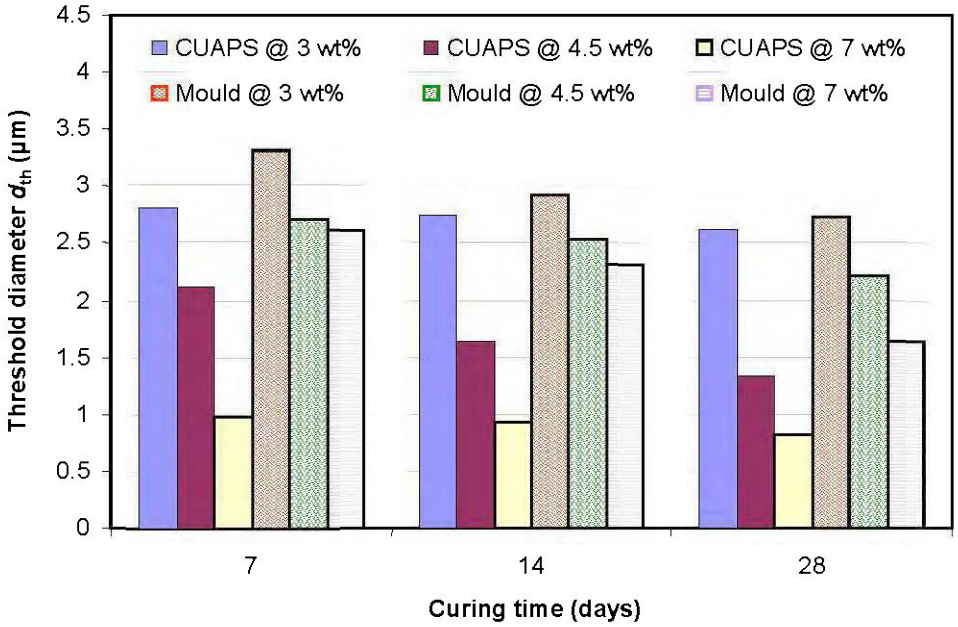

Figure 5.8 Change in threshold diameter with curing time for both CUAPS-consolidated and unconsolidated-undrained CPB samples using binder contents of 3, 4.5, and 7 wt%.

5.3.3 Effect of curing conditions on the compressive strength development of CPB

Figure 5.9 shows the change in uniaxial compressive strength (UCS) of CUAPS-consolidated samples and mould unconsolidated-undrained samples with curing time. It is apparent that curing conditions (with and without pressure) impact the compressive strength development of CPB samples. Consolidated samples always produce higher UCS than unconsolidated-undrained samples for a given binder content. In comparison, the UCS value of consolidated samples having a binder content of 3 wt% is respectively 57.9%, 64.3%, and 58.2% higher than that of unconsolidated-undrained samples for curing times of 7, 14, and 28 days. With binder contents of 4.5 and 7 wt%, UCS is 52.3%, 54.4%, and 51.8% higher, and 50.5%, 27.1%, and 19.8% higher, respectively. The higher UCS for consolidated CPB samples can be explained by the combined effects of applied consolidation pressures during curing and the removal of excess pore water, which accelerates the binding reaction, thereby producing higher mechanical strengths (UCS).

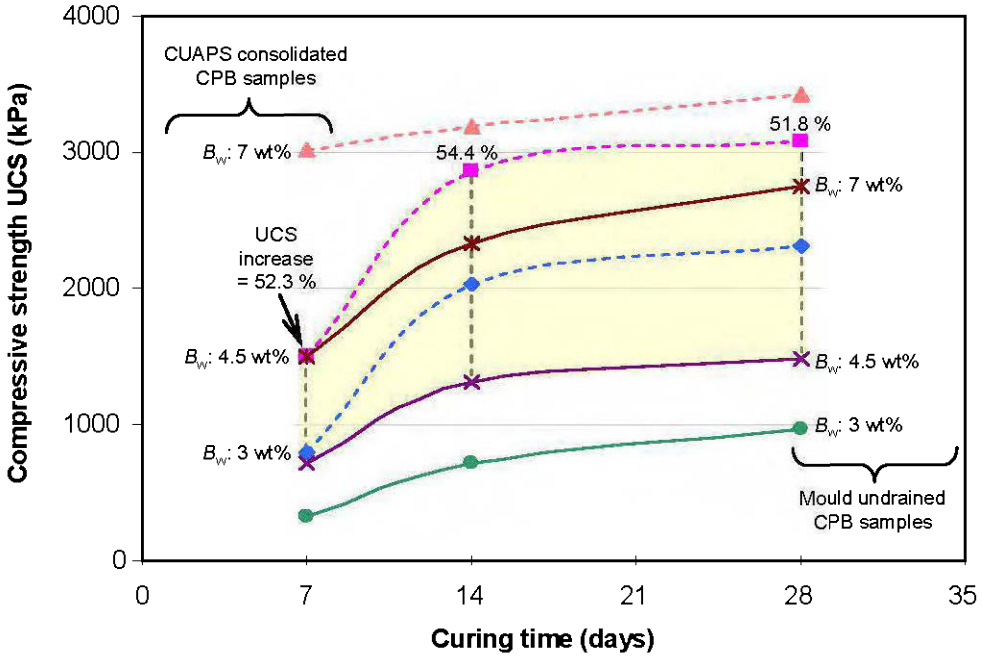

Figure 5.9 Change in uniaxial compressive strength (UCS) with curing time for mould unconsolidated-undrained and CUAPS-consolidated CPB samples. Coloured area shows UCS compared between CUAPS-consolidated samples and mould unconsolidated-undrained samples based on a binder content of 4.5 wt%.

Previous works (Belem et al., 2001, 2008a; Benzaazoua et al., 2004; Fall et al., 2005; Ouellet et al., 2006; El Aatar et al., 2007; Yilmaz et al., 2008a, 2009) have pointed out that the drainage of excess free water within the CPB samples positively affects binder hydration. As hydration progresses, the resulting cement products intrude into the CPB pore space (i.e., pore sizes become smaller), producing higher strength. Consequently, increased curing time and decreased *w/c* ratio result in lower porosity (see Table 5.5). In addition, some phases (such as sulfates) could have reached saturation more easily, as lower water contents were observed in the consolidated paste backfill samples, and no (or negligible) cement species were lost during drainage (Belem et al., 2008a). This would lead to more dense cementitious matrices (i.e., pore spaces were filled with cementitious phases), which in turn gave rise to better cohesion. The hardening process of fresh paste backfill materials during curing is addressed well elsewhere (Benzaazoua et al., 2004).

5.3.4 Effect of curing conditions on specific surface area of CPB

Figure 5.10 shows the change in SSA for CUAPS-consolidated paste backfill samples and plastic mould-undrained samples with curing time. Overall, SSA increases with increasing binder content and curing time. For 3 wt% binder content, SSA values are 5594, 6981, and 7729 m^2/kg for consolidated samples and 5967, 7320, and 8297 m^2/kg for unconsolidated-undrained samples for curing times of 7, 14, and 28 days, respectively. For 7 wt% binder content, SSA values are 8590, 9418, and 9826 m^2/kg for CUAPS-consolidated samples and 10120, 10748, and 11327 m^2/kg for conventional plastic mould-unconsolidated samples.

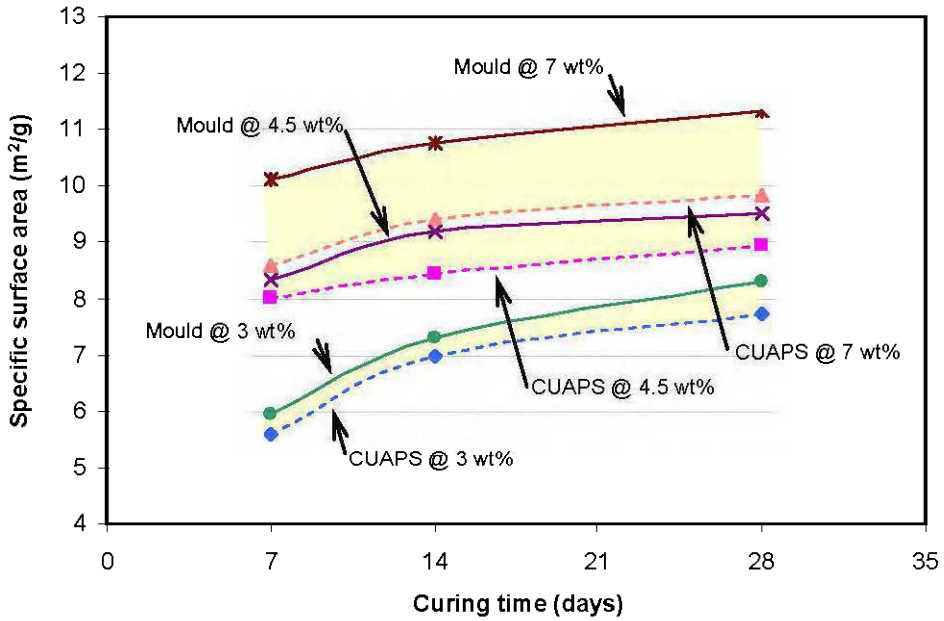

Figure 5.10 Change in specific surface area (SSA) with curing time for unconsolidated-undrained and CUAPS-consolidated CPB samples using binder contents of 3, 4.5, and 7 wt%. Coloured areas in the graph represent the difference observed between CUAPS-consolidated samples and mould unconsolidated-undrained samples.

Overall, the unconsolidated CPB samples consistently produce higher SSA than consolidated samples for a given binder content and curing time, confirming previous findings by Belem et

al. (2002). Moreover, after 28 days of curing, as binder content increases from 3 to 7 wt%, SSA increases from 7729 to 9826 m^2/kg for consolidated CPB samples and from 8297 to 11327 m^2/kg for unconsolidated-undrained CPB samples. This significant increase in material fineness can be partly explained by the gradual formation of cement hydration products. These observations are in addition supported by earlier SSA tests performed on unconsolidated backfills cured for 91 days (Benzaazoua et al., 2000).

5.4 RELATIONSHIPS BETWEEN UCS AND MIP PARAMETERS

The microstructure of CPB samples is directly related to their physical and mechanical properties (Aligizaki, 2006). Among the factors determining the UCS of a cementitious material are 1) the composition of binders and tailings GSD, 2) the *w/c* ratio of the mix, 3) mixing conditions, and 4) curing conditions, especially RH, temperature, and time (Taylor, 1990). UCS is the most often used index parameter for CPB mix optimization and stability design. Thus, it is particularly relevant to evaluate how this index parameter is affected by changes in the pore structure of hardened CPB. Many attempts have been made to express the empirical and semi-analytical relationships between the UCS and porosity of different types of cement-based materials such as cement pastes, concrete, mortars, and CPB (Kendall et al., 1983; Hakkinen, 1993; Takahashi et al., 1997; Zhang, 1998; Kumar and Bhattacharjee, 2003b; Lee et al., 2003; Li and Aubertin, 2003; Ouellet et al., 2007, 2008).

These studies showed that UCS development within cement-based material is a function of the number, shape, and distribution of the void space and porosity. It is generally accepted that the relationship between strength and porosity can be simply and empirically represented by a linear plot (Vodak et al., 2004). Nevertheless, nonlinear regression correlations using exponential, power law, and yield-density models are also commonly used. Relationships between UCS and porosity are found in the literature for a given cemented material. Some of these relations use total porosity $n_{Hg\text{-}tot}$ while others use fractional pore size or partial porosity derived from MIP cumulative curves. Most relationships also use strength at zero porosity or porosity at zero strength parameters, which can be difficult to estimate (Matusinović et al.,

2003). Ouellet et al. (2007) proposed a generalized model that distinguishes between the contribution of porosity and size-dependent porosity (based on 0.3 µm pore size) for CPB. In the following subsections, results from this study and the Ouellet et al. (2007) equation are first compared. Some simple expressions, based on microstructural parameters (MIP meso- and macroporosity, threshold diameter and specific surface area) and UCS are proposed using various regression (best fit) analyses.

5.4.1 Ouellet et al.'s power law model

Ouellet et al. (2007) proposed a predictive equation to estimate the compressive strength of different CPB materials using MIP total and partial porosities (Eq. 5.2), in which the effect of microstructural evolution is evaluated by two fractional size distributions (fine and coarse pore sizes) based on a fixed diameter d (0.3 µm). The equation can be expressed as:

$$\sigma_{cn} = \sigma_{n_{\min}} \left[\frac{(1-n)}{(1-n_{\min})} \right]^{u} \cdot \left[\frac{(1-n_{\geq d})}{(1-n_{<d})} \right]^{V} \tag{5.2}$$

where σ_{cn} is the uniaxial compressive strength UCS (kPa) for a given MIP total porosity n, σ_{nmin} is the reference compressive strength UCS at minimum porosity n_{min}, $n_{\geq d}$ is the cumulative MIP porosity for pore sizes larger than diameter d (considered as 0.3 µm), $n_{<d}$ is the cumulative MIP porosity for pore sizes smaller than diameter d, and u and V are exponents used to define the non-linearity of the two functions in brackets.

In this equation, a reference UCS value of 4080 kPa is considered for CPB having n_{min} = 0.25. This specific value is based on the minimum n values measured on underground hard rock mine tailings (Bussière, 1993; Brackebusch, 1994; Aubertin et al., 1996; Amaratunga and Yaschyshyn, 1997; Cayouette, 2003) and on an additional porosity reduction mainly due to the formation of cementitious phases within the backfill. The model was developed using CPB samples (prepared in standard moulds) made of non-sulphidic material (ground silica

having a GSD similar to typical mine tailings) mixed with three binder types (100% ordinary Portland cement GU, a mix of 20% GU and 80% ground granulated blast furnace slag, and a mix of 70% GU and 30% fly ash) at 5% wt, and three water types (deionised water and two ore treatment waters containing 4613 pap and 7549 pap of sulfates). More information on the CPB recipes tested to develop Eq. (5.2) can be found in Ouellet et al. (2007).

Eq. (5.2) implies that the final UCS is related to the difference between MIP total porosity and minimum porosity (first term of Eq. 5.2) and to the ratio between the pore fractions greater than 0.3 μm and the fraction lower than 0.3 μm. The weight of each term is conditioned by the u and V exponents. These constant exponents control the non-linearity of the strength–porosity relationship. Based on their data, in which no significant change in MIP total porosity was observed for all specimens tested, Ouellet et al. (2007) suggested values of 1 and 5.2 for the u and V exponents, while mentioning that these two parameters were obtained by fitting.

To obtain a good fit between the results obtained in the present study and Eq. (5.2), parameter u was kept at 1 and parameter V was changed to 3.2. This new fitting gives more weight to a slight change in total porosity (first term in brackets in Eq. 5.2). This is consistent with the slight change in total MIP porosity observed with curing time in the present study (see Fig. 4), although this effect was not observed by Ouellet et al. (2007). A possible explanation for the need to slightly reduce the value of exponent V from V = 5.2, as used in Ouellet et al. (2007), would be differences in tailings mineralogy and GSD, mixing water geochemistry, hydraulic binder types, and their proportions and curing conditions (under pressure or not). Hence, for each CPB recipe, the u and V parameters in Eq. (5.2) must be verified and adjusted. Figure 5.11 presents a comparison between laboratory measured and calculated UCS values using Eq. (5.2), showing that about 80% of the measurements for CPB samples are predicted within a precision range of ±25%. Considering that this type of tool is usually used for preliminary evaluation when only small amounts of material are available, the precision obtained with Eq. (5.2) can be considered acceptable. In Ouellet et al. (2007), it is worth mentioning that the proposed estimation method could not replace an appropriate

experimental investigation in order to adequately determine the unconfined and confined characteristics of CPB materials for purposes of design or quality control monitoring.

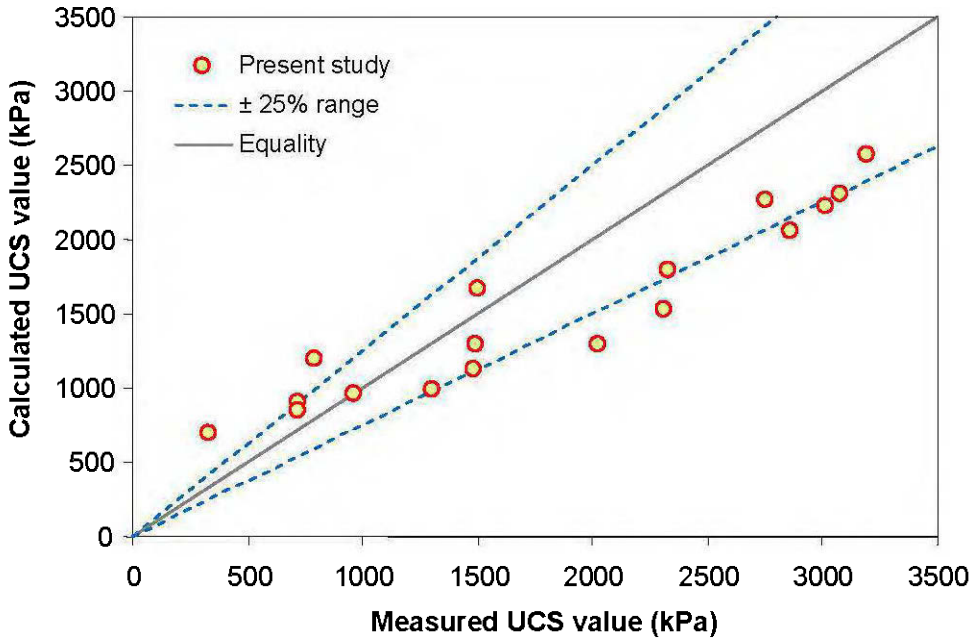

Figure 5.11 Comparison of laboratory measured and calculated UCS values using Eq. (2) with the MIP total and partial porosity data obtained from this study.

5.4.2 Proposed relationships between UCS and MIP parameters for CPB

The previous sections have shown that for the CPB samples tested in this study, the partial porosity obtained with MIP correlates well with strength. In the following subsections, some empirical relationships are presented in more detail and also in Appendix G.

5.4.2.1 Relationships between UCS and meso- and macroporosity

As mentioned above, the pore system in cement-based materials consists mainly of three pore types: gel micropores (pores within the C-S-H gel or hydrated products), capillary mesopores (residual pores from cement hydration), and larger macropores (IUPAC, 1972).

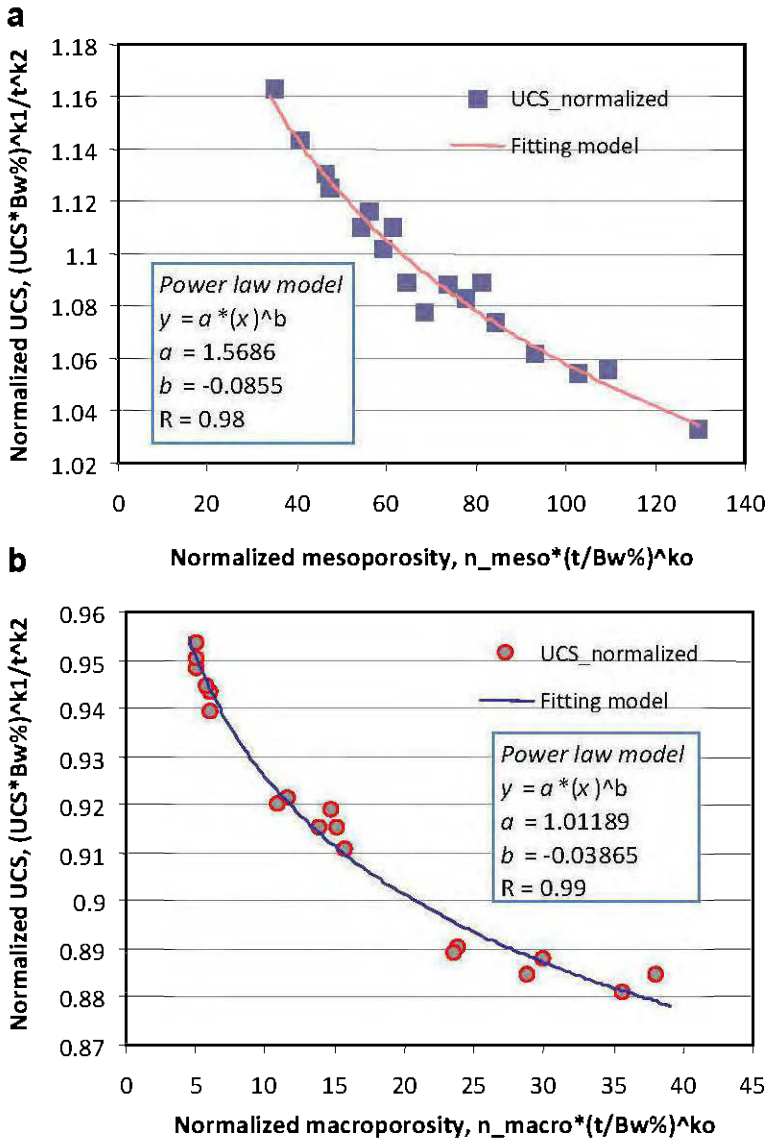

Figure 5.12 Graphical representation of Eq. (3) showing the relationship between (a) normalized UCS versus normalized mesoporosity and (b) normalized UCS versus normalized macroporosity for CPB samples.

Kendall et al. (1983) demonstrated that gel pores are too small to initiate cracking under relatively low stress, and therefore do not detract from the strength of cement-based material. Capillary pores and other larger pores, however, are responsible for reductions in strength

and elasticity (Cook and Hover, 1999; Taylor, 1990; O'Farrell et al., 2001). Capillary pores are thus sufficient to initiate cracking, hence reducing the strength gain of cemented-based materials (Kendall et al., 1983). The pore structure parameters considered here are mesopores (between 0.002 μm and 0.05 μm) and macropores (larger than 0.05 μm).

Figure 5.12 shows the relationship of normalized UCS [$y = (UCS * B_{w\%})^{\beta_1} / (t)^{\beta_2}$] as a function of normalized meso/macroporosity [$x = n_{meso,\,macro} * (t / B_{w\%})^{\beta_0}$] for the combined data obtained from both CUAPS-consolidated and unconsolidated-undrained CPB samples. Substituting the normalized variables into a power law relationship [$y = a*x\hat{}b$] yields the empirical relationship between UCS and n_{meso}/n_{macro}, given in Eq. (5.3) as follows:

$$UCS = \alpha \cdot (n_{meso,\,macro})^{\beta_0} \cdot \frac{t^{\beta_1}}{(B_{w\%})^{\beta_2}} \tag{5.3}$$

where UCS = compressive strength (kPa), $n_{meso,\,macro}$ = meso- or macroporosity (%), t = curing time (days), $B_{w\%}$ = binder content (wt%), and α, β_0, β_1, and β_2 are empirical constants. For the binder used (GU-Slag@20:80), α = 6.62E+07, β_0 = –3.4201, β_1 = 0.29, and β_2 = –0.71 for n_{meso}, and α = 10.6528, β_0 = –7.7293, β_1 = 2.2706, and β_2 = –6.7293 for n_{macro}, with a coefficient of correlation r = 0.98 (n_{meso}) and = 0.99 (n_{macro}), respectively. This equation can be used for other binder types simply by adjusting the fitting constants.

5.4.2.2 Relationship between UCS and threshold diameter

Diamond (2000) suggested that, due to limitations in the interpretation of MIP results, the effective diameter d_{eff} or threshold diameter d_{th} should be used to compare pore structures of cement-based materials. In this view, Figure 5.13 presents a general yield-density fitting relationship of normalized UCS [$y = (UCS * B_{w\%})^{k_1} / (t)^{k_2}$] as a function of normalized threshold diameter [$x = d_{th} * (t / B_{w\%})^{k_0}$] for the combined data obtained from CUAPS-

consolidated and undrained samples. This figure shows that as d_{th} decreases, UCS increases. Substituting the normalized variables into a yield-density model [$y = 1/(a+b*x\hat{}c)$] yields the empirical relationships between UCS and d_{th}, given in Eq. (5.4) as follows:

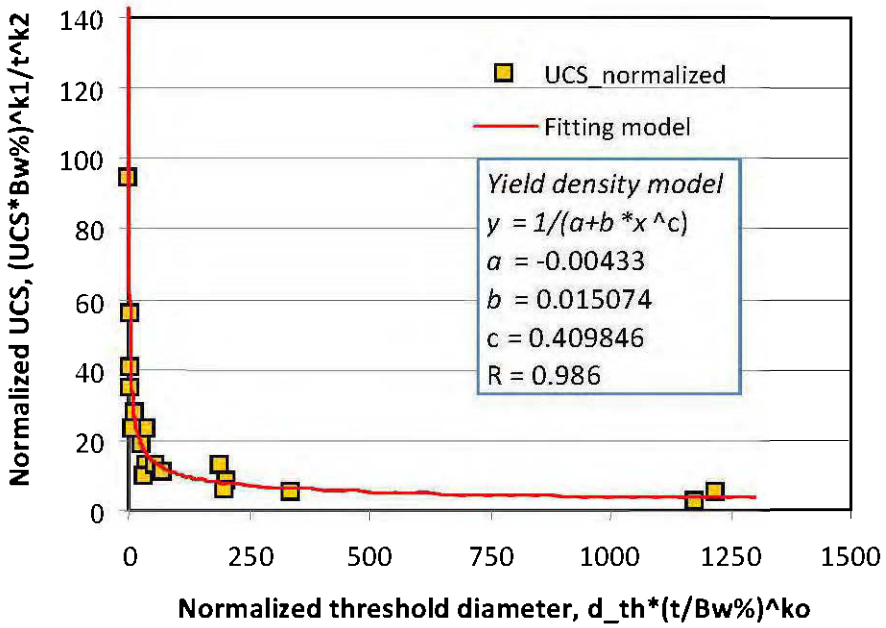

Figure 5.13 Graphical representation of Eq. (4) showing the relationship between normalized UCS and normalized threshold diameter for CPB samples.

$$UCS = \frac{(t)^{\alpha_0}}{B_{w\%}\left(a + b\cdot(d_{th})^{c}\cdot\left(\frac{t}{B_{w\%}}\right)^{\alpha_1}\right)^{\alpha_2}} \tag{5.4}$$

where UCS = unconfined compressive strength (kPa), d_{th} = threshold diameter (μm), t = curing time (days), $B_{w\%}$ = binder content (wt%), and α_0, α_1, α_2, a, b, and c are empirical constants. For the binder type used (GU-Slag@20:80), $\alpha_0 = 2$, $\alpha_1 = 1.1270$, $\alpha_2 = 1.3333$, $a = -0.0043$, $b = 0.015$, and $c = 0.4098$, with a coefficient of correlation $r = 0.99$. Again, this equation can be used for other CPB types by adapting the fitting constants.

5.4.2.3 Relationship between UCS and specific surface area

Specific surface area (SSA), which is a fineness parameter, provides indirect information about the microstructure of CPB samples during curing. Therefore, SSA can be closely related to the UCS development of CPB (Belem et al., 2002, 2006; Benzaazoua et al., 2000). Figure 5.14 shows the change in UCS for both CUAPS-consolidated and unconsolidated-undrained CPB samples as a function of SSA, indicating a proportionality between SSA and the binder content used within the CPB, and therefore UCS development.

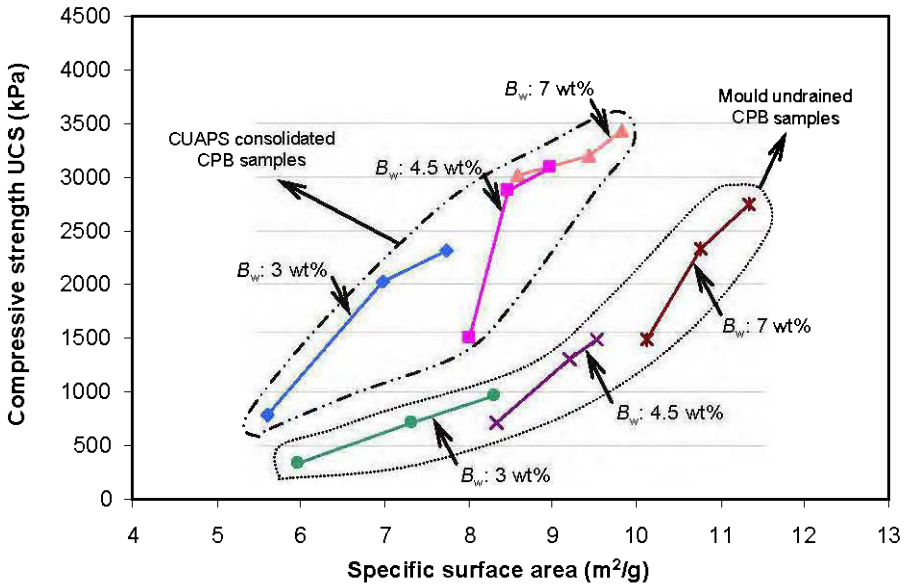

Figure 5.14 Change in compressive strength with specific surface area for all CPB samples.

It is generally accepted that increasing the fineness of cement particles can increase the hydration rate. Hence, increasing the hydration rate also increases the degree of hydration, which in turn produces higher strength development. However, it is observed from Figure 5.14 that SSA is not the only parameter that controls UCS development. In fact, consolidated backfills often show higher UCS and surprisingly lower SSA than unconsolidated-undrained backfills for a given binder content. This unexpected observation is probably due to the

combined effects of the gradual formation of precipitated cement hydrates and the particle rearrangement process at the early stages of compaction (removal of water leads to solid density increase or decrease in the voids present within the CPB material).

Figure 5.15 shows a linear relationship of normalized UCS [$y = \ln\left[(UCS * B_{w\%})^{k_1} / (t)^{k_2}\right]$] as a function of normalized SSA [$x = \ln\left[SSA * (t / B_{w\%})^{k_0}\right]$] for the combined data obtained from CUAPS-consolidated and unconsolidated-undrained CPB samples. This figure shows that as normalized SSA increases, UCS increases proportionally.

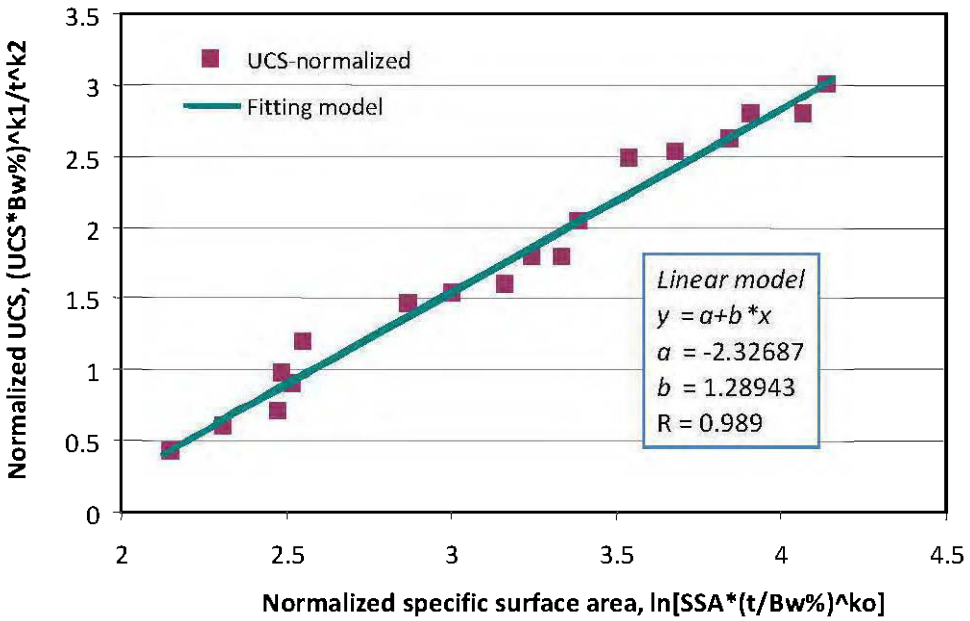

Figure 5.15 Graphical representation of Eq. (5) showing the relationship between normalized UCS and normalized SSA for CPB samples.

Substituting the normalized variables into a linear model [y = a+b*x] yields the relationships between strength (UCS) and specific surface (SSA), given in Eq. (5.5) as follows:

$$UCS = \lambda \cdot (SSA)^{\alpha} \cdot \left(B_{w\%}\right)^{\beta_0} t^{\beta_1} \tag{5.5}$$

where UCS = unconfined compressive strength (kPa), SSA = specific surface area (m^2/g), t = curing time (days), $B_{w\%}$ = binder content (wt%), and λ, α, β_0, and β_1 are empirical constants. For the binder type used (GU-Slag@20:80 wt%), λ = 9.074E-05, α = 5.1577, β_0 = –5.6677, and β_1 = –1.3322, with a coefficient of correlation r = 0.99. This equation can be used for other CPB types by adapting the fitting constants.

5.5 CONCLUSIONS

This paper presents the results of an experimental investigation of the microstructure of different mixtures of CPB samples (binder contents of 3, 4.5, and 7 wt%) characterized by mercury intrusion porosimetry (MIP) and specific surface area (SSA) measurement. Two types of backfill samples, consolidated (using a recently developed consolidometer, an improved CUAPS apparatus (curing under applied pressure system) and mould undrained samples were prepared. Total porosity n_{tot}, pore size distribution PSD, threshold diameter d_{th}, and compressive strength UCS of the samples were determined for 3, 4.5, and 7 wt% binder contents and for 7, 14, and 28-day curing times. Based on the obtained results, the following conclusions can be drawn:

- MIP total porosity n_{tot} decreased slightly from 41% to 38% for CUAPS-consolidated backfills and from 47% to 45% for unconsolidated-undrained backfills, depending on the *w/c* ratio and curing time. Longer curing times and lower *w/c* ratios therefore result in lower total porosity values.

- Binder content and curing time play a significant role in the resultant CPB pore size distribution. Increased binder content (from 3 wt% to 7 wt%) caused PSD curves to shift towards lower pore size, resulting in decreased porosity and threshold diameters.

- Threshold diameter d_{th} of CUAPS-consolidation backfills ranged from 2.81 µm to 0.82 µm while d_{th} of unconsolidated-undrained backfills ranged from 3.31 µm to 1.63 µm. For a given CPB, longer curing times (up to 28 days) and lower *w/c* ratios therefore result in lower threshold diameter.

- ❖ UCS data reveal that consolidated backfills consistently produced higher strength than mould unconsolidated-undrained backfills, mainly due to the consolidation that refines the pore structure during curing. A clear relationship was found between MIP pore-size parameters (< 0.3 μm, meso- and macroporosity) and uniaxial compressive strength.

- ❖ From the SSA data, it was inferred that specific surface area was indirectly related to UCS development for each backfill specimen. This implies that the greater the SSA, the higher the volume of cement hydration products, resulting in considerably increased UCS of CPB samples.

Despite these interesting results, further laboratory tests are needed to better characterize the pore structure of CPB materials and to develop more generalized relationships between pore structure parameters and mechanical strength.

5.6 ACKNOWLEDGEMENTS

The authors would like to express their appreciation to the NSERC (Natural Sciences and Engineering Research Council of Canada) Discovery Grant Prog-ram, the Industrial NSERC-Polytechnique-UQAT Chair on Environment and Mine Wastes Management, and the Canadian Research Chair on Integrated Management of Sulphidic Mine Mailings using Backfill Technology for their generous financial support for this research study. The Canada Foundation for Innovation (CFI) is gratefully acknowledged for the manufacture of the ten CUAPS apparatuses. Special thanks are extended to Pierre Trudel of G+ Plus Industrial Plastic Inc. for his collaborative assistance in modifying the CUAPS apparatus, to David Bouchard, Yvan Poirier, and Nil Gaudet (UQAT-URSTM technicians) for their technical support, and to Nathan Mutch of Lafarge North America Inc. for kindly providing the cement materials. The authors are also grateful to Dr. Serge Ouellet of Agnico-Eagle Mines Ltd. (Technical Services Division) and to the two anonymous reviewers for their helpful and constructive comments on the earlier version of the manuscript.

5.7 REFERENCES

Ait-Mokhtar, A., Amiri, O., Dumargue, P., Sammartino, S., 2002. A new model to calculate water permeability of cement-based materials from MIP results. *Advanced Concrete Research,* Vol. 13, No. 1, No. 1–7.

Aligizaki, A.K., 2006. Pore structure of cement-based materials: testing, interpretation and requirement. Modern Concrete Technology. Series; v.12, Taylor and Francis.

ASTM Designation D1557, 1991. Standard test method for liquid limit, plastic limit, and plasticity index of soils. In: *Annual Book of ASTM Standards,* Vol. 04-02, ASTM International, West Conshohocken, PA, pp. 573–583.

ASTM Designation C39, 2002. Standard test method for compressive strength of cylindrical concrete specimens. In: *Annual Book of ASTM Standards,* Vol. 04-02, ASTM International, West Conshohocken, PA, pp. 15–23.

ASTM Designation D4404, 2002. Standard test method for determination of pore volume and pore volume distribution of soil and rock by mercury intrusion porosimetry. In: *Annual Book of ASTM Standards,* Vol. 04-08, ASTM International, West Conshohocken, PA, pp. 582–586.

ASTM Designation D6556, 2009. Standard test method for carbon black-total and external surface area by nitrogen adsorption. In: *Annual Book of ASTM Standards,* Vol. 04-08, ASTM International, West Conshohocken, PA, pp. 411–428.

Amaratunga, L.M., Yaschyshyn, D.N., 1997. Development of a high modulus paste fill using fine gold mill tailings. *Geotechnical and Geological Engineering,* Vol. 15, No. 3, pp. 205–219.

Aubertin, M., Bussière, B., Chapuis, R.P., 1996. Hydraulic conductivity of homogenized tailings from hard rock mines. *Canadian Geotechnical Journal,* Vol. 33, No. 3, pp. 470–482.

Belem, T., Benzaazoua, M., Bussière, B., 2000. Mechanical behaviour of cemented paste backfill. In: *The 53rd Canadian Geotechnical Conference "geotechnical engineering at the dawn of the third millennium",* vol 1, Montreal, Quebec, Canada, October 15–18, pp. 373–380.

Belem, T., Bussière, B., Benzaazoua, M., 2001. The effect of microstructural evolution on the physical properties of paste backfill. In: *Proceedings of the 8th International conference on Tailings and Mine Waste,* Vail, Forth Collins, Colorado, United States, A.A. Balkema, pp. 365–374.

Belem, T., Benzaazoua, M., Bussière, B., Dagenais, A.M., 2002. Effects of settlement and drainage on strength development within mine paste backfill. In: *Proceedings of the 9th International conference on Tailings and Mine Waste,* Vail, Forth Collins, Colorado, United States, January 27–30, pp. 139–148.

Belem, T., El Aatar, O., Bussière, B., Benzaazoua, M., Fall, M., Yilmaz, E., 2006. Characterization of self-weight consolidated paste backfill. In: *Proceedings of the 9th International Seminar on Paste and Thickened Tailings,* Limerick, Ireland, April 3–7, pp. 333–345.

Belem, T., El Aatar, O., Benzaazoua, M., Bussière, B., Yilmaz, E., Hydro-geotechnical and geochemical characterization of column consolidated cemented paste backfill. In: *Proceedings of the 9th International Symposium on Mining with Backfill,* CIM, Montreal, Quebec, Canada, April 29–May 2, pp. 162–171.

Belem, T., Benzaazoua, M., 2008a. Design and application of underground paste backfill technology. *Geotechnical and Geological Engineering,* Vol. 26, No. 2, pp. 147–174.

Belem, T., Benzaazoua, M., 2008b. Predictive models for pre-feasibility cemented paste backfill mix design. In: *Post-Mining'08, GISOS: Research Group for the Impact and Safety of Underground Works,* Nancy, France, February 6-8, pp. 155–169.

Benzaazoua, M., 1996. Caractérisation physico-chimique et minéralogique de produits miniers sulfures en vue de la réduction de leur toxicité et de leur valorisation. *Ph.D. Thesis,* Institut national polytechnique de Lorraine, Nancy, France.

Benzaazoua, M., Ouellet, J., Servant, S. Newman, P., Verburg, R., Cementitious backfill with high sulfur content: physical, chemical and mineralogical characterization. *Cement and Concrete Research,* Vol. 29, No. 5, pp. 719–725.

Benzaazoua, M., Belem, T., Jolette, D., 2000. Investigation de la stabilité chimique et de son impact sur la qualité des remblais miniers cimentés. In: *Institut de Recherche Robert-Sauvé en Santé et en Sécurité du Rravail Report No R–260,* Canada, pp. 1–172.

Benzaazoua, M., Belem, T., Bussière, B., 2002. Chemical factors that influence the performance of mine sulphidic paste backfill. *Cement and Concrete Research,* Vol. 32, No. 7, pp. 1133–1144.

Benzaazoua, M., Fall, M., Belem, T., 2004. A contribution to understanding the hardening process of cemented pastefill. *International Journal of Minerals Engineering,* Vol. 17, No. 2, pp. 141–152.

Benzaazoua, M., Belem, T., Yilmaz, E., Novel lab tool for paste backfill. *Canadian Mining Journal,* Vol. 127, No. 3, pp. 31–31.

Brackebusch, F.W., 1994. Basics of paste backfill systems. *Mining Engineering,* Vol. 46, No. 10, pp. 1175–1178.

Bussière, B., Colloquium 2004, 2007. Hydrogeotechnical properties of hard rock tailings from metal mines and emerging geoenvironmental disposal approaches. *Canadian Geotechnical Journal,* Vol. 44, No. 9, pp. 1019–1052.

Bussière, B., 1993. Evaluation des propriétés hydrogéologiques de résidus miniers utilisés comme barrières de recouvrement. *M.Sc. Thesis,* Université de Montréal École Polytechnique, Québec, Canada.

Cayouette, J., 2003. Optimization of the paste backfill plant at Louvicourt mine. *Canadian Institute of Mining, Metallurgy and Petroleum Bulletin,* Vol. 96, No. 175, pp. 51–57.

Cook, R., Hover, K., 1999. Mercury porosimetry of hardened cement pastes. *Cement and Concrete Research,* Vol. 29, No. 6, pp. 933–943.

Deschamps, T., Benzaazoua, M., Bussière, B., Aubertin, M. Belem, T., 2008. Microstructural and geochemical evolution of paste mine tailings in surface disposal. *Minerals Engineering,* Vol. 21, No. 4, pp. 341–353.

Diamond, S., 2000. Mercury porosimetry: an inappropriate method for the measurement of pore size distributions in cement-based materials. *Cement and Concrete Research,* Vol. 30, No. 10, pp. 517–1525.

El Aatar, O., Belem, T., Bussiere, B., Benzaazoua, M., Yilmaz, E., 2007. Microstructural properties of column consolidated paste backfill. In: *Proceedings of the 60th Canadian Geotechnical Conference and the 8th Joint CGS/IAH-CNC Groundwater Conference,* Ottawa, Ontario, Canada, October 21–24, pp. 45–52.

El Aatar, O., 2009. Consolidation behavior of cemented paste backfill material. *Unpublished M.Sc. Thesis,* Université du Québec en Abitibi-Témiscamingue (UQAT), Rouyn-Noranda, Québec, Canada.

Ercikdi, B., Kesimal, A., Cihangir, F., Deveci, H., Alp, I., 2009. Cemented paste backfill of sulphide-rich tailings: Importance of binder type. *Cement and Concrete Research,* Vol. 31, No. 4, pp. 268–274.

Fall, M., Benzaazoua, M., Ouellet, S., 2005. Experimental characterization of the influence of tailings fineness and density on the quality of cemented paste backfill. *International Journal of Minerals Engineering,* Vol. 18, No. 1, pp. 41–44.

Fall, M., Samb, S.S., 2008. Pore structure of cemented tailings materials under natural or accidental thermal loads. *Material Characterization,* Vol. 59, No. 5, pp. 598–605.

Fourie, A.B., Fahey, H., Helinski, M., 2007. Using effective stress theory to characterize the behaviour of backfill. *Canadian Institute of Mining, Metallurgy and Petroleum Bulletin,* Vol. 100, No. 1103, pp. 1–9.

Galle, C., 2001. Effect of drying on cement-based materials pore structure as identified by mercury intrusion porosimetry: A comparative study between oven, vacuum, and freeze–drying. *Cement and Concrete Research,* Vol. 31, No. 10, pp. 1467–1477.

Garboczi, E.J., 1990. Permeability, diffusivity, and microstructural parameters: A critical review. *Cement and Concrete Research,* Vol. 20, No. 4, pp. 591–601.

Godbout, J., 2005. Évolution des propriétés hydriques des remblais miniers cimentés en pâte durant le curage. *M.Sc. Thesis,* École Polytechnique, Québec, Canada.

Grabinsky, M.W., Bawden, F.W., 2007. In situ measurements for geomechanical design of cemented pastefill systems. *Canadian Institute of Mining, Metallurgy and Petroleum Bulletin,* Vol. 100, No. 1103, pp. 1–8.

Hakkinen, T., 1993. Effect of slag content on microstructure, permeability and mechanical properties of concrete. Part 1 Microstructural studies and basic mechanical properties. *Cement and Concrete Research,* Vol. 23, No. 2, pp. 407–421.

Helinski, M., Fourie, A.B., Fahey, M., 2006. Mechanics of early age cemented paste backfill. In: *Proceedings of the 9th International Seminar on Paste and Thickened Tailings,* Limerick, Ireland, April 3–7, pp. 313–322.

Helinski, M., Fourie, A.B., Fahey, M., 2009. Prelimary results from an investigation into the effect of application of effective stress to cemented paste backfill during curing. *Australian Centre for Geomechanics Newsletter,* Vol. 31, No. 12, pp. 10–13.

IUPAC, 1972. Manual of symbols and terminology. Appendix 2, Part 1: Colloid and surface chemistry. *Journal of Pure Applied Chemistry,* Vol. 31, No. 1, pp. 578–593.

Kendall, K., Howard, A.J., Birghall, J., 1983. The relation between porosity, microstructure and strength, and the approach to advanced cement-based materials. *International Journal of Philosophical Transactions of the Royal Society B: Biological Sciences,* Vol. 310, No. 2, pp. 139–153.

Kesimal, A., Ercikdi, B., Yilmaz, E., 2003. The effect of desliming by sedimentation on paste mine backfill performance. *International Journal of Minerals Engineering,* Vol. 16, No. 10, pp. 1009–1011.

Kesimal, A., Yilmaz, E., Ercikdi, B., 2004. Evaluation of paste backfill mixtures consisting of sulphide-rich mill tailings and varying cement contents. *Cement and Concrete Research,* Vol. 34, No. 10, pp. 1817–1822.

Kesimal, A., Yilmaz, E., Ercikdi, B., Alp, I., Deveci, H., 2005. Effect of properties of tailings and binder on the short and long terms strength and stability of cemented paste backfill. *Material Lettters,* Vol. 59, No. 28, pp. 3703–3709.

Kumar, R., Bhattacharjee, B., 2003a. Study on some factors affecting the results in the use of MIP in concrete. *Cement and Concrete Research,* Vol. 33, No. 3, pp. 417–424.

Kumar, R., Bhattacharjee, B., 2003b. Porosity, pore size distribution and in situ strength of concrete. *Cement and Concrete Research,* Vol. 33, No. 1, pp. 155–164.

le Roux K.-A., 2004. In situ properties and liquefaction analysis of cemented paste backfill. *Ph.D. Thesis,* The University of Toronto, Ontario, Canada.

Lee, C.Y., Lee, H.K., Lee, K.M., 2003. Strength and microstructural characteristics of fly ash–cement systems. *Cement and Concrete Research,* Vol. 33, No. 3, pp. 425–431.

Li, L., Aubertin, M., 2003. A general relationship between porosity and UCS of engineering materials. *Canadian Journal of Civil Engineering,* Vol. 30, No. 4, pp. 644–658.

Matusinović, T., Šipušić, J., Vrbos, N., 2003. Porosity–strength relation in calcium aluminate cement pastes. *Cement and Concrete Research,* Vol. 33, No. 11, pp. 1801–1806.

McCarthy, D.F., 2007. *Essentials of soil mechanics and foundations: Basic geotechnics (7th edn).* Pearson-Prentice Hall, Canada.

O'Farrell, M., Wild, S., Sabir, B.B., 2001. Pore size distribution and compressive strength of waste clay brick mortar. *Cement Concrete Composites,* Vol. 23, No. 1, pp. 81–91.

Ouellet, S., 2006. Mineralogical characterization, microstructural evolution and environmental behaviour of cemented paste backfills. *Ph.D. Thesis,* Université du Québec en Abitibi-Témiscamingue (UQAT), Rouyn-Noranda, Québec, Canada.

Ouellet, S., Bussière, B., Mbonimpa, M., Benzaazoua, M., Aubertin, M., 2006. Reactivity of an underground mine sulphidic cemented paste backfill. *Minerals Engineering,* Vol. 19, No. 5, pp. 407–419.

Ouellet, S., Bussière, B., Aubertin, M., Benzaazoua, M., 2007. Microstructural evolution of cemented paste backfill: Mercury intrusion porosimetry test results. *Cement and Concrete Research,* Vol. 37, No. 12, pp. 1654–1665.

Ouellet, S., Bussière, B., Aubertin, M., Benzaazoua, M., 2008. Characterization of cemented paste backfill pore structure using SEM and IA analysis. *Bulletin of Engineering Geology and the Environment,* Vol. 67, No. 2, pp. 139–152.

Petrolito, J., Anderson, R.M., Pigdon, S.P., 2005. A review of binder materials used in stabilized backfills. *Canadian Institute of Mining, Metallurgy and Petroleum Bulletin,* Vol. 98, No. 1085, pp. 1–7.

Potvin, Y., Thomas, E.H., Fourie, A.B., 2005. *Hand Book on Mine Fill.* Perth, Australia.

Penumadu, D., Dean, J., 2000. Compressibility effect in evaluating the pore size distribution of kaolin clay using mercury intrusion porosimetry. *Canadian Geotechnical Journal,* Vol. 37, No. 2, pp. 393–405

Ramlochan, T., Grabinsky, M.W., Hooton, D.H., 2004. Microstructural and chemical investigations of cemented paste backfills. In: *Proceedings of the 11th International Conference on Tailings and Mine Waste,* Vail, Forth Collins, Colorado, United States, A.A. Balkema, October 10–13, pp. 293–304.

Takahashi, T., Yamamoto, M., Ioku, K., Goto, S., 1997. Relationship between compressive strength and pore structure of hardened cement pastes. *Advanced Cement Research,* Vol. 9, No. 33, pp. 25–30.

Taylor, H.F.W., 1990. *Cement Chemistry.* Academic Press, New York.

Vodak, F., Trtik, K., Kapicková, O., Hoskova, S., Demo, P., 2004. The effect of temperature on strength-porosity relationship for concrete. *Construction and Building Materials,* Vol. 18, No. 7, pp. 529–534.

Washburn, E., 1921. Dynamics of capillary flow. *Physical Rev.,* Vol. 17, No. 3, pp. 273–283.

Winslow, D.N., Diamonds, S., 1970. A mercury porosimetry study of the evolution of porosity in general use Portland cement. *International Journal of Materials,* Vol. 5, No. 3, pp. 564–585.

Xu, Y., 2004. Surface irregularity of soils in molecular domain. *Chaos, Solitons & Fractals,* Vol. 21, No. 2, pp. 435–444.

Yilmaz, E., El Aatar, O., Belem, T., Benzaazoua, M., Bussière, B., 2006. Effect of consolidation on the performance of cemented paste backfill. In: *Proceedings of the 21st Under-ground Mine Support Conference,* Val d'Or, Quebec, Canada, April 11–12, pp. 1–14.

Yilmaz, E., Belem, T., Benzaazoua, M., Kesimal, A., Ercikdi, B., 2007. Evaluation of the strength properties of deslimed tailings paste backfill. *Minerals Resources Engineering,* Vol. 12, No. 2, pp. 129–144.

Yilmaz, E., Belem, T., Benzaazoua, M., Bussière, B., 2008a. Experimental characterization of the influence of curing under stress on the hydromechanical and geotechnical properties of cemented paste backfills. In: *Proceedings of the 12th International Conference on Tailings and Mine Waste,* Vail, Forth Collins, Colorado, United States, A.A. Balkema, October 18–23, pp. 139–152.

Yilmaz, E., Belem, T., Bussière, B., Benzaazoua, M., 2008b. Consolidation characteristics of early age cemented paste backfil. In: *Proceedings of the 61st Canadian Geotechnical Conference and the 9th Joint CGS/IAH-CNC Groundwater Conference,* Edmonton, Alberta, Canada, September 21–24, pp. 797–804.

Yilmaz, E., Belem, T., Bussière, B., Benzaazoua, M., 2008c. Evaluation of strength, microstructure and consolidation properties of cemented paste fill using new lab equipment. In: *Proceedings of the 3rd International Symposium on Mines and the Environment,* Rouyn-Noranda, Quebec, Canada, November 2–5.

Yilmaz, E., Benzaazoua, M., Belem, T., Bussière, B., 2009. Effect of curing under pressure on compressive strength development of cemented paste backfill. *International Journal of Minerals Engineering,* Vol. 22, No. 9-10, pp. 772–785.

Yilmaz, E., 2010. Investigating the hydrogeotechnical and microstructural properties of cemented paste backfills using the CUAPS apparatus. *Ph.D. Thesis,* Université du Québec en Abitibi-Témiscamingue (UQAT), Rouyn-Noranda, QC, Canada.

Yilmaz, E., Belem, T., Benzaazoua, M., Bussière, B., 2010a. Assessment of the modified CUAPS apparatus to estimate in situ properties of cemented paste backfill. *Geotechnical Testing Journal,* Vol. 33, No. 5, pp. 351–362.

Yilmaz, E., Belem, T., Bussière, B., Mbonimpa, M., Benzaazoua, M., 2010b. Evaluation of the one-dimensional consolidation behaviour of early age cemented paste backfills. *Canadian Geotechnical Journal* (submitted in January 2010).

Zhang, B., 1998. Relationship between pore structure and mechanical properties of concrete under bending fatigue. *Cement and Concrete Research,* Vol. 28, No. 5, pp. 699–711.

CHAPTER VI

SUMMARY, CONCLUSIONS AND RECOMMENDATIONS

6.0 GENERAL SUMMARY

Cemented paste backfill (CPB) technology is now widely used by most modern underground hard rock mines in Canada, Australia, the United States, South Africa and Turkey. It provides an efficient and environmentally non-destructive] tailings management technique due to its technical, operational and environmental advantages over the other backfill methods (i.e., hydraulic and rock fills). The most attractive features of this technique are that it allows mine operators to use the total mine tailings without desliming for CPB production, it significantly reduces surface tailings disposal by placing them securely in underground stopes, eliminating potential damages due to environmentally harmful sulphide-rich mill tailings in the form of acid mine drainage, and it reduces post-mining rehabilitation costs.

Most studies to date have focused on the physico-chemical, mineralogical, mechanical and microstructural properties of CPB using conventional plastic (non-perforated) moulds and test procedures. In fact, the overall design of CPB is usually based on materials that are prepared, cured and tested in the laboratory. However, laboratory curing conditions have

been proven to differ from field conditions. The laboratory-prepared CPB samples using conventional moulds consistently underestimate some performance properties (e.g., strength and consolidation) of the paste backfill placed in underground stopes. Consequently, a proper laboratory system to assess the effects of in situ placement and curing conditions could assist in laboratory simulations of field conditions. This study investigates CPB with two different tailings streams (coarse-grained tailings from a European mine and fine-grained tailings from a Canadian mine) categorized as non-plastic silt (ML) using a recently designed laboratory apparatus called CUAPS (curing under applied pressure system) that estimates in situ CPB conditions. The CUAPS apparatus has been demonstrated as a practical and cost-effective tool that effectively replaces the traditional approach using non-perforated plastic moulds. The results obtained with the CUAPS apparatus will contribute to improve the safety of mines and miners and provide a better understanding of CPB. Each section of this thesis represents an original contribution to the science and engineering of CPB. This thesis provides some theoretical and experimental bases for designing paste backfill mixes in terms of cost savings and safety and for incorporating in situ backfill behaviour and properties.

The thesis is divided into six chapters. The first chapter states the problem and reviews the recent literature on the issues of interest. The research objectives and scope are presented along with the organization of the thesis. The second chapter presents the hydromechanical, geotechnical and geochemical properties of coarse-grained tailings CPB determined in parallel using the original CUAPS apparatus and conventional moulds. The third chapter describes the improved CUAPS apparatus and presents the results obtained from a series of tests performed on medium-grained tailings CPB: one-dimensional consolidation, pore water pressure dissipation, saturated hydraulic conductivity and curing under vertical pressure. The fourth chapter focuses on the one-dimensional consolidation properties of early age paste backfill samples prepared with medium-grained tailings as well as measured and back-calculated permeability. The fifth chapter presents the microstructural properties of medium-grained tailings CPB samples using both mercury intrusion porosimetry (MIP) and specific surface area (SSA) measurements. The sixth chapter presents a summary, the general conclusions and some directions for future research. The following section provides an overview of the body of the thesis.

6.1 OVERVIEW OF THESIS MANUSCRIPTS

6.1.1 Chapter 2

This chapter presents a study undertaken to better characterize the hydromechanical, physical and geochemical properties of laboratory-prepared CPB material under self-weight or time-dependent loads during curing. The mine tailings used (coarse-grained) to prepare the CPB mixtures were sampled from a European polymetallic mine (Garpenberg, Sweden). Two different testing procedures were used: i) a recently designed laboratory apparatus called CUAPS that allows the backfill sample to consolidate under pressure and ii) conventional plastic non-perforated moulds (undrained samples). CUAPS and moulds were used separately to assess the properties of CPB prepared with sulphide-rich and coarse-grained mine tailings prepared with two different types of binder: general use Portland cement GU (or PCI) alone and slag blended binder (GU or PCI-Slag@20:80 wt%) at binder contents varying from 3 to 10 wt%. The effects of vertical pressure (simulating different filling rates and stope heights) on compressive strength development and geotechnical index (bulk properties) parameters of CPB samples were analyzed in detail. Results indicate that CUAPS-consolidated backfills consistently produce better performance than that obtained with mould-undrained backfills, which could explain the CPB strength differences observed between laboratory-prepared samples (using conventional moulds) and in situ backfill materials. This chapter therefore makes an original contribution to the understanding of cemented backfills in terms of reliable data collection for the preliminary and final design of CPB systems.

However, this chapter also shows that the original CUAPS apparatus does not have the capacity to measure vertical deformations, which would allow one-dimensional consolidation testing, or the effective stresses that gradually develop within backfill that is cured under pressure, which greatly affect the overall CPB strength and stability. To overcome these shortcomings, the original CUAPS was improved by adding some instrumentation to allow further testing, as explained in the following chapter.

6.1.2 Chapter 3

This chapter assesses some improvements in the design of the original CUAPS apparatus. Currently, it can be used to conduct the following tests: i) one-dimensional consolidation with or without pore water pressure (PWP) measurement, ii) PWP dissipation test, iii) permeability (saturated hydraulic conductivity) test and iv) curing under constant and variable vertical pressures. The improved CUAPS apparatus is equipped with a linear variable transducer (LVDT) on the top rigid loading plate to monitor the vertical deformation of the sample with increasing pressure and a pore water pressure transducer (PWPT) to measure the change in effective stress within the backfill sample during curing. The PWPT is equipped with a ceramic high entry pressure filter to prevent potential corrosion. To prevent uncontrolled water loss and to conduct permeability tests on CPB samples before and/or after consolidation, a free drainage system port (Swagelok tube fitting) is also plugged into the top and bottom of the apparatus. In addition, porous stones are placed at the bottom and on top of the CPB testing sample to facilitate drainage during the one-dimensional consolidation test and to prevent solid losses. To assess and validate the functionality of the improved CUAPS apparatus, two different materials were tested: uncemented mine tailings (control samples) and CPB containing a single binder content of 4.5 wt%. The mine tailings used for CPB preparation were medium-grained tailings from a Canadian polymetallic mine (northwestern Quebec, one of the world's largest gold mines), categorized as low plastic silt (ML) in keeping with the Unified Soil Classification System (USCS). The binding agent was a blend of 20 wt% general use Portland cement (GU) and 80 wt% blast furnace slag (Slag). After mixing, the prepared paste was poured into both conventional moulds with $D \times H$ = 10 cm × 20 cm (4" × 8") and lubricated Perspex moulds having $D \times H$ = 10 cm × 20 cm (4" × 8") and 10 cm × 10 cm (4" × 4") to determine the scale effect. The lubricant used was silicon grease in order to facilitate post-testing CPB sample extrusion with minimal deterioration.

Preliminary test results confirm the accuracy, usefulness and capacity of the improved CUAPS apparatus. This apparatus enables reproducing practical and more realistic CPB properties than what are currently obtained from conventional moulds, which consistently

give lower UCS for a given paste backfill mix recipe. However, a limitation of the improved CUAPS apparatus is that the pressure loading system can apply a maximum pressure of 600 kPa (simulating a stope height range of only 25–30 m, depending on the tested material's unit weight) and a diameter-to-height ratio of 0.5 (limiting the representation of in situ backfilled stope samples). The versatility of the CUAPS could be enhanced by overcoming these technical limitations, thereby allowing an improved test protocol for backfill researchers and practitioners seeking to better understand the properties of laboratory-prepared backfills.

6.1.3 Chapter 4

The originality of Chapter 4 lies in the examination of the consolidation characteristics (e.g., compression index C_c and coefficient of consolidation c_v) of early age CPB samples using the improved CUAPS apparatus over an effective stress range of 0.5–400 kPa. A slag blended binder (GU-Slag@20:80 wt%) was used to prepare the CPB mixtures with five different binder contents: 0 – control, 1, 3, 4.5 and 7 wt%. CPB samples were cured under atmospheric conditions for four different curing times of 0, 1, 3 and 7 days. The change in saturated hydraulic conductivity was considered based on control and CPB samples prepared with a binder content of 4.5 wt%. A single empirical predictive model of compressibility parameters is also proposed and discussed.

Results show that adding binder to the CPB mixture in proportion to the cement hydration greatly affects the initial void ratio and increases the initial consolidation resistance. Binder hydration during curing in turn increases the stiffness or rigidity of the CPB material. This increased stiffness means less deformation of the paste material, which prevents the effective stress from increasing. Consequently, less water volume needs to be removed to dissipate the pore water pressure. Medium-grained tailings were tested, which may retard consolidation (and therefore lower drainage capacity). In general, the compression index reduces over curing time, whereas the coefficient of consolidation increases with increasing binder content due to decreased compressibility. Permeability decreases with increasing compressibility as the applied pressure is gradually increased to 400 kPa. This chapter describes a pioneering experimental study on the consolidation of cured CPB samples. It shows how knowledge of

the one-dimensional consolidation behaviour of CPB samples can advance the understanding of placement methods and curing conditions in underground stopes. More importantly, this chapter sheds light on the influence of consolidation on the behaviour of cured CPB, information that mine operators can use to design efficient CPB mixtures and methods for underground hard rock mines.

6.1.4 Chapter 5

This chapter presents an experimental investigation of the influence of curing conditions on the change in microstructure and compressive strength of CPB samples. Two different CPB, consolidated backfill samples (cured under applied pressure during curing using the modified CUAPS apparatus) and undrained CPB samples (cured under no pressure using conventional plastic moulds) were prepared with a slag blended binder consisting of 80 wt% blast furnace slag (Slag) and 20 wt% general use Portland cement type 1 (GU or PCI). Three different binder contents (3, 4.5 and 7 wt%) and curing times (7, 14 and 28 days) were considered to compare the CPB microstructural parameters (total porosity, mesoporosity, macroporosity, threshold diameter and critical pore size) investigated by mercury intrusion porosimetry (MIP) and specific surface area (SSA) measurements. The MIP results indicate that the microstructure strongly depends on the water-to-cement (*w/c*) ratio and effective curing conditions. It was observed that as *w/c* ratio decreases or as curing time increases (hence as the degree of hydration increases), total porosity is reduced, mainly attributable to the reduction in larger sized pores that have been filled by cementitious phases. From the SSA measurements, it was inferred that specific surface area is closely related to the compressive strength development within the CPB. This means that the higher the SSA, the higher the UCS of the CPB. Overall, consolidation reduces the porosity of CPB compared to undrained backfill samples. As the cement hydrates grow over time, the fines content within the CPB fills in void space that is used for flow, thereby reducing the permeability. Some empirical predictive models are proposed to predict UCS from MIP porosity (total and partial) and specific surface area measurements of CPB samples.

Despite these encouraging results, further experimental tests are needed to better characterize the pore structure of CPB materials. To understand the properties of the different binder types and to determine the effect of compression rates simulating the different stope heights, it is crucial to study the microstructural properties of CPB to determine how it is affected by the different *w/c* mixing proportions and how the backfill pore structure is affected during the cement–water reaction with different curing times.

6.2 SUMMARY OF RESEARCH RESULTS

The conclusions of this thesis are drawn from an analysis of the experimental investigations and observations on CPB samples prepared with two different size tailings, using both the improved CUAPS apparatus and conventional plastic (non-perforated) moulds. The major conclusions are outlined below:

- Consolidated backfills (before complete cementation) consistently develop higher UCS than unconsolidated backfills, regardless of binder type, binder content or curing time. This is mainly attributable to particle rearrangement (i.e., removal of excess water within the backfill increases the density or decreases the void ratio or porosity) due to applied pressure and the gradual formation of cement bonds during hydration.

- The application of effective stress to early-age CPB, simulating placement conditions after underground stope filling, produces more cementitious matrices (the filling of pore voids due to hydration), which in turn produces better cohesion and consequently accelerated mechanical strength development and higher ultimate strength.

- The magnitude of the mechanical strength increase of CPB is usually based on the rate at which effective stress is applied to the samples during curing. This largely explains why the mechanical strength of in situ CPB material is always higher than laboratory-prepared backfills for the same recipes and curing times. In general, conventional moulds do not exhibit substantial change in effective stress (except for the presence of self-desiccation, which progressively reduce the pore water pressure), nor do they allow samples to cure

under stress. Consequently, there is no excess water removal, which can lead to the formation of acid and sulphate at later curing times.

- The improved CUAPS apparatus can be used to do a series of tests: one-dimensional consolidation, PWP dissipation, saturated hydraulic conductivity and curing under constant or variable pressure. In this way, the improved CUAPS enables new procedures to better understand the behaviour and quality performance of CPB material in proposed mix designs. It would therefore enable mine operators to benefit from savings in cement amounts used in the mixtures, without introducing an additional risk of CPB instability.

- The one-dimensional consolidation tests (application of pressure increments) show that the initial void ratio (after a given curing time simulating the CPB post-placement) is significantly reduced due to the effective stress applied to the cemented paste backfill. In addition, the amount of the cement added to the mix affects the void ratios at pressures experienced during cement hydration.

- The permeability (saturated hydraulic conductivity k_{sat}) results show a nearly constant value for uncemented tailings (control samples) with curing time. However, with the addition of binder, the permeability decreases very quickly during the early ages of curing (less than 3 days) due to the formation of cement hydrates, which gradually fill in the initial voids or porosity. Permeability appears to reduce thereafter at a slower rate or stabilize after curing times greater than 3 days. The greater the amount of binder used, the lower the permeability of the CPB materials.

- The mercury intrusion porosimetry (MIP) results indicate that total porosity reduces substantially with increased binder content for both CUAPS-cured and undrained mould-cured CPB samples. As *w/c* ratio decreases, or as curing time increases, total porosity is reduced, mainly due to the reduction in larger size pores that have been filled by the precipitation of hydrates (mainly C-S-H gel), replacing the originally water-filled space. The final *w/c* ratio values of consolidated backfills are reduced as a result of the removal of excess water from samples due to applied pressure during curing.

- The effective curing conditions (based on the combined effects of applied pressure and water drainage, considered for consolidated samples using CUAPS) accelerate the cement hydration rate, which leads to the formation of more hydrated products and a consequent lower porosity of the cement matrix. However, conventional moulds in which samples are cured under no pressure and are not allowed to drain tend to reduce the rate of the hydration reactions due to a nearly constant *w/c* ratio. Hence, undrained backfills show much greater porosity than consolidated backfills due to inadequate hydration.

6.3 DIRECTIONS FOR FUTURE RESEARCH

The investigation presented in this thesis has not only provided a better understanding of the in situ properties of laboratory-prepared CPB using the CUAPS apparatus, but it has also identified areas of interest for further research on methods that can be used in most CPB operations. These areas include:

- Further investigations into the effects of curing and stress application schemes on hydromechanical and bulk properties of CPB samples using the improved CUAPS apparatus. There is a lack of information in the literature on the significant influence of placement and curing conditions in the overall performance of in situ CPB material. For instance, the additional effect of the presence of sulphate (quality of mixing water) and clayey minerals needs to be clarified.

- An assessment of the stope depth effect on in situ properties of stope-filled CPB samples could be performed using CUAPS testing and field data collection. It is well known that the strength and stability of backfill material placed at different heights in an underground stope vary greatly from top to bottom as a result of self-weight and/or time-dependent consolidation. Different equivalent stope heights (using different vertical pressures applied to CPB samples) could be simulated using different mixtures prepared with different binder types and binder contents over different curing times.

- Experimental studies are needed to determine the influence of curing under different loading rates on CPB microstructure using the CUAPS apparatus. The results would be affected not only by the paste backfill microstructure, but also by the experimental parameters. Four different loading rates can be applied to the samples during curing: extra slow (ES), slow (SL), fast (FL) and extra fast (EFL). It would be useful to understand how these loading rates affect the pore structure and strength of CPB prepared with different binder types and contents over different curing times.

- An examination of the effects of sample size and drainage conditions on the compressive strength performance of CPB samples could be undertaken to assess the scale effect. In fact, some of the observed differences between the strength properties of laboratory and in situ samples are probably due to the scale effect, placement and curing conditions. To investigate this aspect, three conventional plastic mould sizes with $D \times H$ of 10 cm × 20 cm (4" × 8"), 7.6 cm × 15.2 cm (3" × 6") and 5 cm × 10 cm (2" × 4"), and four different curing conditions could be well simulated such as: capped-drained; uncapped-drained; capped-undrained; and uncapped-undrained. The results could be valuably compared to CUAPS-consolidated paste backfill samples.

APPENDICES

APPENDIX A

PROPERTIES OF CEMENTITIOUS MATERIALS: CEMENT AND CEMENT PASTE

Luca Bertolini, Bernhard Elsener, Pietro Pedeferri, Rob B. Polder

The first chapter of the book entitled

Corrosion of Steel in Concrete: Prevention, Diagnosis, Repair, Wiley-VCH Verlag GmbH & Co. KGaA, Weinheim, ISBN: 978-3-527-30800-2, 409 pages, March 2004

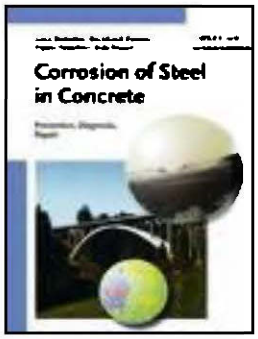

A.0 CEMENTS AND CEMENT PASTE

Concrete is a composite material made of aggregates and the reaction product of the cement and mixing water, i.e. the porous cement paste. The structure and composition of the cement paste determines the durability and the long-term performance of concrete. Concrete is normally reinforced with steel bars. The protection that concrete provides to the embedded steel and, more in general, its ability to withstand various types of degradation, also depends on its structure. This chapter shows the properties of the most utilised cements and the micro structure of hydrated cement pastes.

A.1 CEMENT TYPES AND HYDRATION REACTION

Cements are fine mineral powders that, when they are mixed with water, form a paste that sets and hardens due to hydration reactions. Portland cement is the basis for the most widely used cements (Taylor, 1990; Neville, 1995, Metha and Monterio, 1993; Collepardi, 2002). It is produced by grinding clinker, which is obtained by burning a suitable mixture of limestone and clay raw materials. Its main components are tricalcium and dicalcium silicates (C_3S and C_2S), the aluminate and ferroaluminate of calcium (C_3A and C_4AF respectively) (In the chemistry of cement, the following abbreviations are used: CaO = C; SiO_2 = S; Al_2O_3 =A; Fe_2O_3 = F; H_2O = H; SO_3 = S.). Gypsum (CS) is also added top clinker before grinding, to control the rate of hydration of aluminates. Table A.1 shows the typical ranges of variation of these constituents of Portland cement. Other components, such as sodium and potassium oxides, are present in small but various amounts.

Table A.1 Main components of Portland cement and typical percentages by mass

Component name	Equation	Abbreviation	Value (%)
Tricalcium silicate (alite)	$3CaO.SiO_2$	C_3S	45–60
Dicalcium silicate (belite)	$2CaO.SiO_2$	C_2S	5–30
Tricalcium aluminate	$3CaO.Al_2O_3$	C_3A	6–15
Tetracalcium ferroaluminate	$4CaO.Al_2O_3.Fe_2O_3$	C_4AF	6–8
Gypsum	$CaSO_4.2H_2O$	CS	3–5

In the presence of water, the compounds of Portland cement form colloidal hydrated products of very low solubility. Aluminates react first, and are mainly responsible for setting, i.e. solidification of the cement paste. The hydration of C_3A and C_4AF, in the presence of gypsum, mainly gives rise to hydrated sulfoaluminates of calcium. Hardening of cement paste, i.e. the development of mechanical strength that follows solidification, is governed by the hydration of silicates. The hydration of C_3S and C_2S gives rise to calcium silicate hydrates forming a rigid gel indicated as C–S–H. It is composed of extremely small particles with a layer structure that tend to aggregate in formulations a few μm in dimension, characterized by interlayer spaces of small dimensions (< 2nm) and by a large surface area (100–700 m^2/g). Figure A.1 shows a model proposed to describe this structure. Due to the high surface area, C–S–H can give considerable strength to the cement paste. Its chemical composition is not well defined since the ratio between the oxides may vary as the degree of hydration, the water-to-cement ratio, and temperature vary (for instance the C/S ratio may pass from 1.5 to 2). However, upon complete hydration, it tends to correspond to the formula $C_3S_2H_3$ usually used in stoichiometric calculations. C–S–H represents approximately 50–60 % of the volume of the completely hydrated cement paste.

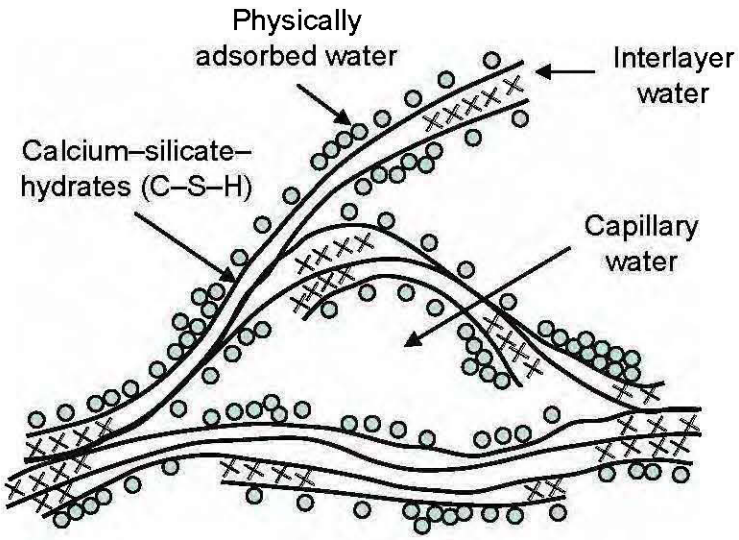

Figure A.1 Feldman–Sereda model for C–S–H (Neville, 1995).

Hydration of calcium silicates produces hexagonal crystals of calcium hydroxide ($Ca(OH)_2$, Portlandite). These have dimensions of the order of a few μm and occupy 20 to 25 % of the volume of solids. They do not contribute to the strength of cement paste. However, $Ca(OH)_2$, NaOH and KOH that are present in small amounts, are important with regard to protecting the reinforcement, because they cause an alkaline pH up to 13.5 in the pore liquid.

The hydration reactions of tricalcium and dicalcium silicates can be illustrated as follows (Eqs. A1 and A2):

$$2C_3S + 6H = C_3S_2H_3 + 3Ca(OH)_2 \quad (A.1)$$

$$2C_2S + 4H = C_3S_2H_3 + Ca(OH)_2 \quad (A.2)$$

The reaction products are the same, but the proportions are different. The ratio between C–S–H and Portlandite, passing from the hydration of C_3S to that of C_2S changes from 61/39 to 82/18, and the amount of water required for hydration from 23 % to 21%. In principle, C_2S should lead to a higher ultimate strength of the cement paste by producing a higher amount of C–S–H. Nevertheless, the rate of hydration is much lower for C_2S compared with C_3S, and the strength of cement paste after 28 days of wet curing is mainly due to C_3S. Therefore the larger the amount of C_3S in a Portland cement, the higher the rate of hydration and strength development of its cement paste. Increasing the fineness of cement particles can also increase the rate of hydration. The reactions leading to hydration of Portland cement are exothermic; hence increasing the rate of hydration increases the rate of generation of heat of hydration.

A.2 POROSITY AND TRANSPORT PROCESSES

The cement paste formed by the hydration reactions always contains interconnected pores of different sizes, as shown in Figure A.2. The pores can be divided into macropores, capillary pores and gel pores. The interlayer spacing within C–S–H (gel pores) have a volume equal to about 28 % of the gel and dimensions ranging from a few fractions of a nm to several nm. These do not affect the durability of concrete and its protection of the reinforcement because they are too small to allow significant transport of aggressive species.

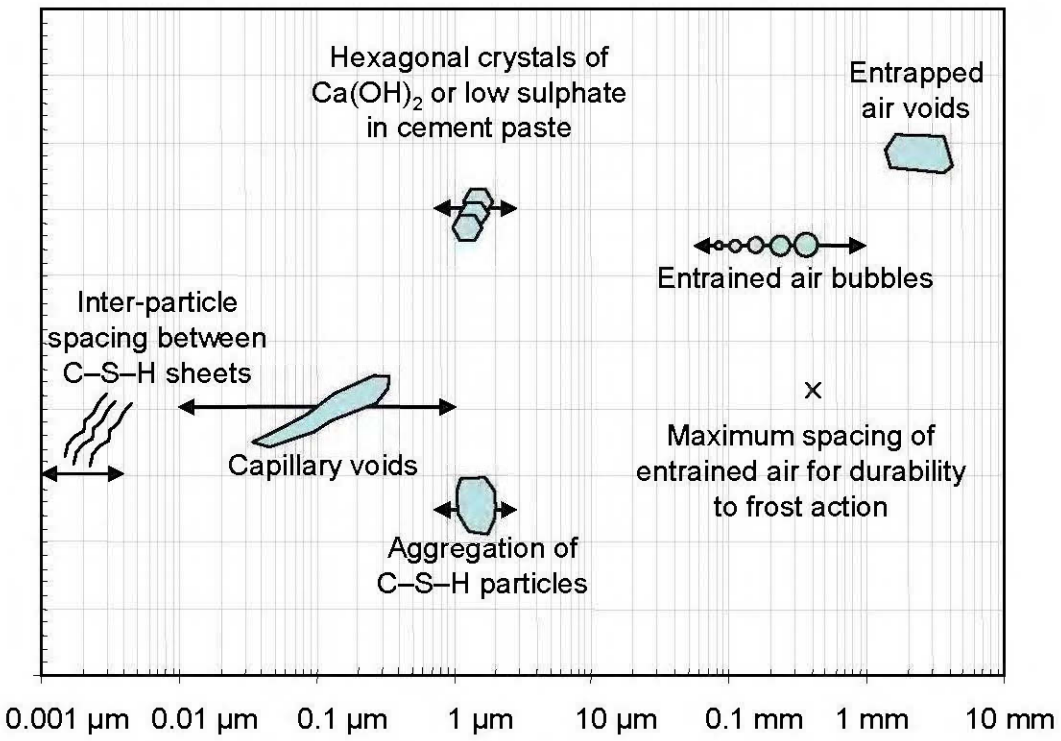

Figure A.2 Dimensional range of solids and pores in hydrated cement paste (Metha and Monterio, 1993).

The capillary pores are the voids not filled by the solid products of hydration of hardened cement paste. They have dimensions of 10 to 50 nm if the cement paste is well hydrated and produced using low water/cement ratios (*w*/*c*), but can reach up to 3–5 µm if the concrete is made using high *w*/*c* ratios or it is not well hydrated. Larger pores of dimensions of up to a few mm are the result of the air entrapped during mixing and not removed by compaction of fresh concrete. Air bubbles with diameters of about 0.05–0.2 mm may also be introduced in the cement paste intentionally through air-entraining mixtures, so as to produce resistance to freeze-thaw cycles. Both capillary pores and entrapped air are relevant to the durability of concrete and its protection of the rebars. Entrapped air can be reduced by providing adequate workability to the fresh concrete and proper compaction.

A.2.1 Water/cement ratio and curing

During the hydration of cement paste, the gross volume of the mixture practically does not change, so that the initial volume, equal to the sum of the volumes of mixed water (V_m) and cement (V_c) is equal to the volume of the hardening product. As indicated in Figures A.3 from Neville and Brooks (1990), this consists in the sum of the volume of cement that has not yet reacted (V_{uc}), the hydrated cement ($V_p + V_{gw}$), the capillary pores that are filled by water (V_{cw}) or by air (V_{ec}). The volume of the products of hydration can be assumed to be roughly double that of the cement: during hydration these products fill the space previously occupied by the cement that has hydrated and part of the surrounding space initially occupied by water. Thus, if the cement paste is kept moist, the hydration proceeds and the volume of capillary pores decreases and will reach a minimum when the hydration of cement has completed.

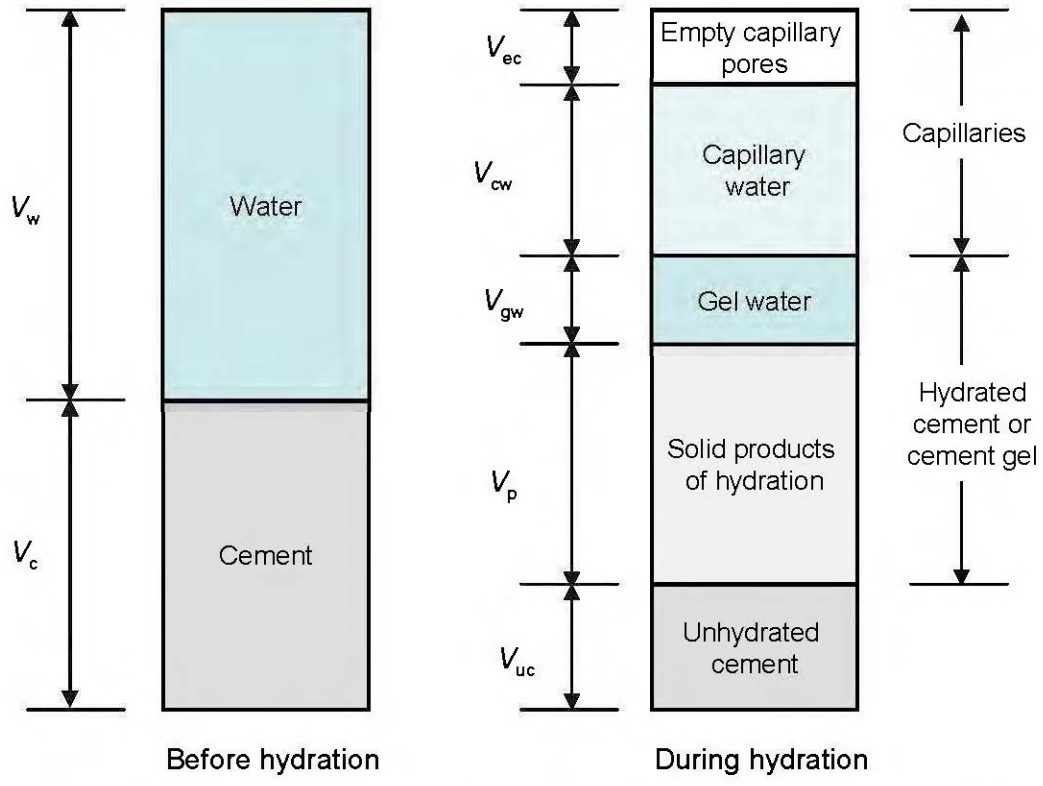

Figure A.3 Schematic representation of the volumetric proportions in cement paste before and during hydration (Neville and Brooks, 1990).

Nevertheless, the value reached after complete hydration will be greater in proportion to the initial distance between the cement particles and thus to the amount of mixing water.

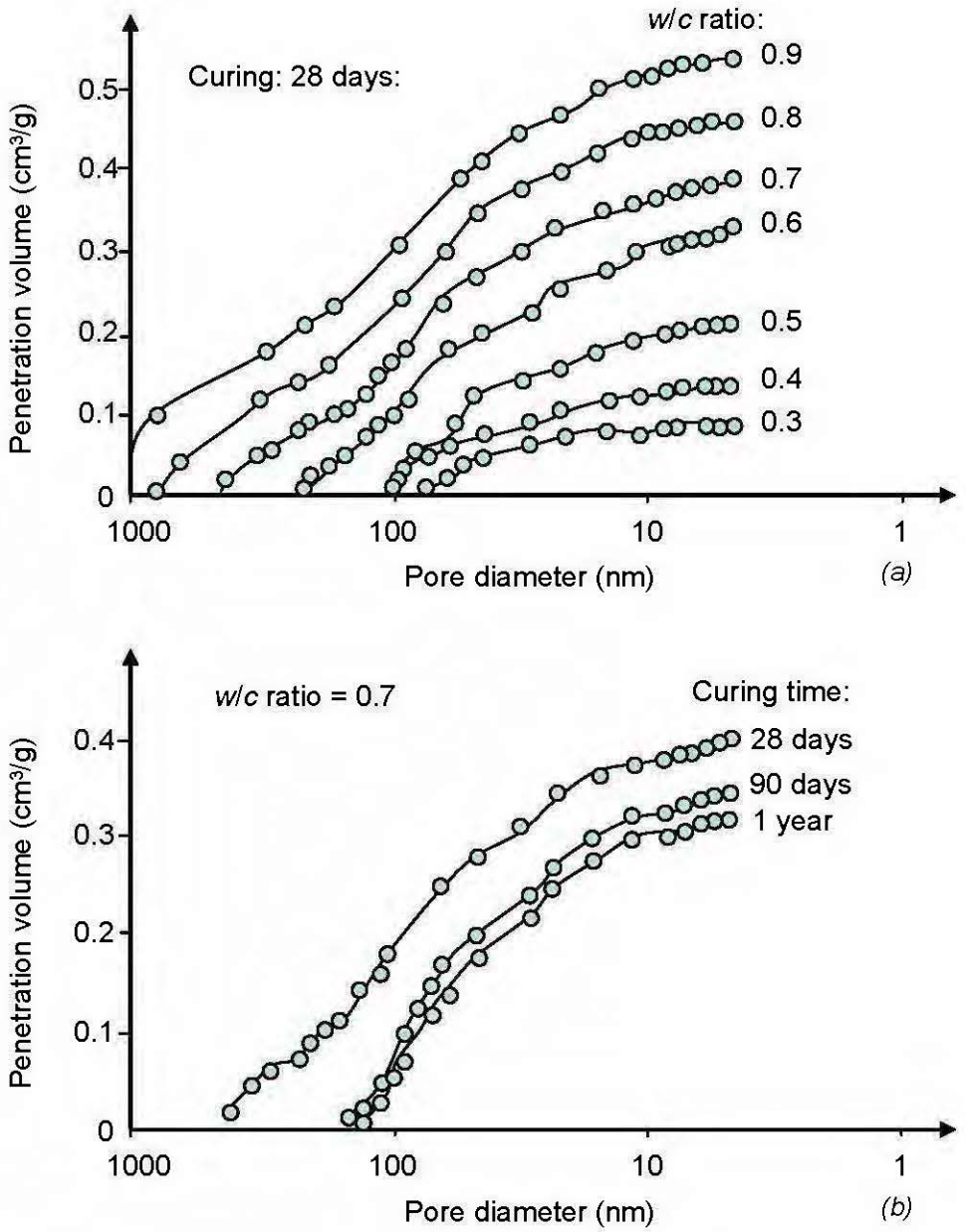

Figure A.4 Influence of the water/cement ratio (a) and curing (b) on the distribution of pore size in hydrated cement pastes (Metha and Monterio, 1993).

Figure A.4 shows that the pore-size distribution, measured by mercury intrusion porosimetry (MIP), depends on *w/c* ratio and curing. It can be observed that as the *w/c* ratio decreases or as the curing time increases (and consequently also the degree of hydration increases), the reduction of porosity is mainly due to the reduction in pores of larger dimensions that have been filled or have been connected only by C–S–H gel pores.

In conclusion, the volume of the capillary pores (V_{cp}) in the cement paste increases with the amount of water used in the paste and thus with the water/cement ratio (w/c) and decreases with the degree of hydration (h), i.e. the fraction of hydrated cement. The volume of capillary pores (V_{cp} in litres per kg of cement) can be calculated with the following formula (Eq. A.3), proposed by Powers (1958):

$$V_{cp} = (w/c - 0.36h) \qquad \text{(A.3)}$$

When concrete is considered instead of cement paste, the water/cement ratio and the degree of hydration remain the main factors that determine the capillary porosity. Nevertheless, concrete is more complex because of the presence of the aggregates and the transition zone between aggregate and the cement matrix, where the structure of cement paste tends to be more porous (Neville, 1995, Metha and Monterio, 1993).

A.2.2 Porosity, permeability and percolation

In determining the resistance to degradation of concrete and its role in protecting the embedded steel, not only should the total capillary porosity (i.e. the percentage of volume occupied by capillaries) be considered but also the size and the interconnection of capillary pores. Figure A.5 shows the relation between the transport properties of cement paste (expressed as coefficient of water permeability) and the compressive strength as a function of the w/c ratio and degree of hydration (Powers, 1958). The decrease in capillary porosity increases the mechanical strength of the cement pastes and reduces the permeability of the hydrated cement paste (Figure A.5). A distinction should be made between capillary pores of

larger dimensions (> 50 nm), or macropores, and pores of smaller dimensions, or micropores (Metha and Monterio, 1993). The reduction in porosity of both the macro- and the micro-pores plays an essential role in increasing mechanical strength.

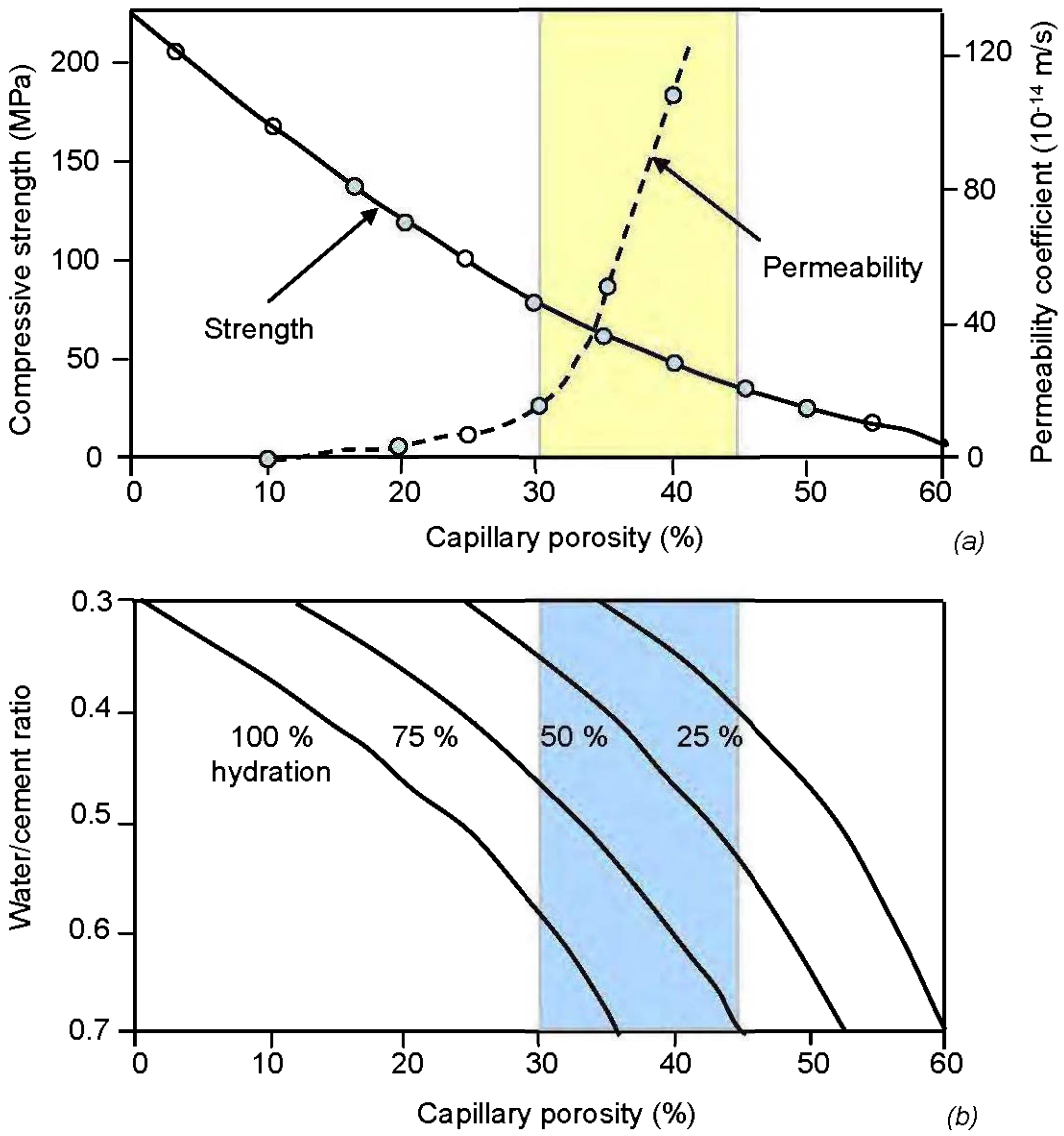

Figure A.5 Influence of capillary porosity on strength and permeability of cement paste (a). Capillary porosity derives from a combination of water/cement ratio and degree of hydration (b) (Powers (1958) from (Metha and Monterio, 1993).

On the other hand, the influence of porosity on the transport processes cannot be explained simply by the pore volume, but the concept of connectivity or the degree of continuity of the pore system has to be taken into account. At high porosities the interconnected capillary pore system extends from the concrete surface to the bulk of concrete. Permeability is high (Figure A.5) and transport processes like, e.g., capillary suction of (chloride-containing) water can take place rapidly. With decreasing porosity the capillary pore system loses its connectivity, thus transport processes are controlled by the small gel pores.

Consequently, water and chlorides will penetrate only a short distance into concrete. This influence of structure (geometry) on the transport properties can be described with the percolation theory (Stauffer, 1985): below a critical porosity, p_c, the percolation threshold, the capillary pore system is not interconnected (only finite clusters are present); above pc the capillary pore system is continues (infinite clusters). The percolation theory has been used to design numerical experiments and applied to transport processes in cement paste and mortars (Elsener et al., 2000).

The steep increase of the water permeability above around 25% porosity (corresponding to a w/c ratio of 0.45 with a degree of hydration of 75%, Figure A.5) is the background of the specified values in the codes of practice for high quality concrete. For instance, Table A.2 shows the relationships between water/cement ratio and degree of hydration in order to achieve segmentation of the macropores in a paste of Portland cement.

Table A.2 Curing times necessary to achieve a degree of hydration capable of segmenting the macropores in Portland cement (Powers from Neville 1995)

Water/cement ratio	Degree of hydration (%)	Curing time
0.40	50	3 days
0.45	60	7 days
0.50	70	14 days
0.60	92	6 months
0.70	100	1 year
> 0.70	100	impossible

A.3 BLENDED CEMENTS

Nowadays blended cements are normally used, which are obtained by inter-grinding or blending Portland cement with particular mineral substances. Among these, those with the addition of pozzolanic materials or ground granulated blast furnace slag are of particular interest with regard to durability of reinforced concrete.

A.3.1 Pozzolanic materials

Pozzolanic materials can be either natural, like pozzolana, or artificial, like fly ash and silica fume (Neville, 1995). They are mainly glassy siliceous materials that may contain aluminous compounds but have a low lime (calcium hydroxide) content. In themselves they do not have binding properties, but acquire them in the presence of lime, giving rise to hydration products similar to those of Portland cement. The reaction between pozzolanic materials, lime and water is known as the pozzolanic reaction, as follows (Eq. A.4):

$$\text{pozzolana} + \text{water} + Ca(OH)_2 \rightarrow C\text{–}S\text{–}H \qquad (A.4)$$

In cements containing the pozzolanic additions, the lime needed to react with pozzolana is provided by the hydration of Portland cement. The hardened cement paste (compared to that obtained with ordinary Portland cement) has a lower lime content and higher content of C–S–H. The amount of pozzolanic addition to Portland cement generally ranges from 20 to 40 % of the total cement content: it should be adjusted to the amount of lime produced in the hydration of Portland cement. Any excess of the pozzolanic addition will not react and thus will behave as an inert addition.

Natural pozzolana: This is a sedimentary material, usually of piroclastic origin, that is derived from the sediment of volcanic eruptions that have produced incoherent deposits or compact deposits that have been chemically transformed with time (such as Italian pozzolana, which was used by the Romans). Pozzolanic materials may also have other origins, such as diatomaceous earth composed of the siliceous skeleton of micro-organisms. The pozzolanic

activity of these materials is related to their siliceous component in the vitreous state and to their fineness. There are pozzolanas that are obtained by calcinations of natural substances.

Fly ash: Fly ash (also called pulverised fuel ash, PFA) is a by-product of the combustion of coal powder in thermoelectric power plants. In consists of very fine and spherical particles (dimensions from 1 to 100 μm and a Blaine fineness or specific surface area of 300–600 m^2/kg) that are collected from exhaust gases with electrostatic or mechanical filters. Its composition depends on the type of coal it derives from; the most common PFA is mainly siliceous. Because of the high temperature at which it is formed, it subsequently undergoes rapid cooling so that its structure is mainly amorphous (glassy) and thus reactive.

Silica fume: Silica fume (SF) is a waste product of manufacturing ferro-silicon alloys. It consists of an extremely fine powder of amorphous silica. Average particle diameter is about 100 times smaller than that of normal Portland cement and the Blaine specific surface area is neroumous:13 000–30 000 m^2/kg compared to 300–400 m^2/kg for common Portland cements. Silica fume shows an elevated pozzolanic activity and is also a very effective filler. For these reasons, addition of silica fume to Portland cement may lead to a very low porosity of the cement paste, increasing the mechanical strength and lowering the permeability. It is usually added in the proportion of 5 to 10 % and it is combined with the use of a superplasticizer in order to maintain adequate workability of the fresh concrete.

A.3.2 Ground granulated blast furnace slag

Production of pig iron generates great quantities of liquid slag, which is composed, like Portland cement, of lime, silica, and alumina, although in different proportions. The slag acquires hydraulic properties if it is quenched and transformed into porous granules with an amorphous structure. This is then ground to obtain a powder whose fineness is comparable to that of cement, which is called ground granulated blast furnace slag (GGBS).

Unlike pozzolanic materials, which hydrate only in the presence of lime, slag has hydraulic characteristics and thus might be used as a hydraulic binder. The rate of hydration of this

process is, however, too slow for practical purposes. This material shows good hardening properties when mixed with Portland cement, because the hydration of Portland cement creates an alkaline environment that activates the reaction of GGBS. Nevertheless, even when activated by Portland cement, the hydration of GGBS is slower than that of Portland cement. For achieving a high early strength, the slag content should be relatively low (35–50 %). The hydration of GGBS, however, refines the pore structure of the cement paste; in order to achieve an optimal densification of the cement paste the GGBS content should be higher than 65%.

A few years ago, a blast furnace slag cement with improved properties with regard to both early strength and density was introduced. It is a CEM III/A 52.5 containing 57% finely ground slag and rapid-hardening Portland cement. Various laboratory tests showed that it has a better resistance to carbonation than CEM II/B, and a similarly good resistance to chloride penetration and alkali-silica reactions. Its relatively high early strength makes it suitable for use in the precast concrete industry.

A.3.3 Properties of blended cements

Cement paste obtained with blended cements differs considerably from that obtained with Portland cement. The hydration of pozzolanic materials or GGBS consumes lime and thus reduces its amount with respect to a cement paste obtained with Portland cement. Figure A.6 outlines the microstructures of hardened cement pastes made of Portland cement and blended cements. It can be observed that the addition of PFA or GGBS leads to the formation of very fine products of hydration that lead to a refinement of pores. Consequently, an increase in the resistance to penetration of aggressive agents can be obtained. However, the reactions of pozzolanic materials or GGBS are slower than the hydration of Portland cement; hence this effect will be achieved only if the wet curing of the concrete is long enough.

The rate of reaction of blast furnace slag and fly ash differs strongly. To show this, Figure A.7 compares electrical resistivity measurements of wet cured concrete with a water/cement ratio of 0.45 made with Portland, Portland fly ash and blast furnace slag cements.

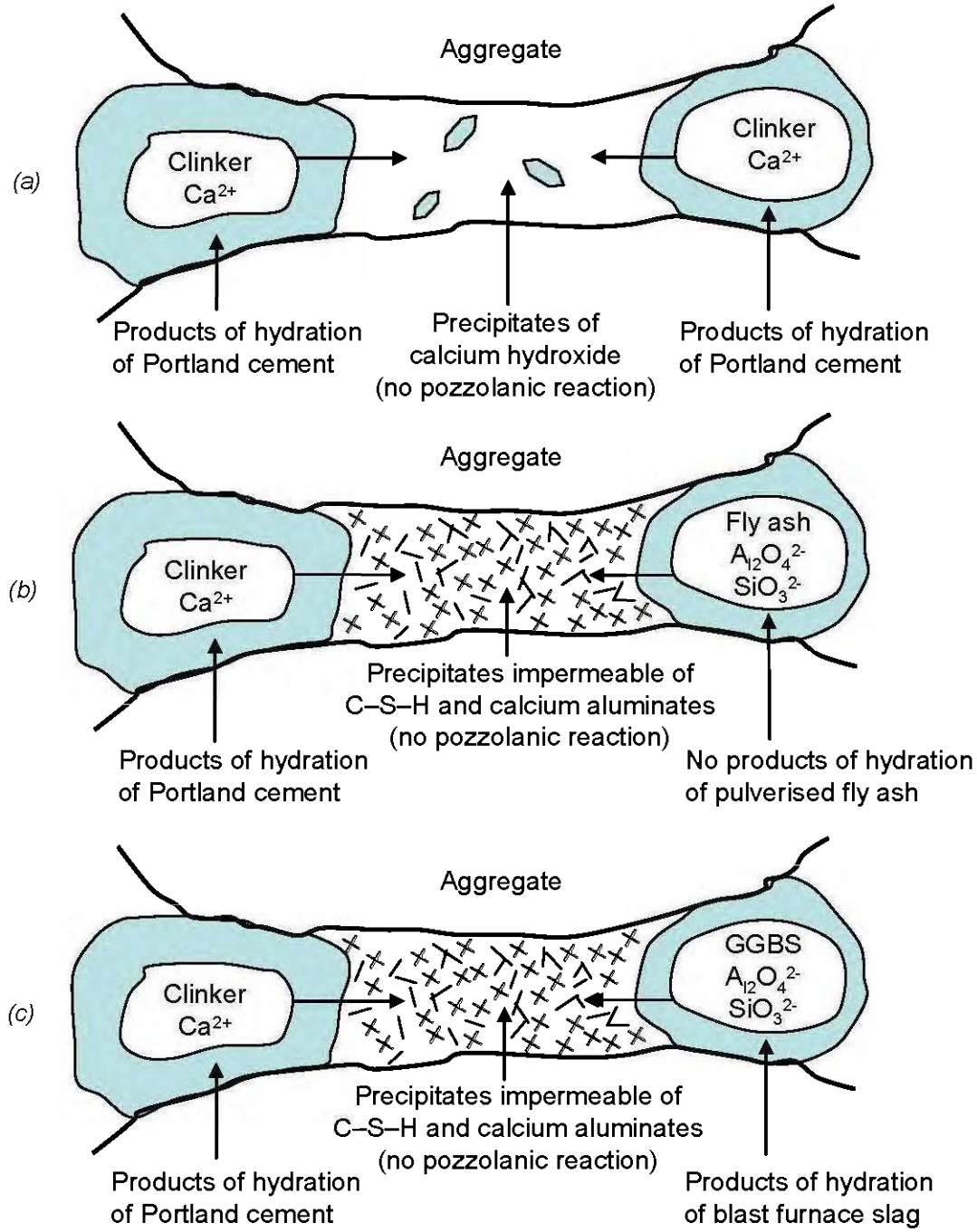

Figure A.6 Microstructure of hydration of Portland cement (a), and cements with addition of pulverised fly ash PFA (b) and ground granulated blast furnace slag GGBS (c) (Bakker from Schiessl (1988).

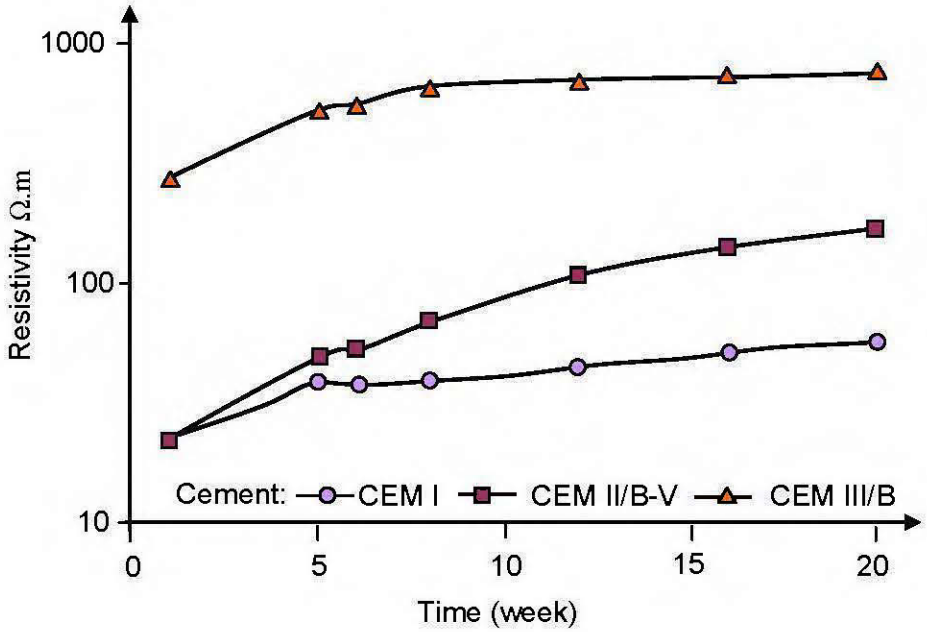

Figure A.7 Electrical resistivity of concrete made with different cements from 7 days age while exposed in a fog room (w/c = 0.45, 2 % chloride mixed-in), from (Polder, 2000).

The development of resistivity of concrete at an early age shows the changes that occur in the microstructure of cement paste. From the age of one week on, the resistivity of blast furnace slag cement (CEM III/B) was more than three times higher than for Portland cement (CEM I) and Portland fly ash (CEM II/B-V) cement (Polder, 2000). The resistivity of PFA concrete became significantly higher than that of ordinary Portland cement concrete from about eight weeks of age. It appears then, that the refinement of the pore structure by GGBS starts as early as a few days, while the effect of PFA takes several weeks to months to develop. Silica fume is also known to react quickly.

A.4 COMMON CEMENTS

According to the European standard EN 197-1 (EN 197, 2000), Portland cement and blended cements can be classified on the basis of composition and performance (strength) at 28 days. As far as composition is concerned, five main types of cement can be considered:

Table A.3 Types of cement according to EN 197-1 and their composition (% by mass)

Type of cement		Notation	Clinker	Blast furnace slag	Silica fume	Pozzolana		Fly ash		Burnt shale	Lime stone	Minor additional constituents [a]
						natural	calcined	siliceous	calcareous			
			K	S	D[b]	P	Q[c]	V	W	T	L	
I	Portland cement	I	95–100	–	–	–	–	–	–	–	–	0–5
	Portland-slag cement	II/A-S	80–94	6–20	–	–	–	–	–	–	–	0–5
		II/B-S	65–79	21–35	–	–	–	–	–	–	–	0–5
	Portland-silica fume cement	II/A-D	90–94	–	6–10	–	–	–	–	–	–	0–5
II	Portland-pozzolana cement	II/A-P	80–94	–	–	6–20	–	–	–	–	–	0–5
		II/B-P	65–79	–	–	21–35	–	–	–	–	–	0–5
		II/A-Q	80–94	–	–	–	6–20	–	–	–	–	0–5
		II/B-Q	65–79	–	–	–	21–35	–	–	–	–	0–5
	Portland-fly ash cement	II/A-V	80–94	–	–	–	–	6–20	–	–	–	0–5
		II/B-V	65–79	–	–	–	–	21–35	–	–	–	0–5
		II/A-W	80–94	–	–	–	–	–	6–20	–	–	0–5
		II/B-W	65–79	–	–	–	–	–	21–35	–	–	0–5
	Portland-burnt shale cement	II/A-T	80–94	–	–	–	–	–	–	6–20	–	0–5
		II/B-T	65–79	–	–	–	–	–	–	21–35	–	0–5
	Portland-limestone cement	II/A-L	80–94	–	–	–	–	–	–	–	6–20	0–5
		II/B-L	65–79	–	–	–	–	–	–	–	21–35	0–5
	Portland-composite cement	II/A-M	80–94	←	———	———	6	20 [d]	———	———	——— →	0–5
		II/B-M	65–79	←	———	———	21	35 [d]	———	———	——— →	0–5
III	Blast furnace cement	III/A	35–64	36–65	–	–	–	–	–	–	–	0–5
		III/B	20–34	66–80	–	–	–	–	–	–	–	0–5
		III/C	05–19	81–95	–	–	–	–	–	–	–	0–5
IV	Pozzolanic cement	IV/A	65–89	–	←—	———	11–35	——→	–	–	–	0–5
		IV/B	45–64	–	←—	———	36–55	——→	–	–	–	0–5
V	Composite cement	V/A	40–64	18–30	–	←———	18–30	——→	–	–	–	0–5
		V/B	30–39	31–50	–	←———	31–50	——→	–	–	–	0–5

[a] Minor additional constituents may be fillers or one or more of the main constituents, if these have not been included as main constituents; [b] The proportion of silica fume is limited to 10%, [c] The proportion of non-ferrous blast furnace slag is limited to 15%; and [d] The proportion of filler is limited to 5%.

- CEM I (Portland cement), with at least 95 % of clinker (by total binder mass),
- CEM II (Portland-composite cements), with addition of up to 35 % of another single constituent,
- CEM III (blast furnace cement) with addition of 36–95 % blast furnace slag,
- CEM IV (pozzolanic cement) with addition of 11–35% pozzolanic materials,
- CEM V (composites cement) with concurrent additions of slag and pozzolana (18–50%).

Table A.3 shows the composition and the notation of the types of cement provided by EN 197-1. For CEM II and CEM V, additions of substance that do not contribute to hydration, such as limestone, is also allowed. In ach type of cement, minor additional constituents (such as fillers, which are finely ground natural or artificial inorganic materials that are added to improve the physical properties of cement such as its workability or to achieve requirements of mechanical strength) may be added up to 5 % by mass.

To evaluate the performance of a cement at 28 days of moist curing, i.e. when the strength of concrete is normally tested, the standard strength classes have been introduced. These are conventionally defined on the basis of the characteristic compressive strength measured on mortar cubes with a w/c ratio equal to 0.5 and a sand/cement ratio of 3, cured for 28 days in moist conditions. For each type of cement, three classes of 28-day strength are potentially available; furthermore, depending on early strength each class is then divided into normal (*N*) or high-early strength (*R*), as shown in Table A.4.

Table A.4 Strength classes of cement according to EN 197-1

Class	Compressive strength (MPa)			
	Early strength		Standard strength	
	2 days	7 days	28 days	
32.5 N	–	≥ 16	≥ 32.5	≤ 52.5
32.5 R	≥ 10	–	≥ 32.5	≤ 52.5
42.5 N	≥ 10	–	≥ 42.5	≤ 62.5
42.5 R	≥ 20	–	≥ 42.5	≤ 62.5
52.5 N	≥ 20	–	≥ 52.5	
52.5 R	≥ 30	–	≥ 52.5	

The strength classes are essentially a measure of the rate of hydration of the cement: the higher the strength at a given time, the higher the rate of hydration. Notation of cement indicates the cement type (Table A.3) and the strength class (Table A.4). For instance, CEM II/A-S 42.5N indicates Portland-slag cement with addition of blast furnace slag in the range of 6–20 % and strength class 42.5 with normal early strength. EN 197-1 also provides other requirements of cement such as setting times, or chemical properties. Methods of testing these properties are described in the European standard EN 196.

A.5 OTHER TYPES OF CEMENT

Other types of cement than those of Table A.3 are available for special uses. These are for instance: low heat cements to be used when low heat of hydration is desired such as in massive structures, sulfate-resisting cements to be used to increase the resistance of concrete to sulfate attack, expansive cements, quick setting cements, white or coloured cements, etc (Neville, 1995).

Mention should however be made of high alumina cement. In fact, although nowadays it is generally not used for structural purposes, in the past its use has caused problems of durability (as well as from the structural point of view), especially in countries like Spain and the United Kingdom where it was extremely used.

High alumina cement (HAC): This is obtained by melting a suitable mixture of limestone and bauxite (mainly consisting of alumina) at about 1600 ºC. Its primary constituent is $CaO.Al_2O_3$ (CA). The hydration reaction ($CA + 10H = CAH_{10}$) mainly produces CAH_{10}, which is unstable. In humid environments whose temperature exceeds 25 ºC a process of conversion occurs: hydration products transform into another compound (C_3AH_6). This transformation induces a considerable increase in porosity, and thus a drastic loss of strength and a decrease in the resistance to aggressive agents, especially to carbonation. The degree to which the porosity will increase and related consequences occur, depends on the *w/c* ratio used, and is much greater when this ratio exceeds 0.4.

In some countries, HAC has more recently been used to obtain acid-resistant (sewage) pipe or lining. During production, the w/c is kept below 0.4 and thermal treatment is applied during the manufacturing process, deliberately forcing the conversion to the stable compound (C_3AH_6). If the strength and density of the converted material are adequate, the durability is good. The stable product has a high resistance against attack by acids. HAC concrete also has good properties for high-temperature applications (furnaces).

A.6 REFERENCES

Collepardi, M., 2002. *The new concrete (in Italian),* Tintoretto, Villorba (I).

Elsener, B., Fluckiger, D., Bohni, H., 2000. A percolation model for water sorption in porous cementitous materials. In: *Materials for Building and Structures,* Euromat, Vol. 6, F.H. Wittmann (Ed.), Wiley-VCH, Weinheim, pp. 163–169.

EN 197-1 (2000). *Cement- Part 1: Composition, specifications and conformity for common cements,* European Committee for Standardization.

Metha, P.K., Monteiro, P.J.M., 1993. *Concrete: structure, properties, and materials,* 2nd Edn., Prentice Hall.

Neville, A.M., 1995. *Properties of concrete,* 4th Edn., Longman Group Limited, Harlow.

Neville, A.M., Brooks, J.J., 1990. *Concrete technology,* Longman Scientific and Technical, Harlow.

Poers, T.C., 1958. Structure and physical properties of hardened Portland cement paste. *Journal of American Ceramic Society,* Vol. 41, No. 1, pp. 1–6.

Polder, R.B., 2000. Simulated de-icing salt exposure of blended cement concrete- chloride penetration. In: *Proceedings of the 2nd International RILEM Workshop Testing and Modeling the Chloride Ingress into Concrete,* C. Andrade, J. Kropp, (Eds.), PRO 19, RILEM publications, pp. 189–202.

Schiessl, P., 1988. *Corrosion in construe,* Rilem Technical Comminute 60-CSC, Chapmann and Hall, London.

Stauffer, D., 1985. *Introduction to percolation theory,* Taylor and Francis, London.

Taylor, H.F.W., 1990. *Cement chemistry,* Academic Press Inc., London.

APPENDIX B

CONSOLIDATION CHARACTERISTICS OF EARLY AGE CEMENTED PASTE BACKFILL

Erol Yilmaz, Tikou Belem, Bruno Bussière, and Mostafa Benzaazoua

Paper presented at the 61st Canadian Geotechnical Conference

Proceedings of the 61st Canadian Geotechnical Conference and the 9th Joint CGS/IAH-CNC Groundwater Specialty Conference, Edmonton, Alberta, Canada, September 21–24, pp. 797–804

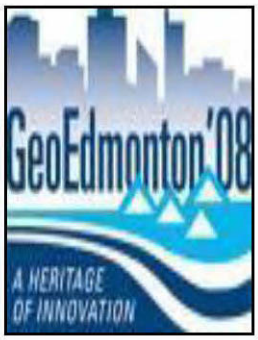

B.0 RÉSUMÉ

Les matériaux à grains fins saturés tels que le remblai cimenté en pâte (RCP) peuvent subir un tassement significatif dû à leur consolidation pendant les jeunes âges. La connaissance de ce phénomène est tout à fait importante pour développer des systèmes de remblayage bien conçus. La plupart des études ont été faites en se concentrant sur l'effet des propriétés physiques, chimiques et minéralogiques des ingrédients du RCP (résidus miniers, liant et eau de mélange) sur leur comportement mécanique et microstructural. Cependant, les aspects reliés aux propriétés in situ et les conditions qui affectent la performance à court, moyen et long termes du RCP n'ont pas été suffisamment étudiés. En fait, les effets des conditions pendant et après la mise en place sur la qualité et le comportement des RCP frais et/ou durcis curés en condition gravitaire ou avec surcharge n'ont pas beaucoup été expérimentés. Ce article présente une étude en laboratoire entreprise pour comprendre l'effet de la teneur en liant sur les caractéristiques de la consolidation unidimensionnelle du RCP (par exemple, détermination du coefficient de consolidation c_v, de l'indice de compression C_c et de récompression C_r) et les propriétés physiques résultantes (par exemple, indice des vide final e_f, teneur en eau finale w_f et degré de saturation final S_{rf}). L'évolution des propriétés de consolidation des remblais sous une séquence de chargement incrémental de 0.5, 25, 50, 100, 200 et 400 kPa est comparée pour cinq teneurs en liant (0- échantillon témoin, 1, 3, 4.5 et 7%) et quatre temps de cure (0, 1, 3 et 7 jours). Les résultats d'essai montrent que le comportement en consolidation 1-D est considérablement affecté par la quantité de liant ajoutée au RCP. L'indice de compression C_c varie de 0.06 à 0.54 tandis que celui de récompression C_r varie entre 0.0019 et 0.0081. Le coefficient de consolidation c_v diminue de 2.73×10^{-3} à 3.46×10^{-3} cm^2/s avec le temps dû à la formation progressive des liens de cimentation pendant l'hydratation.

B.0 ABSTRACT

Saturated fine-grained materials such as cemented paste backfill (CPB) can undergo significant consolidation settlement during the early curing ages. Understanding this phenomenon is vital in designing effective mine backfill systems. Most studies have focused on the effects of the physical, chemical and mineralogical properties of CPB ingredients (tailings, binder and water) on its mechanical and micro-structural behaviour. However, aspects linked to in situ properties and conditions that affect short, mid- and long-term backfill performance have not been sufficiently studied. In fact, the effects of during- and after-placement conditions on the quality and behaviour of fresh and/or hardened CPB cured under either self-weight or time-dependant load have not been experimentally investigated. This paper presents a laboratory study undertaken to understand the effect of binder contents on the one-dimensional (1-D) consolidation characteristics (coefficient of consolidation c_v, compression index C_c and recompression index C_r) and the resultant final bulk properties (void ratio e_f, water content w_f and degree of saturation S_{rf}) of CPB. The change in consolidation properties of CPB materials under an example loading sequence of 0.5, 25, 50, 100, 200 and 400 kPa is compared for five binder contents (0 – control, 1, 3, 4.5 and 7%) and four curing times (0, 1, 3 and 7 days). Results show that the behaviour of 1-D consolidation under time-dependent loading is greatly affected by the amount of binder added to CPB material. C_c varies from 0.06 to 0.54 while C_r is between 0.0019 and 0.0081 and c_v decreases from 2.73×10^{-3} to 3.46×10^{-3} cm^2/s over time due to the gradual formation of cement bonds during hydration.

B.1 INTRODUCTION

Every day, a vast amount of sulphide-rich mill tailings are generated in mineral processing plants worldwide. These tailings can cause harmful impacts on the environment if they are not properly managed. Therefore, how to treat such tailings effectively and economically has always been a major issue facing all mining operations (Aubertin et al., 2002; Yilmaz, 2007). Due to its rapid rate of delivery and placement (as compared to other forms of backfill such as hydraulic fill and rock fill) and the fact that mill tailings are recycled as backfill, cemented paste backfill (CPB) is a promising tailings management technique for mines.

From an ever higher density dewatered tailings (65–90 wt% solids content), CPB are produced by mixing them with a hydraulic binding agent which can be a blend of two or more cements and mineral additives (0–10 wt%) to provide mechanical strength and stability, and water (typically lake water, recycled process water or tap water) to obtain the desired slump consistency (152–254 mm or 6–10") allowing the safe transport and placement of the final CPB material to the underground mine stopes (Landriault, 2001; Benzaazoua et al., 2004, Belem and Benzaazoua, 2008a). CPB offers numerous operational, environmental, and economic benefits: lower operating and rehabilitation costs, higher regional and local ground support, the option of placing a part (up to 60 wt%) of mine tailings to the stopes (thus reducing the volume of tailings to be stored on the surface), and the control of environmental pollution associated with the safe storage of sulphide-rich mine tailings under atmospheric conditions allowing the formation and release of acidic waters and heavy metals (Hassani and Archibald, 1998; Aubertin et al., 2002; Bussiere, 2007). As a result of these facts, CPB is now in quite wide use by most mines as an efficient and beneficial backfill method.

A number of studies regarding the physical, chemical and mineralogical characteristics of CPB ingredients (i.e. tailings, binder and water) on the strength gain and micro-structural properties have been conducted by focussing on the inter-relationship between particle size distribution, solids concentration, binder type and content, curing time and temperature, and pore structure (Benzaazoua et al., 1999; 2004; Belem et al., 2000, 2002; Kesimal et al., 2005; Klein and Simon, 2006; Ouellet et al., 2007; Fall et al., 2008, Belem and Benzaazoua,

2008b). However, aspects linked with in situ properties and conditions that affect the paste backfill performance are not known sufficiently. The effects of during- and after-placement conditions (i.e. enhanced consolidation) on the quality and behaviour of fresh and hardened CPB samples being cured under time-dependent loads are not sufficiently investigated (e.g., Belem et al., 2002, 2006).

It is common practice at most underground mines to place CPB sequentially (plug fill and residual fill), except for small-scale mines where fill placement is continuous and governed by a constant filling rate based on the plant capacity. In general, it is necessary for pouring an initial "plug-fill" of CPB material and then let it cure under self-weight consolidation during a couple of days (typically 2-7 days) for achieving a good cement bonding and to prevent a barricade failure during subsequent residual filling. Due to the gradual reduction of void ratio after consolidation, the stiffness of the backfill increases over time (Bussiere, 1993; Belem et al., 2002, 2006; Cayouette, 2003; le Roux, 2004; Grabinsky and Bawden, 2007). In some cases, a "continuous" filling application may damage cement bonds and/or give rise to barricade failures due to excess strain and stress developed within the CPB during placement (Yumlu and Guresci, 2007). Consequently, it is of a great importance to understand self-weight and surcharge load consolidation characteristics of fresh CPB materials.

In this study, a new laboratory consolidation apparatus named CUAPS (curing under applied pressure system) that allows one-dimensional consolidation testing on the CPB materials was developed (Benzaazoua et al., 2006). The originality of this work is that it focuses on the relations between the effects of curing, void ratio, and binder content on the CPB quality and behaviour. More specifically, the influence of binder proportion and curing time on the one-dimensional consolidation characteristics (e.g. coefficient of consolidation c_v, coefficients of compression index C_c and recompression index C_r) as well as the consequential physical and geotechnical properties (e.g. void ratio e_f, degree of saturation S_f, water content w_f, settlement S_p, vertical strain ε_v and specific surface S_s). Five binder proportions (0-control sample, 1, 3, 4.5, and 7 wt%) and four curing times (0, 1, 3 and 7 days) were considered.

B.2 MATERIALS AND METHODS

B.2.1 Tailings sample characterization

Sulphide-rich mill tailings sample was collected from LaRonde mine in Quebec, Canada. The sample was received in sealed plastic containers to avoid any oxidation. The laboratory analysis results show that the tailings sample has an average water content w of 23.4 wt%, a specific gravity G_s of 3.7, a specific surface S_s of 2.17 m^2/g, an optimum water content w_{opt} of 9.1 wt%, a maximum dry unit weight γ_{dmax} of 24.9 kN/m^3, a relative compaction R_c of 91 wt%, a liquid limit w_L of 23 wt%, a plastic limit w_P of 18 wt%, a liquidity index LI of 1 wt%, a plastic index PI of 5 wt%, and a clay activity A (simply defined as the PI divided by the percent of clay-sized particles present, < 2 μm) of 1. The Atterberg limit results showed that the tailings sample would be designated as ML. A laser diffraction-type particle size analyzer (Malvern Mastersizer) was used to determine the grain size distribution (GSD) curves of mine tailings, as shown in Figure B.1.

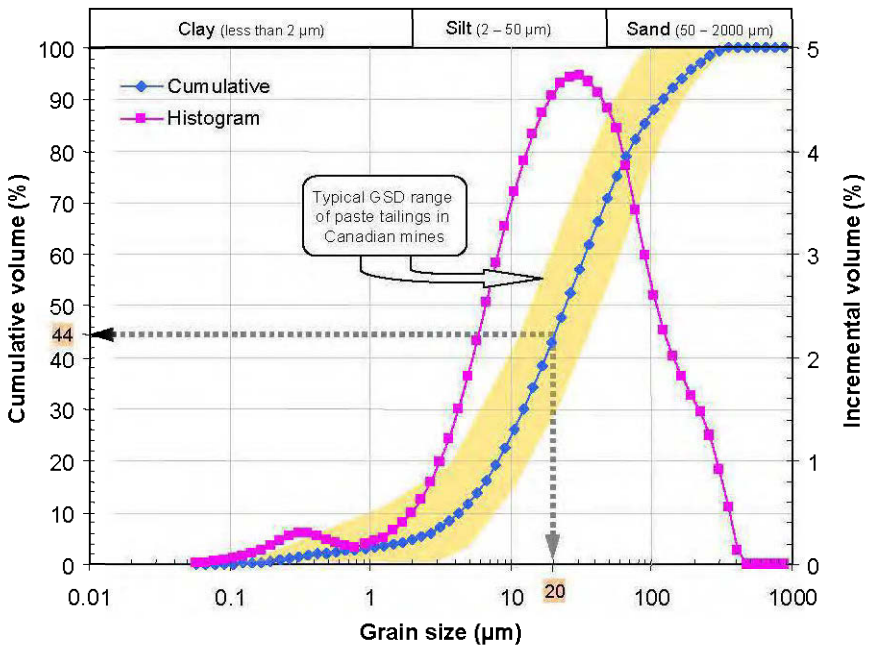

Figure B.1 Grain size distribution (GSD) curves of the tailings sample, comparing to a typical range of PSD curves of 11 mine tailings sampled from Canadian mines.

The GSD results show that the sample contained only 4.7% of clay-sized particles. The most GSD fell in medium to fine sand and silt-sized particles. With the fines (< 20 μm) content of 44%, the mine tailings sample is classified as a medium size tailings material (Landriault, 2001). The uniformity coefficient (C_u = D_{60}/D_{10}) and curvature coefficient (C_c=$D_{30}^2/D_{60}\times D_{10}$) of the mine tailings sample are 7.9 and 1.1, respectively. Based on the USCS classification (Das, 2002), the tested tailings material is a low plasticity silt (ML).

Table B.1 tabulates X-ray diffraction (XRD) analysis and ICP-AES analysis results of the studied tailings sample. It can be concluded from XRD analysis that the sample contains a high proportion of pyrite (47.05 wt%), mainly responsible for the high G_s of the tailings (3.7). The other major minerals are quartz (31.6 wt%), chlorite (8.9 wt%), paragonite (7.31 wt%) and muscovite (4.60 wt%). The ICP-AES analysis also indicates iron Fe (27.4 wt%) and sulphur S (24.9 wt%) are the most abundant elements identified within the tailings sample.

Table B.1 Chemical and mineralogical analyses results of the tailings sample used

Element (ICP)	Grade (%)	Mineral (XRD)	Grade (%)
Aluminum, Al	2.8	Pyrite	47.05
Calcium, Ca	0.57	Quartz	31.6
Iron, Fe	27.4	Chlorite	8.9
Sodium, Na	0.3	Paragonite	7.31
Lead, Pb	0.1	Muscovite	2.92
Sulphur, S	20.6	Talc	1.34
Potassium, K	0.2	Gypsum	0.84
Zinc, Zn	0.35	Albite	0.04

B.2.2 Binding agent

The binder used for CPB preparation was a blend of 20 wt% of ordinary Portland cement (type I or PCI) and 80 wt% of ground granulated blast furnace slag (Slag). Five different binder contents were considered for each test series: 0 (control sample), 1, 3, 4.5 and 7 wt%. Table B.2 tabulates the main chemical and physical properties of the binding agent used in the paste backfill mixtures.

Table B.2 Chemical composition and physical properties of the binder used

Properties	CPI	Slag	PCI-Slag (20-80 wt%)
G_s	3.08	2.89	2.92
S_s (m^2/g)	1.58	3.54	2.84
Al_2O_3 (%)	4.86	10.24	8.39
CaO (%)	65.76	31.41	42.82
Fe_2O_3 (%)	2.44	0.55	0.64
MgO (%)	2.21	11.29	6.19
Na_2O (%)	2.11	2.01	2.03
SO_3 (%)	3.67	3.27	3.35
SiO_2 (%)	19.51	36.22	30.91
Hydraulic modulus	2.28	0.66	1.07

The hydraulic modulus [$CaO/(SiO_2+Al_2O_3+ Fe_2O_3)$] values of the binders are 2.28 and 0.66 for PCI and Slag binders, respectively. Metallurgists classify slag as either basic or acidic: the more basic the slag, the greater its hydraulic activity in the presence of alkaline activators (Hewlett, 2001). Physical characterization indicates that the BET specific surface area S_s and the specific gravity G_s for Slag binder and PCI are 3.54 m^2/g and 1.58, and 2.89 m^2/g and 3.08, respectively.

B.2.3 Mixing water

Two types of water, the mine recycled process water and tap water were used for preparing CPB mixtures and their chemical and geochemical compositions are listed in Table B.3. The mine recycled process water is very highly aggressive with respect to sulphate content (4882.8 ppm) but also contains calcium Ca of 559 ppm because of the addition of lime during the milling. Tap water used within the CPB mixture contains a Ca concentration of 40.9 ppm and a magnesium Mg concentration of 2.27 ppm. A Benchtop pH/ISE meter Orion Model 920A coupled with a Thermo Orion Triode combination electrode (Pt-Ag-AgCl; Orion Inc.) was utilised for the pH, redox potential (Eh) and electrical conductivity (EC) measurements. In addition, Table B.3 tabulates the pH, Eh and EC parameters for recycled process and tap waters used in this study.

Table B.3 Chemical and geochemical analyses results of the mixing waters used

Parameter	Recycled process water	Tap water
Al (ppm)	0.212	0.01
Ca (ppm)	559	40.9
Fe (ppm)	0.011	0.066
Mg (ppm)	1.83	2.27
Si (ppm)	0.891	0.901
SO_4^{2-} (ppm)	4882.8	137.8
pH	9.41	7.82
EhN (mV)	146.6	430.7
EC (mS/cm)	7.42	0.274

B.2.4 Mixing, pouring, and curing of paste backfills

The required amounts of CPB ingredients such as mine tailings, cement and water) were prepared in a Hobart mixer (Model No D 300-1). The mixing procedure was as follows: to ensure the homogeneity of the final paste material, tailings, accompanied by little water were first mixed by a rigid "B" stainless beater for 4 minutes at a low speed of 54 rpm (speed 1), then added the cement and mixed by a floppy "D" wire whip for 4 minutes at a medium speed of 100 rpm (speed 2) and later added the remaining water to the premixed materials, and mixed with the same beater for 4 minutes at a high speed of 183 rpm (speed 3). Therefore, the total mixing time for CPB materials was 12 minutes. Each CPB mix has a typical water content of 28.2 wt% (corresponding to a solids concentration of 78 wt%) and diverse binder contents (0, 1, 3, 4.5 and 7%). CPB containing 1, 3, 4.5 and 7 wt% binders have a water-to-cement ratio of 27.8, 9.7, 6.5 and 4.3, respectively.

Each CUAPS cell or apparatus is then poured with CPB material into a Perspex transparent cylinder in three equal thickness layers of ~68 mm. Each layer is rammed in 25 blows using a ¼" diameter steel rod in order to eliminate any large trapped air bubbles within the sample. After the paste was poured into cylinders, the top porous stone, the loading piston and platen connected with a pneumatic pressure line are then placed (Figure B.2).

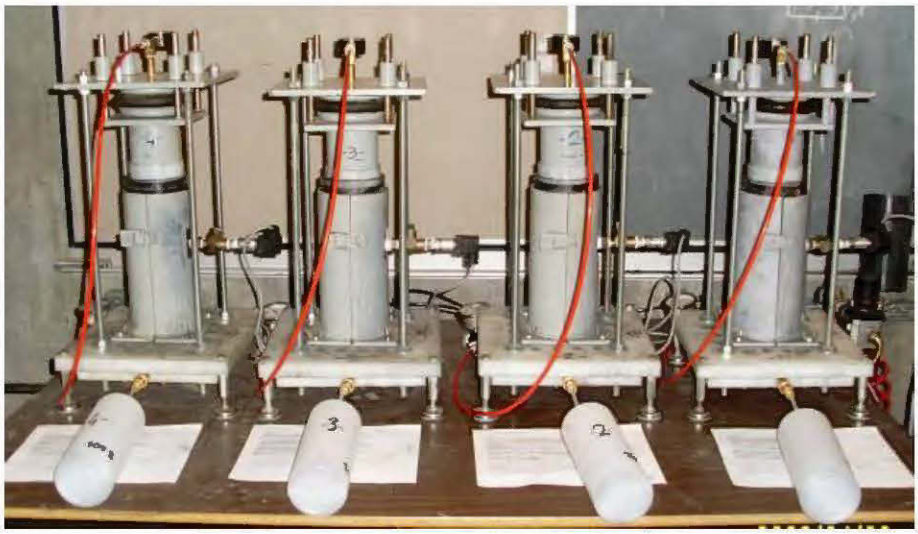

Figure B.2 A series of the one-dimensional consolidation tests conducted on CPB samples being cured for 0, 1, 3 and 7 days.

A total of 20 test samples (16 cemented tailings and 4 uncemented tailings as control sample), having 4" (101.6 mm) in diameter and 8" (203.2 mm) height was prepared and cured for 0, 1, 3 and 7 days at a room temperature of 20-25°C and at a relative humidity greater than 70%. It has been observed that, for a given binder content, the slump (paste consistency) values measured by means of the Abrams cone slump test (ASTM C143 standard) ranged between 165 mm and 254 mm. The slump in this range was suitable for the safe placement without segregation, as testified by a number of underground mines worldwide (Hassani and Archibald, 1998).

B.2.5 One-dimensional consolidation tests

One-dimensional (1-D) consolidation tests, based on the ASTM D2435 and D4186 standards were performed by using CUAPS (curing under applied pressure system) cells in order to investigate the effects of binder content and curing time on the evolution of CPB micro-structure and to simulate in situ placement of lab-prepared CPB. Basically, the CUAPS cell is a consolidometer having a polycarbonate cylinder as the CPB sample holder and a pneumatic pressure system, including porous stone discs to cover the top and bottom ends of the backfill

sample to enable pore water to escape from CPB as compression is taking place. A complete description of the CUAPS cell employed in the experiments is beyond the scope of this paper. Further information on this multiple-aim laboratory tool and some related works can be found in Benzaazoua et al. (2006) and Yilmaz et al. (2006, 2008).

1-D consolidation tests are carried out on CPB under time-dependent loading. Immediately after samples are placed into the consolidometer, a pre-contact pressure of 15 kPa is applied in order to put the piston and the top porous stone in contact. Then, the pressure sequence of 0.5, 25, 50, 100, 200 and 400 kPa is applied to the CPB and vertical displacement is recorded following a time interval of 0, 2, 4, 6, 8, and 10 hours. The load increment ratio (LIR) is 1 ($\Delta\sigma/\sigma$, where $\Delta\sigma$ = increase in pressure and σ = pressure before the increase). Pressure is applied following this LIR until the maximum pressure of 400 kPa is reached. During consolidation tests, test data such as pressure, deformation and time are concurrently and continuously recorded and stored in a data logging system. These data can be recovered and downloaded on a laptop for time duration of 7 days. In the tests, at first samples are allowed to cure under self-weight consolidation until prefixed curing time, and, later incrementally applied the pressure varying from 0,5 to 400 kPa to simulate time-dependent consolidation.

B.3 RESULTS

B.3.1 Effect of binder content on consolidation properties

Variations in the initial void ratio e_0 of uncemented and cemented backfills during 1-D consolidation tests versus applied pressure ($log\ p$) are presented in Figure B.3. Once can say from Figure B.3 that, in spite of the major difference in the magnitude, the overall trend of the variation in the void ratio (Δe) versus pressure are similar and decreases with curing time. Table B.4 summarizes the variation of the difference between the initial (e_0) and the final (e_f) void ratios for four binder contents and curing times. It can be observed that for a given curing time, Δe decreases with increasing binder. For a given binder content, Δe decreases with increasing curing time.

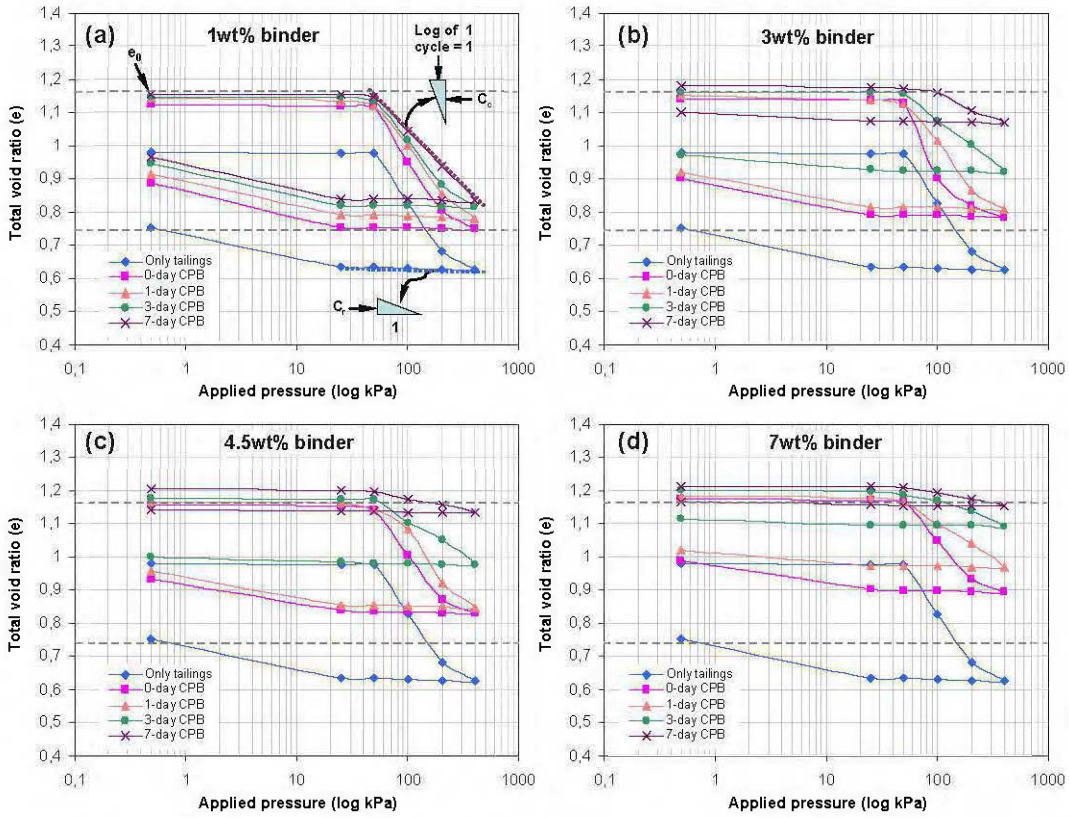

Figure B.3 Consolidation curves of CPB samples containing different binder content: a) 1 wt%, b) 3 wt%, c) 4.5 wt% and d) 7 wt%.

Table B.4 Magnitude of variation of void ratio for CPB samples

Curing time	$\Delta e = e_0 - e_f$			
	1 wt%	3 wt%	4.5 wt%	7 wt%
0-day	0.25	0.24	0.23	0.18
1-day	0.24	0.23	0.21	0.17
3-day	0.21	0.19	0.18	0.08
7-day	0.20	0.08	0.06	0.05

Let us consider Δe as «resistance to consolidation» of CPB material. Consequently, a low Δe value means high resistance to consolidation, while a high Δe value means low resistance to consolidation. It can be noticed that this resistance to consolidation is highest for the 7-day

curing time which can be explained by the strength development because of the gradual formation of cement bonds during hydration

B.3.2 Evolution of compressibility parameters

The compressibility parameters (i.e. compression index C_c, recompression index C_r, and coefficient of consolidation c_v) are obtained from the linear portions of consolidation curves in Figure B.3.

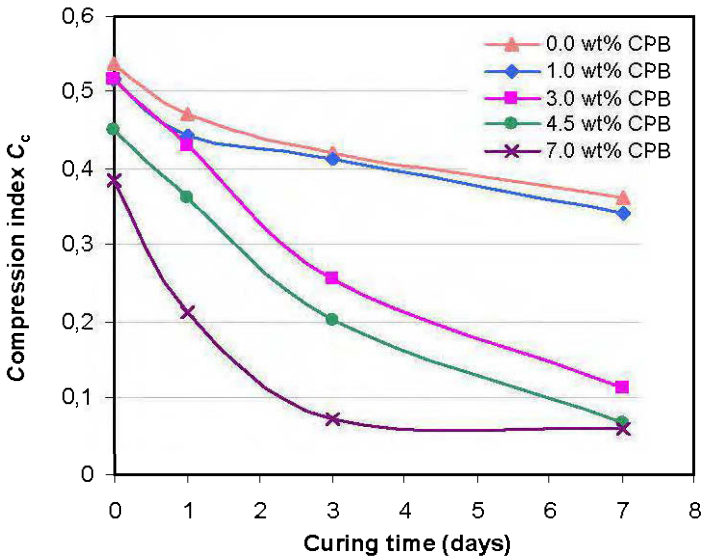

Figure B.4 Change in compression index with curing time for tailings and CPB samples.

Figure B.4 shows that the compression index C_c of CPB material decreases non-linearly with the increase of curing time, regardless of the binder content. In the other hand, the rate of decrease in C_c with curing time is higher with the increase of the binder content because the CPB matrix becomes increasingly rigid. By increasing the binder content from 0 wt% to 7 wt%, the C_c value is reduced by about 30% and 83% for 0-day and 7-day curing time, respectively. For the CPB with binder content of 7 wt%, the C_c value is reduced by 82% while for the binder content of 1 wt% this reduction is about 34%.

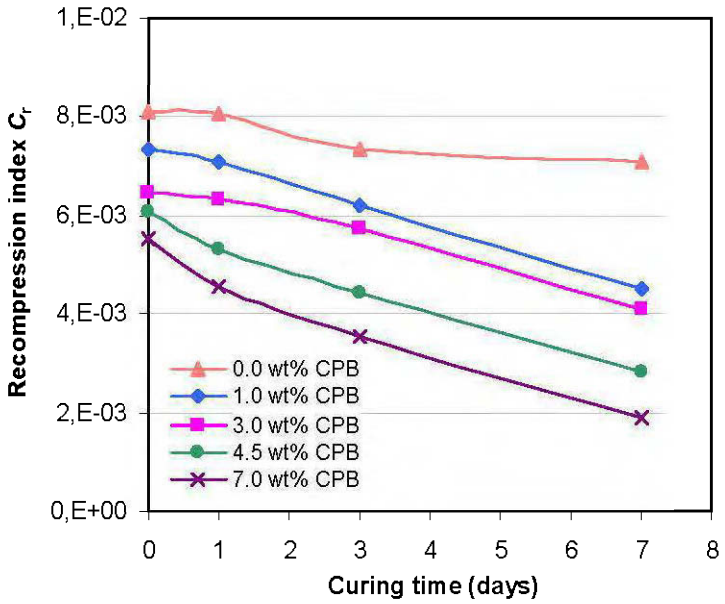

Figure B.5 Change in recompression index with curing time for tailings and CPB samples.

Figure B.5 shows the variation of C_r with curing time. It can be observed that the C_r value decreases linearly with the increase of curing time, regardless of the binder proportion. This linearity seems to relate the evolution of C_r to the elastic properties of CPB material. Calculated C_r values are very low compared to C_c values. This can be explained by the fact that once the CPB is compressed (packed) the recompression phase affects very little its skeleton.

B.4 DISCUSSION

B.4.1 Calculated coefficient of consolidation

Figure B.6 shows the variation of coefficient of consolidation c_v with curing time. c_v was estimated from the square root of time or Taylor's method ($c_v = 0.848*H_{dr}^2/t_{90}$). It can be observed that value c_v decreases with the increase in curing time, regardless of the binder content. In addition, for a given curing time, the c_v value slightly increases with the increase of binder content.

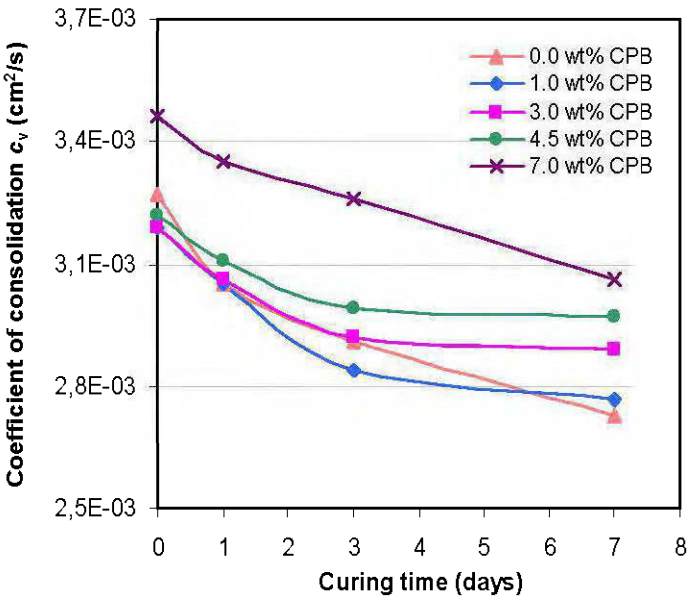

Figure B.6 Change in coefficient of consolidation with time for tailings and CPB samples.

B.4.2 Calculated hydraulic conductivity

Figure B.7 shows the calculated CPB saturated hydraulic conductivity k_{sat} ($=c_v*m_v*\gamma_w$) from values c_v and coefficient of volume compressibility m_v (Taylor's method) values. The overall trend is similar to that of the variation in compression index (C_c) with curing time (see Figure B.4). It can be noted that for the binder content varying from 0% to 4.5% by dry mass, the calculated k_{sat} decrease quasi-linearly with the increase of curing time. This k_{sat} decrease becomes non-linear when the binder content used in CPB mix is of 7 wt%. Previous work done by Godbout (2005) showed that the measured k_{sat} decreases non-linearly with the increase of curing time in the contrary of what was calculated in this study. Though, data presented in Figure B.7 are overall in the same orders of magnitude as those obtained by Godbout (2005) for identical binder type, binder content and curing times, even if they are slightly lower. But in the literature it is stated that calculated k_{sat} is lower than measured k_{sat}. It should however be noted that the samples tested in the study done by Godbout (2005) were not consolidated in the contrary of the samples tested in the present study.

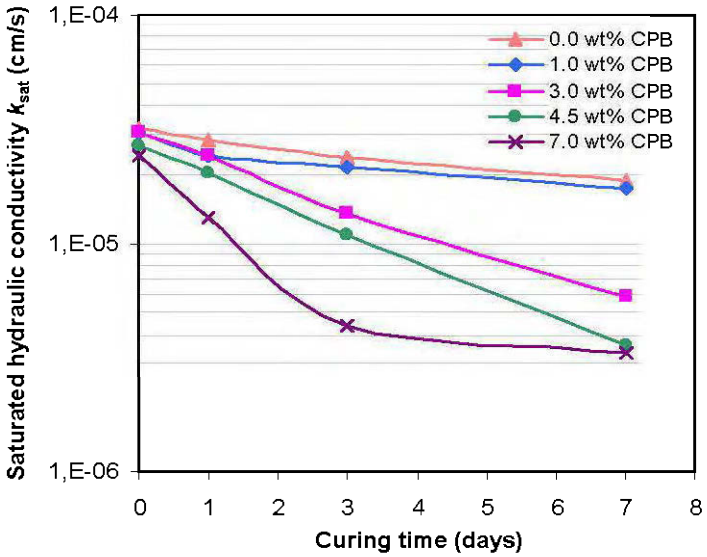

Figure B.7 Change in saturated hydraulic conductivity with curing time for CPB samples.

B.4.3 Evolution of the physical parameters

Figures B.8 and B.9 show an evolution of the different final physical index parameters calculated after 1-D consolidation tests performed on both tailings and CPB. Figure B.8a shows that binder content strongly affects the final void ratio e_f of consolidated samples. Also, the increase in curing involves the increase of the final void ratio e_f. This is probably due to the precipitation and the formation of the hydration products in CPB. As an example, for 7wt% binder, e_f increases from 0.99 to 1.17 as curing time increases from 0 to 7 days. Figure B.8b shows a variation of water content w_f with time. As the curing time increases from 0 to 7 days, CPB with 1 and 7wt% binders reduces the w_f value from 23.5 wt% to 20.6 wt% and from 19.2 wt% to 14.1 wt%, respectively. Knowing that the initial water content w_0 is 28.2 wt%, the first major drop of water content can be explained by water drainage due to stress application (0.25 to 400 kPa). In terms of degree of saturation (S_{rf}) this corresponds to a reduction of the initial degree of saturation (S_{ri} = 100%) by 10% for 1wt% binder and by 21% for 7wt% binder. The rest of the reduction (~7% and 15% for binder contents of 1 wt% and 7wt%, respectively) can be attributed to binder hydration. It can also be noted that the binder type used and especially 7wt% binder seems to support the water drainage of fresh CPB.

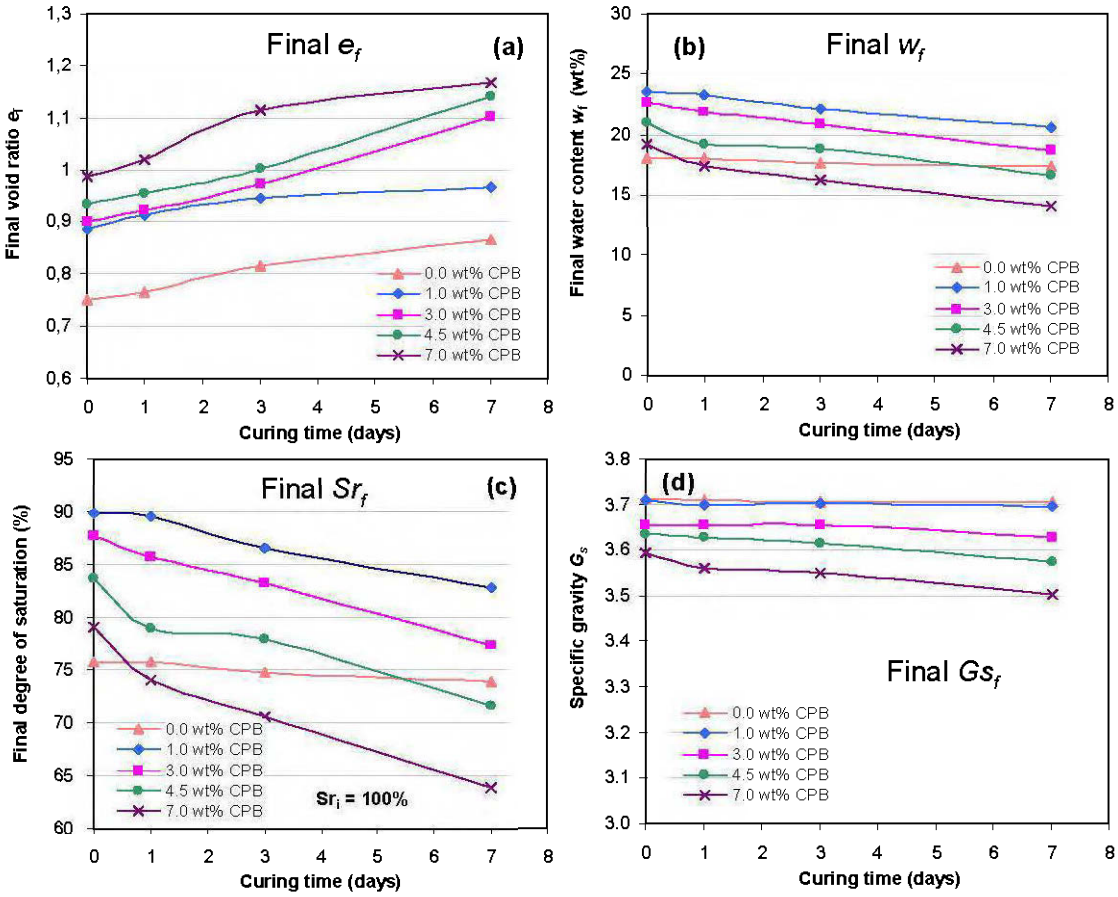

Figure B.8 Evaluation of the CPB final index properties as a function of curing time: a) void ratio, b) water content, c) degree of saturation, and d) specific gravity.

The reduction of water within CPB via drainage, in fact, gives rise to a more dense structure having a lower final degree of saturation S_r, as shown in Figure B.8c. It can be observed that as the binder content increases from 1 to 7 wt%, S_r decreases from 98% to 72% for 0-day curing time, and 79% to 64% for 7-day curing time. Figure B.8d shows that the specific gravity varies very slightly and remains almost constant with the curing time and binder content. For example after 7 days curing time, G_s slightly decreases from 3.7 to 3.64 when the binder content is increased from 0 to 7 wt%. Figure B.9a shows that vertical strain ε_v decreases with increasing curing time, depending a lot on the amount of binder used in the CPB mixture. This is because there is a progressive formation of cement bonds with curing

time and which develop the material stiffness and prevent the deformation. The exactly same observations were made for the primary settlement (Figure B.9b). Figure B.9c shows the evolution of cumulative drainage water W_d as a function of curing time. It can be observed that as for the vertical strain ε_v, the cumulative drainage water significantly decreases with the increase of curing time and depends much on the binder proportion. This is most probably due to the increase of CPB matrix stiffness with curing time, which allows less drainage water volume to be collected once the pressure was applied (p = 400 kPa) and, at early ages (< 5 days), hydration reactions took place. For the CPB sample containing 7wt% binder, W_d decreases drastically from 18.6% to about 3% when time increases from 0 to 7 days.

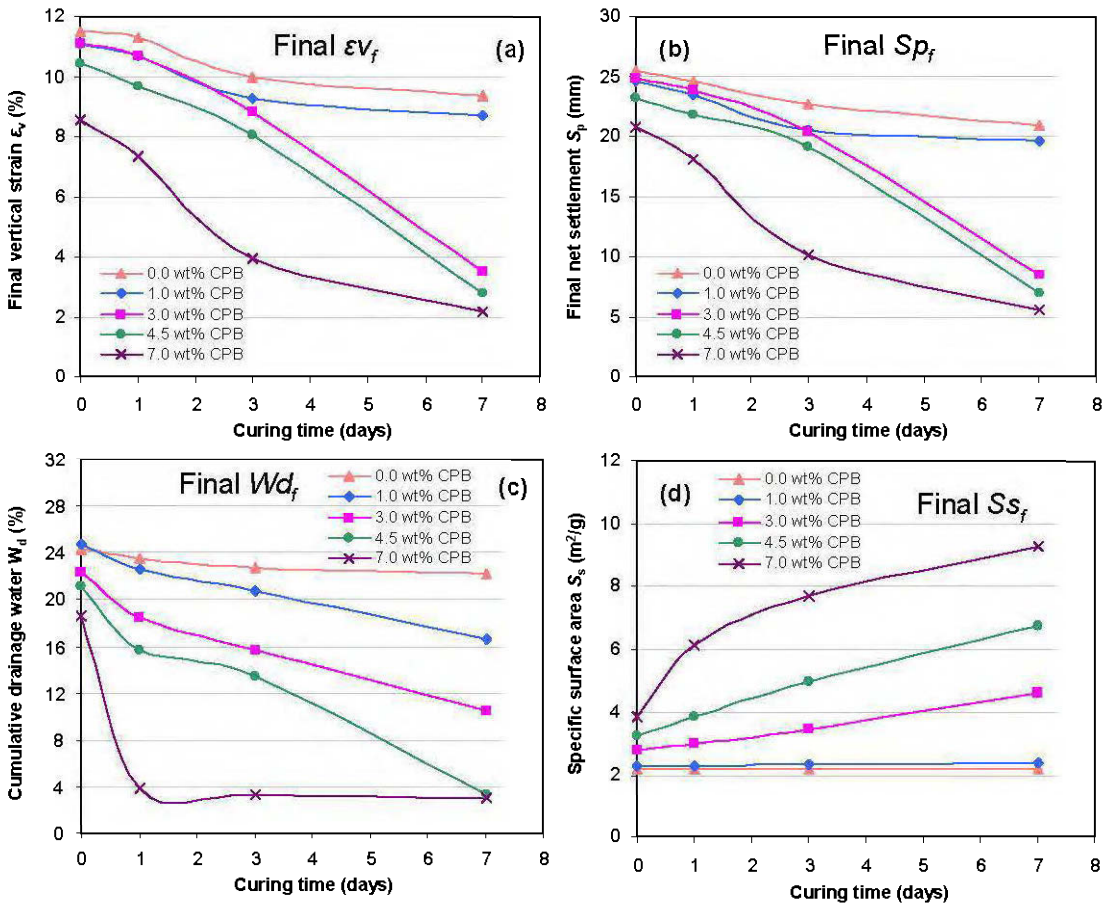

Figure B.9 Evaluation of the CPB final index properties as a function of curing time: a) strain, b) settlement, c) cumulative drainage water, and d) specific surface.

Finally, the variation of the specific surface area S_s of CPB samples as a function of curing time is illustrated in Figure B.9d. The overall trend is that S_s value increases proportionally with increasing binder content because of the gradual formation of the cement hydration products which eventually filled the void space.

B.5 CONCLUSIONS

This study presents the effects of curing time and binder content on consolidation properties and resulting hydraulic properties (e.g. saturated hydraulic conductivity k_{sat} and degree of saturation S_r) of early age CPB. The main conclusions from this work are as follows: 1) Coefficient of consolidation c_v is greatly affected by the CPB binder content as a function of curing time. Overall trend is that the c_v decreases with increasing binder content and curing time, 2) Compressibility parameters such as compression index C_c and recompression index C_r decreases as the curing time increases, and 3) calculated saturated hydraulic conductivity k_{sat} (based on Taylor's method) and degree of saturation S_r decrease with increased curing time and are in good agreement with the measured values from the literature. Finally, this study has shown that the knowledge of 1-D consolidation of CPB materials can effectively help on the understanding of their placement and curing process during backfilling. More importantly, it brings a light on the effect of consolidation on CPB properties that can help operators to make a very efficient CPB design for under-ground hard rock mines.

B.6 ACKNOWLEDGEMENTS

This research was partly financed by the Canada research chair on Integrated management of sulphidic mine wastes using backfill and the NSERC-Polytechnique-UQAT industrial chair on Environment and mine wastes management. The authors would like to thank the financial support provided for the manufacture of lab setups by Canadian Foundation for Innovation. Special thanks are due to Pierre Trudel of G+Plus Industrial Plastics Inc. for his collaboration and help during setups' modification. Special thanks are extended to URSTM chemists and technicians, principally David Bouchard and Nil Gaudet for their technical support.

B.7 REFERENCES

Aubertin, M., Bussière, B., Bernier, L., 2002. *Environ-nement et gestion des résidus miniers.* Presses Inter-nationales Polytechnique, Montréal, Quebec, Canada.

Belem, T., Benzaazoua, M., Bussière, B., 2000. Mechanical behavior of cemented paste backfill. In: *Proceedings of the 53rd Canadian Geotechnical Conference,* Montreal, Quebec, Canada, Vol 1. pp. 373–380.

Belem, T., Benzaazoua, M., Bussière, B., Dagenais, A.M., 2002. Effects of settlement and drainage on strength development within mine paste backfill. In: *Proceedings of the 9th International Conference on Tailings and Mine Waste,* Vail, Forth Collins, Colorado, USA, pp. 139–148.

Belem, T., El Aatar, O., Bussière, B., Benzaazoua, M., Fall, M., Yilmaz, E., 2006. Characterization of self-weight consolidated paste backfill. In: *Proceedings of the 10th International Seminar on Paste and Thickened Tailings,* Limerick, Ireland, pp. 333–345.

Belem, T., Benzaazoua, M., 2008a. Design and application of underground mine paste backfill technology. *Geotechnical and Geological Engineering,* Vol. 26, No. 2, pp. 147–174.

Belem, T., Benzaazoua, M., 2008b. Predictive models for prefeasibility cemented paste backfill mix design. In: *Post-Mining 2008,* GISOS: Research Group for the Impact and Safety of Underground Works, Nancy, France, February 6–8, pp. 1–13.

Benzaazoua, M., Ouellet, J., Servant, S., Newman, P., Verburg, R., 1999. Cementitious backfill with sulphur content: physical, chemical and mineralogical characterization. *Cement and Concrete Research,* Vol. 29, No. 5, pp. 719–725.

Benzaazoua, M., Fall, M., Belem, T., 2004. A contribution to understanding the hardening process of cemented paste fills. *Minerals Engineering,* Vol. 17, No. 2, pp. 141–152.

Benzaazoua, M., Belem, T., Yilmaz, E., 2006. Novel lab tool for paste backfill. *Canadian Mining Journal,* Vol. 127, No. 3, pp. 31–31.

Bussière, B., 1993. Evaluation des propriétés hydro-géologiques de résidus miniers utilisés comme barrières de recouvrement. *M.Sc. Thesis,* Université de Montréal, École Polytechnique, Canada, pp. 1–171.

Bussière, B., 2007. Colloquium 2004: Hydro-geotechnical properties of hard rock tailings from metal mines and emerging geo-environmental disposal approaches. *Canadian Geotechnical Journal,* Vol. 44, No. 9, pp. 1019–1052.

Cayouette, J., 2003. Optimization of the paste backfill plant at Louvicourt mine. *CIM Bulletin,* Vol. 96, No. 1075, pp. 51–57.

Das, B.M., 2002. *Soil mechanics laboratory manual,* 6th ed., Oxford University Press, New York, USA.

Fall, M., Benzaazoua, M., Saa, E., 2008. Mix proportioning of underground cemented tailings backfill. *Tunnelling and Underground Space Technology,* Vol. 23, No. 1, pp. 80–90.

Helinski, M., Fahey, F., Fourie, A.B., 2007. Numerical modeling of cemented paste backfill deposition. *Journal of Geotechnical and Geoenvironmental Engineering,* Vol. 13, No. 10, pp. 1308–1319.

Godbout, J., 2005. Évolution des propriétés hydriques des remblais miniers cimentés en pâte durant le curage. *M.Sc. Thesis,* Ecole Polytechnique de Montréal, pp. 1–213.

Grabinsky, M.W.F., Bawden, W.F., 2007. In situ measurements for geo-mechanical design of cemented paste backfill systems. *CIM Bulletin,* Vol. 100, No. 1103, pp. 1–8.

Hassani, F.P., Archibald, J.F., 1998. *Mine Backfill,* CIM, Quebec, Canada.

Hsu, T.W., Lu, S., 2006. Behavior of one-dimensional consolidation under time-dependent loading. *Journal of Engineering Mechanics,* Vol. 132, No. 4, pp. 457–462.

Kesimal, A., Yilmaz, E., Ercikdi, B., Alp, I., Deveci, H., 2005. Effect of properties of tailings and binder on the short and long terms strength and stability of cemented paste backfill. *Materials Letters,* Vol. 59, No. 28, pp. 3703–3709.

Klein, K., Simon, D., 2006. Effects of specimen composition on the strength development in cemented paste fill. *Canadian Geotechnical Journal,* Vol. 43, No. 3, pp. 310–324.

Landriault, D., 2001. *Backfill in underground mining: Underground mining methods engineering basics and case studies,* Littleton, USA, Chapter 69, pp. 601–614.

Hewlett, P., 2001. *Lea's chemistry of cement and concrete,* 4th ed., Butterworth-Heinemann.

le Roux, K.-A., 2004. In situ properties and liquefaction potential of cemented paste backfill. *Ph.D. Thesis, The University of Toronto,* pp. 1–271.

Ouellet, S., Bussière, B., Aubertin, M., Benzaazoua, M., 2007. Microstructural evolution of cemented paste backfill: MIP results. *Cement and Concrete Research,* Vol. 37, No. 3, pp. 1654–1665.

Yilmaz, E., El Aatar, O., Belem, T., Benzaazoua, M., Bussière, B., 2006. Effect of consolidation on performance of cemented paste backfill. In: *The 21st Underground Support'06,* AMQ, Val d'Or, Quebec, Canada, pp. 1–14.

Yilmaz, E., 2007. How efficiently the volume of wastes produced from mining operations can be reduced without causing any important environmental impact? *Environmental Synthesis Report,* UQAT, Quebec, Canada, pp. 1–45.

Yilmaz, E., Benzaazoua, M., Belem, T., Bussière, B., 2008. Influence of applied pressure on the hydro-mechanical properties of cemented paste backfill. *Geotechnical and Geological Engineering,* (submitted in January 2008).

Yumlu, M., Guresci, M., 2007. Paste backfill bulkhead monitoring: A case study from Inmet's Cayeli Mine, Turkey. *CIM Bulletin,* Vol. 100, No. 1103, pp. 1–10.

APPENDIX C

EXPERIMENTAL CHARACTERIZATION OF THE INFLUENCE OF CURING UNDER STRESS ON THE HYDROMECHANICAL AND GEOCHEMICAL PROPERTIES OF CEMENTED PASTE BACKFILL

Erol Yilmaz, Tikou Belem, Mostafa Benzaazoua and Bruno Bussière

Paper presented at the 12th International Conference on Tailings and Mine Waste

Proceedings of the 12th International Conference on Tailings and Mine Waste, Vail, Forth Collins, Colorado, USA, October 19–22, pp. 139–152.

C.0 RÉSUMÉ

La performance en résistance en compression uniaxiale (UCS) des remblais cimentés en pâte (RCP) placés dans des ouvertures souterraines (par exemple, chantiers miniers) ont souvent tendance à surestimer les résistances mécaniques obtenues en laboratoire en utilisant des moules classiques non perforés, même dans des conditions similaires de température et d'humidité pendant la cure. Cette différence est probablement due à la consolidation gravitaire ou avec surcharge, les contraintes de cure, les conditions de drainage, l'effet d'arche, et la pression de confinement du toit et des mûrs des chantiers miniers remblayés. Dans cette étude, l'effet de la cure sous contrainte sur les propriétés hydromécaniques et géochimique des RCP a été étudié. Un équipement de laboratoire améliorées appelé CUAPS (système de cure sous pression appliqué) qui imite les conditions de mise en place et de cure in situ des RCP a été utilisé en parallèle avec les moules conventionnels non perforés. Une grande différence a été observée entre l'UCS obtenus à partir des échantillons de RCP consolidés au CUAPS et ceux non consolidés des moules classiques en plastique. L'évolution des propriétés physico-chimiques et géochimiques du RCP est comparée pour trois teneurs en liant 3, 4,5 et 7 wt% et pour trois temps de cure de 7, 14 et 28 jours. Les résultats ont montré que le drainage des eaux en raison de la consolidation a un effet avantageux sur le durcissement du RCP. Par conséquent, la performance globale des remblais consolidés au CUAPS est toujours plus réaliste que celle des moules conventionnels en plastique non perforés dans lesquels le RCP n'est pas consolidés, dont les résistances sont connues pour être sous-estimées.

C.0 ABSTRACT

The uniaxial compressive strength (UCS) performance of cemented paste backfill (CPB) placed in underground openings (e.g., mine stopes) tends to be underestimated based on mechanical strengths obtained using conventional non-perforated moulds in the laboratory, even under similar curing conditions of temperature and humidity. This difference is attributable to self-weight consolidation and/or time-dependent surcharge consolidation, curing under stresses, drainage conditions, the arching effect, and roof and wall confinement pressure encountered in backfilled mine stopes. In this study, the effect of curing under stress on the hydromechanical and geochemical properties of CPB materials was investigated. An improved laboratory apparatus called CUAPS (curing under applied pressure system) that mimics the in situ placement and curing conditions of CPB material was used, along with conventional non-perforated mould samples. A substantial difference was observed between the UCS obtained on CUAPS-consolidated CPB and conventional mould-unconsolidated CPB samples. Changes in the physico-chemical and geochemical properties of the CPB material are compared for binder contents of 3, 4.5 and 7 wt% and curing times of 7, 14 and 28 days. Results show that water drainage due to consolidation has an advantageous effect on CPB hardening. Consequently, the overall performance of CUAPS-consolidated CPB is consistently more realistic than the performance of conventional non-perforated mould-unconsolidated CPB, whose strength is known to be underestimated.

C.1 INTRODUCTION

The mining industry uses mine waste materials (mainly tailings and waste rocks) for the preparation of backfill, which fills underground voids created by ore extraction. The choice of mine backfill systems such as rock fill, slurry fill or paste backfill plays a major role in the productivity, safety, and economic benefits of operating underground mines (Hassani and Archibald, 1998; Bussiere, 2007). However, compared with other backfill systems, cemented paste backfill (CPB) has begun to be increasingly used by most modern mines worldwide, due to its significant cost advantages and the potential for placing the full plant sulphidic tailings in underground stopes (Landriault, 2001).

CPB is usually prepared by mixing the tailings, binder and mixing water to form a composite construction material. After its hardening, the CPB material acts as secondary ground support. Physico-chemical and mineralogical properties of CPB ingredients greatly affect both strength and stability performance (Amaratunga and Yaschyshyn, 1997; Archibald et al., 1999; Benzaazoua et al., 1999, 2002, 2004; Belem et al., 2000; Mohamed et al., 2001; Yilmaz, 2003; Yilmaz et al., 2003; Kesimal et al., 2004, 2005; Godbout, 2005; Klein and Simon, 2006; Ouellet, 2007). The uniaxial compressive strength (UCS) is the key index parameter mostly utilised for CPB stability design (Stone, 1993; Belem and Benzaazoua, 2008a, b). The UCS requirements are closely related to the assortment of roles undertaken by CPB. Overall, the typical target UCS values for CPB vary from 0.25 to 4.35 MPa for a wide range of applications varying from mine tailings disposal to roof support in underground mines (Hassani and Bois, 1992; Belem and Benzaazoua, 2008a).

CPB design is frequently based on the evaluated properties of laboratory-prepared backfill material (conventional plastic mould samples). However, experience indicates that it is not easy to ensure that all the physical and mechanical conditions prevailing underground are observed when the CPB sample is prepared, cured and tested in the laboratory (Servant, 2001). Besides, the mechanical and curing properties of in situ CPB material vary appreciably, depending on the methods of preparation, placement and the conditions of the mine environment (Belem et al., 2002; le Roux et al., 2005). In order to obtain a more

realistic mechanical response of CPB material, it is very important to take into account the intrinsic and extrinsic factors affecting in situ backfill performance. Previous studies indicate that the UCS magnitudes of in situ CPB material are often 2 to 4 times higher than those obtained from laboratory-prepared samples of identical batch mix and curing time (Servant, 2001; Belem et al., 2002; Cayouette, 2003; Revell, 2004; le Roux et al., 2005). The UCS discrepancy may be attributed to the fact that the hardening of CPB material cured under an effective field stress increases the rate of strength development and the ultimate strength, as reported recently by a number of authors (Belem et al., 2002, 2006; Helinski et al., 2006; Fourie et al., 2006; Grabinsky and Simms, 2006; Yilmaz et al., 2006, 2008a). As well, Revell (2004) has indicated that scale effects have a large impact on CPB strength performance. To the knowledge of the authors, there is no suitable laboratory apparatus and/or standardized test procedure for CPB that mimics the field mixing, placement and curing conditions on a laboratory scale. Moreover, only few studies showed that consolidation both under self-weight and time-dependent surcharge loading could have a notable effect on the overall performance and quality of CPB materials (Belem et al., 2002, 2006, 2007; Benzaazoua et al., 2004; le Roux et al., 2005; Yilmaz et al., 2006, 2008a, b). In the literature, there is a lack of knowledge about the characteristics of CPB cured under constant and/or variable applied pressure. Consequently, an understanding of the influence of curing under stress on CPB performance is required, for a more reliable and better quality of backfill design.

The main objective of this study is to evaluate the effects of binder content and curing time on CPB hydromechanical performance, as well as to observe the resulting geochemical properties. To achieve this objective, a new laboratory consolidometer named CUAPS (curing under applied pressure system) that allows for the simulation of the in situ placement and curing conditions of CPB materials is used (Benzaazoua et al., 2006). A comparative analysis of the above-mentioned properties of the CPB cured in both conventional plastic moulds and under variable applied pressures was performed using three different binder contents (3, 4.5 and 7 wt%) and curing times (7, 14 and 28 days).

C.2 MATERIALS AND METHODS

C.2.1 Characteristics of paste backfill ingredients

Tailings: the tailings sample used in this study was taken from a Canadian gold mine, located in the western part of the province of Quebec. The sample's grain size distribution (GSD) was determined using a Malvern Mastersizer laser diffraction-type particle size analyser (Figure C.1), fitting with a typical range of GSD curves of 11 mine tailings sampled from the underground mines located in the provinces of Quebec and Ontario, Canada (Ouellet, 2006).

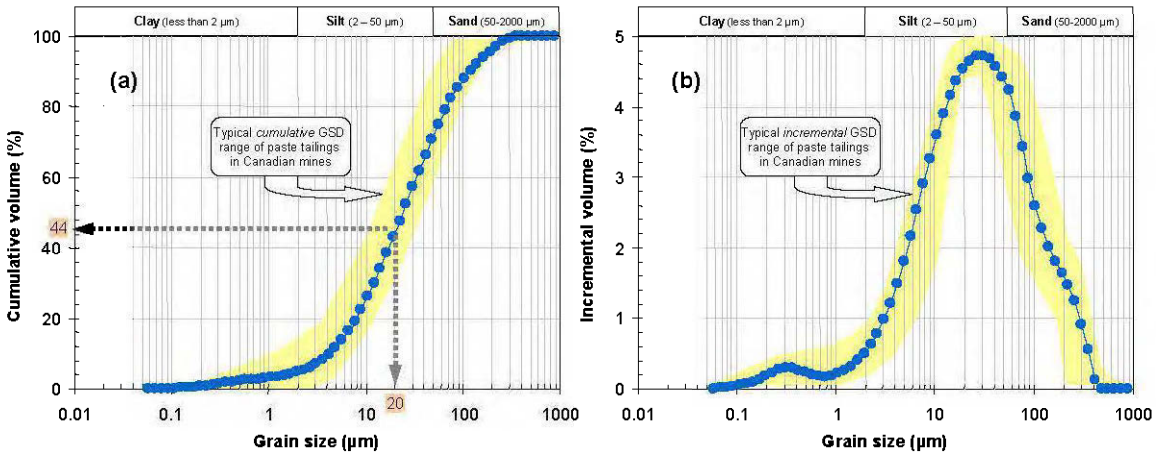

Figure C.1 GSD curves of the tailings used: a) cumulative, b) incremental.

Table C.1 also shows the main physico-chemical characteristics of the tailings sample. It can be observed that fines content (–20 µm) is 44 wt% which corresponds to medium size tailings, according to Landriault (2001). Mine tailings are well-graded with a coefficient of uniformity C_u (= D_{60}/D_{10}) of 8 and with a coefficient of curvature C_c (= $D_{30}^2/D_{60}*D_{10}$) of 1.1. Based on the Unified Soil Classification System, the tailings are classified as low plasticity silt (ML). The specific gravity G_s that was measured with a Micromeritics® Accupyc 1330 helium gas pycnometer is 3.7, reflecting a relatively high content of metal-barren sulphides.

The chemical composition analyses of metals and total sulphur (S_{total}) were conducted on the mine tailings sample using a Perkin-Elmer® Model Optima 3100 RL ICP-AES (inductively coupled plasma-atomic emission spectroscope) after complete acid digestion by HNO_3, Br_2, HF and HCl. Dilute HCl was used to extract sulfates and the solution obtained was analyzed by ICP-AES. From the chemical composition analysis carried out on the tailings sample, it can be observed that the contents of iron Fe, sulphur S, aluminium Al, and calcium Ca were 27.4 wt%, 20.6 wt%, 2.8 wt% and 0.57 wt%, respectively.

Table C.1 Main physico-chemical characteristics of the tailings sample used

Parameter	S_s (m^2/g)	G_s	D_{10} (µm)	Fines (<20µm)	C_u (wt%)	C_c (wt%)	Al (wt%)	Ca (wt%)	Fe (wt%)	S_{total} (wt%)
Tailings	2.17	3.7	4.26	44 wt%	8	1.1	2.8	0.57	27.4	20.6

S_s: specific surface; D_{10}: effective particle diameter

Binding agent: the binder used for the preparation of CPB samples is a blend of Ordinary Portland cement or Type I (PCI) and ground granulated blast furnace slag (Slag). The blending ratio of PCI to Slag is 20/80. Three different binder proportions of 3, 4.5 and 7 wt% were chosen to evaluate the effect of curing conditions on the UCS performance of CPB samples. Proportions were calculated on the basis of weight, relative to the total dry tailings. Moreover, the chemical composition analyses were conducted on the studied binder samples using ICP-AES method, as explained well in the previous section. Table C.2 shows the main chemical composition and physical properties of the binding agents used in the experiments.

Table C.2 Chemical composition and some physical properties of the binders used

Parameter	S_s (m^2/g)	G_s	Al_2O_3 (wt%)	CaO (wt%)	Fe_2O_3 (wt%)	K_2O (wt%)	MgO (wt%)	Na_2O (wt%)	SO_3 (wt%)	SiO_2 (wt%)
PCI	1.58	3.1	4.86	65.76	2.44	0.83	2.21	2.11	3.67	19.51
Slag	3.54	2.8	10.24	31.41	0.55	0.51	11.3	2.01	3.27	36.22
PCI-Slag	2.84	2.9	4.26	42.82	0.64	0.55	6.19	2.03	3.35	30.91

Mixing water: two types of water: namely, as-received tailings pore water and tap mixing water were chemically analyzed using ICP-AES method. Table C.3 summarizes the results of the chemical and geochemical analyses. It can be observed that the pore water is highly aggressive in terms of sulphate content (SO_4^{2-} content around 4880 ppm) but also contains calcium (Ca content about 560 ppm). While Ca comes from the lime added during ore treatment, sulphates can come from cyanide elimination process (tailings are treated before backfilling), and those produced from sulphide reactivity (Benzaazoua et al., 2004).

Table C.3 Chemical and geochemical analysis results of pore and tap waters

Parameter / element	*EC* (mS/cm)	pH	Eh (v)	SO_4^{2} (ppm)	Si (ppm)	Mg (ppm)	Al (wt%)	Ca (ppm)	Fe (wt%)
Pore water	7.42	9.4	0.147	4883	0.891	1.83	0.212	559	0.011
Tap water	0.274	7.8	0.431	138	0.901	2.27	0.01	40.9	0.066

Additionally, the values in terms of pH, Eh (redox potential) and EC (electrical conductivity) of pore and tap waters were 9.41, 0.147 volt and 7.42 mS/cm, and 7.82, 0.431 volt and 0.274 mS/cm, respectively. The relatively high value of EC within the pore water of as-received tailings indicates the presence of many dissolved conducting ions.

C.2.2 Experimental program

Consolidometer: An innovative laboratory apparatus named CUAPS (curing under applied pressure system) was developed for simulating field placement and curing conditions of laboratory-prepared CPB materials. The CUAPS apparatus has been described previously by Benzaazoua et al. (2006). The CUAPS allows the operator to estimate the more realistic UCS values of the CPB materials cured under constant or variable pressure up to 400 kPa. The operating principle of the CUAPS is that CPB are one-dimensionally consolidated by axial pressure applied over time. A Polycarbonate Perspex tube in the CUAPS apparatus forms a highly resistant portion against volume change after a series of pressure is applied. Following an increase in total pressure, excess pore water within CPB material is expulsed through a

drainage port located at the bottom of CUAPS. During curing, drainage water is collected to calculate drainage rate and to analyze the chemical composition for the different recipes.

Backfill sample preparation: The CPB ingredients (i.e. mine tailings, cement and water) were thoroughly mixed using a double spiral mixer for about 7 minutes. After mixing, the measured slump of all mixtures was set to approximately 7 inches by adding more or less mixing water. The slump test was conducted according to ASTM C143 standard. The initial gravimetric water content w_g for all CPB samples was kept constant at 28.2 wt%.

Table C.4 lists the initial bulk properties of each CPB batch mixture. These values represent volumetric binder content B_v, solids concentration C_w, volumetric concentration C_v, water-to-cement ratio w/c, specific gravity G_s, void ratio e, wet density ρ, density ρ_d, and volumetric water content θ. It can be observed from Table C.4 that the w/c ratios reduce from 9.68 to 4.31 when the amount of binder added to the CPB batch is increased from 3 to 7 wt%. Also, ρ_d value was 1810, 1800, and 1790 kg/m^2 for 3, 4.5 and 7wt% binder contents, respectively.

Table C.4 Initial bulk properties of the CPB materials prepared for a given batch mix

Parameter	ρ (kg/m^2)	B_v (wt%)	C_w (wt%)	C_v (wt%)	G_s	w/c	e	ρ_d (kg/m^2)	S_r (wt%)	θ
3.0 wt%	2320	3.8	78	49.1	3.68	9.68	1.04	1810	100	0.5
4.5 wt%	2310	5.7	78	49.2	3.66	6.55	1.03	1800	100	0.5
7.0 wt%	2300	8.8	78	49.3	3.64	4.31	1.03	1790	100	0.5

Immediately after mixing, the prepared paste materials were poured into both conventional plastic moulds and transparent polycarbonate round tubes (CUAPS cell samples holders). Tubes and moulds have a shape factor of 2 that corresponds to height-to-diameter ratio. CPB samples were then sealed and stored in a humidity chamber maintained at ~80% relative humidity and 24 °C ± 2 °C in order to mimic curing conditions similar to those observed in the underground stopes of the mine under investigation. Figure C.2 shows consolidated CPB samples and mould-unconsolidated CPB samples being cured in a humidity chamber.

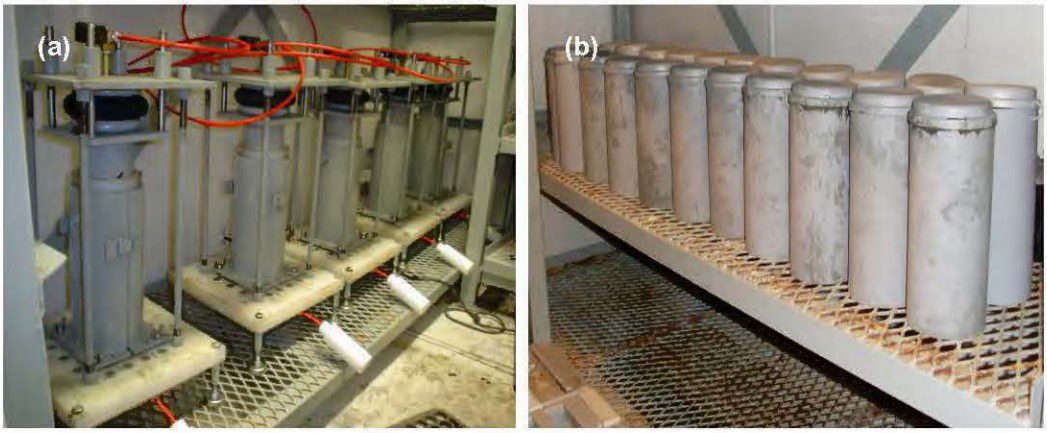

Figure C.2 Photos of (a) CUAPS-consolidated CPB samples and (b) conventional mould-unconsolidated CPB samples curing in a humidity chamber.

One-dimensional consolidation tests: as part of the present investigation, one-dimensional consolidation tests, inspired by ASTM D2435 and D4186 standards were carried out. CPB samples were consolidated using the CUAPS apparatus which allows a pressure range of 0–500 kPa. Before running the tests, a seating pressure of 15 kPa was applied to provide contact between sample and loading platen. Then, an example pressure sequence of 0.5, 25, 50, 100, 200 and 400 kPa, based on a load increment ratio LIR of 1, was applied to CPB samples and the axial deformations during each pressure increment were measured with LVDTs (linear displacement variable transducers) through a HOBO U12-4 data logger at a time interval of 0, 2, 4, 6, 8, and 10 hours. All pressures were incrementally applied during the first day of curing and unloaded down to 0.5 kPa after the desired curing time.

Unconfined compression tests: A total of 36 CPB samples, 9 CUAPS-consolidated and 27 conventional mould-unconsolidated samples were cured for uniaxial compressive strength (UCS) tests after periods of 7, 14, and 28 days. After curing, all CPB samples were subjected to the UCS tests according to ASTM C39 using a computer–controlled MTS 10/GL press, which has a nominal loading capacity of 50 kN and a displacement speed of 1 mm/min. The UCS magnitude of each sample is recorded (peak or ultimate stress) along with the elasticity modulus of deformation. For a given binder proportion and curing time, only one-test is done

for CUAPS-consolidated backfill samples whereas the average of three tests is taken for conventional plastic mould-unconsolidated backfill samples.

Bulk properties determination: after UCS testing, the calculated and/or measured CPB geotechnical index (bulk properties) parameters are determined as follows: gravimetric water content w (%), solids specific gravity G_s, degree of saturation S_r (%), void ratio e (or porosity n), volumetric water content, dry density ρ (g/cm^3), solid concentration C_w (%) and specific surface area S_s (m^2/kg). The S_s parameter, based on the BET (Brunauer, Emmett, and Teller) method, is evaluated by the nitrogen N_2 isotherm adsorption using a Micromeritics® surface analyzer model Gemini III.

Chemical and geochemical analysis: during the consolidation tests, a quantity of water is collected from each consolidated CPB samples at a specific time interval. After the acidifying process, analysis of the chemical composition of the collected water is carried out using a Perkin-Elmer ICP–AES (Optima 3100 RL). Also, the pH, redox potential (Eh) and electrical conductivity (EC) parameters are also measured using a Benchtop pH/ISE meter Orion Model 920A coupled with a Thermo Orion Triode combination electrode (Pt-Ag-AgCl).

C.3 RESULTS

C.3.1 Drainage water of consolidated CPB samples

Figure C.3 shows the evolution of cumulative drainage water W_d versus elapsed time for CUAPS-consolidated CPB samples prepared with a binder content of 3, 4.5 and 7 wt% as a function of elapsed time (7, 4.5 and 7 days of curing). It can be observed from Figure C.3 that the W_d parameter is greatly affected by the hardening process, depending on the amount of binder added to the CPB mixtures. The drainage rate decreases with increases of both binder content and curing time.

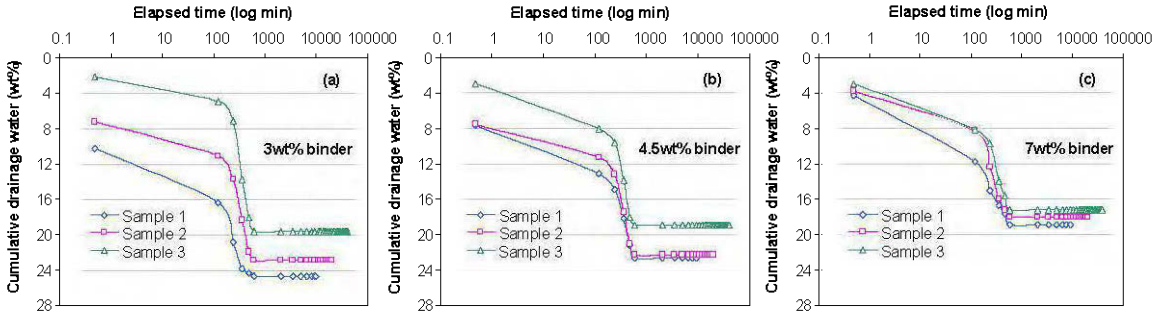

Figure C.3 Change in cumulative drainage water with elapsed time for different binder content CPB samples: a) 3 wt%, b) 4.5 wt%, and c) 7 wt% binder content.

For a 28-day curing time, the volume of drainage water for CPB with 3, 4.5 and 7 wt% binder was 19.6 wt% (253.5 mL), 18.8 wt% (242.7 mL) and 17.1 wt% (217.8 mL), respectively. As well, the pressure varying from 0.5 to 400 kPa plays a key role in the volume of water collected from samples. Overall, a pressure of 100, 200 and 400 kPa that corresponds to an elapsed time varying between 120 and 600 minutes induced a major gap in the magnitude of W_d. However, a lower pressure of 0.5, 25 and 50 kPa did not have a big influence on the water collection, even at early curing times (up to 7 days).

C.3.2 Vertical strain of consolidated CPB samples

Figure C.4 shows the evolution of the vertical strain ε_v (= ΔH*100/H_0) of consolidated CPB being cured under variable pressures as a function of binder content (3, 4.5 and 7 wt%). For a given applied pressure, Figure C.4 shows that the total ε_v observed from CPB samples containing 3 wt% binder is slightly greater than those observed from CPB samples containing the 4.5 and 7 wt% binder content. For pressure greater than 200 kPa, the settlement behaviour is relatively similar. For a binder content of 3, 4.5 and 7 wt%, the observed ε_v value varies from 12.5 to 13.4%, from 12.2 to 13.3%, and from 11.2 to 12.1 for CPB samples 1, 2 and 3, respectively. The shape of the curves is different particularly for pressure less than 200 kPa. As the amount of binder added to CPB material increases, the ε_v value (for pressure less than 200 kPa) decreases mainly because of binder hydration during the first day.

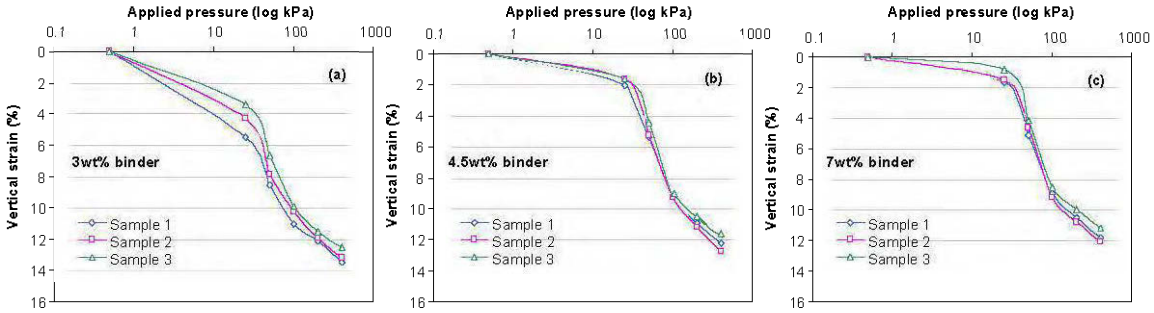

Figure C.4 Change in vertical strain with applied pressure for different binder content CPB samples: a) 3 wt%, b) 4.5 wt%, and c) 7 wt% binder content.

For a given applied pressure, Figure C.4 shows that the total ε_v observed from CPB samples containing 3 wt% binder is slightly greater than those observed from CPB samples containing the 4.5 and 7 wt% binder content. For pressure greater than 200 kPa, the settlement behaviour is relatively similar. For a binder content of 3, 4.5 and 7 wt%, the observed ε_v value varies from 12.5 to 13.4%, from 12.2 to 13.3%, and from 11.2 to 12.1 for paste backfill samples 1, 2 and 3, respectively. The shape of the curves is different particularly for pressure less than 200 kPa. As the amount of binder added to CPB material increases, the ε_v value (for pressure less than 200 kPa) decreases mainly because of binder hydration during the first day.

C.3.3 Characterization of CPB mechanical strength

Figure C.5 shows the difference in terms of the mechanical strength development between CUAPS-consolidated CPB samples and plastic mould-unconsolidated CPB samples as a function of binder content and curing time. Strength proportionally increases with binder content as expected. Generally, consolidated CPB samples systematically produce higher mechanical strength (higher UCS value) than conventional mould-unconsolidated samples, regardless of the curing time. This difference is of 57.9%, 64.3% and 58.2% for 3 wt% binder content, 52.3%, 54.3% and 51.8% for 4.5 wt% binder content, and 50.5%, 27.1% and 19.8% for 7 wt% binder content (Figures C.5a, C.5b, and C.5c). The highest UCS gap was obtained for CPB with 3 wt% binder content. One of the reasons for such a high UCS variation could

be the high drainage of excess water from these mixtures during the consolidation process, which reduces the corresponding porosity and permeability. During the drainage, the stiffness of consolidated samples increases as a function of increasing density.

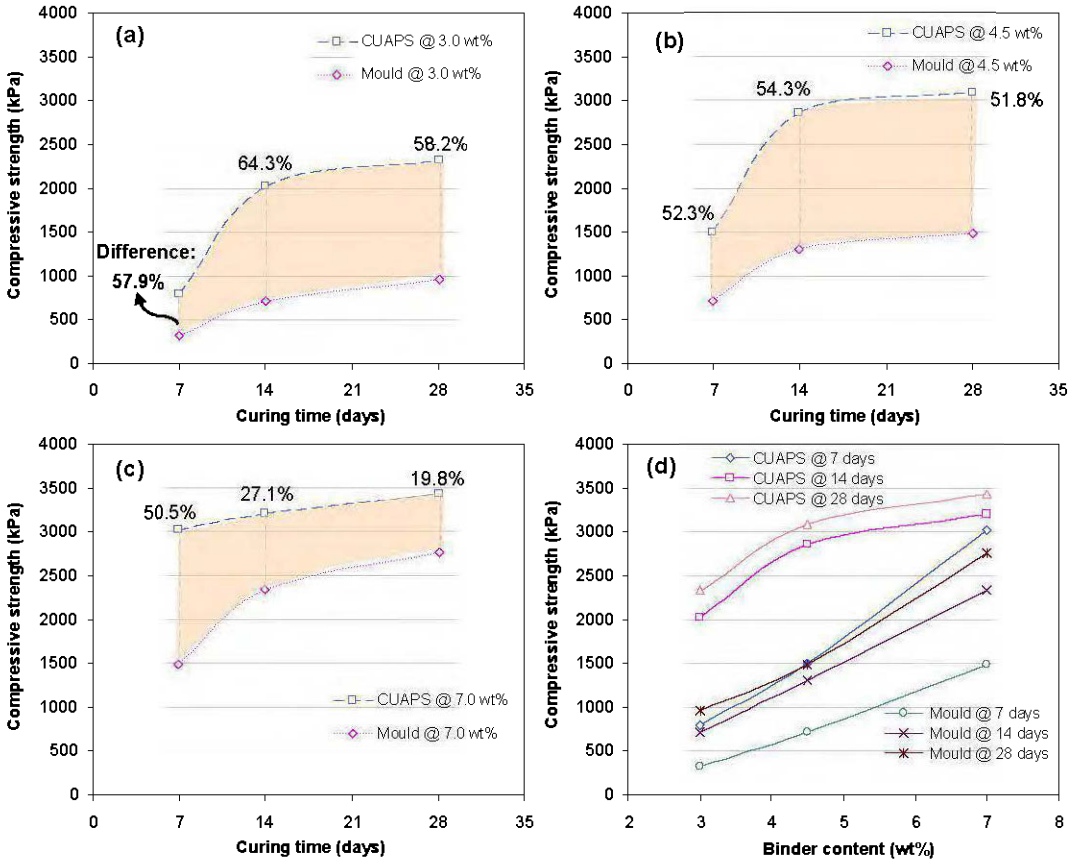

Figure C.5 Comparison of CPB mechanical strengths as a function of curing time: a) 3 wt%, b) 4.5 wt%, c) 7 wt%, and d) mixed results.

Another reason is that the hardening of CPB materials being cured under different effective stresses greatly contributes to the CPB strength. If a series of effective stress is applied just before the commencement of curing which contributes to hardening, as is being practiced in the present investigation, the rate of strength increase (short-term property), ultimate strength (mid-term property) and durability (long-term property) will be greater, compared to the

application of pressure after the completion of hydration. It has been experimentally shown from Belem et al. (2002) and Yilmaz et al. (2006, 2008a) that the primary bonds in cement in CPB may be broken due to hydrates damage caused by the applied pressure (overloading) in early stages of strength development, which thus reduces the strength and stiffness.

C.3.4 Characterization of CPB geotechnical index parameters

Figure C.6 shows the variation of the geotechnical index (bulk properties) parameters of CUAPS-consolidated samples and conventional plastic mould-unconsolidated CPB samples containing a binder content of 3, 4.5 and 7 wt% as a function of curing time. The measured geotechnical index parameters are as follows: the gravimetric water content w_g (%), dry density ρ_d (g/cm^3), specific surface S_s (m^2/kg), degree of saturation S_r (%) and void ratio e.

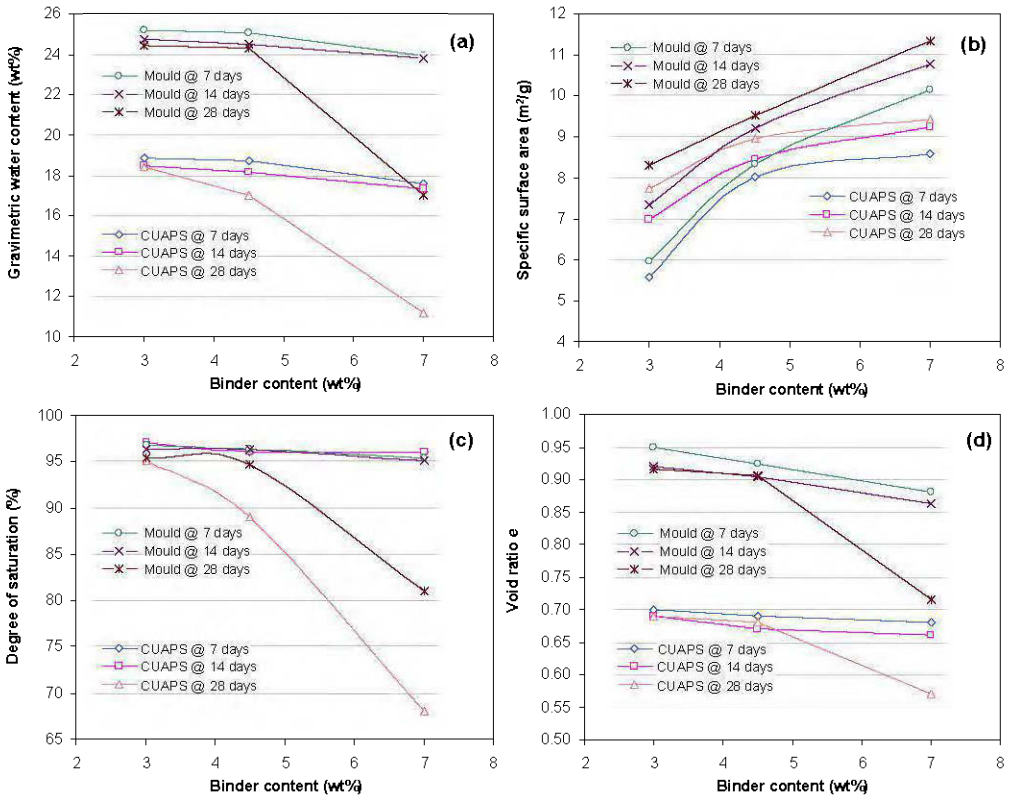

Figure C.6 Evolution of CPB bulk properties as function of binder content and curing time

There is a notable variation in water content, density and void ratio. Consolidated samples have a w_g value varying between 18.8–11.2 wt%, a ρ_d value varying between 2.13–2.08 g/cm^3, a void ratio e value varying between 0.7–0.57 while unconsolidated samples have a w_g value varying between 25.2–17%, a ρ_d value varying between 1.85–1.87 g/cm^3, a void ratio e value varying between 0.95–0.71. As well, the final water content w_g and degree of saturation S_r are highly influenced by the drainage ability of CPB material. The highest binder content (7 wt%) exhibits the lowest w_g and S_r. This could be basically explained by the different initial w/c ratios (see Table C.4) and the amounts of water required for binder hydration.

It was also shown by a number of authors (Belem et al., 2002, 2006; Benzaazoua et al., 2004; Yilmaz et al., 2006; 2008a, b) that drainage of the excess water existing within the CPB sample contributes to a better hardening process (water trapped during the cement hydration and/or hydrated phase precipitation as gypsum) for CPB material and therefore, the reduction of void ratio of backfilling. Moreover, the rate of water drainage is significantly affected by the settling (i.e. improved consolidation and/or density increase) of CPB sample being cured under a series of pressure during the first step of curing, and so higher strengths. Specific surface area S_s is closely related to the hardening phase formation during curing, and the ultimate mechanical strength. The higher the binder content used, the greater the overall S_s value of the CPB due to hydrate growth, becomes. UCS increase with the increasing S_s values for a given binder content, Overall, one can say that the consolidated samples give lower w_g and S_r, and higher UCS than those obtained using unconsolidated samples due to the variation in the initial void ratio e_0 and the influence of time–dependent consolidation settlement.

C.4 DISCUSSION

C.4.1 Correlation between the mechanical strength

From the compression test results shown in Figure C.7, it seems that a strong correlation exists between the UCS obtained from CUAPS-consolidated CPB samples (UCS_{CUAPS}) and the UCS obtained from conventional plastic mould-unconsolidated CPB samples (UCS_{mould}).

After normalizing the UCS values for binder content and curing time, it was possible to observe the correlation between the two sets of UCS data. This normalization consisted of multiplying each UCS variable by the binder content/curing time ratio (UCS*$B_{w\%}$/t). Figure C.7 shows the relationship between UCS_{CUAPS} and UCS_{mould}.

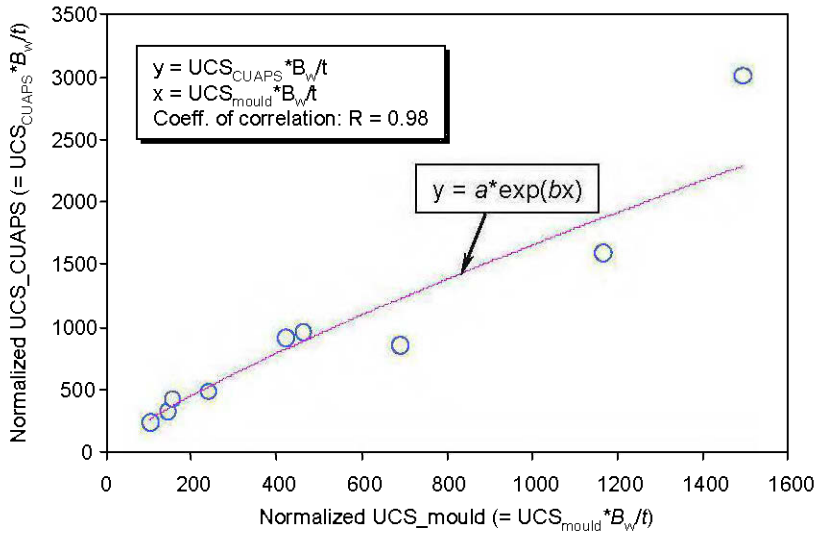

Figure C.7 Correlation between UCS_{CUAPS} and UCS_{mould} for different CPB samples.

It should be noted that at first approximation, it appears that this relationship could be well-described by an exponential function such as $y = a^*\exp(b^*x)$. Indeed, a coefficient of correlation $R = 0.98$ was obtained, thus indicating the strong relationship existing between the two types of UCS variables. The exponential relationship describing the correlation between these two types of variables (UCS_{CUAPS}, UCS_{mould}) is as follows (Eq. C.1):

$$UCS_{CUAPS} \times \left(\frac{B_{w\%}}{t} \right) = 360.952 \times \exp\left(0.001399 \times \left[UCS_{mould} \times \frac{B_{w\%}}{t} \right] \right) \qquad \text{(C.1)}$$

where $B_{w\%}$ = binder content (wt%); t = curing time (day); UCS values are in kPa.

Finally, the predictive CUAPS-consolidated backfill samples equation from known mould-unconsolidated backfill samples is given as follows (Eq. C.2):

$$UCS_{CUAPS} = \left(\frac{360.952 \times t}{B_{w\%}}\right) \times \exp\left(UCS_{mould} \times \frac{0.001399 \times B_{w\%}}{t}\right) \quad \text{(C.2)}$$

The above equations are specific to the CPB tested and to the loading sequence applied in this study (see the relevant section on consolidation tests). However, ongoing research on the influence of different pressure loading rates on the CPB consolidation characteristics, and consequently on its strength development, is underway. After these tests, it would be possible to develop a more general equation that could be used to improve prediction of CPB strength.

C.4.2 Chemical analysis of drainage water

Table C.5 shows the variation of chemical analysis of drainage water obtained from CUAPS-consolidated CPB samples during consolidation tests. Overall, the calcium Ca, silicon Si and sulphates SO_4^{2-} concentrations of CPB samples containing 3, 4.5 and 7 wt% binder content decrease with increasing curing time. The variation in terms of chemical composition can be explained by the different chemical compositions of both binder and tailings pore water and tap water (see Table C.3) used for CPB, relating to the hydration and precipitation process at early ages. However, the variation is due to the fact that the denser the cementitious matrix is, the more this later act as a filter of colloidal species from the pore waters. It can be observed from Table C.5 that, for a given binder content, calcium Ca concentration is higher at early ages (7 days) and begins to reduce when time is increased up to 28 days.

Table C.5 Chemical composition of water collected from CUAPS-consolidated samples

Binder content	Curing (day)	*Al* (ppm)	*Ca* (ppm)	*Fe* (ppm)	Mg (ppm)	Si (ppm	SO_4^{2-} (ppm)
	7	0.03	436	0.07	0.08	13.3	6692
3.0 wt%	14	0.02	429	0.13	0.04	12.5	6411
	28	0.03	284	0.15	0.05	11.7	4945
	7	0.01	420	0.06	0.02	15.0	6390
4.5 wt%	14	0.02	302	0.12	0.05	14.0	6100
	28	0.03	247	0.17	0.01	13.5	3056
	7	0.01	412	0.08	0.02	28.0	6279
7.0 wt%	14	0.03	251	0.13	0.78	27.5	5572
	28	0.04	194	0.22	0.18	26.7	2885

The reason for this phenomenon can be explained by the dissolution of Ca-bearing mineral within the cement during early hydration stages. At this time, Ca remains trapped in porous media. The dissolved Ca is expulsed from the sample along with drainage water as a function of pressure. In a similar manner, Si concentration is reduced with increased curing time, but at lower rates than Ca, due to the fact that Si occurs as gel phases in solid form. One can also say that sulphate concentration is relatively higher (6692, 6390, and 6279 ppm for 3, 4.5 and 7 wt% binder, respectively at 7 days of curing) than the one observed from the tailings pore water (4883 ppm, also Table C.3). This means that sulphate concentration increases during mixing at early curing ages due to aeration contributing to sulphide oxidation by oxygen intake. Also, the sulphates can come from the sulphated mineral dissolution from the binder.

C.4.3 Geochemical analysis of drainage water

Figure C.8 shows the variation in the geochemical analyses of water collected from the CUAPS-consolidated CPB samples containing a binder content of 3, 4.5 and 7 wt%. The measured parameters are pH, redox potential (Eh) and electrical conductivity (EC). For all CPB mixtures, as the amount of binder used in the tailings material sample increases, the pH and EC parameter decreases as a function of curing time. However, the Eh value increases with increasing binder content and curing time. In terms of magnitude, the highest pH change (from 11.5 at 7-day curing to 7.9 at 28-day curing) is observed for the sample containing 7 wt% binder content (Figure C.8a). This shows that pH decreases with increasing binder content and curing time. Furthermore, the Eh values, as shown in Figure C.8b, indicate that the CUAPS-consolidated CPB sample that contains 7 wt% binder acts differently while a binder content of both 3 wt% and 4.5 wt% acts in the same manner. After 7 days of curing, all the Eh values are almost the same (0.141, 0.148, 0.154 volts for 3, 4.5 and 7 wt% binder contents, respectively). In addition, pH reduces while Eh increases with increased curing time, due to the enhanced reactivity of sulphide during the sample preparation and mixing. Oxidation of pyrite accelerates acidity (i.e. the decrease of pH) and gives rise to a loss of strength over time. Degree of saturation S_r is closely related to the Eh parameter. Eh increases with the decrease of S_r which contributes to the increase of oxidation by molecular oxygen diffusing through CPB samples.

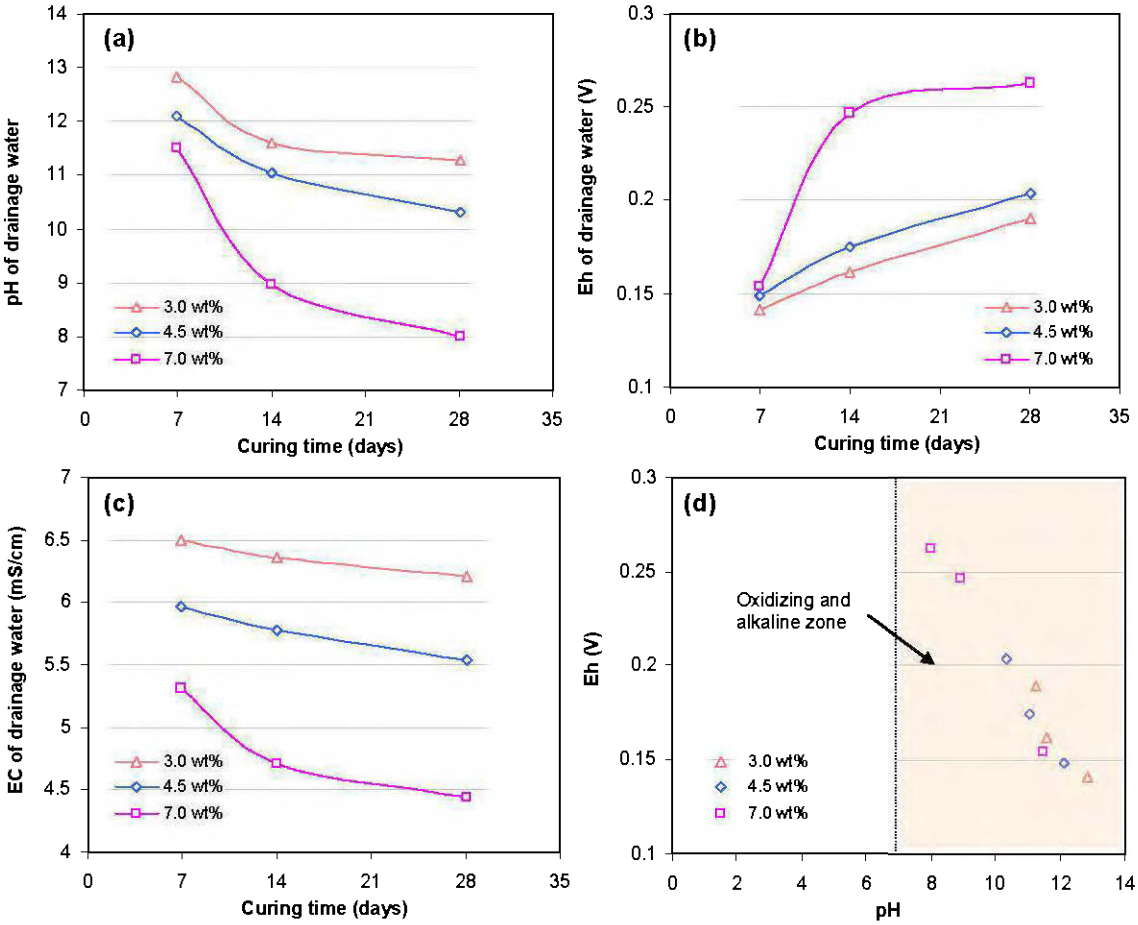

Figure C.8 Geochemical analysis of drainage water: a) pH, b) redox potential (Eh), electrical conductivity (EC), and d) pH versus Eh.

At the highest binder content (7 wt%), the S_r value is much lower compared to other binder contents (3 and 4.5 wt%) and the Eh value becomes higher, as can be seen in Figure C.8b. However, as curing time increases, the gap observed between 7 and 4.5 wt% binder contents increases from 0.17 to 0.25 after 14 days, from 0.2 to 0.26 after 28 days. The electrical conductivity EC value decreases from 6.5 to 6.2 mS/cm, from 5.9 to 5.5 mS/cm, and from 5.3 to 4.4 mS/cm when curing time is increased from 7 to 28 days (Figure C.8c). Also, Eh versus pH curve, as indicated in Figure C.8d, shows the drainage water exhibits an oxidizing and alkaline medium.

C.5 CONCLUSIONS

This paper presents comparative results of laboratory testing conducted in order to better understand the hydromechanical and geochemical properties of consolidated (using a new laboratory apparatus called CUAPS) and unconsolidated (by conventional plastic moulds) CPB samples. From the tests performed, one can say that the one-dimensional consolidation of CPB samples being cured under a series of pressure increments is essential to a better understanding of events linked to placement and curing conditions occurring in underground stopes during the backfilling process. Consolidated backfills always give higher mechanical strengths than those obtained from undrained samples for a given binder content and curing time. Geotechnical index parameters show that void ratio is dramatically reduced when CPB samples are prepared using CUAPS cells that allow drainage during a curing time of 7, 14 and 28 days. The reduction of void ratio leads to a stiffer, and consequently more resistant, CPB material. From chemical composition analysis, it can be said that the concentrations of sulphate SO_4^{2-} continuously decrease over time, depending on binder content used in the CPB mixture. Geochemical analyses have also shown that drainage water exhibits an alkaline to neutral oxidizing medium, based on relationship between pH and Eh. These results showed that CUAPS apparatus gives higher CPB strength than UCS values from laboratory–prepared CPB samples (often considered an underestimation of the true value). Thus, more realistic strength results can be obtained using this new apparatus. More work is underway to validate the values obtained by the CUAPS apparatus and in situ results.

C.6 ACKNOWLEDGEMENTS

This research was partly financed by the Canada Research Chair on "Integrated Management of Sulphide Mine Waste using Fill Technology" and the Industrial NSERC-Polytechnique-UQAT Chair on "Environment and Mine Wastes Management". The authors would like to express their appreciations to the Canadian Foundation for Innovation for the financial support provided for designing and manufacturing the CUAPS setups used in the present study. Special thanks go to URSTM chemists and technicians, principally Mélanie Bélanger and Mélinda Gervais for their technical support on chemical and geochemical analyses.

C.7 REFERENCES

Amaratunga, L.M., Yaschyshyn, D.N., 1997. Development of a high modulus paste fill using fine gold mill tailings. *Geotechnical and Geological Engineering,* Vol. 15, No. 3, pp. 205–219.

Archibald, J.F., Chew, J.L., Lausch, P., 1999. Use of ground waste glass and normal Portland cement mixtures for improving slurry and paste backfill support performance. *CIM Bulletin,* Vol. 92, No. 1030, pp. 74–80.

ASTM Designation D2435, 1999. Standard test method for one-dimensional consolidation properties of soils. In: *Annual Book of ASTM Standards,* Vol. 04.08, ASTM International, West Conshohocken, PA, pp. 207–216.

ASTM Designation D4186, 1999. Standard test method for one-dimensional consolidation properties of soils using controlled-strain loading. In: *Annual Book of ASTM Standards,* Vol. 04.08, ASTM International, West Conshohocken, PA, pp. 477–481.

ASTM Designation D806, 1999. Standard test method for cement content of soil-cement mixtures. In: *Annual Book of ASTM Standards,* Vol. 04.08, ASTM International, West Conshohocken, PA, pp. 85–87.

ASTM Designation C143, 1999. Standard test method for slump of hydraulic cement concrete. In: *Annual Book of ASTM Standards,* Vol. 04.08, ASTM International, West Conshohocken, PA, pp. 68–76.

ASTM Designation C39, 1999. Standard test method for compressive strength of cylindrical concrete specimens. In: *Annual Book of ASTM Standards,* Vol. 04.08, ASTM International, West Conshohocken, PA, pp. 15–23.

Belem, T., El Aatar, O., Bussière, B., Benzaazoua, M., Fall, M., Yilmaz, E., 2006. Characterization of Self weight consolidated paste backfill. In: *Proceedings of the 9th International Seminar on Paste and Thickened Tailings*, Limerick, Ireland, ACG, April 3–7, pp. 333–345.

Belem, T., Benzaazoua, M., 2008a. Design and application of underground mine paste backfill technology. *Geotechnical and Geological Engineering,* Vol. 26, No. 2, pp. 147–174.

Belem, T., Benzaazoua, M., 2008b. Predictive models for prefeasibility cemented paste backfill mix design. In: *International Symposium on Post-Mining 2008,* Nancy, France, February 6–8, pp. 1–13.

Belem, T., Benzaazoua, M., Bussière, B., 2000. Mechanical behaviour of cemented paste backfill. In: *Proceedings of the 53rd Canadian Geotechnical Conference and the 1st Joint IAH-CNC Conference,* Montréal, Canadian Geotechnical Society, September 18–20, pp. 373–380.

Belem, T., Benzaazoua, M., Bussière, B., Dagenais, A.M., 2002. Effects of settlement and drainage on strength development within mine paste backfill. In: *Proceedings of the 9th International Conference on Tailings and Mine Waste,* Vail, Colorado, USA, Balkema: Rotterdam, January 27–30, pp. 139–148.

Belem, T., El Aatar, O., Benzaazoua, M., Bussière, B., Yilmaz, E., 2007. Hydro-geotechnical and geochemical characterization of column consolidated cemented paste backfill. In: *Proceedings of the 9th International Symposium in Mining with Backfill*, Montreal, Quebec, April 29 – May 2, pp. 1–10 (Paper 2523).

Benzaazoua, M., Ouellet, J., Servant, S., Newman, P., Verburg, R., 1999. Cementitious backfill with sulfur content: physical, chemical and mineralogical characterization. *Cement and Concrete Research,* Vol. 29, No. 5, pp. 719–725.

Benzaazoua, M., Belem, T., Bussière, B., 2002. Chemical factors that influence the performance of mine sulphidic paste backfill. *Cement and Concrete Research,* Vol. 32, No. 7, pp. 1133–1144.

Benzaazoua, M., Belem, T, Yilmaz, E., 2006. Novel lab tool for paste backfill. *Canadian Mining Journal,* Vol. 127, No. 3, pp. 31–31.

Benzaazoua, M., Fall, M., Belem, T., 2004. A contribution to understanding the hardening process of cemented pastefill. *Minerals Engineering,* Vol. 17, No. 2, pp. 141–152.

Bussière, B., 2007. Colloquium 2004: Hydrogeotechnical properties of hard rock tailings from metal mines and emerging geoenvironmental disposal approaches. *Canadian Geotechnical Journal,* Vol. 44, No. 9, pp. 1019–1052.

Cayouette, J., 2003. Optimization of the paste backfill plant at Louvicourt mine. *CIM Bulletin,* Vol. 96, No. 1075, pp. 51–57.

Fourie, A., Helinski, M., Fahey, M., 2006. Filling the gap – a geomechanics perspective. *Australian Centre for Geomechanics Newsletter,* Vol. 26, No. 5, pp. 1–4.

Godbout, J., 2005. Évolution des propriétés hydriques des remblais miniers cimentés en pate durant le curage. *M.Sc. Thesis,* Université de Montréal, Québec, pp. 1–190.

Grabinsky, M., Simms, P., 2006. Self-desiccation of cemented paste backfill and implications for mine design. In: *Proceedings of the 9th International Seminar on Paste and Thickened Tailings*, Limerick, Ireland, ACG, April 3–7, pp. 323–332.

Hassani, F., Archibald, J., 1998. *Mine Backfill.* Canadian Institute of Mining, Metallurgy and Petroleum, Montreal, Quebec, Canada, pp. 1–263.

Hassani, F.P., Bois, D., 1992. Economic and technical feasibility for backfill design in Quebec underground mines. Final report 1/2, *Canada-Quebec Mineral Development Agreement, Research and Development in Quebec Mines.* Contract No. EADM 1989 – 1992, File No. 71226002.

Helinski, M., Fahey, F., Fourie, A.B., 2007. Numerical modelling of cemented paste backfill deposition. *ASCE Journal of Geotechnical and Geoenvironmental Engineering,* Vol. 13, No. 10, pp. 1308–1319.

Kesimal, A., Yilmaz, E., Ercikdi, B., 2004. Evaluation of paste backfill test results obtained from different size slumps with varying cement contents for sulphure rich tailings. *Cement and Concrete Research,* Vol. 34, No. 5, pp. 1817–1822.

Kesimal, A., Yilmaz, E., Ercikdi, B., Alp, I., Deveci, H., 2005. Effect of properties of tailings and binder on short-and long-term strength and stability of cemented paste backfill. *Materials Letters,* Vol. 59, No. 28, pp. 3703–3709.

Klein, K., Simon, D., 2006. Effect of specimen composition on the strength development in cemented paste backfill. *Canadian Geotechnical Journal,* Vol. 43, No. 3, pp. 310–324.

Landriault, D., 2001. *Backfill in underground mining: Underground mining methods engineering fundamentals and international case studies.* Littleton, Colorado, Society for Mining, Metallurgy and Exploration, Chapter 69, pp. 601–614.

le Roux, K.A., Bawden, W.F., Grabinsky, M.W.F., 2005. Field properties of cemented paste backfill at the Golden Giant mine. *Mining Technology: IMM Transactions section A,* Vol. 114, No. 2, pp. 65–80.

Mohamed, A., Hossein, M., Hassani, F., 2001. Hydromechanical evaluation of stabilized mine tailings. *Environmental Geology,* Vol. 41, No. 7, pp. 749–759.

Ouellet, S. 2007. Mineralogical characterization, microstructural evolution and environmental behaviour of cemented paste backfills. *Ph.D. Dissertation,* University of Quebec at Abitibi-Témiscamingue, Rouyn-Noranda, Quebec, Canada pp. 1–310.

Revell, M.B., 2004. Paste – How strong is it? In: *The 8th International Symposium on Mining with Backfill*, Beijing, China, September 19–21, pp. 286–294.

Servant, S., 2001. Détermination des paramètres mécaniques des remblais miniers faits de résidus ciments. *M.Sc. Thesis,* McGill University, Montreal, Quebec, pp. 1–53.

Stone, D.M., 1993. The optimization of mix designs for cemented rockfill. In: *Proceedings of 5th International Symposium on Mining with Backfill,* Johannesburg, South Africa, October 15–20, pp. 249–253.

Yilmaz, E., 2003. Experimental investigaton of the compressive strength behaviour of the cemented paste backfill samples prepared from sulphidic mine tailings. *M.Sc. Thesis,* Black Sea Technical University (KTU), Trabzon, Turkey, pp. 1–117.

Yilmaz, E. Kesimal, A., Ercikdi, B., 2003. Strength properties in varying cement dosages for paste backfills. In: *Proceedings of the 10th International Conference on Tailings and Mine Waste,* October 12–15, Vail, Fort Collins, Colorado, pp. 109–114.

Yilmaz, E., Benzaazoua, M., Belem, T., Bussière, B., 2008a. Influence of applied pressure on hydro-mechanical properties of cemented paste fill. *Geotechnical and Geological Engineering,* (submitted in January 2008).

Yilmaz, E., Belem, T., Bussière, B., Benzaazoua, M., 2008b. Consolidation characteristics of early age cemented paste fill. In: *Proceedings of the 61st Canadian Geotechnical Conference,* Edmonton, Alberta, Canada, September 21–24, pp. 797–804.

Yilmaz, E., El Aatar, O., Belem, T., Benzaazoua, M., Bussière, B., 2006. Effect of consolidation on the performance of cemented paste backfill. In: *The 21st Annual Underground Mine Support Conference*, Val d'Or, Quebec, April 11–12, pp. 1–14.

APPENDIX D

SUMMARY OF THE ONE-DIMENSIONAL CONSOLIDATION RESULTS

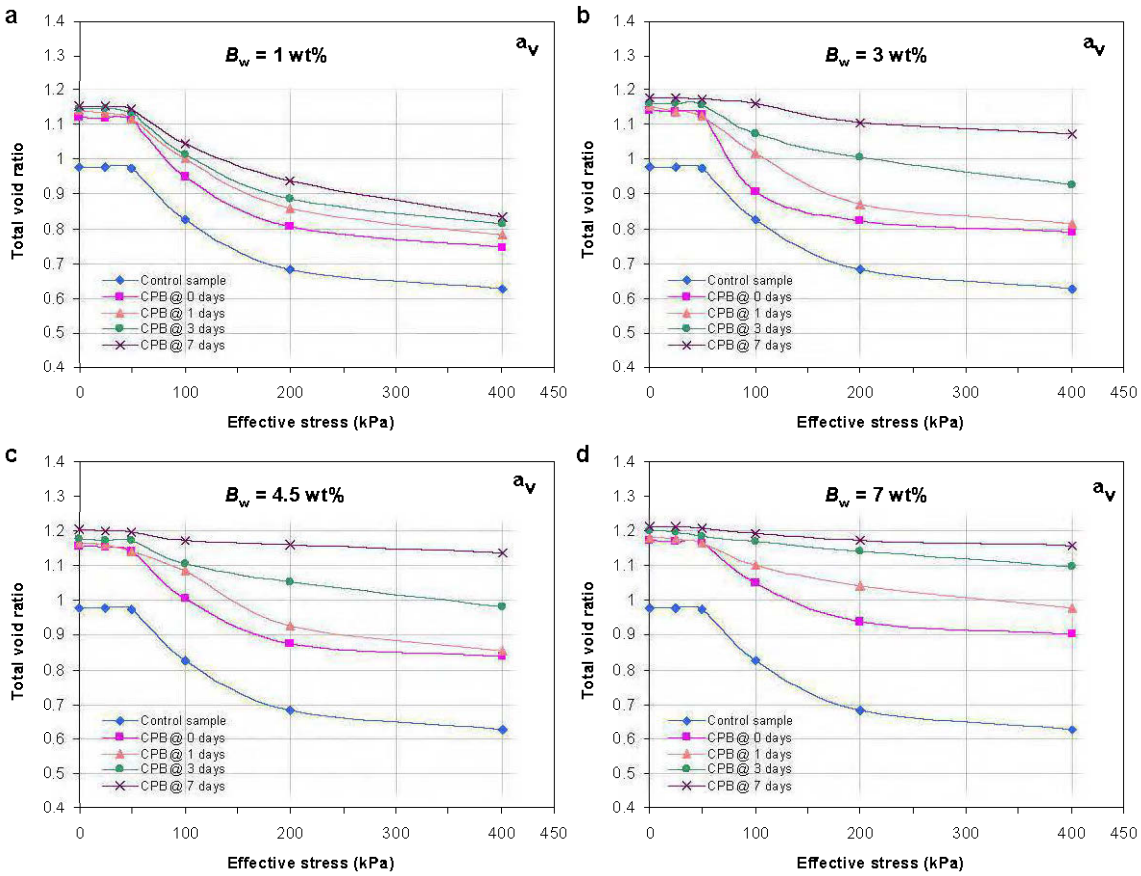

D.1 Variation in total void ratio with effective stress for the coefficient of compressibility a_v of CPB samples having binder contents of (a) 1 wt%, (b) 3 wt%, (c) 4.5 wt% and (d) 7 wt%. CPB samples are compared to control samples (tailings without binder).

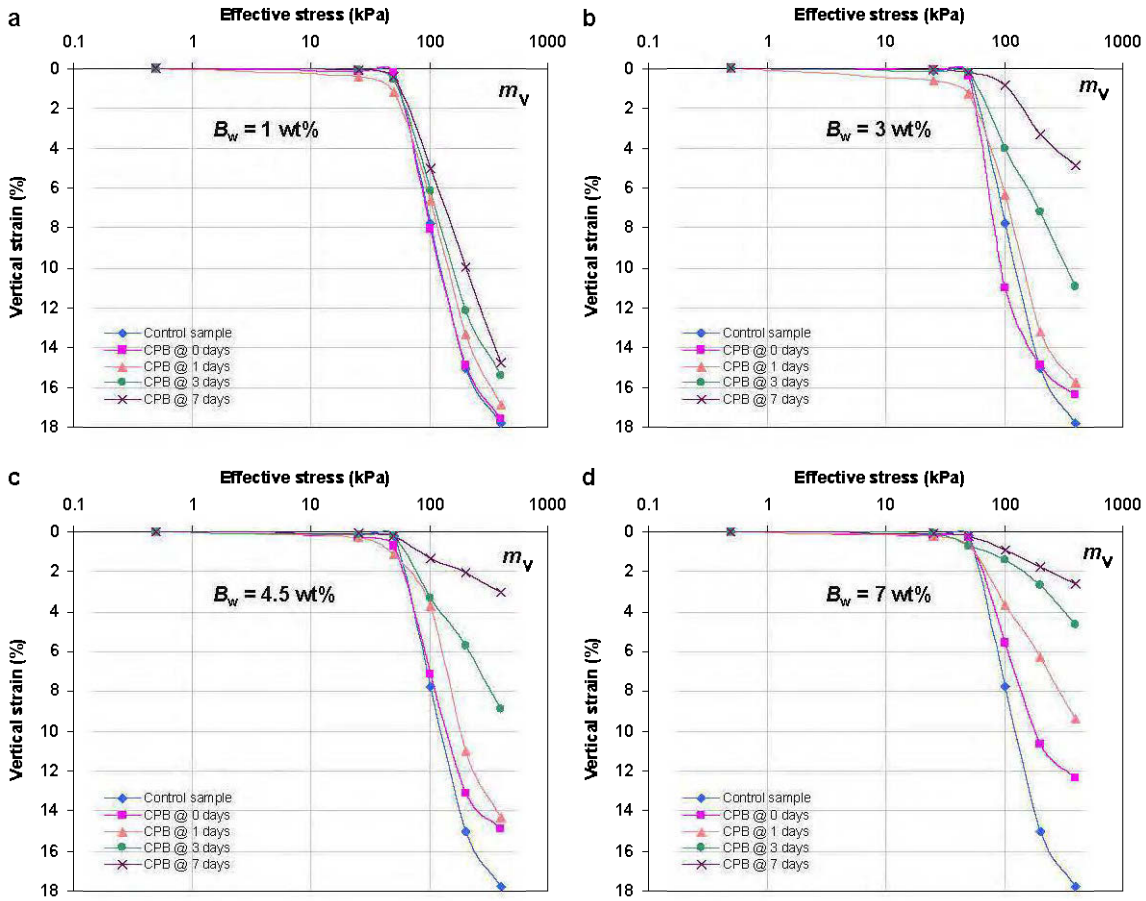

D.2 Variation in vertical strain with effective stress for the coefficient of volumetric compressibility m_v of CPB samples having binder contents of (a) 1 wt%, (b) 3 wt%, (c) 4.5 wt% and (d) 7 wt%. CPB samples are compared to control samples (tailings without binder).

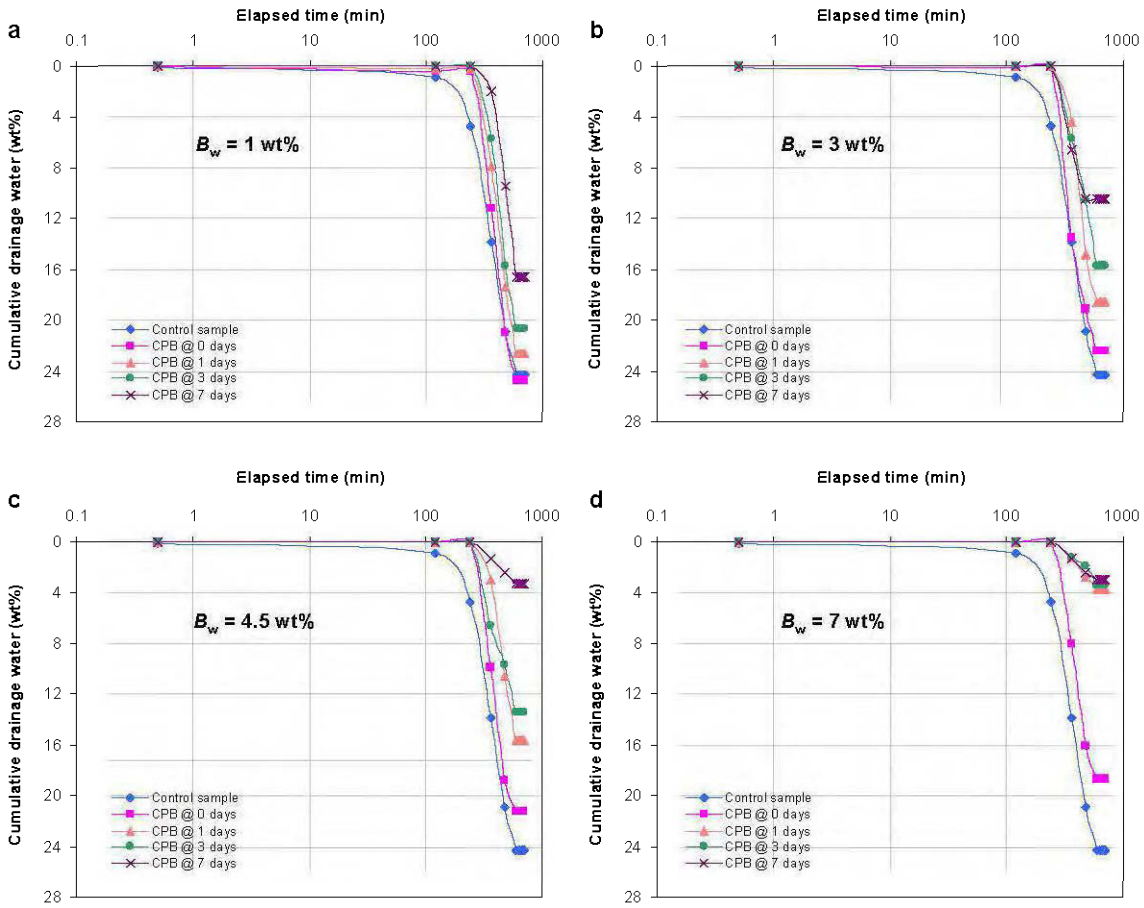

D.3 Variation in cumulative drainage water with elapsed time for CPB samples having binder contents of (a) 1 wt%, (b) 3 wt%, (c) 4.5 wt%, and (d) 7 wt%. CPB samples are compared to control samples (tailings without binder).

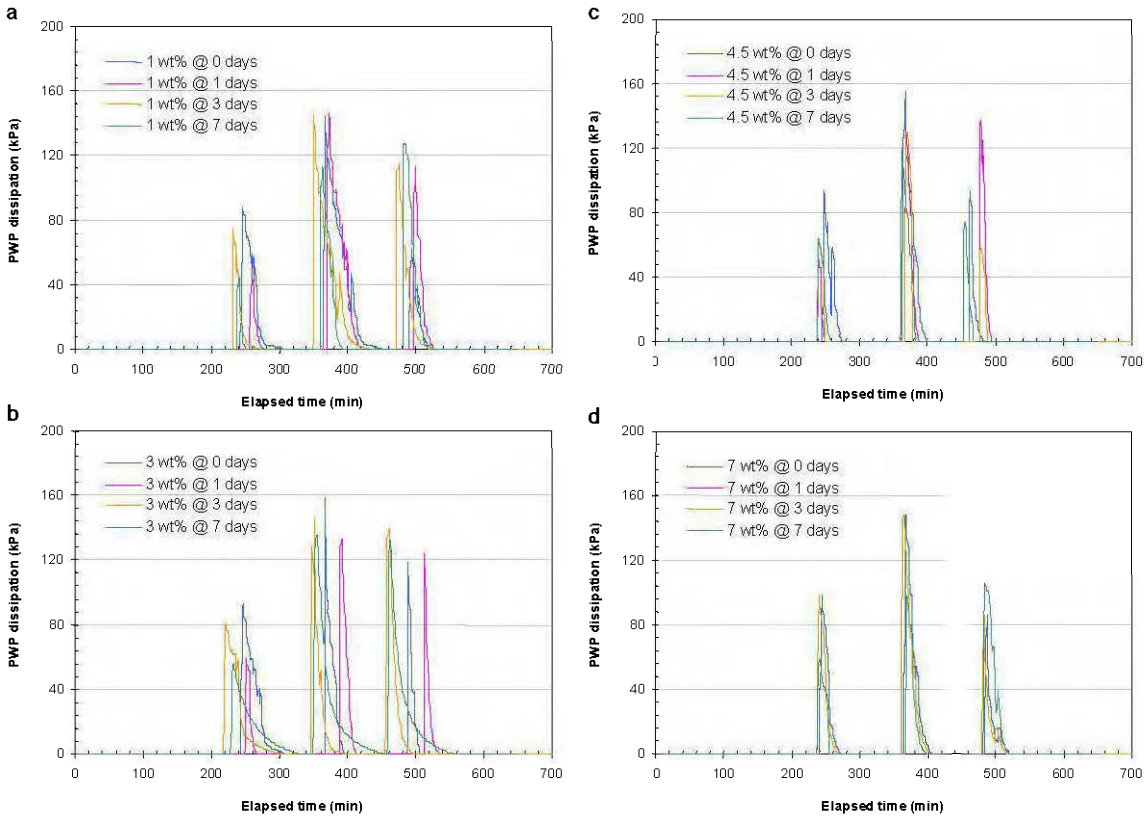

D.4 Change in pore water pressure dissipation with elapsed time for CPB samples having binder contents of (a) 1 wt%, (b) 3 wt%, (c) 4.5 wt%, and (d) 7 wt%.

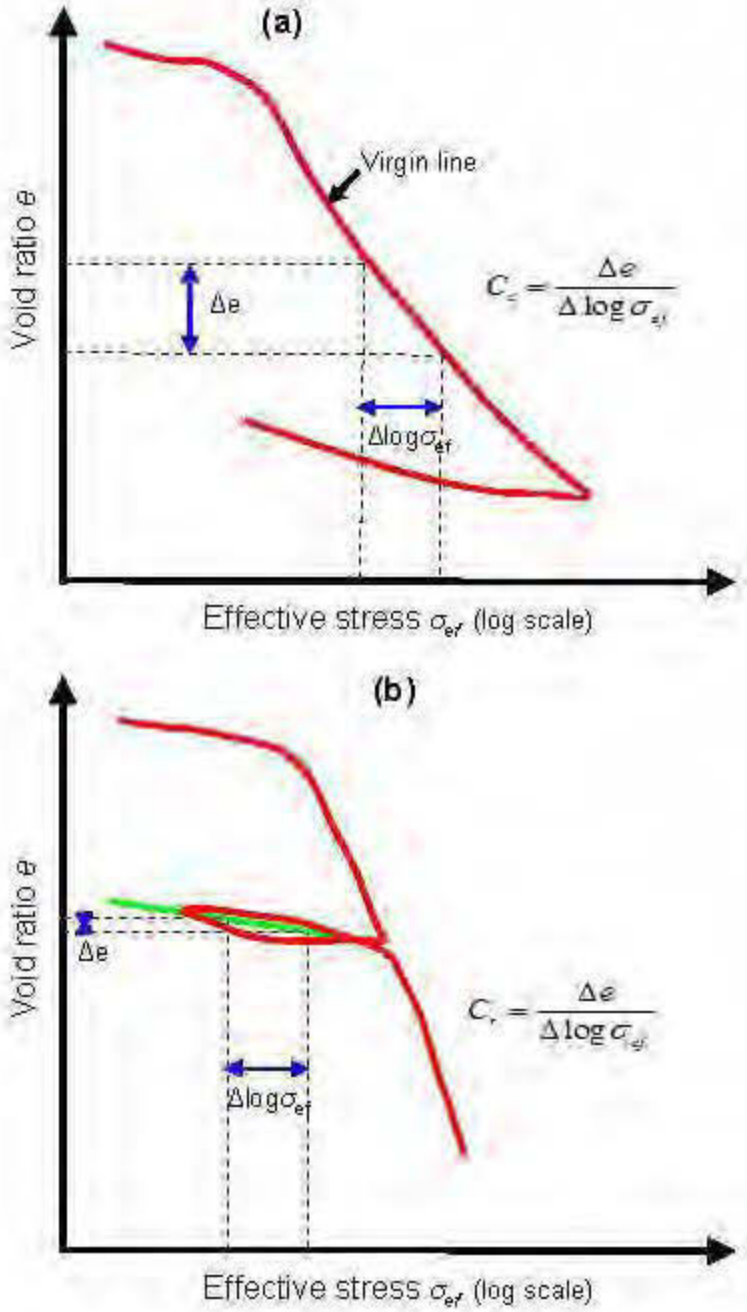

D.5 Description of compression parameters: (a) compression index C_C; (b) re-compression index C_{Cr}.

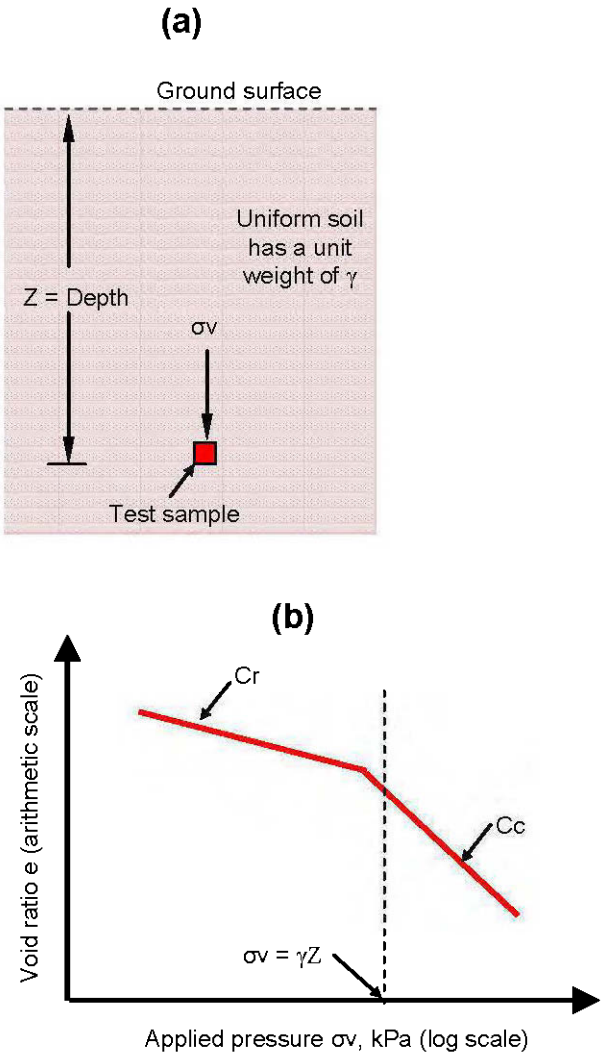

D.6 Description of conditions applying to compression test samples: (a) location of soil sample obtained for compression test; (b) compression test result.

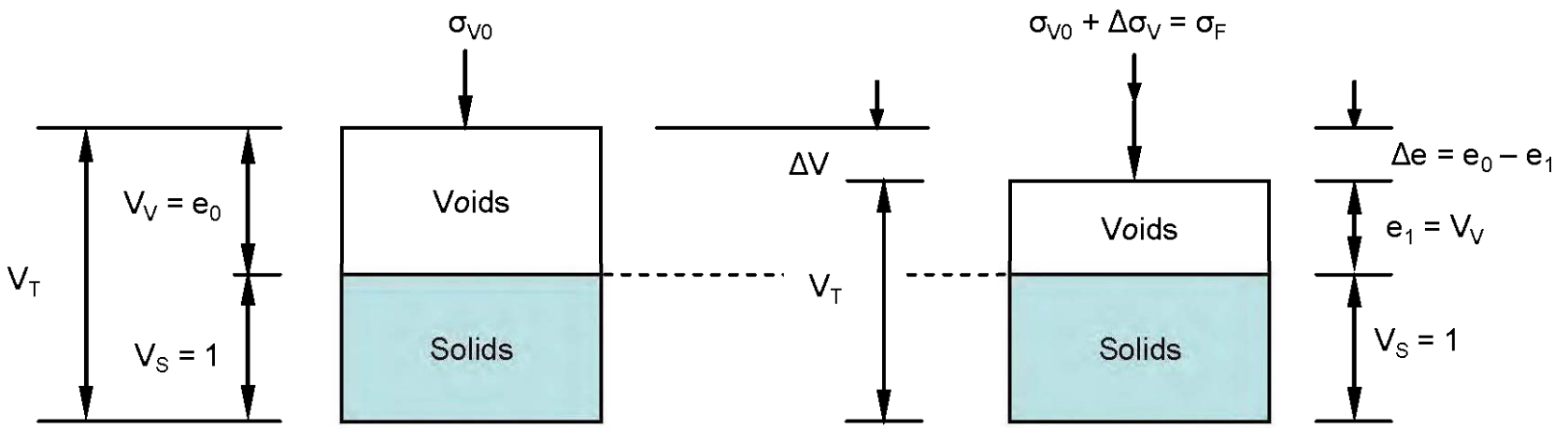

D.7 Phase diagram illustrating the change in soil volume with loading increase.

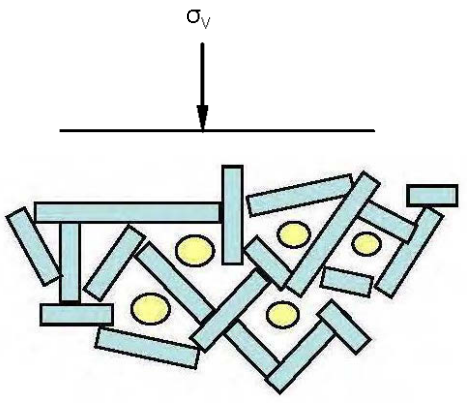

Fine-grained soil deposit; soil deposit is 100% saturated. Before construction, a compressive stress due to the soil overburden exists (is imposed onto the soil particles); $\sigma_{v0} = \gamma z$. Water pressure in soil void spaces is normal hydrostatic pressure.

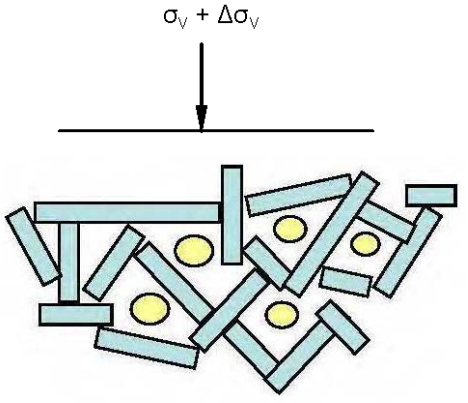

Construction loading causes a stress increase in the soil deposit. Due to effect of the new stress $\Delta\sigma_v$, particles attempt to shift into a more compact or tighter arrangement (so as to develop more compressive resistance as necessary for stability). However, water occupies the void spaces and prevents the soil particles from moving into those void spaces. The compressive stress increase, $\Delta\sigma_v$, therefore is imposed onto the water trapped in the void spaces, and not onto the soil particles. The result is that the void water is under an "excess" pressure (pressure greater than normal hydrostatic pressure expected from the position of the groundwater table).

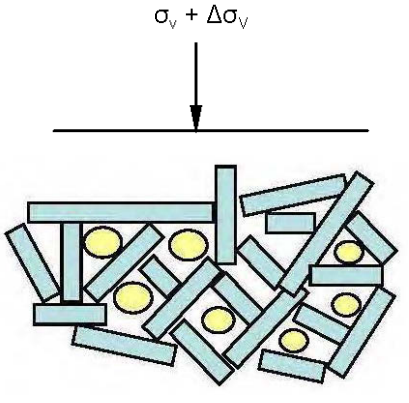

Because void water is subject to excess pressure created by $\Delta\sigma v$, the water gradually flows to locations of lesser water pressure (toward location of "normal" water pressure). The rate of flow depends on soil permeability. As void water pressure is dissipated, the soil particles gradually shift and the $\Delta\sigma v$ stress is slowly transferred from the void water over to the soil particles (that is, onto the "soil skeleton" for the soil deposit). The process of stress being slowly transferred onto the soil skeleton as void water is being expelled or squeezed from the stressed region of the soil deposit, and related gradual compression of the soil deposit is "consolidation".

D.8 Sequence of foundation loading transferred onto soil particles (soil skeleton) due to consolidation (McCarth, 2007).

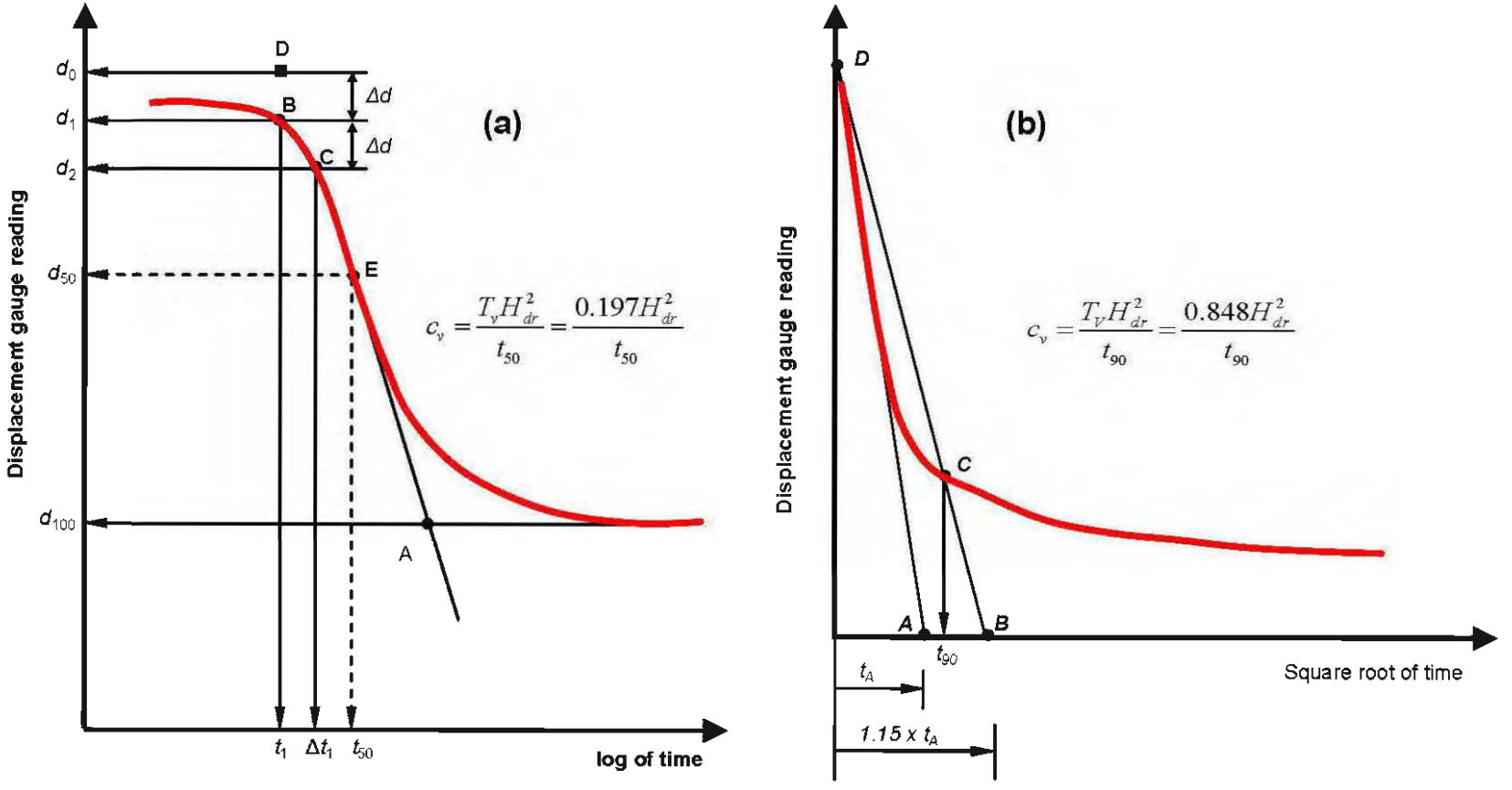

D.9 Schematic illustration of (a) logarithm of time fitting method (Casagrande's) and (b) square root of time fitting method (Taylor's).

APPENDIX E

SUMMARY OF GEOCHEMICAL RESULTS

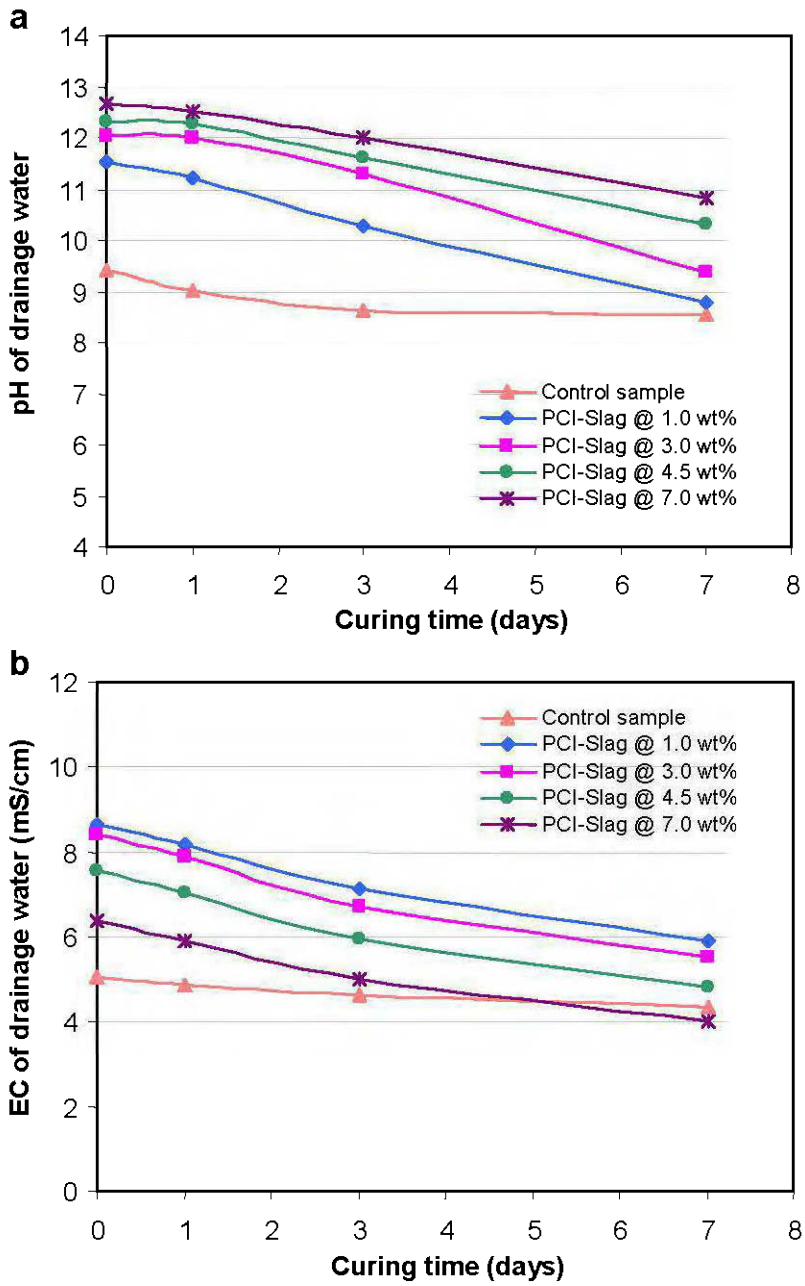

E.1 Change in (a) pH and (b) electrical conductivity (EC) of drainage water collected from consolidated CPB samples containing slag-based binder (PCI-Slag@20:80 wt%) with curing time as a function of binder content.

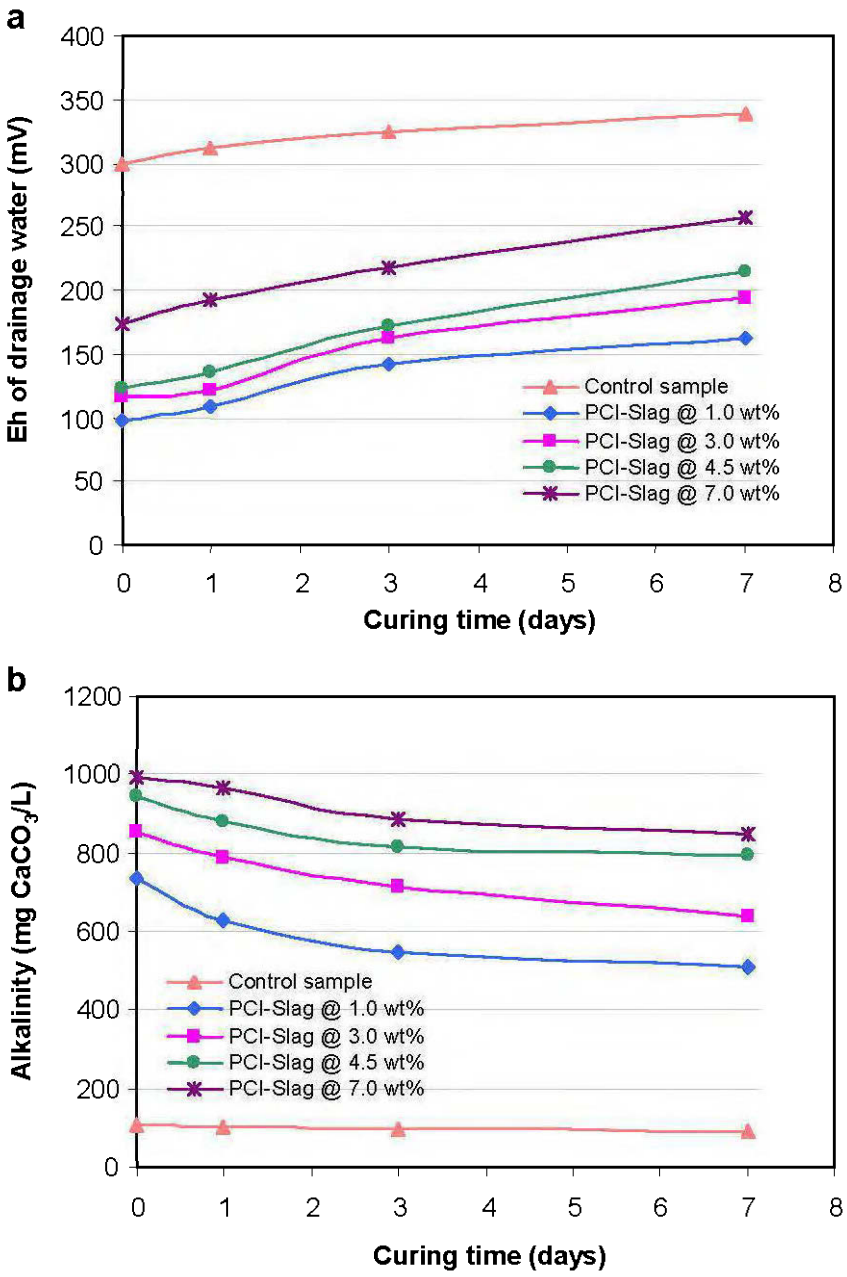

E.2 Change in (a) redox potential (Eh) and (b) alkalinity of drainage water collected from consolidated CPB samples containing slag-based binder (PCI-Slag@20:80 wt%) with curing time as a function of binder content.

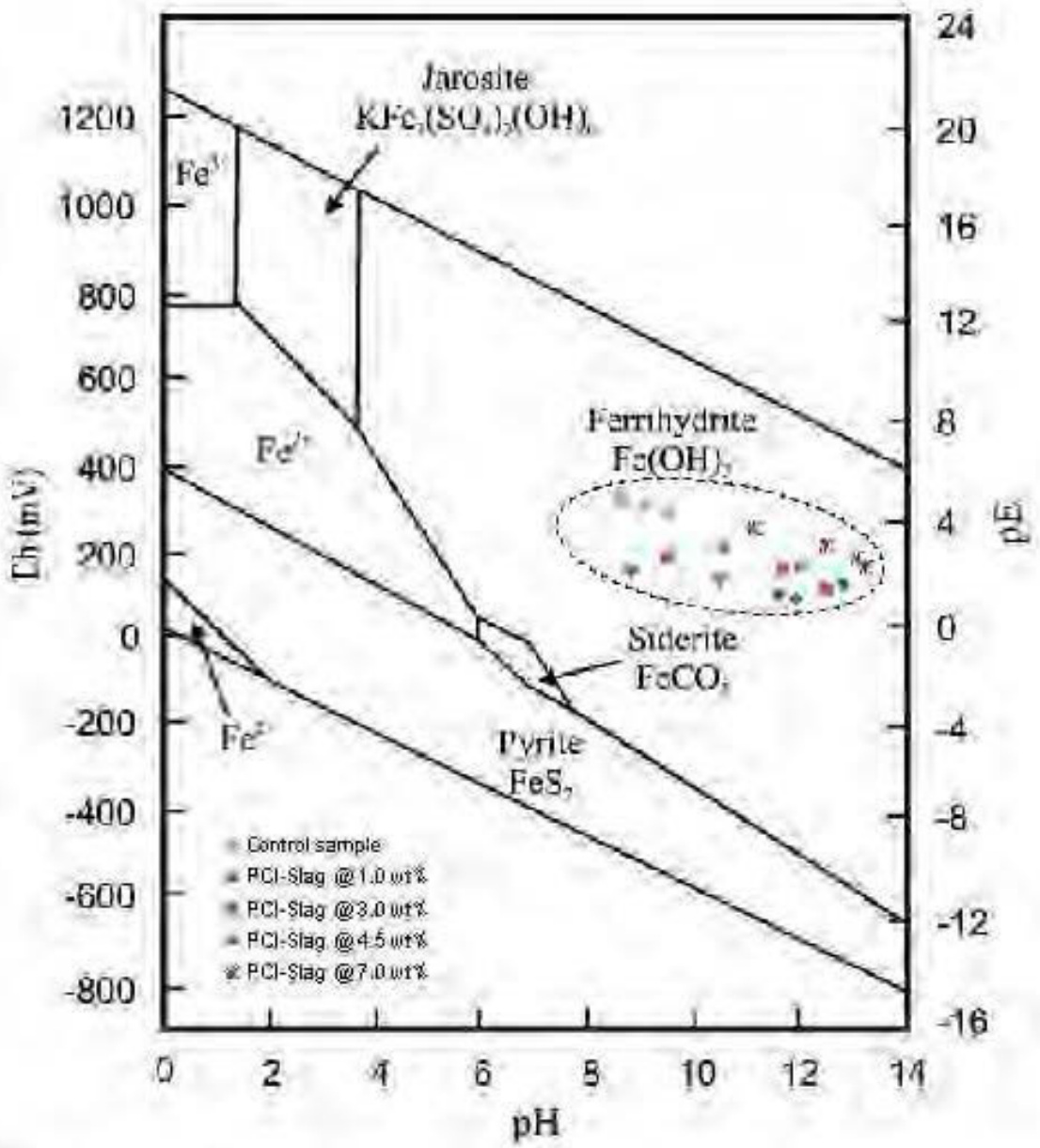

E.3 Illustration of the pE-pH diagram for the iron-carbon dioxide-water system for CPB samples containing slag-based binder (PCI-Slag@20:80 wt%).

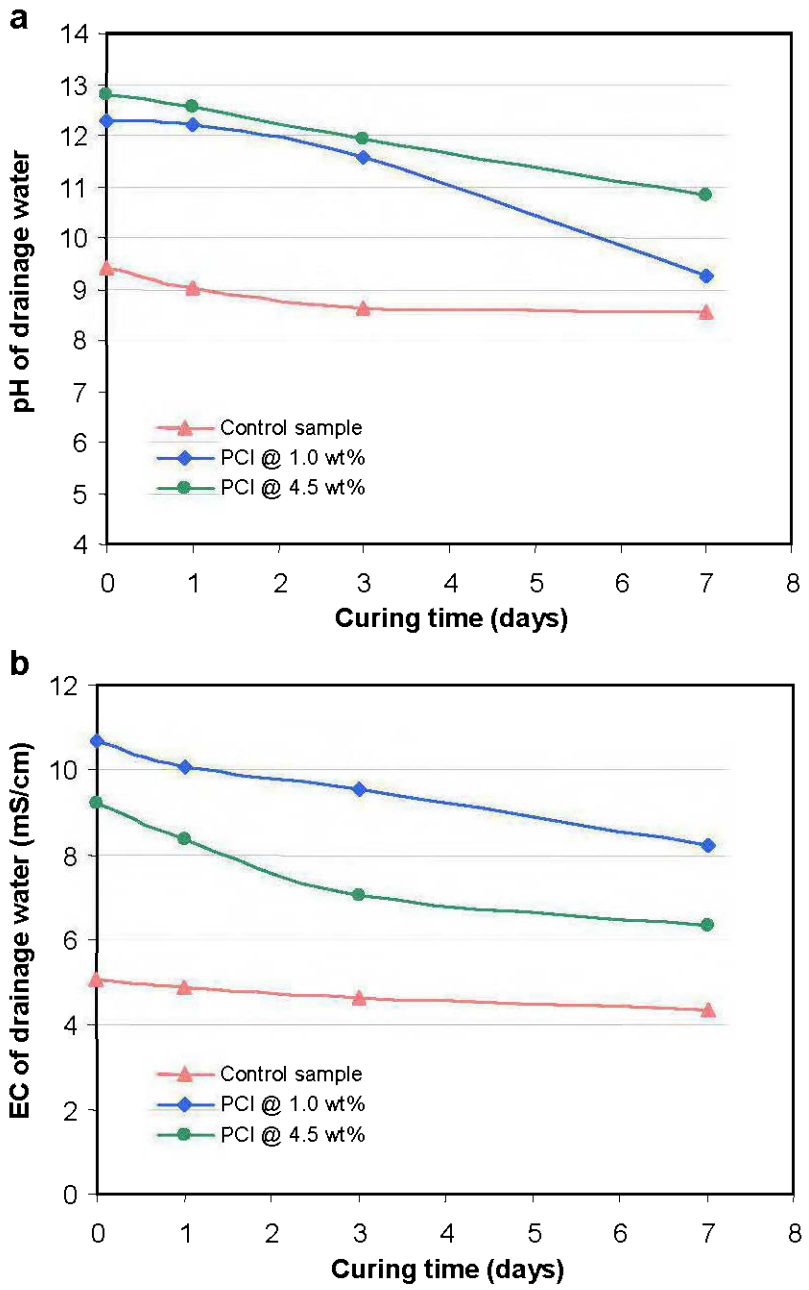

E.4 Change in (a) pH and (b) electrical conductivity (EC) of drainage water collected from consolidated CPB samples containing general use Portland cement (PCI@100 wt%) with curing time as a function of binder content.

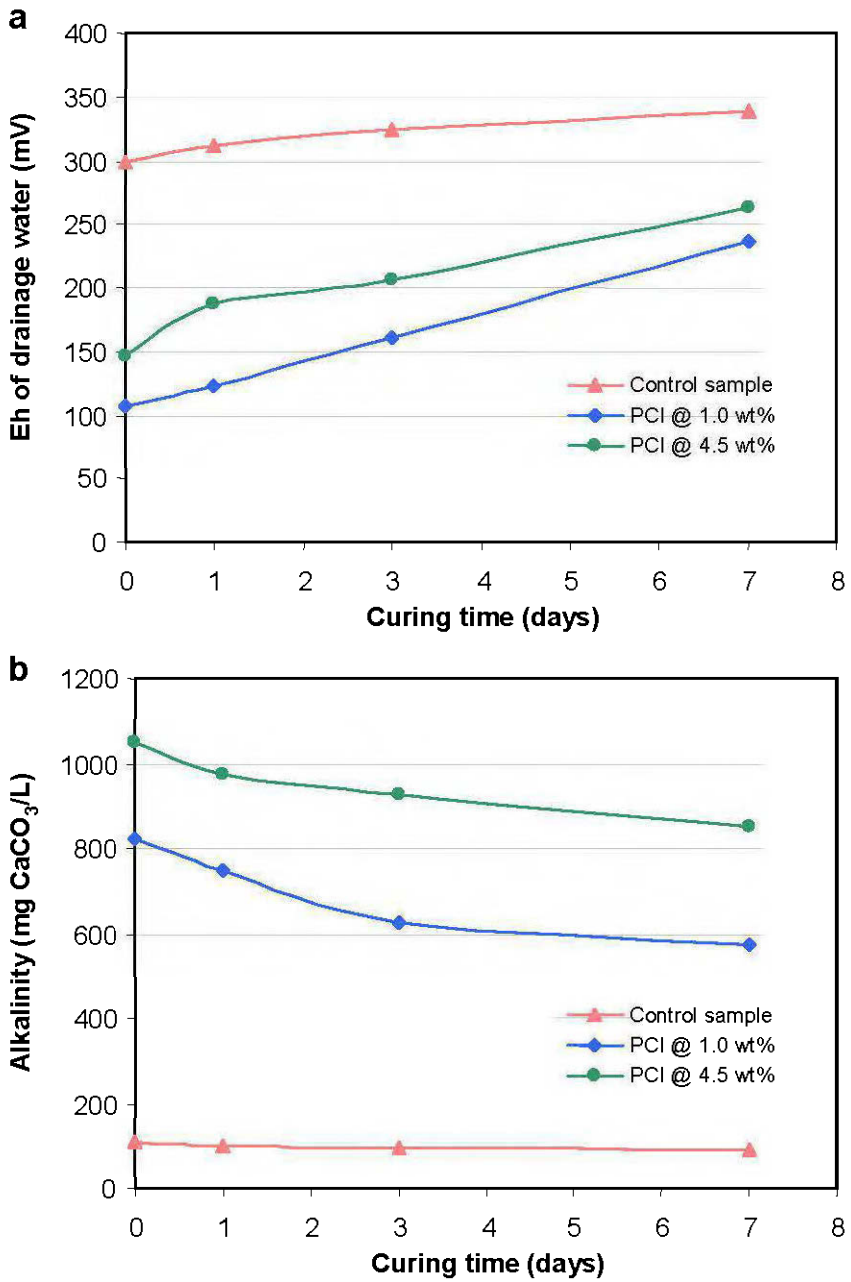

E.5 Change in (a) redox potential (Eh) and (b) alkalinity of drainage water collected from consolidated CPB samples containing general use Portland cement (PCI@100 wt%) with curing time as a function of binder content.

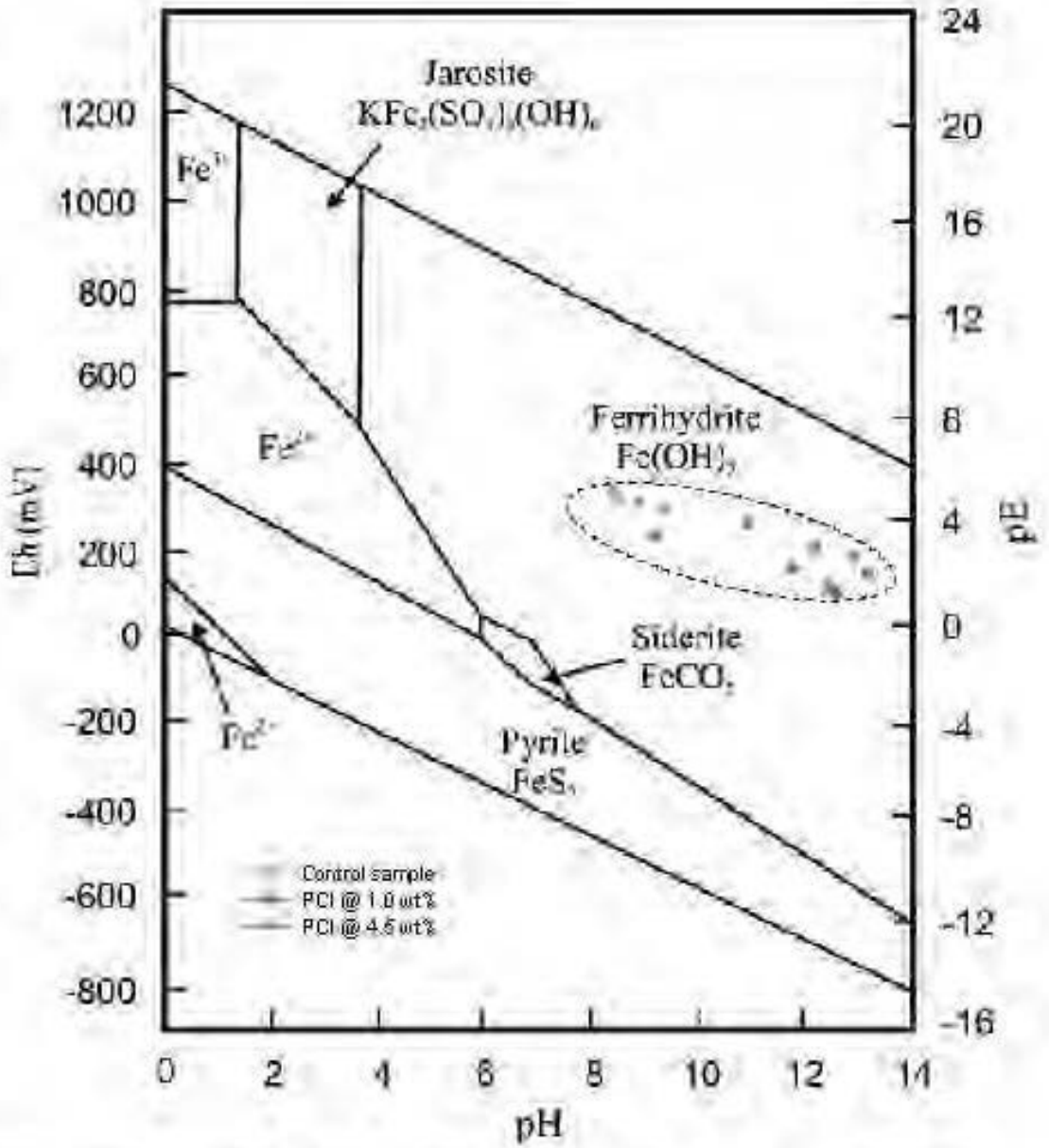

E.6 Illustration of the pE-pH diagram for the iron-carbon dioxide-water system for CPB samples containing general use Portland cement (PCI@100 wt%)

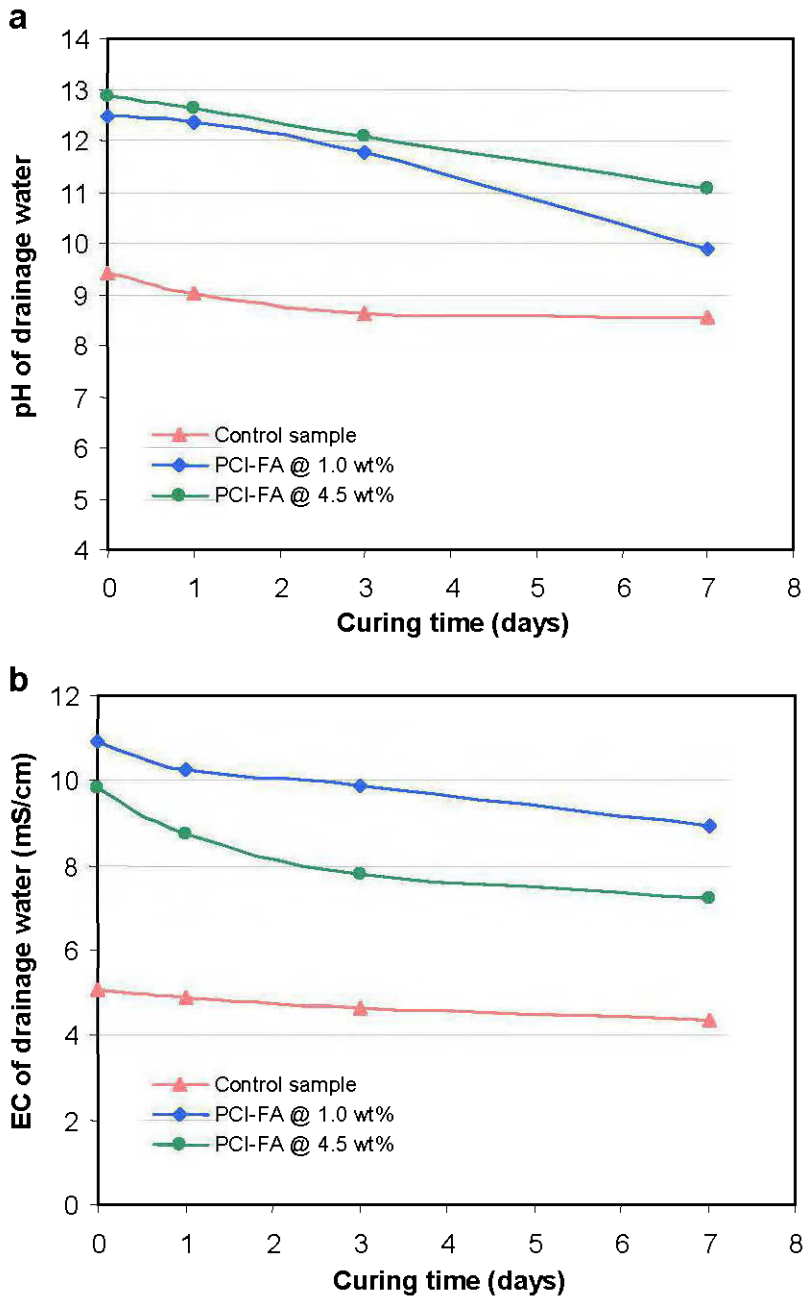

E.7 Change in (a) pH and (b) electrical conductivity (EC) of drainage water collected from consolidated CPB samples containing fly ash-based binder (PCI-FA@60:40 wt%) with curing time as a function of binder content.

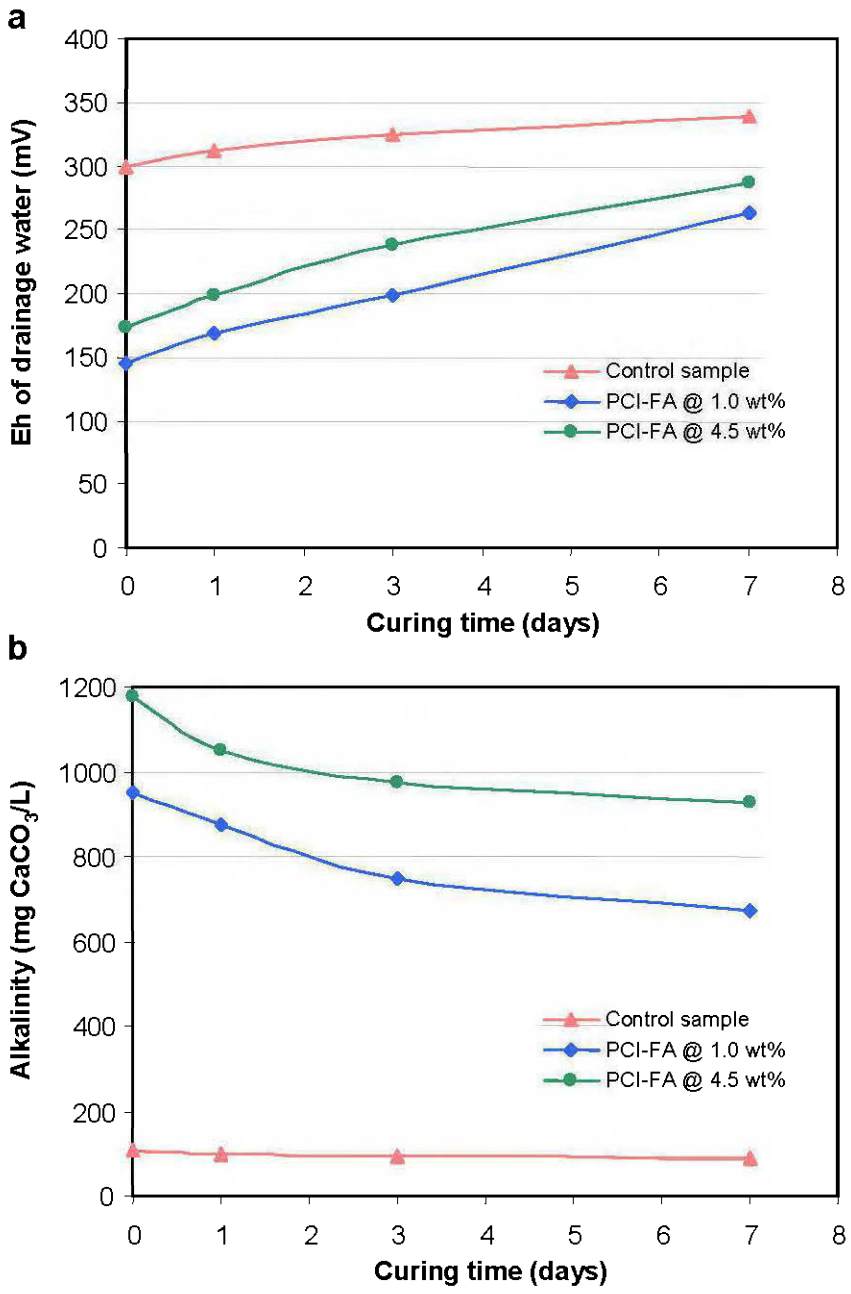

E.8 Change in (a) redox potential (Eh) and (b) alkalinity of drainage water collected from consolidated CPB samples containing fly ash-based binder (PCI-FA@60:40 wt%) with curing time as a function of binder content.

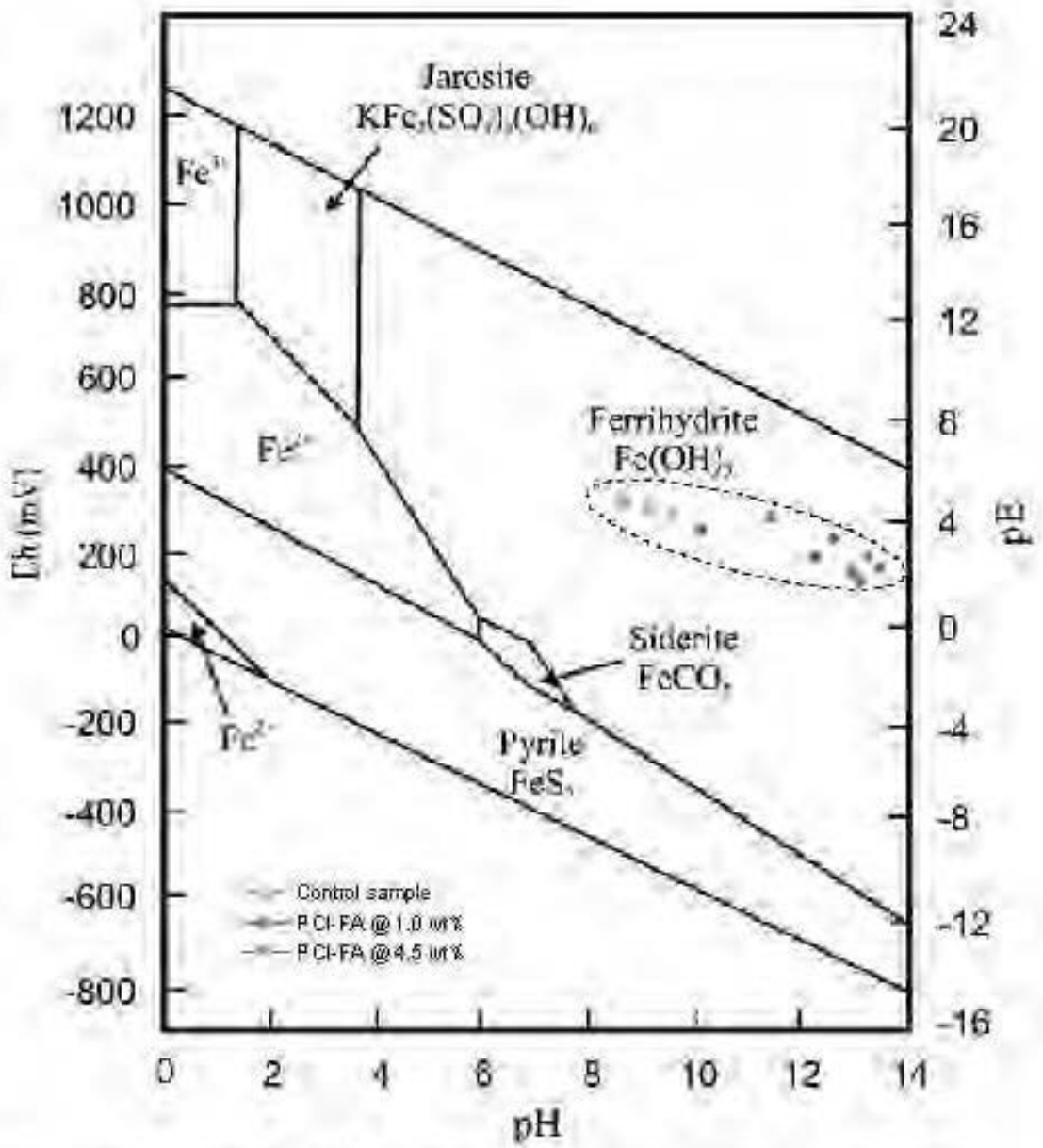

E.9 Illustration of the pE-pH diagram for the iron-carbon dioxide-water system for CPB samples containing fly ash-based binder (PCI-FA@60:40 wt%)

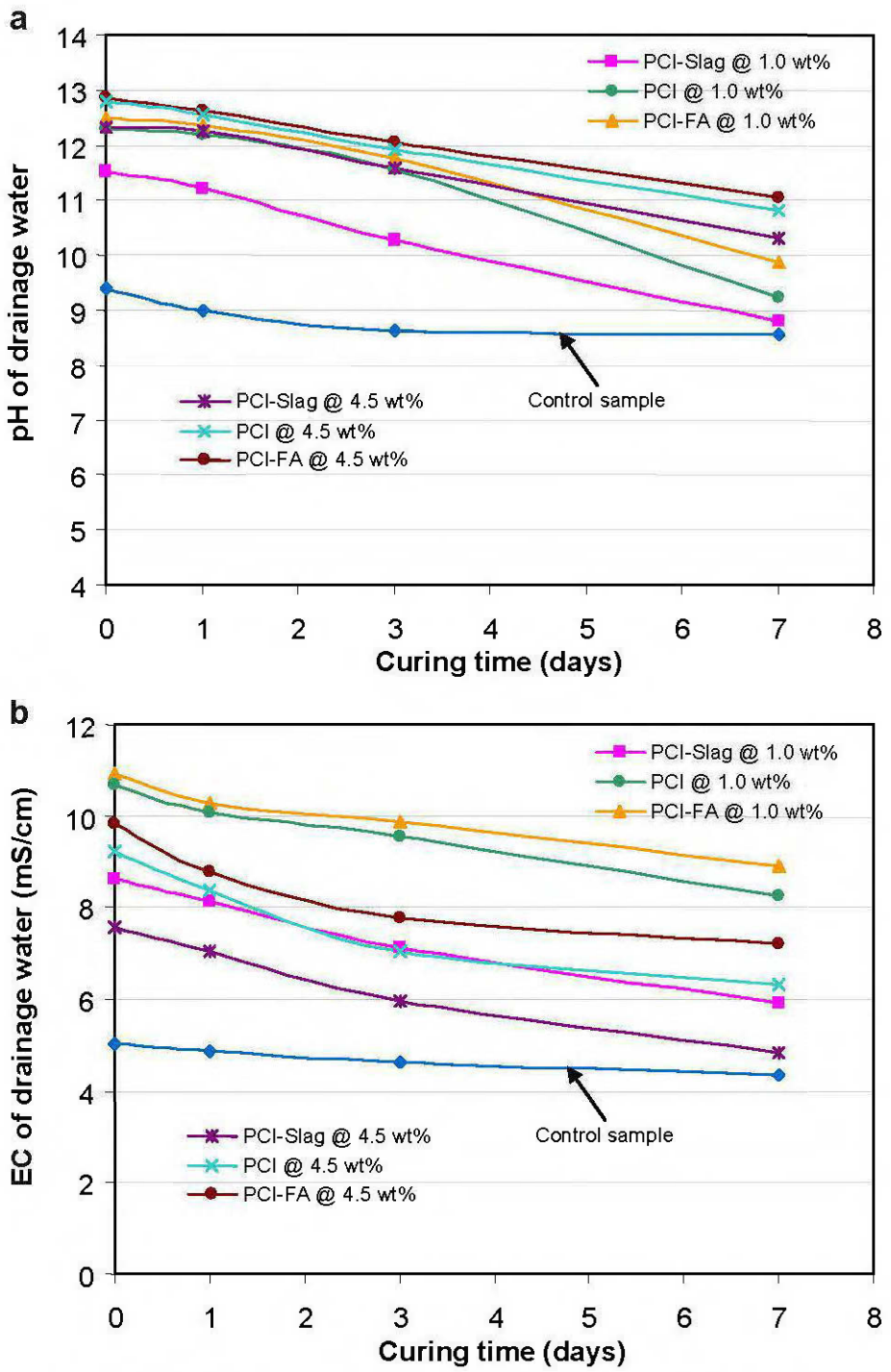

E.10 Comparison of (a) pH and (b) electrical conductivity (EC) of drainage water collected from consolidated CPB samples containing a binder content of 1 and 4.5 wt% with curing time as a function of binder content.

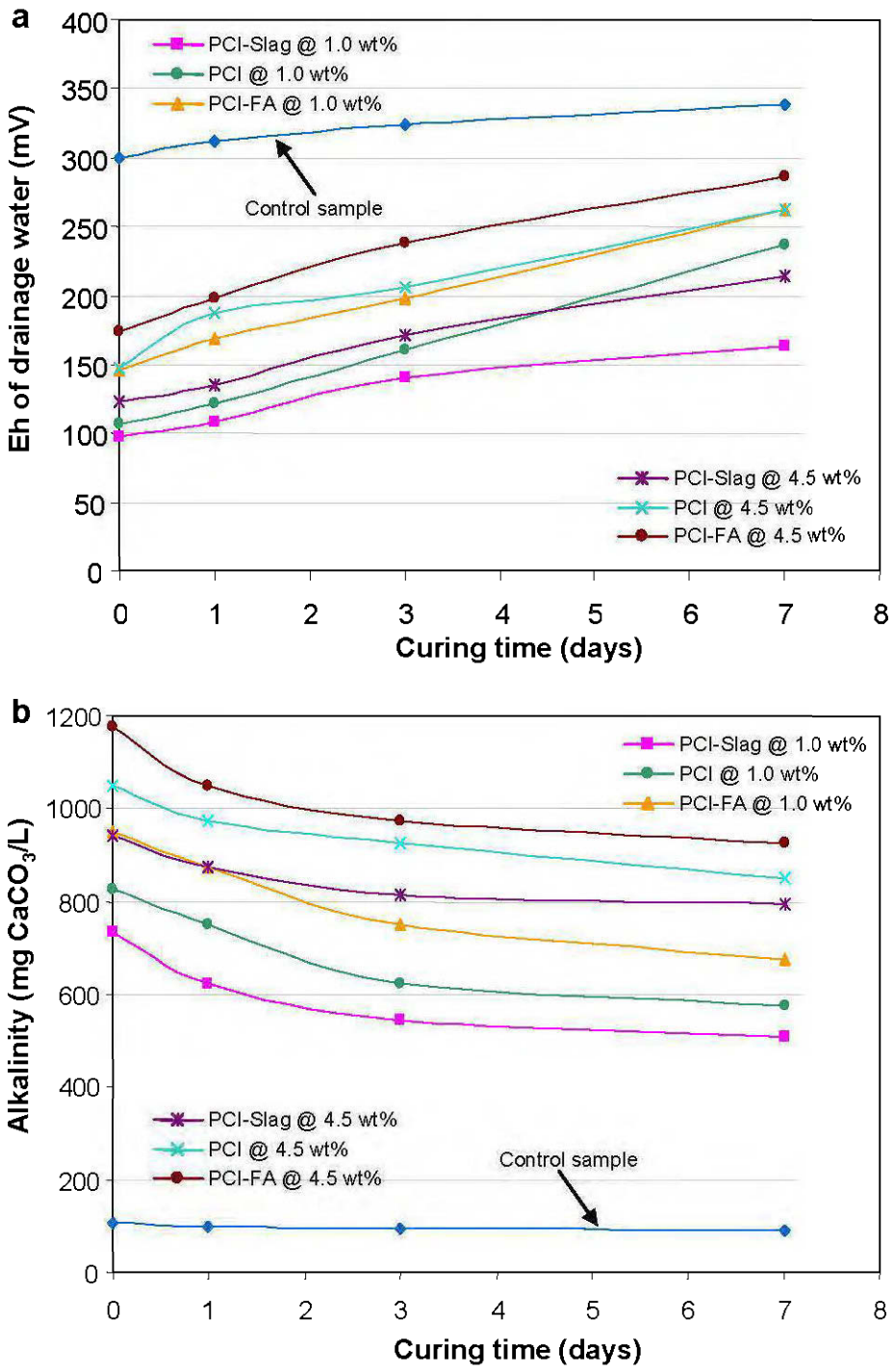

E.11 Comparison of (a) redox potential (Eh) and (b) alkalinity of drainage water collected from consolidated CPB samples containing a binder content of 1 and 4.5 wt% with curing time as a function of binder content.

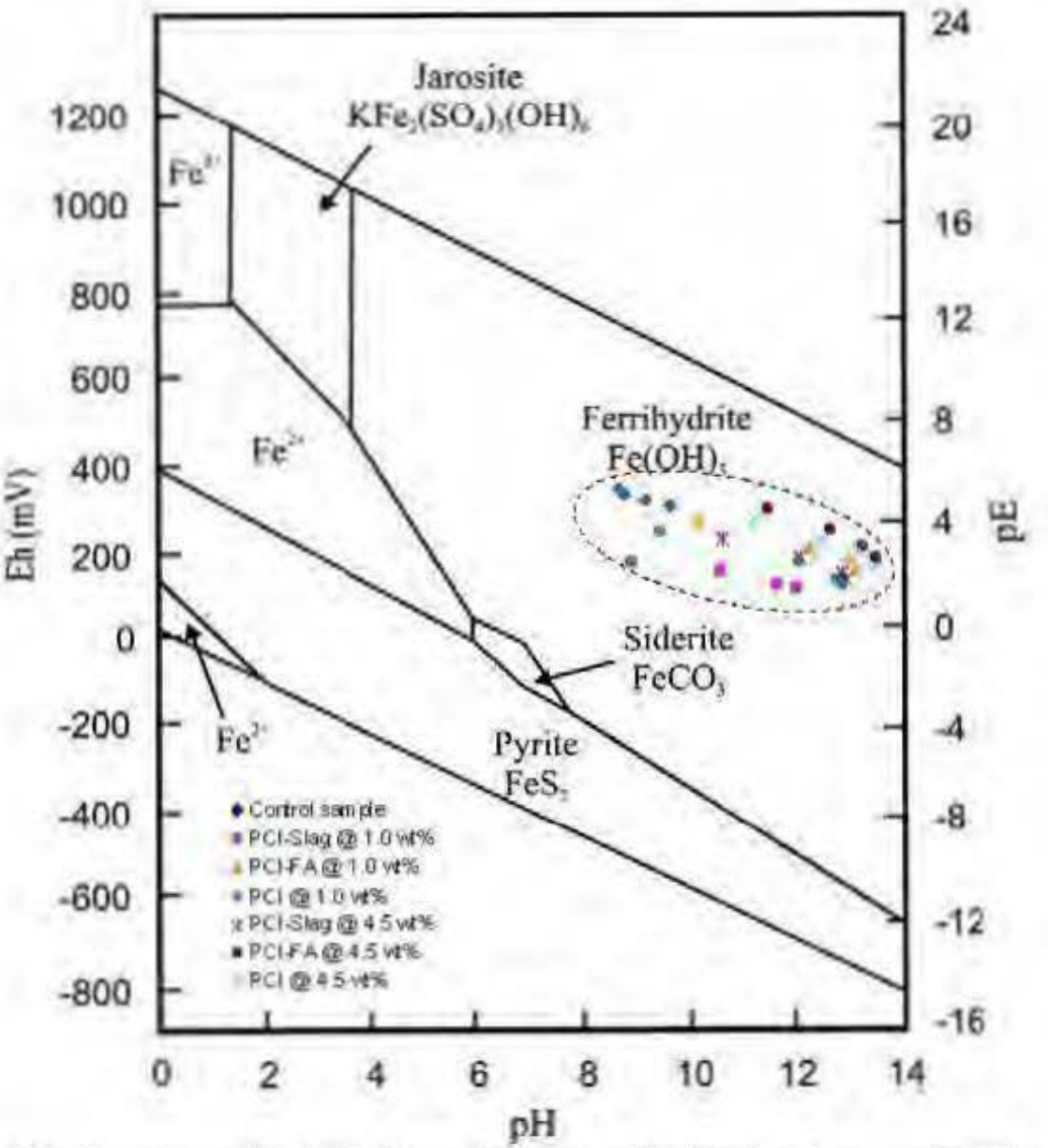

E.12 Comparison of the pE-pH diagram for the iron-carbon dioxide-water system for CPB samples containing a binder content of 1 and 4.5 wt%.

APPENDIX F

SUMMARY OF ICP-AES (INDUCTIVELY COUPLED PLASMA ATOMIC EMISSION SPECTROSCOPY) RESULTS

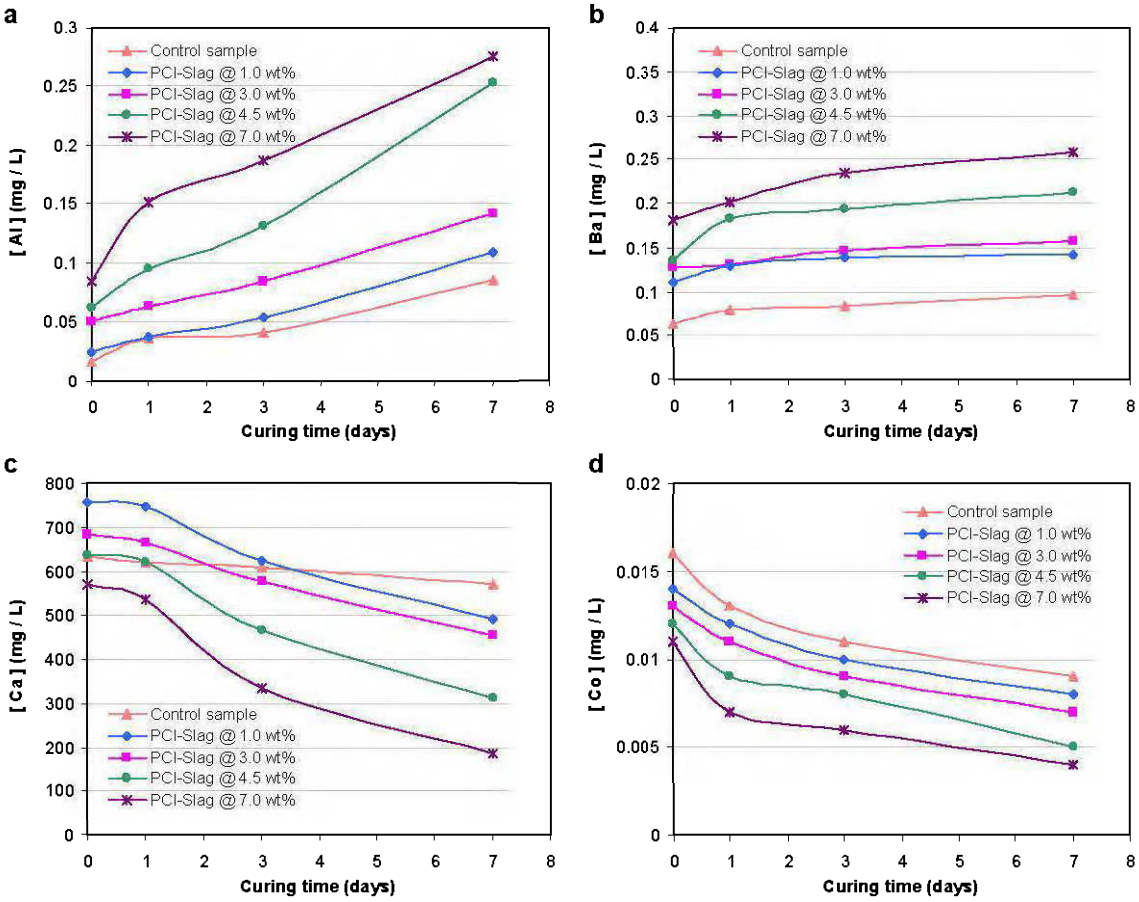

F.1 Change in (a) aluminium Al, (b) barium Ba, (c) calcium Ca, and (d) cobalt Co content in drainage water collected from consolidated CPB samples containing slag-based binder (PCI-Slag@20:80 wt%) with curing time as a function of binder content.

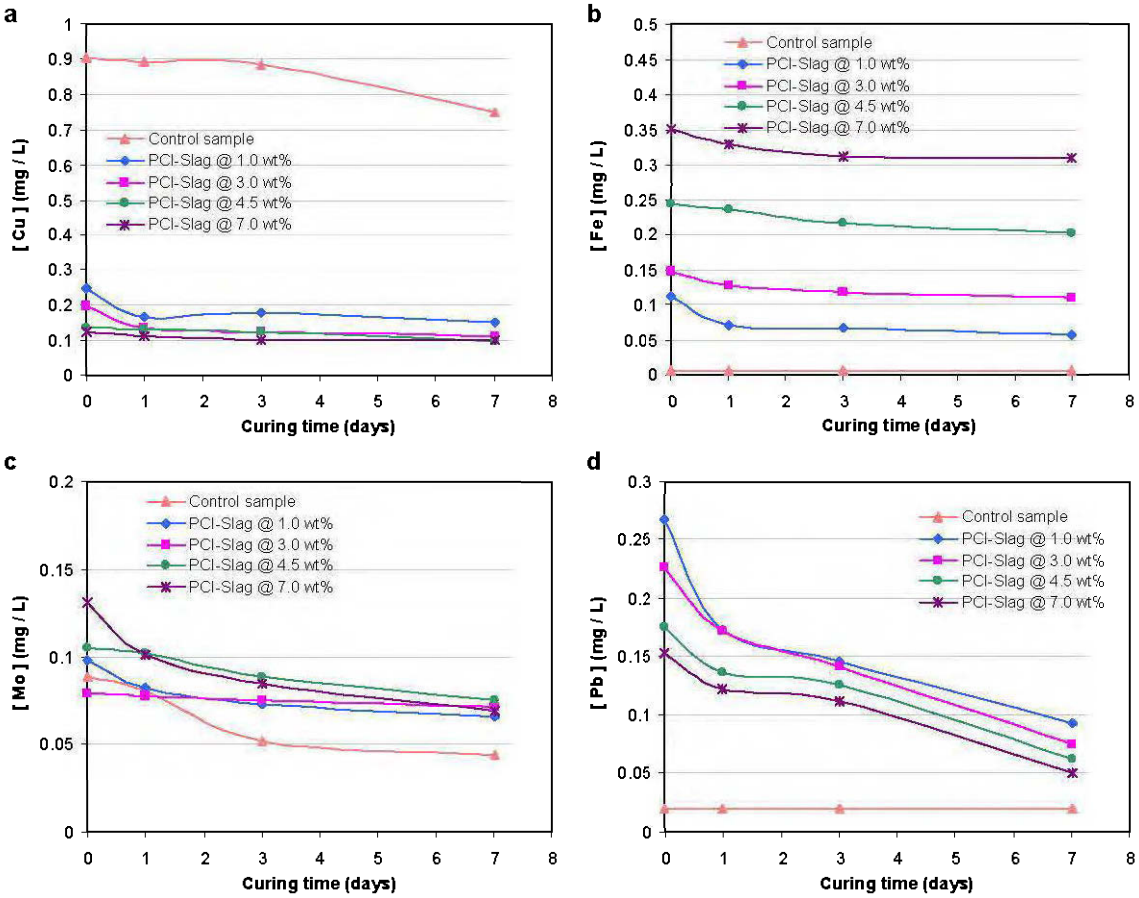

F.2 Change in (a) copper Cu, (b) iron Fe, (c) molybdenum Mo, and (d) lead Pb content in drainage water collected from consolidated CPB samples containing slag-based binder (PCI-Slag@20:80 wt%) with curing time as a function of binder content.

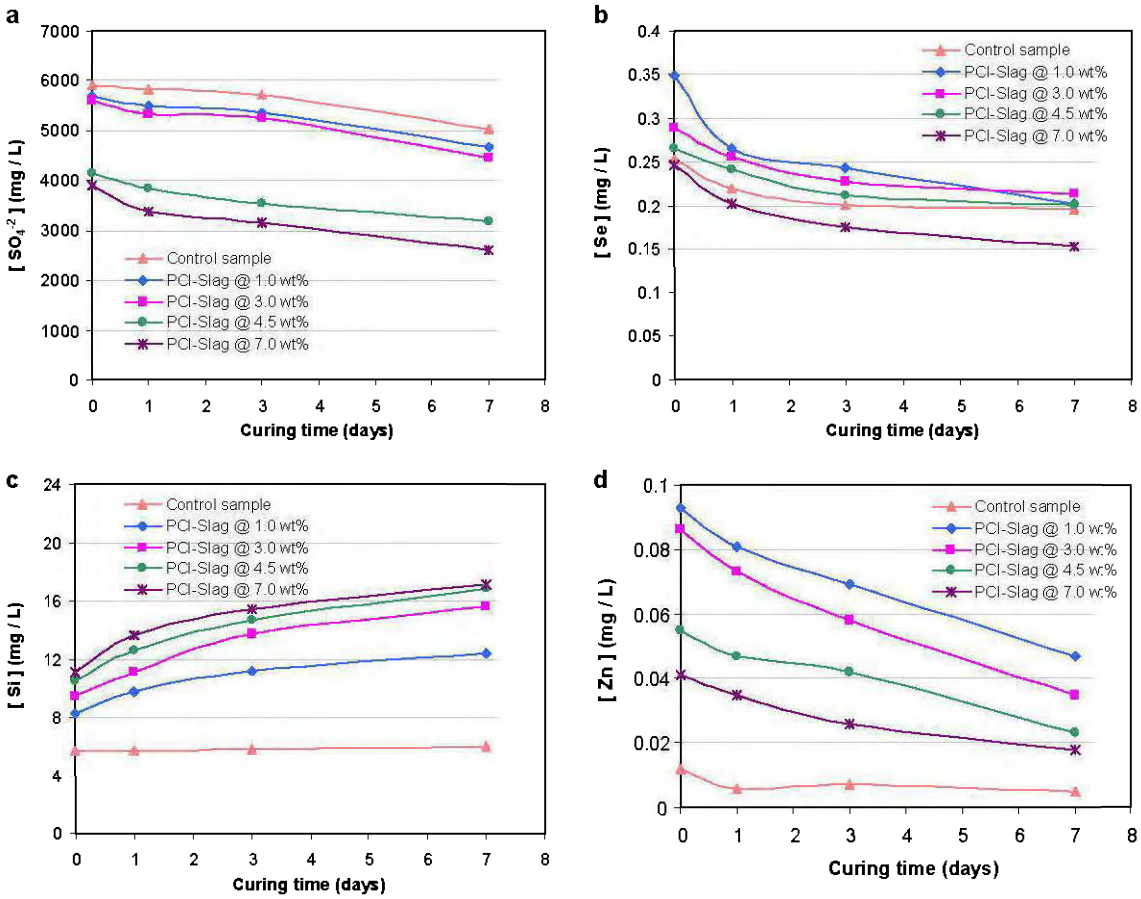

F.3 Change in (a) sulphate SO_4^{-2}, (b) selenium Se, (c) silicon Si, and (d) zinc Zn content in drainage water collected from consolidated CPB samples containing slag-based binder (PCI-Slag@20:80 wt%) with curing time as a function of binder content.

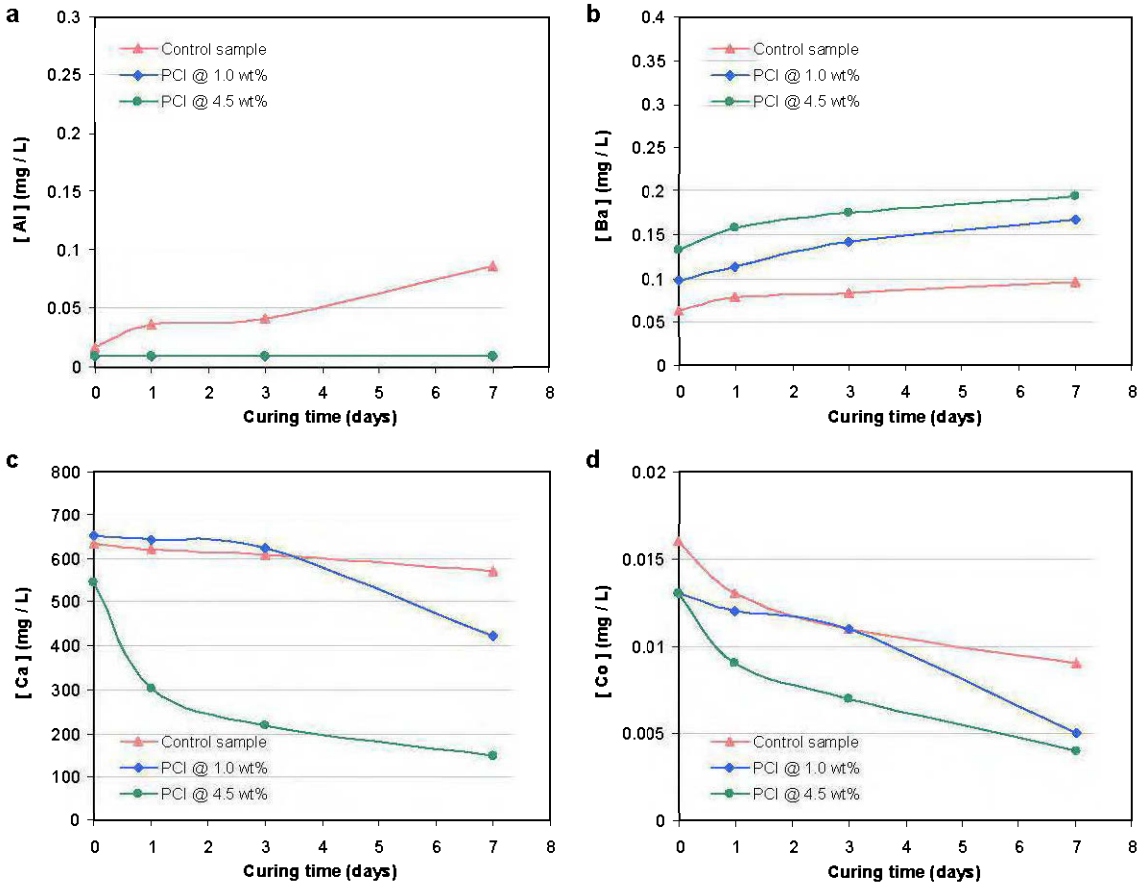

F.4 Change in (a) aluminium Al, (b) barium Ba, (c) calcium Ca, and (d) cobalt Co content in drainage water collected from consolidated CPB samples containing general use Portland cement (PCI@100 wt%) with curing time as a function of binder content.

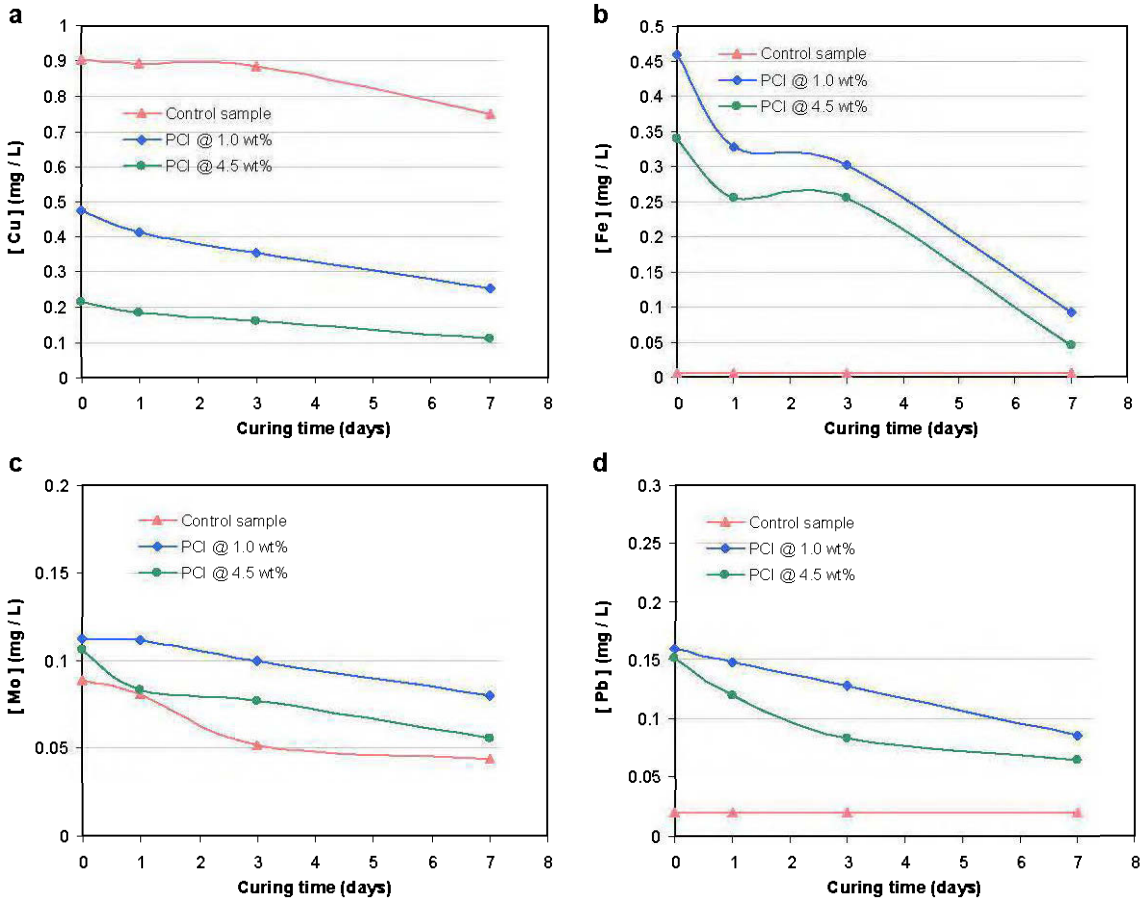

F.5 Change in (a) copper Cu, (b) iron Fe, (c) molybdenum Mo, and (d) lead Pb content in drainage water collected from consolidated CPB samples containing general use Portland cement (PCI@100 wt%) with curing time as a function of binder content.

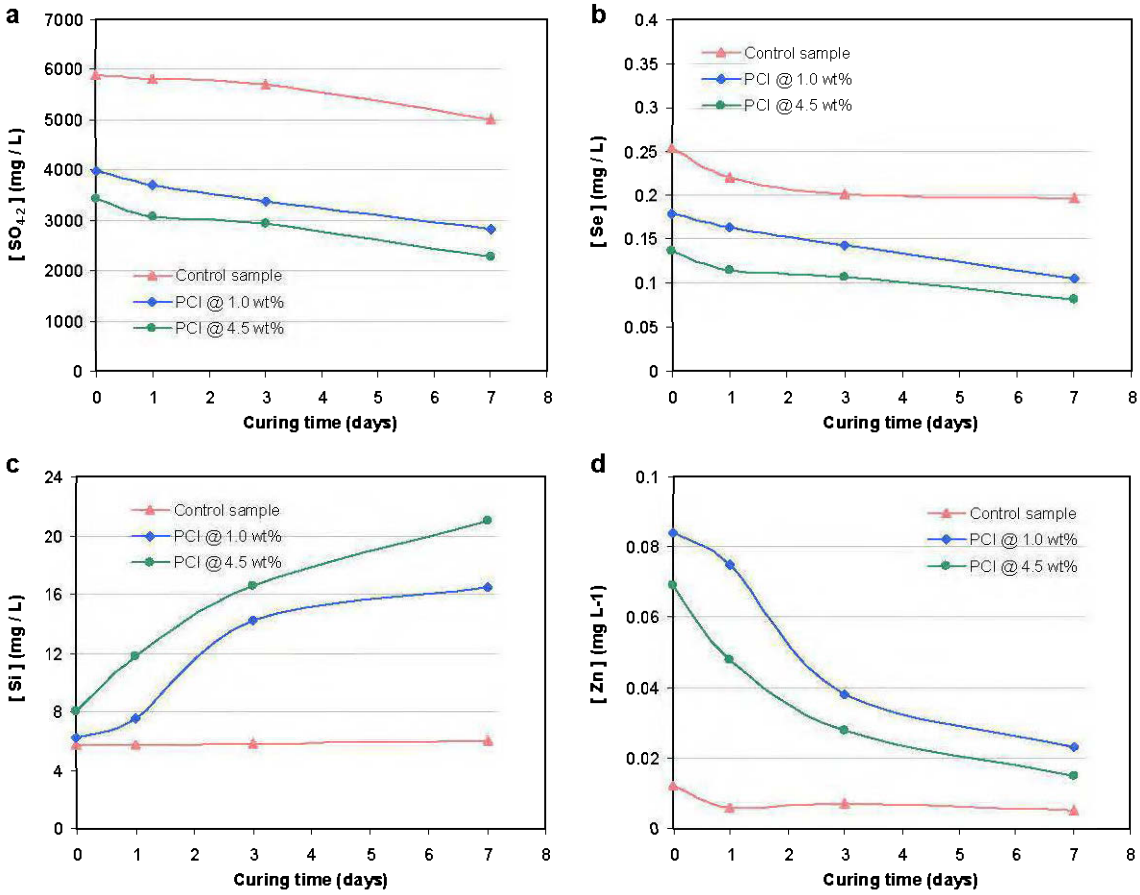

F.6 Change in (a) sulphate SO_4^{-2}, (b) selenium Se, (c) silicon Si, and (d) zinc Zn content in drainage water collected from consolidated CPB samples containing general use Portland cement (PCI@100 wt%) with curing time as a function of binder content.

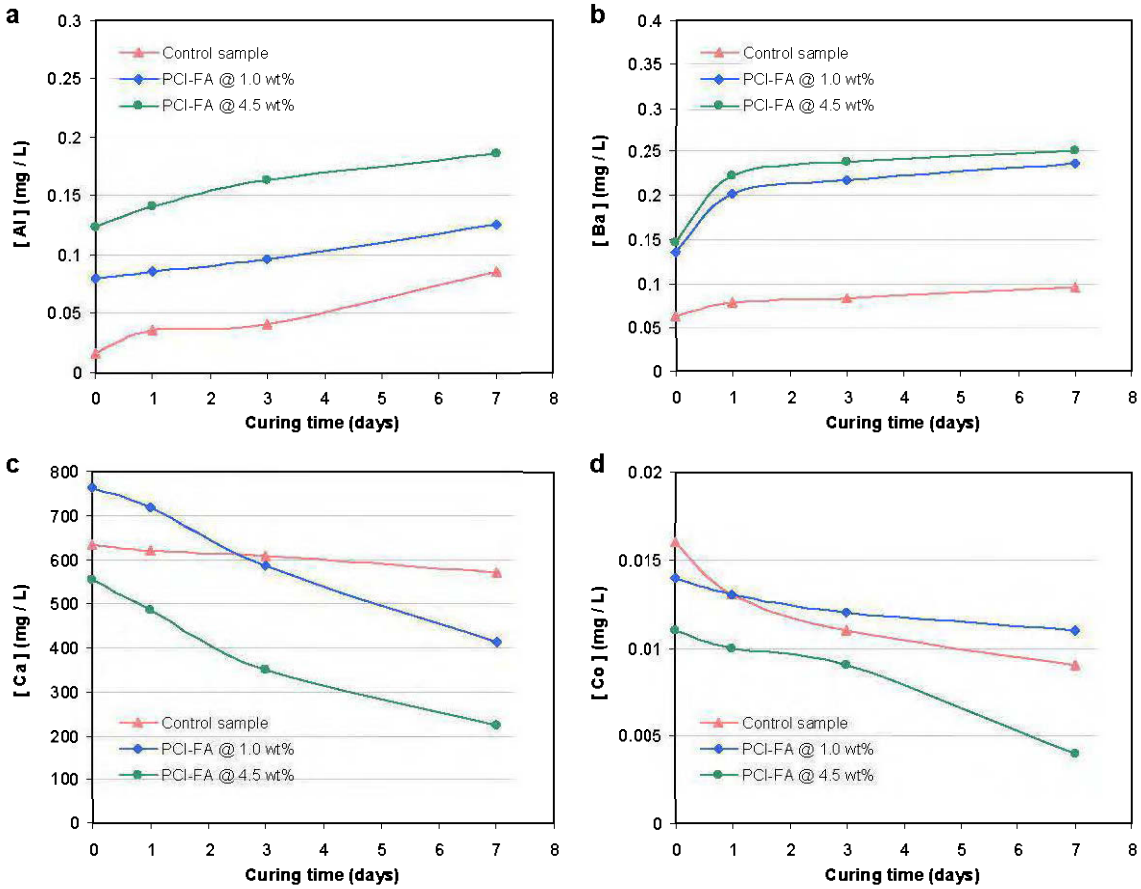

F.7 Change in (a) aluminium Al, (b) barium Ba, (c) calcium Ca, and (d) cobalt Co content in drainage water collected from consolidated CPB samples containing fly ash-based binder (PCI-Slag@60:40 wt%) with curing time as a function of binder content.

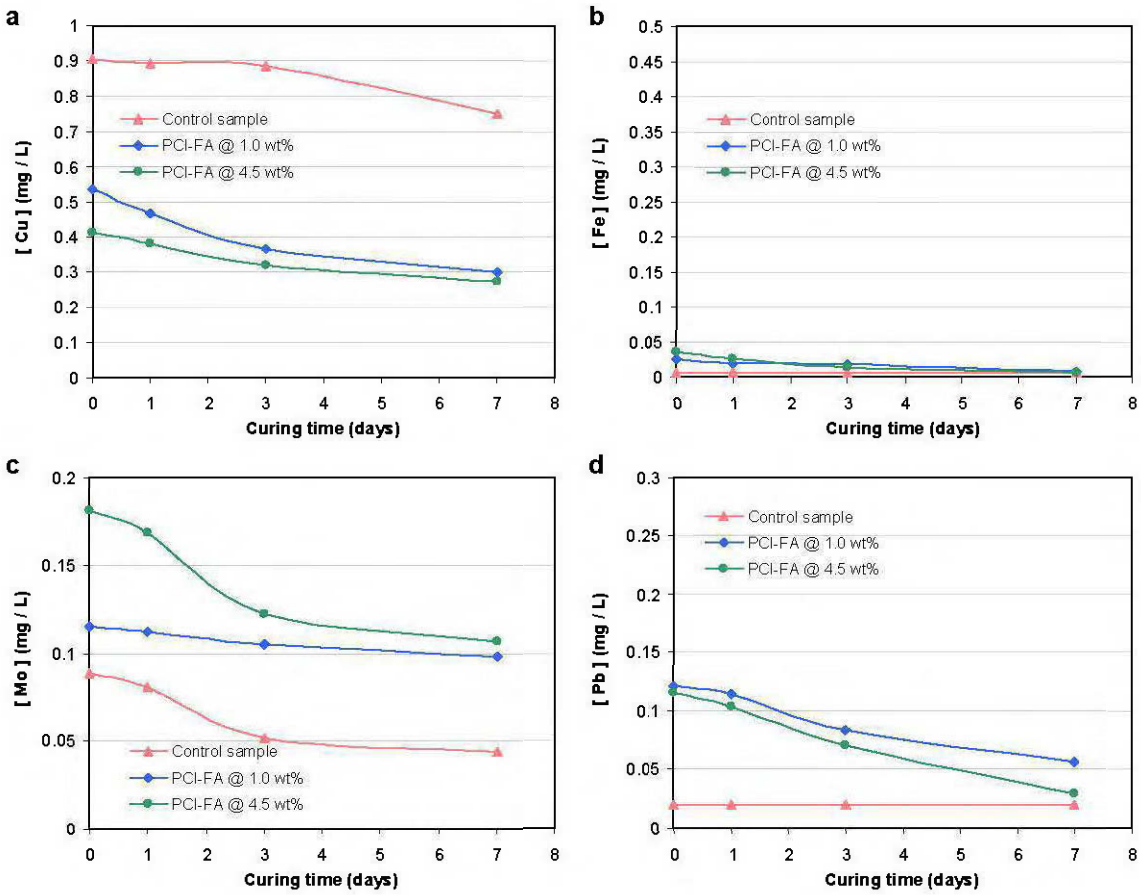

F.8 Change in (a) copper Cu, (b) iron Fe, (c) molybdenum Mo, and (d) lead Pb content in drainage water collected from consolidated CPB samples containing fly ash-based binder (PCI-Slag@60:40 wt%) with curing time as a function of binder content.

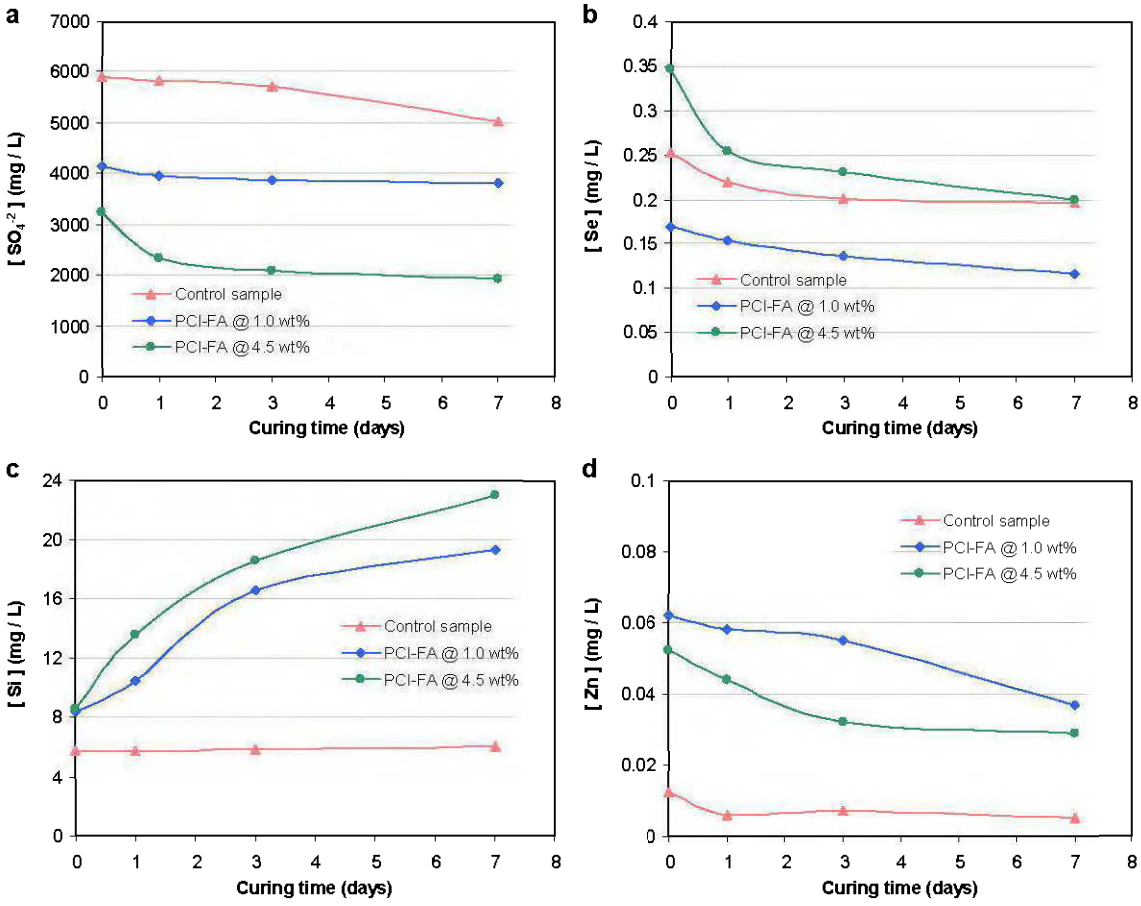

F.9 Change in (a) sulphate SO_4^{-2}, (b) selenium Se, (c) silicon Si, and (d) zinc Zn content in drainage water collected from consolidated CPB samples containing fly ash-based binder (PCI-Slag@60:40 wt%) with curing time as a function of binder content.

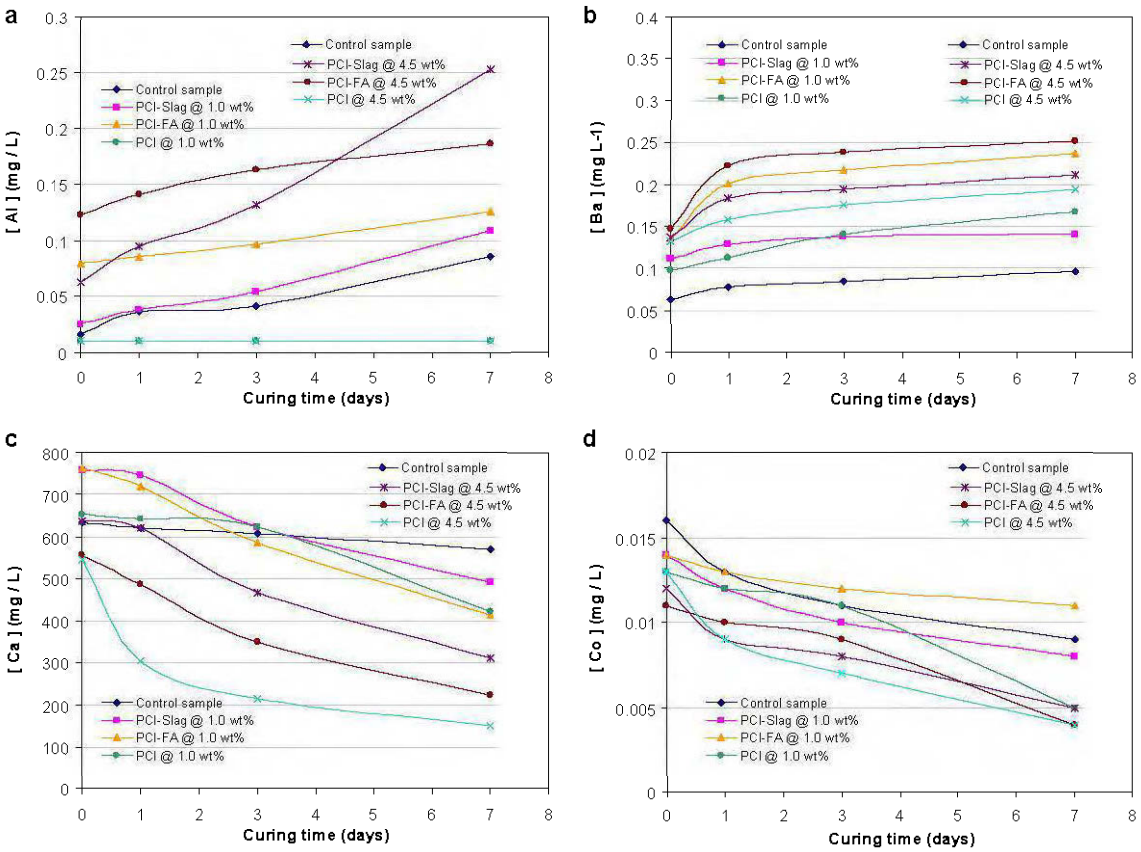

F.10 Comparison of (a) aluminium Al, (b) barium Ba, (c) calcium Ca, and (d) cobalt Co content in drainage water collected from consolidated CPB samples containing a binder content of 1 and 4.5 wt% with curing time as a function of binder content.

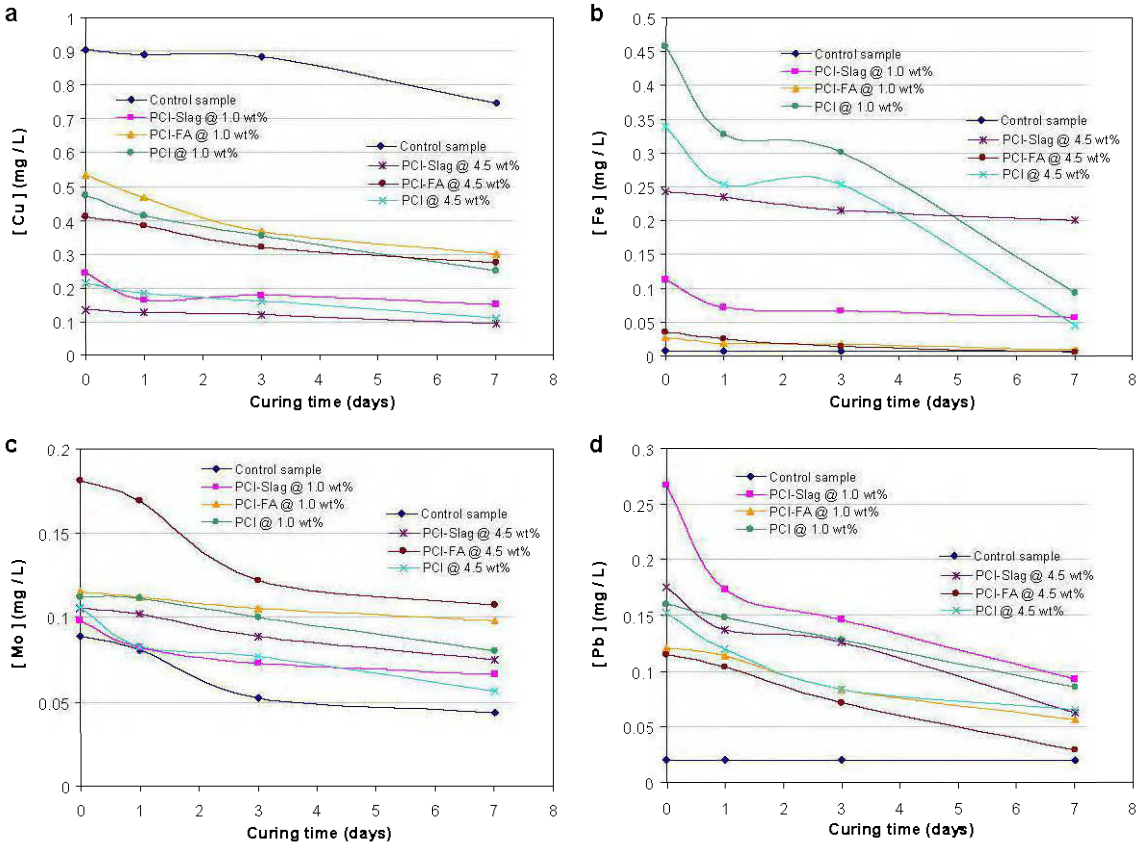

F.11 Comparison of (a) copper Cu, (b) iron Fe, (c) molybdenum Mo, and (d) lead Pb content in drainage water collected from consolidated CPB samples containing a binder content of 1 and 4.5 wt% with curing time as a function of binder content.

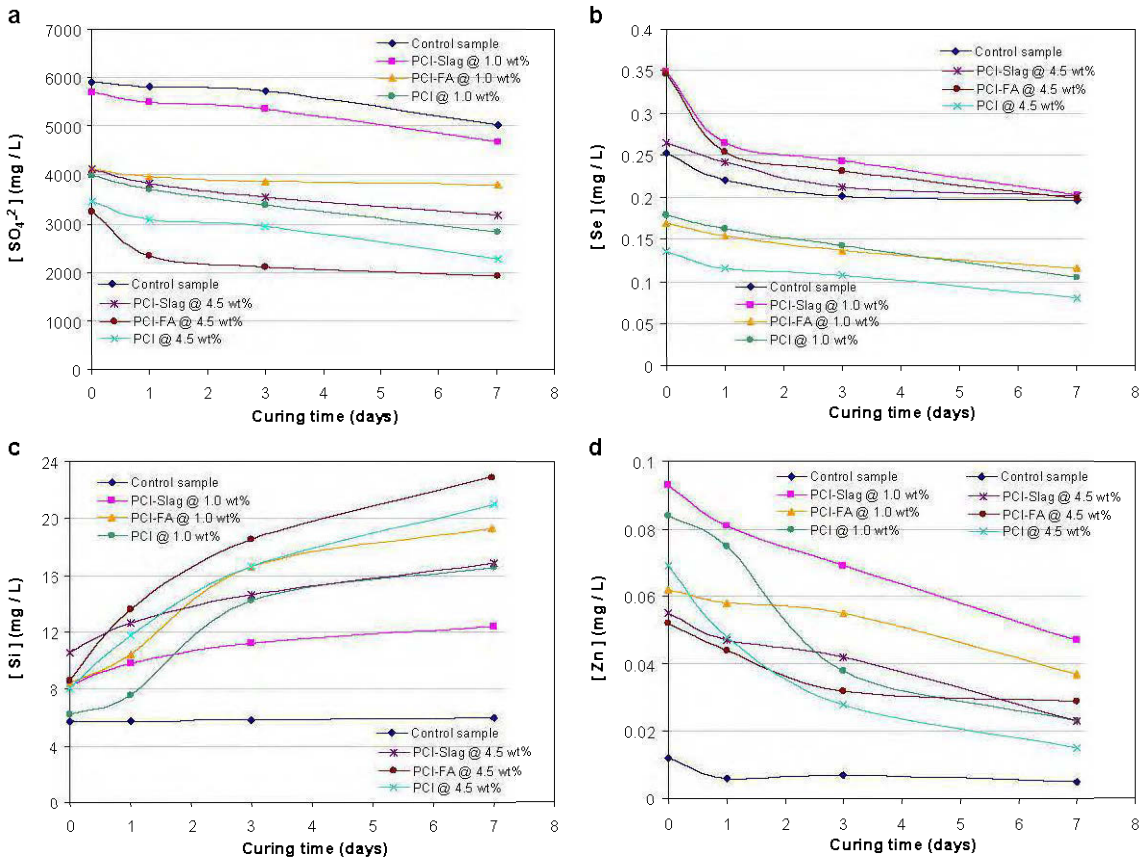

F.12 Comparison of (a) sulphate SO_4^{-2}, (b) selenium Se, (c) silicon Si, and (d) zinc Zn content in drainage water collected from consolidated CPB samples containing a binder content of 1 and 4.5 wt% with curing time as a function of binder content.

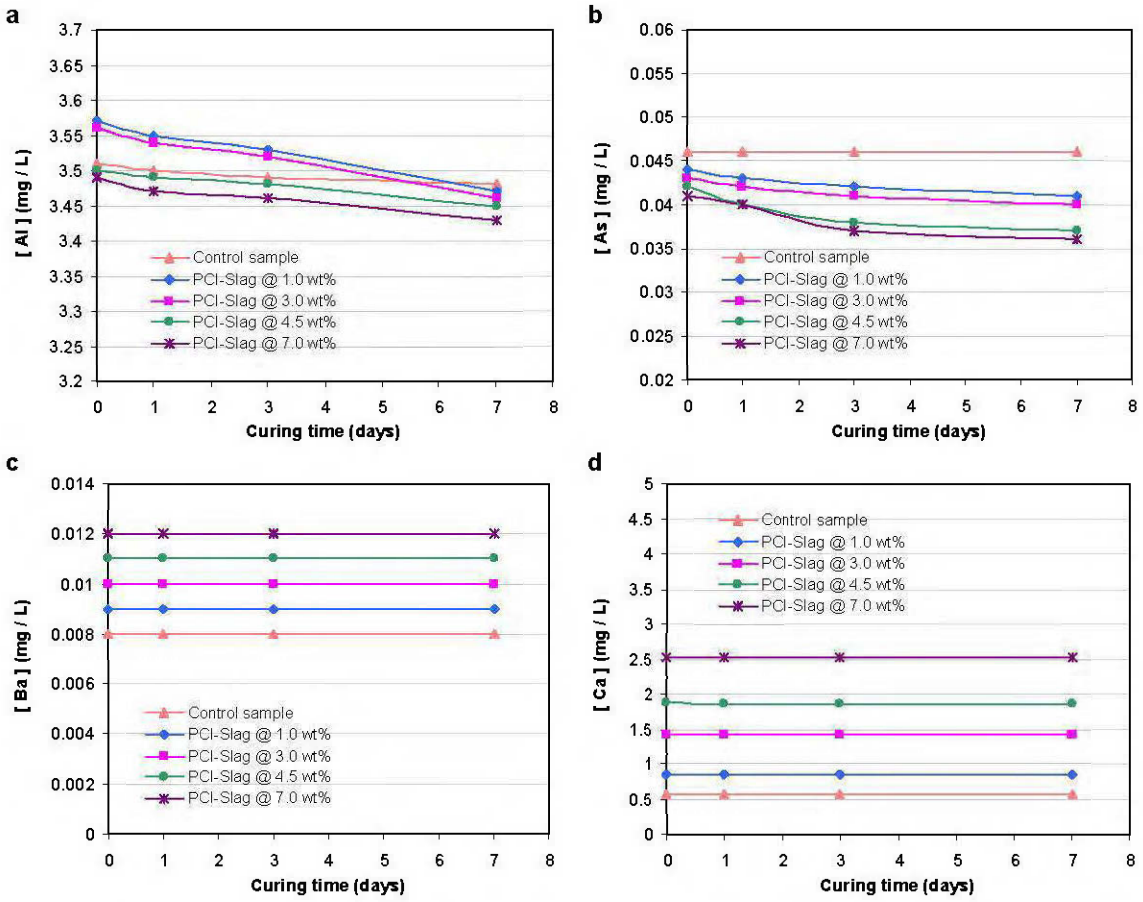

F.13 Change in (a) aluminium Al, (b) arsenic As, (c) barium Ba, and (d) calcium Ca of CPB samples containing slag-based binder (PCI-Slag@20:80 wt%) with curing time as a function of binder content.

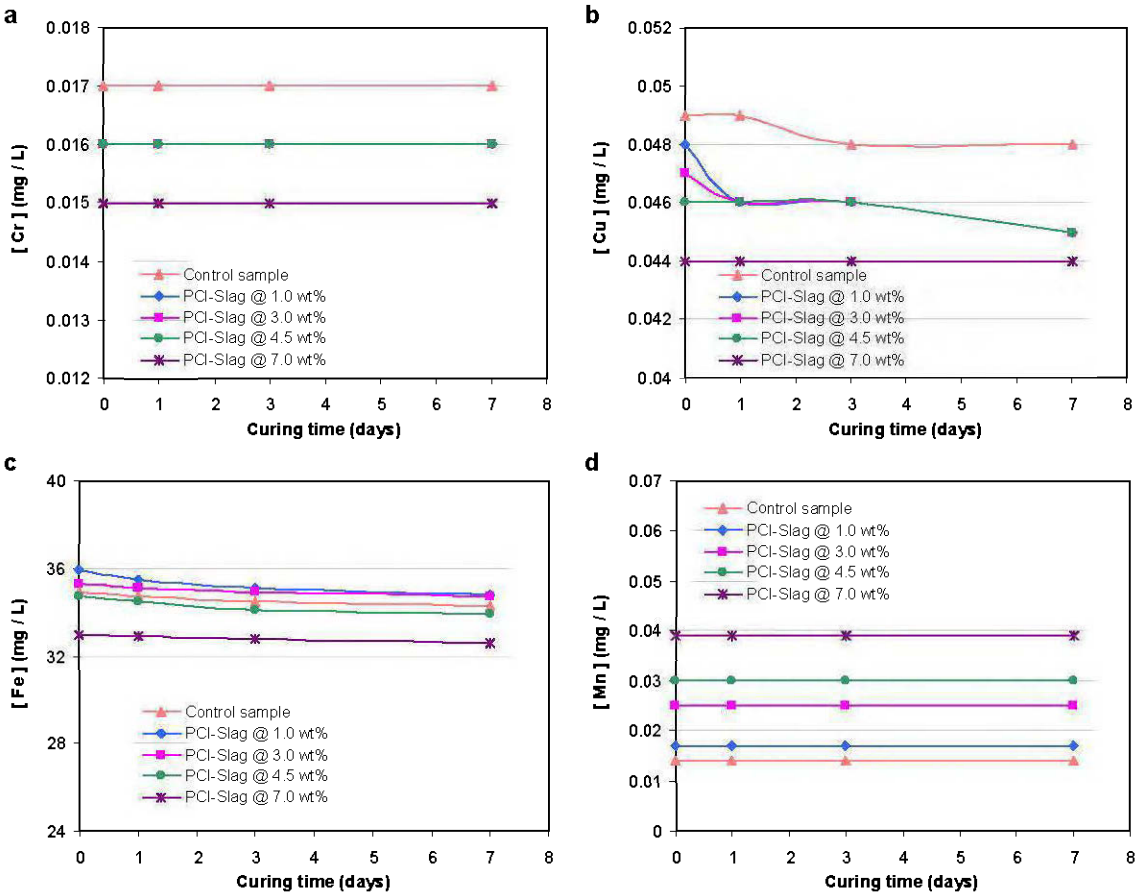

F.14 Change in (a) chromium Cr, (b) copper Cu, (c) iron Fe, and (d) molybdenum Mo of CPB samples containing slag-based binder (PCI-Slag@20:80 wt%) with curing time as a function of binder content.

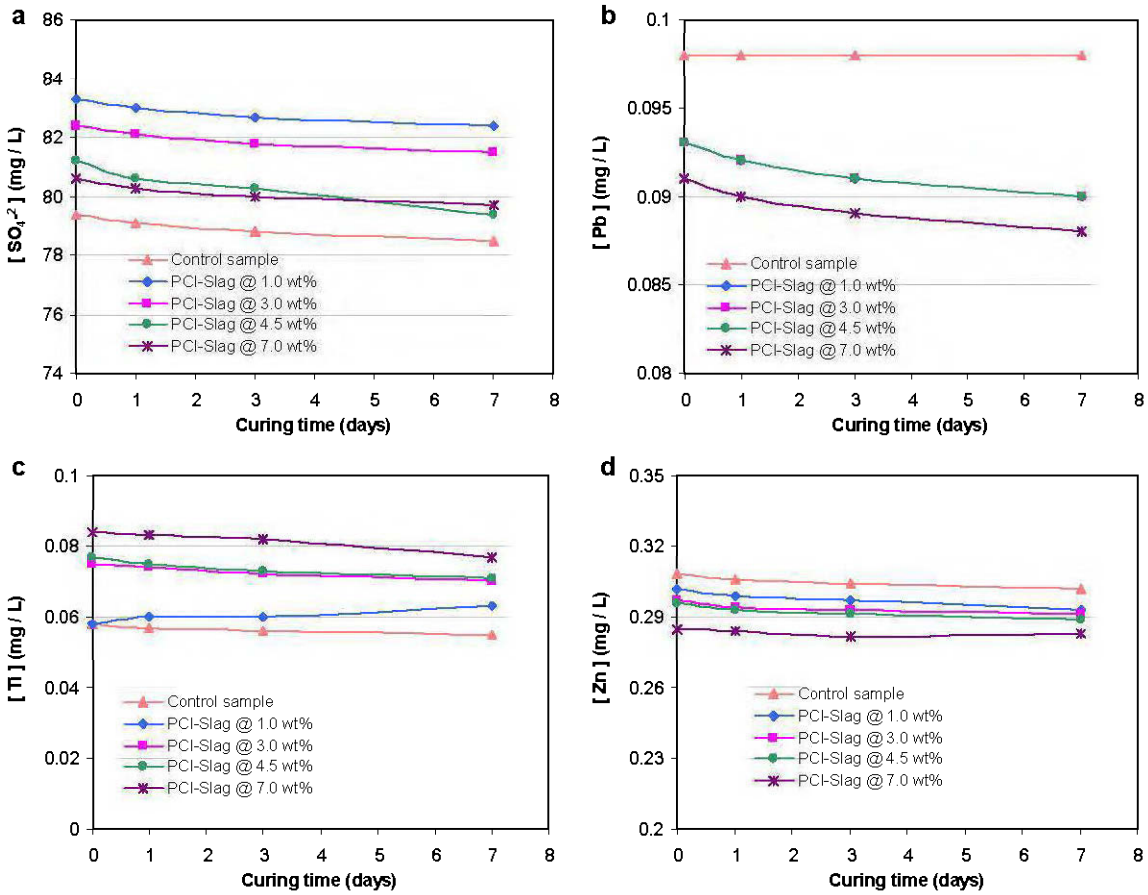

F.15 Change in (a) sulphate SO_4^{-2}, (b) lead Pb, (c) titanium Ti, and (d) Zinc Zn of CPB samples containing slag-based binder (PCI-Slag@20:80 wt%) with curing time as a function of binder content.

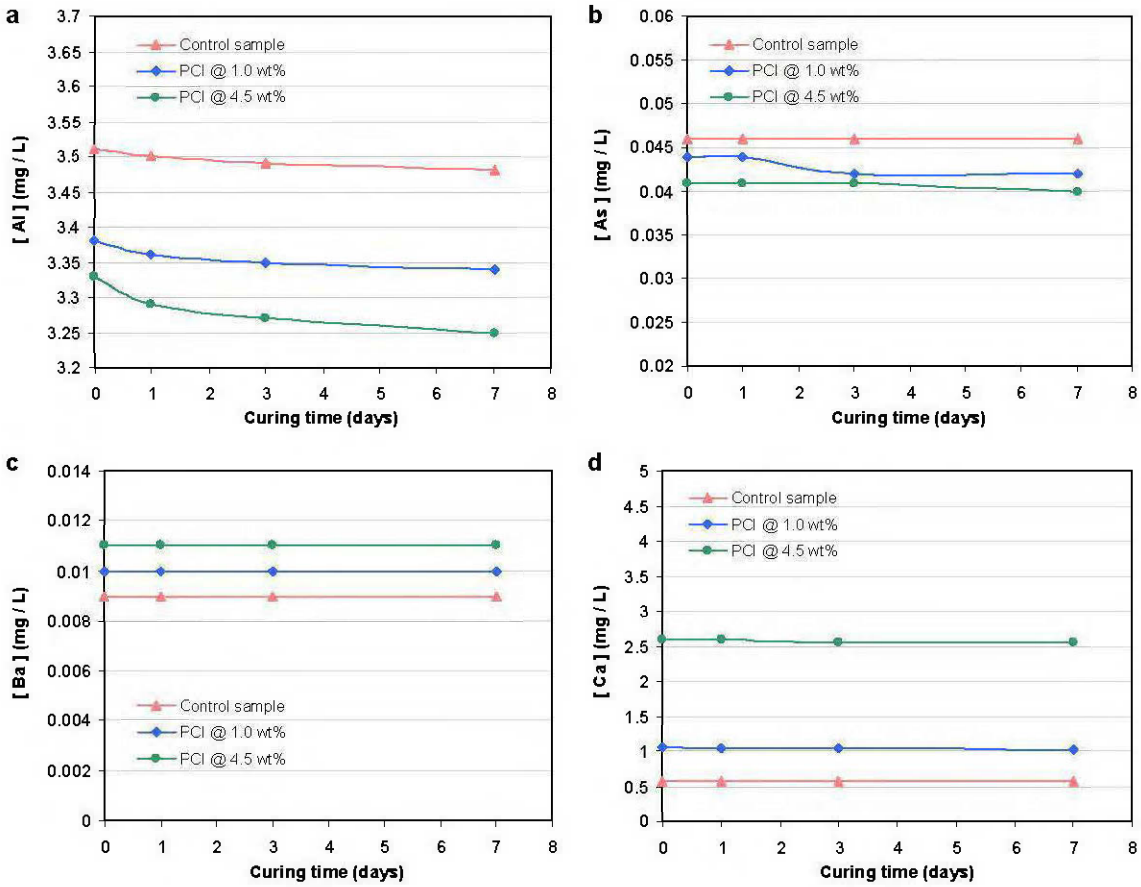

F.16 Change in (a) aluminium Al, (b) arsenic As, (c) barium Ba, and (d) calcium Ca of CPB samples containing general use Portland cement (PCI@100 wt%) with curing time as a function of binder content.

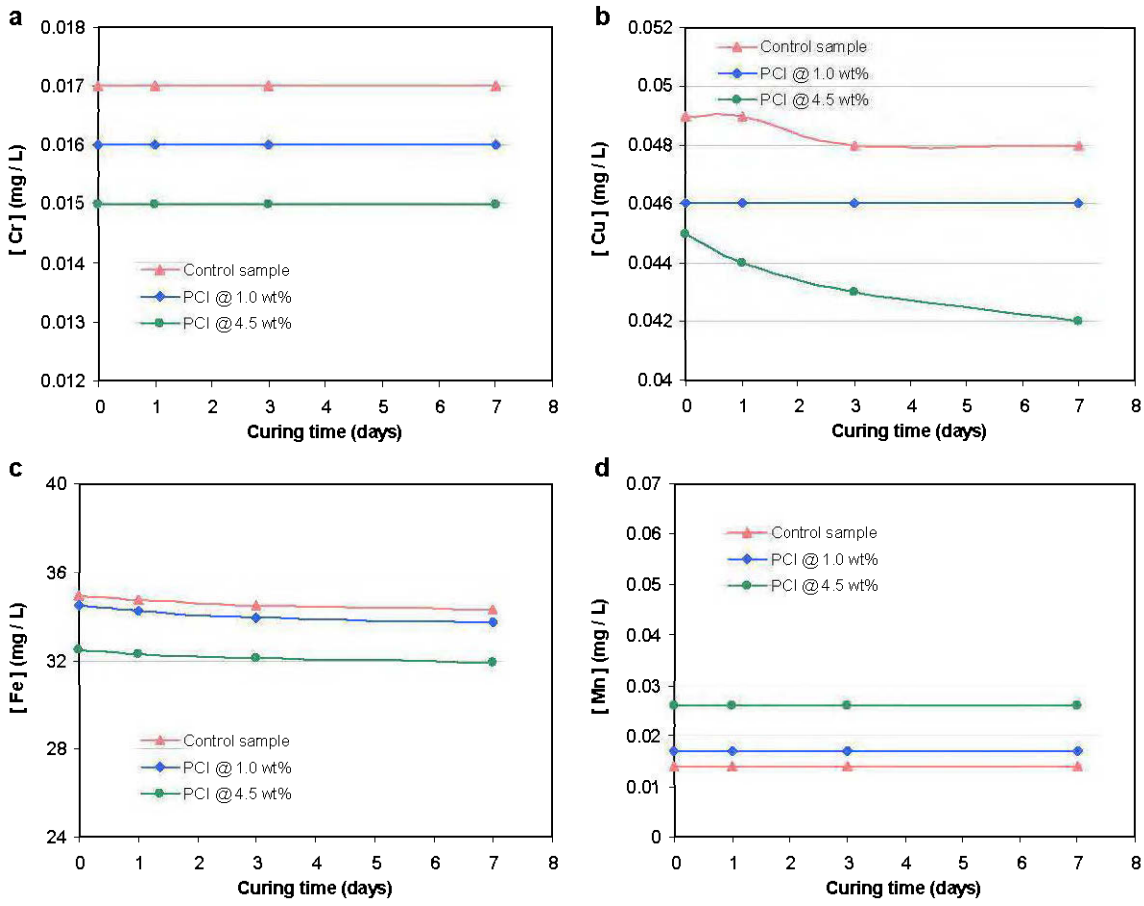

F.17 Change in (a) chromium Cr, (b) copper Cu, (c) iron Fe, and (d) molybdenum Mo of CPB samples containing general use Portland cement (PCI@100 wt%) with curing time as a function of binder content.

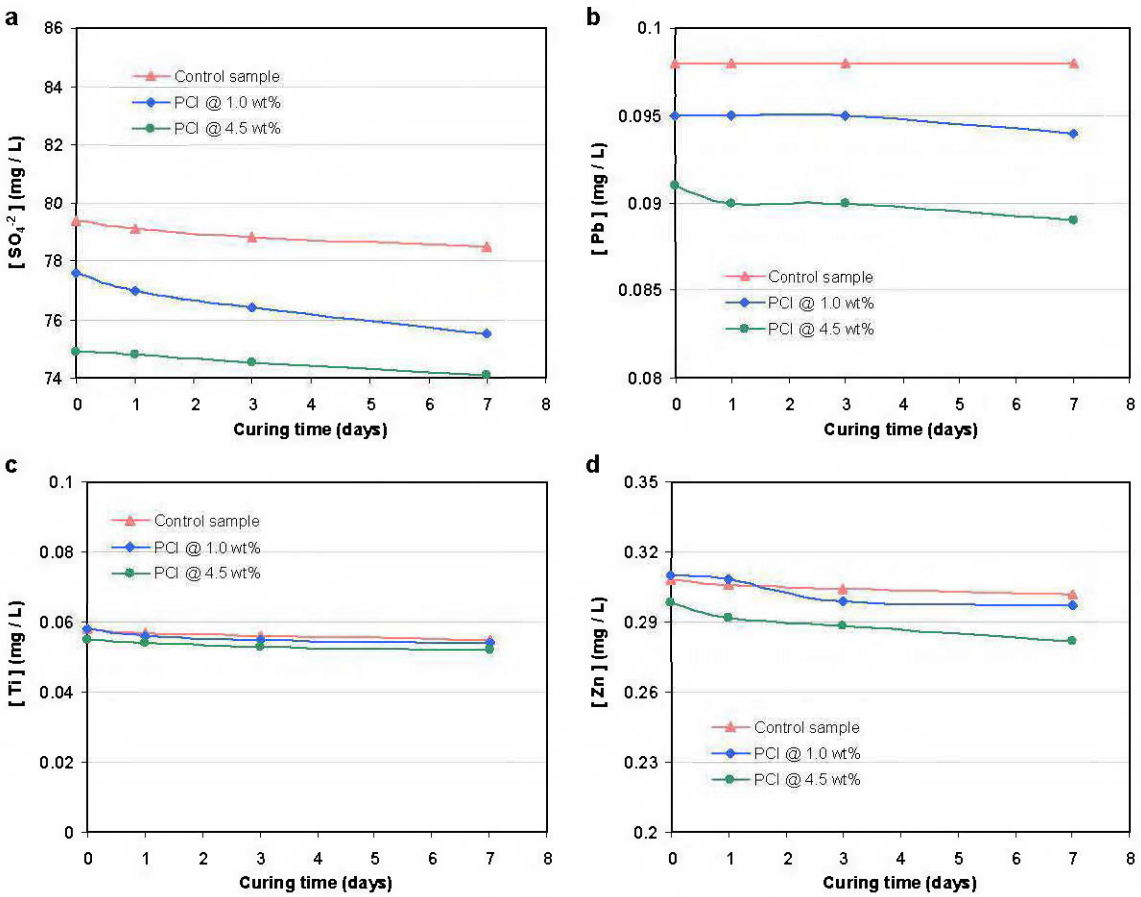

F.18 Change in (a) sulphate SO_4^{-2}, (b) lead Pb, (c) titanium Ti, and (d) Zinc Zn of CPB samples containing general use Portland cement (PCI@100 wt%) with curing time as a function of binder content.

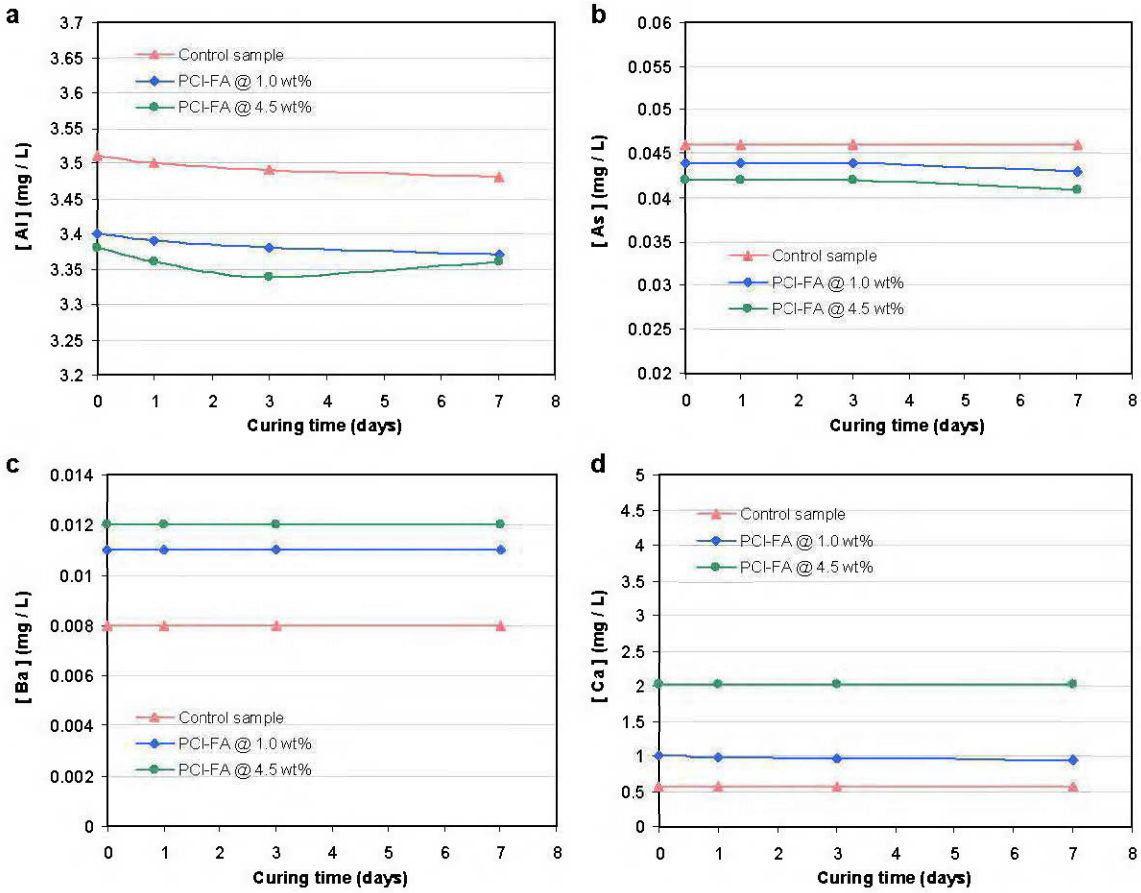

F.19 Change in (a) aluminium Al, (b) arsenic As, (c) barium Ba, and (d) calcium Ca of CPB samples containing fly ash-based binder (PCI-FA@60:40 wt%) with curing time as a function of binder content.

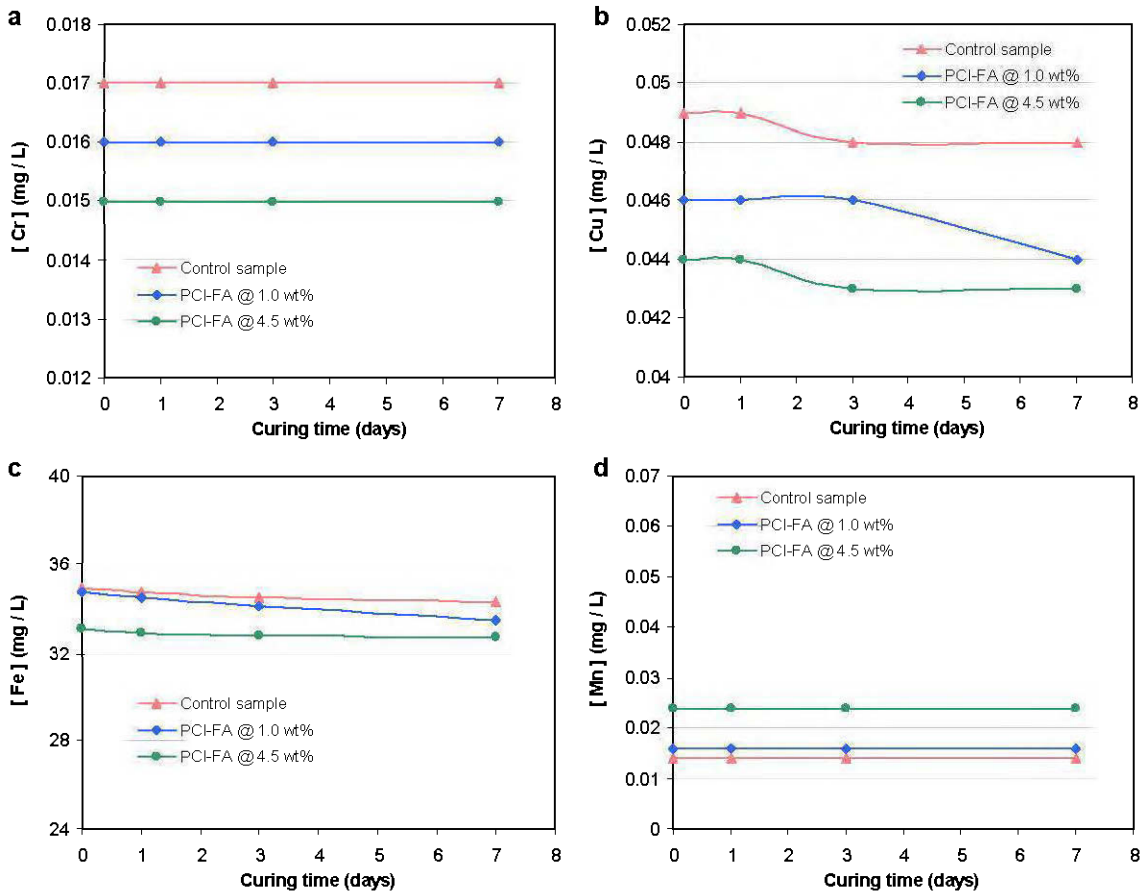

F.20 Change in (a) chromium Cr, (b) copper Cu, (c) iron Fe, and (d) molybdenum Mo of CPB samples containing fly ash-based binder (PCI-FA@60:40 wt%) with curing time as a function of binder content.

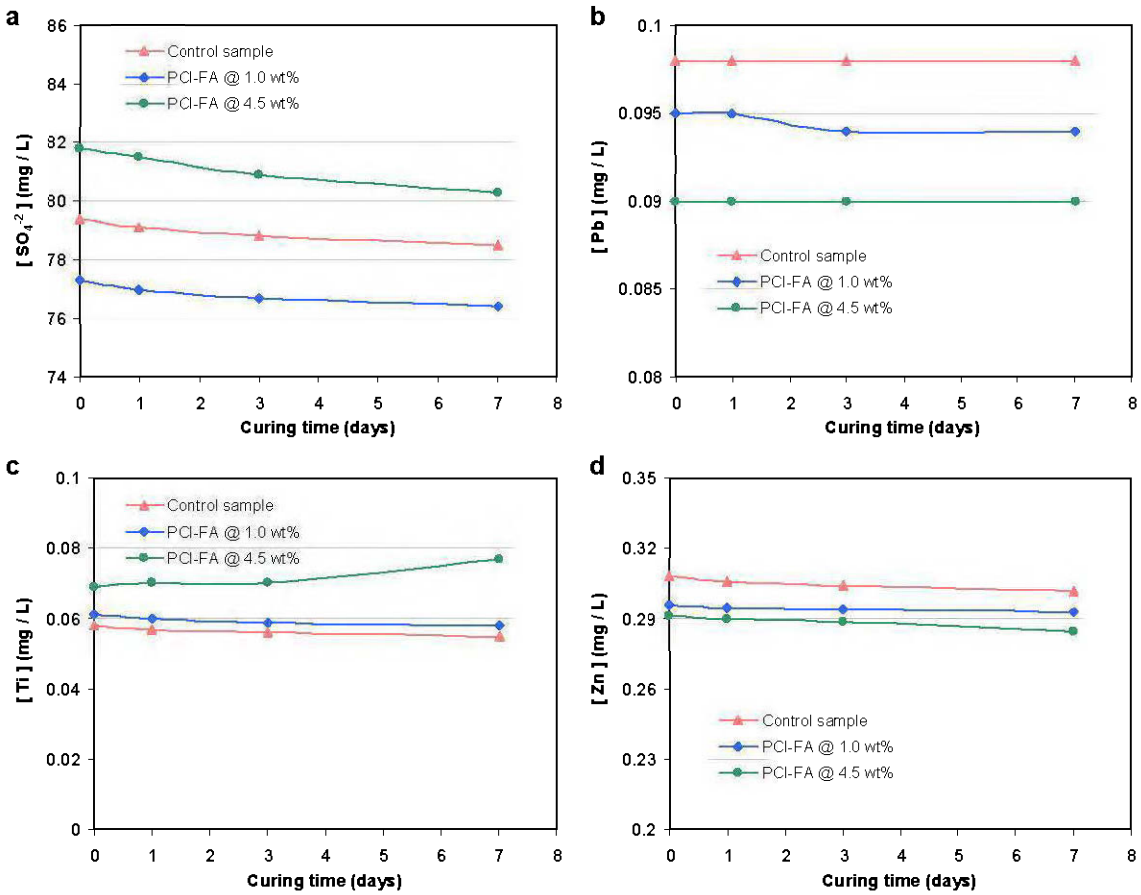

F.21 Change in (a) sulphate SO_4^{-2}, (b) lead Pb, (c) titanium Ti, and (d) Zinc Zn of CPB samples containing fly ash-based binder (PCI-FA@60:40 wt%) with curing time as a function of binder content.

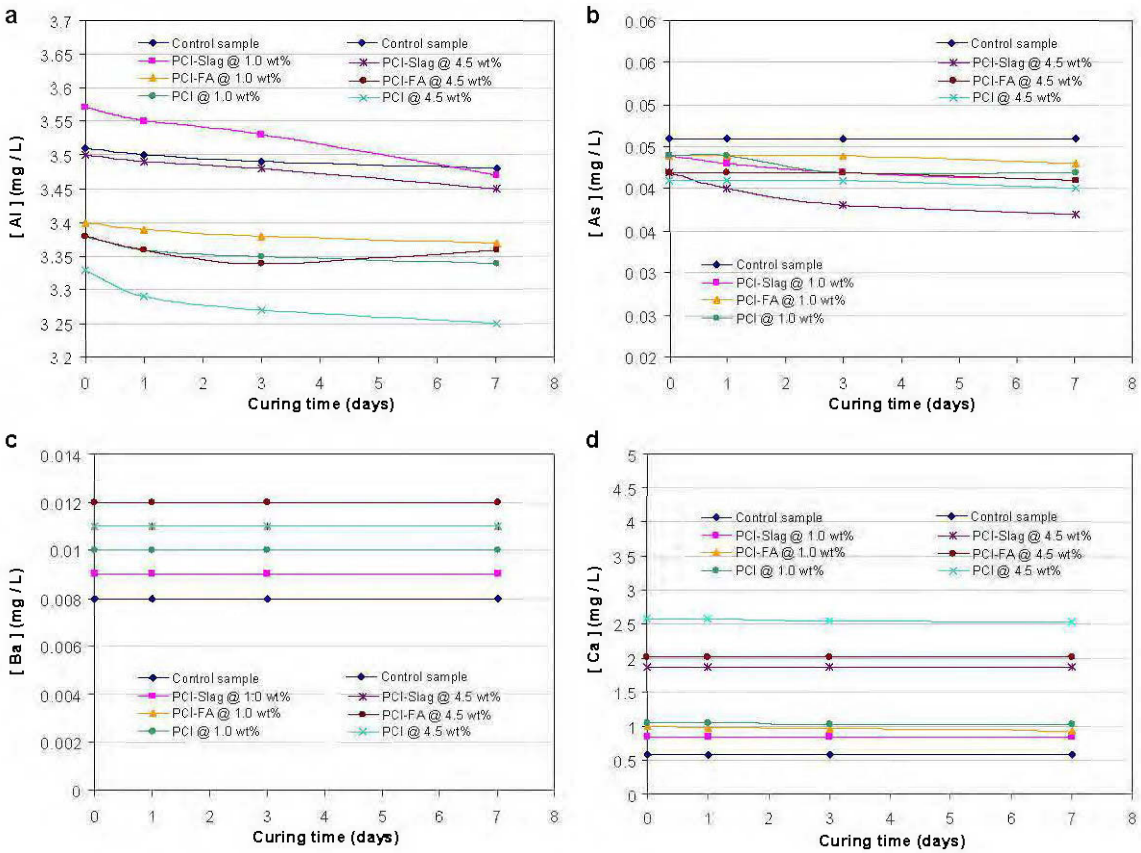

F.**22** Comparison of (a) aluminium Al, (b) arsenic As, (c) barium Ba, and (d) calcium Ca of CPB samples containing a binder content of 1 and 4.5 wt% with curing time as a function of binder content.

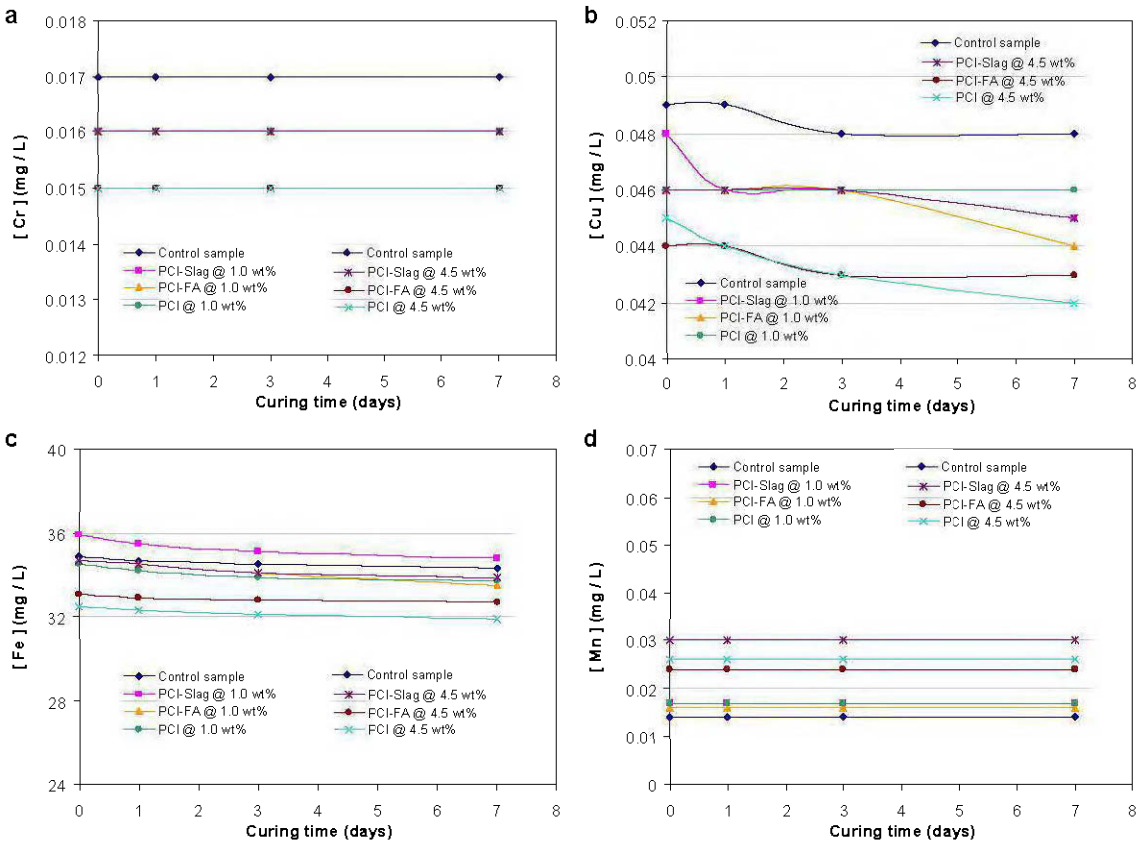

F.23 Comparison of (a) chromium Cr, (b) copper Cu, (c) iron Fe, and (d) molybdenum Mo of CPB samples containing a binder content of 1 and 4.5 wt% with curing time as a function of binder content.

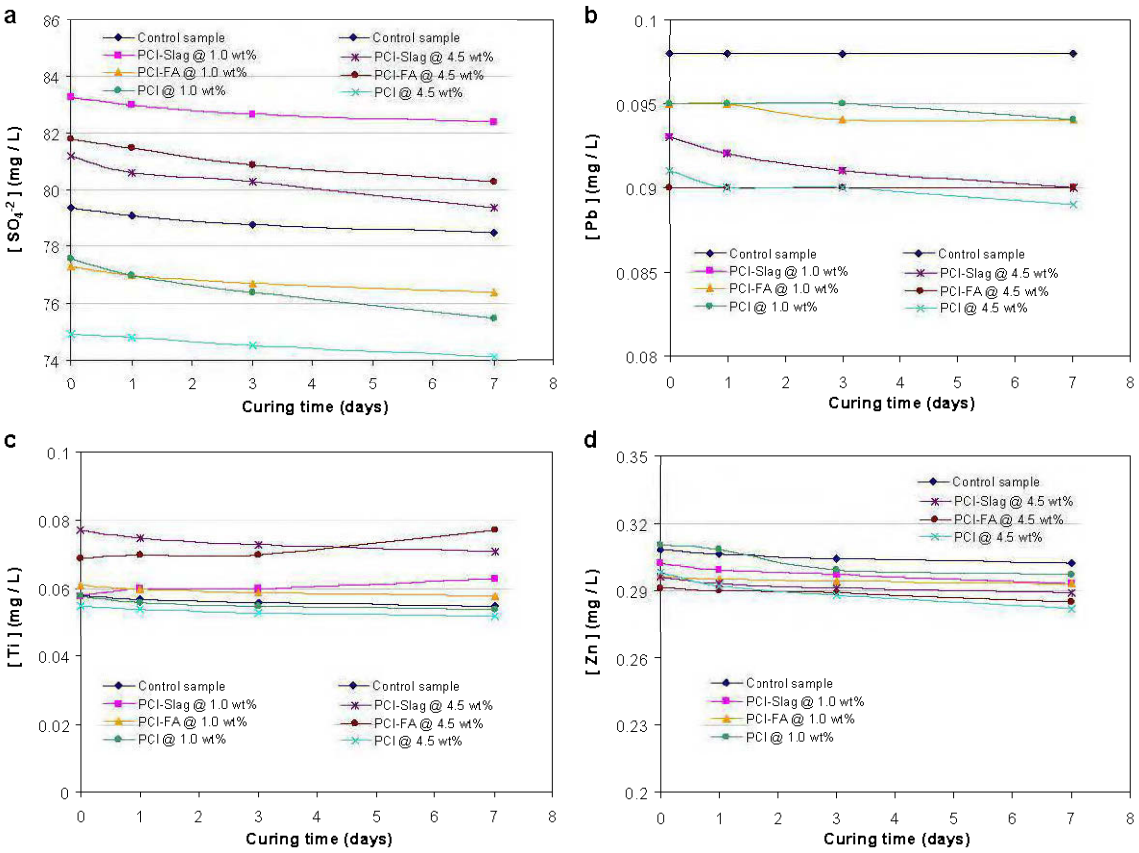

F.24 Comparison of (a) sulphate SO_4^{-2}, (b) lead Pb, (c) titanium Ti, and (d) Zinc Zn of CPB samples containing a binder content of 1 and 4.5 wt% with curing time as a function of binder content.

APPENDIX G

SUMMARY OF MERCURY INTRUSION POROSIMETRY (MIP) RESULTS

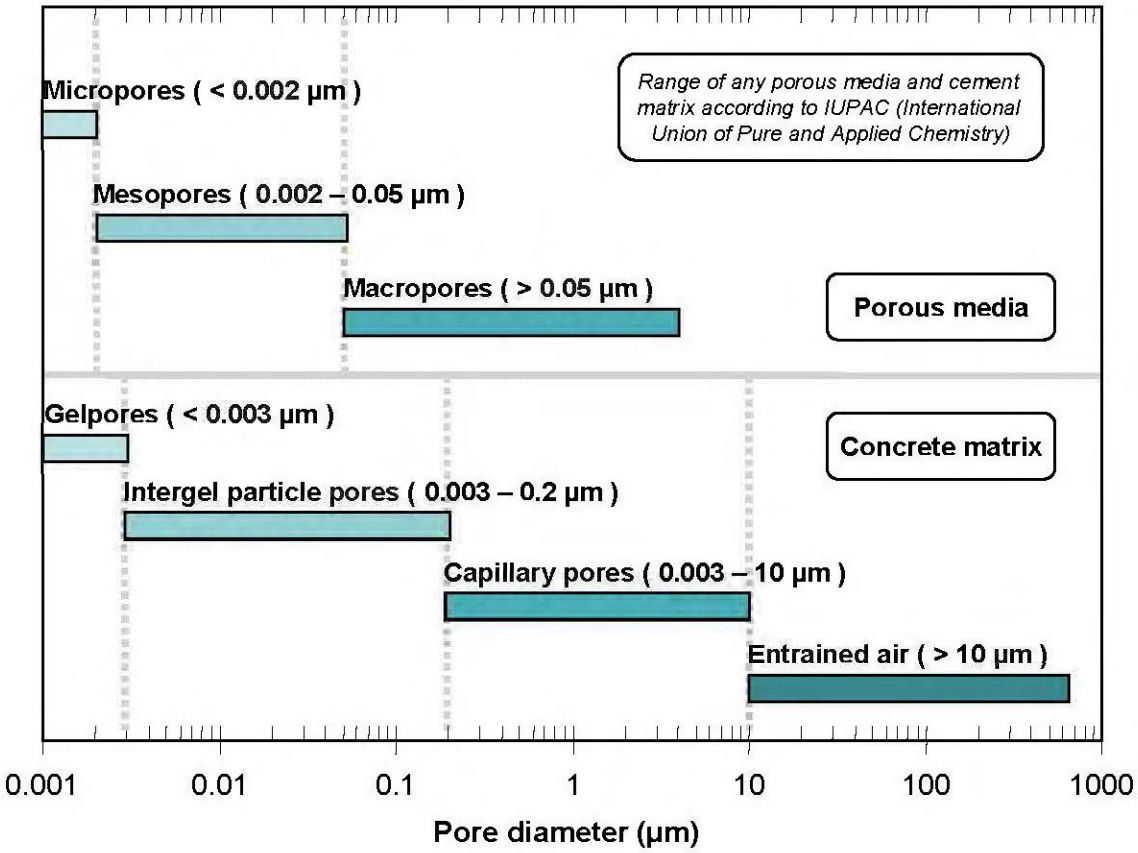

G.1 Classification of pore sizes according to IUPAC convention and concrete science terminology.

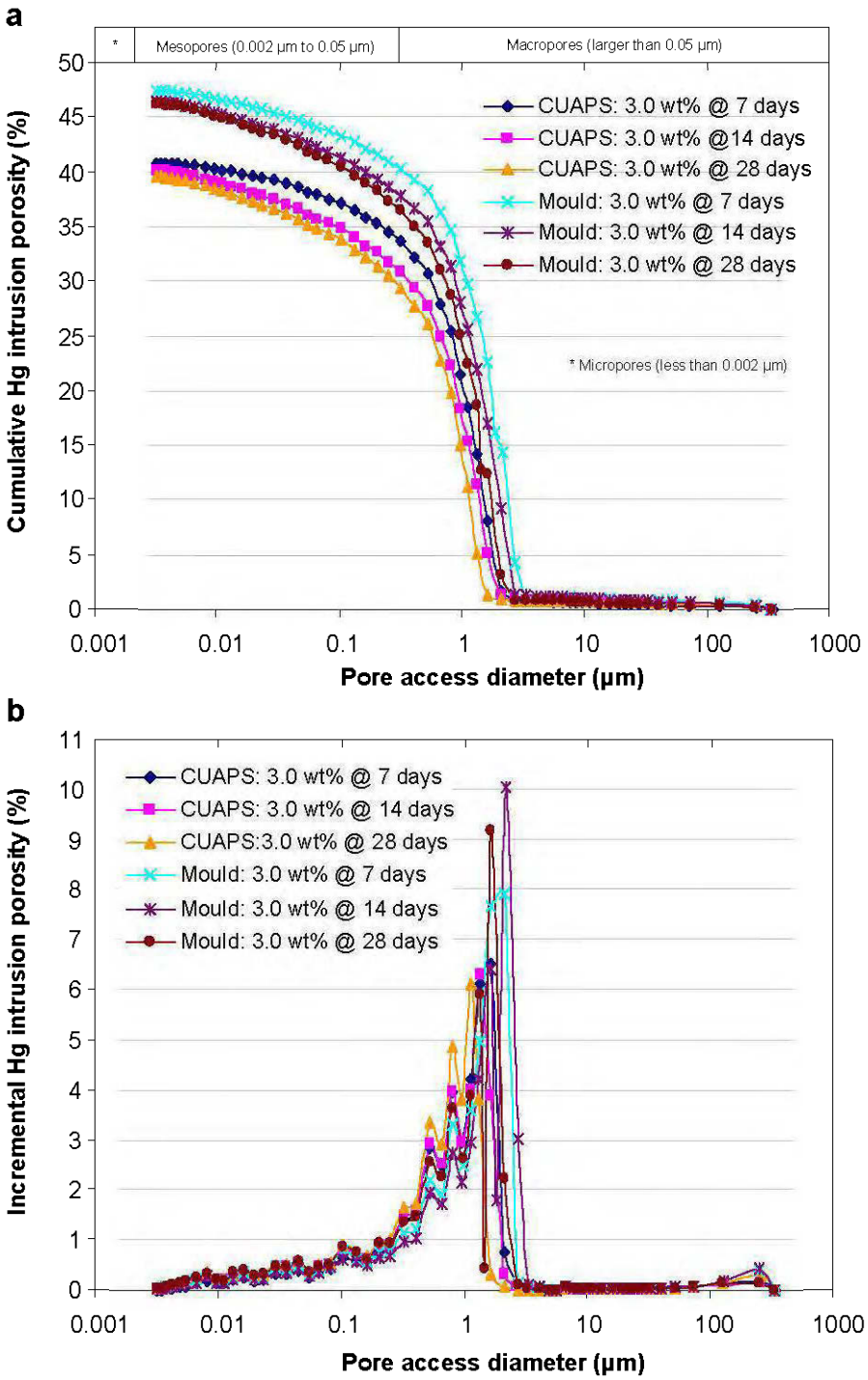

G.2 Cumulative (a) and incremental (b) mercury intrusion porosimetry curves for CUAPS-consolidated and mould-undrained CPB samples with 3 wt% binder content after curing times of 7, 14 and 28 days.

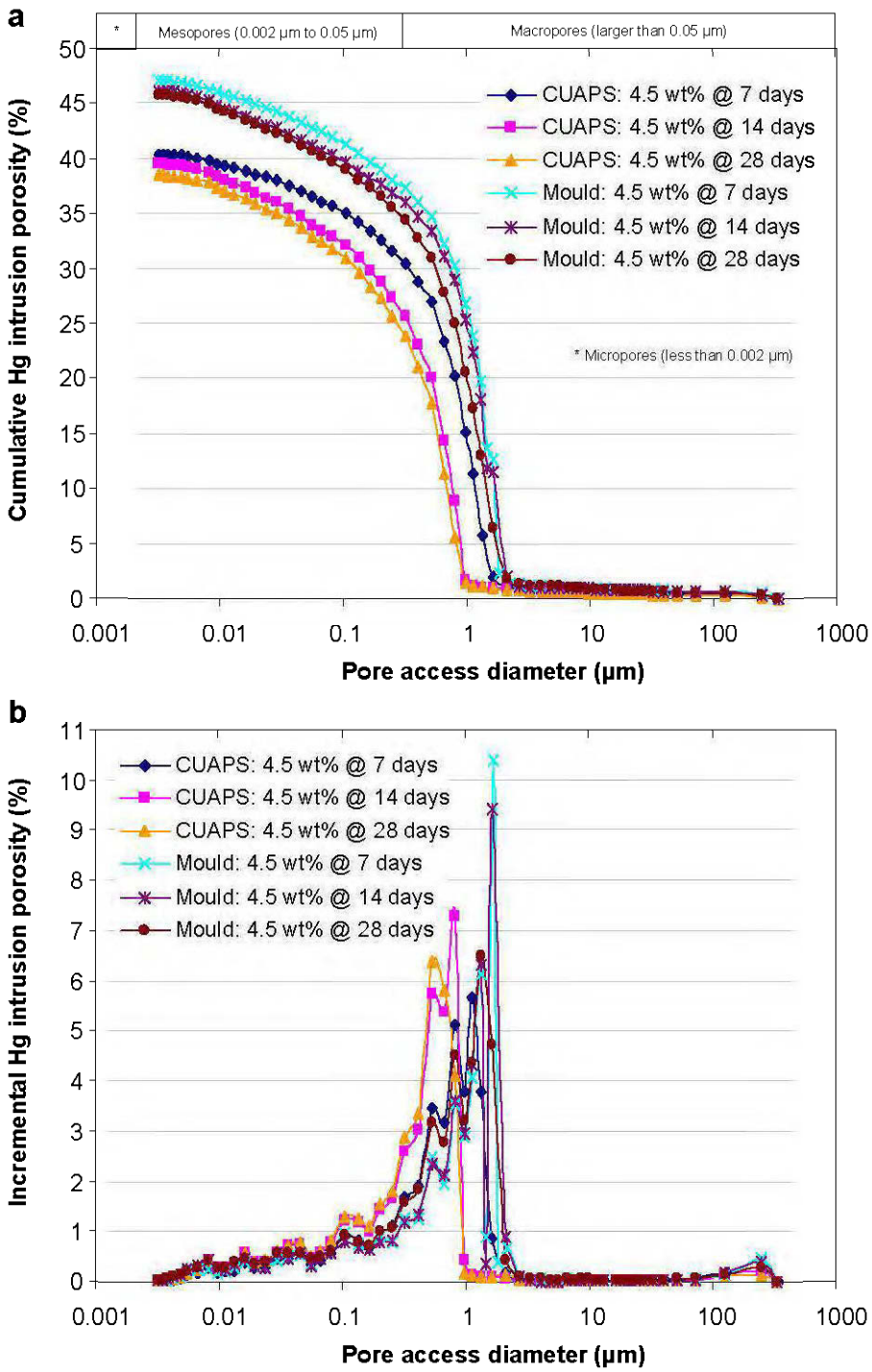

G.3 Cumulative (a) and incremental (b) mercury intrusion porosimetry curves for CUAPS-consolidated and mould-undrained CPB samples with 4.5 wt% binder content after curing times of 7, 14 and 28 days.

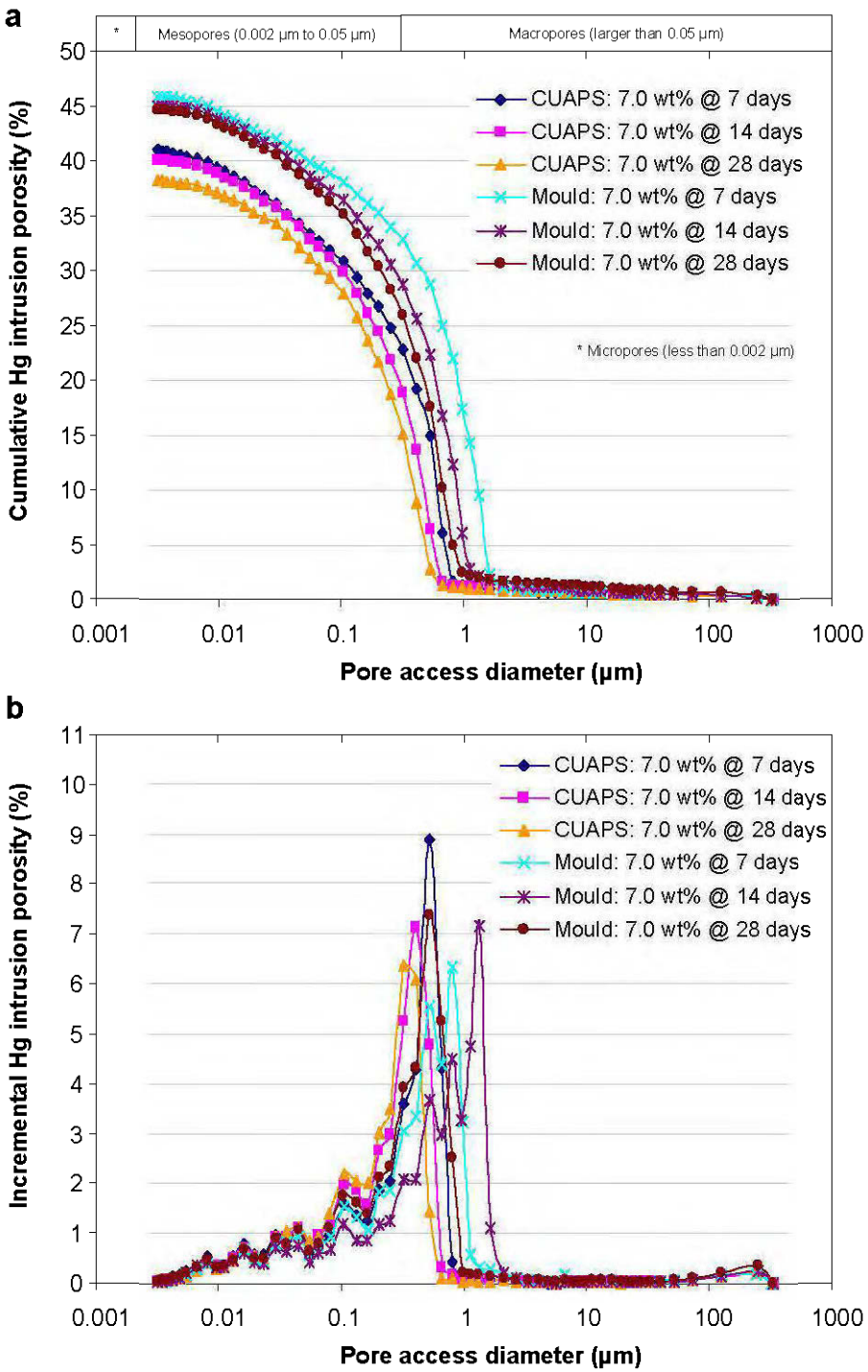

G.4 Cumulative (a) and incremental (b) mercury intrusion porosimetry curves for CUAPS-consolidated and mould-undrained CPB samples with 7 wt% binder content after curing times of 7, 14 and 28 days.

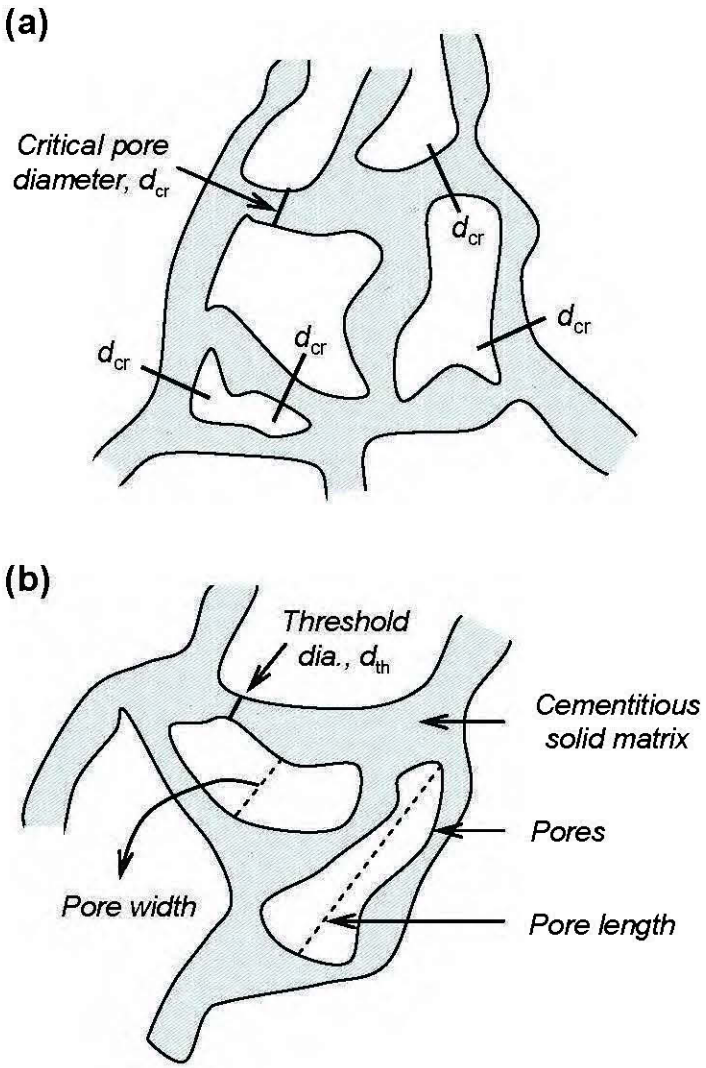

G.5 Schematic drawing of a pore structure and network: (a) critical pore diameter d_{cr} and (b) threshold diameter d_{th} (Aligizaki, 2006).

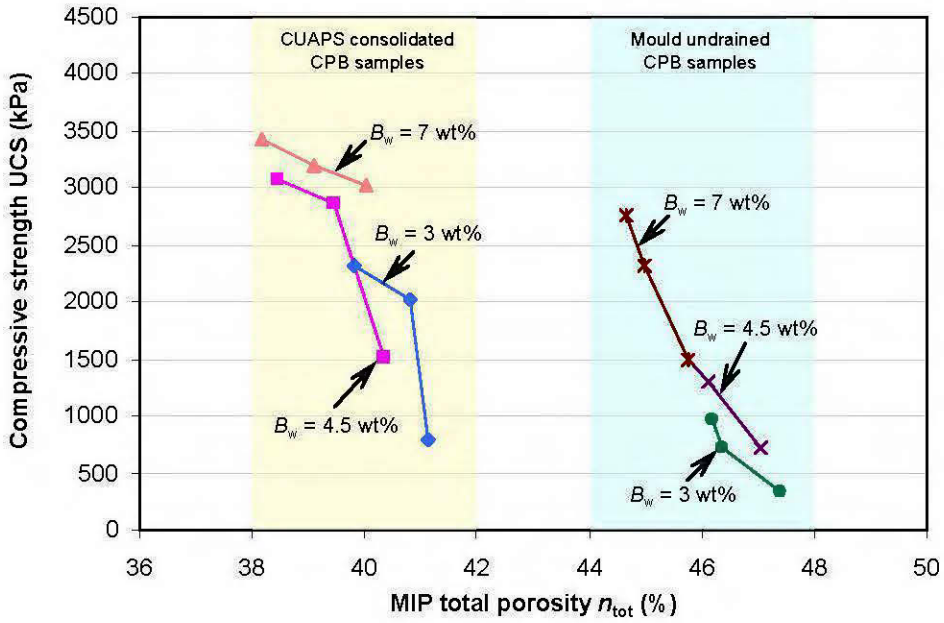

G.6 Change in uniaxial compressive strength (UCS) with MIP total porosity for unconsolidated-undrained and CUAPS-consolidated CPB samples.

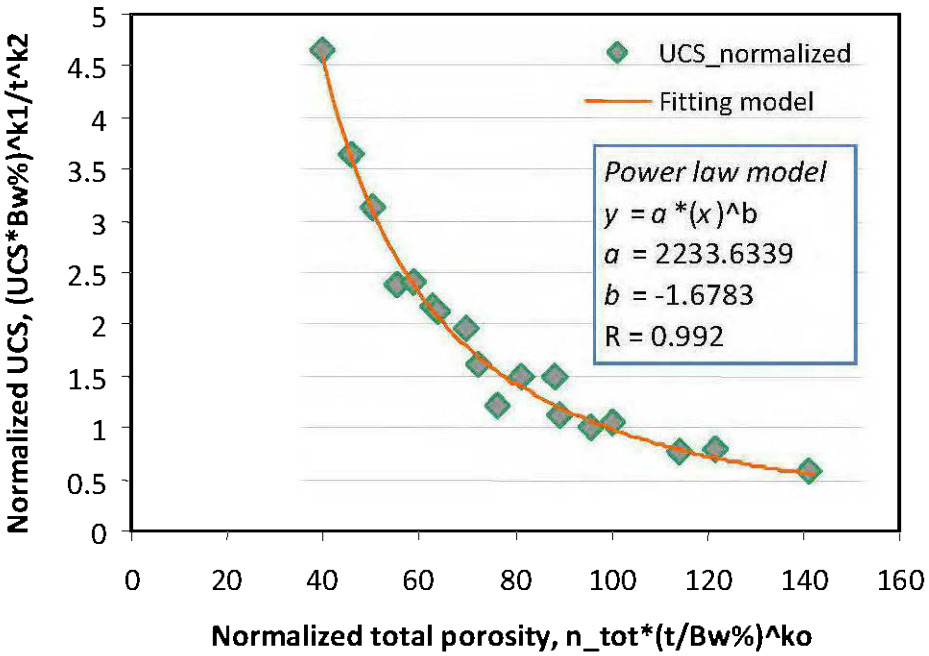

$$UCS = A \cdot (n_{tot})^{k_0} \cdot \frac{(t)^{k_1}}{(B_{w\%})^{k_2}}$$

G.7 Graphical representation of the regression analysis of normalized variables for deriving predictive models for normalized UCS vs. normalized total porosity.

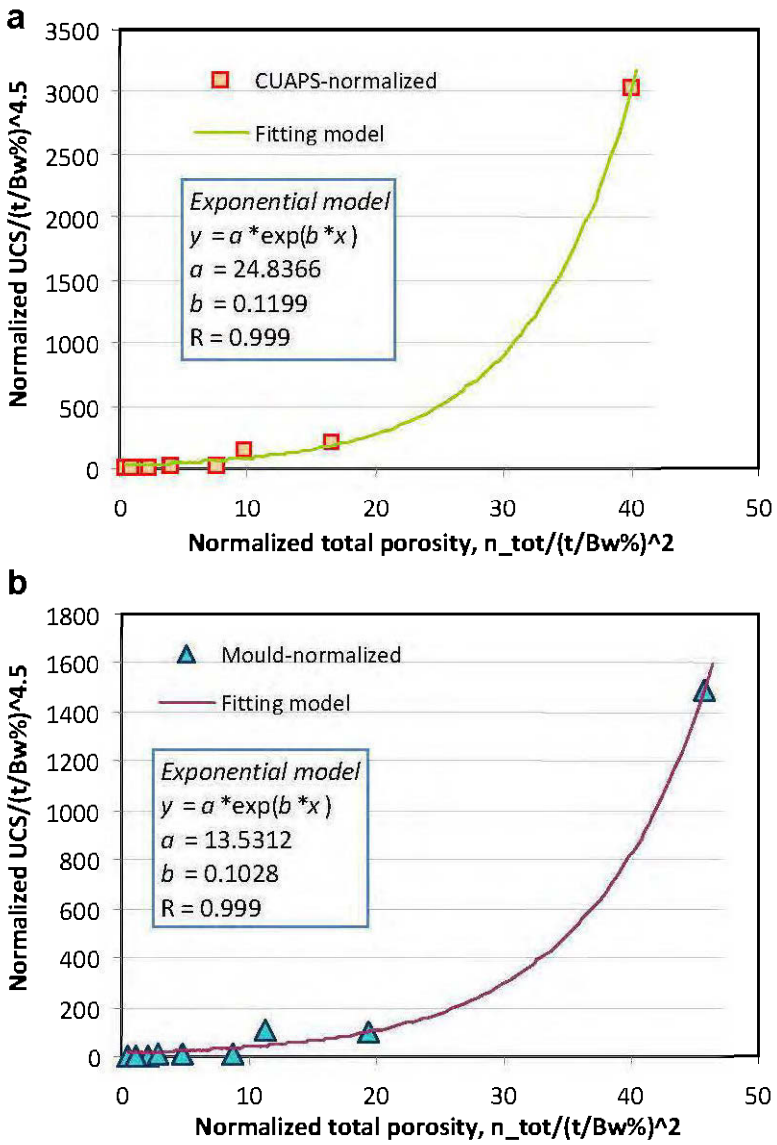

$$UCS_{cuaps,\,mould} = \left(\frac{t}{B_{w\%}}\right)^{4.5} * \left[a * \exp\left(b * \left(n_{tot\_cuaps,\,mould} * \left[\frac{B_{w\%}}{t}\right]^2\right)\right)\right]$$

G.8 Graphical representation of regression analysis of normalized variables for deriving predictive models for: (a) UCS of CUAPS-consolidated CPB sample knowing n_{tot} and (b) UCS of undrained CPB sample knowing n_{tot}.

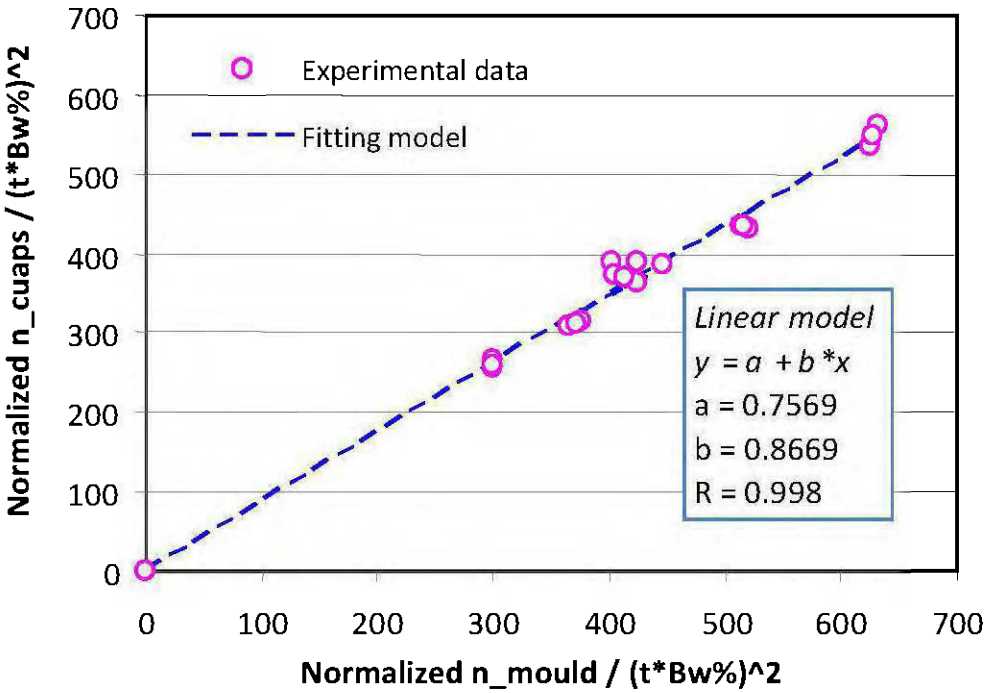

$$n_{tot-cuaps} = \left(t * B_{w\%}\right)^2 * \left[a + b * \left(\frac{n_{tot-mould}}{\left(t * B_{w\%}\right)^2}\right)\right]$$

G.9 Graphical representation of the regression analysis of normalized variables for deriving predictive models for n_{tot}-CUAPS knowing n_{tot}-mould.

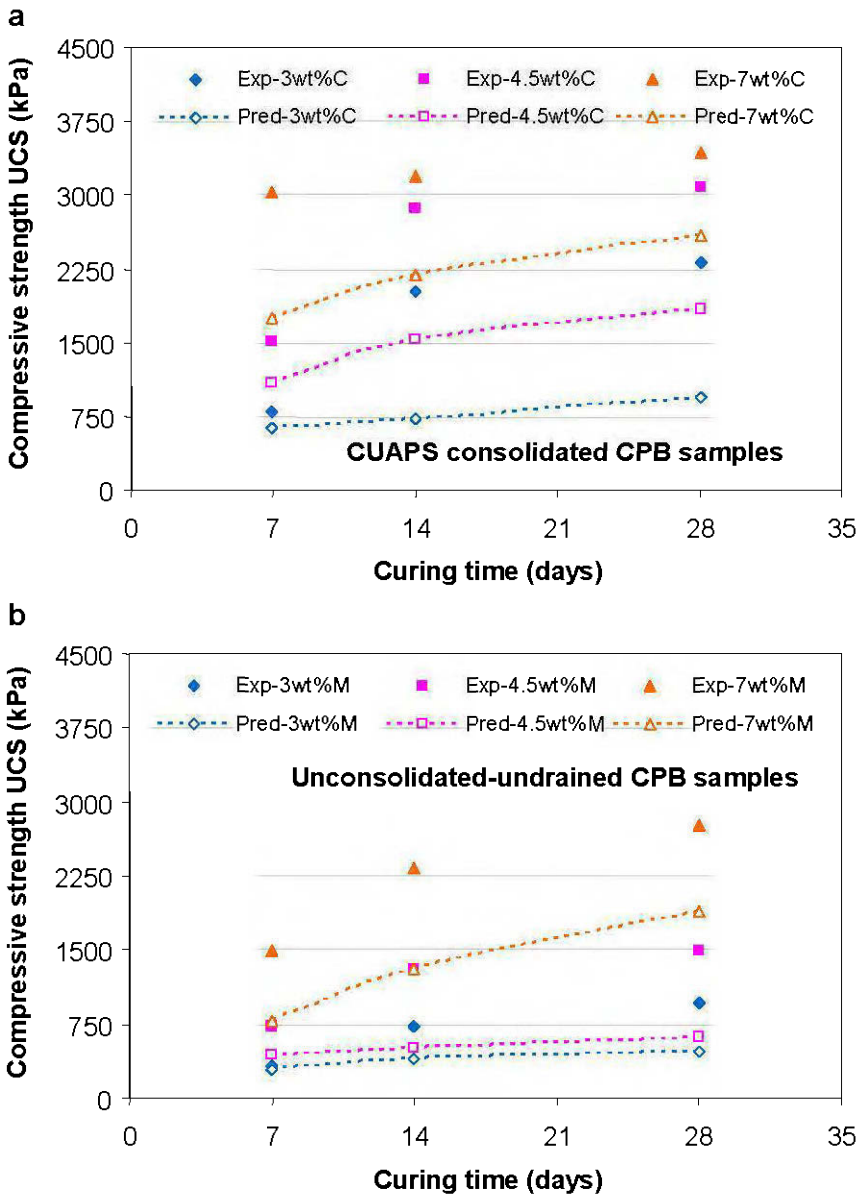

G.10 Change in UCS with curing time for (a) CUAPS-consolidated and (b) mould-undrained CPB samples as a function of binder content (3, 4.5 and 7 wt%) compared to predicted UCS values using Ouellet et al.'s model (2007).

APPENDIX H

SUMMARY OF SEM-EDS (SCANNING ELECTRON MICROSCOPY WITH ENERGY DISPERSIVE X-RAY SPECTROSCOPY) RESULTS

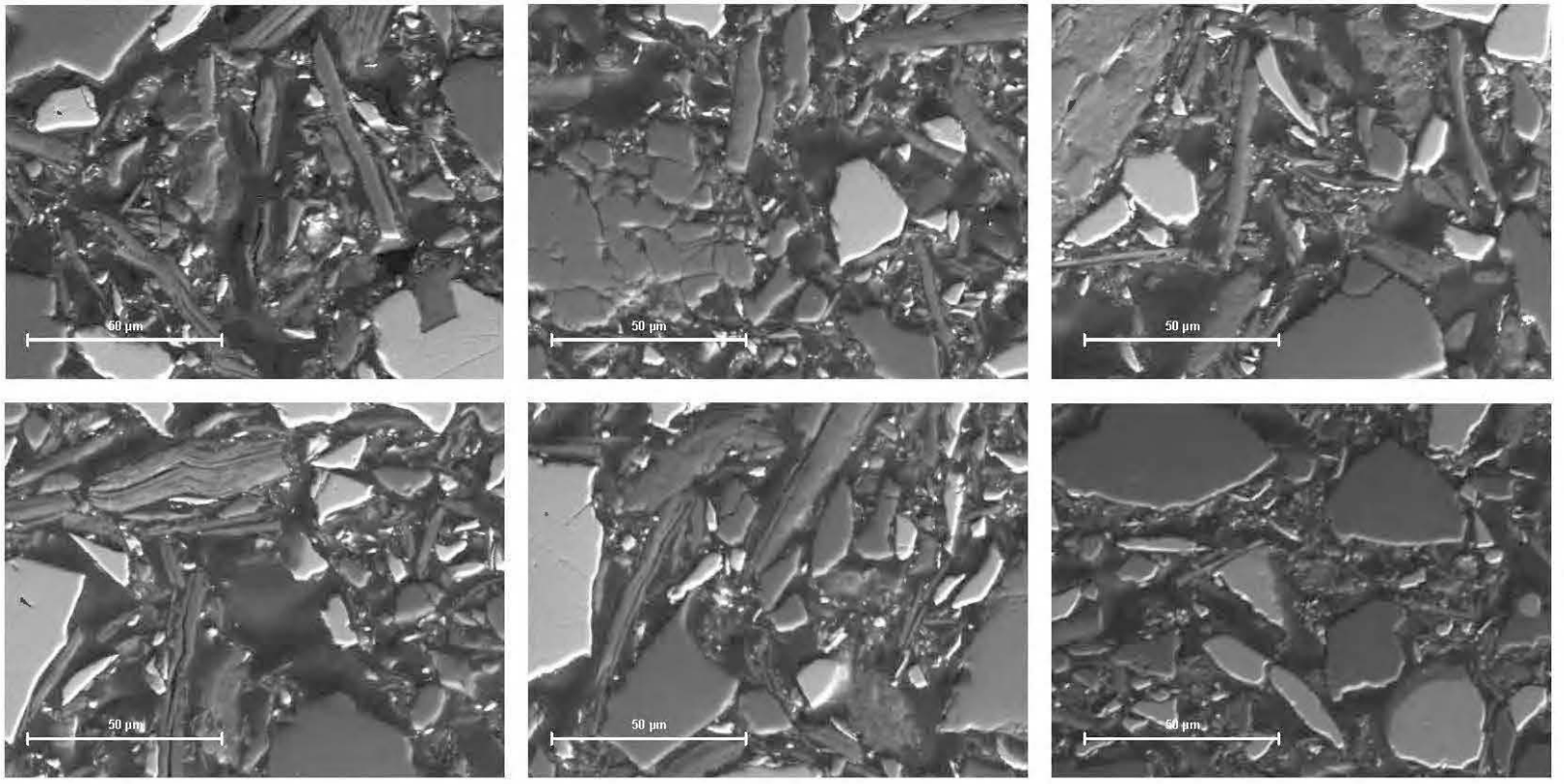

H.1 Scanning electron microscopy (SEM) micrographs of the polished section of uncemented mine tailings.

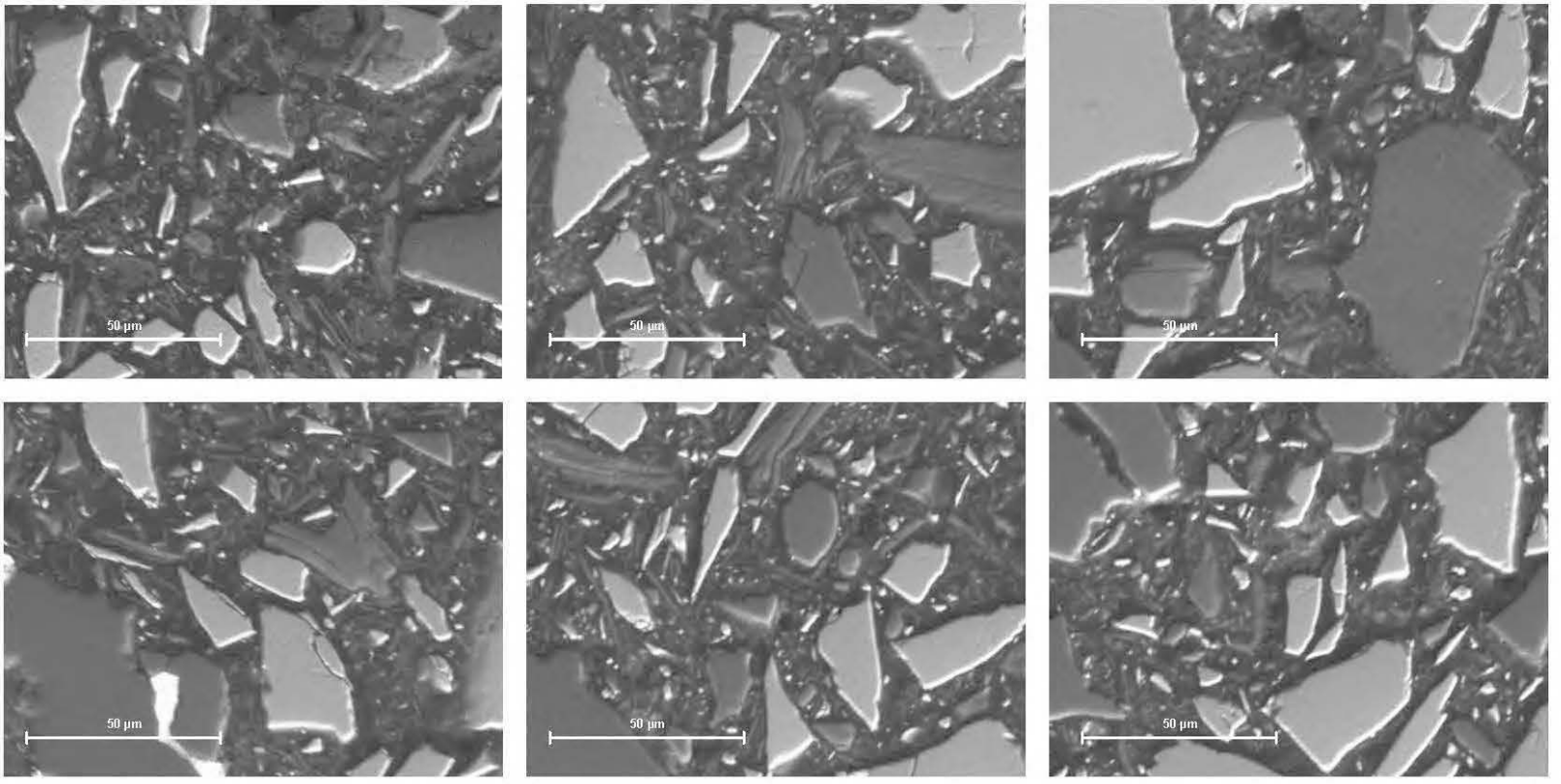

H.2 Scanning electron microscopy (SEM) micrographs of the polished section of conventional plastic mould-CPB samples prepared with GU@100 wt% and cured under no applied pressure during curing. Samples contain a binder content of 4.5 wt% and show a curing time of 28 days.

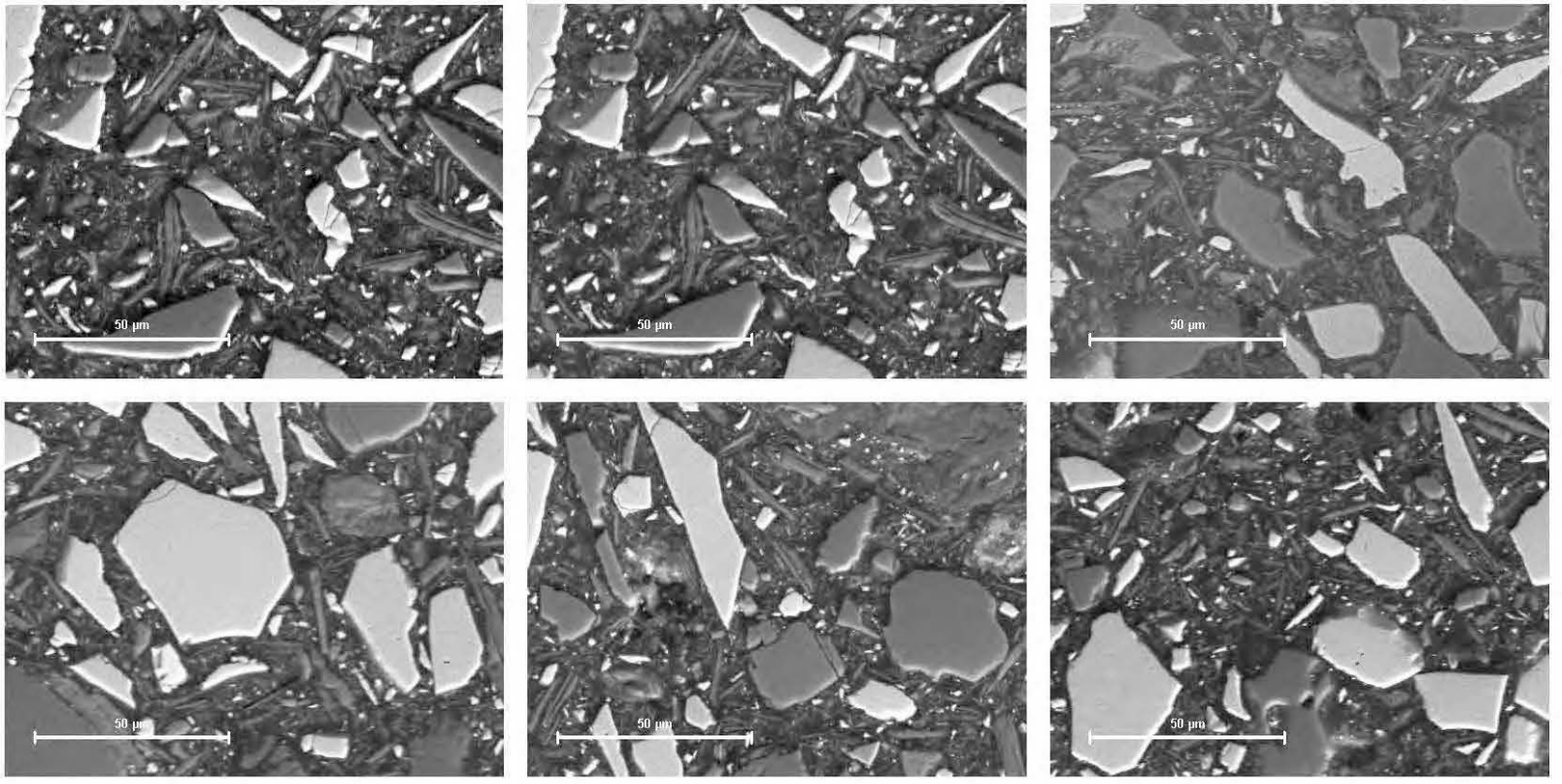

H.3 Scanning electron microscopy (SEM) micrographs of the polished section of CUAPS-consolidated CPB samples prepared with GU@100 wt% and cured under an applied pressure of 400 kPa during curing. Samples contain a binder content of 4.5 wt% and show a curing time of 28 days.

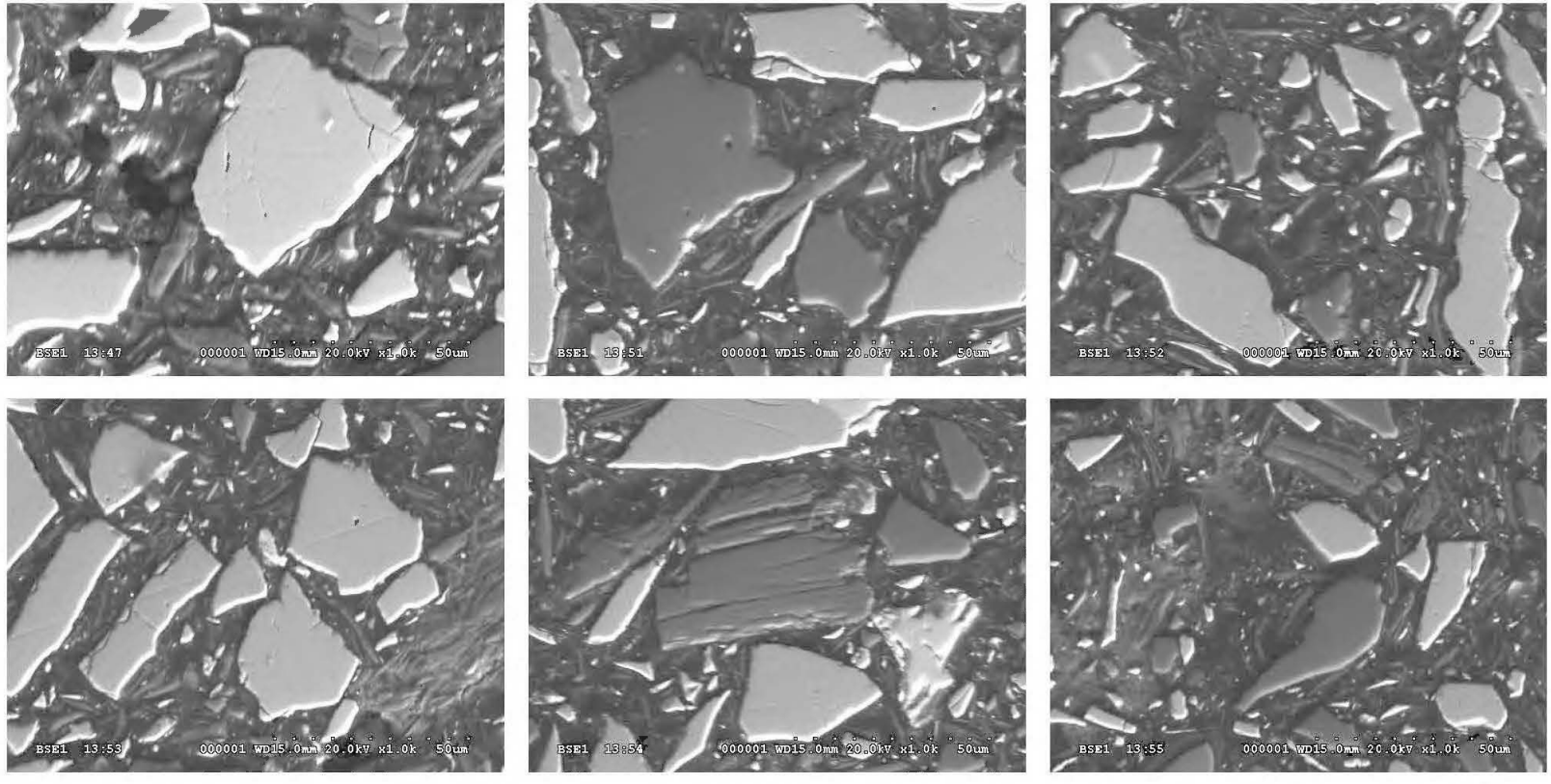

H.4 Scanning electron microscopy (SEM) micrographs of the polished section of conventional plastic mould-CPB samples prepared with GU-Slag@20:80 wt% and cured under no applied pressure during curing. Samples contain a binder content of 4.5 wt% and show a curing time of 28 days.

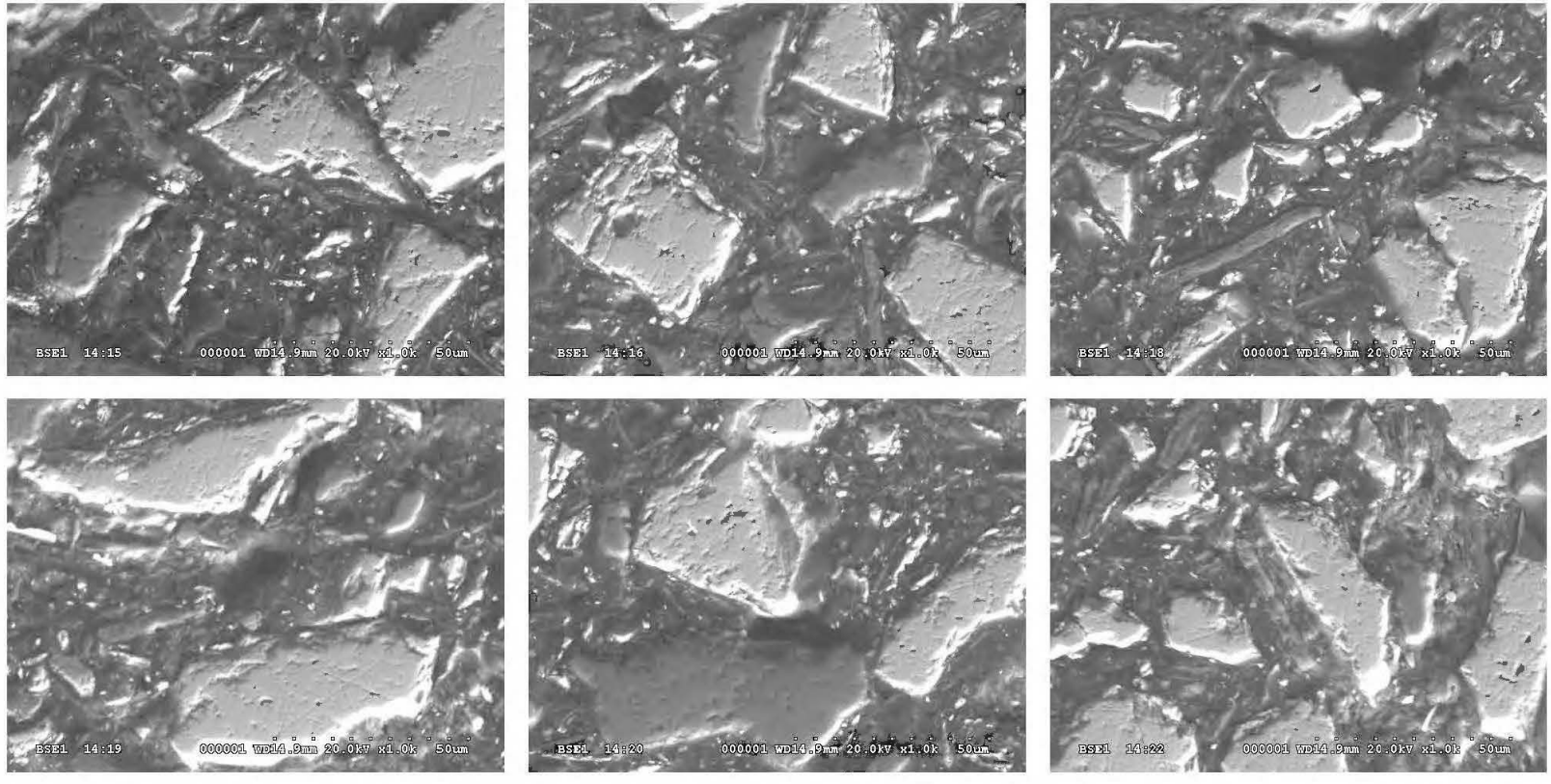

H.5 Scanning electron microscopy (SEM) micrographs of the polished section of CUAPS-consolidated CPB samples prepared with GU-Slag@20:80 wt% and cured under an applied pressure of 400 kPa during curing. Samples contain a binder content of 4.5 wt% and show a curing time of 28 days.

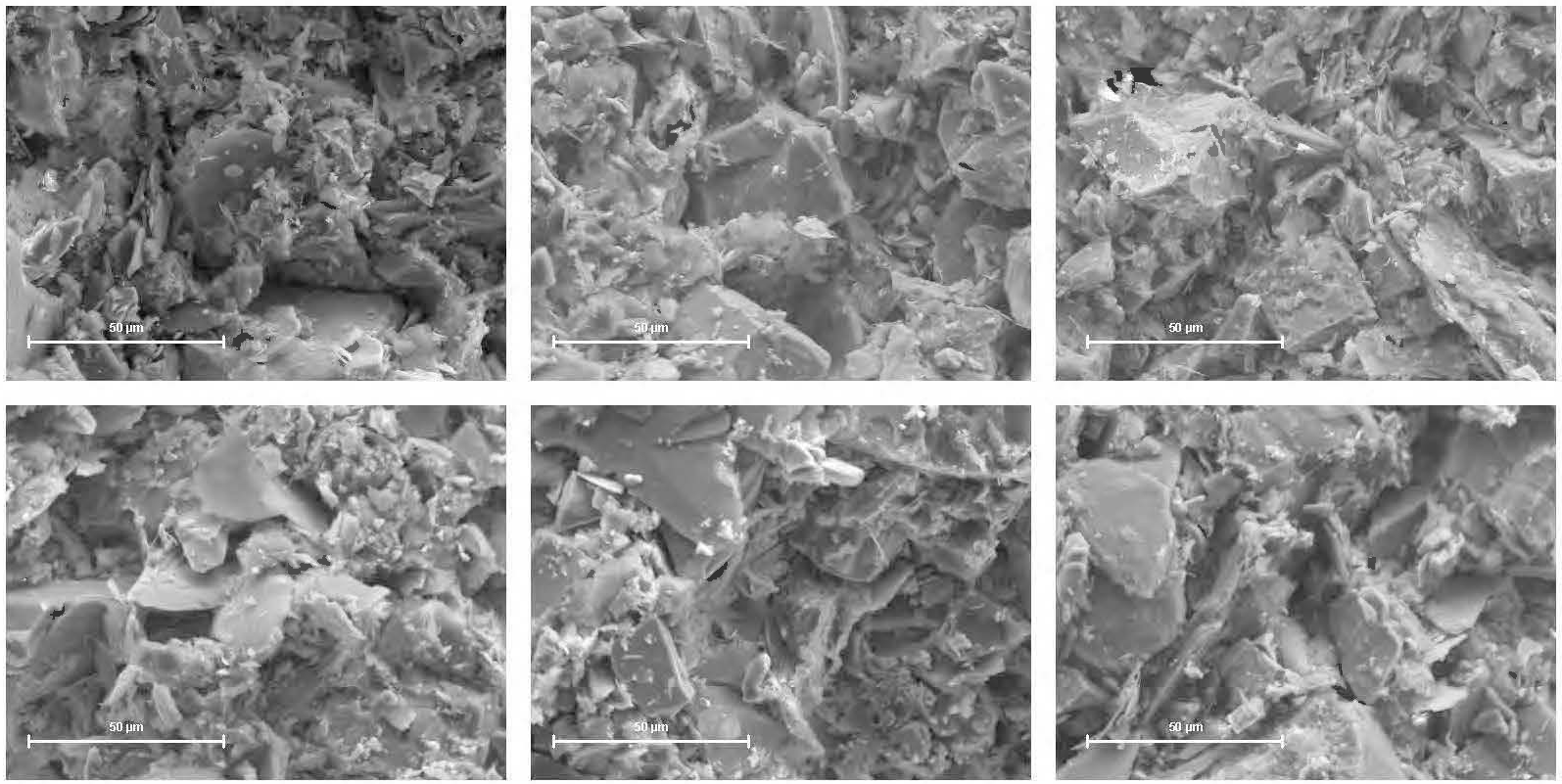

H.6 Scanning electron microscopy (SEM) micrographs of the freshly-fractured surface of uncemented mine tailings.

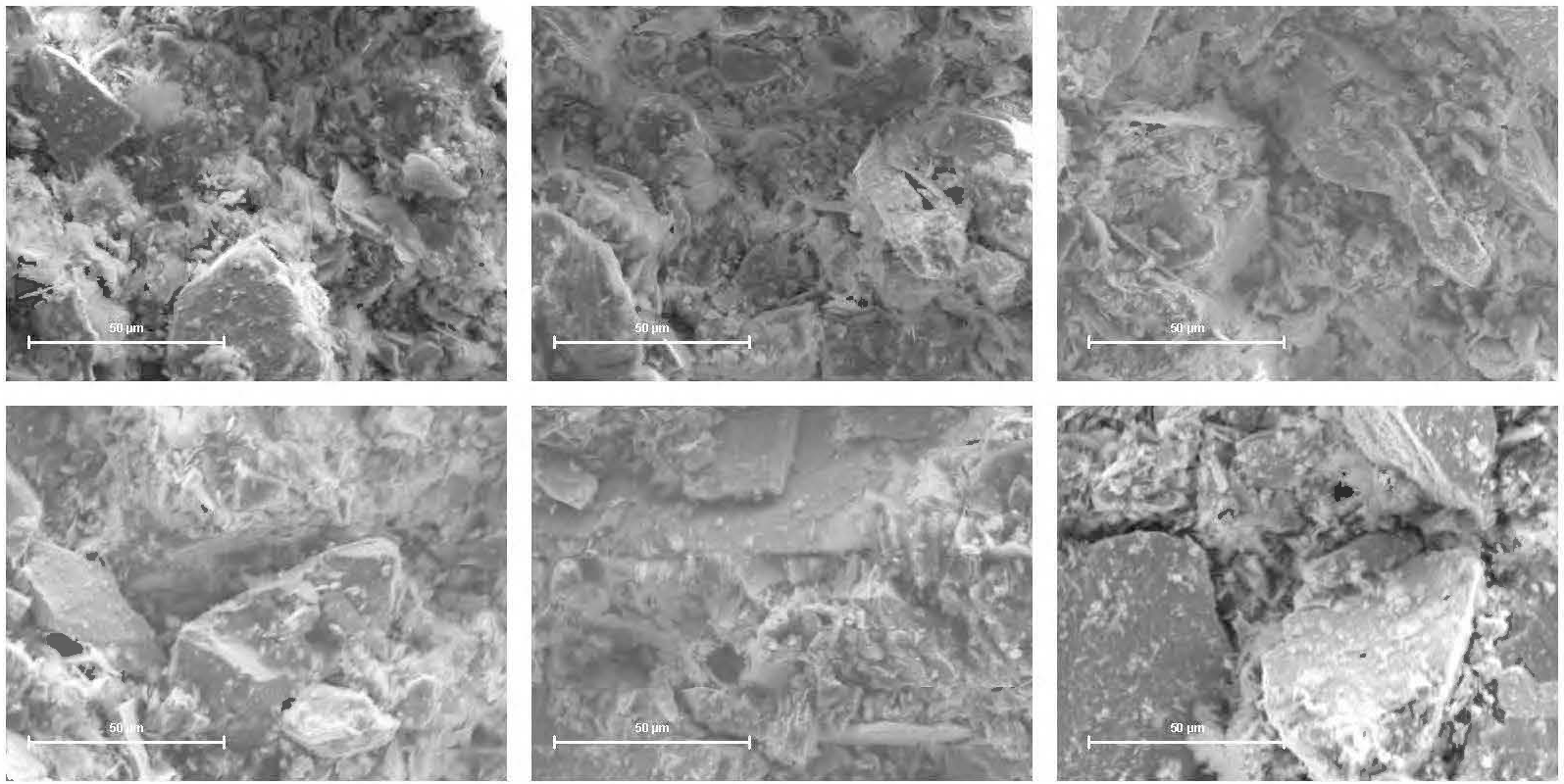

H.7 Scanning electron microscopy (SEM) micrographs of the freshly-fractured surface of conventional plastic mould-CPB samples prepared with GU@100 wt% and cured under no applied pressure during curing. Samples contain a binder content of 4.5 wt% and show a curing time of 28 days.

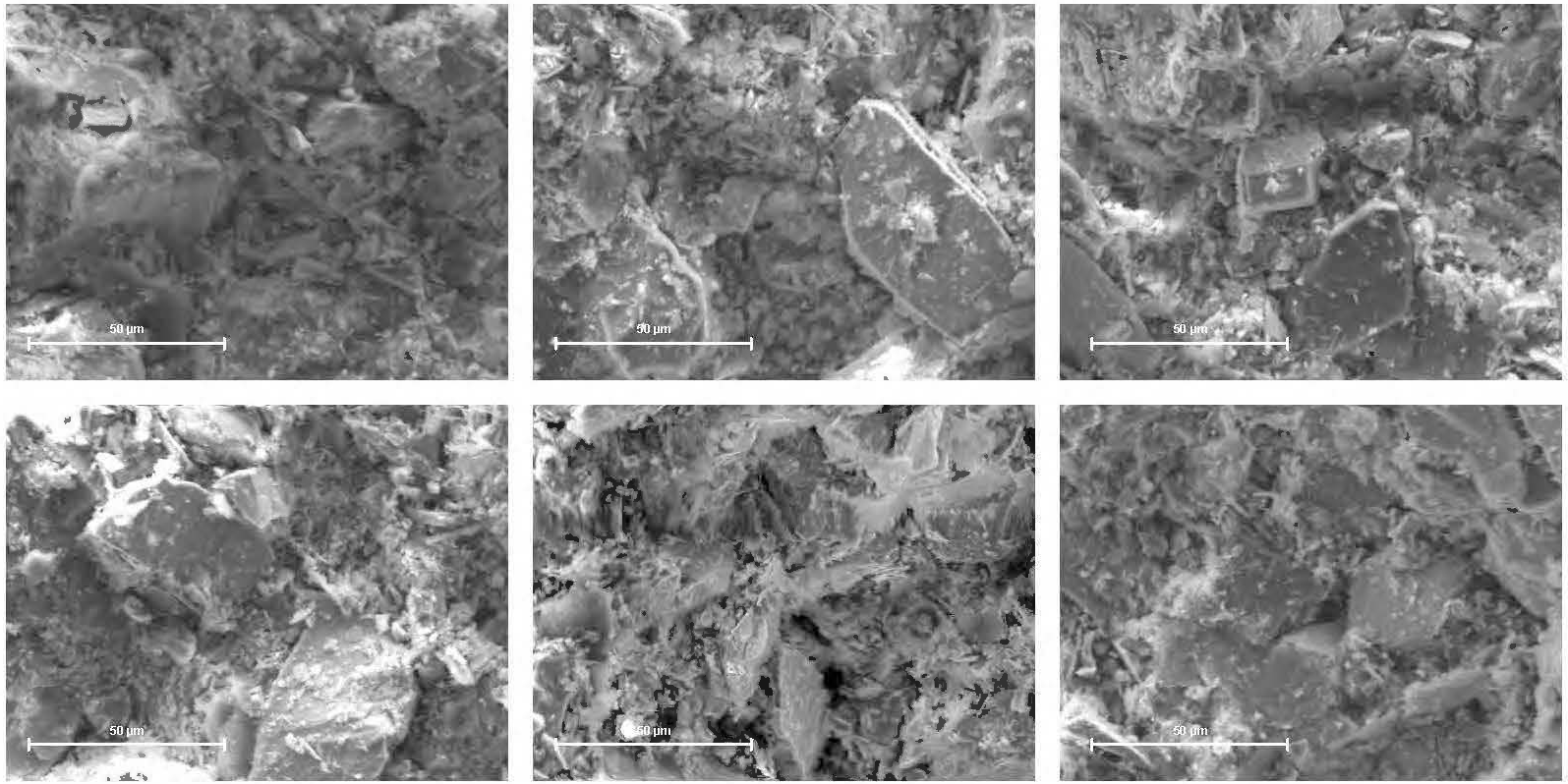

H.8 Scanning electron microscopy (SEM) micrographs of the freshly-fractured surface of CUAPS-consolidated CPB samples prepared with GU@100 wt% and cured under an applied pressure of 400 kPa during curing. Samples contain a binder content of 4.5 wt% and show a curing time of 28 days.

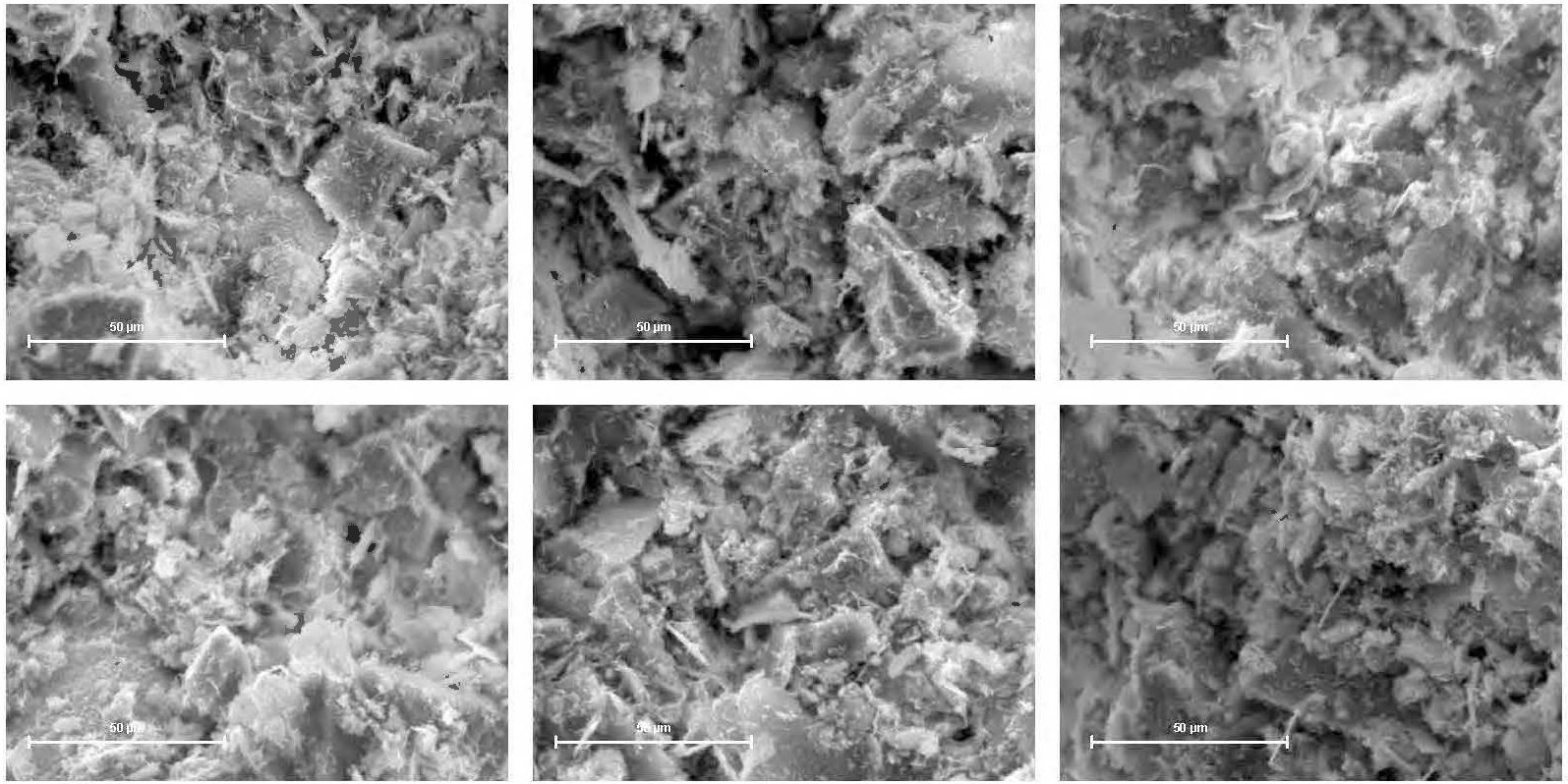

H.9 Scanning electron microscopy (SEM) micrographs of the freshly-fractured surface of conventional plastic mould-CPB samples prepared with GU-Slag@20:80 wt% and cured under no applied pressure during curing. Samples contain a binder content of 4.5 wt% and show a curing time of 28 days.

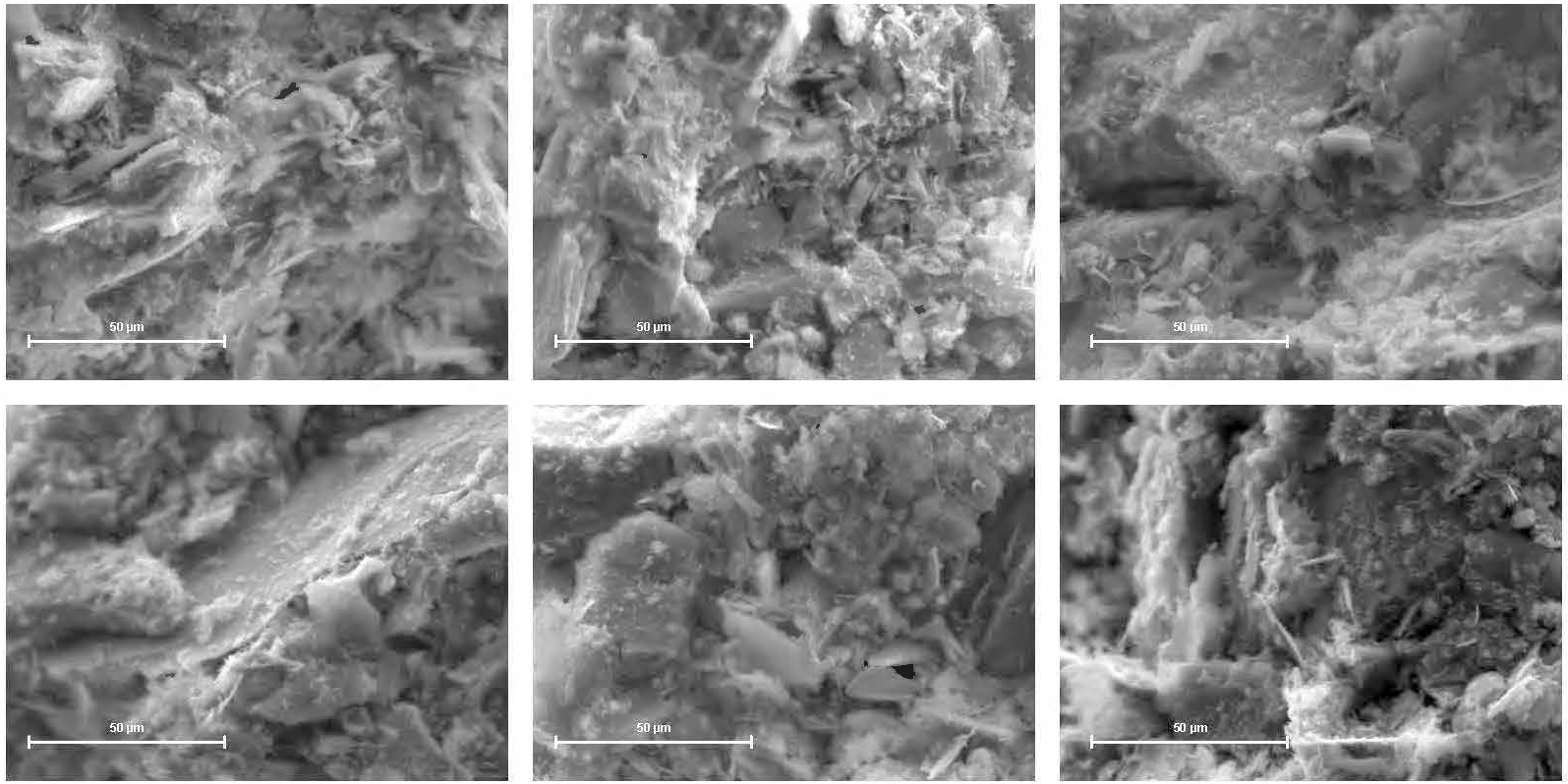

H.10 Scanning electron microscopy (SEM) micrographs of the freshly-fractured surface of CUAPS-consolidated CPB samples prepared with GU-Slag@20:80 wt% and cured under an applied pressure of 400 kPa during curing. Samples contain a binder content of 4.5 wt% and show a curing time of 28 days.

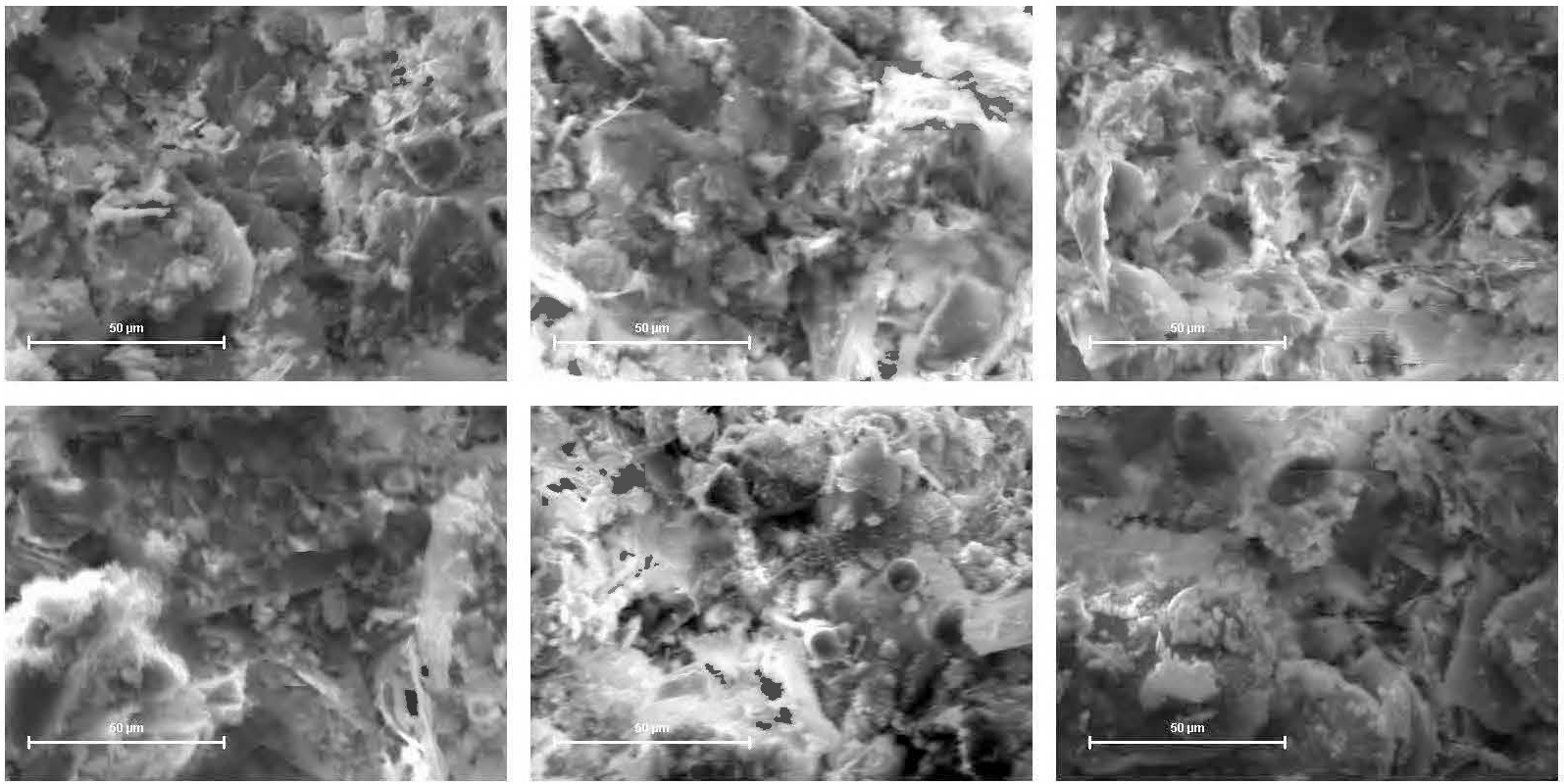

H.11 Scanning electron microscopy (SEM) micrographs of the freshly-fractured surface of conventional plastic mould-CPB samples prepared with GU-FA@40:60 wt% and cured under no applied pressure during curing. Samples contain a binder content of 4.5 wt% and show a curing time of 28 days.

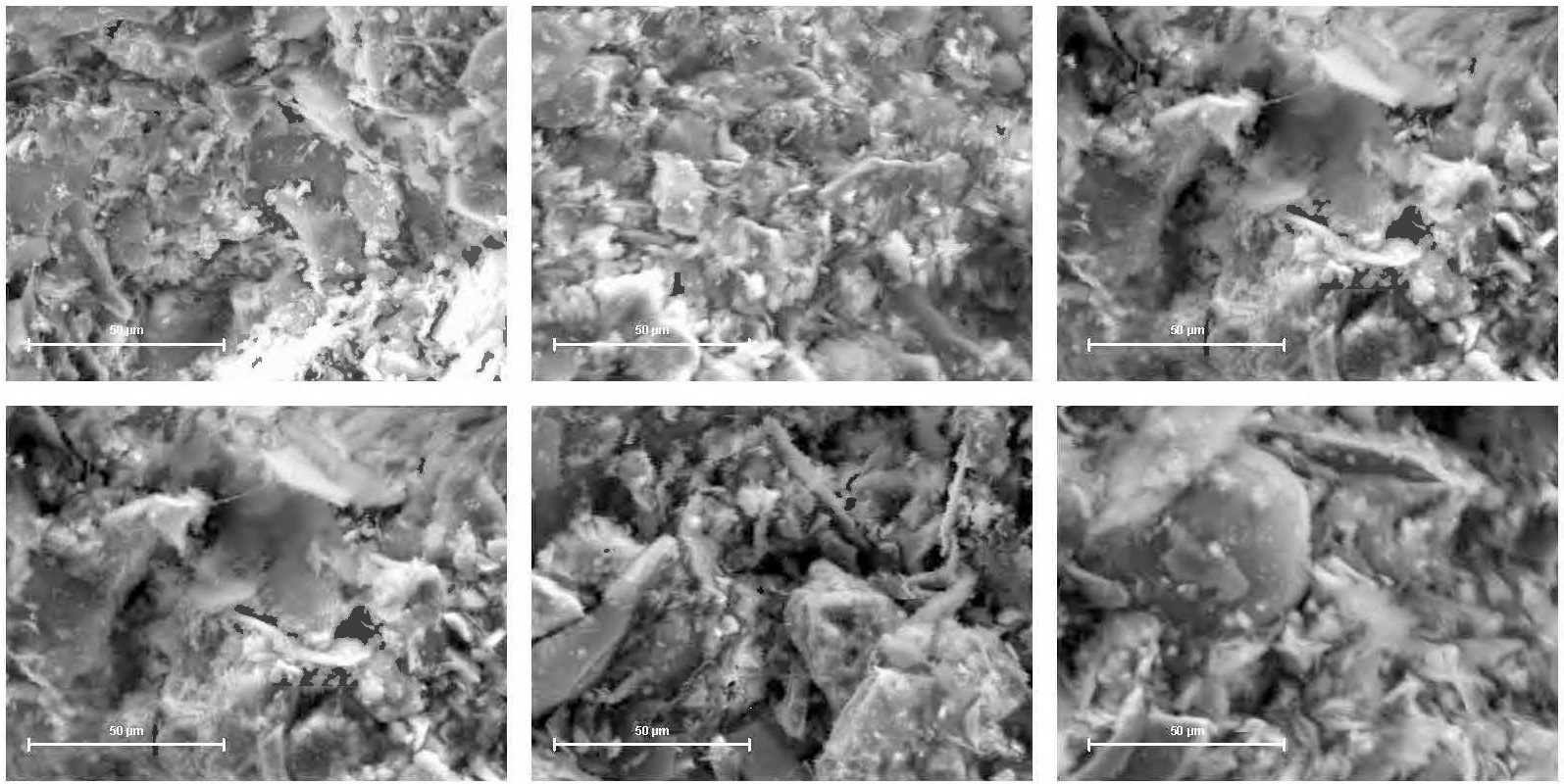

H.12 Scanning electron microscopy (SEM) micrographs of the freshly-fractured surface of CUAPS-consolidated CPB samples prepared with GU-FA@40:60 wt% and cured under an applied pressure of 400 kPa during curing. Samples contain a binder content of 4.5 wt% and show a curing time of 28 days.

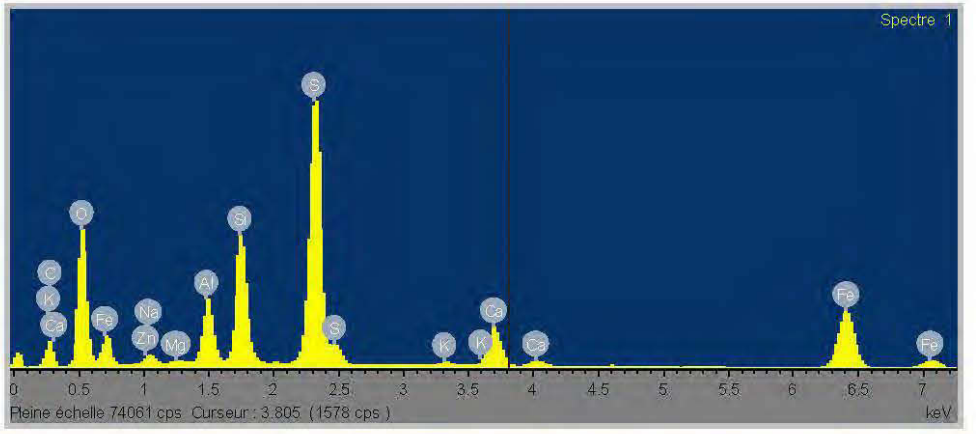

Na	Mg	Al	Si	S	K	Ca	Fe	Cu	Zn	Pb	Ca/Si
1.4	0.26	5.67	16.5	16.86	0.64	0.58	13.71	2.02	1.85	0.57	4%

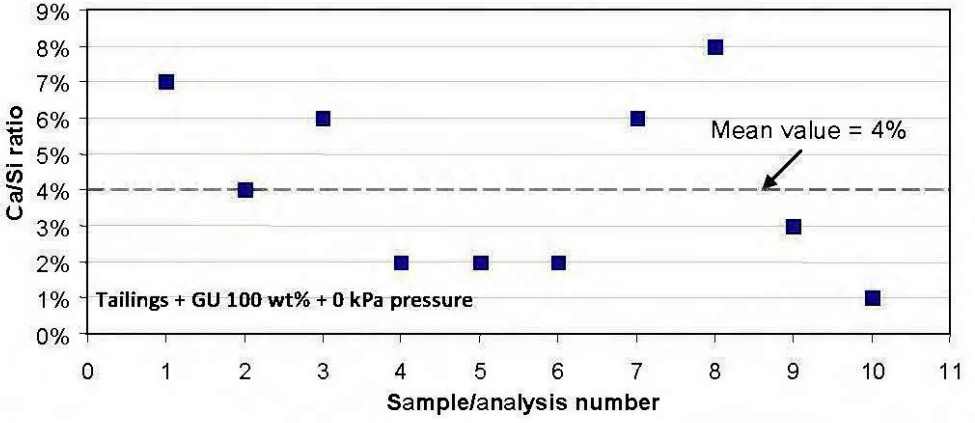

H.13 Energy dispersive X-ray spectroscopy (EDS) analysis and Ca/Si ratio curve of the freshly-fractured surface of uncemented mine tailings.

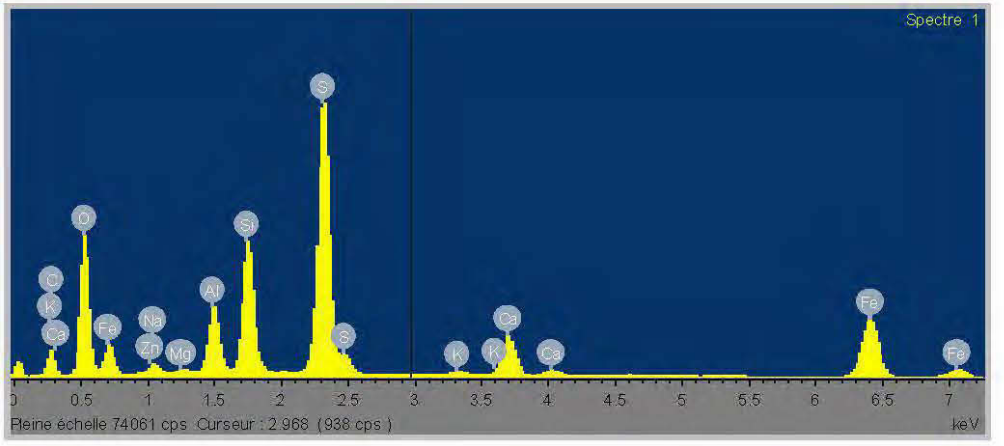

Na	Mg	Al	Si	S	K	Ca	Fe	Cu	Zn	Pb	Ca/Si
1.37	0.5	6.17	11	16.9	0.59	4.96	15.81	0	0.52	0.37	45%

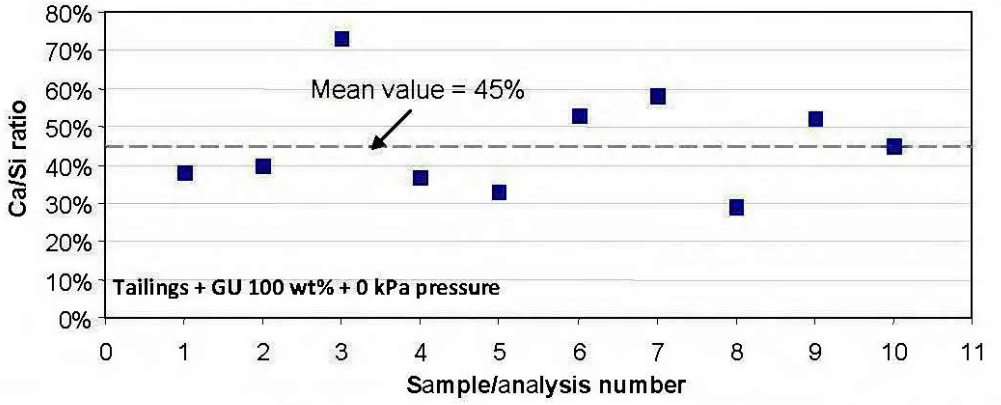

H.14 Energy dispersive X-ray spectroscopy (EDS) analysis and Ca/Si ratio curve of the freshly-fractured surface of conventional plastic mould-CPB samples prepared with GU@100 wt% and cured under no applied pressure during curing. Samples contain a binder content of 4.5 wt% and show a curing time of 28 days.

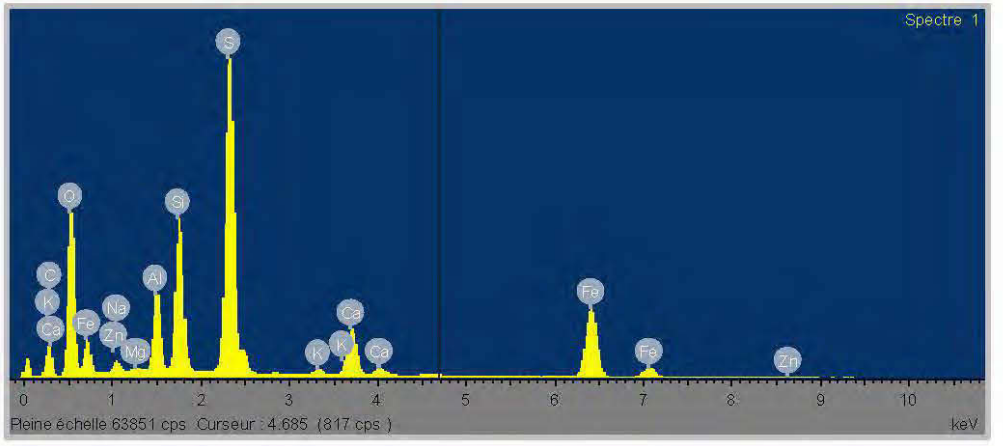

Na	Mg	Al	Si	S	K	Ca	Fe	Cu	Zn	Pb	Ca/Si
1.65	0.48	6.65	11	15.19	0.41	4.54	16.92	0.03	0.96	0.21	41%

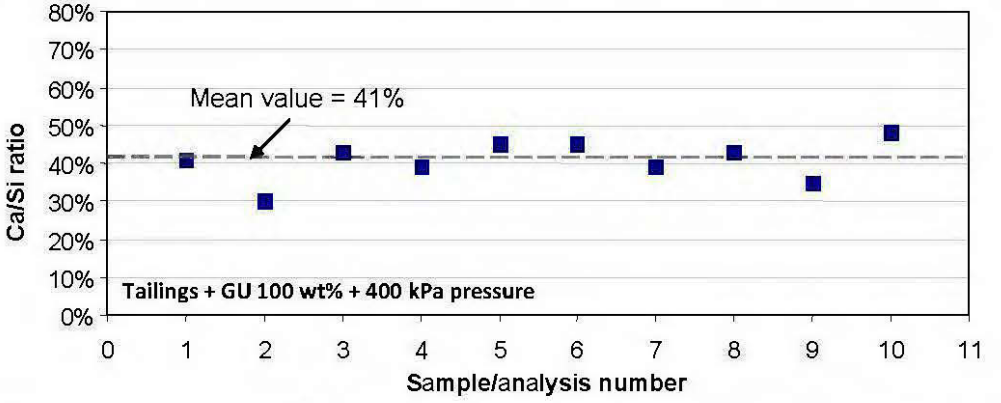

H.15 Energy dispersive X-ray spectroscopy (EDS) analysis and Ca/Si ratio curve of the freshly-fractured surface of CUAPS-consolidated CPB samples prepared with GU@100 wt% and cured under an applied pressure of 400 kPa during curing. Samples contain a binder content of 4.5 wt% and show a curing time of 28 days.

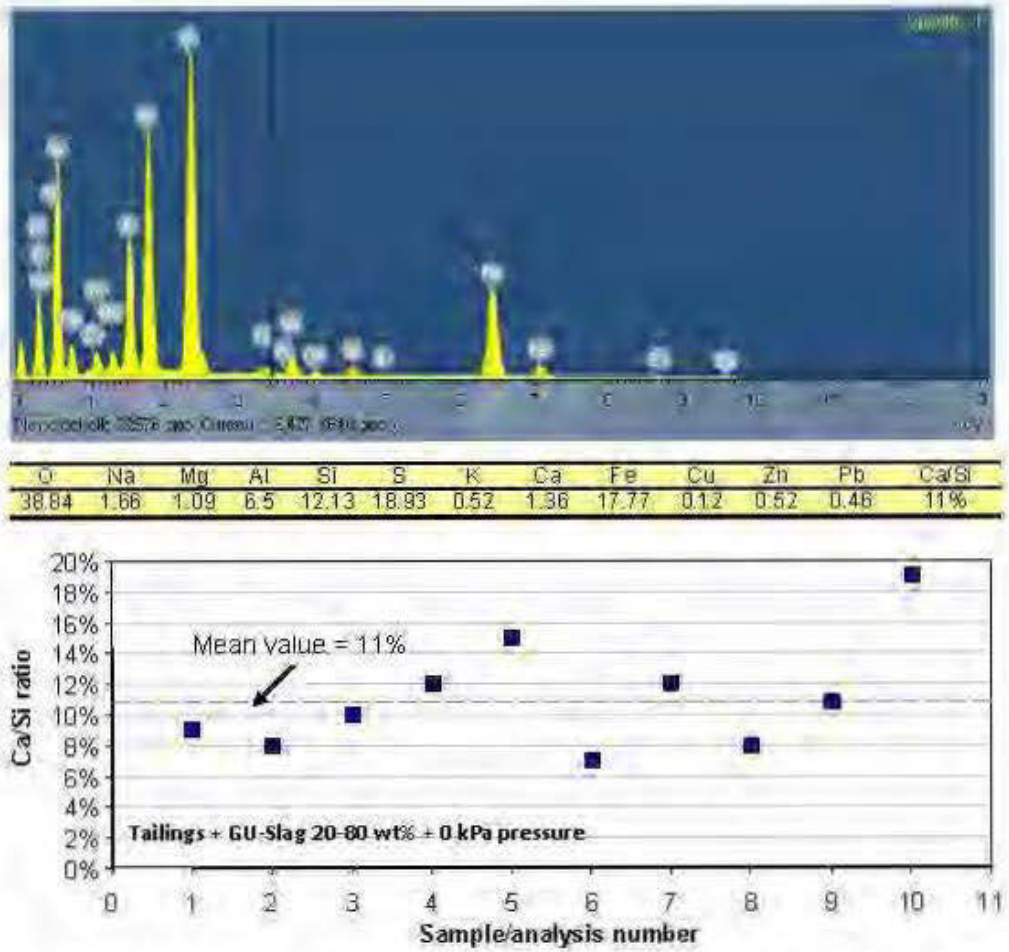

H.16 Energy dispersive X-ray spectroscopy (EDS) analysis and Ca/Si ratio curve of the freshly-fractured surface of conventional plastic mould-CPB samples prepared with GU-Slag@20:80 wt% and cured under no applied pressure during curing. Samples contain a binder content of 4.5 wt% and show a curing time of 28 days.

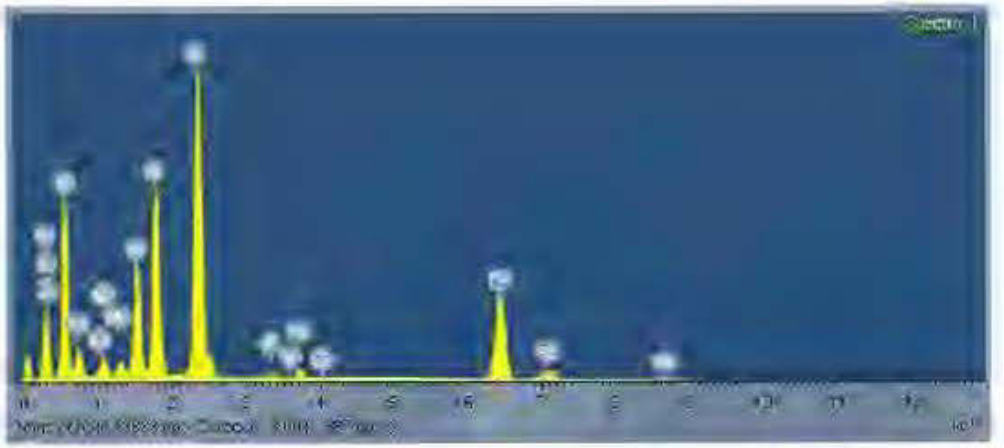

O	Na	Mg	Al	Si	S	K	Ca	Fe	Cu	Zn	Pb	Ca/Si
38.11	1.66	0.92	6.31	11.08	21.2	0.44	0.7	19.15	0.02	0.43	0.02	6%

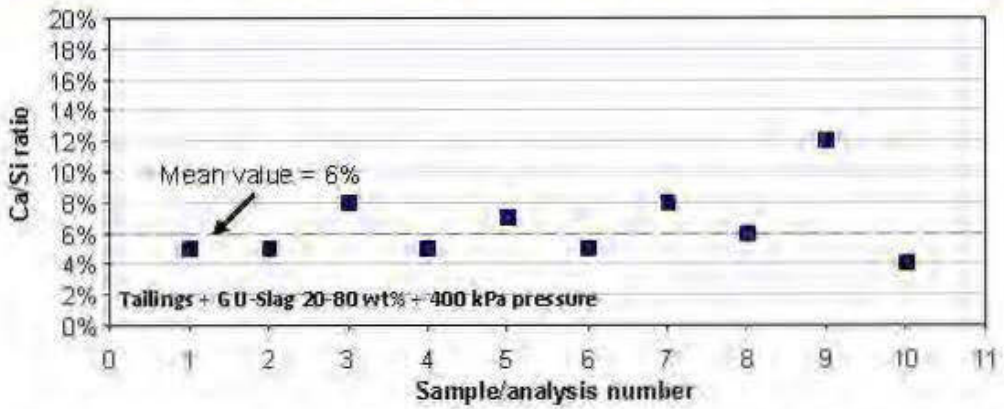

H.17 Energy dispersive X-ray spectroscopy (EDS) analysis and Ca/Si ratio curve of the freshly-fractured surface of CUAPS-consolidated CPB samples prepared with GU-Slag@20:80 wt% and cured under an applied pressure of 400 kPa during curing. Samples contain a binder content of 4.5 wt% and show a curing time of 28 days.

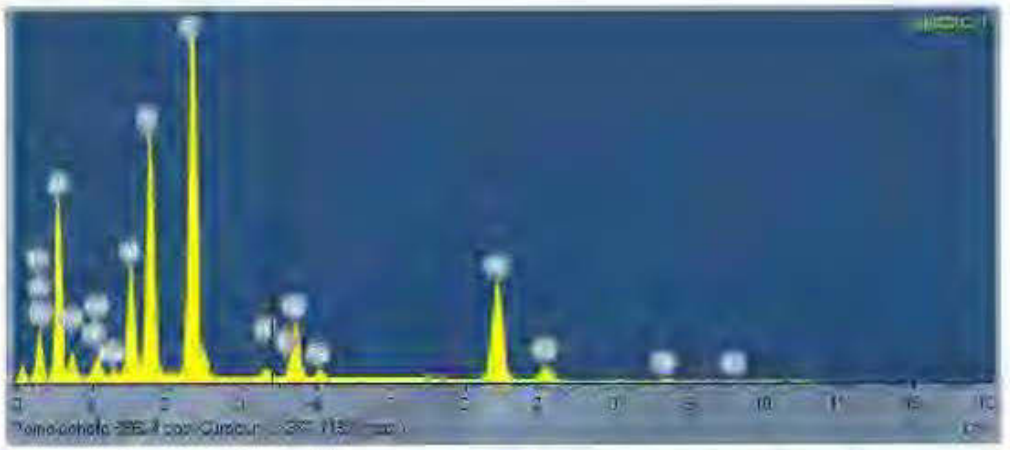

O	Na	Mg	Al	Si	S	K	Ca	Fe	Cu	Zn	Pb	Ca/Si
36.99	1.64	0.21	5.22	11.7	20	0.57	4.43	18.72	0.11	0.53	0.19	38%

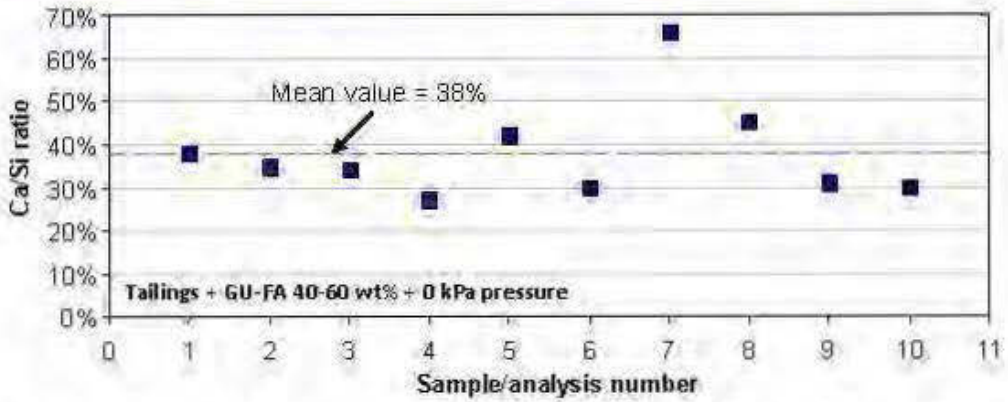

H.18 Energy dispersive X-ray spectroscopy (EDS) analysis and Ca/Si ratio curve of the freshly-fractured surface of conventional plastic mould-CPB samples prepared with GU-FA@40:60 wt% and cured under no applied pressure during curing. Samples contain a binder content of 4.5 wt% and show a curing time of 28 days.

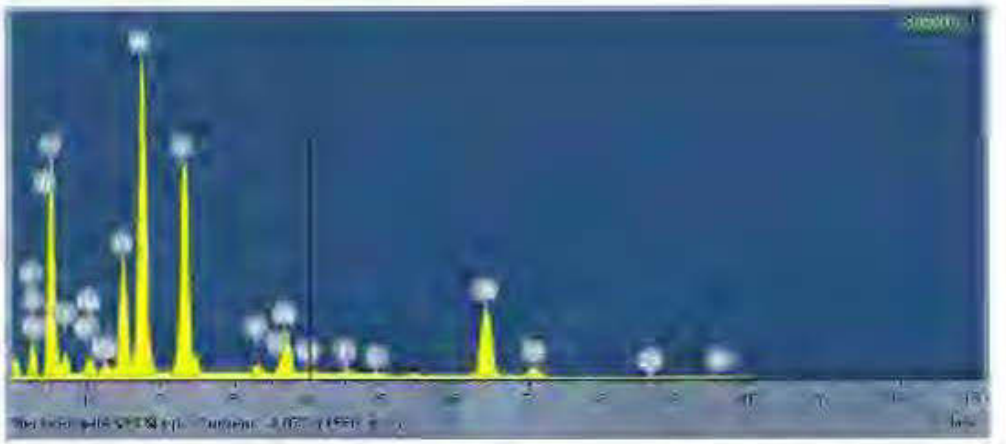

O	Na	Mg	Al	Si	S	K	Ca	Fe	Cu	Zn	Pb	Ca/Si
43.52	1.27	0.4	5.73	16.48	13.22	0.6	3.58	14.34	0.01	0.44	0.52	22%

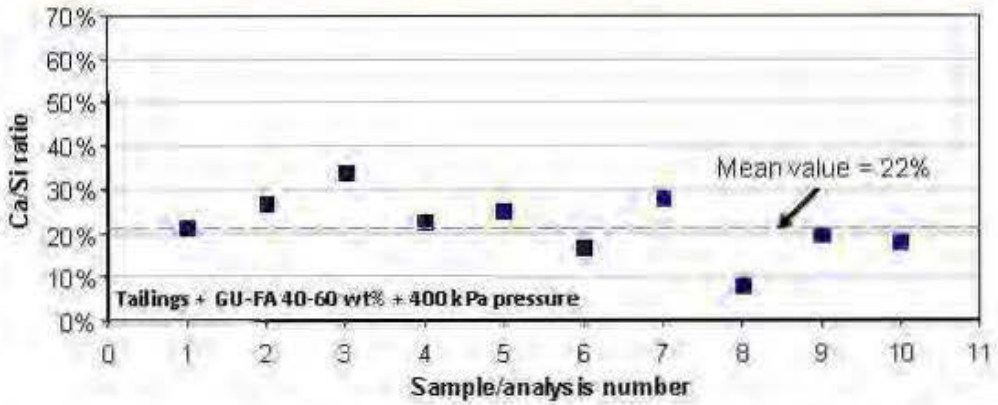

H.19 Energy dispersive X-ray spectroscopy (EDS) analysis and Ca/Si ratio curve of the freshly-fractured surface of CUAPS-consolidated CPB samples prepared with GU-FA@40:60 wt% and cured under an applied pressure of 400 kPa during curing. Samples contain a binder content of 4.5 wt% and show a curing time of 28 days.

APPENDIX I

SUMMARY OF QUANTITATIVE X-RAY DIFFRACTION (XRD) ANALYSIS USING THE RIETVETD FULL-PATTERN FITTING METHOD

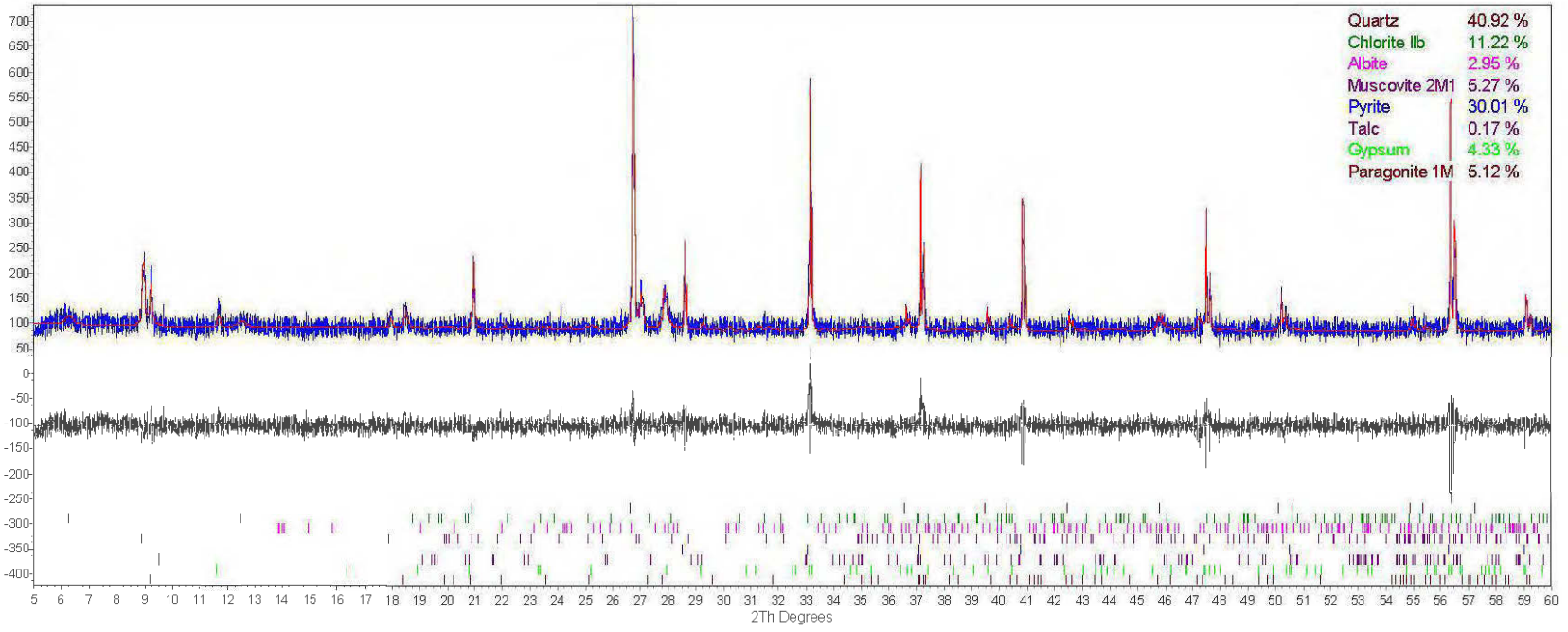

I.1 X-ray diffraction diffractograms of uncemented mine tailings.

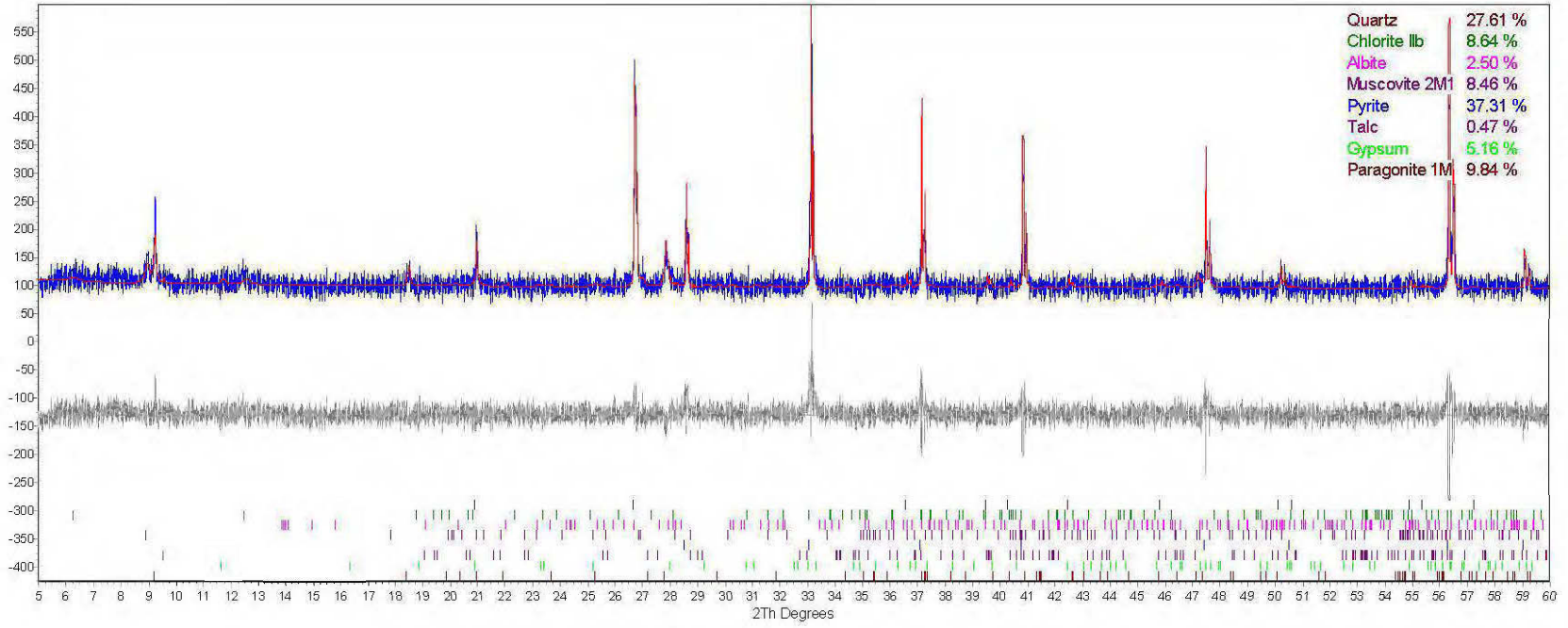

I.2 X-ray diffraction diffractograms of conventional plastic mould-CPB samples prepared with GU@100 wt% and cured under no applied pressure during curing. Samples contain a binder content of 4.5 wt% and show a curing time of 28 days.

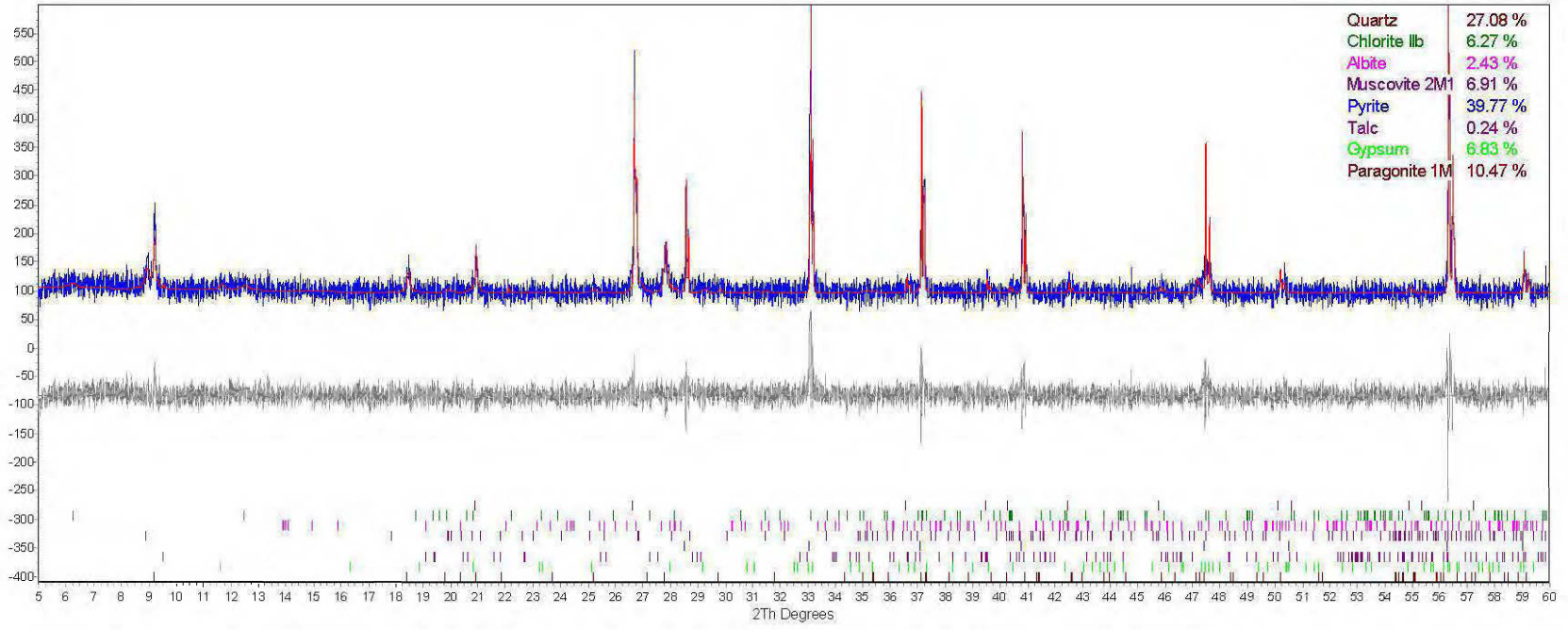

I.3 X-ray diffraction diffractograms of CUAPS-consolidated CPB samples prepared with GU@100 wt% and cured under an applied pressure of 400 kPa during curing. Samples contain a binder content of 4.5 wt% and show a curing time of 28 days.

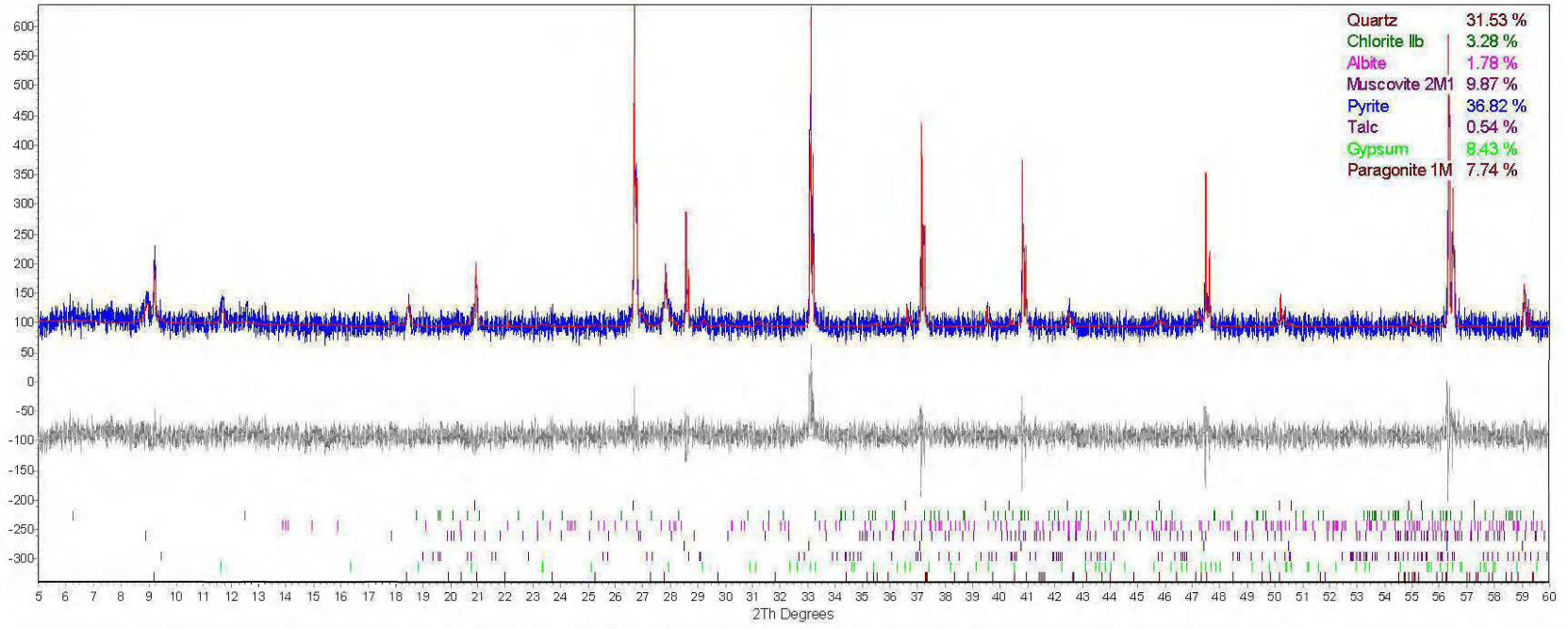

I.4 X-ray diffraction diffractograms of conventional plastic mould-CPB samples prepared with GU-Slag@20:80 wt% and cured under no applied pressure during curing. Samples contain a binder content of 4.5 wt% and show a curing time of 28 days.

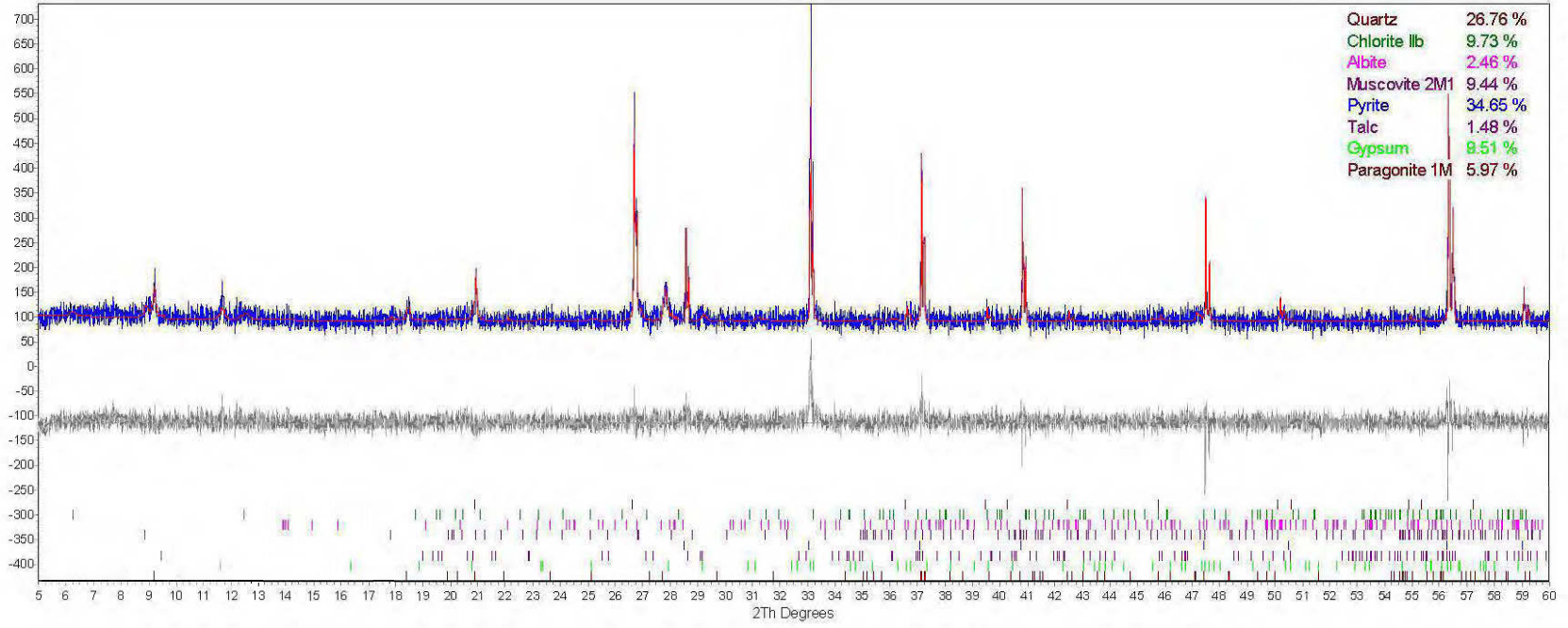

I.5 X-ray diffraction diffractograms of CUAPS-consolidated CPB samples prepared with GU-Slag@20:80 wt% and cured under an applied pressure of 400 kPa during curing. Samples contain a binder content of 4.5 wt% and show a curing time of 28 days.

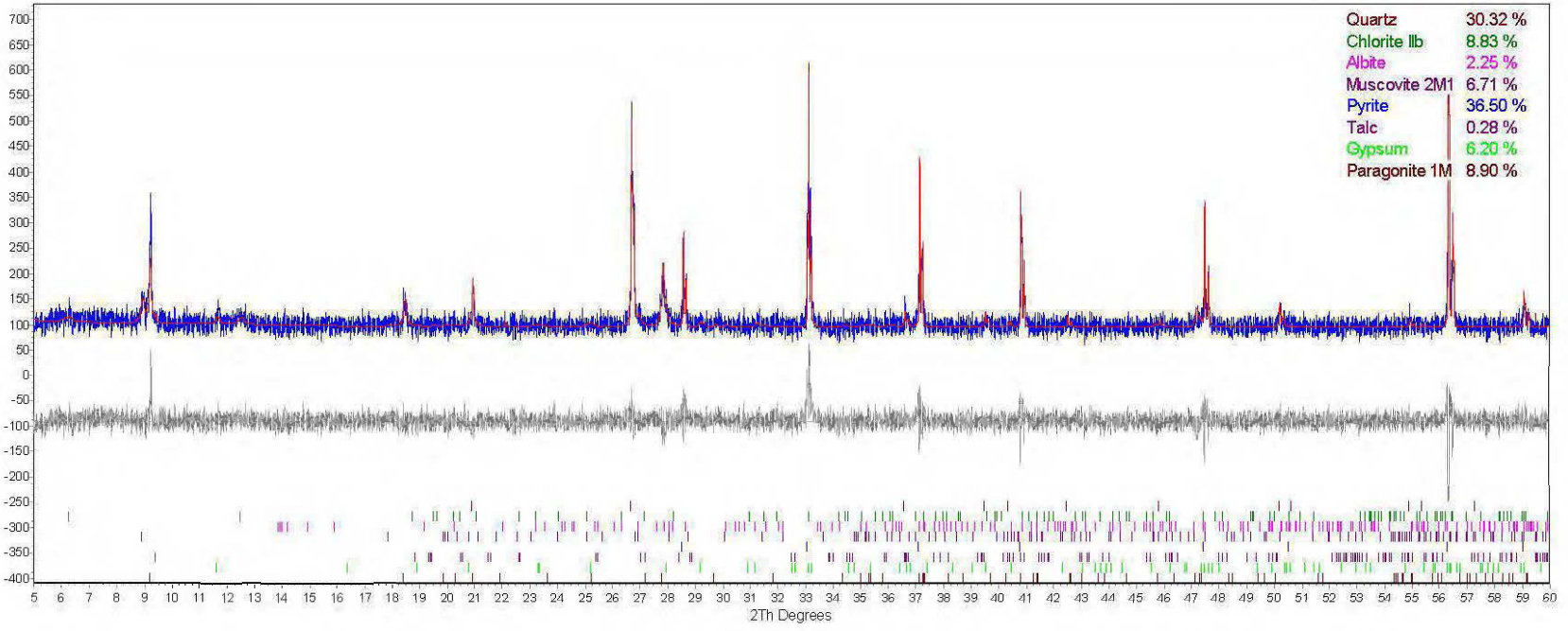

I.6 X-ray diffraction diffractograms of conventional plastic mould-CPB samples prepared with GU-FA@40:60 wt% and cured under no applied pressure during curing. Samples contain a binder content of 4.5 wt% and show a curing time of 28 days.

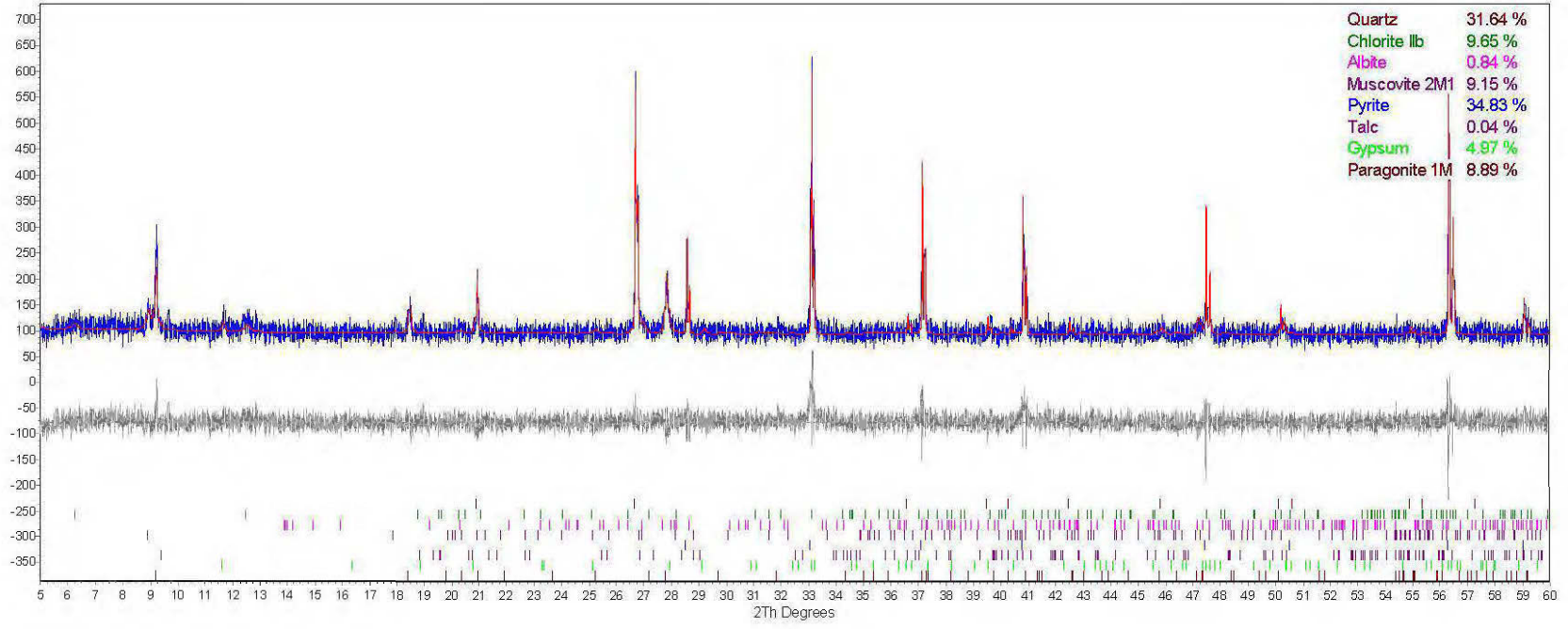

I.7 X-ray diffraction diffractograms of CUAPS-consolidated CPB samples prepared with GU-FA@40:60 wt% and cured under an applied pressure of 400 kPa during curing. Samples contain a binder content of 4.5 wt% and show a curing time of 28 days.

APPENDIX J

LABORATORY EQUIPMENT USED IN THE PH.D. RESEARCH PROJECT AND THESIS

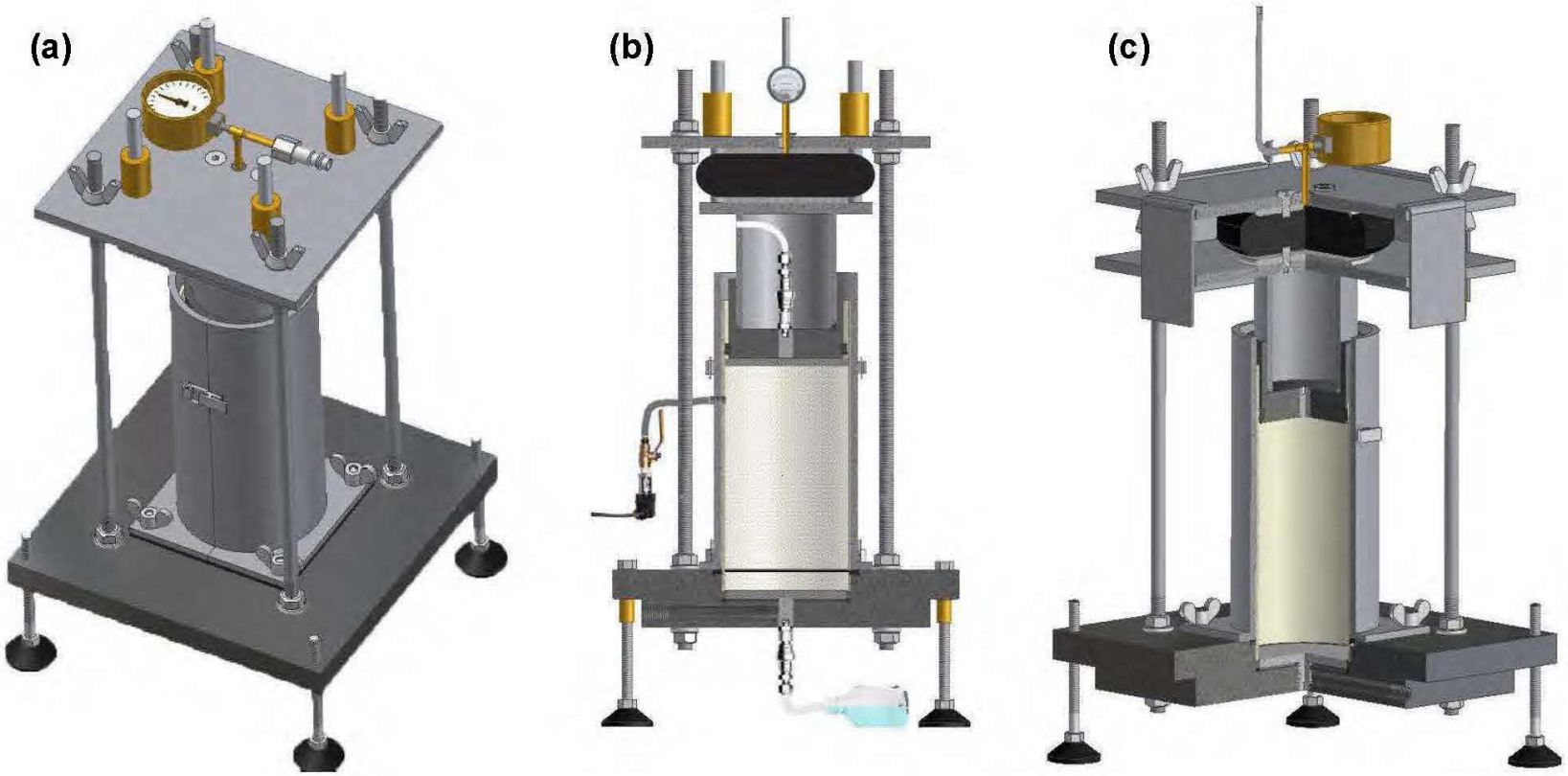

J.1 Schematic illustration of the CUAPS (curing under applied pressure system) apparatus used for consolidation and permeability testing: (a) general view, (b) front view, and (c) internal view.

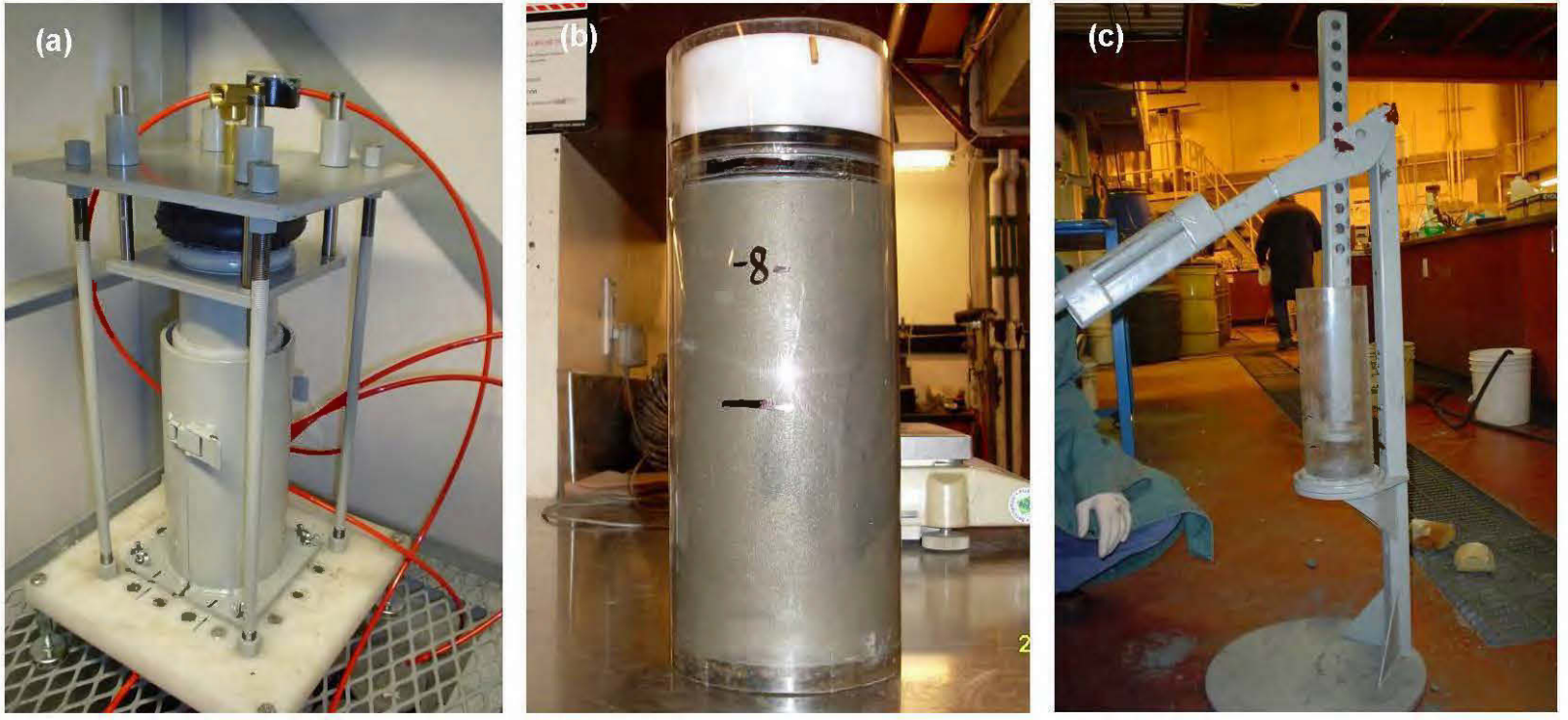

J.2 Photos of (a) the CUAPS apparatus used to characterize in situ properties of laboratory-prepared CPB samples, (b) Perspex cylinder filled with CPB material, showing loading piston, bottom and top porous stones, and (c) its supplementary equipment to extract sample from Perspex moulds filled with CPB material.

J.3 Photos of (a) the HOBART food mixer and (b) the KitchenAid heavy duty mixer for preparing small volume batches and (c) the Mathieu mortar mixer for preparing for large volume batches of paste backfill mixtures.

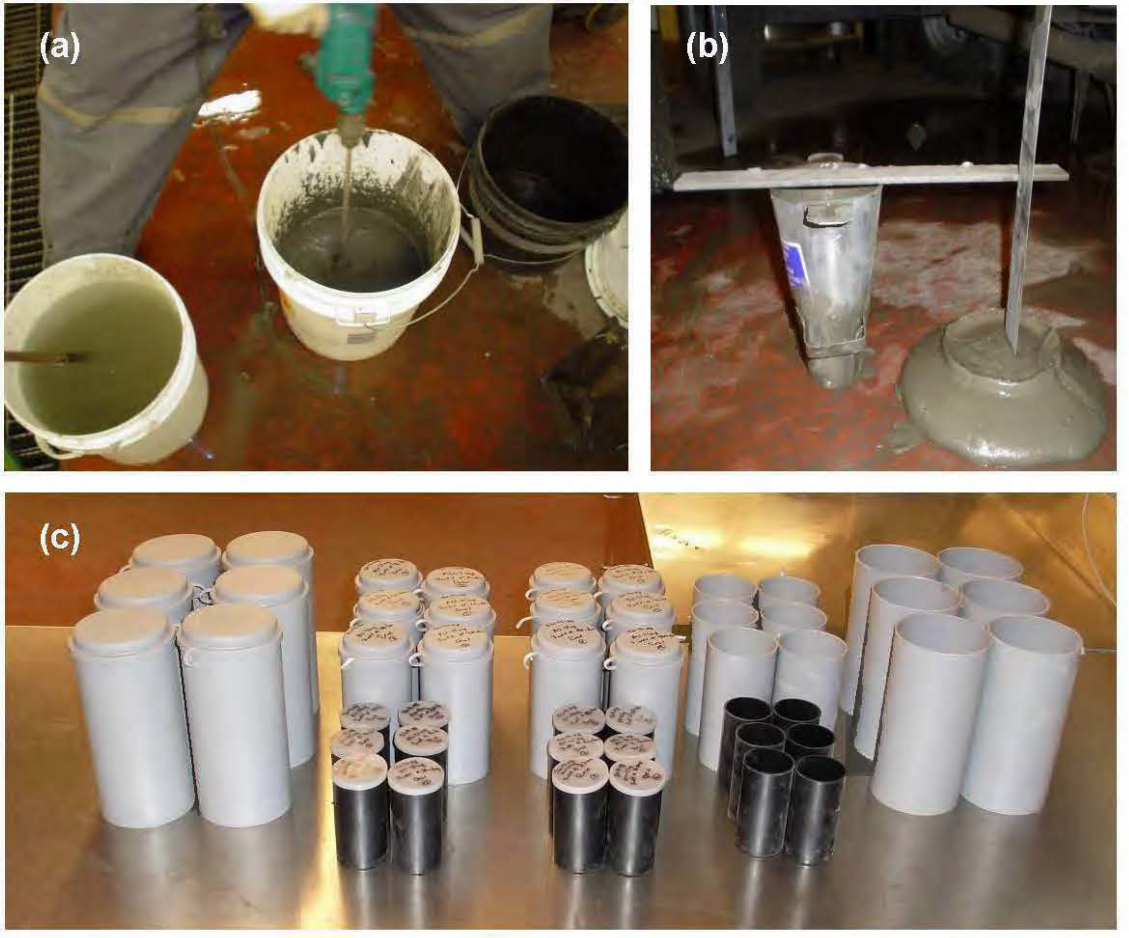

J.4 Photos of (a) an electrical driller with a paint mixer bit in a 20-L pail, (b) the slump test and (c) conventional plastic moulds.

J.5 Photo of the Malvern Mastersizer S200 laser particle size analyzer used to determine the grain size distribution of samples.

J.6 Photo of the Micromeritics AccuPyc 1330 helium pycnometry system used to determine the specific gravity of samples.

J.7 Photo of the Micromeritics Gemini surface analyzer used to determine the specific surface area of samples.

J.8 Photo of the Bruker AXS D8 Advance X-ray diffractometer used to determine the mineralogical composition of samples.

J.9 Photo of the Perkin-Elmer Optima 3100 RL inductively coupled plasma-atomic emission spectroscopy used to determine the chemistry of samples.

J.10 Photo of the Thermolyne Cimarec 2 Stirrer (left) and the Thermo Fisher Scientific Benchtop Orion Model 920A pH/ISE/mV/ORP/Temperature Meter (right).

J.11 Photos of (a) an outside view and (b) inside view of the controlled humidity chamber used to cure paste backfill samples.

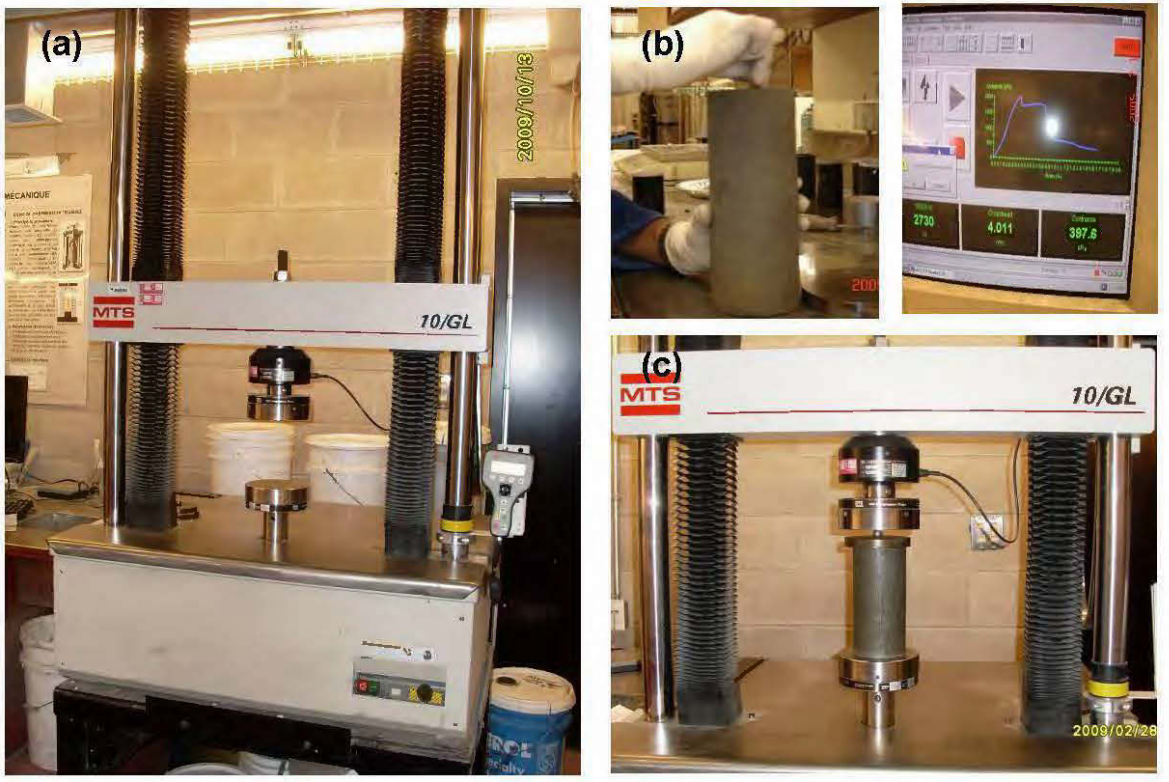

J.12 Photos of (a) the MTS Sintech 10/GL mechanical press, (b) a sample rectification with typical results and (c) paste backfill samples under compression testing.

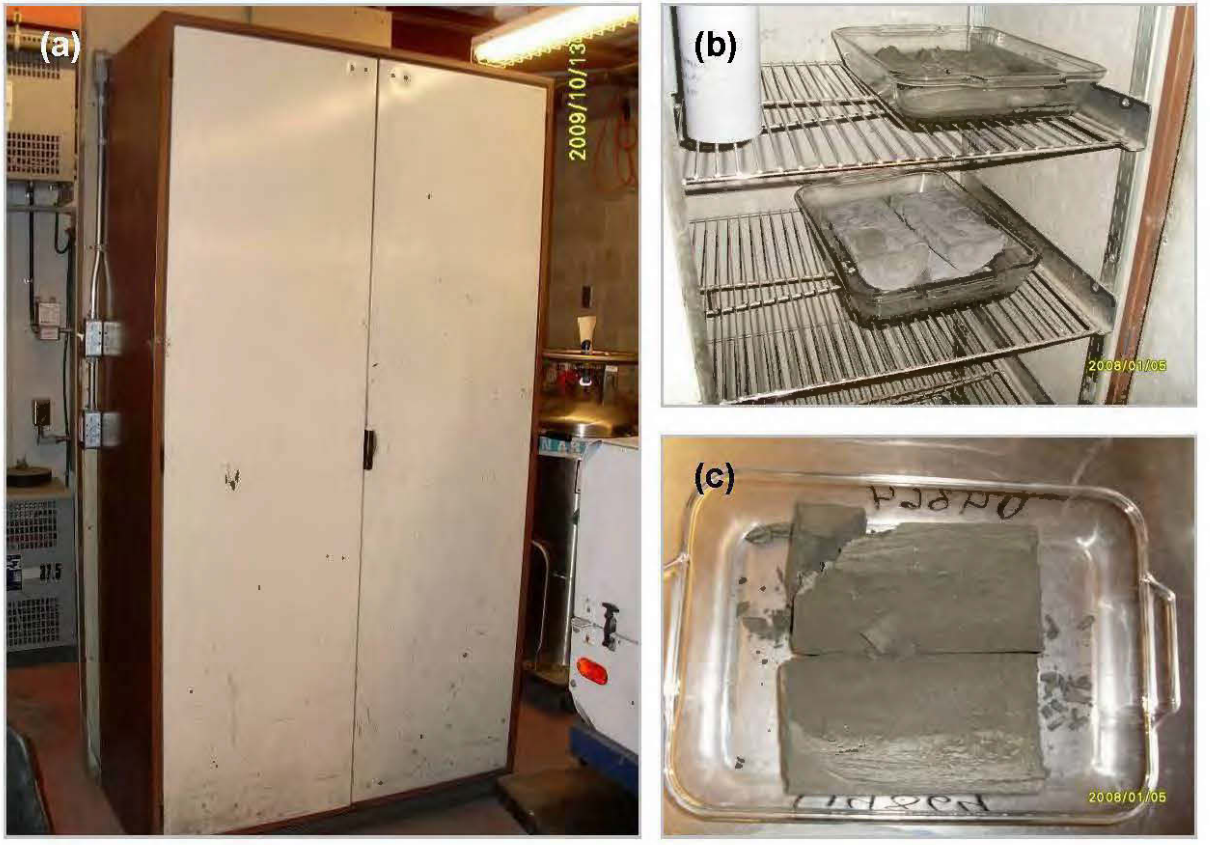

J.13 Photos of (a) the electronic drying cabinet designed to expedite sample drying (b) an inside view of the dry cabinet and (c) a dried sample on a glass plate.

J.14 Photos of (a) a 5 kg assay balance, (b) a 30 kg assay balance and (c) a 1 kg assay balance.

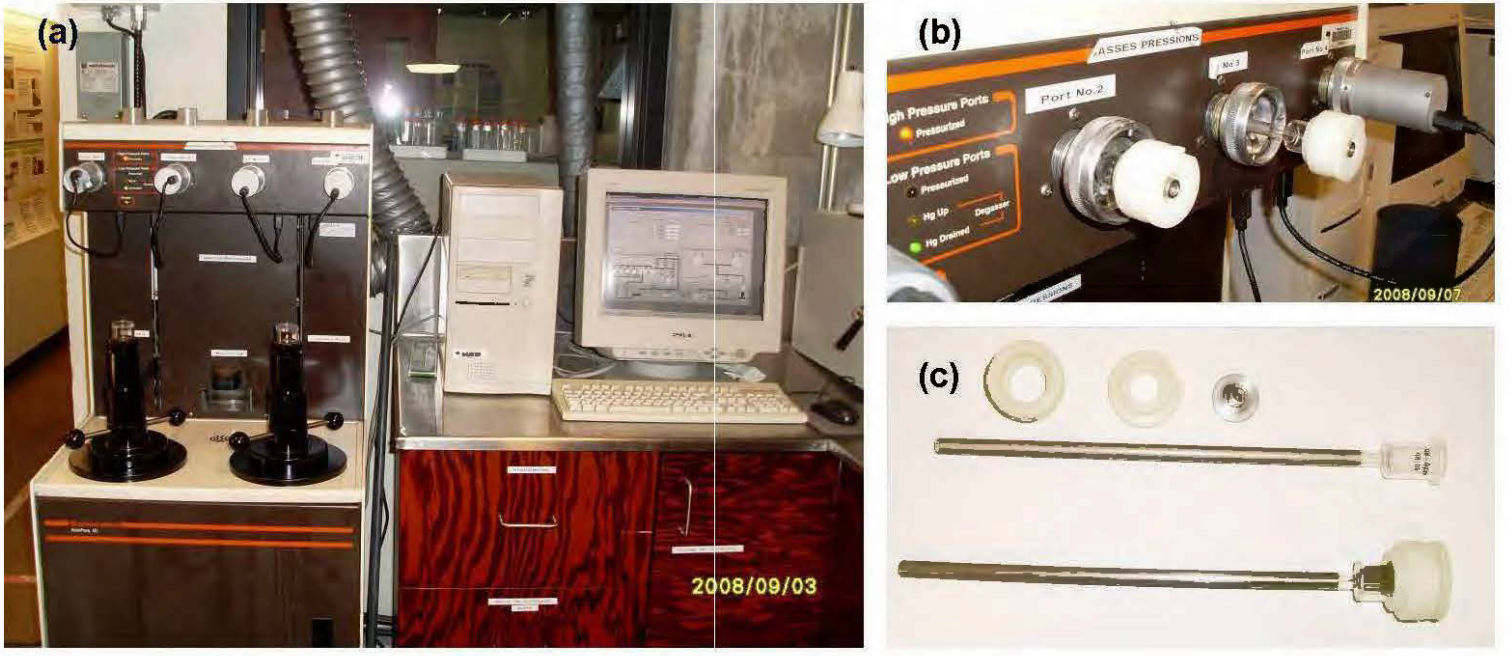

J.15 Photos of (a) the Micromeritics Autopore III Model 9420 mercury intrusion porosimetry (MIP), (b) views of low and high pressure ports and (c) MIP penetrometer.

J.16 Photo of the GENEQ Model 855-AC controlled atmosphere chamber for minimizing samples pore alteration due to hydration product destruction and moisture ingress.

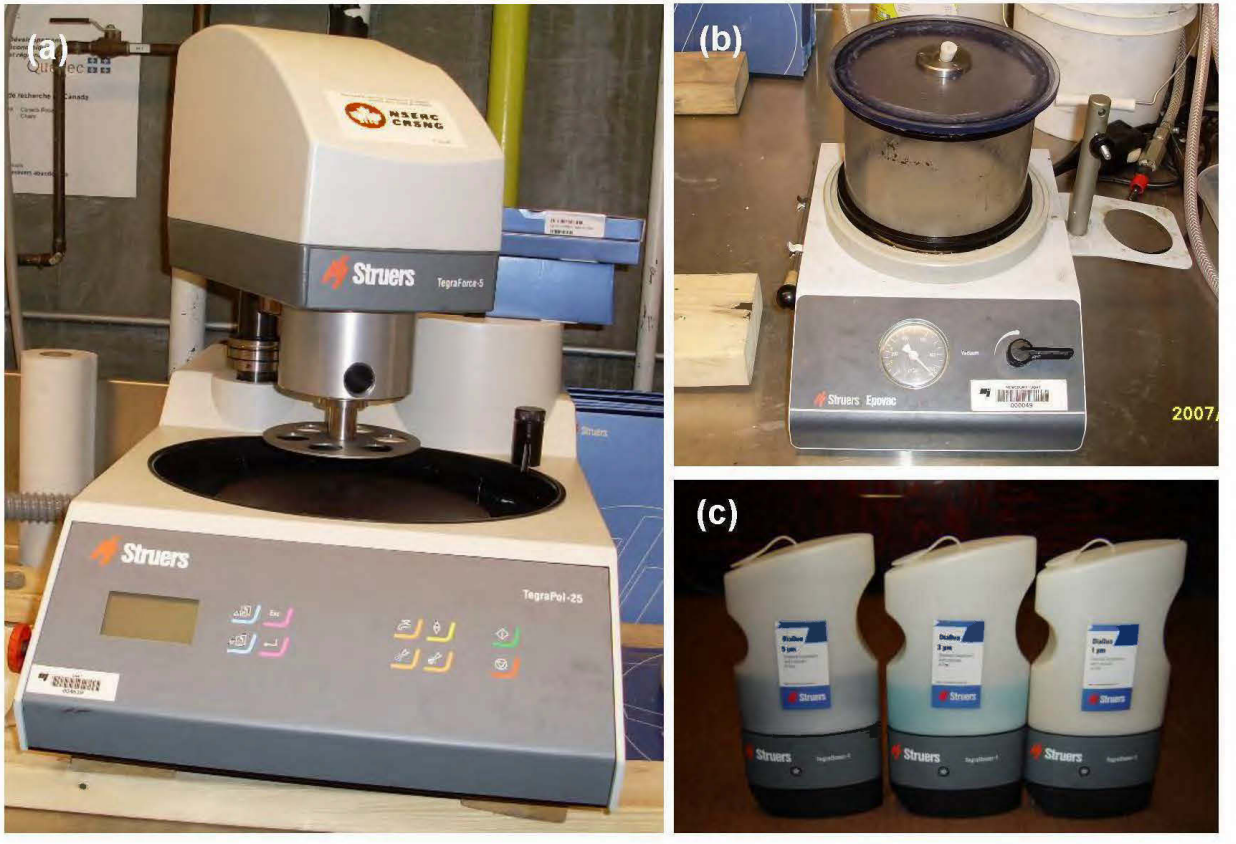

J.17 Photos of (a) Struers TegraPol - 25 grinding / polishing machine, (b) Struers EpoVac vacuum impregnation unit and (c) Struers TegraDoser-1 (DiaDuo 9 µm / 3 µm / 1 µm) diamond suspension and lubricant in one.

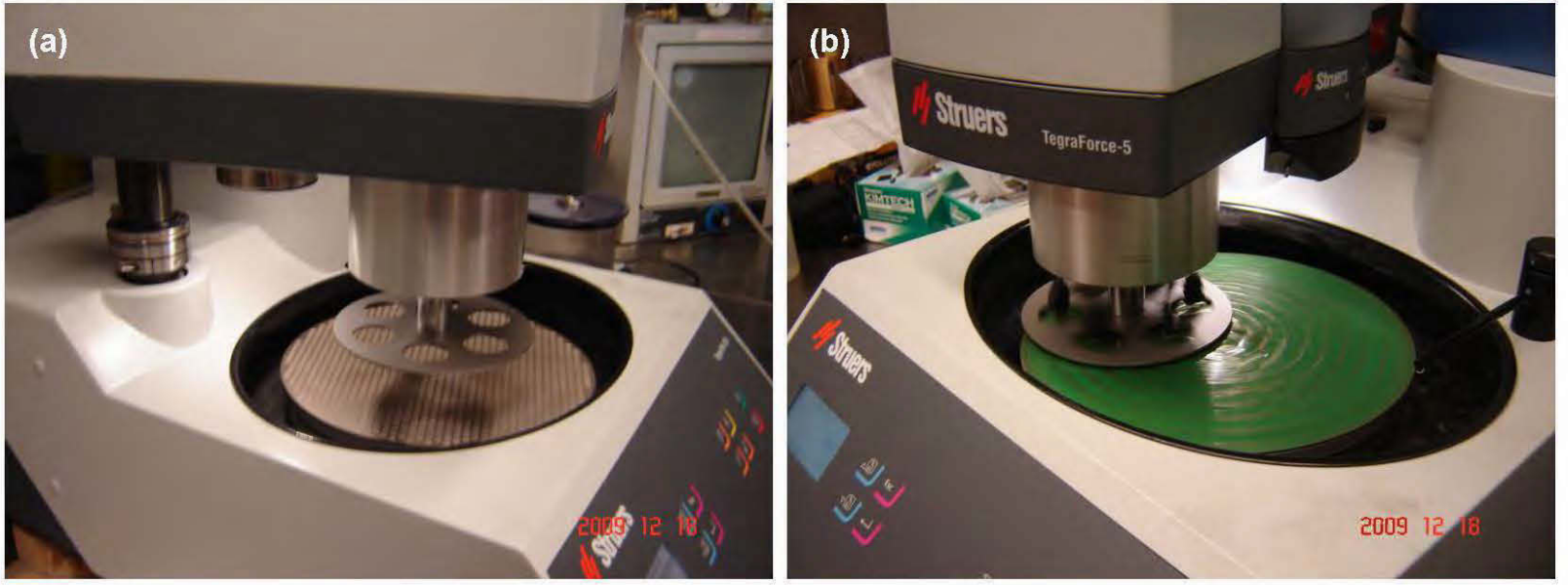

J.18 Photos of (a) resin-bonded diamond grinding disc and (b) maintenance-free composite disc within a polishing machine for grinding and fine polishing of materials.

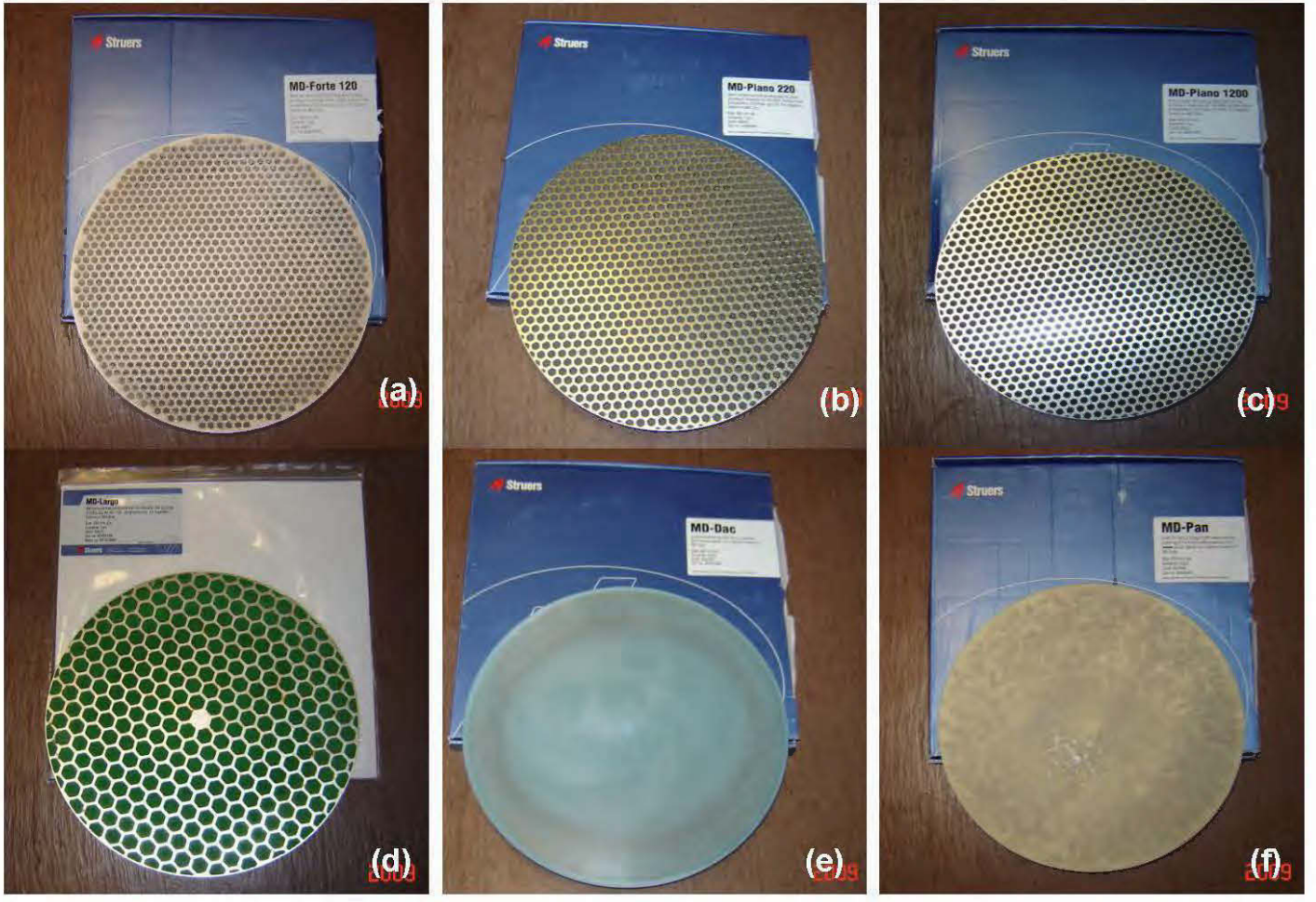

J.19 Photos of (a) MD-Forte 120, (b) MD-piano 220, (c) MD-Piano 1200, (d) MD-largo, (e) MD-Dac, and (6) MD-Pan metal or resin bonded diamond disc for plane grinding and fine polishing of materials.

J.20 Photos of polished section and freshly-fractured surface of both uncemented mine tailings and cemented paste backfills containing different binder types such as GU@100 wt%, GU-Slag@20:80 wt% and GU-FA@40:60 wt%.

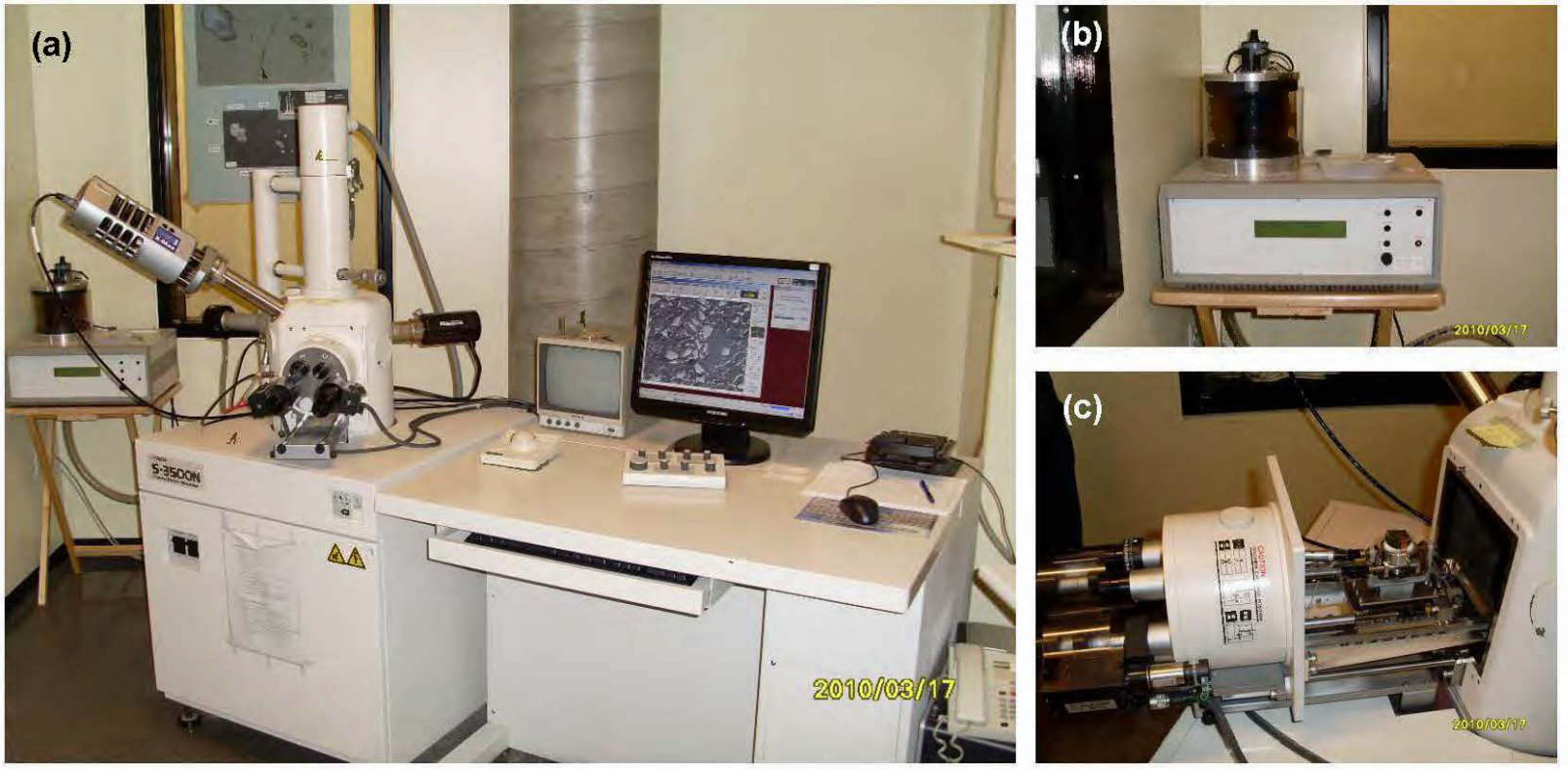

J.21 Photos of (a) scanning electron microscopy with energy dispersive X-ray spectroscopy (SEM-EDS), (b) impregnation unit and (c) internal section of sample placement within the SEM equipment.

GENERAL REFERENCES

Aboshi, H., Yoshikumi, H., Maruyama, S., 1970. Constant loading rate consolidation test. *Soils and Foundations,* Vol. 10, No. 1, pp. 43–56.

Ait-Mokhtar, A., Amiri, O., Dumargue, P., Sammartino, S., 2002. A new model to calculate water permeability of cement-based materials from MIP results. *Advance in Concrete Research,* Vol. 13, No. 1, pp. 1–7.

Aligizaki, K.K., 2006. *Pore structure of cement-based materials: Testing, interpretation and requirements*. Modern Concrete Technology, *v.12,* Taylor and Francis, Canada.

Amaratunga, L.M., Hein, G.G., Yaschyshyn, D.N., 1997. Utilization of gold mill tailings as a secondary resource in the production of a high strength total tailings paste backfill. *CIM Bulletin,* Vol. 90, No. 1012, pp. 83–88.

Amaratunga, L.M., Hmidi, N., 1998. Cold-bond agglomeration of gold mill tailings for backfill using gypsum beta-hemihydrate and cement as low cost binders. *Canadian Metallurgical Quarterly*, Vol. 36, No. 4, pp. 283–288.

Archibald, J.F., Lausch, P., He, Z.X., 1993. Quality control problems associated with backfill use in mines. *CIM Bulletin,* Vol. 86, No. 972, pp. 53–57.

Archibald, J.F., Chew, J.L. Lausch, P., 1999. Use of ground waste glass and normal Portland cement mixtures for improving slurry and paste backfill support performance. *CIM Bulletin,* Vol. 92, No. 1030, pp. 74–80.

Aubertin, M., Bussière, B. Chapuis, R. 1996. Hydraulic conductivity of homogenized tailings from hard rock mines. *Canadian Geotechnical Journal,* Vol. 33, No. 3, pp. 470-482.

Aubertin, M., Bussière, B., Bernier, L., 2002. *Environnement et gestion des résidus miniers.* Montréal: Presses Internationales Polytechnique, Montréal, Québec, Canada.

Barron, R.A., 1948. Consolidation of fine grained soils by drain wells. *Trans. of American Society of Civil Engineers,* Vol. 113, No. 5, pp. 718–734.

Basak, P., 1979. Analytical solution for consolidation of semi-infinite medium with variable permeability. *Indian Geotechnical Journal,* Vol. 9, No. 3, pp. 15–23.

Been, K., Sills, G.C., 1981. Self-weight consolidation of soft soils: An experimental and theoretical study. *Géotechnique,* Vol. 31, No. 4, pp. 519–535.

Belem, T., Benzaazoua, M., Bussière, B., 2000. Mechanical behaviour of cemented paste backfill. In: *Proceedings of the 53rd Canadian Geotechnical Conference,* Montreal, Quebec, Canada, October 15–18, pp. 373–380.

Belem, T., Benzaazoua, M., Bussière, B., Dagenais, A.M., 2002. Effects of settlement and drainage on strength development within paste backfill. In: *Proceedings of the 8th Tailings and Mine Waste.* Vail, Colorado, USA, January 27–30, pp. 139–148.

Belem, T., Bussière, B., Benzaazoua, M., 2001. The effect of microstructural evolution on the physical properties of cemented tailings paste backfill. In: *Proceedings of the 8th International Conference on Tailings and Mine Waste.* Vail, Fort Collins, Colorado, USA, January 16–19, pp. 365–374.

Belem, T., Harvey, A., Simon, R., Aubertin, M., 2004. Measurement and prediction of internal stresses in an underground opening during its filling with cemented backfill. In: *Proceedings of the 5th International Symposium on Ground support in Mining and Underground Construction,* Australia, September 28–30, pp. 619–630.

Belem, T., El Aatar, O., Bussière, B., Benzaazoua, M., Fall, M., Yilmaz, E., 2006. Characterization of self-weight consolidated paste backfill. In: *Proceedings of the 9th Int. Seminar on Paste and Thickened Tailings,* Ireland, April 3–7, pp. 333–345.

Belem, T., Benzaazoua, M., 2007. Design and application of underground mine paste backfill technology. *Geotechnical and Geological Engineering,* Vol. 26, No. 2, pp. 147–174.

Belem, T., El Aatar, O., Benzaazoua, M., Bussière, B., Yilmaz, E., 2007. Hydro-geotechnical and geochemical characterization of column consolidated cemented paste backfill. In: *Proceedings of the 9th International Symposium in Mining with Backfill,* Montreal, Quebec, Canada, April 29–May 2, pp. 151–159.

Belem, T., Benzaazoua, M., 2008. Predictive models for pre-feasibility cemented paste backfill mix design. In: *Proceedings of the 2nd International Symposium on Post-Mining,* Nancy, France, February 6–8, pp. 1–13.

Belem, T., 2009 Développement d'une méthode intégrée d'analyse de stabilité des chantiers miniers remblayés. In: *Institut de Recherche Robert-Sauvé en Santé et en Sécurité du Rravail Report 099-293*, Montreal, Québec, Canada.

Belem, T., Fourie, A.B., Fahey, M., 2010a. Time-depdenet failure criterion for cemented paste backfills. In: *Proceedings of the 13th International Seminar on Paste and Thickened Tailings,* Toronto, Ontario, Canada, May 3–6, pp. 1–14.

Belem, T., Fourie, A.B., Fahey, M., 2010b. Measurement of volume change in cemented mine backfills at early ages. In: *Proceedings of the First International Seminar on the Reduction of Risk in the Management of Tailings and Mine Waste,* Sheraton Perth Hotel, Western Australia, September 29 to October 1, pp. 1–14.

Benkendorff, P.N., 2006. Potential of lead/zinc slag for use in cemented mine backfill. *Mineral Processing and Extractive Metallurgy: Institution of Mining and Metallurgy Transactions Section C,* Vol. 115, No. 3, pp. 171–173.

Benzaazoua, M., 1996. Caractérisation physico-chimique et minéralogique de produits miniers sulfures en vue de la réduction de leur toxicité et de leur valorization. *Ph.D. Thesis,* Institut National Polytechnique de Lorraine (INPL), Nancy, France.

Benzaazoua, M., Ouellet, J., Servant, S., Newman, P., Verburg, R., 1999. Cementitious backfill with sulfur content: physical, chemical and mineralogical characterization. *Cement and Concrete Research,* Vol. 29, No. 5, pp. 719–725.

Benzaazoua, M., Belem, T., Bussière, B., 2002. Chemical factors that influence the performance of mine sulphidic paste backfill. *Cement and Concrete Research,* Vol. 32, No. 7, pp. 1133–1144.

Benzaazoua, M., Fall, M., Belem, T., 2004a. A contribution to understanding the hardening process of cemented paste backfill. *International Journal of Minerals Engineering,* Vol. 17, No. 2, pp. 141–152.

Benzaazoua M., Marion P., Picquet, I., Bussière B., 2004b. The use of paste backfill as a solidification and stabilization process for control of acid mine drainage. *Minerals Engineering,* Vol. 17, No. 2, pp. 233-243.

Benzaazoua, M., Belem, T., Yilmaz, E., 2006. Novel lab tool for paste backfill. *Canadian Mining Journal,* Vol. 127, No. 3, pp. 31–31.

Bertrand, V.J., Monroy, M.G., Lawrence, R.W., 2000. Weathering characteristics of cemented paste backfill: mineralogy and solid phase chemistry. In: *Proceedings of the 5th International Conference on Acid Rock Drainage,* Denver, Colorado, USA, May 21–24, pp. 863–876.

Bernier, R.L., Li, M.G., Moerman, A., 1999. Effects of tailings and binder geochemistry on physical strength of paste fill. In: *Proceedings of the 2nd International Conference on Mining and the Environment*, Sudbury, September 13–17, pp. 1113–1122.

Biot, M.A., 1941. General theory of three-dimensional consolidation. *Journal of Applied Physics,* Vol. 12, No. 2, pp. 155–168.

Biot, M.A., 1955. Theory of elasticity and consolidation for a porous anisotropic solid. *Journal of Applied Physics,* Vol. 20, No. 2, pp. 182–185.

Bo, M.W., Arulrajah, A., Choa, V., Na, Y.M., 1999. One-dimensional compression of slurry with radial drainage. *Japanese Geotechnical Society: Soils and Foundations,* Vol. 39, No. 5, pp. 9–17.

Bo, M.W., 2008. Have we understood enough on consolidation theory? In: *Proceedings of the 61st Canadian Geotechnical Conference,* Edmonton, Alberta, Canada, September 21–24, pp. 339–346.

Brackebusch, F.W., 1994. Basics of paste backfill systems. *Mining Engineering,* Vol. 46, No. 10, pp. 1175–1178.

Bussière, B., 1993. Evaluation des propriétés hydrogéologiques de résidus miniers utilisés comme barrières de recouvrement. *M.Sc. Thesis,* École Polytechnique de Montreal, Québec, Canada.

Bussière, B., 2007. Colloquium 2004: Hydrogeotechnical properties of hard rock tailings from metal mines and emerging geoenvironmental disposal approaches. *Canadian Geotechnical Journal,* Vol. 44, No. 9, pp. 1019–1052.

Carillo, N., 1942. Simple two and three dimensional cases in the theory of consolidation of soils. *Journal of Mathematics and Physics*, Vol. 2, No. 3, pp. 1–5.

Carrier, W.D., 1985. Consolidation parameters derived from index tests. *Geotechnique,* Vol. 35, No. 2, pp. 211–213.

Casagrande, 1., 1964. Effect of preconsolidation on settlement. *ASCE Journal of Geotechnical Engineering,* Vol. 90, Vol. 1, pp.15–32.

Cayouette, J. 2003. Optimization of the paste backfill plant at Louvicourt mine. *CIM Bulletin,* Vol. 96, No. 1075, pp. 51–57.

Celestin, J.C., 2008. Performance properties of cemented paste tailings and paste fill barrier systems under various thermal loading conditions. *M.Sc. Thesis,* The University of Ottawa, Ontario, Canada pp. 1–222.

Chan, A.H.C., 2003. Determination of coefficient of consolidation using a least squares method. *Geotechnique* Vol. 53, No. 7, pp. 673–678.

Chapuis, R.P., Aubertin, M., 2003. On the use of the Kozeny-Carman equation to predict the permeability of soils. *Canadian Geotechnical Journal,* Vol. 40, No. 3, pp. 616–628.

Cihangir, F., Yilmaz, E., Ercikdi, B., Kesimal, A., 2008. The effect of tailings particle size on the strength and microstructure of paste backfill. In: *Proceedings of the 9th Regional Rock Mechanics Symposium,* Izmir, Turkey, October 30–31, pp. 108–115.

Cincilla, W.A., Landriault, D.A., Verburg, R., 1997. Application of paste technology to surface tailings disposal of mineral wastes. In: *Proceedings of the 4th Tailings and Mine Waste,* Vail, Colorado, USA, January 13–16, pp. 343–356.

Consoli, N.C., Rotta, G.V., Prietto, P.D. 2000. Influence of curing stress on the triaxial response of cemented soils. *Géotechnique,* Vol. 50, No. 1, pp. 99–105.

Consoli, N., Rotta, G., Prietto, P., 2006. Investigation of yielding-compressibility-strength relationship for an artificially cemented soil cured under stress. *Géotechnique,* Vol. 56, No. 1, pp. 69-72.

Consoli, N.C., Rotta, G., Foppa, D., Fahey, M. 2007. Mathematical model for compression behaviour of cemented soil cured under stress. *Geomechanics and Geoengineering: An International Journal,* Vol. 2, No. 4, pp. 269–280.

Cook, R., Hover, K., 1999. Mercury porosimetry of hardened cement pastes. *Cement and Concrete Research,* Vol. 29, No. 6, pp. 933–943.

Cooke, R., 2007. Backfill pipeline distribution systems: Design methodology review. *CIM Bulletin,* Vol. 100, No. 1103, pp. 1–8 (Paper 20).

Cour, F.R., 1971. Inflection point method for computing c_v, *Journal of Soil Mechanics and Foundation Engineering,* Vol. 5, No. 2, pp. 827–831.

Davis, E.H., Raymond, G.P., 1965. A non-linear theory of consolidation. *Géotechnique,* Vol. 15, No. 2, pp. 161–173.

Deschamps, T., Benzaazoua, M., Bussière, B., Aubertin, M., Belem T., 2008. Microstructural and geochemical evolution of paste tailings in surface storage. *Minerals Engineering,* Vol. 21, No. 4, pp. 341–353.

Deschamps, T., 2009. Study of the physical and hydrogeochemical behaviour of surface paste disposal. *Ph.D. Thesis,* University of Quebec at Abitibi-Temiscamingue (UQAT), Rouyn-Noranda, Quebec, Canada, pp. 1–295.

Diamond, S., 2000. Mercury porosimetry: An inappropriate method for the measurement of pore size distributions in cement-based materials. *Cement and Concrete Research,* Vol. 30, No. 10, pp. 1517–1525.

Dirige, A.P.E., De Souza, E., 2007. Engineering design of backfill systems in undercut mining. *CIM Bulletin,* Vol. 100, No. 1103, pp. 1–7 (Paper 23).

Dirige, A.P.E., Archibald, J.F., Clarke, R., Hilkewich, T., Frank, T., 2008. The effect of different mixing techniques on strength behaviour of paste backfill. In: *The 42nd U.S. Rock Mechanics Symposium,* San Francisco, USA, June 29 – July 2, pp. 1–7.

Duncan, J.M. 1993. Limitations of conventional analysis of consolidation settlement. *ASCE Journal of Geotechnical Engineering,* Vol. 119, No. 9, pp. 1333–1359.

El Aatar, O., Belem, T., Bussiere, B., Benzaazoua, M., Yilmaz, E., 2007. Microstructural properties of column consolidated paste fill. In: *Proceedings of the 60th Canadian Geotechnical Conference,* Ottawa, Ontario, October 21–24, pp. 45–52.

El Aatar, O., 2009. Consolidation behavior of cemented paste backfill material. *M.Sc. Thesis,* Université du Québec en Abitibi-Témiscamingue, Québec, Canada.

Ercikdi, B., Kesimal, A., Cihangir, F., Deveci, H., Alp, I., 2009a. Cemented paste backfill of sulphide-rich tailings. *Cement Concrete Composites,* Vol. 31, No. 4, pp. 268–274.

Ercikdi, B., Cihangir, F., Kesimal, A., Deveci, H., Alp, I., 2009b. Utilization of industrial waste products as pozzolanic material in cemented paste backfill of high sulphide mill tailings. *Journal of Hazardous Materials,* Vol. 168, No. 2–3, pp. 848–856.

Ercikdi, B., Cihangir, F., Kesimal, A., Deveci, H., Alp, I., 2009c. Effect of natural pozzolanas as mineral admixture on the performance of cemented –paste backfill of sulphide-rich tailings. *Waste Management and Research,* Vol. 31, No. 4, pp. 268–274.

Evans, R., Ran, J., Allan, R., 2007. Application of mine backfill at Barrick Gold. *CIM Bulletin,* Vol. 100, No. 1103, pp. 1–8 (Paper 30).

Fahey, M., Helinski, M., Fourie, A.B., 2009. Some aspects of the mechanics of arching in the paste backfilled stopes. *Canadian Geotechnical Journal,* Vol. 46, No. 11, pp. 1322–1336.

Fall, M., Benzaazoua, M., 2005. Modeling the effect of sulphate on strength development of paste backfill and binder mixture optimization. *Cement and Concrete Research,* Vol. 35, No. 2, pp. 301–314.

Fall, M., Benzaazoua, M., Ouellet, S., 2005. Experimental characterization of the influence of tailings fineness and density on quality of cemented paste backfill. *Minerals Engineering,* Vol. 18, No. 1, pp. 41–44.

Fall, M., Belem, T., Samb, S., Benzaazoua, M., 2007. Experimental characterization of the stress–strain behaviour of cemented paste backfill in compression. *International Journal of Materials Sciences,* Vol. 42, No. 11, pp. 3914–3992.

Fall, M., Benzaazoua, M., Saa E.G., 2008. Mix proportioning of underground cemented backfill. *International Journal of Tunnelling and Underground Space Technology*, Vol. 23, No. 1, pp. 80–90.

Feng, T.W., Lee, Y.J., 2001. Coefficient of consolidation from the linear segment of the t 1/2 curve, *Canadian Geotechnical Journal,* Vol. 38, No. 2, pp. 901–909.

Fredlund, D.G., Hasan, J.U., 1979. One-dimensional consolidation theory: unsaturated soils. *Canadian Geotechnical Journal,* Vol. 16, No. 3, pp. 521–531.

Fourie, A.B., Helinski, M., Fahey, M., 2006. Filling the gap – a geomechanics perspective. *Australian Centre for Geomechanics Newsletter,* Vol. 26, No. 5, pp. 1–4.

Fourie, A.B., Fahey, H., Helinski, M., 2007. Using effective stress theory to characterize the behaviour of backfill. *CIM Bulletin,* Vol. 100, No. 1103, pp. 1–9 (Paper 27).

Galle, C., 2001. Effect of drying on cement-based materials pore structure as identified by mercury intrusion porosimetry: A comparative study between oven, vacuum, and freeze–drying. *Cement and Concrete Research,* Vol. 31, No. 10, pp. 1467–1477.

Gibson, R.E., England, G.L., Hussey, M., 1967. The theory of one-dimensional consolidation of saturated clays, I. Finite nonlinear consolidation of thin homogenous layers. *Géotechnique,* Vol. 17, No. 3, pp. 261–273.

Gibson, R.E., Schiffman, R., Cargill, K., 1981. The theory of one-dimensional consolidation of saturated clays, II. Finite non-linear consolidation of thick homogeneous layers. *Canadian Geotechnical Journal*, Vol. 18, No. 3, pp. 280–293.

Godbout, J., 2005. Évolution des propriétés hydriques des remblais miniers cimentés en pate durant le curage. *M.Sc. Thesis,* University of Montreal, Quebec, Canada.

Godbout, J., Bussiere, B., Aubertin, M., Belem, T., 2007. Evolution of cemented paste backfill saturated hydraulic conductivity at early curing time. In: *Proceedings of the 60th Canadian Geotechnical Conference,* Canada, October 21–24, pp. 1–7.

Godbout, J., Bussiere, B. Benzaazoua, M. Aubertin, M., 2009. Influence of pyrrhotite content on the physico-chemical behavior of cemented mine fill. In: *Proceedings of the 62nd Canadian Geotechnical Conference,* Nova Scotia, September 20–24, pp. 1–8.

Grabinsky, M.W., Therieult, J., Welch, D., 2002. An overview of paste thickened tailings disposal on surface. In: *Proceedings of the Symposium 2002 sur l'environnement et les mines: Défis et perspectives (Mine and the Environment`02),* Rouyn-Noranda, Quebec, Canada, November 3–5, pp. 1–8.

Grabinsky, M., Simms, P., 2006. Self-desiccation of cemented paste fill and implications for mine design. In: *Proceedings of the 9th International Seminar on Paste and Thickened Tailings,* Limerick, Ireland, April 3–7, pp. 323−332.

Grabinsky, M.W., Bawden, W.F., 2007. In situ measurements for geomechanical design of cemented paste fill systems. *CIM Bulletin,* Vol. 100, No. 1103, pp. 1–8 (Paper 21).

Grabinsky, M., Bawden, W., Simon, D., Thompson, B., 2008. In situ properties of cemented paste fill in an Alimak Stope. In: *Proceedings of the 61st Canadian Geotechnical Conference,* Edmonton, Alberta, Canada, Canadian Geotechnical Society, September 21–24, pp. 790–796.

Grice, T., 1998. Underground mining with backfill. In: *Proceedings of 2nd Annual Summit-Mine Tailings Disposal Systems,* Brisbane, Australia, November 24–25, pp. 1–14.

Harvey, A. 2004. Étude comparative des contraintes triaxiales dans le remblai en pâte selon la portée des chantiers. *M.Sc. Thesis,* École Polytechnique de Montréal, Quebec, Canada, pp. 1–136.

Hassani, F.P., Archibald, J.F., 1998. *Mine Backfill Handbook*. Canadian institute of Mining, Metallurgy and Petroleum (CIM), Montreal, Quebec, Canada.

Hassani, F.P., Ouellet, J., Hossein, M., 2001. Strength development in underground high-sulphate paste backfill operation. *CIM Bulletin,* Vol. 94, No. 1050, pp. 57–62.

Hassani, F., Ouellet, J., Zhu, Z., Roy, A., 2004. Paste backfill behaviour in a narrow vein mine: in situ stress and strain monitoring. In: *Proceedings of the 8th International Symposium on Mining with Backfill*, Beijing, China, September 19–21, pp. 257–267.

Hassani, F., Razavi, S.M., Isagon, I., 2007. A study of physical and mechanical behaviour of gel fill. *CIM Bulletin,* Vol. 100, No. 1103, pp. 1–7 (Paper 28).

Helinski, M., Fourie, A.B., Fahey, M., 2006. Investigation of the mechanical behaviour of early age cemented paste backfill. In: R. Jewell, S. Lawson and P. Newman (eds), *Proceedings of the 9th International Seminar on Paste and Thickened Tailings,* Limerick, Ireland, Australian Centre for Geomechanics (ACG), Perth, Western Australia, Australia, April 3–7, pp. 313–322.

Helinski, M., Fahey, M., Fourie, A., 2007a. Numerical modelling of cemented paste backfill deposition. *Journal of Geotechnical and Geoenvironmental Engineering,* Vol. 13, No. 10, pp. 1308–1319.

Helinski, M., Fourie, A.B., Fahey, F., Ismail, M., 2007b. Assessment of the self-desiccation process in cemented mine backfills. *Canadian Geotechnical Journal,* Vol. 44, No. 10, pp. 1148–1156.

Helinski, M., Fahey, M., Fourie, A.B., 2007c. An effective stress approach to modeling mine backfilling. *CIM Bulletin,* Vol. 100, No. 1103, pp. 1–8 (Paper 29).

Helinski, M., Fourie, A.B., Fahey, M., 2009. Preliminary results from an investigation into the effect of application of effective stress to cemented paste backfill during curing. *Australian Centre for Geomechanics Newsletter,* Vol. 31, No. 12, pp. 10–13.

Henderson, A., Revell, M., 2005. *Basic Mine Fill Materials.* In: Y. Potvin, E. Thomas and A.B. Fourie (eds), Handbook on Mine Fill, Australian Centre for Geomechanics (ACG), Western Australia, Australia, Chapter 2, pp. 13–19.

Henderson, A., Revell, M.B., Landriault, D.A., Coxon, J., 2005. *Paste fill.* In: Y. Potvin, E. Thomas, A. Fourie (eds.), Handbook on Mine Fill, Australian Centre for Geo-mechanics (ACG), Western Australia, Australia, Chapter 6, pp. 83–97.

Hsu, T.W., Lu, S.C., 2006. Behavior of one-dimensional consolidation under time-dependent loading. *Journal of Engineering Mechanics,* Vol. 132, No. 4, pp. 457–462.

Janbu, N., 1965. Consolidation of clay layers based on nonlinear stress-strain. In: *Proceedings of the Sixth International Conference on Soil and Mechanics and Foundation Engineering,* Vol. 2, Montreal September 12–15, pp. 83–87.

Jones, D.R., Li, H., Waite, T., Fenton, B., 2001. Hydrochemical and geotechnical properties of cemented uranium paste tailings. In: *Proceedings of 8th International Conference on Tailings and Mine Waste.* Vail, Colorado, USA, January 16–19, pp. 401–409.

Justnes, H., Reyniers, B., Van Loo, D., Sellevold, E.J., 1994. An evaluation of methods for measuring chemical shrinkage of cementitious paste. *Nordic Concrete Research,* Vol. 14, No. 3, pp. 45–61.

Justnes, H., Van Gemert, A., Verboven, F., Sellevold, E.J., 1996. Total and external chemical shrinkage of low *w/c* ratio cement pastes. *Advanced Cement Research,* Vol. 8, No. 31, pp. 121–126.

Kesimal, A., Ercikdi, B., Yilmaz, E., 2003. The effect of desliming by sedimentation on paste backfill performance. *Minerals Engineering,* Vol. 16, No. 10, pp. 1009–1011.

Kesimal, A., Yilmaz, E., Ercikdi, B., 2004. Evaluation of paste backfill test results obtained from different size slumps with varying cement contents for sulphur rich mill tailings. *Cement and Concrete Research,* Vol. 34, No. 10, pp. 1817–1822.

Kesimal, A., Yilmaz, E., Ercikdi, B., Alp, I., Deveci, H., 2005. Effect of properties of tailings and binder on short and long terms strength and stability of cemented paste backfill. *Materials Letters,* Vol. 59, No. 28, pp. 3703–3709.

Klein, K., Simon, D., 2006. Effect of specimen composition on the compressive strength development of cemented paste backfill. *Canadian Geotechnical Journal,* Vol. 43, No. 3, pp. 310–324.

Kumar, R., Bhattacharjee B., 2003. Porosity, pore size distribution and in situ strength of concrete. *Cement and Concrete Research,* Vol. 33, No. 1, pp. 155–164.

Kwong, J.Y.T., 2004. Chemical stability of two tailings backfill materials with two types of binders. In: *Proceedings of the 8th International Symposium on Mining with Backfill-Minefill 2004*, Beijing, China, September 19–21, pp. 219–223.

Laloui, L., Leroueil, S., Chalindar, S., 2008. Modeling the combined effect of strain rate and temperature on one-dimensional compression of soils. *Canadian Geotechnical Journal,* Vol. 45, No. 12, pp. 1765–1777.

Landriault, D.A, 1995. Paste backfill mix design for Canadian underground hard rock mines. In: *Proceedings of the 97th Annual General Meeting of the CIM Rock Mechanics and Strata Control,* Halifax, Nova Scotia, Canada, May 14–18, pp. 1–13.

Landriault, D.A, 2001. *Backfill in Underground Mining.* In: W. Hustrulid and R. Bullock (eds), Underground Mining Methods Engineering Fundamentals and International Case Studies, Society of Mining Engineers (SME), Littleton, Colorado, USA, Chapter 69, pp. 601–614.

Lee, K., Sills, G C., 1981. The consolidation of a soil stratum, including self-weight effects and large strains. *International Journal for Numerical and Analytical Methods in Geomechanics*, Vol. 5, No. 2, pp. 405–428.

Lekha, K.R., Krishnaswamy, N.R., Basak, P., 2003. Consolidation of clays for variable permeability and compressibility. *Journal of Geotechnical and Geoenvironmental Engineering,* Vol. 129, No. 11, pp. 1001–1009.

Leroueil, S., 1996. Compressibility of clays: fundamental and practical aspects. *Journal of Geotechnical Engineering,* Vol. 122, No. 7, pp. 534–543.

Leroueil, S., Kabbaj, M., Tavenas, F., Bouchard, R. 1985. Stress–strain-strain rate relation for the compressibility behavior of natural sensitive clays. *Géotechnique,* Vol. 35, No. 2, pp. 159–180.

le Roux, K.-A., Bawden, W.F., Grabinsky, M.F., 2002. Comparison of the material properties of in situ and laboratory prepared cemented paste backfill. In: *Proceedings of the 104th CIM Annual General Meeting,* Vancouver, British Columbia, Canada, April 27 to May 3, pp. 1–13.

le Roux, K.-A. 2004. In situ properties and liquefaction analysis of cemented paste backfill. *Ph.D. Dissertation,* University of Toronto, Ontario, Canada, pp. 1–204.

le Roux, K.-A., Bawden, W.F., Grabinsky, M.W. 2005. Field properties of cemented paste backfill at the Golden Giant mine. *Mining Technology: Institution of Mining and Metallurgy Transactions Section A,* Vol. 114, No. 2, pp. 65–80.

Levens, R.L., Marcy, A.D., Boldt, C.M.K., 1996. *Environmental impacts of cemented mine waste backfill.* Report of Investigations RI 9599, USA, pp. 1–23.

Lottermoser, B., 2007. *Mine wastes: characterization, treatment and environmental impacts.* 2nd ed., Germany: Springer-Verlag Berlin Heidelberg.

Lowe, J., Jonas, E., Obrician, V., 1969. Controlled gradient consolidation test. *ASCE Journal of the Soil Mechanics and Foundation Division,* Vol. 95, No. 1, pp. 77–97.

Martin, V., Aubertin, M., McMullen, J., 2006. Surface disposal of paste tailings. In: *Proceedings of the 5th ICEG Environmental Geotechnics: Opportunities, Challenges and Responsibilities for Environmental Geotechnics,* vol. 2, Cardiff, Wales, United Kingdom, Thomas Telford Services Ltd., International Congresses on Environmental Geotechnics (ICEG), June 26–30, pp. 1471–1478.

Mbonimpa, M., Aubertin, M., Chapuis, R. Bussière, B. 2002. Practical pedotransfer functions for estimating the saturated hydraulic conductivity. *Geotechnical and Geological Engineering,* Vol. 20, No. 3, pp. 235–259.

McCarthy, D.F., 2007. Essentials of soil mechanics and foundations: Basic geotechnics (7th edn), *Pearson Prentice Hall,* Toronto, Canada, pp. 1–864.

Mesri, G., Rokhsar, A., 1974. Theory of consolidation for clays. *ASCE Journal of Geotechnical Engineering,* Vol. 100, No. 8, pp. 889–904.

Mesri, G., Shahein, M., 1999. Coefficient of consolidation by the inflection point method. *ASCE Journal of Geotechnical and Geoenvironmental Engineering,* Vol. 125, Vol. 8, pp.716–718.

Mitchell, R.J., Smith, J.D., 1979. Mine backfill design and testing. *Canadian Institute of Mining, Metallurgy and Petroleum Bulletin,* Vol. 72, No. 8018, pp. 82–89.

Mitchell, R.J, Olsen, R., Smith, J.D, 1982. Model studies on cemented tailings used in mine backfill. *Canadian Geotechnical Journal,* Vol. 19, No. 1, pp. 14–28.

Moerman, A., Rogers, K., Cooper, M., Li, M., 2001. Operating and technical issues in the implementation of paste backfill at the Brunswick Mine. In: *Proceedings of the 7th International Symposium on Mining with Backfill,* Littleton, Colorado, United States, September 17–19, pp. 237–250.

Mohammed, A.M.O., Hossein, M., Hassani, F.P., 2002. Hydromechanical evaluation of stabilized mine tailings. *International Journal of Environmental Geology,* Vol. 41, No. 7, pp. 749–759.

Mohamed, A.M.O., Hassani, F., Hossein, M. 2003. Role of fly ash and aluminum addition on ettringite formation in lime-remediated mine tailings. *Journal of Cement, Concrete and Aggregates (CCA),* Vol. 25, No. 2, pp. 49–58.

Morris, P.H., 2002. Analytical solution of linear finite-strain one-dimensional consolidation of the soils. *ASCE Journal of Geotechnical and Geoenvironmental Engineering,* Vol. 128, No. 4, pp. 319–326.

Nasir, O., 2008. Modeling of coupled process in hydrating cemented paste backfill structures and application to the analysis of their performance. *M.Sc. Thesis,* University of Ottawa, Ontario, Canada, pp. 1–130.

Nehdi, M., Tarig, A., 2007. Stabilization of sulphidic mine tailings for prevention of metal release and acid drainage using cementitious materials: a review. *Journal of Environmental Engineering and Science,* Vol. 6, No. 4, pp.423–436.

Olson, R.E., 1977. Consolidation under time-dependent loading. *ASCE Journal of Geotechnical Engineering,* Vol. 103, No. 1, pp. 55–60.

Ouellet, J., Benzaazoua, M., Servant, S. 1998. Mechanical, mineralogical and chemical characterization of paste backfill. In: *Proceedings of the 5th International Conference on Tailings and Mine Waste,* Vail, Colorado, USA, January 26–29, pp. 139–146.

Ouellet, J., Servant, S., 2000. In-situ mechanical characterization of a paste backfill with self-boring pressuremeter. *CIM Bulletin,* Vol. 93, No. 1042, pp. 110–115.

Ouellet, S., 2006. Investigation of mineralogical characterization, microstructural evolution and environmental behaviour of cemented paste backfills. In: *Ph.D. Dissertation,* University of Quebec at Abitibi-Temiscamingue (UQAT), Rouyn-Noranda, Quebec, Canada, pp. 1–287.

Ouellet, S., Bussière, B., Mbonimpa, M., Benzaazoua, M., Aubertin, M., 2006. Reactivity and mineralogical evolution of an underground mine sulphidic cemented paste backfill. *Minerals Engineering,* Vol. 19, No. 5, pp. 407–419.

Ouellet, S., Bussiere, B., Aubertin, M., Benzaazoua, M. 2007. Microstructural evolution of cemented paste backfill: Mercury intrusion porosimetry test results. *Cement and Concrete Research,* Vol. 37, No. 12, pp. 1654–1665.

Ouellet, S., Bussière, B., Aubertin, M., Benzaazoua, M., 2008. Characterization of cemented paste backfill pore structure using SEM and IA analysis. *Bulletin of Engineering Geology and the Environment,* Vol. 67, No. 2, pp. 139–152.

Pandian, N., Nagaraj, T., Sivakumar Babu, G.L., 1992. Generalized state parameter for partly saturated soils. *Journal of Geotechnical Engineering,* Vol. 118, No. 5, pp. 622–627.

Parkin, A.K., 1978. Coefficient of consolidation by the velocity method. *Géotechnique,* Vol. 28, No. 4, pp. 472–474.

Petrolito, J., Anderson, R.M., Pigdon, S.P., 2005. A review of binder materials used in stabilized backfills. *CIM Bulletin,* Vol. 98, No. 1085, pp. 1–7.

Pierce, M.E., 1997. Laboratory and numerical analysis of the strength and deformation behavior of paste fill. *M.Sc. Thesis,* Queens University, Canada, pp. 1–195.

Pierce, M.E., Bawden, W.F., Paynter, J.T. 1998. Laboratory testing and stability analysis of paste backfill at the Golden Giant Mine. In: *Proceedings of the 6th International Symposium on Mining with Backfill,* Brisbane, Australia, The Australasian Institute of Mining and Metallurgy, April 14–16, pp. 159–165.

Potvin, Y., Thomas, E.H., Fourie, A.B., 2005. *Handbook on Mine Fill.* Australian Centre for Geomechanics (ACG), Western Australia, Perth, Australia.

Raju, N., Pandian P.S.R., Nagaraj, T., 1995. Analysis and estimation of coefficient of consolidation. *Geotechnical Testing Journal,* Vol. 18, No. 2, pp. 252–258.

Ramlochan, T., Grabinsky, M.W., Hooton, D.H., 2004. Microstructural and chemical investigations of cemented paste backfills. In: *Proceedings of the 11th International Conference on Tailings and Mine Waste.* Vail, Fort Collins, Colorado, United States, October 10–13, pp. 293–304.

Rankine, K.J., Sivakugan, N., Cowling, R.M., 2006. Emplaced geotechnical characteristics of hydraulic fills in a number of Australian mines. *Geotechnical and Geological Engineering,* Vol. 24, No. 1, pp. 1–14.

Rendulic, L., 1936. Porenziffer und porenwasserdruck in tonen. *Der Bauingenieur,* Vol. 17, No. 2, pp. 559–564.

Revell, M. 2004. Paste - how strong is it? In: *Proceedings of the 8th International Symposium on Mining with Backfill*, Beijing, China, September 19–21, pp. 286–294.

Robinson, R.G., Allam, M.M., 1996. Determination of coefficient of consolidation from early stage of log *t* plot. *Geotechnical Testing Journal,* Vol. 19, No. 3, pp. 316–320.

Rotta, G.V., Consoli, N.C., Prietto, P.D.M., Coop, M.R., Graham, J. 2003. Isotropic yielding in a cemented soil cured under stress. *Géotechnique,* Vol. 53, No. 5, pp. 493–501.

Sainsbury, D.P., Revell, M.B., 2007. Advancing paste fill bulkhead design using numerical modelling. *CIM Bulletin,* Vol. 100, No. 1103, pp. 1–10 (Paper 25).

Schiffman, R.L., Pane, V., Gibson, R.E., 1984. The theory of one-dimensional consolidation of saturated clays. IV. An overview of non-linear finite strain sedimentation and consolidation, In: *Sedimentation consolidation Models - Predictions and Validation,* Eds. R.N. Yong & F.C. Townsend, pp. 1–29.

Servant, S., 2001. Détermination des paramètres mécaniques des remblais miniers faits de résidus ciments. *M.Sc. Thesis,* McGill University, Montreal, Quebec, Canada.

Shuttleworth, J.A., Thomson, B.J., Wates, J.A., 2005. Surface paste disposal at Bulyanhulu – practical lessons learned. In: *Proceedings of the 8th International Seminar on Paste and Thickened Tailings,* Santiago, Chili, April 20–22, pp. 207–218.

Simms, P., Grabinsky, M., 2009. Direct measurement of matric suction in triaxial tests on early-age cemented paste backfill. *Canadian Geotechnical Journal,* Vol. 46, No. 1, pp. 93–101.

Sivakugan, N., Rankine, K.J., Rankin, K.S., 2005. Geotechnical consideration in mine backfilling in Australia. *J. Cleaner Production,* Vol. 14, No. 12–13, pp. 1168–1175.

Smith, R.E., Wahls, H.E., 1969. Consolidation under constant rate of strain. *ASCE Journal of the Soil Mechanics and Foundation Division,* Vol. 95, No. 2, pp. 519–539.

Sridharan, A., Murthy, N.S., Prakash, K., 1987. Rectangular hyperbola method of consolidation analysis. *Géotechnique,* Vol. 37, No. 3, pp. 355–368.

Sridharan, A., Nagaraj, H.B., 2004. Coefficient of consolidation and its correlation with index properties of soils. *Geotech. Testing J.,* Vol. 27, No. 5, pp. 108–116.

Sridharan, A., Prakash, K., Asha, S.R., 1995. Consolidation behavior of soils. *Geotechnical Testing Journal,* Vol. 18, No. 1, pp. 56–68.

Sridharan, A., Rao, A.S., 1981. Rectangular hyperbola fitting method for one dimensional consolidation. *Journal of Geotechnical Engineering,* Vol. 4, No. 4, pp. 161–168.

Stone, D., 2007. Factors that affect cemented rock fill quality in Nevada mines. *CIM Bulletin,* Vol. 100, No. 1103, pp. 1–6 (Paper 24).

Tarig, A., Nehdi, M. 2007. Developing durable paste backfill from sulphidic tailings. *Waste Resources and Management,* Vol. 160, No. 4, pp. 155–166.

Taylor, D.W., 1948. Fundamental of soil mechanics, John Wiley & Sons, New York.

Terzaghi, K. 1936. The Shearing resistance of saturated soils. In: *Proceedings of the First International Conference on Soil Mechanics,* Vol. 1, pp. 54–56.

Terzaghi, K., 1923. Die berechnun der durchlassigkeitziffer des tons aus dem verlauf der hydrodynamicschen spannungserscheinungen. Vol. 132, No. 34, pp. 125–318.

Terzaghi, K., 1943. *Theoretical Soil Mechanics,* John Wiley, New York.

Terzaghi, K., Peck, R.B., Mesri, G., 1996. *Soil Mechanics in Engineering Practice,* 3rd Ed., John Wiley and Sons, New York, 223–229.

Wissa, A.E.Z., Christian, J.T., Davis, E.H., Heiberg, S., 1971. Consolidation at constant rate of strain. *Journal of Soil Mechanics & Foundation,* Vol. 97, No. 10, pp. 1393–1413.

Witteman, M., Simms, P., 2010. Hydraulic response of cemented paste backfill during and after hydration. In: *Proceedings of the 13th International Seminar on Paste and Thickened Tailings*, Toronto, Ontario, Canada, May 3-6, pp. 199–208.

Verburg, R.B.M., 2002. Paste technology for disposal of acid-generating tailings. *Mining Environmental Management,* Vol. 13, No. 7, pp. 14–18.

Yilmaz, E., 2003. Experimental investigation of the compressive strength behaviour of the cemented paste backfill samples prepared from sulphidic mine tailings. *M.Sc. Thesis,* Black Sea Technical University (KTU), Trabzon, Turkey, pp. 1–117.

Yilmaz, E., Kesimal, A., Ercikdi, B., 2003a. The factors affecting the strength and stability of paste backfill. *Turkish Journal of Earth Sciences,* Vol. 28, No. 2, pp. 155–169.

Yilmaz, E., Kesimal, A., Ercikdi, B., 2003b. Strength properties in varying cement dosages for paste backfill samples. In: *Proceedings of the 10th International Symposium on Tailings and Mine Waste*, Vail, Colorado, USA, October 12–15, pp. 109–114.

Yilmaz, E., Kesimal, A., Ercikdi, B., 2004a. Evaluation of acid producing sulphidic mine tailings as a paste backfill. *Earth Science Review,* Vol. 17, No. 1, pp. 11–19.

Yilmaz, E., Kesimal, A., Ercikdi, B., 2004b. Strength development of paste backfill samples at long term by using two different binders. In: *Proceedings of the 8th International Symposium on Mining with Backfill*, Beijing, China, Sept. 19–21, pp. 281–285.

Yilmaz, E., Kesimal, A., Ercikdi, B., Benzaazoua, M., Belem, T., Bussière, B., 2005. Short and long terms strength performance of cemented paste backfill. In: *Proceedings of the 19th International Mining Congress,* Izmir, Turkey, June 9–12, pp. 11–17.

Yilmaz, E., El Aatar, O., Belem, T., Benzaazoua, M., Bussière, B., 2006. Effect of consolidation on performance of cemented paste backfill. In: *Proceedings of the 21st Underground Mine Support Conference,* Val d'Or, Quebec, April 11–12, pp. 1–14.

Yilmaz, E., Belem, T., Benzaazoua, M., Kesimal, A., Ercikdi, B., 2007. Evaluation of the strength properties of deslimed tailings paste backfill. *The International Journal of Minerals Resources Engineering,* Vol. 12, No. 2, pp. 129–144.

Yilmaz, E., 2007. How efficiently the volume of wastes produced from mining operations can be reduced without causing any important environmental impact? *Environmental Synthesis Report,* University of Quebec at Abitibi-Temiscamingue (UQAT), Rouyn-Noranda, Quebec, Canada, pp. 1–45.

Yilmaz, E., Belem, T., Benzaazoua, M., Bussière, B., 2008a. Experimental characterization of the influence of curing under stress on the hydromechanical and geotechnical properties of cemented paste backfill. In: *Proceedings of the 15th Int. Conference on Tailings and Mine Waste,* Vail, Colorado, USA, October 18–23, pp. 139–152.

Yilmaz, E., Belem, T., Bussière, B., Benzaazoua, M., 2008b. Consolidation characteristics of early age cemented paste backfill. In *Proceedings of the 61st Canadian Geotechnical Conference,* Edmonton, Alberta, Canada, September 21–24, pp. 797–804.

Yilmaz, E., Benzaazoua, M., Belem, T., Bussière, B., 2009a. Effect of curing under pressure on compressive strength development of cemented paste backfill. *Minerals Engineering,* Vol. 22, No. 9–10, pp. 772–785.

Yilmaz, E., Belem, T., Bussière, B., Benzaazoua, M., 2009b. Relationships between porosity, microstructure and compressive strength of consolidated and unconsolidated cement paste backfills. *Cement and Concrete Composites* (submitted in October 2009).

Yilmaz, E., Belem, T., Bussière, B., Mbonimpa, M., Benzaazoua, M., 2010a. Evaluation of the one-dimensional consolidation behaviour of early age cemented paste backfills. *Canadian Geotechnical Journal* (submitted in January 2010).

Yilmaz, E., Belem, T., Benzaazoua, M., Bussière, B., 2010b. Assessment of the improved CUAPS apparatus to estimate in situ properties of cemented paste backfill. *Geotechnical Testing Journal,* Vol. 33, No. 5, pp. 351–362.

Yumlu, M., Guresci, M., 2007. Paste backfill bulkhead failures and pressure monitoring at Cayeli Mine. *CIM Bulletin,* Vol. 100, No. 1103, pp. 1–10 (Paper 22).

Zhuang, Y., Xie, K., Li, X., 2005. Analysis of consolidation with variable compres-sibility and permeability. *J. Zhejiang University Science,* Vol. 6, No. 3, pp. 181–187.